

Jie Ren  
*Editor*

# Biodegradable Poly (Lactic Acid)

Synthesis, Modification, Processing  
and Applications



**TSINGHUA**  
UNIVERSITY PRESS



Springer

Jie Ren

**Biodegradable Poly(Lactic Acid): Synthesis, Modification,  
Processing and Applications**

Jie Ren

# **Biodegradable Poly(Lactic Acid): Synthesis, Modification, Processing and Applications**

With 150 figures



*Author*

Prof. Jie Ren

Institute of Nano and Bio-Polymeric Materials

Tongji University, 200438, Shanghai, China

ISBN 978-7-302-23601-6

Tsinghua University Press, Beijing

ISBN 978-3-642-17595-4

e-ISBN 978-3-642-17596-1

Springer Heidelberg Dordrecht London New York

Library of Congress Control Number: 2010927590

© Tsinghua University Press, Beijing and Springer-Verlag Berlin Heidelberg 2010

This work is subject to copyright. All rights are reserved, whether the whole or part of the material is concerned, specifically the rights of translation, reprinting, reuse of illustrations, recitation, broadcasting, reproduction on microfilm or in any other way, and storage in data banks. Duplication of this publication or parts thereof is permitted only under the provisions of the German Copyright Law of September 9, 1965, in its current version, and permission for use must always be obtained from Springer. Violations are liable to prosecution under the German Copyright Law.

The use of general descriptive names, registered names, trademarks, etc. in this publication does not imply, even in the absence of a specific statement, that such names are exempt from the relevant protective laws and regulations and therefore free for general use.

*Cover design:* Frido Steinen-Broo, EStudio Calamar, Spain

Printed on acid-free paper

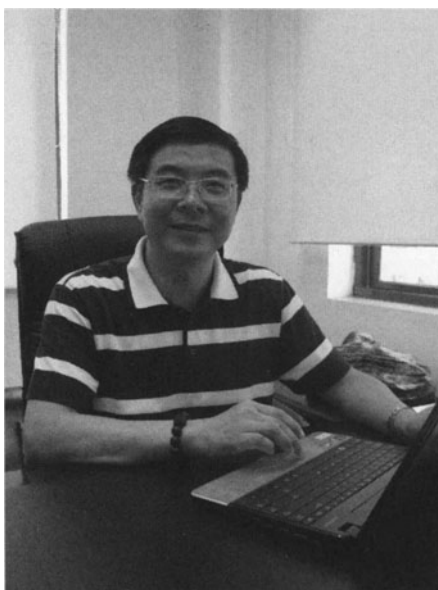
Springer is part of Springer Science+Business Media ([www.springer.com](http://www.springer.com))

---

## About Author

---

**Jie Ren** Born in 1965, PhD, a professor at the Institute of Nano and Bio-Polymeric Materials, Tongji University in Shanghai. He holds the position of the director of the institute and serves as a council member of Chinese Materials Research Society, a vice chairman of Council of Degradable Plastic, China Plastics Processing Industry Association, an expert of new materials forecast designated by Shanghai municipal government, a member of Biological Material Committee in Shanghai Society of Biology and Medical Science, the director of Degradable Materials Committee in Shanghai Society of Advanced Materials, an editor of “Plastics” and “Journal of Building Materials”.



He has concentrated on the research of biodegradable material, controllable drug delivery system and tissue engineering scaffold. In the field of biodegradable material, the main projects he has undertaken include special project for technological innovation of the 2010 Shanghai World Exposition, special project for biomass engineering high-tech industrialization of National Development and Reform Commission, project of the National High Technology Research and Development Program of China (863 Program), Shanghai Key Scientific and Technological Project, Shanghai Key Nano Science and Technology Project, and some international cooperation projects(cooperated with Boeing.etc). His research

was supported by Program for New Century Excellent Talents in MOE of China in 2005. In 2007 he was chosen to be one of the “Shanghai Subject Chief Scientist”.

He has published a few monographs and more than 160 papers, including over 50 SCI papers which are cited over 300 times. He has achieved 42 China patents and 1 US patents.

---

# Preface

---

Polymers with biodegradability and renewability have attracted much attention due to the environmental concerns and sustainability issues associated with petroleum-based polymers. At present the depletion of oil resources has been a large concern all over the world and “white pollution” is becoming a serious problem threatened the human health and the environment. Therefore, the low-carbon economy has been put on the agenda. Poly(lactic acid) (PLA) is one of the most important environment-friendly biodegradable thermoplastic polyester with extensive application. Because of its renewable resources, low toxicity and its environment-friendly characteristics along with performance comparable with many petroleum-based plastics, much attention has been paid for its use in service ware, grocery, waste-composting bags, mulch films, ideal material for food packaging, engineering plastics and other consumer products.

This book is written for indicating the importance of PLA in material field. The production and properties of lactic acid and the monomeric building block of PLA are described in detail in this book; the synthesis and manufacture of PLA are described, too. In addition, the book aims at introducing the recent developments in preparation of the linear, graft or branch, star-shaped, and dendritic PLA copolymers and the catalysts used in copolymerization. The processing of PLA, such as injection, spinning, blowing, foaming, is also discussed. A variety of products including bottles, fibers, film, and foam can be manufactured from PLA. Furthermore, PLA can be applied in the field of medical industry used as tissue engineering scaffold, controllable drug delivery system, and so on. The standard and test methods of PLA are discussed in the end of the book.

Some my colleagues and doctoral candidates have taken part in the writing of this book. These colleagues are professor Shuying Gu, associate professor Hua Yuan, associate professor Tianbin Ren, Dr. Qingang Tan. And the doctoral candidates

Dakai Chen, Jianbo Li, Yang Cao, Qinfeng Wang, Naiwen Zhang, Tao Yu, Minghao Gu have also joined the above writing.

I also express my thanksgiving to the professor Guofang Gu, associate professor Weizhong Yuan, and the doctoral candidates Yan Liu, Yang Qu, Zhonghai Zhang for their help during the completion of this book. Without their help this book wouldn't be published so easily.



# Contents

<b>1</b>	<b>Introduction</b> .....	1
<b>2</b>	<b>Lactic Acid</b> .....	4
2.1	Introduction .....	4
2.2	Properties.....	4
2.3	Preparation.....	7
2.3.1	Chemical Synthesis.....	7
2.3.2	Fermentation.....	7
2.4	Separation and Purification of LA.....	9
2.4.1	Esterification and Hydrolysis.....	10
2.4.2	Crystallization.....	10
2.4.3	Molecular Distillation.....	11
2.5	Application .....	12
2.5.1	Raw Materials of PLA .....	12
2.5.2	Additives in Foods.....	12
2.5.3	Applications in Cosmetics .....	13
2.5.4	Applications in Detergents.....	13
	References .....	14
<b>3</b>	<b>Synthesis and Manufacture of PLA</b> .....	15
3.1	Direct Polycondensation of Lactic acid.....	15
3.2	Azeotropic Dehydrative Polycondensation of LA.....	21
3.3	Polycondensation Kinetics of LA.....	23
3.4	Ring-Opening Polymerization of Lactide.....	23
3.4.1	Cationic Ring-Opening Polymerization of Lactide.....	24
3.4.2	Anionic Ring-Opening Polymerization of Lactide .....	26
3.4.3	Coordination-Insertion Polymerization of Lactide .....	28
3.4.4	Enzymatic Ring-Opening Polymerization of Lactide .....	33
	References .....	35
<b>4</b>	<b>Modification of PLA</b> .....	38
4.1	Copolymerization of PLA .....	38
4.1.1	Random and alternating copolymers of PLA.....	39
4.1.2	Block Copolymers of PLA.....	45

4.1.3	Multi-Block Copolymers of PLA .....	52
4.1.4	Graft or Branched Copolymers of PLA .....	54
4.1.5	Star-Shaped Copolymers of PLA.....	56
4.1.6	Dendritic Copolymers of PLA .....	65
4.2	PLA Blending .....	68
4.2.1	PLA/HA.....	69
4.2.2	PLA/PEG .....	72
4.2.3	PLA/PHB.....	78
4.2.4	PLLA/PDLA.....	81
4.2.5	PLLA and PDLA/PCL.....	85
4.2.6	PLA /PBS.....	91
4.2.7	PLA /PHEE.....	94
4.2.8	PLA /PMMA.....	95
4.2.9	PLA /PVA .....	95
4.2.10	PLA/ PBAT .....	97
4.3	Composites .....	99
4.4	Additives.....	100
4.4.1	Additives for PLA.....	100
4.4.2	PLA Crystallization Behavior and Nucleating Agents.....	124
4.5	New Modifiers for PLA.....	129
4.5.1	Core-Shell Impact Modifiers .....	129
4.5.2	Nanocomposites.....	130
	References .....	136
<b>5</b>	<b>Processing of PLA .....</b>	<b>142</b>
5.1	Injection.....	142
5.1.1	PLA Injection Molding .....	142
5.1.2	Controlling Crystallinity in Injection Molded PLA.....	146
5.1.3	Mechanical Properties of Injection-Molded Poly ( <i>L</i> -Lactic Acid) .....	147
5.1.4	Porous Lamellar Poly ( <i>L</i> -Lactic Acid) Scaffolds Made by Conventional Injection Molding Process.....	148
5.1.5	Shear Controlled Orientation in Injection Molding of PLLA.....	150
5.2	Spinning.....	152
5.2.1	Melt Spinning of PLA.....	153
5.2.2	Dry Spinning of PLA .....	161
5.2.3	Wet Spinning of PLA.....	167
5.2.4	Dry-Jet-Wet Spinning of PLA.....	168
5.2.5	Dyeing of PLA Fibers.....	170
5.2.6	Electrospinning of PLA Fibers.....	173
5.3	Blowing .....	179

5.3.1	Properties for Packaging .....	179
5.3.2	Process of Blown Film.....	184
5.3.3	Modification of Blown Film .....	185
5.4	Foaming.....	186
5.4.1	Modification of PLA and Its Foam .....	187
5.4.2	Starch/PLLA Hybrid Foams.....	190
5.4.3	PLA /PBAT Blend Foams .....	195
5.4.4	PLA Nanocomposite Foams .....	201
	References .....	204
<b>6</b>	<b>Application in the Field of Commodity and Industry Product.....</b>	<b>208</b>
6.1	Packaging Materials .....	208
6.2	Fiber and Nonwoven .....	209
6.2.1	PLA Fibers .....	209
6.2.2	Application of PLA Fibers.....	210
6.3	Engineering Plastic .....	220
6.4	Disposable Ware .....	222
6.4.1	What Is the Difference Between Biodegradable and Compostable? .....	223
6.4.2	About PLA for Disposable Use.....	224
6.4.3	Commercial PLA Disposable Ware .....	226
6.5	Biodegradable Hot Melt Adhesive Based on PLA and Other Biodegradable Polymer.....	229
6.5.1	Biodegradable PLA and/or PCL Based Biodegradable HMAs .....	229
6.5.2	PHBV and PEA Based on Biodegradable HMAs .....	231
6.5.3	Natural Polymer Based on Biodegradable HMAs .....	233
	Reference.....	236
<b>7</b>	<b>Application in the Field of Biomedical Materials.....</b>	<b>240</b>
7.1	Tissue Engineering Scaffold.....	240
7.1.1	Design Principles of Tissue Engineering Scaffold .....	240
7.1.2	PLA Materials and Modification for Tissue Engineering Scaffold Application .....	241
7.1.3	Surface Hydrophilicity Modifications .....	244
7.1.4	Biomimetic ECM Modification .....	245
7.1.5	PLA/Apatite Composite.....	248
7.1.6	Preparation of Tissue Engineering Scaffolds .....	250
7.1.7	Thermally Induced Phase Separation.....	251
7.1.8	Solvent Casting/Particulate Leaching.....	251
7.1.9	Gas Foaming .....	252
7.2	Controllable Drug Delivery Based on PLA.....	253

7.2.1	Introduction to Drug Delivery Based on PLA .....	253
7.2.2	Science of Controllable Drug Delivery.....	254
7.3	Other Biomedical Appliances.....	260
7.3.1	PLA Used For Surgical Sutures .....	260
7.3.2	Ideal Filler for Soft Tissue Augmentation.....	261
7.3.3	Mesh Insertion for Groin Hernia Repair .....	264
	Reference.....	267
<b>8</b>	<b>Standard and Test Methods.....</b>	<b>273</b>
8.1	Biodegradation of PLA.....	274
8.1.1	Definition of Biodegradation .....	274
8.1.2	Factors Affecting the Biodegradation Behaviour of PLA.....	274
8.1.3	Abiotic Degradation.....	275
8.1.4	Biotic Degradation .....	280
8.2	Biodegradation Standards and Certification Systems.....	283
8.2.1	Biodegradation Standards .....	283
8.2.2	Different Certification Systems .....	289
8.3	Introduction to Some Test Methods.....	291
8.3.1	Visual Observation.....	291
8.3.2	Gravimetry .....	292
8.3.3	Enzyme Assays .....	292
8.3.4	Plate Tests .....	292
8.3.5	Respiration Tests.....	292
8.3.6	Controlled Composting Test .....	294
	Reference.....	295
	<b>Index.....</b>	<b>297</b>

# 1 Introduction

Recently, biodegradable and renewably derived polymers have attracted much attention due to the environmental concerns and sustainability issues associated with petroleum-based polymers. Such a polymer is poly (lactic acid) (PLA), a biodegradable and bioabsorbable, renewably derived thermoplastic polyester extensively investigated over the lastest several decades. PLA is a compostable polymer derived from renewable sources.

Until the lastest decade, the main uses of PLA have been limited to medical applications such as implant devices, tissue scaffolds, and internal sutures, because of its high cost, low availability and limited molecular weight. Recently, new techniques which allow economical production of high molecular weight PLA polymer have broadened its uses. Since PLA is compostable and derived from sustainable sources, it has been viewed as a promising material to reduce the societal solid waste disposal problem. Its low toxicity, along with its environmentally benign characteristics, has made PLA an ideal material for food packaging and for other consumer products.

PLA development initiated with the lactide production formulas published by Bischoff and Walden in 1893. In 1932, Carothers and coworkers produced low molecular weight PLA. E. I. Du Pont de Nemours and Ethicon, Inc. began marketing PLA in medical applications for sutures, implants, and drug-delivery systems in 1954. Shimadzu Corporation and Kanebo Gohsen Ltd., Japan produced PLA fibers by melt spinning in the laboratory in 1992 and Kanebo Gohsen Ltd., Japan started commercial production of PLA fibers under the trade name Lactron in 1994. Fiberweb France S. A., France started commercial production of PLA fibers under the trade name Deposa in 1997. Cargill Dow LLC, USA started commercial production of PLA from starch under the trade name Nature Works at a capacity of 140 000 t/a in 2002. In 2003, Cargill Dow LLC introduced PLA fiber Ingeo TM spun from the Nature Works TM polymer. Dow sold its share to Cargill in 2005, which renamed their PLA business Nature Works LLC.

For PLA, there are many advantages: (1) Eco-friendly—Apart from being derived from renewable resources, PLA is biodegradable, recyclable, and compostable. Its production also consumes carbon dioxide. These sustainability and eco-friendly characteristics make PLA an attractive biopolymer. (2) Biocompatibility—The most attractive aspect of PLA, especially with respect to biomedical applications, is its biocompatibility. A biocompatible material should not produce toxic or carcinogenic effects in local tissues. Also, the degradation products should not interfere with tissue healing. PLA hydrolyzes to its constituent  $\alpha$ -hydroxy acid

## **Biodegradable Poly(Lactic Acid): Synthesis, Modification, Processing and Applications**

when implanted in living organisms, including the human body. It is then incorporated into the tricarboxylic acid cycle and excreted. Moreover, PLA degradation products are non-toxic (at a lower composition) making it a natural choice for biomedical applications. The Food and Drug Administration (FDA) in USA has also approved PLA for direct contacting with biological fluids.

(3) Processibility—PLA has better thermal processibility compared to other biopolymers such as poly(hydroxyl alcanoates) (PHAs), poly(ethylene glycol) (PEG), poly( $\alpha$ -caprolactone) (PCL), etc. It can be processed by injection molding, film extrusion, blow molding, thermoforming, fiber spinning, and film forming, with PLA resins for these methods commercialized by Nature Works LLC.

(4) Energy savings—PLA requires 25% – 55% less energy to produce than petroleum-based polymers, and this can be further reduced to less than 10% in the future. Lower energy use makes PLA production potentially advantageous with respect to cost as well. However, there are many limitations: (1) Poor toughness—PLA is a very brittle material with less than 10% elongation at break. Although its tensile strength and elastic modulus are comparable to poly(ethylene terephthalate) (PET), the poor toughness limits its use in the applications that need plastic deformation at higher stress levels (e.g., screws and fracture fixation plates). (2) Slow degradation rate—PLA degrades through the hydrolysis of backbone ester groups and the degradation rate depends on the PLA crystallinity, molecular weight, molecular weight distribution, morphology, water diffusion rate into the polymer, and the stereoisomeric content. The degradation rate is often considered to be an important selection criterion for biomedical applications. The slow degradation rate leads to a long life time in vivo, which could be up to years in some cases. There have been reports of a second surgery almost 3 years after implantation to remove a PLA-based implant. The slow degradation rate is a serious problem with respect to disposal of consumer commodities as well. (3) Hydrophobicity—PLA is relatively hydrophobic, with a static water contact angle of approximately 80°. This results in low cell affinity, and can elicit an inflammatory response from the living host upon direct contact with biological fluids. (4) Lack of reactive side-chain groups—PLA is chemically inert with no reactive side-chain groups making its surface and bulk modifications a challenging task. The successful implementation of PLA in consumer and biomedical applications relies not only on mechanical properties being better than or comparable to conventional plastics, but also on controlled surface properties (such as hydrophilicity, toughness, and reactive functionalities). PLA has been bulk modified mainly to improve toughness and degradation rate. The surface modification of PLA has been attempted to control hydrophilicity, toughness, and to introduce reactive groups. The toughness improvement is a crucial necessity for many consumer applications, while the improvements in hydrophilicity and introduction of reactive groups are beneficial to biomedical applications. The improvements in degradation rate could be important in both consumer and biomedical applications.

Therefore, in this book, the production and properties of lactic acid, the monomeric building block of PLA, are described in detail (Chapter 2). The synthesis and manufacture of PLA are very important. These polymers can be produced using several techniques, including direct polycondensation, azeotropic dehydrative polycondensation, and ring-opening polymerization of lactide. By and large, commercially available high-molecular-weight PLA resins are mainly produced via the ring-opening polymerization route of lactide (Chapter 3). Unitary structure and poor properties of PLA such as the inherent brittleness, poor melt strength, low heat deflection temperature (HDT), narrow processing window and low thermal stability pose considerable scientific challenges and limit their large-scale applications. There is a pressing need to enhance the versatility of PLA bioplastics, so that they can compete with conventional polymers. The most common strategy to overcome this limit is to prepare the copolymers. By copolymerization of lactic acid (or lactide) with hydroxyl acid, amino acid or polymers such as poly(ethylene glycol), starch, etc., the strength, toughness, hydrophilic and controlled-degradable properties of PLA can be significantly improved, and at the same time, numerous new copolymers in different macromolecular architectures can be obtained. These materials are attracting considerable interest in materials science research. PLA copolymers can be synthesized by several kinds of well-known polymerization techniques, including polycondensation, anionic, cationic, and coordination-insertion ring-opening polymerization. Chapters 3 and 4 in the book aim at highlighting on recent developments in preparation of the linear, graft or branch, star-shaped, and dendritic PLA copolymers and the catalysts used in copolymerization. The processing of PLA, such as injection, spinning, blowing, foaming, is discussed in Chapter 5. The bottles, fibers, film, and foam of PLA can be manufactured. In addition, PLA can be applied in the field of commodity and industry product (Chapter 6). For example, PLA material can be used as packaging material, fiber and nonwoven, and engineering plastic. PLA processes good compatibility and degradability. PLA can be used as tissue engineering scaffold, controllable drug delivery system, and so on (Chapter 7). In Chapter 8, the standard and test methods of PLA are discussed.

## 2 Lactic Acid

**Abstract** Lactic acid (LA) is an organic acid found in many products of natural origin. The first reports on isolation of lactic acid from milk can be found in as early as 1780 and the solidification by self-esterification some years later. Lactic acid can be manufactured by chemical synthesis or carbohydrate fermentation. And, lactic acid can be purified either by precipitation of metal lactates followed by a neutralizing reaction with sulfuric acid or by esterification with alcohol, distillation and hydrolysis of the formed ester, or by electro-dialysis. Nowadays, lactic acid based polymers, a good alternative for substituting conventional plastic produced from petroleum oil because of low emission of carbon dioxide that contributes to global warming, have been widely used.

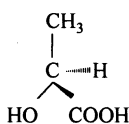
**Keywords** biodegradable, lactic acid (LA), poly (lactic acid) (PLA), synthesis, fermentation purification, crystallization ,molecular distillation

### 2.1 Introduction

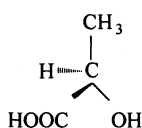
Lactic acid (chemically, 2-hydroxypropanoic acid, LA), also known as milk acid, is the most widely occurring carboxylic acid in nature. It was first isolated in 1780 by a Swedish chemist, Carl Wilhelm Scheele, but it was first produced commercially by Charles E. Avery at Littleton, Massachusetts, USA in 1881.

### 2.2 Properties

LA is a three carbon organic acid: one terminal carbon atom is part of an acid or carboxyl group; the other terminal carbon atom is part of a methyl or hydrocarbon group; and a central carbon atom having an alcohol carbon group attached. Lactic acid exists in two optically active isomeric forms. One is known as *L*-lactic acid or (*s*)-lactic acid and the other, its mirror image, is *D*-lactic acid or (*r*)-lactic acid. *L*-Lactic acid is the biologically important isomer.



*L*-lactic acid



*D*-lactic acid



LA has a hydroxyl group adjacent to the carboxyl group, making it an alpha hydroxy acid (AHA). In solution, it can lose a proton from the acidic group, producing the lactate ion  $\text{CH}_3\text{CH}(\text{OH})\text{COO}^-$ . It is miscible with water or ethanol, and is hygroscopic. It exhibits low volatility. Other identification and physical-chemical properties of lactic acid are summarized in Table 2.1. And, the thermodynamic characteristics of lactic acid are listed in Table 2.2.

**Table 2.1** Identification and physical-chemical properties

Identification	Physical & chemical properties		
CAS number	D/L: [50-21-5] L: [79-33-4] D: [10326-41-7]	Melting point	L: 53°C D: 53°C D/L: 16.8°C
Einecs No.	200-018-0	Boiling point	122°C (12 mmHg)
H.S. Code	2918.11	Specific gravity	1.2 g/mL
Formula	$\text{CH}_3\text{CH}(\text{OH})\text{COOH}$	Molar mass	90.08 g/mol

**Table 2.2** Thermodynamic characteristics of lactic acid

Items	Characteristics
Dissociation constant ( $K_a$ )	0.000 137 (at 25°C)
Heat of dissociation ( $\Delta H$ )	-63 cal/mol (at 25°C)
Free energy of dissociation ( $\Delta F$ )	5000 cal/mol
Heat of solution ( $\Delta H$ )	1868 cal/mol (for crystalline L(+) lactic acid at 25°C)
Heat of dilution ( $\Delta H$ )	-1000 cal/mol (for dilution with a large volume of water)
Heat of fusion ( $\Delta H$ )	2710 cal/mol (for racemic lactic acid) 4030 cal/mol (for L(+) lactic acid)
Entropy of solution ( $\Delta S$ )	6.2 cal/mol/°C
Entropy of dilution ( $\Delta S$ )	-3.6 cal/mol/°C
Entropy of fusion ( $\Delta S$ )	9.4 cal/mol/°C (for racemic lactic acid) 12.2 cal/mol/°C (for L(+) lactic acid)
Heat of combustion ( $\Delta H_{c0}$ )	-321 220 cal/mol (for crystalline L(+) lactic acid at 25°C) -325 600 cal/mol (for liquid racemic lactic acid at 25°C)
Heat of formation ( $\Delta H_{f0}$ )	-165 890 cal/mol (for crystalline L(+) lactic acid at 25°C) -163 000 cal/mol (for liquid lactic acid) -164 020 cal/mol (for lactic acid in dilute solution) -164 080 cal/mol (for dissociated and diluted lactic acid)
Heat capacity ( $C_p$ )	0.338 cal/g/°C (for crystalline lactic acid at 25°C) 0.559 cal/g/°C (for liquid lactic acid at 25°C)
Absolute entropy ( $S_0$ )	34.0 cal/mol/°C (for crystalline L(+) lactic acid at 25°C) 45.9 cal/mol/°C (for liquid racemic lactic acid at 25°C)
Entropy of formation ( $\Delta S_{f0}$ )	-137.2 cal/mol/°C (for crystalline lactic acid at 25°C) -125.3 cal/mol/°C (for liquid lactic acid at 25°C)
Free energy of formation ( $\Delta F_{f0}$ )	-124 980 cal/mol (for crystalline L(+) lactic acid at 25°C) -126 500 cal/mol (for liquid racemic lactic acid at 25°C)

## **Biodegradable Poly(Lactic Acid): Synthesis, Modification, Processing and Applications**

The various reactions characteristic of an alcohol which lactic acid (or its esters or amides) may undergo are xanthation with carbon bisulphide, esterification with organic acids and dehydrogenation or oxygenation to form pyruvic acid or its derivatives. The acid reactions of lactic acid are those that form salts. It also undergoes esterification with various alcohols.

LA can be analyzed by  $\text{NAD}^+$  linked lactate dehydrogenase enzyme assay. A colorimetric method has been described in many papers. Gas chromatography can be used after esterification of lactic acid but is unsatisfactory for quantitative. Liquid chromatography and its various techniques can be used for quantitative analysis and separation of its optical isomers. Lactic acid is used as acidulant/ flavouring/ pH buffering agent or inhibitor of bacterial spoilage in a wide variety of processed foods. In contrast to other food acids it has a mild acidic taste. It is non-volatile and odorless, and is classified as generally regarded as safe (GRAS) by FDA in the US. It is a very good preservative and pickling agent. Addition of lactic acid aqueous solution to the packaging of poultry and fish increases their shelf life [1].

The esters of lactic acid are used as emulsifying agents in baking foods (stearoyl-2-lactylate, glyceryl lactostearate, glyceryl lactopalmitate). The manufacture of these emulsifiers requires heat stable lactic acid, hence only the synthetic or the heat stable fermentation grades can be used for this application [2, 3].

Technical grade lactic acid is used as an acidulant in vegetable and leather tanning industries. Various textile finishing operant and acid dyeing of food require low cost technical grade lactic acid to compete with cheaper inorganic acid. LA is being used in many small scale applications like pH adjustment hardening baths for cellophanes used in food packaging, terminating agent for phenol formaldehyde resins, alkyd resin modifier, solder flux, lithographic and textile printing developers, adhesive formulations, electroplating and electropolishing baths, detergent builders.

LA has many pharmaceutical and cosmetic applications and formulations in topical ointments, lotions, anti acne solutions, humectants, parenteral solutions and dialysis applications as anti carries agent. Calcium lactate can be used for calcium deficiency therapy and as anti caries agent. Its biodegradable polymer has medical applications as sutures, orthopaedic implants, controlled drug release etc. Polymers of lactic acids are biodegradable thermoplastics. These polymers are transparent and their degradation can be controlled by adjusting the composition and the molecular weight. Their properties are comparable with those of petroleum derived plastics. Lactic acid esters like ethyl/butyl lactate can be used as green solvents. They are high boiling, non-toxic and degradable components. Poly (*L*-lactic acid) (PLLA) with low degree of polymerization can help in controlled release or degradable mulch films for large-scale agricultural applications [2].

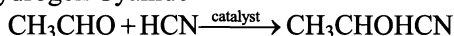
## 2.3 Preparation

Lactic acid can be manufactured by (a) chemical synthesis or (b) carbohydrate fermentation.

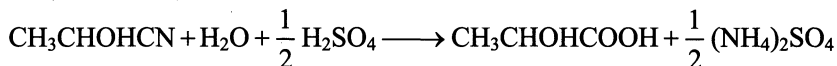
### 2.3.1 Chemical Synthesis

The commercial process for chemical synthesis is based on lactonitrile. Hydrogen cyanide is added to acetaldehyde in the presence of a base to produce lactonitrile. This reaction occurs in liquid phase at high atmospheric pressures. The crude lactonitrile is recovered and purified by distillation. It is then hydrolyzed to lactic acid, either by concentrated HCl or by H<sub>2</sub>SO<sub>4</sub> to produce the corresponding ammonium salt and lactic acid. Lactic acid is then esterified with methanol to produce methyl lactate which is then isolated and purified by distillation and hydrolyzed by water under acid catalyst to produce lactic acid and the methanol that is recycled. This process is represented by the following reactions.

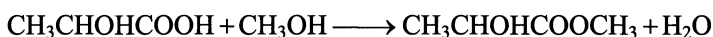
(a) Addition of Hydrogen Cyanide



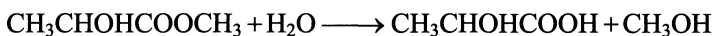
(b) Hydrolysis by H<sub>2</sub>SO<sub>4</sub>



(c) Esterification



(d) Hydrolysis by H<sub>2</sub>O



A racemic mixture of lactic acid is produced in the chemical synthesis method. Two companies Musashino, Japan and Sterling Chemicals Inc., USA [4] are using this technology.

### 2.3.2 Fermentation

Lactic acid fermentation is a biological process by which sugars such as glucose, fructose and sucrose are converted into cellular energy and the metabolic product fermental acid. It is the anaerobic form of respiration that occurs in some bacteria and animal cells in the absence of oxygen. During homolactic acid fermentation, one molecule of glucose is ultimately converted to two molecules of lactic acid. In heterolactic acid fermentation, sometimes referred to as the phosphoketolase pathway, the products of fermentation are one molecule of carbon dioxide, one molecule of ethanol, and one molecule of lactic acid.

### 2.3.2.1 Lactic Acid Bacteria

Lactic acid bacteria have the property of producing lactic acid from sugars by a process called fermentation. The genera *Bacillus*, *Leuconostoc*, *Pediococcus* and *Streptococcus* are important members of this group. The taxonomy of lactic acid bacteria has been based on the gram reaction and the production of lactic acid from various fermentable carbohydrates.

Lactobacilli are gram positive and vary in morphology from long, slender rods to short coccobacilli, which frequently form chains [5, 6]. Their metabolism is fermentative; some species are aerotolerant and may utilize oxygen through the enzyme flavoprotein oxidase, while others are strictly anaerobic. While spore bearing *Bacillus coagulans* are facultative anaerobes, the rest are strictly anaerobic. The growth is optimum at pH 5.5-5.8 and the organisms have complex nutritional requirements for amino acids, peptides, nucleotide bases, vitamins, minerals, fatty acids and carbohydrates.

The genus is divided into three groups based on fermentation patterns:

- A. Homofermentative: to produce more than 85% lactic acid from glucose.
- B. Heterofermentative: to produce only 50% lactic acid and considerable amounts of ethanol, acetic acid and carbon dioxide.
- C. Less well known heterofermentative species which produce DL-lactic acid, acetic acid and carbon dioxide.

The species which have been therapeutically used are:

- *L-sporogenes*\*
- *L-acidophilus*
- *L-plantarum*
- *L-casei*
- *L-brevis*
- *L-delbruckii*
- *L-lactis*

### 2.3.2.2 Fermentation Process

By glycolysis 2 molecules of ATP are produced, 2 molecules of  $\text{NAD}^+$  to NADH are reduced, and 2 three-carbon molecules of pyruvate are formed. Most of the chemical energy (about 95%) of the glucose is still trapped in pyruvate. The complete breakdown of glucose to  $\text{CO}_2$  requires the oxidation of pyruvate through the Krebs cycle and electron transport system (ETS). When the Krebs cycle and ETS are working at capacity (this action requires oxygen [7]), further local ATP needs can be achieved by increasing glycolysis. The resulting pyruvate is converted to lactic acid through lactic acid fermentation.

The conversion of pyruvate to lactate regenerates  $\text{NAD}^+$ , which allows glycolysis to continue. Lactate diffuses out of the cell and into the blood. The lactate in the bloodstream is converted back into pyruvate in the liver for use when oxygen is once again present.

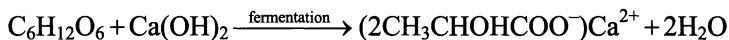
Certain cells, such as cardiac muscle cells, are highly permeable to lactate. Lactate is converted into pyruvate and metabolised normally (ie: via the Krebs cycle). Since these cells are highly oxygenated, it is unlikely that lactate would accumulate (such as the case in oxygen-starved muscle cells). This also allows circulating glucose to be available to muscle cells.

Any excess lactate is taken up by the liver, converted into pyruvate and then into glucose. This, along with the production of lactate from glucose in muscle cells, constitutes the Cori cycle.

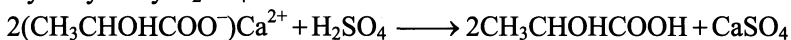
Phosphofructokinase (PFK) is inhibited by a low pH and this prevents the formation of excess lactate and/or lactic acidosis (sudden drop in blood pH). PFK catalyses an irreversible step in glycolysis.

Though a racemic mixture is produced through chemical synthesis, stereo specific acid can be made by carbohydrate fermentation depending on the strain being used. It can be described by following reactions.

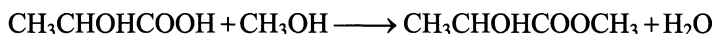
(a) Fermentation and neutralization



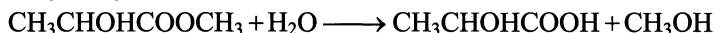
(b) Hydrolysis by  $\text{H}_2\text{SO}_4$



(c) Esterification



(d) Hydrolysis by  $\text{H}_2\text{O}$



The broth containing calcium lactate is filtered to remove cells, carbon treated, evaporated and acidified with sulphuric acid to get LA and  $\text{CaSO}_4$ . The insoluble  $\text{CaSO}_4$  is removed by filtration; LA is obtained by hydrolysis, esterification, distillation and hydrolysis.

## 2.4 Separation and Purification of LA

LA solution obtained initially from a fermentation medium or any other source cannot be used directly, which need to be concentrated and purified.

LA can be purified either by precipitation of metal lactates followed by a neutralizing reaction with sulfuric acid [8] or by esterification with alcohol, distillation and hydrolysis of the formed ester, or by electro-dialysis. A more recent purification process is to extract LA by liquid-liquid extraction making use of at least one organic solvent not miscible with water in the presence or not of at least one Lewis base such as a ternary amine for instance. With this process, lactic acid must be recovered in a second step with a liquid-liquid back-extraction. This step allows to re-transfer the lactic acid to water. Finally, LA in acid- and/or ammonium lactate or metal lactate-form may be purified by processing it on cationic and/or anionic ion-exchange columns.

### **2.4.1 Esterification and Hydrolysis**

LA is easily produced in bacterial fermentations, but a substantial processing and cost are involved in extraction and purification of LA in the fermentation broth. Conversion of LA or ammonium lactate ( $\text{NH}_4\text{LA}$ ) into esters and subsequent hydrolysis of the purified ester into LA is a widely accepted way to extract and purify because by using this method highly pure LA can be obtained. In a study, using two reactors with a rectifying Column were used to carry out recovery of LA from the fermentation broth.  $\text{NH}_4\text{LA}$  obtained by fermentation was used directly to produce butyl lactate by reacting with butanol for 6 h, and the esterification yield of  $\text{NH}_4\text{LA}$  was 87.7%. In this procedure, a cation exchange resin which was modified by  $\text{SnCl}_2$  replaced sulphuric acid as a catalyst, and neutral  $\text{NH}_4\text{LA}$  replaced former LA as a starting material, so that not only corrosion of the reactor was eliminated, but also generation of calcium salts as a by-product was avoided. Then butyl lactate was rectified, and the purified butyl lactate was subsequently hydrolyzed into LA in the presence of cation exchange resin in the  $\text{H}^+$  form as a catalyst for 4 h. and the hydrolysis yield was 89.7% and the purity of recovered LA was 90%. In the recovery process, the liberated butanol in hydrolysis procedure and unreacted butanol in esterification procedure can be recycled to the above esterification, and the recovery rate of butanol was 85.6%.

### **2.4.2 Crystallization**

In principle, the known techniques can be employed for crystallization of LA. An example of such a technique is melt crystallization (cooling crystallization), which involves direct cooling of the condensed, liquid concentrate or distillate containing (*s*)- or (*r*)-lactic acid in the molten state, so that the (*s*)- or (*r*)-lactic acid crystallizes out. It is preferable to keep the temperature at which crystallization occurs (the crystallization temperature) as low as possible, so that the formation of oligomers and polymers of lactic acid is limited as less as possible.

Melt crystallization is a process in which a crystalline material is obtained from a melt of the material to be crystallized. The greatest advantage of melt crystallization, compared with distillation, is that much less energy is required, as the enthalpy of fusion of organic compounds is generally lower than the enthalpy of evaporation. Furthermore, another advantage of melt crystallization compared with distillation is that the process generally can be carried out at much lower temperatures, which is advantageous if the organic compound is thermally unstable.

The melt crystallization can be carried out with the aid of a suspension crystallization or a layer crystallization, possibly in conjunction with a wash column or a centrifuge, or some other purification technique [9 – 11].

It has also been found that crystallization from an aqueous solution gives very

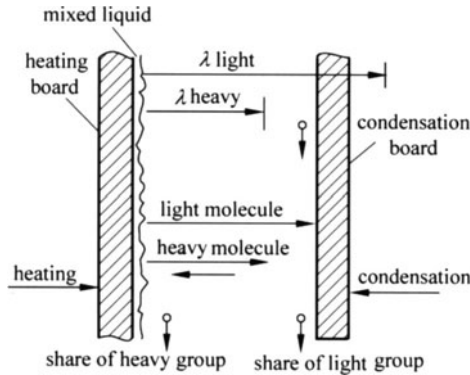
good results. With this crystallization treatment, the concentrated lactic acid solution is diluted with water and is then subjected to one or more cooling and/or evaporation crystallization steps. With these techniques, the concentrate or distillate is cooled directly (cooling crystallization) or concentrated by evaporation of the solvent that is usually water (evaporation crystallization). The driving force for the crystallization in the case of cooling crystallization technique is super-saturation in the concentrated lactic acid solution brought about by lowering temperature of the concentrated lactic acid solution. Owing to the lower temperature of the solution, the solubility decreases, and super-saturation may be resulted. The driving force for crystallization in evaporation crystallization technique is super-saturation in the concentrated lactic acid solution brought about by evaporation of solvent (increasing the concentration at constant temperature). This means that cooling or evaporation of solvent (usually water) results in effective removal of the heat of crystallization. During cooling or evaporation of water, crystallization of lactic acid then take place.

Another highly suitable crystallization technique is adiabatic crystallization where the driving force for crystallization is the of super-saturation in the concentrated lactic acid solution brought about by heat neither being removed nor supplied. This involves lowering the temperature of the concentrated solution (solvent evaporates) and increasing the concentration of LA (two effects: (a) solvent evaporates and (b) the temperature of the concentrated LA solution drops, as a result of which the solubility decreases and super-saturation may be resulted).

### 2.4.3 Molecular Distillation

Molecular distillation (MD) is a kind of high vacuum distillation method which is suitable for the separation of high boiling point, heat sensitive and viscous products. Molecular distillation is a special liquid-liquid separation technology which is different from the separation principle of traditional distillation depending on boiling point difference. It is depending on the difference of molecular mean free path to separate different matters. Here, molecular mean free path ( $\lambda$ ) is referred to the path between a molecule strikes two times.

When the liquid mixture flows along the heating board and is heated, light and heavy molecule will leave the surface of liquid and enter the vapor phase. Because of different mean free path of light and heavy molecule, different matters have different moving distance. Supposing a condensation board is put at the proper position, light molecule can reach the board and will be condensed, then be discharged along the condensation board; while the heavy molecule will not reach the board and be discharged along the heating board. Therefore, the objective of separation is achieved [12].



**Figure 2.1** Principle of molecular distillation

## 2.5 Application

### 2.5.1 Raw Materials of PLA

Two molecules of lactic acid can be dehydrated to form lactide, a cyclic lactone. A variety of catalysts can be used to polymerise lactic acid to either heterotactic or syndiotactic PLA, which as biodegradable polyesters with valuable (inter alia) medical properties are currently attracting much attention.

Nowadays, lactic acid is used as a monomer for producing PLA which has wide application as biodegradable plastic. This kind of plastic is a good option for substituting conventional plastic produced from petroleum oil because of low emission of carbon dioxide that contributes to global warming. The commonly used process in producing lactic acid is fermentation, and later the polymerization process follows to obtain PLA.

### 2.5.2 Additives in Foods

LA is primarily found in sour milk products, such as: koumiss, leban, yogurt, kefir, and some cottage cheeses. The casein in fermented milk is coagulated (curdled) by LA.

Although it can be fermented from lactose (milk sugar), most commercially used LA is derived by using bacteria such as *Streptococcus thermophilus*, *Lactobacillus acidophilus*, or *Lactobacillus delbrueckii* subsp. *bulgaricus* (formerly known as *Lactobacillus bulgaricus*) to ferment carbohydrates from nondairy sources such as cornstarch, potatoes, and molasses. Thus, although it is commonly known as “ilk acid” vegan products can contain LA as an ingredient.



LA may also be found in various processed foods, usually either as a pH-adjusting ingredient or as a preservative (either as antioxidant or for control of pathogenic micro-organisms). It may also be used as a fermentation booster in rye and sourdough breads.

Potassium lactate, sodium lactate, and calcium lactate are the neutralized salts of LA. Potassium lactate is used in many fresh and cooked meat products for shelf life control, color preservation, and reduction of sodium content. Sodium lactate has a mild saline taste and is therefore suitable for flavor enhancement in meat products. Sodium lactate is being produced in solution as well as dry. Calcium lactate is popular for fortification and improved texture in emulsified meat products like frankfurters. Ready-to-eat meat and poultry products commonly contain sodium or potassium lactate to control *Listeria monocytogenes*. LA is also present in wheat beers, especially lambic, due to the activity of *Pediococcus damnosus*.

LA is widely used for reducing the number of pathogenic bacteria like *E.coli*, *Salmonella*, *Campylobacter* and *Listeria* on animal carcasses like beef, pork, and poultry during the slaughtering process.

### 2.5.3 Applications in Cosmetics

Both racemic and *D*-lactic acid are less suitable for cosmetic applications because they are not as mild as the *L* form.

The *L* form is the form which is present in the human body (e.g., skin, hair and muscles). Every day the human body produces about 120 g of LA. LA is also part of the natural moisturizing factor (NMF) that retains moisture in the skin.

Being a natural ingredient and a natural constituent of the human body, LA and lactates fit perfectly in today's trend towards natural and safer formulations. With their multi-functionality (moisturizing, pH-regulation, humectancy, antimicrobial), LA and lactates are ideal standard ingredients in the formulation of a good base for cosmetic products. In addition to their multi-functionality, *L*-lactic acid and lactates also possess special features (e.g., skin lightening) that make them very useful as active ingredients.

### 2.5.4 Applications in Detergents

LA has gained importance in the detergents industry in the last couple of years. Being a good descaler, soap-scum remover and being a registered anti-bacterial agent, lactic acid becomes a safer and natural ingredients.

## **References**

- [1] Anon. Chemical Engineering News. 20. August, 1992.
- [2] Datta R. FEMS Microbiology Reviews, 16, 221 (1995).
- [3] Borgardt P., Krischke W., Trosch W., et al. Bioprocess Engineering, 19, 321 (1998).
- [4] Ajioka I., Enomoto K., Suzuki K., et al. Journal of Environmental Polymer Degradation, 3, 225 (1995).
- [5] Skory C. D., Freer S. N., Bothast V. Biotechnology Letters, 20, 191 (1998).
- [6] Porro D., Bianchi M. M., Brambilla L., et al. Applied and Environmental Microbiology, 65, 4211 (1997).
- [7] Sparks S. Science, 277, 459 (1997).
- [8] Maesato K., Komori A. Taki Chem. Co. (JP), 6, 272, 646 (Sep. 25, 1985).
- [9] Kirt-Othmer. Encyclopedia of Chemical Technology (4th Ed.), 7, 723 (1993).
- [10] Mullin J. W. Crystallization (3rd Revised Ed.). Butterworth-Heinemann Ltd., 309, (1993).
- [11] Ullrich J., Kallies B. Current Topics in Crystal Growth Research, 1, (1994).
- [12] Lao Hanzhang, Sun Jianrong, Wang Jian, et al. China Patent, CN101007756.

### 3 Synthesis and Manufacture of PLA

**Abstract** PLA belongs to the family of aliphatic polyesters derived from  $\alpha$ -hydroxy acids. The basic building block of PLA, lactic acid, (2-hydroxy propionic acid), can exist in optically active *D*- or *L*-enantiomers, which can be produced by carbohydrate fermentation or chemical synthesis. Depending on the proportion of the enantiomers, PLA of with variable material properties can be derived. This allows the production of a wide spectrum of PLA polymers to match performance requirements.

**Keywords** synthesis, PLA, polycondensation, azeotropic dehydrative polycondensation, ring-opening polymerization, enzyme-catalyzed polymerization, molecular weight, kinetics, mechanism

Commercial PLA are homopolymer of poly(*L*-lactic acid) (PLLA) or copolymer of poly(*D,L*-lactic acid) (PDLLA), which are produced from *L*-lactic acid and *D,L*-lactic acid. The *L*-isomer constitutes the main fraction of PLA derived from renewable sources since the majority of lactic acid from biological sources exists in this form. Recently, the stereocomplex of PLLA and PDLA has drawn attention, and the importance of *D*-lactic acid and PDLA production is increasing. One of the main drivers for the recent expanded use of PLA is attributable to the economical production of high-molecular-weight (greater than 100 000 Da) PLA polymers. These polymers can be produced using several techniques, including direct polycondensation, azeotropic dehydrative polycondensation, and ring-opening polymerization of lactide (Fig. 3.1). By and large, commercially available high-molecular-weight PLA resins are mainly produced via the ring-opening polymerization route of lactide [1].

#### 3.1 Direct Polycondensation of Lactic acid

Direct polycondensation of lactic acid is usually performed in bulk by distillation of condensation water with or without a catalyst, while vacuum and temperature are progressively increased. The polymer obtained has a low molecular weight, because it is hard to remove water completely from the highly viscous reaction mixture; therefore a polymer of a molecular weight of a few ten thousands is obtained. The polymer of low molecular weight is the main disadvantage of

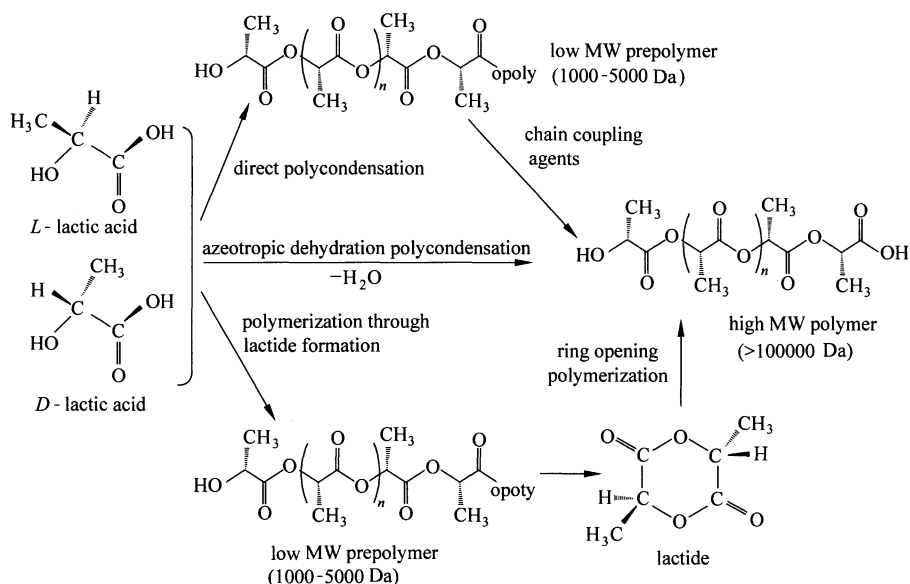
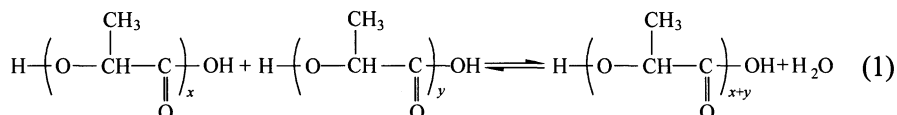


Figure 3.1 Synthesis of PLA from L- and D-lactic acids [2]

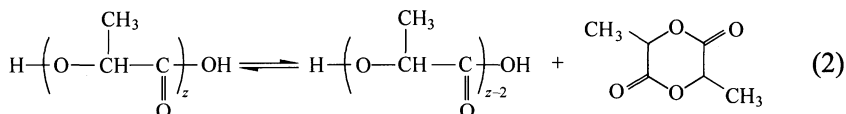
direct polycondensation and it restricts its use. Moreover, the stereoregularity cannot be controlled during the course of polymerization. The polymer thus possesses inferior mechanical properties. So, this method is employed only if the polymer of low molecular weight is required [3].

Different strategies have been suggested in the literature to increase the molecular weight of the polymer produced through direct polycondensation. For example Chen et al. [4] recently implemented different operational strategies by controlling the decompression and esterification rate to produce high molecular weight polymer. They reported for the first time that very high molecular weight of PLA (130 000 Da) by the direct bulk polycondensation using titanium (IV) butoxide as a catalyst at different polymerization time. The duration of the decompression of the reaction pressure to 1 torr is important to produce high-molecular-weight PLLA. When the polymerization reactor was decompressed extremely slowly step by step for 7 h, the molecular weight of PLLA reached as high as 130 000. Increase of the time for the esterification reaction from 3 to 7 h also raised the molecular weight of PLLA from 30 000 to 120 000.

The polycondensation system of LA involves two reaction equilibria: dehydration equilibrium for esterification and ring-chain equilibrium involving the depolymerization of PLA into lactide (Eq. 1 and 2):



### 3 Synthesis and Manufacture of PLA



Keki et al. [5] studied the ring-chain equilibrium of direct polycondensation of *D, L*-lactic acid by using the MALDI-TOF MS method, which has been proved to be a useful method for characterizing the ring-chain equilibrium, at temperatures ranging from 100 to 220°C. At low temperature, i.e., up to 120°C, linear, and at higher temperature both linear and cyclic oligomers were formed. The ring-chain equilibrium was investigated in detail and the concentration-based equilibrium constants ( $K_x$ ) and their dependence on the degree of polycondensation and on the temperature were determined. It was also found that the molecular size distribution of the linear chain oligomers obeys to “the most probable distribution”. A detailed investigation also showed that the ring size distribution of the cyclic oligomers follows the Jacobson-Stockmayer theory.

For obtaining a high molecular weight PLA, dehydration equilibrium and ring-chain equilibrium should be controlled in parallel. Under typical reaction conditions with high temperature and high vacuum to promote the dehydrative polycondensation, the evaporation of lactide is also favorable to induce depolymerization. In the solution polycondensation of the Mitsui process [6], the lactide formed in the ring-chain equilibrium can efficiently be fed back to the reaction system together with the refluxed solvent to allow continuous dehydration without undergoing depolymerization of PLA. In the direct polycondensation, however, such an efficient technique is not available. One possible way to promote polycondensation is to activate the dehydrative reaction and deactivate the formation of lactide by the possible selection of a catalyst.

On the basis of this consideration, Moon et al. [7] made an intensive screening test to find an adequate catalyst for the direct polycondensation of *L*-lactic acid. In this catalyst screening, they found that the polarity of the reaction system was greatly altered with the progress of the condensation, resulting in an ultimate change in the catalyst activity. The starting *L*-lactic acid and its primary condensates contained both carboxyl and hydroxyl groups in a high ratio, causing a high polarity for the reaction system, whereas the resultant PLLA consisted of less polar ester groups, leading to a great decrease in polarity. This polarity change was the main cause of the deterioration of catalyst activity. In some catalyst systems, the activity was completely lost when they were directly added to the starting *L*-lactic acid. Therefore, they first prepared oligo (*L*-lactic acid) (OLLA) with a sufficient degree of polymerization by the non-catalytic dehydration of *L*-lactic acid, and then the catalyst was added to it for the continuation of its polycondensation.

The polycondensation with OLLA was examined with various catalysts: metallic and nonmetallic, organic and inorganic, and homogeneous and heterogeneous. Typical results are shown in Table 3.1. This screening test revealed that tin oxide

and chloride were particularly effective for increasing the molecular weight of PLLA among the metal and metal oxide catalysts frequently adopted for ordinary esterification reactions, although the polymer yield was relatively low. The activity of both the tin oxide and chloride was almost identical. In carrying out the polycondensation, the balance of the reaction temperature and pressure was also important for preventing the evaporation of *L*-lactide formed in equilibrium with PLLA from the system. they obtained a high molecular weight of PLLA ( $M_w \geq 100\ 000$ ) through the melt polycondensation of *L*-lactic acid with Sn (II) catalysts activated by proton acids within a short reaction time. However, when the melt polycondensation was conducted above  $T_m$  of PLLA at reduced pressure, the polymer yield became about 60% relative to the starting *L*-lactic acid because of the evaporation of lactide formed by the ring (*L*-lactide)/chain (PLLA) equilibrium.

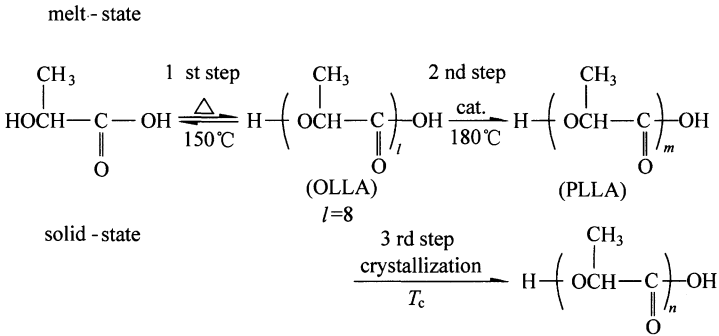
**Table 3.1** Typical results of the catalyst screening test for the direct polycondensation of OLLA [7]

Run	Catalyst	Catalyst/OLLA (wt%)	Temperature (°C)	Time (h)	Pressure (torr)	$M_w^a$	Yield (%)
1	GeO <sub>2</sub>	0.8	180	20	10	28 000	73
2	Sb <sub>2</sub> O <sub>3</sub>	0.1	200	30	20	20 000	25
3	ZnO	0.1	200	30	20	36 000	35
4	Fe <sub>2</sub> O <sub>3</sub>	0.1	200	8	1	20 000	23
5	Al <sub>2</sub> O <sub>3</sub>	8.5	200	30	20	27 000	42
6	SiO <sub>2</sub>	0.8	180	20	10	11 000	58
7	TiO <sub>2</sub>	0.8	180	20	10	11 000	64
8	SnO	0.2	180	20	10	50 000	36
9	SnCl <sub>2</sub> ·2H <sub>2</sub> O	0.4	180	20	10	41 000	43
10	TSA	0.34	180	10	10	17 000	70

<sup>a</sup> Determined by GPC relative to a polystyrene standard with chloroform as the eluent.

Moreover, the molecular weight remained around 100 000 Da, being much lower than that of the PLLA obtained by the ring-opening polymerization of *L*-lactide. Therefore, they examined the melt/solid polycondensation of lactic acid in which the melt polycondensation of *L*-lactic acid was subjected to solid-state polycondensation below  $T_m$  of PLLA [8]. In solid state, the polymerization reaction can be favored over the depolymerization or other side reactions. Particularly, in the process of crystallization of the resultant polymer, both monomer and catalyst can be segregated and concentrated in the noncrystalline part to allow the polymer formation to reach 100% [9]. Figure 3.2 shows the whole process of this melt/solid polycondensation of *L*-lactic acid. In this process, a polycondensation with a molecular weight of 20 000 Da is first prepared by

ordinary direct polycondensation, crystallized by heat-treatment around 105°C, and heated at 140 or 150°C for 10–30 h for further polycondensation. A high-quality polymer of PLLA can be obtained in high yield in a relatively short reaction time and its molecular weight exceeds 500 000 Da. As a result, they successfully obtained a high-molecular-weight PLLA by the melt/solid polycondensation of *L*-lactic acid catalyzed by a tin chloride dihydrate/*p*-toluenesulfonic acid binary system. The molecular weight of PLLA which is comparable with that of the PLLA obtained by the lactide method reached over 600 000 Da in a relatively short reaction time.



**Figure 3.2** The whole process of the melt/solid polycondensation of *L*-lactic acid

Ren et al. [10–11] presented a direct condensation process for the production of high-molecular-weight PLLA. It constitutes two steps: pre-polymerization in melt state and chain extending reactions. First, the lactic acid monomer was oligomerized to low molecular weight hydroxyl-terminated prepolymer; the molecular weight was then increased by chain extension. The results showed that the obtained polymer had 1.0–1.5 dL/g.

Another interesting example is that Yoda et al. [12] have conducted the direct synthesis of PLLA from an *L*-lactic acid oligomer in supercritical carbon dioxide (scCO<sub>2</sub>) by using an esterification promoting agent, dicyclohexyldimethylcarbodiimide (DCC), and 4-dimethylaminopyridine (DMAP) as a catalyst. PLLA with  $M_n$  of 13 500 Da was synthesized in 90% yield at 3500 psi (lb/in<sup>2</sup>, equal to 6.894 kPa and 80°C after 24 h. The molecular weight distribution of the products was narrower than PLLA prepared with melt-solid phase polymerization under conventional conditions. Both DCC and DMAP showed high solubility in scCO<sub>2</sub> (DCC: 7.6 wt% ( $1.63 \times 10^{-2}$  mol/mol CO<sub>2</sub>) at 80°C, 3385 psi, DMAP: 4.5 wt% ( $1.62 \times 10^{-2}$  mol/mol CO<sub>2</sub>) at 80°C, 3386 psi) and supercritical fluid extraction was found to be effective at removing excess DMAP and DCC after the polymerization was complete.

Since the polycondensation of LA is accompanied by the release of water, and both lactic acid and its oligomers are polar in nature, it is reasonable to expect microwave irradiation to influence the reaction. Keki et al. [13] studied the

polycondensation of *D,L*-lactic acid upon microwave irradiation. The results of polycondensation by means of microwave were compared to those obtained from conventional heating of LA at 100°C, and it was found that the molecular mass of the PLA formed under microwave irradiation increased with irradiation time. But it also was found that cyclic oligomers formed after 20 min of reaction time and only linear oligomers with a molecular weight of 500–2000 g/mol were yielded. Nagahata et al. [14] reported that the synthesis of PLA by a microwave-assisted single-step direct polycondensation of LA can be achieved effectively by use of microwave irradiation and the reaction time can be shortened considerably compared to conventional polycondensation at the same temperature. The tin catalysts and the reduced pressure were found to be strikingly effective to obtain polymers with a molecular weight higher than 10 000. Among the catalysts tested, the SnCl<sub>2</sub>/*p*-TsOH binary catalyst showed the highest activity. By use of a binary catalyst of SnCl<sub>2</sub>/*p*-TsOH, PLA with a  $M_w$  of 16 000 was obtained within 30 min under a reduced pressure of around 30 mmHg.

In syntheses of biodegradable and bioresorbable polymers, efficient metal-free catalysts are very desirable as the resulting products may be more biocompatible. For example Wang et al. [15] have tried to use the most commonly used ionic liquids, 1,3-dialkylimidazolium salts as single-component catalysts in the melt polycondensation of *L*-lactic acid for the first time. It has been found that less bulky substituents on the imidazolium ring are conducive to catalytic activity. PLLA with molar mass of about 20 000 g/mol was synthesized at high yield (over 70%) in the presence of various 1,3-dialkylimidazolium salts. The product exhibits satisfactory color (white to slightly yellow), optical purity (89%–95%) and crystallinity (40%–55%). As compared with the well-known binary catalyst system SnCl<sub>2</sub>·2H<sub>2</sub>O/toluene sulfonic acid, the catalysts used in this investigation were better in terms of increasing PLLA yield and preventing discoloration and comparable in terms of racemization.

In addition, to aim at developing practical and economical technologies for effectively producing PLLA, Miyoshi et al. [16] carried out continuous melt-polymerization experiments using the combination of a batch type stirred reactor and an intermeshed twin screw extruder. As a result, they have obtained PLLA with higher molecular weight of up to  $M_w = 150\,000$  from LA by a continuous melt-polycondensation process.

The melt/solid polycondensation of LA has been extensively studied by many researchers. This process usually leads to high molecular weight products, however, is not usually used commercially due to low production rates and mixing problems experienced in the process.

On the other hand, a polymer of high molecular weight can be obtained by the use of chain coupling agents. The coupling agent joins the polymer chain of low molecular weight to the chain of high molecular weight. Since the self-condensation of LA results in a low-molecular-weight polymer with an equimolar concentration of hydroxyl and carboxyl end-groups, chain-coupling agents preferentially react



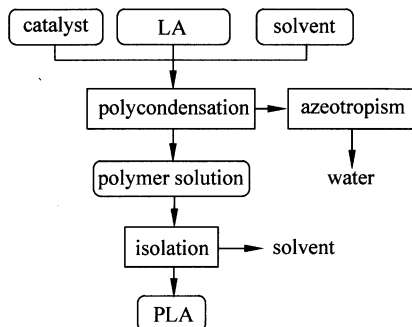
with either the hydroxyl or carboxyl end groups of the polymer. With the use of a bi/multi-functional co-monomer, PLA can be modified to all hydroxyl or carboxyl end group. Hydroxyl terminated PLA can be synthesized by the polymerization of LA in the presence of a small amount of bi/multi-functional hydroxyl compounds such as 2-butene 1,4-diol, glycerol, or 1,4-butanediol, which leads to a preferential hydroxyl end-groups. This same concept can be used to synthesize carboxyl terminated PLA by using bi/multi-functional carboxylic acids such as maleic, succinic, adipic, or itaconic acid, leading to all carboxyl-end functional polymer [17 – 19]. PLA can also be post-reacted with acid anhydrides such as maleic or succinic anhydride to convert the hydroxyl group to a carboxylic end group [19]. The reaction of bi/multi-functional PLA with a suitable coupling agent like di/polyacids or isocyanates to form copolyester or poly(lactic acid-co-urethane), respectively results in an increase in the length of the polymer chain.

Although, high molecular weight polyesters with good mechanical properties are not easy to obtain, the properties of LA oligomers, which can be further used as intermediates in the synthesis of polyurethanes, can be controlled by the use of different catalysts and functionalization agents, as well as by varying the polymerization conditions. This approach was used by Carothers and is still used by Mitsui Toatsu Chemicals Inc. to manufacture a low to intermediate molecular weight polymer [20].

## 3.2 Azeotropic Dehydrative Polycondensation of LA

The direct polycondensation process has restrained the equilibrium between free acids, water, and polyesters and the viscous polyester melt, causing difficulty in removing by-produced water. If too high a temperature for the reaction is employed, the rate of depolymerization becomes higher than the rate of polymerization. Until 1995, it was believed that a high molecular weight of PLA could not be prepared by the polycondensation of LA because of the difficulty in driving the dehydrative equilibrium to the direction of esterification or the formation of PLA with a sufficiently high molecular weight. The azeotropic dehydrative polycondensation developed by Mitsui Chemicals Co. brought a breakthrough in increasing the molecular weight of the polycondensation of LA. This method can afford PLA with a high molecular weight after a relatively long reaction time [21 – 23]. Solvents with high boiling point are used for the removal of the dissociated water by means of the so-called azeotropic distillation technique (Fig. 3.3).

Takasu et al. [24] reported that scandium trifluoromethanesulfonate [Sc(OTf)<sub>3</sub>] and scandium trifluoromethanesulfonimide [Sc(NTf<sub>2</sub>)<sub>3</sub>] are effective for one-step dehydration polycondensation of *L*-lactic acid. Bulk polycondensation of *L*-lactic acid was carried out at 130–170 °C to give PLLA with  $M_n$  of  $5.1 \times 10^4$  –  $7.3 \times 10^4$  (yield 32% – 60%). However, the solution polycondensation was



**Figure 3.3** Flow diagram of the azeotropic dehydrative polycondensation of LA

performed at 135 °C for 48 h to afford PLLA with  $M_n$  of  $1.1 \times 10^4$  with good yield (90%). The catalyst was recovered easily by extraction with water and reused for polycondensation.

Fukushima et al. [25] developed a two-step polycondensation process so as to produce economically PLLA with high molecular weight. The process was composed of both melt polycondensation under the lactide-reflux and solid-phase polycondensation. First they studied a direct polycondensation of *L*-lactic acid with a small amount of solvent, using a mixture of *L*-lactic acid as raw material, diphenyl ether as solvent, Tin (II) chloride dihydrate as catalyst, and *p*-toluene sulfonic acid as a discoloration prevention agent. After the dehydrative oligomerization of *L*-lactic acid, the polycondensation of the oligocondensates and solid-phase post-polycondensation, PLLA of  $M_w = 266\ 000$  was obtained. Then, they carried out direct bulk polycondensation tests from *L*-lactic acid without any solvent added. After optimization of the reaction conditions, PLLA with  $M_w = 134\ 000$  was produced by the melt polycondensation of *L*-lactic acid accompanied by solid-phase post-polycondensation. In both systems, the lactide-reflux was indispensable for promoting dehydration/water removal. The reflux lactide was taken into the polymer-chain by trans-esterification reaction hiring the melt-polycondensation. Furthermore, the catalyst was allowed to deactivate and stabilize hiring the solid-phase polymerization to cause the  $M_w$  growth.

Ajioka et al. [26] have synthesized PLA with a  $M_w$  higher than 300 000 by azeotropic dehydrative polycondensation of LA in the presence of a catalyst and an organic solvent. These polymers have good mechanical properties and can be processed into products such as cups, film, and fiber, which can be used as compostable materials.

The polymerization process by azeotropic dehydrative condensation of LA seems promising for obtaining a high molecular weight PLA with improved cost performance. However, the use of solvents such as diphenyl ether results in multiple reactors and complex facilities of the process control, leaving the price of PLA expensive. Also, it is hard to remove solvent completely from the end product. Meanwhile, the azeotropic dehydrative condensation process inherits the

problems with involvement of organic solvents which makes the processes ecologically unattractive.

### 3.3 Polycondensation Kinetics of LA

Harshe et al. [27] developed a dynamic model for the polycondensation of LA accounting for water removal by diffusion. The model and the corresponding parameter values were validated by comparing the model simulation results with the experimental results. The developed model was found to predict with reasonable accuracy the time evolution of average polymer properties. The model was also used to study the effects of different operating conditions on the performance of the system. It was found that the reaction proceeds very close to the case of instantaneous removal of water, and hence there is no effect of decompression and/or decompression profile on the molecular weight of the produced polymer. For the specific reactor under examination, large catalyst activities were essential to achieve high molecular weights.

Furthermore, polycondensation of LA with and without catalyst under closed and open conditions at different temperatures has been studied [28]. The experimental results are used to estimate the polymerization rate constant and the equilibrium constant. Accounting for the actual rate of water removal, the model encompasses all possible situations and, in particular, the two limiting cases of complete water removal (ideal irreversible polycondensation) and no water removal (ideal reversible polycondensation).

The mathematical model developed with the assumption of a simple kinetic scheme and estimated kinetic parameters is instrumental to understand and to predict effects of different operating conditions on the polymer properties. Though the model results differ from the experimental results in terms of the polymer MWDs measured by GPC, the model predicted average polymer properties are in fairly good agreement with the experimental values. To improve the model predictions a better understanding of possible side reactions is most likely needed. Finally, in contrast to earlier literature results [29], no dependence of the polymer properties on the reactor pressure and/or pressure reduction rate is found through both the model simulations and experiments.

### 3.4 Ring-Opening Polymerization of Lactide

While direct polycondensation of LA should be the cheapest route to PLA, the ring-opening polymerization (ROP) of lactide is the method used commercially. Though the ROP of lactide was first studied long back (1932), only low molecular weight polymer was produced until lactide purification techniques were devised by DuPont in 1954. Over the past decades, many researchers have studied the

ROP of lactide, and numerous patents [30–33] which describe methods to produce PLA by the ROP of lactide have been filed. Furthermore, Nature Works LLC has developed a solvent-free, low-cost continuous process for the production of PLA from corn-derived dextrose. The resulting PLA, commercially branded as Ingeo™ biopolymer, is the first synthetic polymer to be produced from annually renewable resources.

Lactide, the cyclic dimer formed by condensation of lactic acid, is produced by the thermal degradation of oligolactic acid (formed by polycondensation). It is a useful monomer as now it can be easily purified by vacuum sublimations to remove water and acid impurities. The ring-opening polymerization of lactide can be initiated by metal complexes, organic compounds, or enzymes, with/without alcohol, to yield high molecular weight PLA in excellent conversion and purity. The most striking aspect of ROP was theoretically elucidated by Flory; the invariant number of propagating chains in the ROP results in the generation of nearly monodisperse polymers at a high degree of polymerization (DP). The benefits of ROP in conjunction with a “living” method have enabled the controlled synthesis of block, graft, and star polymers, which leads to a present consensus that living ROP is a powerful and versatile addition-polymerization method.

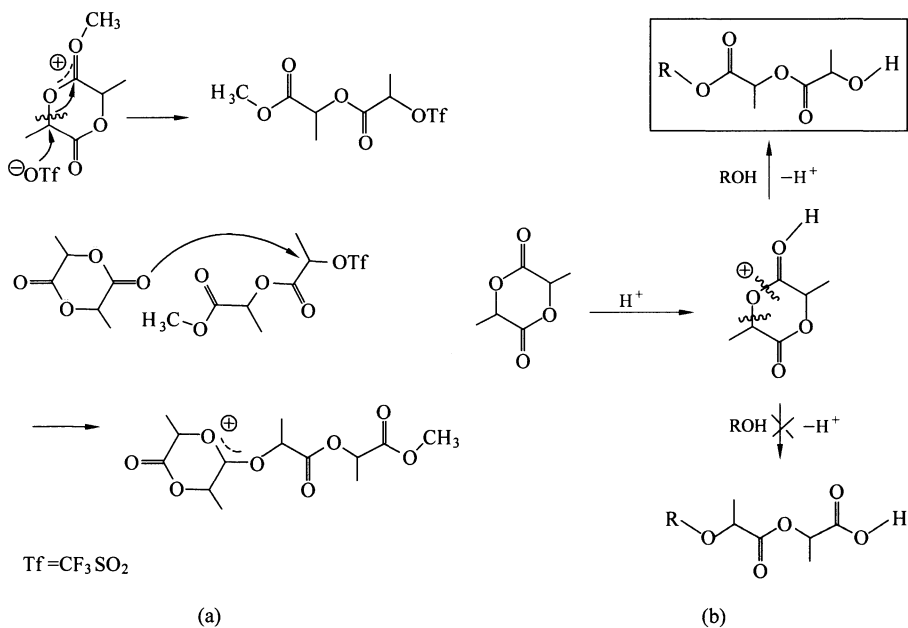
The thermodynamic driving force is the enthalpy of ring-opening polymerization and specifically the relief of ring strain ( $\Delta H=22.1$  kJ/mol for 1 mol/L solution of lactide at room temperature). This enables the unfavorable entropy of polymerization to be overcome [34]. Whilst the polymerization equilibrium is determined thermodynamically, the polymerization control, stereoselectivity, and rate are governed by the choice of initiator. The most common initiators are metal alkoxide or amide coordination compounds (sometimes formed in situ by reaction of metal precursor complex with the appropriate alcohol that is referred to as an initiating system), which are especially useful due to their tolerance, selectivity, rate, and lack of side reactions. On the other hand, for some biomedical applications metal residues are undesirable and in these cases low toxicity organocatalytic or enzyme initiating systems are favorable (initiating system refers to the use of an organocatalyst/enzyme with added alcohol).

### 3.4.1 Cationic Ring-Opening Polymerization of Lactide

Cationic polymerization has been applied for the ROP of a variety of cyclic heterocycles [35]. The cationic ROP of lactones has been achieved using alkylating agents, acylating agents, Lewis acids, and protic acids. For example, alkylating agents such as methyl triflate were reported by Kricheldorf and coworkers in a series of papers in the 1980 s for the cationic polymerization of various lactones, including  $\beta$ -propiolactone (PL),  $\epsilon$ -caprolactone (CL), valerolactone (VL), glycolide (GA), and lactide (LA) [36–39]. Acylating agents have been reported by Hofman et al. for the cationic ROP of CL and PL [40]. A variety of Lewis acids have been screened for the bulk and solution cationic ROP of monomers such as

1,5-dioxepan-2-one (DXO) by Albertsson and Palmgren [41].

Early attempts reported in 1971 by Dittrich and Schulz to polymerize LA with cationic compounds were unsuccessful [42]. In 1986, Kricheldorf and coworkers screened a variety of acidic compounds, among which only trifluoromethanesulfonic acid (triflic acid, HOTf) and methyl triflate (MeOTf) proved to be useful initiators for the cationic ROP of LA [43,44]. The polymerization rates were significantly higher in nitrobenzene than in chlorinated solvents with 50°C being found to be the optimum reaction temperature (lower temperatures result in modest yields, and higher temperatures lead to dark-colored samples). End-group analysis by  $^1\text{H}$  NMR indicates methyl ester groups when methyl triflate is used as the initiator, suggesting that the polymerization proceeds by cleavage of the alkyl-oxygen bond rather than the acyloxygen bond. Polymerizations of *L*-lactide performed under 100°C using HOTf and MeOTf initiators result in 100% optically active PLLA. A two-step propagation mechanism has been proposed involving activation of the monomer by methylation with methyl triflate followed by  $\text{S}_{\text{N}}2$  attack of the triflate anion on the positively charged LA ring with inversion of stereochemistry. Propagation is proposed to proceed by nucleophilic attack by LA on the activated cationic chain end with inversion, leading to net retention of the configuration (Fig. 3.4(a)). Regardless of the monomer-to-initiator ratio (50 – 400), the reported polymer viscosities are all quite similar, suggesting that the polymerization is not living under the reported optimized conditions [44].



**Figure 3.4** (a) Proposed pathway for cationic ROP of lactide; (b) proposed activated monomer pathway for cationic ROP of LA [45]

Recently, Bourissou et al. [46] reported the controlled cationic polymerization of LA by using a combination of the triflic acid (as the catalyst) and a protic reagent (water or an alcohol) as an initiator. Reactions were performed in  $\text{CH}_2\text{Cl}_2$  solution at room temperature and required only a few hours for high monomer conversion. In the absence of a protic initiator, monomer conversion reached only 23% after 2 h. Weaker acids such as  $\text{HCl}\cdot\text{Et}_2\text{O}$  or  $\text{CF}_3\text{COOH}$  were reportedly inactive toward LA polymerization after 2 h under the same conditions. PLAs with molar masses up to 20 000 g/mol with PDIs ranging from 1.13 to 1.48 were obtained using the HOTf catalyst/protic initiator system with quantitative incorporation of the protic initiator confirmed by  $^1\text{H}$  NMR and ESI mass spectrometry. The controlled character of the polymerization is suggested by the linear relationship of the molecular weight versus monomer conversion and monomer-to-initiator ratio. The controlled cationic ring-opening polymerization is believed to proceed by an “activated cationic polymerization” mechanism as described by Penczek [35], where the acid would activate the cyclic ester monomer and the alcohol would be the initiator of polymerization. Polymerization is, therefore, thought to proceed by protonation of LA by triflic acid followed by nucleophilic attack by the initiating alcohol or that of the growing polymer chain, as shown in Fig. 3.4(b). The presence of isopropyl ester chain ends from the initiating isopropyl alcohol (observed by  $^1\text{H}$  NMR) suggests that polymerization proceeds by acyl bond cleavage, not by alkyl bond cleavage.

Bowden and coworkers [47] reported the bulk ROP of LA by using ethanol as the alcohol initiator and diphenylammonium triflate (DPAT) as an acidic-proton catalyst. Bulk polymerization at  $130^\circ\text{C}$  by using 5 mol% DPAT catalyst relative to initiator resulted in molecular weights up to 12 000 Da and PDIs ranging from 1.24 to 1.51. The high PDIs are likely due to transesterification with prolonged reaction times ( $> 4$  days). Similar to the previously described acid-catalyzed ROP of LA, polymerization is thought to proceed through a cationic activated monomer mechanism.

### 3.4.2 Anionic Ring-Opening Polymerization of Lactide

Anionic ROP of lactide has been much less investigated than the coordination insertion approach. Although higher activities might be anticipated for anionic promoters that typically display strong nucleophilic and/or basic character, the deleterious contribution of transesterification and racemization reactions might be expected to be significantly more important when naked or loosely bonded anionic species are involved [48].

Kricheldorf et al. [49] demonstrated the anionic ROP of *L*-lactide in solution at room temperature with potassium *tert*-butoxide and butyllithium. They found that the monomer conversion did not exceed 80%, and the anionic initiator and

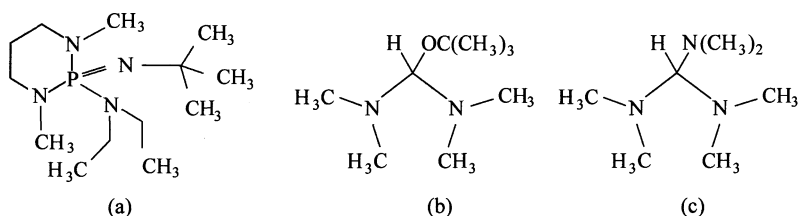
alkoxide growing chain were both found to induce racemization regardless of solvent and temperature. Significantly higher yields could be obtained by in situ generation of secondary and primary lithium and potassium alkoxides [50–52]. Although these promoters required temperatures of 50 °C to achieve the polymerization, the extent of racemization was found to be rather low, especially for the lithium alkoxides, and isotactic PLLA with optical purity up to 95% could be prepared. When potassium methoxide was used as a promoter [53], the ROP of *L*-lactide could be conveniently achieved in THF, with almost quantitative yields being obtained after 10–135 min at room temperature for initial monomer concentrations of 1.3–2.0 mol/L and monomer-to-initiator ratios of 50–300. Under these conditions, polymers with molecular weights in agreement with the monomer-to-initiator ratios and relatively narrow molecular weight distribution (PDI ranging from 1.3 to 1.4) were obtained. Moreover, microstructural analysis by optical rotation measurements and <sup>13</sup>C NMR spectroscopy indicated a high degree of isotacticity for the resulting PLA. All these data suggest that potassium methoxide allows for minimization of both transesterification and racemization reactions.

Kasperczyk et al. [54, 55] demonstrated that the use of lithium *tert*-butoxide as a promoter is also interesting for the stereocontrolled polymerization of *rac*-lactide, via chain-end control, leading to highly heterotactic microstructures with stereoselectivities of 90% at room temperature and 94% at –20 °C. However, these results were obtained at only 35% monomer conversion, and due to transesterification reactions, the regular microstructure of the chain tended to be significantly reduced when the monomer conversion was increased.

In addition, dibutylmagnesium has also been reported as an efficient promoter for ROP of *L*-lactide in toluene/THF solution at 0 °C [56]. The polymerization is typically completed within a few days for an initial monomer concentration of 4 mol/L and monomer-to-initiator ratios up to 400. Polymers with almost complete optical purity but rather high polydispersity indexes (about 2) are obtained, indicating that these polymerization conditions minimize epimerization but not transesterification reactions. Moreover, the stereocontrolled polymerization of *rac*-lactide has been also investigated with dibutylmagnesium and butyllithium [57]. Although significant extents of heterotactic microstructures could be observed by <sup>13</sup>C NMR (about 60%–70%), transesterification reactions are found to have a strongly deleterious effect, as is the case with lithium *tert*-butoxide.

Recently, Zhang et al. [58] reported that the commercially available phosphazene base, 2-*tert*-butylimino-2-diethylamino-1,3-dimethylperhydro-1,3, 2-diazaphosphorine (BEMP, Fig. 3.5(a)), are active organocatalyst for the living ring-opening polymerization (ROP) of *L*-lactide and *rac*-lactide. The catalytic activity of the phosphazene base was studied in dry toluene at room temperature for polymerizations with targeted monomer-to-initiator ratios of 100 by using 1-pyrene-butanol as the initiator. For example, at a 1 mol% catalyst BEMP-to-monomer ratio, polymerization of *L*-LA reached 78% conversion in 23 h to

give PLLA with  $M_n$  of 13 100 Da and a narrow PDI (1.08). A plot of  $M_n$  versus monomer conversion showed a linear correlation, characteristic of a living polymerization. The PDI decreases slightly as the conversion approaches 70% and then increases. The increase of molecular weight distribution at high conversion attributed to the is transesterification as the monomer supply is depleted. In an effort to minimize adverse transesterification reactions, the reaction was quenched by the addition of benzoic acid. Polymerization of *rac*-lactide yields isotacticeriched PLA with the probability of isotactic propagation ( $P_1=0.70$ ).



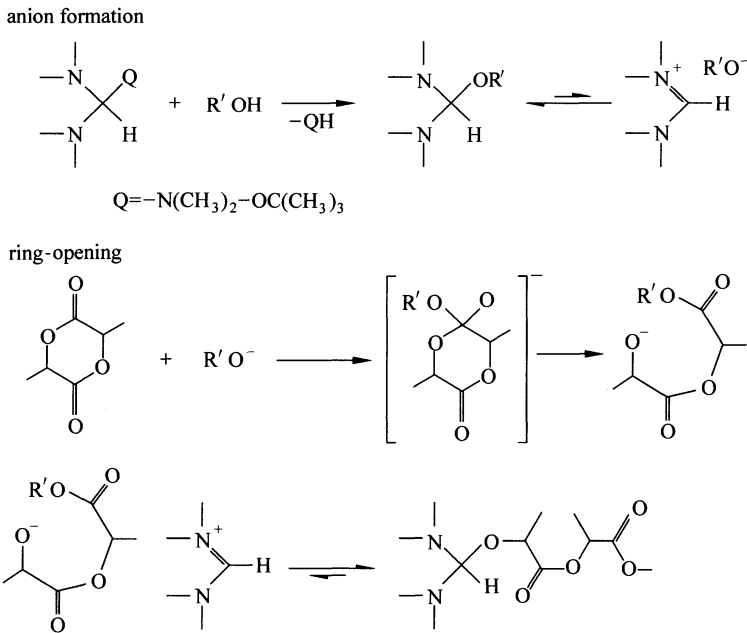
**Figure 3.5** (dimethylamino) methane, and (c) tris (dimethylamino) methane

The commercially available compounds, *tert*-butoxybis-(dimethylamino)methane (also known as Brederick's reagent, Fig. 3.5(b)) and tris(dimethylamino)methane (Fig. 3.5(c)), have been also investigated for the ROP of LA [59] because they are reminiscent of other protected forms of *N*-heterocyclic carbenes (NHCs) and are expected to show similar reactivities. The ROP of LA with commercially available Brederick-type reagents in the presence or absence of alcohol initiators is an efficient method for the synthesis of PLA with controlled molecular weight and narrow PDIs. High monomer conversion is reached after 3 h at 70°C in THF solution or in several minutes when vacuum is applied. Although these compounds are initially envisioned as precursors to stabilized carbenes, alternative mechanisms involving heterolytic cleavage to alkoxides are proposed, suggesting that these reagents can function as latent anionic initiators for ring-opening polymerization reactions. As shown in Fig. 3.6, the ring-opening of the LA by the alkoxide provides a propagating anion. This anion can continue to ring open LA through an anionic mechanism. Because the formamidinium counterion is also an electrophile, it is possible that the propagating anion is reversibly captured by the counterion, leading to reversible deactivation of the propagating anion.

### 3.4.3 Coordination-Insertion Polymerization of Lactide

The three-step coordination-insertion mechanism for the ROP of cyclic esters was first formulated in 1971 by Dittrich and Schulz [60]. The first experimental





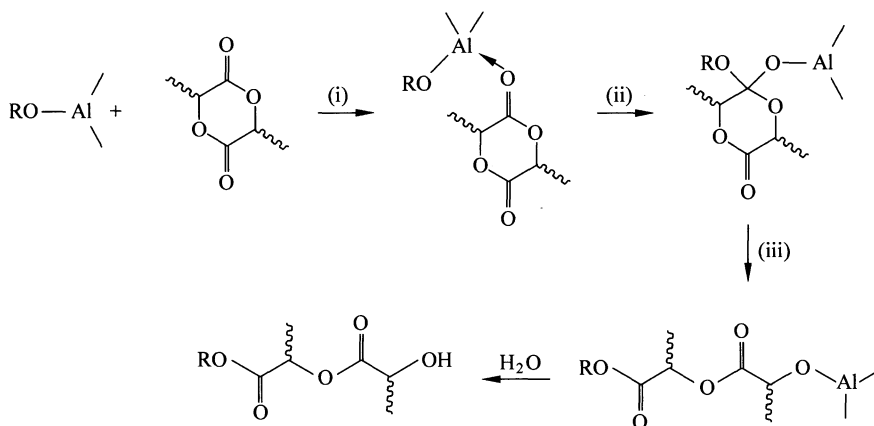
**Figure 3.6** Proposed mechanism for anionic ring-opening polymerization of lactide by Bredereck-type reagents [59]

proof for such a mechanism in the  $Al(Oi-Pr)_3$ -initiated polymerization of lactide was independently reported in the late 1980 s by Kricheldorf et al. [61] and Teyssié et al. [62]. Recently, further support for such a mechanism has been provided by experimental [63 – 65] as well as theoretical [66, 67] studies. The living character of the polymerization in toluene at  $70^\circ C$  has also been deduced from the linear dependence of the mean DP on the monomer-to-initiator molar ratio calculated for the actual monomer conversion [62].

The first step of the coordination-insertion mechanism (I) consists of the coordination of the monomer to the Lewis-acidic metal center (Fig. 3.7). The monomer subsequently inserts into one of the aluminum-alkoxide bonds via nucleophilic addition of the alkoxy group on the carbonyl carbon; (II) followed by ring opening via acyl-oxygen cleavage; (III) hydrolysis of the active metal-alkoxide bond leads to the formation of a hydroxyl end group, while the second chain end is capped with an isopropyl ester, as indicated by  $^1H$  NMR characterization of the resulting polymers [48].

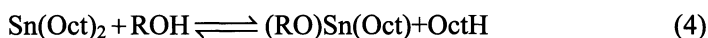
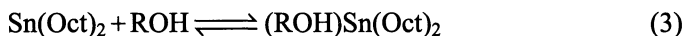
Calculations have revealed the critical influence of the aluminum substituents. Significantly lower activation barriers are predicted for trialkoxides relative to the corresponding monoalkoxides [66]. The sensitivity of aluminum initiators toward steric bulk has also been noted and is attributed to the shortness of the aluminum-oxygen bonds [67]. Accordingly, the activation barrier for the insertion step is found to be about 40% higher for lactide than for glycolide for the

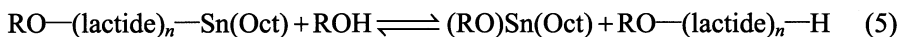
model complex  $\text{AlMe}_2(\text{OMe})$ . These data nicely parallel the higher polymerizability of glycolide compared to lactide, an activity ratio  $r_G/r_L$  of about 10 being typically observed experimentally [68].



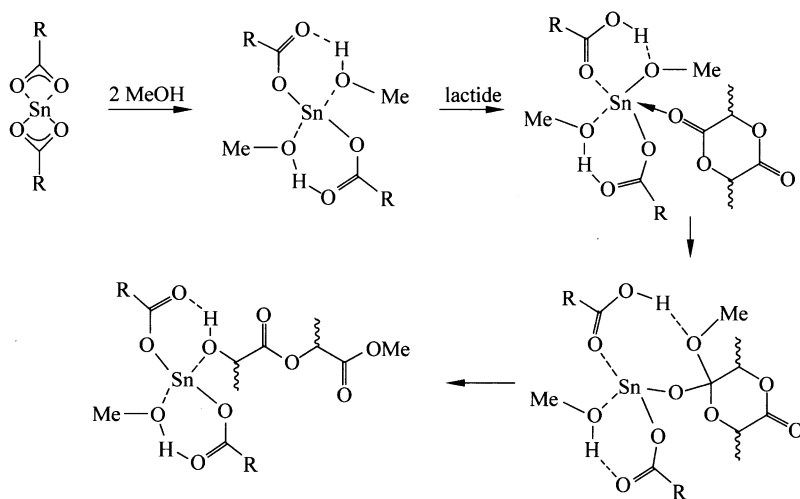
**Figure 3.7** Coordination-insertion mechanism for the  $\text{Al}(\text{O}i\text{-Pr})_3$ -catalyzed ROP of lactide [48]

$\text{Sn}(\text{Oct})_2$  is inherently more active than  $\text{Al}(\text{O}i\text{-Pr})_3$ , but the polymerization is found to be even faster and better controlled when  $\text{Sn}(\text{Oct})_2$  is combined with a protic reagent such as an alcohol. The mechanism for the  $\text{Sn}(\text{Oct})_2$ -catalyzed ROP has been the subject of much more controversy. Recent investigations [69, 70] have allowed for the characterization of several intermediate tin complexes and strongly support a coordination-insertion mechanism rather than a cationic or activated-monomer mechanism [71 – 74]. However, the most debatable question concerns the very nature of the initiating complex. Although it is generally accepted that protic reagents such as alcohols react with  $\text{Sn}(\text{Oct})_2$  to form covalent tin (II) alkoxides [75,76], this coordination step can occur with retention of the octanoate ligands (Eq. (3)) [77] or with liberation of octanoic acid (Eq. (4)) [69, 78 – 81], and the reaction conditions (in terms of temperature, alcohol-to-tin ratio, solvent, etc.) are believed to strongly influence these processes. It is also widely accepted that impurities present in the monomer (alcohols, lactic acid, water, etc.) may act as co-initiators, especially when  $\text{Sn}(\text{Oct})_2$  is used without protic additives. Last, it should not be underestimated that besides their involvement in polymerization initiation, protic agents may also be involved in reversible chain transfer with the growing chain (Eq. (5)), making it essential that the  $\text{ROH}$  to  $\text{Sn}(\text{Oct})_2$  ratio is carefully optimized [70].





Support for the coordination-insertion mechanism has recently been obtained theoretically (Fig. 3.8) [82]. Two molecules of methanol are found to coordinate to  $\text{Sn}(\text{OAc})_2$  as a model for  $\text{Sn}(\text{Oct})_2$ . Both coordinations are favored by about 59–63 kJ/mol and occur in an associative fashion, i.e., with retention of the two octanoate moieties (hydrogen bonds are formed between the alcohol and octanoate ligands). A weak complexation of lactide is predicted (coordination enthalpy of 16 kJ/mol). Notably, the latter coordination step induces a proton migration from methanol to the nearby octanoate ligand, so that the alcohol ligand is converted into an alkoxide. Subsequently, the insertion occurs in two steps, namely, nucleophilic attack of this alkoxide on the coordinated lactide followed by ring opening, resulting formally in the insertion of a lactide moiety into the O—H bond of a coordinated methanol. These calculations suggest that the octanoic acid remains coordinated to tin during propagation, but taking into consideration of both the entropic term and the reaction temperature, it might also be possible that the octanoic acid dissociates from the tinalkoxide complex during ROP.



**Figure 3.8** Predicted mechanism for the  $\text{Sn}(\text{Oct})_2$ -catalyzed ROP of lactide in the presence of methanol [82]

Comparatively, the mechanism of  $\text{Zn}(\text{Lact})_2$ -catalyzed ROP has been much less studied. However, the combination of  $\text{Zn}(\text{Lact})_2$  with a primary alcohol is demonstrated to increase its activity and allows for a better control of the polymerization, as in the case of  $\text{Sn}(\text{Oct})_2$  [83]. Thus, it seems rather likely that the polymerization proceeds with  $\text{Zn}(\text{Lact})_2$  in a similar way to that discussed above for  $\text{Sn}(\text{Oct})_2$ . In such coordination-insertion polymerizations the efficiency

of the molecular-weight control depends on the ratio  $k_{\text{propagation}}/k_{\text{initiation}}$ , but also on the extent of transesterification side reactions. These transesterification reactions can occur both intramolecularly (backbiting leading to macrocyclic structures and shorter chains) and intermolecularly (chain redistributions) [84, 85]. The polymerization/depolymerization equilibrium should also be taken into account as a particular case of intramolecular transesterification reaction. All of these side reactions result in broader molecular-weight distributions, sometimes making the molecular weights of the resulting polymers irreproducible. The extent of these undesirable transesterification reactions is found to strongly depend on the metallic initiator [61, 84, 85]. Side reactions occur from the very beginning of the polymerization with  $\text{Sn}(\text{Oct})_2$ , leading to rather broad molecular weight distributions (PDI indexes around 2) but only at high or even complete conversion with  $\text{Al}(\text{O}i\text{-Pr})_3$ , lower PDI indexes (less than 1.5) is yielded [63, 64]. The promising results obtained with  $\text{Sn}(\text{Oct})_2$ ,  $\text{Al}(\text{O}i\text{-Pr})_3$ , and  $\text{Zn}(\text{Lact})_2$  have given rise to a growing interest in metal-based initiators that would display higher catalytic activity and better control of the extent of the undesirable transesterification reactions.

A variety of initiators and catalysts have been employed in the ring-opening polymerization of lactide. Among them, the most frequently used catalyst for the industrial preparation of PLA is undoubtedly tin(II) bis(2-ethylhexanoate). This derivative, usually referred to as tin(II) octanoate,  $\text{Sn}(\text{Oct})_2$ , is commercially available, easy to handle, and soluble in common organic solvents and in melt monomers. It is highly active (typical reaction times in bulk at 140–180°C range from minutes to a few hours) and allows for the preparation of high-molecular-weight polymers (up to  $10^5$  or even  $10^6$  Da in the presence of alcohol) [63]. Although  $\text{Sn}(\text{Oct})_2$  has been accepted as a food additive by the U.S. FDA, the toxicity associated with most tin compounds is a considerable drawback in the case of biomedical applications.

Aluminum alkoxides have also proved to be efficient catalysts for the ROP of cyclic esters. The archetypal example, namely,  $\text{Al}(\text{O}i\text{-Pr})_3$ , has been largely used for mechanistic studies. However, it has been revealed to be significantly less active than  $\text{Sn}(\text{Oct})_2$  (in bulk at 125–180°C, reaction time of several days is usually required and molecular weight is generally lower than  $10^5$  Da) [63]. Moreover, an induction period of a few minutes is systematically observed with  $\text{Al}(\text{O}i\text{-Pr})_3$ . This feature has been attributed to aggregation phenomenon [86]. For all these reasons,  $\text{Al}(\text{O}i\text{-Pr})_3$  is much less used for the preparation of biodegradable polyesters, and especially since aluminum ions do not belong to the human metabolism and are suspected of supporting Alzheimer's disease.

Much interest has thus been devoted to zinc derivatives as potential nontoxic catalysts. Zinc powder itself is a relatively good polymerization catalyst that is used industrially [87, 88]. With reaction times of several days at 140°C in bulk, it is roughly as active as  $\text{Al}(\text{O}i\text{-Pr})_3$ . Numerous zinc salts have also been investigated [89, 90]. So far, the best results regarding lactide conversion and

degree of polymerization are observed with zinc(II) lactate,  $\text{Zn}(\text{Lact})_2$ , which is commercially available and can be readily obtained from ZnO and ethyl lactate or lactide. Notably,  $\text{Zn}(\text{Lact})_2$  allows for a better control of the molecular weight of the resulting polymers compared with zinc powder.

Continuous efforts have been devoted to the development of new catalysts for ring-opening polymerization of lactide. In particular, the biomedical applications of polylactide necessarily require low levels of impurities, and therefore, there is a great impetus for the development of highly active catalysts with low toxicity. Noteworthy advances about catalysts, for example, metal-alkoxides catalysts and ligands, organocatalysts for ROP of lactide to generate PLA have been made and thoroughly reviewed by Dechy-Cabaret et al. [48] and Kamber et al. [45]. The reader is referred to these for further discussion.

#### 3.4.4 Enzymatic Ring-Opening Polymerization of Lactide

A vast number of enzymes catalyze metabolic reactions via biosynthetic pathways in living cells. Natural polymers such as polysaccharides, proteins, polyesters etc. are synthesized in nature by enzymes. A conservative estimate is that over 10<sup>12</sup> t cellulose, starch and related biomaterials are generated on our planet each year due to natural processes [91]. The use of enzymes for in vitro polymer synthesis has been actively pursued in the last decade. Enzymatic polymerization is an in vitro polymerization via non-biosynthetic pathways catalyzed by an isolated enzyme [9]. This approach is found to be effective in the synthesis of natural polymers and has been extended to the synthesis of biodegradable polymers such as aliphatic polyesters [93]. The field of enzyme-catalyzed ring-opening polymerization has grown since the initial application of a lipase catalyst for ring-opening of lactones by the independent groups of Kobayashi et al. [94, 95] and Knani et al. [96]. Enzymes exhibit high stereo-, reaction-, and substrate specificity and come from renewable resources that can be easily recycled.

The enzymatic ring-opening polymerization of lactide was first conducted using lipase as the catalyst by Matsumura et al. [97–99]. They reported the lipase catalyzed polymerization of *L*-, *D*-, and *D,L*-lactides at a temperature between 80 and 130°C in bulk to yield the corresponding PLA. It was found that polymerization occurred with all the commercially available lipases tested except for Novozyme 435. Among the lipases tested, lipase PS (*Pseudomonas fluorescens*) showed the best results with respect to both the polymerization rate and the molecular weight of the resultant polylactide ( $M_w$  of up to 126 000 Da) [97]. And, the polymerization results of the *D,L*-lactide were better than those of the *D*- and *L*-lactides (Table 3.2). Furthermore, they also reported the polymerization of *L*-, *D*-, and *D,L*-lactides by using lipase PS in the temperature range from 80 to 130°C, and obtained polylactide (PLA) with a molecular weight

## Biodegradable Poly(Lactic Acid): Synthesis, Modification, Processing and Applications

of 270 000 Da with rather narrow distributions (PDI=1.1 – 1.3) [98]. Although the enzyme and oligomers were easily removed from the resulting PLA upon workup, the isolated yields were fairly low (<16%). The formation of these oligomer fractions along with the observed induction periods are characteristic features for lipase-induced polymerizations.

**Table 3.2** Conditions and results of the lipase-catalyzed ring-opening polymerization of lactide<sup>a</sup>

Entry <sup>b</sup>	Lactide	Lipase <sup>c</sup>	Concentration of lipase (wt%) based on monomer	Temp. (°C)	time (d)	Monomer conversion (%) <sup>d</sup>	Polymer yield (wt%) based on monomer	$M_w^e$	$M_w/M_n^f$
1	<i>D,L</i> -	Novo	3	80	7	0	0	–	–
2	<i>D,L</i> -	PPL	3	80	7	37	29	7 500	1.2
3	<i>D,L</i> -	CC	3	80	7	30	19	8 300	1.2
4	<i>D,L</i> -	Pro	3	80	7	40	40 <sup>g</sup>	1900	1.2
5	<i>D,L</i> -	PS	3	80	7	7	3	27 000	1.2
6	<i>D,L</i> -	PS	10	80	7	83	10	36 000	1.2
7	<i>D,L</i> -	PS	10	80	14	99	16	52 000	1.1
8	<i>D,L</i> -	PS	3	100	7	82	8	69 000	1.2
9	<i>D,L</i> -	PS	3	130	7	100	16	126 000	1.1
10	<i>L,L</i> -	PS	3	80	7	77	10	15 000	1.3
11	<i>L,L</i> -	PS	10	80	7	86	10	37 000	1.1
12	<i>L,L</i> -	PS	3	100	7	82	8	48 000	1.2
13	<i>D,D</i> -	PS	3	80	7	44	5	13 000	1.3
14	<i>D,D</i> -	PS	10	80	7	73	7	25 000	1.2
15	<i>D,D</i> -	PS	3	100	7	96	5	59 000	1.2
16	<i>D,L</i> -	–	–	80	7	0	0	–	–
17	<i>D,L</i> -	–	–	100	7	0	0	–	–
18	<i>D,L</i> -	–	–	130	7	100	100 <sup>g</sup>	3300	1.6
19	<i>L,L</i> -	–	–	100	7	0	0	–	–
20	<i>D,D</i> -	–	–	100	7	0	0	–	–

<sup>a</sup> Polylactide was prepared by the reaction of lactide (500 mg) and lipase in bulk.

<sup>b</sup> Entries 16-20: blank tests.

<sup>c</sup> Novo: Novozyme 435; PPL: porcine pancreatic lipase; CC: *Candida cylindracea* lipase; Pro: Proteinase K; PS: Lipase PS.

<sup>d</sup> Monomer conversion as determined by <sup>1</sup>H NMR of the reaction mixture.

<sup>e</sup>  $M_w$ : Weight-average molecular weight.

<sup>f</sup>  $M_w/M_n$ : Ratio of weight- to number-average molecular weight.

<sup>g</sup> Oligomeric fraction was only produced.

Fujioka et al. [100] conducted the ring-opening polymerization of *L*-lactide by using immobilized lipase *Candida Antarctica* (Novozym 435) as a catalyst at a

temperature of 100°C in bulk. This process was found to yield the corresponding PLLA with weight-average molecular weight of about 2440 and a polydispersity index of 2.63. It was observed that the increase of the reaction time and amount of enzyme catalyst resulted in the polylactides with higher molecular weights.

Very recently, Numata et al. [101] reported the synthesis of branched Poly lactide by enzymatic polymerization. They synthesized various linear and branched PLA using lipase PS (*Pseudomonas fluorescens*)-catalyzed ring-opening polymerization (ROP) of lactide monomers having different stereochemistries (*L*-lactide, *D*-lactide, and *D,L*-lactide). Five different alcohols were used as initiators for the ROP, and the monomer-to-initiator molar feed ratio was varied from 10 to 100 and 1000 for each branch in the polymer architecture. In each polymerization by lipase PS, the molecular weight of the samples increased with decreasing initiator concentration. These molecular weights did not however agree perfectly with the monomer-to-initiator ratio of the enzymatic polymerization, especially in the case of the 1:1000 of monomer-to-initiator ratio, because the conversion did not reach 100%. And then they studied the effects of the number of molecular branches (chain ends) and the stereochemistry of PLA on the enzymatic degradation and alkaline hydrolysis.

## References

- [1] Lim L. T., Auras R., Rubino M. Prog. Polym. Sci., 33, 820 (2008).
- [2] Auras R., Harte B., Selke S. Macromol. Biosci., 4, 835 (2004).
- [3] Gupta A. P., Kumar V. Eur. Polym. J., 43, 4053 (2007).
- [4] Chen G. X., Kim H. S., Kim E. S., et al. Eur. Polym. J., 42, 468 (2006).
- [5] Keki S., Bodnar I., Borda J., et al. J. Phys. Chem. B, 105, 2833 (2001).
- [6] Ajioka M., Enomoto K., Suzuki K., et al. Bull. Chem. Soc. Jpn., 68, 2125 (1995).
- [7] Moon S. I., Lee C. W., Miyamoto M., et al. J. Polym. Sci. Part A: Polym Chem., 38, 1673 (2000).
- [8] Moon S. I., Lee C. W., Taniguchi I., et al. Polymer, 42, 5059 (2001).
- [9] Shinno K., Miyamoto M., Kimura Y., et al. Macromolecules, 30, 6438 (1997).
- [10] Ren Jie, Wang Qinfeng. China Patent, ZL 03115321.6
- [11] Ren Jie, Wang Qinfeng, Zhang Naiwen. China Patent, ZL 200410017212.7
- [12] Yoda S., Bratton D., Howdle S. M. Polymer, 45, 7839 (2004).
- [13] Keki S., Bodnar I., Borda J., et al. Macromol. Rapid Commun., 22, 1063 (2001).
- [14] Nagahata R., Sano D., Suzuki H., et al. Macromol. Rapid Commun., 28, 437 (2007).
- [15] Wang W., Wu L., Huang Y., et al. Polym. Int., 57, 872 (2008).
- [16] Miyoshi R., Hashimoto N., Koyanagi K., et al. Int. Polym. Proc., 11, 320 (1996).
- [17] Bonsignore P. V. U. S. Pat. 5,470,944 (1995).
- [18] Spinu M. L-D. U. S. Pat. 5,270,400 (1993).
- [19] Ibay A. C., Tenney L. P. U. S. Pat. 5,206,341 (1993).
- [20] Mehta R., Kumar V., Bhunia H., et al. J. Macromol. Sci. Polym. Rev. C, 45, 325 (2005).

- [21] Ajioka M., Enomoto K., Suzuki K., et al. *Bull. Chem. Soc. Jpn.*, 68, 2125 (1995).
- [22] Koyanagi K., Fukushima T., Sumihiro Y., et al. *Polym. Prep. Jpn.*, 45, 3565 (1996).
- [23] Shin G. I., Kim J. H., Kim S. H., et al. *J. Korea Polym.*, 5, 19 (1997).
- [24] Takasu A., Narukawa Y., Hirabayashi T. *J. Polym. Sci. Pol. Chem.*, 44, 5247 (2006).
- [25] Fukushima T., Sumihiro Y., Koyanagi K., et al. *Int. Polym. Proc.*, 15, 380 (2000).
- [26] Ajioka M., Enomoto K., Suzuki K., et al. *J. Environ. Polym. Degrad.*, 3, 225 (1995).
- [27] Harshe Y. M., Storti G., Morbidelli M., et al. 9th International Workshop on Polymer Reaction Engineering, 116. Hamburg, Germany (2007).
- [28] Harshe Y. M., Storti G., Morbidelli M., et al. *Macromol. React. Eng.*, 1, 611 (2007).
- [29] Chen G. X., Kim H. S., Kim E. S., et al. *Eur. Polym. J.*, 42, 468 (2006).
- [30] Grubber P. R., Paul St., Hall E. S., et al. U. S. Pat. 5,142,023 (1992).
- [31] Grubber P. R., Paul St., Hall E. S., et al. U. S. Pat. 5,274,073 (1993).
- [32] Enomoto K., Ajioka M., Yamaguchi A. U. S. Pat. 5,310,865 (1994).
- [33] Maeda H., Shimizu K., Miyakawa Y., et al. U. S. Pat. 5,866,677 (1999).
- [34] Duda A., Penczek S. ACS Symposium Series, 764,160 (2000).
- [35] Penczek S. *J. Polym. Sci., Part A: Polym. Chem.*, 38, 1919 (2000).
- [36] Kricheldorf H. R., Jonte J. M., Dunsing R. *Makromol. Chem.*, 187, 771 (1986).
- [37] Kricheldorf H. R., Dunsing R., Serra A. *Macromolecules*, 20, 2050 (1987).
- [38] Kricheldorf H. R., Dunsing R. *Makromol. Chem.*, 187, 1611 (1986).
- [39] Kricheldorf H. R., Kreiser I. *Makromol. Chem.*, 188, 1861 (1987).
- [40] Hofman A., Szymanski R., Slomkowski S., et al. *Makromol. Chem.*, 185, 655 (1984).
- [41] Albertsson A. C., Palmgren R. *J. Macromol. Sci., Pure Appl. Chem.*, A33, 747 (1996).
- [42] Dittrich W., Schulz R. C. *Angew. Makromol. Chem.*, 15, 109 (1971).
- [43] Kricheldorf H. R., Dunsing R. *Makromol. Chem.*, 187, 1611 (1986).
- [44] Kricheldorf H. R., Kreiser I. *Makromol. Chem.*, 188, 1861 (1987).
- [45] Kamber N. E., Jeong W., Waymouth R. M., et al. *Chem. Rev.*, 107, 5813 (2007).
- [46] Bourissou D., Martin-Vaca B., Dumitrescu A., et al. *Macromolecules*, 38, 9993 (2005).
- [47] Atthoff B., Hilborn J., Bowden T. *PMSE Prepr.*, 88, 369 (2003).
- [48] Dechy-Cabaret O., Martin-Vaca B., Bourissou D. *Chem. Rev.*, 104, 6147 (2004).
- [49] Kricheldorf H. R., Kreiser-Saunders I. *Makromol. Chem.*, 191, 1057 (1990).
- [50] Kricheldorf H. R., Boettcher C. *Makromol. Chem.*, 194, 1665 (1993).
- [51] Kricheldorf H. R., Boettcher C. *Makromol. Chem., Macromol. Symp.*, 73, 47 (1993).
- [52] Xie W., Chen D., Fan X., et al. *J. Polym. Sci., Part A: Polym. Chem.*, 37, 3486 (1999).
- [53] Jedlinski Z., Walach W., Kurcok P., et al. *Makromol. Chem.*, 192, 2051 (1991).
- [54] Kasperczyk J. E. *Macromolecules*, 28, 3937 (1995).
- [55] Bero M., Dobrzynski P., Kasperczyk J. *J. Polym. Sci., Part A: Polym. Chem.*, 37, 4038 (1999).
- [56] Kricheldorf H. R., Lee S. R. *Polymer*, 36, 2995 (1995).
- [57] Kasperczyk J., Bero M. *Polymer*, 41, 391 (2000).
- [58] Zhang L., Nederberg F., Pratt R. C., et al. *Macromolecules*, 40, 4154 (2007).
- [59] Csihony S., Beaudette T. T., Sentman A. C., et al. *Adv. Synth. Catal.*, 346, 1081 (2004).
- [60] Dittrich W., Schulz R. C. *Angew. Makromol. Chem.*, 15, 109 (1971).
- [61] Kricheldorf H. R., Berl M., Scharnagl N. *Macromolecules*, 21, 286 (1988).
- [62] Dubois P., Jacobs C., Jérôme R., et al. *Macromolecules*, 24, 2266 (1991).
- [63] Degée P., Dubois P., Jérôme R., et al. *Macromol. Symp.*, 144, 289 (1999).



- [64] Degée P., Dubois P., Jérôme R. *Macromol. Symp.*, 123, 67 (1997).
- [65] Degée P., Dubois P., Jérôme R. *Macromol. Chem. Phys.*, 198, 1973 (1997).
- [66] Eguiburu J. L., Fernandez-Berridi M. J., Cossío F. P., et al. *Macromolecules*, 32, 8252 (1999).
- [67] Von Schenk H., Ryner M., Albertsson A. C., et al. *Macromolecules*, 35, 1556 (2002).
- [68] Gilding D. K., Reed A. M. *Polymer*, 20, 1459 (1979).
- [69] Kricheldorf H. R., Kreiser-Saunders I., Stricker A. *Macromolecules*, 33, 702 (2000).
- [70] Kowalski A., Duda A., Penczek S. *Macromolecules*, 33, 7359 (2000).
- [71] Nijenhuis A. J., Grijpma D. W., Pennings A. J. *Macromolecules*, 25, 6419 (1992).
- [72] Du Y. J., Lemstra P. J., Nijenhuis A. J., et al. *Macromolecules*, 28, 2124 (1995).
- [73] In't Veld P. J. A., Velner E. M., van de Witte P., et al. *J. Polym. Sci., Part A: Polym. Chem.*, 35, 219 (1997).
- [74] Schwach G., Coudane J., Engel R., et al. *J. Polym. Sci., Part A: Polym. Chem.*, 35, 3431 (1997).
- [75] Duda A., Penczek S., Kowalski A., et al. *Macromol. Symp.*, 153, 41 (2000).
- [76] Kowalski A., Libiszowski J., Duda A., et al. *Macromolecules*, 33, 1964 (2000).
- [77] Kricheldorf H. R., Kreiser-Saunders I., Boettcher C. *Polymer*, 36, 1235 (1995).
- [78] Zhang X., MacDonald D. A., Goosen M. F. A., et al. *J. Polym. Sci., Part A: Polym. Chem.*, 32, 2965 (1994).
- [79] Kricheldorf H. R. *Macromol. Symp.*, 153, 55 (2000).
- [80] Majerska K., Duda A., Penczek S. *Macromol. Rapid Commun.*, 21, 1327 (2000).
- [81] Pack J. W., Kim S. H., Park S. Y., et al. *Macromolecules*, 36, 8923 (2003).
- [82] Ryner M., Stridsberg K., Albertsson A. C., et al. *Macromolecules*, 34, 3877 (2001).
- [83] Kricheldorf H. R., Kreiser-Saunders I., Damrau D. O. *Macromol. Symp.*, 159, 247 (2000).
- [84] Baran J., Duda A., Kowalski A., et al. *Macromol. Symp.*, 123, 93 (1997).
- [85] Penczek S., Duda A., Szymanski R. *Macromol. Symp.*, 132, 441 (1998).
- [86] Kowalski A., Duda A., Penczek S. *Macromolecules*, 31, 2114 (1998).
- [87] Chabot F., Vert M., Chapelle S., et al. *Polymer*, 24, 53 (1983).
- [88] Schwach G., Coudane J., Engel R., et al. *Polym. Int.*, 46, 177 (1998).
- [89] Kricheldorf H. R., Damrau D. O. *Macromol. Chem. Phys.*, 198, 1753 (1997).
- [90] Kreiser-Saunders I., Kricheldorf H. R. *Macromol. Chem. Phys.*, 199, 1081 (1998).
- [91] Vogl R.R., Matheson K., Matyjaszewski G. D. *Prog. Polym. Sci.*, 26, 1337 (2001).
- [92] Kobayashi S. *J. Polym. Sci., Part A: Polym. Chem.*, 37, 3041 (1999).
- [93] Albertsson A. C., Srivastava R. K. *Adv. Drug Deliver. Rev.*, 60, 1077 (2008).
- [94] Uyama H., Kobayashi S. *Chem. Lett.*, 1149 (1993).
- [95] Uyama H., Takeya K., Kobayashi S. *Proc. Jpn. Acad., Ser. B: Phys. Biol. Sci.*, 69, 203 (1993).
- [96] Knani D., Gutman A. L., Kohn D. H. *J. Polym. Sci., Part A: Polym. Chem.*, 31, 1221 (1993).
- [97] Matsumura S., Mabuchi K., Toshima K. *Macromol. Rapid Commun.*, 18, 477 (1997).
- [98] Matsumura S., Mabuchi K., Toshima K. *Macromol. Symp.*, 130, 285 (1998).
- [99] Matsumura S., Tsukada K., Toshima K. *Int. J. Biol. Macromol.*, 25, 161 (1999).
- [100] Fujioka M., Hosoda N., Nishiyama S., et al. *Sen-i. Gakkaishi.*, 62, 63 (2006).
- [101] Numata K., Srivastava R. K., Finne-Wistrand A., et al. *Biomacromolecules*, 8, 3115 (2007).

## 4 Modification of PLA

**Abstract** PLA widely used in many fields has gained enormous attention because of its biodegradable and biocompatible properties. However, unitary structure and poor properties of PLA such as the inherent brittleness, poor melt strength, low heat deflection temperature (HDT), narrow processing window and low thermal stability have posed considerable scientific challenges and limited their large-scale applications. This section of the book aims at highlighting recent developments in modification of PLA including copolymerization, blending, compounding and additives to improve relevant properties of PLA.

**Keywords** modification, copolymerization, stereocomplex, blending, composites, additives, modifiers, mechanical properties, crystallization

### 4.1 Copolymerization of PLA

PLA widely used in many fields have gained enormous attention because of its biodegradable and biocompatible properties. However, unitary structure and poor properties of PLA such as the inherent brittleness, poor melt strength, low heat deflection temperature (HDT), narrow processing window and low thermal stability pose considerable scientific challenges and limit their large-scale applications. There is a pressing need to enhance the versatility of PLA bioplastics, so that they can compete with conventional polymers. The most common strategy to overcome this limit is to prepare the copolymers. Copolymerization of lactic acid (or lactide) with hydroxyl acid, amino acid or polymers such as PEG, starch, etc., can markedly improve the strength, toughness, hydrophilic and controlled-degradable properties of PLA, and at the same time numerous new copolymers in different macromolecular architectures (linear, branch, star and dendron) can be obtained. These materials are attracting considerable interest in materials science research. In the past several decades, extensive work has been carried out to synthesize the desired PLA copolymers for drug delivery, hydrogels, nanoparticles, microparticles, implants, micelles, etc. PLA copolymers can be synthesized by several kinds of well-known polymerization techniques, including polycondensation, anionic, cationic, and coordination-insertion ring-opening polymerization. This section of the book aims at highlighting on recent developments in preparation of

the linear (random, alternating or block), graft or branch, star-shaped, and dendritic PLA copolymers and the catalysts (system) used in copolymerization.

#### 4.1.1 Random and alternating copolymers of PLA

Random polymers are the statistical arrangement of comonomer in their backbone. Numerous monomers have been used to copolymerize with LA, such as lactones, cyclic carbonates, hydroxyl acid, amino acid, and so on, to improve the flexibility, thermal stability, degradability, biocompatibility, hydrophilicity, functionality, etc. The most widely used technique to synthesize random copolymers of PLA is controlled/"living" ring-opening polymerization.

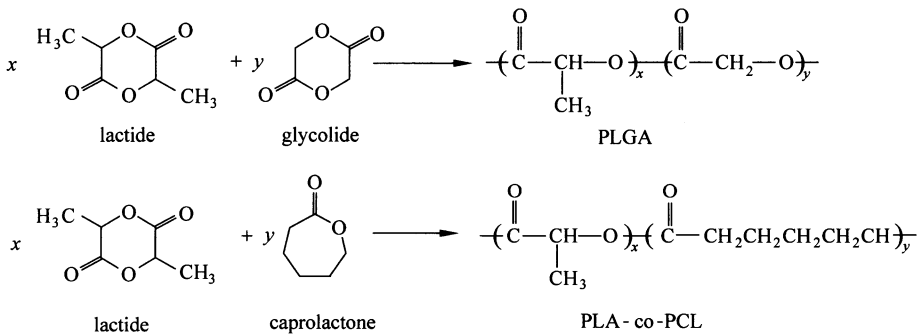
Aliphatic copolyesters derived from LA and glycolic acid (GA) belong to the renowned biodegradable materials widely used in medicine and pharmacy. They were synthesized early in the 1950's, when most of the commercial polymers were launched on the market. However, no attention was paid to these polyesters because of their poor hydrolytic and thermal stabilities. But, their hydrolytic instability recently has turned into an exciting advantage and made these materials suitable for a wide variety of surgical and pharmaceutical applications [1]. Since 1970, poly(glycolic acid) has been commercially available as the surgical suture, Dexon, and the copolymer made of 92 mol% GA and 8 mol% LA has had a limited application as the competitive suture, Vicryl, since 1975 [1, 2]. Poly(glycolic acid-co-lactic acid) (PLGA) can be prepared by simple polycondensation reaction of glycolic acid and LA [3]. However, because of thermal instability of the polymers formed and the equilibrium nature of the reaction as well as difficulties associated in removing water from the viscous polymer mass, only low molecular weight copolymers are obtainable which lack the optimum properties for most applications. The preferred method for producing high-molecular-weight copolymers is the ring-opening polymerization of the cyclic dilactons, lactide and glycolide [1, 4, 5]. Their synthesis is carried out generally with the use of tin compounds as initiators [6]. However, complete elimination of highly toxic tin compounds from the polymer is practically impossible. As a result, tin compounds are slowly penetrating into the patient's blood circulation. It is known that these compounds even in trace amounts are especially dangerous for small children and endanger proper functioning of tissues sensitive to toxication (e.g., brain tissue, nerve tissue). To avoid the side effects several attempts have been undertaken with the use of less toxic initiators, mainly zinc, calcium, zirconium, etc. [7]. For instance, Bero and colleagues describes the copolymerization of glycolide with L-lactide with the use of low toxic compounds, such as  $Zr(acac)_4$ ,  $Fe(acac)_3$  and  $Fe(OEt)_3$ , as initiators, which enable one to obtain copolymers with yields up to 100% and possessing good mechanical

properties [6, 7]. In addition, Rebert's group [8] has successfully synthesized an alternating version of poly(lactic acid-co-glycolic acid) (50:50) by the condensation polymerization of *O*-(2'-bromopropionyl)glycolic acid, in order to overcome the variable properties of PLGA attributed the variability to the random nature of the polymer.

Poly(*D,L*-lactic acid) (PDLA) is an amorphous material with half-life of a few weeks *in vivo* and hardly permeable to most drugs. In contrast, poly( $\epsilon$ -caprolactone) (PCL) is a semicrystalline polymer with a half-life of about one year *in vivo* and can be permeable to many kinds of drugs. It has been demonstrated that the degradation rate and drug permeability of copolymers of  $\epsilon$ -caprolactone and *D,L*-lactic acid can be adjusted by their compositions [9 – 11]. However, ring-opening copolymerization of CL and LA is usually carried out using stannous octoate as catalysts. To void the highly toxic tin compounds for biomedical applications, some low toxic compounds, such as aluminum isopropoxide, zinc alkoxide, rare earth chloride-propylene oxide (PO) system [9], and zirconium (IV) acetylacetonate [Zr(acac)<sub>4</sub>] [12], etc. have been adopted as the initiators. Furthermore, CL and LA appear to be suitable comonomers for the preparation of copolymers with mechanical properties ranging from elastomeric to rigid. Their elasticity and hydrolyzability combine to make these copolymers suitable for biomedical applications where flexibility and biodegradability are required in the same product. However, the distribution of the CL and LA units along the copolymer chain has a profound influence on the properties of these copolymers [13]. Hiljanen-Vainio et al. [14] reported the synthesis of LA/CL copolymers with different compositions using Sn(Oct)<sub>2</sub> as initiator. Their mechanical and thermal properties varied considerably with the varying sequence lengths of the caproyl (Cap) and lactidyl (LL) units in the copolymer chain. Bero et al. [15] found that longer average sequence lengths of both units could be obtained when Sn(Oct)<sub>2</sub> was employed at only moderate temperatures of around 70°C. Despite many studies have focused on how the polymerization parameters and initiating system affect the bulk properties of block and random LA/CL copolymers, it is still unclear how the monomer sequence distribution could be related to the observed thermal properties. Meanwhile, some attention has been paid to how the synthesis conditions influence the chain microstructure, especially the sequence distribution of Cap and LL units along the copolymer chain [15 – 18]. Nalampang and colleagues [13] reported that thermal properties including stability depended on both composition and chain microstructure which could be controlled by the method of synthesis. Clearly, transesterification processes are extremely important in LA/CL copolymerization and have to be taken into account since they randomize the monomer sequencing, thus change the copolymer microstructure [15, 19]. Brostrom and coworkers [20] reported on the modulation of phase morphology, plasticization properties, and thermal stability of films of partly

branched PLLA-co-PCL copolymer with additions of low molecular weight compounds, namely, triethyl citrate ester, diethyl phthalate, diepoxy polyether (poly-(propylene glycol) diglycidyl ether), and with epoxidized soybean oil (ESO). The PLLA-co-PCL/polyether films show significant stability against thermal depolymerization, high film flexibility, and good plasticizing properties, probably due to cross-linking and chain branching formation between diepoxy groups with both the end carboxyl and hydroxyl groups of the PLLA copolymer (initially present or generated during the degradation process) to produce primary ester and ether bonds, respectively.

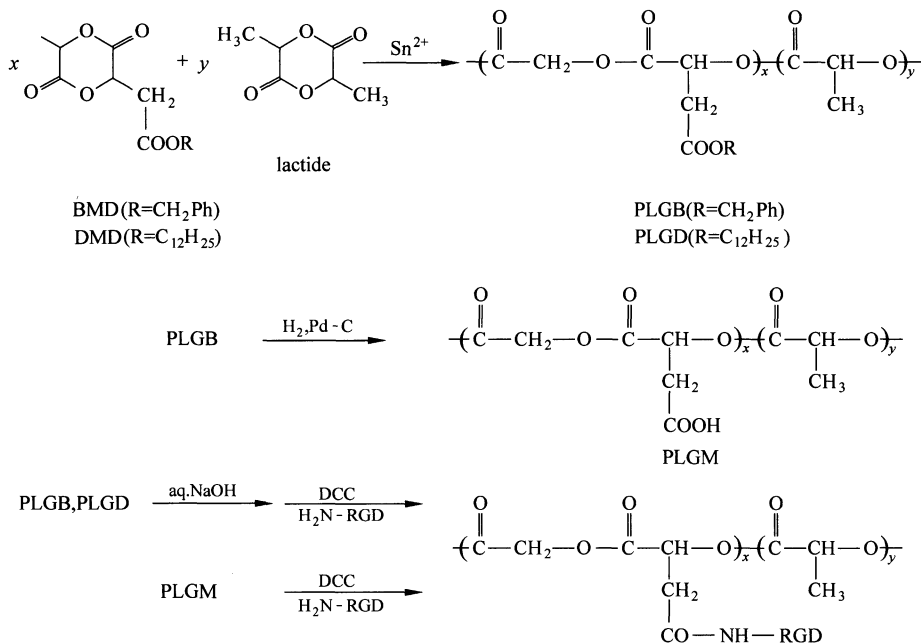
The highly crystalline and hydrophobic nature of PLLA has interfered with modulation of their degradation rate and mechanical properties. It has also been difficult to impart functionality to these polymers by application of the ordinary chemical modification methods. Kimura and coworkers have developed a cyclic diester monomer, 3-(*s*-[(benzyloxycarbonyl)methyl]-1,4-dioxane-2,5-dione (BMD) and 3-(*s*-[(dodecyloxycarbonyl)methyl]-1,4-dioxane-2,5-dione (DMD) which consist of both glycolate and  $\alpha$ -malate components. The aliphatic polyesters synthesized by their polymerization and copolymerization are functionalized with pendant ester groups that are derived from the  $\alpha$ -malate units [21].



**Figure 4.1** Synthesis of PLGA and PLA-co-PCL copolymers

The copolymerization of BMD and *L*-lactic acid could be carried out in bulk with stannous 2-ethylhexanoate as the catalyst. The resulting copolymers are subjected to hydrogenolysis at atmospheric pressure in the presence of a palladium on charcoal catalyst to remove the pendant benzyl groups quantitatively. The deprotected copolymers consists of *L*-lactic (L), glycolic (G) and  $\alpha$ -malic acid (M) repeating units [22, 23], then the RGD oligopeptides can be immobilized onto the PLGM copolymers through the action of deprotected  $\beta$ -carboxyl groups of the  $\alpha$ -malate units for the purpose of developing a novel biodegradable polymer scaffold which can be utilized for cell and tissue engineering (Fig. 4.2 ) [21].

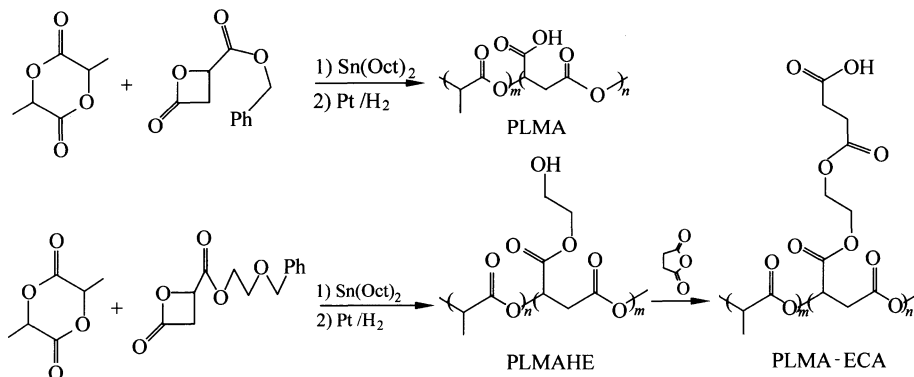
## Biodegradable Poly(Lactic Acid): Synthesis, Modification, Processing and Applications



**Figure 4.2** Synthesis of the copolymers of *L*-lactic acid and BMD and DMD functionalized with pendant ester group and immobilized with cell-binding arg-gly-asp tripeptide (RGD) [21]

To improve cell affinity and hemocompatibility of PLA, some researchers have copolymerized  $\beta$ -maleic acid with lactide to improve the hydrophilicity of PLA and to introduce bioactive functional groups at its carboxyl side [25, 26]. Wang et al. [25] have synthesized the functional PLA with hydroxyl side groups and poly (lactic acid-co- $\beta$ -maleic acid) pendant hydroxyl arms (PLMAHE), and reported that the pendant hydroxyl arms could improve the affinity of the polymer to cells (EVC-304) and that cells grown on the polymer with 10% functional monomer displayed the best morphology. Furthermore, they derived this PLMAHE to a new PLMA-based copolymer with extended carboxyl arms (PLMA-ECA) (Fig. 4.3), which have an interval arm between the carboxyl group and the PLMA main chain. They investigated its structure, composition, as well as hydrophobic / hydrophilic, degradable, and thermal properties, and showed its great improvement in both blood compatibility and cell affinity compared with the PLA and PLMAHE. Their results demonstrated the best reduction in the platelet adhesion and activation, and the great compatibility with human ECs for PLMA-ECA [24].

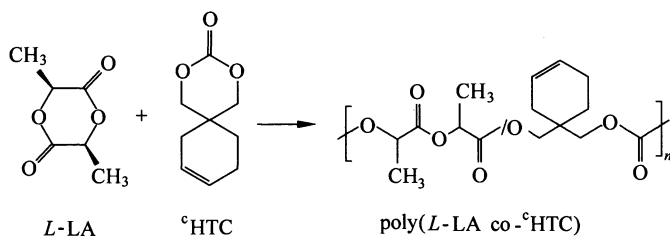
Copolymers containing carbonate units are very interesting for many biomedical applications because of their increased flexibility, the reduced acidity of the degradation products, and the distinctive profile of hydrolytic degradation [28]. These materials can be obtained through polycondensation [29, 30],



**Figure 4.3** The synthesis route of functional copolymers PLMA-ECA [24]

terpolymerization reactions of carbon dioxide with epoxides and cyclic lactones [31], and enzymatically initiated reactions [32]. In some cases, however, the applied materials have to possess a high purity and high molecular weight to provide the appropriate mechanical features required for example in biomedical applications (cell and tissue carriers in tissue engineering techniques, degradable implants, fibers and threads, and drug carriers). For these reasons, the ring-opening polymerization of cyclic monomers, such as lactides and cyclic carbonates, seems to be a general method for the synthesis of materials intended for these applications [33, 34]. Trimethylene carbonate (TMC) is one of the interesting comonomers for copolymerisation with lactides. Poly(trimethylene carbonate) (PTMC) is a rubber, can be hydrolysed both *in vivo* and *in vitro*, and has longer shelf life than PLA [35]. Because of the useful properties of TMC, many attentions have been pay to the copolymerization of TMC and lactide in order to control the copolymer properties, such as melting and glass transition temperatures, biodegradability and toughness. The methods used to obtain copolymers of TMC and lactide have been presented in many patents [36, 37] and publications [33]. Lactide/TMC copolymers as well as products made of these materials are commercially available under the trademarks Resomer LT, Inion Optima, and others. Similarly, the most often used catalysts or initiators in the production process of these copolymers are tin and aluminum compounds. For instance, Chen et al. [27] prepared the six-membered cyclic carbonate monomer 2,2-[2-pentene-1,5-diyl]trimethylene carbonate (<sup>c</sup>HTC) which bears cyclohexene side groups. They have conducted the ring-opening bulk copolymerizations of *L*-lactide with <sup>c</sup>HTC by using AlR<sub>3</sub>-H<sub>2</sub>O (R = ethyl, isobutyl), Al(O<sup>i</sup>Pr)<sub>3</sub>, ZnEt<sub>2</sub>-H<sub>2</sub>O and Sn(Oct)<sub>2</sub> as catalysts. Different organometallic catalysts were evaluated for the copolymerization of *L*-LA and <sup>c</sup>HTC. High molecular weight poly(*L*-LA-co-<sup>c</sup>HTC) copolymers were prepared having controlled <sup>c</sup>HTC contents (Fig. 4.4). Furthermore, copolymerizations of lactides and trimethylene carbonates were also conducted using some low-toxicity

catalysts including diethyl zinc [27, 38, 39], zirconium(IV) acetylacetonate [28], and so on. In addition, water-soluble polyphosphate was also introduced into the PLA chains by ring-opening copolymerization of *D,L*-lactic acid and 2-hydroxy-2-oxo-1,3,2-dioxaphosphorinane to prepare hydrophilic copolymer using the similar method [40].



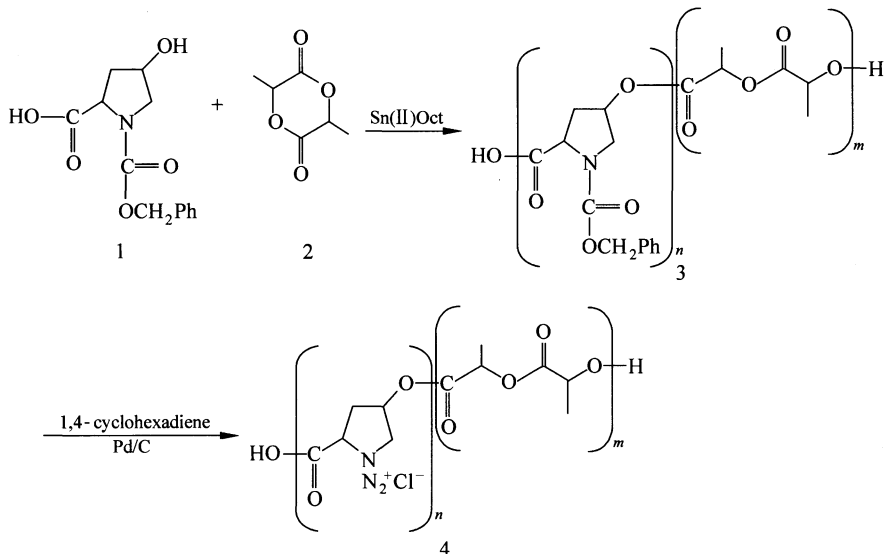
**Figure 4.4** Scheme of ring-opening copolymerization of *L*-lactic acid and cyclic carbonate monomer °HTC [27]

Polydepsipeptides, copolymers of  $\alpha$ -amino acids and  $\alpha$ -hydroxy acids, are one of the newest classes of biodegradable polymers, having the advantages of being nontoxic, biodegradable, biocompatible, and having pendant functional groups on their backbones [42]. The main potential medical applications for synthetic  $\alpha$ -amino acid-based polymers are bioresorbable sutures, screws or plates, and drug delivery systems (controlled release and targeting) [43]. Polydepsipeptides are generally synthesized by means of ring-opening polymerization of  $\alpha$ -amino acid *N*-carboxyanhydrides (NCA) initiated by primary amine. To produce a polydepsipeptide, it was first necessary to synthesize a monomer that could polymerize by the same mechanism as the monomer used for PLA synthesis (Fig. 4.5) [41].

Polydepsipeptides synthesized by the NCA method generally form strong intrachain or interchain hydrogen bonds so that they are insoluble in many organic or inorganic solvents. Actually, they have not been utilized so much for practical applications due to difficulty in handling them, although they possess a structure related to those of proteins [43]. Thus, to overcome their shortcomings and enhance the ability of PLA materials to interact biospecifically with cells, over the last decade, many studies have been devoted to synthesize copolymers of PLA containing polydepsipeptides in order to combine their advantages and introduce the functional groups in PLA. For instance, poly(lactic-co-glycolic acid-co-lysine) (PLGAL) by ring-opening polymerization have been synthesized [44]. And the arginine-glycine-aspartic acid (RGD) peptides were covalently attached to the polymer chains. Liu and coworkers [45] report the synthesis of poly(*D,L*-lactic acid-co-*L*-lysine) (PLAL) random copolymer by copolymerization of amino acid-*N*-carboxyl anhydride (NCA) with LA anhydrosulphite (LAAS) in







**Figure 4.6** Condensation copolymerization of trans-4-hydroxy-*N*-CBz-*L*-proline and *L*-lactide [42]

of the chemical properties of the main components, and the physical properties of the resulted copolymers can be tailored by adjusting the molecular weights and the composition of the constituting blocks. Therefore, many studies have been carried out in an attempt to manipulate their amphiphilic behavior, mechanical and physical properties by adjusting the ratio of the constituting block or adding new blocks of desired properties. A large number of monomers have been used to conduct the copolymerization with lactides or lactic acids by some well-known polymerization techniques, including polycondensation, ring-opening polymerization, ionic polymerization, living radical polymerization, and macromolecular coupling reactions. In addition, a very interesting example presented by Hwang et al. [52] is that PLLA and its block copolymers were synthesized by a ring-opening polymerization of *L*-lactide in supercritical  $\text{CO}_2$  by using 1-dodecanol,  $^1\text{H}$ ,  $^1\text{H}$ -perfluoro-1-decanol, monomethoxy polyethyleneglycol (mPEG-OH), poly(dimethylsiloxane) mono hydroxy terminated (PDMS-OH), and polypropyleneglycol monobutylether (buPPG-OH) as initiators. The homopolymer and diblock copolymers could be prepared with fairly low molecular weight distribution (1.11 – 1.18) as analyzed by GPC.

To modify the hydrophilic properties of PLA, PEG, also known as PEO with high molecular weights, is the most commonly used polymer. PEG is an uncharged, hydrophilic, non-toxic, and nonimmunogenic polymer and has long been considered an attractive biomaterial because of its ability to resist protein adsorption and as a spacer facilitating the formation of a receptor-ligand complex [53]. Typically, PEG with molecular weights of 4000 amu is 98% excreted in humans [54]. Thus, many efforts have been made to form a new family of block

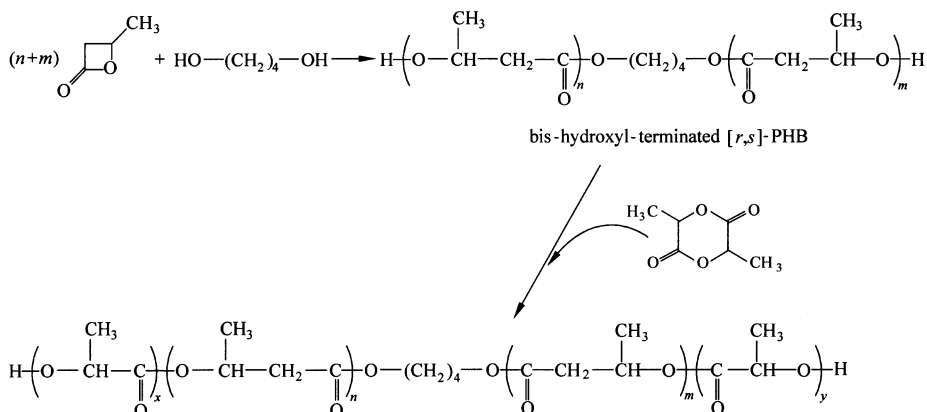
copolymers comprising PEG and PLA. The bright part of this family is that one can modulate the biodegradation rate and hydrophilicity of polymer by adjusting the ratio of its hydrophilic and hydrophobic constituents. Ferruti et al. [55] reported the synthesis of high molecular weight block copolymers containing PLGA and PEG segments by polycondensation. This process involves the reaction of PEG with phosgene followed by polycondensation of the resulting  $\alpha,\omega$ -bis(chloroformates) with PLGA oligomers. The intrinsic viscosity of PLGA-*b*-PEG block copolymers was in the range of 1.74–2.16 dL/g. Lee and coworkers [56] synthesized PEO-*b*-PLA-*b*-PEO triblock copolymers, in which each block was connected by an ester bond, by a coupling reaction between PLA and PEO. However, the most widely used technique to synthesize block copolymers of PLA-PEG is controlled/“living” ring-opening polymerization. For example, Jedlinski et al. [57] conducted the anionic polymerization of *L*-lactide in the presence of sodium poly(ethylene glycol)ate in tetrahydrofuran at 25°C and yielded “tailored” ABA triblock copolymers having the expected compositions and molecular weights. During the polymerization, a slight racemization of *L*-lactide was observed. Xiong and colleagues [58] succeeded in the synthesis of block copolymer from *D,L*-lactide and poly(tetramethylene ether glycol) (PTMG) in bulk with an isotributyl aluminum-water-phosphoric acid complex catalyst as the initiator. Lemmouchi et al. [59] reported the synthesis of PLA-*b*-PEG and PLA-*b*-PEG-*b*-PLA block copolymers by the anionic ring-opening polymerization of lactides in the presence of PEG methyl ether or PEG and potassium hexamethyldisilazide as a catalyst. The polymerization in toluene at room temperature was very fast, yielding copolymers of controlled molecular weights and tailored molecular architectures. Furthermore, some researchers have attempted to introduce bioactive molecular or functional group into the PLA-PEG block copolymers to create new polymer materials and promote cell attachment and function. For instance, Yasugi et al. [60] synthesized a PEG-PLA block copolymer having a site specifically protected-sugar group at the PEG chain end through a successive ROP of ethylene oxide and *D,L*-lactide using a metalated protected sugar as an initiator. After removal of protective groups, block copolymers having a glucose or galactose residue at the chain end in a regioselective manner were obtained. Also, PLA-*b*-PEG copolymers terminated with biotin [61], cholesterol [53], vinyl sulfone [62], sulfamethazine oligomer [63], etc. have been synthesized successfully. At the same time, continuous efforts have been devoted to the development of new catalysts and initiators for attaching PLA blocks to hydroxyl-terminated PEG, e.g. stannous octoate, SnO, SnO<sub>2</sub>, SnCl<sub>2</sub>, ZnEt<sub>2</sub>, Zn, Sb<sub>2</sub>O<sub>3</sub>, PbO, GeO<sub>2</sub>, La(Ac)<sub>3</sub>, CaH<sub>2</sub>, NaH, and so on [64–70].

As widely usable biodegradable materials, PLA is found to exhibit too hard and too brittle characters. The weakness might be improved when a polymer with lower glass transition temperature is used together [18]. Poly( $\epsilon$ -caprolactone) (PCL) and poly(glycolic acid) (PGA), also known as polyglycolide, are two other

biodegradable and biocompatible aliphatic polyesters which are widely used in the copolymerization modification of PLA. Synthetic aliphatic polyesters derived from LA enantiomers, glycolide (GA), and  $\epsilon$ -caprolactone (CL) are regarded as profitable in the field of temporary therapeutic applications in surgery, sustained drug delivery and tissue engineering. Copolymerization provides worthwhile means to adjust the degradation rate, as well as physical and mechanical properties. PCL is a biocompatible and biodegradable polymer with high permeability to drugs. Its low melting temperature ( $T_m \approx 60^\circ\text{C}$ ) and high decomposition temperature ( $T_d \approx 350^\circ\text{C}$ ) provide a wide processing range. Due to the lower glass transition temperature of PCL, the elongation at the break is very large ( $\geq 600\%$ ). However, this polymer degrades very slowly due to its high hydrophobicity and crystallinity [71]. Therefore many studies have been carried out on the copolymerization of CL and/or GA with LA to combine the chemical properties of the main components and tailor the degradable, physical and mechanical properties of the resulted copolymers. Numerous block copolymers, for example, AB, ABA, ABC and ABCBA types have been synthesized by several polymerization techniques, mainly sequential ring-opening polymerization [18, 72 – 77].

Copolymerization of PLA with an elastomer may lead to a large variety of materials ranging from reinforced thermoplastics to thermoplastic elastomers. For example, rubbery materials may be useful for the design of soft implants and microcapsules used in oral drug delivery. Bacterially produced poly(3-hydroxyalkanoates) (PHA) have been convinced to be the promising biodegradable polymers that can be utilized as bioplastics. Meanwhile, chemical synthesis of PHA and their derivatives has also been an important subject of polymer science. Hori and coworkers [78, 79] have succeeded in preparing a high polymer of poly(3-*r*-hydroxybutyrate) (*r*-PHB) by ring-opening polymerization of four-membered *r*- $\beta$ -butyrolactone (*r*- $\beta$ BL) with distannoxanes as the initiators where the ring-opening of *r*- $\beta$ BL proceeds with retention of the configuration or with little or no racemization. Polymerization of racemic monomer *r,s*- $\beta$ BL with the same catalysts has given an atactic- or syndiotactic- rich poly(3-*r,s*-hydroxybutyrate) (*r,s*-PHB) [8]. Unlike the optically active *r*-PHB, *r,s*-PHB is elastomeric. Even the syndiotactic-rich [*r,s*]-PHB (ordinarily 70% syndiotactic diads) shows elastomeric properties because of its low crystallinity. Therefore, the block copolymers consisting of *r,s*-PHB as the soft segment and PLLA as the hard segment can represent the elastomeric biodegradable polymers. For example Hiki et al. [80] have synthesized an ABA type triblock copolyester *r,s*-PHB-*b*-PLLA by the sequential ring-opening polymerization (Fig. 4.7).

Poly(*p*-dioxanone) (PPDO), one of the biodegradable and biocompatible aliphatic polyesters, has high flexibility, good tensile strength and mechanical properties. Due to its good biocompatibility and physical properties, PPDO has been considered as a candidate not only for medical uses but also for universal uses such as films, molded products, laminates, foams, non-woven materials,



**Figure 4.7** Ring-opening polymerization of  $r,s$ -BBL in the presence of 1,4-butanediol and copolymerization with  $L$ -lactide

adhesives and coatings [81, 82]. Although high cost and rigorous synthetic condition of PPDO are the main barriers for the application of PPDO now, it cannot obstruct the development of PPDO as a promising biodegradable material in the future. Copolymerizing PPDO with PLA has been found as a conceivable way to combine the merits of these two polymers. For instance, Stridsberg and Albertsson [83, 84] successfully synthesized a series of novel elastomeric ABA triblock copolymers, poly( $L$ -lactide- $b$ -DXO- $b$ - $L$ -lactide), in a new two-step process. Bhattarai et al. [85 – 88] developed a series of biodegradable copolymer derived from  $p$ -dioxanone (PDO),  $L$ -lactide (LLA), and PEG. In addition, cyclic carbonates such as trimethylene carbonate (TMC) and 2,2-dimethyltrimethylene carbonate (DTC) have also been used to copolymerize with lactides in order to improve the toughness of PLA [89 – 92]. Furthermore, Wang et al. [93] synthesized a polyethylene-poly( $L$ -lactide) diblock copolymer (PE- $b$ -PLLA) containing two semicrystalline blocks by a combination of anionic polymerization, hydrogenation, and coordination-insertion polymerization. The effect of this copolymerization on the morphology and mechanical properties of PLLA/LDPE blends was examined. The tensile and izod impact testing results on the ternary blends showed significantly improved toughness as compared to the PLLA homopolymer or the corresponding PLLA/LDPE binary blends. Polydimethylsiloxane (PDMS) has the lowest  $T_g$  and the highest permeability for oxygen and water among the polymeric materials, and it is biocompatible. It has thus also been chosen as the rubber phase to modify PLLA in some studies [94, 95]. Fluorinated polymeric materials present several unusual properties such as chemical inertia, solvent and high-temperature resistance, barrier properties, low friction coefficient, and low surface tension. Bongiovanni et al. [96] prepared poly[(caprolactone-co-lactide)- $b$ -perfluoropolyether- $b$ -(caprolactone-co-lactide)] copolymers (TXCLLA) by ring-opening polymerization of  $D,L$ -lactide (LA2) and caprolactone (CL) in the presence of  $\alpha,\omega$ -hydroxy terminated perfluoropolyether

(Fomblin Z-DOL TX) as macroinitiator and tin(II) 2-ethylexanoate as catalyst. Then, the effect of the new structures on the crystallization of terpolymers was investigated changing the LA2/CL ratio. The thermal and surface properties are reported and discussed. Boudouris et al. [97] reported the synthesis of a new series of rod-coil block copolymers, regioregular poly(3-alkylthiophene)-*b*-poly(lactic acid) (P3AT-*b*-PLA), where the alkyl chain in the polythiophene moiety is either 6 or 12 carbons in length. In thin films of these materials (ca. 35 nm thickness), microphase separated domains are formed while the crystallinity of the P3AT majority phase is maintained. Upon chemical etching of the PLA block, a nanopitted film where the crystallinity of the P3AT phase remained were observed. The increase in the exposed surface area of the semiconducting polymer (~150% that of the planar film) could be useful in a variety of organic electronic applications.

The self-assembly of block copolymers has been extensively studied due to their abilities to self-assemble into one-, two-, or three-dimensional periodic nanostructures in the bulk with different compositions (i.e., volume fraction). Defined structures can be easily tailored by molecular engineering of synthetic block copolymers, which is very appealing for the applications of nanotechnologies [98]. Wei et al. [99] studied self-assembly morphology effects on the crystalline behavior of asymmetric semicrystalline poly(styrene)-*b*-poly(*L*-lactide) (PS-*b*-PLLA) block copolymer thin film. Fu et al. [100] studied the effects of crystallization of PLLA blocks on the surface orientation and film decomposition upon annealing at the early stage of the film evolution in symmetric polystyrene-block poly(*L*-lactic acid) (PS-*b*-PLLA) semicrystalline block copolymer. Loose semicrystalline rodlike aggregates of PLLA were found to initiate hole nucleation and growth before and after surface orientation of copolymers. Ho et al. [98, 101] examined the chirality effect on self-assembling structures by using a diblock copolymer system constituting both achiral and chiral blocks, poly(styrene)-*b*-poly(*L*-lactide) (PS-*b*-PLLA). Well organized, hexagonally packed PLLA nanohelices with a left-handed helical sense were formed from the self-assembly of PS-*b*-PLLA in the bulk.

Polymeric micelles have recently attracted much attention because of their specific properties for drug delivery systems. In selective solutions, amphiphilic copolymers can self-assemble into a variety of micellar structures at mesoscopic level. The resulting micelles in aqueous medium can significantly enhance the water-solubility of hydrophobic drugs thus improve their bio-availability [102]. Poly(*N*-vinyl-2-pyrrolidone) (PVP) is a well-known water-soluble, biocompatible and relatively amphiphilic polymer. It has been shown that interactions between PVP and DNA protect DNA from degradation by extracellular nucleases and that PVP can serve to stabilize proteins. Like PEG, PVP can increase the circulation time of peptides/proteins and colloids in vivo. Luo et al. [103] reported synthesis of low molecular weight PVP with a hydroxyl group at one end by free radical polymerization of *N*-vinyl-2-pyrrolidone (NVP). Xiong et al. [104] synthesized

ABA triblock copolymers with good biocompatibility and adjustable degradability by ring-opening polymerization, in which *D,L*-lactide polymerized and grew from the two ends of PVP. Benahmed et al. [105] synthesized an amphiphilic diblock copolymer of PVP-*b*-PDLLA capable of self-assembling into polymeric micelles with multiple binding sites and high entrapment efficiency. Polyphosphoester (PPE) is another class of biodegradable polymers with repeated phosphoester linkage in the backbone, where phosphorus is pentavalent and thereby allows introduction of bioactive molecules and extensive modification of the physical and chemical properties of the polymers. It has showed favorable biocompatibility, biodegradability, and relatively controllable hydrophilicity through pendent modification, and attracted increased interest in biomedical applications particularly in drug, gene delivery, and tissue engineering. Yang et al. [106] synthesized amphiphilic triblock copolymers of PPE and PLLA with various compositions and prepared core-shell micelles composed of hydrophobic PLLA core and hydrophilic PPE shell in aqueous solution. Furthermore, block copolymers of PLLA-*b*-PEEP were also synthesized and used to modify the PLLA surface via a spin-coating process, to understand whether surface modification with polyphosphoester-based polymer will be osteoinductive for potential bone tissue engineering applications [107].

Physical responsive behavior is rather typical for biomacromolecules and has been mimicked in fields ranging from advanced artificial devices, smart surfaces and sensors to medicine and biomineralization. Therein, an interesting class of stimuli-responsive materials is thermoresponsive synthetic polymers. They start to collapse at the temperature close to their lower critical solution temperatures (LCST) due to dehydration of the chains, and subsequently form aggregates. The most often investigated thermoresponsive polymers contain poly(*N*-isopropylacrylamide) (PNIPAAm) units, which is a well-known water-soluble polymer showing reversible hydration–dehydration changes in response to small solution temperature changes. Numerous thermally sensitive block copolymer of PIPAAm and PLA have been synthesized by ring-opening polymerization of *D,L*-lactide initiated from hydroxy-terminated PIPAAm [108, 109]. Some hydrophilic comonomers, for example, *N,N*-Dimethylacrylamide (DMAAm) have been used to adjust the LCST values of the amphiphilic PNIPAAm-based copolymers [110]. In addition, block copolymers of PNIPAAm-PLA also can be synthesized by the reversible addition-fragmentation chain transfer (RAFT) polymerization [111]. Thermally sensitive micelles self-assembled from PNIPAAm-PLA block copolymers have been proved to be effective carrier for the controlled delivery of hydrophobic drugs. Poly(*N,N*-dimethylamino-2-ethyl methacrylate) (PDMAEMA) is another stimuli-responsive polymer which has been widely used in drug delivery systems and modification of biomedical polymer surfaces due to its biocompatibility, pH/temperature double responsiveness. Spasova et al. [112] has synthesized well-defined amphiphilic PDLA-*b*-PDMAEMA and PLLA-*b*-PDMAEMA

copolymers by combination of controlled ring-opening polymerization (ROP) and atom transfer radical polymerization (ATRP).

The polypeptide, being a natural material, is a good choice for the design of novel biomaterials. Compared to natural proteins, synthetic polypeptides offer more advantages in stability and processability. Its combination with PLA blocks can enhance the hydrophilicity of PLA and modify the degradation pattern of the polymers because peptidase is required to hydrolyze the peptide bonds [113]. For example, Lavik et al. [114] demonstrated the formation of a block copolymer of poly(lactic-co-glycolic acid) and polylysine via a simple coupling technique using dicyclohexyl carbodiimide (DCC). Deng et al. [115] synthesized biodegradable triblock copolymer, poly(ethylene glycol)-*b*-poly(*L*-lactide)-*b*-poly(*L*-lysine) (PEG-PLA-PLL) by acidolysis of poly(ethylene glycol)-*b*-poly(*L*-lactide)-*b*-poly( $\epsilon$ -benzyloxycarbonyl-*L*-lysine) (PEG-PLA-PZLL) obtained by the ring-opening polymerization (ROP) of  $\epsilon$ -benzyloxycarbonyl-*L*-lysine *N*-carboxyanhydride (ZLys NCA) with amino-terminated PEG-ePLA-NH<sub>2</sub> as a macroinitiator. The pendant amino groups of the lysine residues were modified with a peptide known to modulate cellular functions, Gly-Arg-Gly-Asp-Ser-Tyr (GRGDSY, abbreviated as RGD) in the presence of 1,1'-carbonyldiimidazole (CDI). Yu et al. [116] reported the synthesis of block copolymer of poly(lactic acid-co-lysine)(PLA-*b*-PLL) by a modified method and novel Arg-Gly-Asp (RGD) peptides were chemical conjugated to the primary  $\epsilon$ -amine groups of lysine components.

### 4.1.3 Multi-Block Copolymers of PLA

The syntheses of PLA copolymers have been widely studied, but most efforts have been focused on random, diblock, and triblock copolymers by the ring-open polymerization of lactide that not only affects the properties of copolymers by phase separation but also causes a rather higher cost of production for the lactide as a monomer. However, growing interests have been recently given to a new class of PLA copolymers: multi-block copolymers. Compared to the diblock or triblock copolymers, multiblock copolymer has more and shorter blocks and PLA segments, which alternate in the polymer chain. Consequently, it is possible to get some special properties such as better miscibility between the two components and lower crystallinity. Thus the degradability of the copolymer is expected to be enhanced. Multi-block copolymers can be synthesized by direct polycondensation, coupling reaction or chain-extension reaction of prepolymers.

To improve the properties of PLA copolymers with high-molecular-weights and reduce the cost of production, direct polycondensation of prepolymers has been developed to synthesize multiblock copolymers. For example, Luo et al. [117] synthesized PLLA-PEG multiblock copolymers with predetermined block lengths by polycondensation of PLA diols and PEG diacids. Chen et al. [118]



synthesized copolyester, poly(hexylene terephthalate-co-lactide) (PHTL), via direct polycondensation from terephthaloyl dichloride, 1,6-hexanediol and oligo(lactic acid).

After the synthesis of oligomeric PLA by the condensation reaction of lactic acid, multi-block copolymers can be prepared by coupling reaction between end-groups of oligomeric PLA and other prepolymers. For instance, Chen et al. [119] synthesized multiblock copolymers of PLLA-PEG with high molecular weight by coupling PLLA-PEG-PLLA triblock copolymers with succinic anhydride in the presence of (*N,N*-dimethylamino) pyridine(DMAP) and dicyclohexylcarbodiimide (DCC). Jeon et al. [17] prepared PLLA-PCL multiblock copolymers by using the coupling reaction between the bischloroformates of carboxylated PLLA with PCL-diol in the presence of pyridine. Teng et al. [120] reported the multiblock copolymers derived from PLLA and PCL with the coupling reaction between PLLA and PCL oligomers with —NCO terminals. Huang et al. [121] designed and synthesized multiblock polylactide and aniline pentamer copolymer PLAAP with the condensation polymerization of hydroxyl-capped PLA and carboxyl-capped AP. This biodegradable and electroactive PLA-AP copolymer thus possesses the properties in favor of the long-time application in vivo as nerve repair scaffold materials in tissue engineering.

Chain length of oligomers or prepolymers can be efficiently extended to obtain the corresponding multiblock copolymers in the presence of chain extenders, such as dichloride, aliphatic or aromatic diisocyanate, dianhydride, etc. Nagata et al. [122] synthesized photocurable biodegradable multiblock copolymers from PCL diol and PLLA diol with 4,4'-(adipoyldioxy)-dicinnamic acid (CAC) dichloride derived from adipoyl chloride and 4-hydroxycinnamic acid as a chain extender. Wang et al. [123] synthesized a series of PLA polyurethanes (PLAUs) from PLLA diols, hexamethylene diisocyanate (HDI), and 1,4-butanediol (BDO). By changing the  $M_n$  of the PLA diol and the ratio of the hard-to-soft-segment, their  $T_g$ s and shape-recovery temperatures can be adjusted to the neighborhood of the body temperature. Therefore, these PLAUs are expected to find practical medical applications. Ojha et al. [124] prepared PLLA-polyisobutylene (PIB) multiblock copolymers by chain extension of PLIA-*b*-PIB-*b*-PLLA triblock copolymers. The asynthesized compression molded multiblock copolymers exhibited tensile strengths in the range of 8 – 24 MPa with elongations at break in the range of 2.5% – 400%. Moreover, PLA-PCD multi-block copolymers have been successfully developed using a two-step process with polycondensation and chain extension reactions [125]. The PLA-PCD copolymers exhibit superior mechanical properties with elongation at break above 230%, which is much higher than that of PLA chain-extended products. The products have a good potential for packaging applications.

In addition, Kricheldorf et al. [126] demonstrated the synthesis of *L*-lactide-PEG multiblock copolymers by means of spirocyclic Ge-PEG initiators. Spirocyclic initiators were prepared by condensation of Ge(OEt)<sub>4</sub> and tetra(ethylene glycol),

TEG, or PEG-2000. These spirocycles were used as initiators for the ring-expansion polymerization of *L*-lactide in chlorobenzene at 120°C. The resulting cyclic block co-polymers were reacted in situ with aliphatic dicarboxylic acid dichlorides (ADADs) or with hexamethylene diisocyanate (HMDI) to achieve chain extension.

### 4.1.4 Graft or Branched Copolymers of PLA

The application of renewable resources to synthesize biodegradable polymers with desired physico-chemical and biological properties has recently received increasing interests. Cellulose is the most abundant renewable biomass in the world. But cellulose has poor properties of biodegradability and bioabsorbability. Chen et al. [127] reported the grafting copolymerization of PLA-HEC or PLA-HPC from ring-opening copolymerization of *L*-lactide. Copolymers obtained from lactide and cellulose will combine the advantages of both, and may be used as tissue engineering materials. Yan et al. [128] presented the homogeneous synthesis of thermoplastic cellulose-graft-PLA copolymers by ring-opening polymerization (ROP) in an ionic liquid and mild conditions with 4-Dimethylaminopyridine Catalyst. Dong et al. [129] prepared polymeric micelles in water with the hydrophobic PLLA segments at the cores of micelles and the hydrophilic cellulose segments as the outer shells from the self-assembly of cellulose-*g*-PLLA copolymer. The drug loaded micelles formed by the copolymer in aqueous media show sustained drug release which indicates their potential applicability in drug carrier. Hadano et al. [130] prepared benzylated waste pulps (PBzs) from treated waste pulp and benzyl chloride with phase transfer catalyst (PTC), and then synthesized graft copolymers (PBz-*g*-LA) from PBzs and *L*-lactic acid.

Starch is a potentially useful material for biodegradable plastics because of its natural abundance and low cost. However, the starch-based materials, such as the thermoplastic starch, produced by conventional melt-processing usually exhibit very poor mechanical properties, mainly due to the thermal decomposition of starch before melting, the strong water absorption and the poor interfacial adhesion with other components. Chen et al. [131] prepared PLLA/starch blends by the PLLA grafting starch (PLLA-*g*-St) copolymers as a compatibilizer, and their thermal, mechanical and morphological characterizations were performed to show the better performance of these blends compared to the virgin PLLA/starch blend without the compatibilizer, including PLLA crystallinity, interfacial adhesion between the PLLA matrix and starch dispersive phases, mechanical properties, medium resistance, and contact angle. The 50/50 composite of PLLA/starch compatibilized by 10% PLLA-*g*-St gave a tensile strength of 24.7 MPa and an elongation at break of 8.7%, respectively, vs. 11.3 MPa and 1.5%, respectively, for the simple 50/50 blend of PLLA/starch.

Chitin is one of the most abundant organic materials. Chitin and chitosan and their modified analogs have shown many applications in medicine, cosmetics, agriculture, and biotechnology. Kim et al. [132] synthesized biodegradable copolymers by ring opening polymerization (ROP) of *L*-lactide on chitin in an *N,N*-dimethyl acetamide (DMAc)/lithium chloride (LiCl) solvent system, and chitin was used as macroinitiator to afford new materials. Yao and colleagues [133–135] have grafted oligo(*L*-lactic acid), PLLA and poly(*L*-lactic-co-citric acid) onto chitosan by direct polycondensation without a catalyst or coupling reaction of terminal group of prepolymers and amino groups of chitosan. Degradation of PLA generates acidic degradation products at the implanted site which evokes undesirable tissue reaction. The acidic by-product may lead to local disturbance due to poor vascularization in the surrounding tissue. Chitosan may be combined with acid producing biodegradable polymers, so that local toxicity due to the acidic by-products can be alleviated.

Some research groups have reported the synthesis of PLA grafted dextran copolymers and evaluation of their possibility as biomedical materials. Cai et al. [136] synthesized comb-like biodegradable PLA-grafted dextran copolymer (dextran-*g*-PLA) in a bulk lactide polymerization reaction using dextran derivative as macroinitiator and stannous octoate as catalyst. This dextran-*g*-PLA copolymer was envisioned having good cell affinity and being a good candidate as cell scaffold materials for tissue engineering applications. Nagahama et al. [137] obtained monodisperse stereocomplex nanogels through the self-assembly of an equimolar mixture of dextran-graft-poly(*L*-lactide) (dex-*g*-PLLA) and dextran-graft-poly(*D*-lactide) (dex-*g*-PDLA) amphiphilic copolymers with well-defined composition in a dilute aqueous solution. The stereocomplex nanogel possesses partially crystallized cores of hydrophobic PLA and the hydrophilic dextran skeleton by intra- and/or intermolecular self-assembly between PLLA and PDLA chains. Bang et al. [138] prepared amphotericin B (AmpB)-encapsulated polymeric micelle of poly(*D,L*-lactide-co-glycolide) (PLGA) grafted-dextran (dexLG) copolymer for the cytotoxicity test. These results indicate that AmpB-incorporated polymeric micelle prepared from methanol/water mixture has low cytotoxicity and favorable antimicrobial activity.

Chondroitin sulfate is a physiologically significant glycosaminoglycan (GAGs). It comprises alternating units of  $\beta$ -1,3-linked glucuronic acid and ( $\beta$ -1,4) *N*-acetyl-gal-Na-lactosamine (Ga) with sulfation of either 4- or 6-position of GalNAc. It is present mostly on the surface of the cells and in the extracellular matrix (ECM). It can covalently bind with a core protein, producing a proteoglycan, such as aggregan, versican, neurocan, phosphacan or others. Lee et al. [139] synthesized amphiphilic poly(*L*-lactide)-graft-chondroitin sulfate copolymer using chondroitin sulfate as a hydrophilic segment and PLLA as a hydrophobic segment. Micelles of those copolymers were formed in an aqueous phase. Additionally, the CSn-PLLA micelles can efficiently be transported within the cells via endocytosis as observed from confocal microscopy.

To develop biodegradable polymers that can be modified to tailor their properties for use in a range of applications, while retaining the beneficial properties of the biodegradable polyesters, Hrkach et al. [140] reported the synthesis of poly(*L*-lactic acid-co-*L*-lysine) (PLAL) comb-like graft copolymers by the ring-opening polymerization of  $N^{\epsilon}$ -(carbobenzoxy)-*L*-lysine *N*-carboxyanhydride from the backbone of PLAL. Tasaka et al. [141] reported the synthesis of comb-type biodegradable PLA by graft polymerization of LA onto a depsipeptide-lactide copolymer containing serine residues. The obtained comb-type PLA is of interest as the biodegradable and bioabsorbable biomedical material.

To apply *in situ* gelling systems for drug delivery and tissue engineering, the aqueous polymer solution should be free flowing at a certain temperature and form a gel at the physiological temperature. The resulted gel must have reasonable mechanical strength to persist as a drug-releasing depot over the designed lifetime. Jeong et al. [142] designed and synthesized PEG grafted with poly(lactic acid-co-glycolic acid) (PEG-*g*-PLGA), where hydrophilic PEG was a backbone. Aqueous solutions of poly(*D,L*-lactic acid-co-glycolic acid)-*g*-PEG copolymers exhibited sol-to-gel transition with increasing temperature [143]. They also reported the elegant instrumental methods to determine sol-gel transition temperature and the method to control gel duration [144]. In addition, some thermo-sensitive graft copolymers also were synthesized and used to prepare polymeric micelles for drug delivery [102, 145].

Polyphosphazenes are hybrid macromolecules with a backbone of alternating phosphorus and nitrogen atoms and with two organic side groups linked to each phosphorus atom. Most of the known polyphosphazenes have been synthesized by replacement of the chlorine atoms in poly(dichlorophosphazene) by organic groups. Krogman et al. [146] synthesized polyphosphazenes that contain serine and threonine side groups by the macromolecular substitution technique. Serine and threonine have two different sites for covalent linkage to the polyphosphazene backbone. For one series of polymers, serine ethyl ester and threonine ethyl ester units are linked to the polyphosphazene skeleton via the *N*-terminus. The free hydroxyl groups on each side group are then used to graft PLLA. For the second series of macromolecules, the hydroxyl function of serine or threonine is used as the site for covalent attachment to the polyphosphazene backbone, a process that requires protection of both the *N*- and *C*-termini. Secondary reactions to remove the protective groups then yield side units with free amino and carboxylic acid functions. These polymers are water-soluble over a broad pH range but have the ability to form ionic cross-links in the presence of calcium ions.

### 4.1.5 Star-Shaped Copolymers of PLA

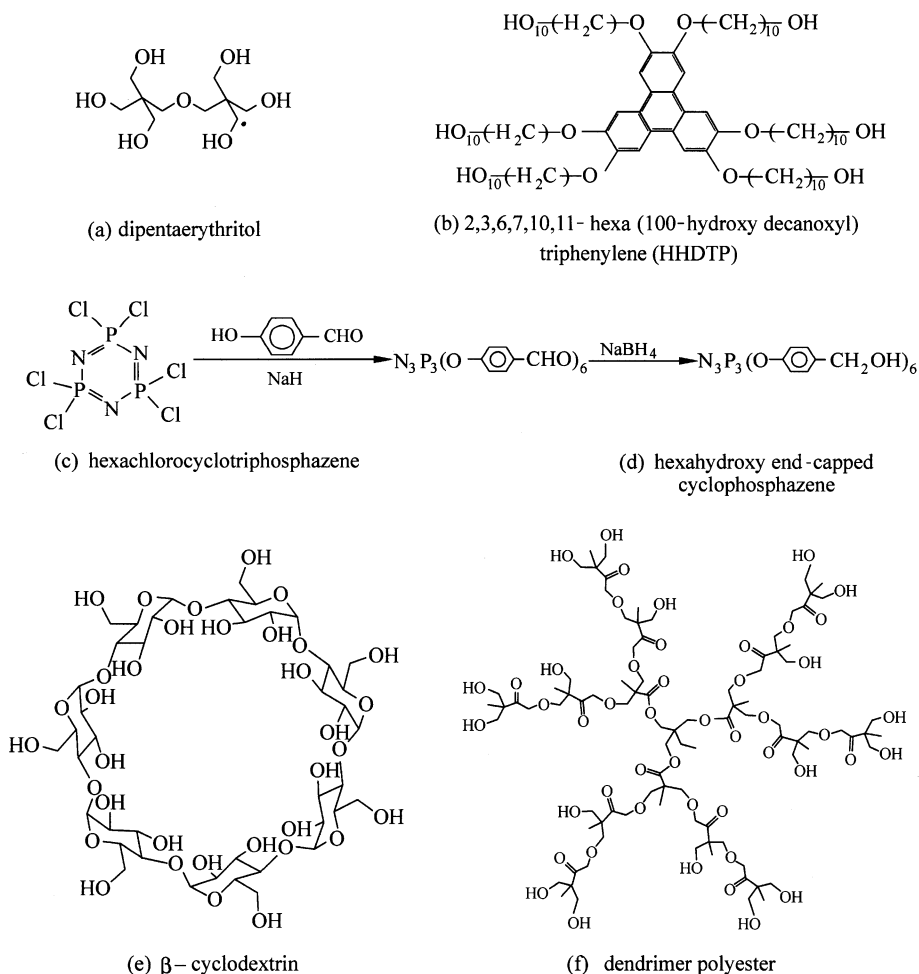
Star polymers have been gaining great attention over the past decades due to their unique three-dimensional shape and properties. Star-shaped and branched

polymeric structures possess interesting rheological and mechanical properties. They can be processed at lower temperatures than linear polymers of comparable molecular weight, since they have a lower melt viscosity. A low melt viscosity is especially advantageous for thermo-labile polymers like PLA. Furthermore, indications have been found that star-shaped structures show enhanced phase separation. Herein, considerable interest has been provoked in the preparation of a variety of star copolymers with varying arm numbers, chemical composition, and chain topology, especially for their potential applications as biomedical materials, such as surgical sutures and controlled drug release systems. Star polymers can be produced either by “arm-first” or “core-first” methods. The arm number of a star polymer is determined by the number of end groups in the core molecule. Till now, star polymers with several arms (arm number < 10) and a larger number of arms (arm numbers > 10) have been reported in a pack of papers.

When dipentaerythritol was used as initiator of star-shaped copolymers of trimethylene carbonate/ $\epsilon$ -caprolactone, a cross-linked star-shaped, poly(TMC-co- $\epsilon$ -CL) rubbers are obtained, that swell in chloroform. This network formation can be understood by “in situ” generation of crosslinked molecules from trimethylene carbonate and initiator. These low molecular weight rubbers can be used as a macro-initiator for the subsequent lactide/glycolide polymerization. Star-shaped lactide/glycolide block copolymers with a poly(TMC-co- $\epsilon$ -CL) rubber core based on *D*-sorbitol show good mechanical properties [147]. At relatively low rubber content ductile tensile behavior is observed indicating extensive toughening. Moreover, Wang et al. [148] synthesized well-defined hexa-armed star-shaped poly( $\epsilon$ -caprolactone)-*b*-poly(*L*-lactide) copolymers (6sPCL-*b*-PLLA) via sequential block copolymerization using dipentaerythritol (Fig. 4.8(a)) as core. The crystallization of both PLLA and PCL blocks within the star-shaped PCL-*b*-PLLA copolymer can be adjusted from the arm length of each block, the PLLA blocks within star-shaped PCL-*b*-PLLA copolymer progressively changes from ordinary spherulites to banded spherulites with increasing arm length ratio of PCL to PLLA. Yu et al. [149] have successively prepared 6-armed star block copolymers, *s*-[poly(*L*-lactide)-*b*-poly(styrene-co-*N*-acryloxysuccinimide)]<sub>6</sub>, with triphenylene (Fig. 4.8(b)) core by the combination of ring-opening polymerization and atom transfer radical copolymerization. The copolymers were used in the self-assembly in tetrahydrofuran, and the micelles with triphenylene core and PLLA as inner layer as well as poly(St-co-NAS) as shell were formed. After shell was cross-linked, PLLA was hydrolyzed in aqueous NaOH solution, the hollow spheres were formed.

Cyclophosphazenes (Fig. 4.8(c)) exhibit interesting properties such as flame retardancy, possibility of forming clathrates, and oil repellence. The usage of these compounds was restricted for long time to act as modifiers such as antioxidants, chain extenders, and compatibilizers. As a matter of fact, it is therefore reasonable to prepare polymers with desired properties inherited from

the phosphazene rings. For example Cui et al. [150] reported the ring-opening polymerization of  $\epsilon$ -caprolactone and *L*-lactide with a hexahydroxy end-capped cyclophosphazene (Fig. 4.8(d)) as initiator. Star-shaped polyesters with AB diblock arms have also been synthesized through a two-step copolymerization method. Yuan et al. [151] synthesized the star-shaped triblock poly( $\epsilon$ -caprolactone)-*b*-Poly(*L*-lactide)-*b*-Poly(*D,L*-lactide-co-glycolide) copolymer from hexakis[*p*-(hydroxymethyl)phenoxy]cyclotriphosphazene initiator via the sequential ring-opening polymerization of  $\epsilon$ -caprolactone (CL), *L*-lactide (*L*-LA), *D,L*-lactide (*D,L*-LA) and glycolide (GA). The triblock copolymer presented a three-phase structure, namely, PCL crystalline, PLLA crystalline, and *D,L*-PLAGA amorphous domains, which made the triblock copolymer different from the



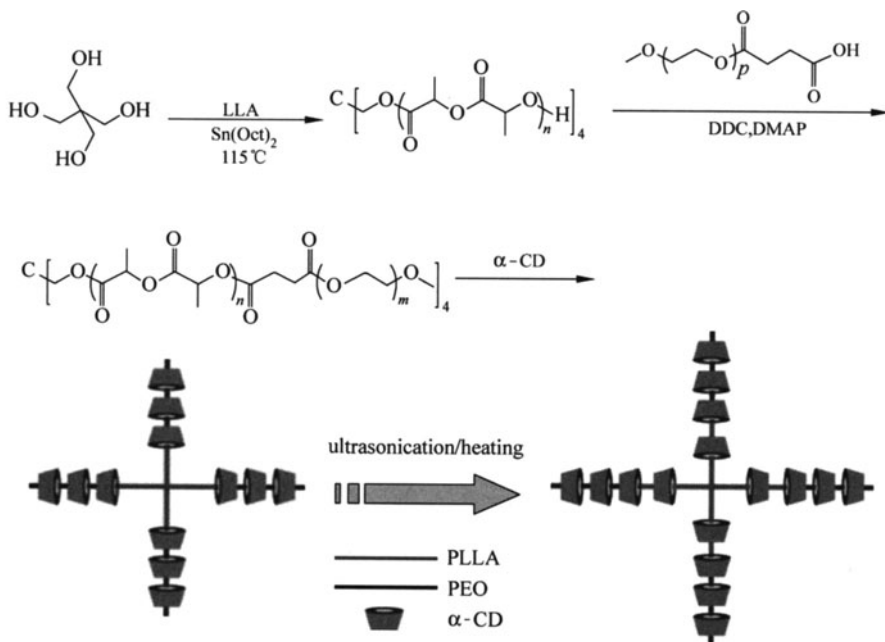
**Figure 4.8** Several multihydroxyl initiators used in the synthesis of star-shaped polymers

diblock copolymer and star-shaped PCL in crystallizability and thermal behaviors. The branched structure and the presence of amorphous copolymer *D,L*-PLAGA led to the lowering of crystallinity of triblock copolymer. Therefore, the water molecule pervaded the molecule of copolymer faster than that of linear PCL, star-shaped PCL, and PCL-*b*-PLLA, which promoted the hydrolytic degradation of the copolymer. In addition,  $\beta$ -cyclodextrin ( $\beta$ -CD) (Fig. 4.8(e)) was also employed as multihydroxyl initiator to synthesize star-shaped PDLLA by the ring-opening polymerization of *D,L*-lactide using triethylamine (Et<sub>3</sub>N) as the catalyst [152].

Amphiphilic block copolymers including PLA-*b*-PEO and PLA-*b*-PEO-*b*-PLA have been intensively studied by different research groups [56]. It is demonstrated that the biodegradable nanoparticles with micellar and vesicular morphologies can be fabricated by adjusting the weight fraction of PEO and/or PLA block. However, these polymeric micelles are not very stable in physiological conditions because of their relatively high critical micelle concentration, thus it is urgent to generate the relatively stable core-shell nanocarrier for drug delivery. In this case, amphiphilic polymers with branched topologies (such as star-shaped, hyperbranched, dendrimer, and dendrons) are expected to generate unimolecular nanoparticles under certain conditions, which have better thermodynamic stability in aqueous solution. Li and Kissel [153] synthesized biodegradable star-block copolymers containing a hydrophilic 4- or 8-arm branched poly(ethylene oxide) (PEO) central unit and hydrophobic PLLA or poly(*L*-lactide-co-glycolide) (PLLG) by solution polymerization in toluene catalyzed by aluminium triethylene. Cai et al. [154, 155] have demonstrated the comparative studies on synthesis, physical properties, and spherulitic growth of PLLA and PLLA-*b*-PEO with different arms (such as one, two, four, and six arms). Moreover, the hydrophilicity, biodegradable nanoparticles, in vitro degradation, and the preliminary drug-release behavior of these PLLA-*b*-PEO block copolymers with different arms also were reported [155]. Lu et al. [156] synthesized branched barbell-like (PLGA)<sub>*n*</sub>-*b*-PEG-*b*-(PLGA)<sub>*n*</sub> (*n* = 1, 2, 4) copolymers by using a series of multihydroxyl (2, 4, and 8) terminated PEGs as initiators. The result of hydrolytic degradation indicated that the rate of degradation increased with the increase of arm numbers or with the decrease of arm lengths. And the thermal properties of barbell-like copolymers depended on the structural variations. Polysorbate 80 (Tween 80) has been widely used as an emulsifier with excellent effects in nanoparticles technology for biomedical applications. So PLA-Tween 80 copolymers also were synthesized by ring-opening polymerization. Then, the paclitaxel-loaded nanoparticles of PLA/Tween 80 copolymers were prepared by the dialysis method without surfactants/emulsifiers involved [157]. Recently, the successful synthesis of a series of inclusion complexes based on  $\alpha$ -CD and star-block PLLA-*b*-PEO amphiphilic copolymers with different PEO chain lengths by two different methods was reported [158]. The results indicated that the activation energy barrier of the inclusion complexation between PLLA guest and  $\alpha$ -CD host and

## Biodegradable Poly(Lactic Acid): Synthesis, Modification, Processing and Applications

the steric hindrance of star-block copolymer could be conquered with heating method and ultrasonication. Namely,  $\alpha$ -CD can be threaded onto the outer PEO block or the PEO and PLLA blocks of star-block copolymers to form inclusion complexes during the alternation of preparing conditions (Fig. 4.9).



**Figure 4.9** Preparation of inclusion complexes of SPLLA-*b*-PEO copolymers and  $\alpha$ -CD [158]

Poly(2-(*N,N*-dimethylamino) ethyl methacrylate) (PDMAEMA) can be potentially used in drug and DNA delivery system owing to its excellent biocompatibility, hydrophilicity and pH sensitivities. Meanwhile, the preparation of PDMAEMA has been carried out by atom transfer radical polymerization (ATRP) and the process of polymerization can be well controlled with this living controllable polymerization. Therefore, Yuan et al. [159] prepared well-defined dendritic star-block PLLA-*b*-PDMAEMA copolymers by the combination of ROP of LLA and ATRP of DMAEMA with hydroxyl-terminated dendrimer polyester (Fig. 4.8(f)) initiator. The investigation of release of model drug chlorambucil indicated that the release rate of the drug could be effectively controlled by altering the pH values of the environment. On the other hand, Kang and Leroux [160] synthesized star-block amphiphilic copolymers, star-poly(*D,L*-lactide)-block-poly(*N*-(2-hydroxypropyl)methacrylamide) and star-poly(*D,L*-lactide)-block-poly(*N*-vinylpyrrolidone), by free radical polymerization of *N*-(2-hydroxypropyl)methacrylamide and *N*-vinyl-2-pyrrolidone in the presence of



biodegradable macromolecular chain-transferring agent, star-poly(*D,L*-lactide) tetrakis-thiol. All copolymers self-assembled in aqueous solution to form supramolecular aggregates of 20 – 180 nm in size. The critical aggregation concentration of the copolymers ranged from 3.9 to 24.1 mg/L, depending on their hydrophobicity. These star-block copolymers could prove useful as nanocarriers for the solubilization and delivery of hydrophobic drugs.

Despite a larger number of star-shaped PLA and its copolymers have been reported in a pack of papers, the synthesis for well-defined star copolymers, especially star block copolymers, have not grown easier until living/controlled free radical polymerization techniques are developed, such as reversible addition fragmentation chain transfer (RAFT) polymerization, atom transfer radical polymerization (ATRP), and nitroxide mediated radical polymerization (NMP). Additionally, the combinations of the living/controlled radical polymerizations and their combinations with living ring opening polymerization (ROP) have also been employed for the preparation of star copolymers.

Sun et al. [161] synthesized a biodegradable Y-shaped copolymer, PLLA<sub>2</sub>-*b*-poly(*g*-benzyl-*L*-glutamic acid) (PLLA<sub>2</sub>-*b*-PBLG) by the ring-opening polymerization (ROP) of *N*-carboxyanhydride of  $\gamma$ -benzyl-*L*-glutamate (BLG-NCA) with centrally amino-functionalized PLLA, PLLA<sub>2</sub>-NH<sub>2</sub> as a macroinitiator in a convenient way (Fig. 4.10). It was found that the self-assembly of the copolymer was dependent on solvent and on relative length of the PBLG block. For a copolymer with PLLA blocks of 26 in total degree of polymerization (DP), if the PBLG block was long enough (e.g., DP=54 or more), the copolymer/toluene solution became a transparent gel at room temperature. In benzyl alcohol solution, only PLLA<sub>2</sub>-*b*-PBLG containing ca. 190 BLG residues could form a gel; those with shorter PBLG blocks (e.g., DP=54) became nano-scale fibrous aggregates and these aggregates were dispersed in benzyl alcohol homogeneously. Copolymers with short PBLG blocks behaved like a pure PLLA both in toluene and in benzyl alcohol. These experimental phenomena are attributed to the helical conformation of PBLG, and to the interactions between the solvents and the PLLA and/or PBLG segments which are responsible for the crystallization or salvation of PLLA segments or for precipitation or dispersion of PBLG  $\alpha$ -helices. On the other hand, Han and Pan [162] synthesized the novel H-shaped copolymers, PLLA<sub>2</sub>-polystyrene-PLLA<sub>2</sub>, by combination of atom transfer radical polymerization (ATRP) with cationic ring-opening polymerization (CROP). The first step of the synthesis was ATRP of styrene using *a,a'*-dibromo-*p*-xylene/CuBr/2,2'-bipyridine as initiating system, and then the PSt with two bromine groups at both chain ends (Br-PSt-Br) were transformed to four terminal hydroxyl groups via the reaction of Br-PSt-Br with diethanolamine in *N,N*-dimethylformamide. The H-shaped copolymers were produced by CROP of LLA, using PSt with four terminal hydroxyl groups as macroinitiator.

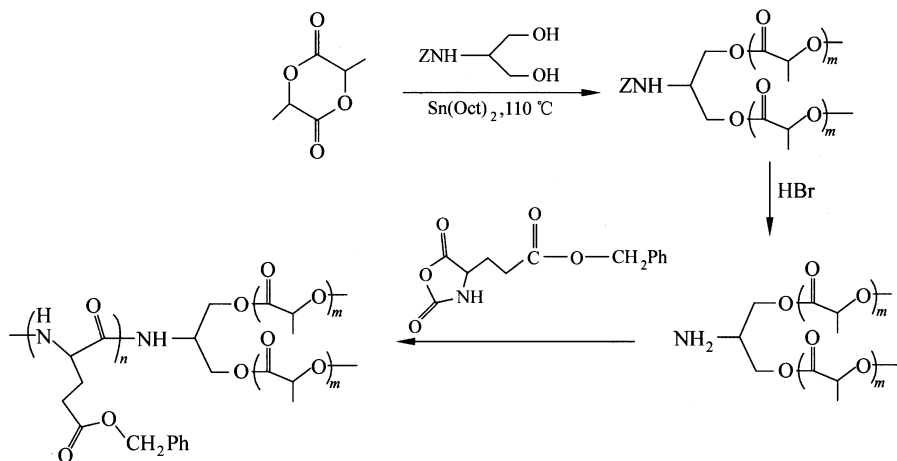


Figure 4.10 Synthesis of Y-shaped copolymer PLLA<sub>2</sub>-b-PBLG

Wei et al. [163] designed and synthesized a seven-arm star block copolymer poly(L-lactide)-star block-poly(*N*-isopropylacrylamide) (PLLA-*sb*-PNIPAAm), comprising one hydrophobic PLLA arm and an average of six hydrophilic poly(*N*-isopropylacrylamide) (PNIPAAm) arms. The amphiphilic copolymer was capable of self-assembling into micelle with diameter of around 100 nm in water. The micelles showed reversible dispersion/aggregation in response to temperature changes through an outer polymer shell of PNIPAAm at around  $31^\circ\text{C}$ . The anticancer drug methotrexate (MTX) as model drug was loaded in the polymeric nano-sized micelles. In vitro release behavior of MTX showed a drastic thermoresponsive fast/slow switching behavior according to the temperature-responsive structural changes of a micellar shell structure. The reversible and sensitive thermoresponse of this micelle might provide opportunities to construct a novel drug delivery system in conjunction with localized hyperthermia. Furthermore, they synthesized a series of star block copolymers PLLA-star block-poly(*N*-isopropylacrylamide-co-*N*-hydroxymethylacrylamide) (PLLA-*sb*-P(NIPAAm-co-HMAAm)) with different molar feed ratios of NIPAAm and HMAAm [164]. Here, the hydrophilic HMAAm was employed to adjust and improve the LCST of the star block copolymer. An ideal P(NIPAAm-co-HMAAm) (13:1) copolymer was found, which exhibited reversible phase transitions at around  $36.8^\circ\text{C}$ , being close to human physiologic temperature ( $37^\circ\text{C}$ ).

Yuan et al. [165] reported the synthesis of well-defined dendrimer-star, block-comb polymers by the combination of living ring-opening polymerization and atom transfer radical polymerization on the basis of a dendrimer polyester. Star-shaped dendrimer PCLs were synthesized by the bulk polymerization of  $\epsilon$ -caprolactone with a dendrimer initiator. The dendrimer PCLs then were converted into macroinitiators via esterification with 2-bromopropionyl bromide. And the star-block copolymer dendrimer poly( $\epsilon$ -caprolactone)-block-poly(2-hydroxyethyl

methacrylate) was obtained by the ATRP of 2-hydroxyethyl methacrylate. Finally, dendrimer-star, block-comb copolymers were prepared with PLLA blocks grafted from poly(2-hydroxyethyl methacrylate) blocks by the ring-opening polymerization of *L*-lactide.

Heteroarm or miktoarm star copolymers have attracted considerable attention in recent years due to the unique properties of these polymers, for example, they exhibit dramatic difference in morphology and solution properties. In comparison with the linear block and star-block copolymers, the synthesis of heteroarm or miktoarm star copolymers has been one of the more challenging projects available. A typical example is that the synthesis of the heteroarm H-shaped terpolymers, [(PLLA)(PS)]-PEO-[(PS)(PLLA)], in which PEO acts as a main chain and PS and PLLA as side arms (Fig. 4.11). The copolymers have been successfully prepared via combination of reversible addition-fragmentation transfer (RAFT) polymerization and ring-opening polymerization (ROP) by Han and Pan [166]. Another interesting example is that Pan et al. [167] successfully

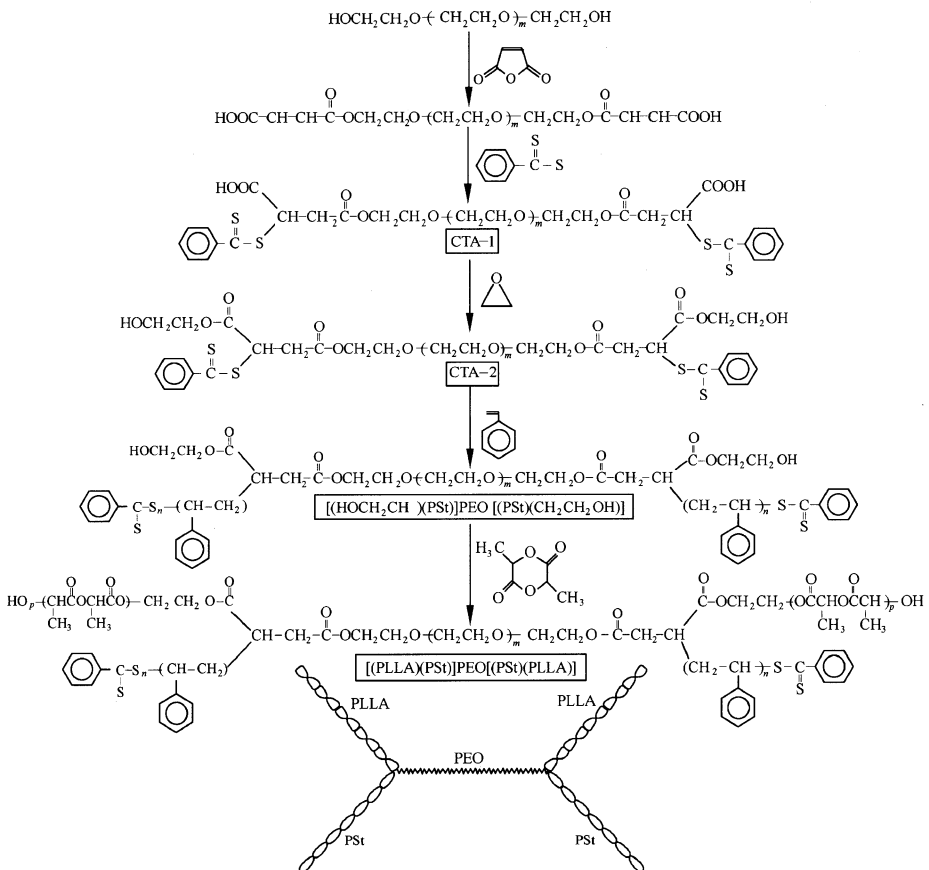
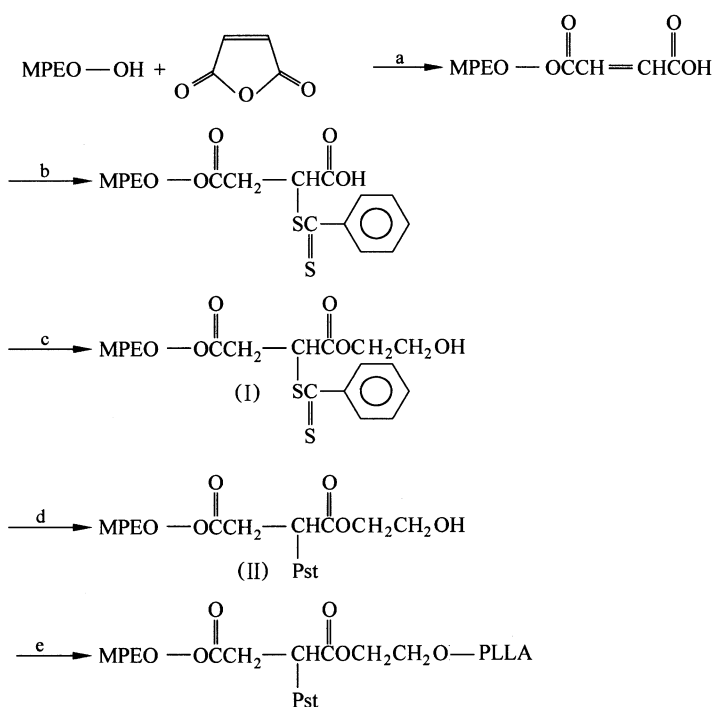


Figure 4.11 Synthetic procedure of heteroarm H-shaped terpolymers [166]

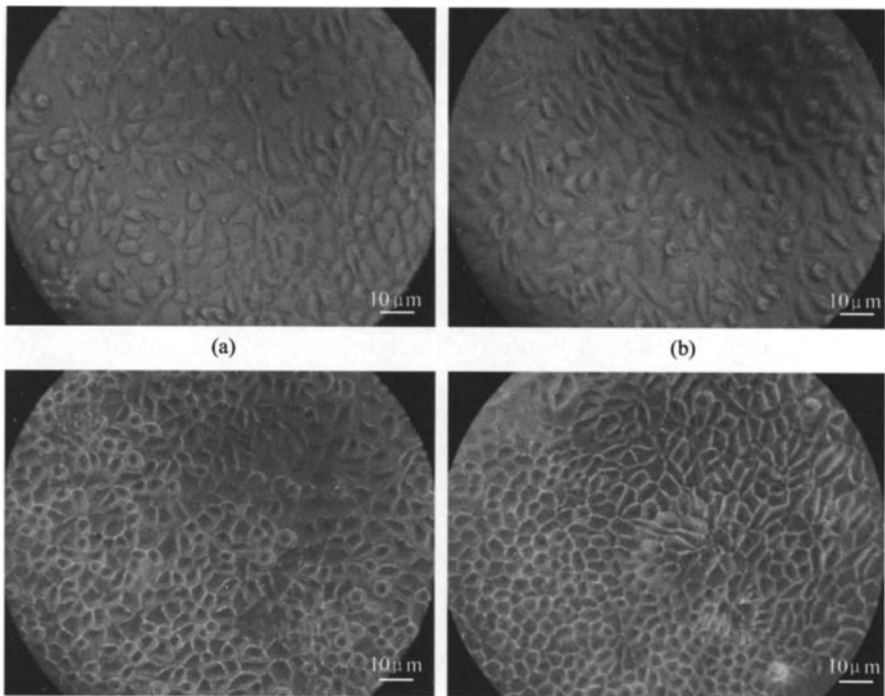
synthesized poly(ethylene oxide) methyl ether/polystyrene/poly(*L*-lactide) (MPEO/PSt/PLLA) ABC miktoarm star copolymers by combination of reversible addition-fragmentation transfer (RAFT) polymerization and ring opening polymerization (ROP) using bifunctional macro-transfer agent, MPEO with two terminal dithiobenzoate and hydroxyl groups (Fig. 4.12). It was prepared by reaction of MPEO with maleic anhydride (MAh), subsequently reacted with dithiobenzoic acid and ethylene oxide. RAFT polymerization of St at 110°C yielded block copolymer, MPEO-*b*-PSt [(MPEO)(PSt)ACH<sub>2</sub>OH], and then it was used to initiate the polymerization of *L*-lactide in the presence of Sn(OCT)<sub>2</sub> at 115°C to produce ABC miktoarm star polymers, *s*-[(MPEO)(PSt)(PLLA)].



**Figure 4.12** Synthesis of ABC miktoarm star copolymers [167]

The stereocomplex of PLLA and PDLA has been expanded by several research groups to block and graft copolymers containing PLLA or PDLA as hydrophobic segments. In addition, biodegradable hydrogels based on stereocomplex formation of PLLA and PDLA in water-soluble amphiphilic copolymers have attracted much attention in recent years for possible biomedical and pharmaceutical applications. These new types of hydrogels created in water through physical cross-linking are expected to show advantageous characteristics for the controlled release of pharmaceutical proteins. For example, Nagahama et al. prepared two water-insoluble biodegradable star-shaped block copolymers of 8-arms

PEG-*b*-PLLA and 8-arms PEG-*b*-PDLA with same chemical component but different stereoregularity [168]. The stereocomplex film exhibited higher Tg and PLA crystallinity than those of original copolymer films. They also analyzed the effects of stereoregularity and stereocomplexation on protein adsorption and L929 cells attachment/proliferation behaviors onto the films. The stereocomplex film was found to exhibit large amount of protein adsorption than original films. Furthermore, cell attachment efficiency and proliferation rate on the film were significantly enhanced by stereocomplexation (Fig. 4.13). This stereocomplex material is expected to be applicable as degradable temporary scaffold for soft tissue regeneration.



**Figure 4.13** Phase contrast images of L929 cells adhering onto (a) 8-arms PEG20K-*b*-PLLA50K film, (b) 8-arms PEG20K-*b*-PDLA46K film, (c) stereocomplex film, and (d) tissue culture polystyrene (TCPS) surfaces at 4 days after cell seeding [168]

#### 4.1.6 Dendritic Copolymers of PLA

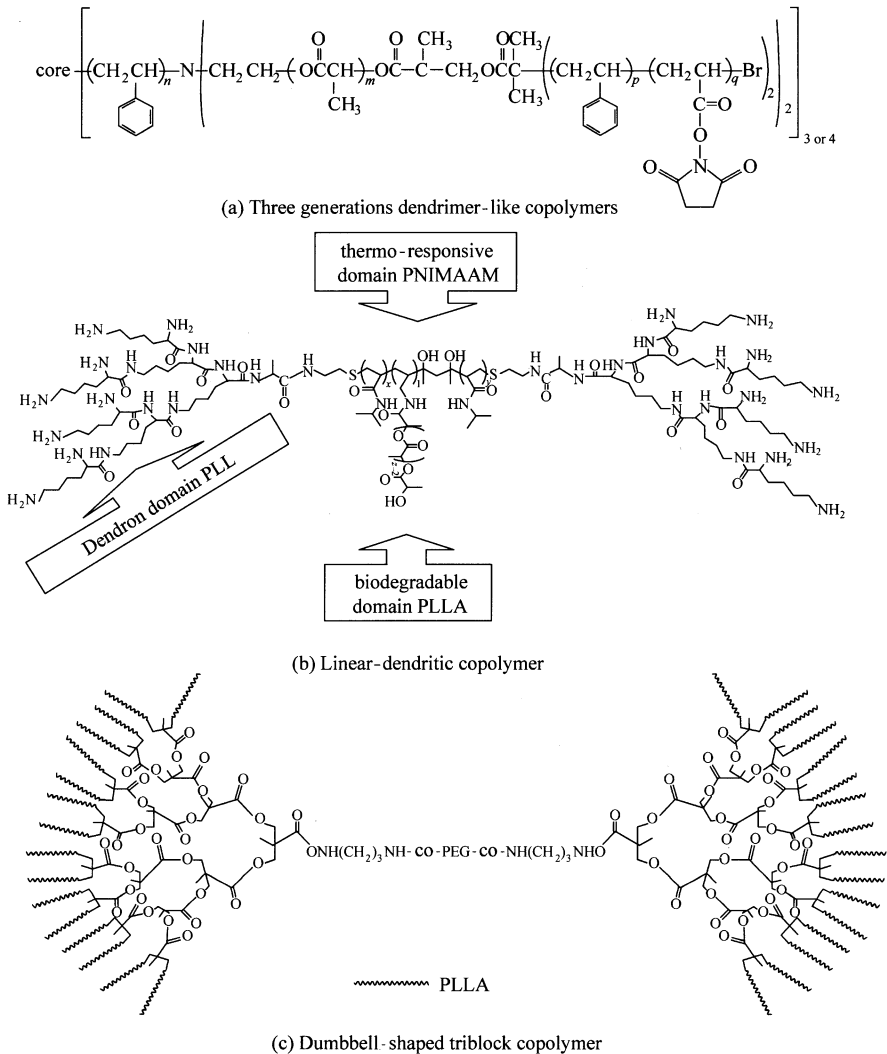
Dendrimers, nanoscale highly branched and reactive three dimensional macromolecules, become increasingly important in biomedical applications due to their specific size, intriguing structural properties such as internal voids and

cavities, and a highly functional terminal surface. Particularly, the spatially arranged functional groups can be used for postformation modifications on the periphery of the dendritic globules with a variety of molecules such as small molecule drugs, DNA and oligonucleotides for drug delivery and gene therapy, targeting molecules such as folic acid to localize drugs to desired tissue sites, hydrophilic molecules such as PEO to increase their blood circulation times, and contrast agents to use in magnetic resonance imaging (MRI). More uniquely, the functional groups of the dendrimers can incorporate two and more functional molecules mentioned above for more compact and efficient therapeutic treatments and diagnostics [169]. The structural character makes them possess some unique physical and chemical properties, which arise great interest of polymer scientists.

Pan's group has successfully synthesized the three generations of dendrimer-like copolymers core-(PSt-*b*-(PLLA-*b*-PSt<sub>2</sub>)<sub>2</sub>)<sub>3</sub>, core-(PSt-*b*-(PLLA-*b*-(PSt-co-PNAS)<sub>2</sub>)<sub>2</sub>)<sub>3</sub> and core-(PSt-*b*-(PLLA-*b*-(PSt-co-PNAS)<sub>2</sub>)<sub>2</sub>)<sub>4</sub> (Fig. 4.14(a)) by combination of ATRP and ROP [170, 171]. Diethanol amine and 2,2-*bis*(methylene-2-bromoisobutyrate) propionyl chloride were used as divergent reagents before preparations of the second and the third generations. Microspheres with average diameter of 295 nm is formed in the solution of the dendrimer-like copolymers in THF with concentration of 1 mg/mL, and the spheres have layered structure and broad size distribution. The shell of the particles then can be cross-linked via substituted reaction of NAS in the shell polymer with ethylene diamine. After cross-linking and aminolysis reactions, precipitation in petroleum ether and drying, hollow microspheres with one hole and seldom two holes on the surface of every particle are obtained due to removal of hydrolyzed small molecules and evaporation of solvents inside the particles. After the microspheres are preserved for long time, the hole on the surface becomes big. The hollow particles should have potential application in catalysis and bioengineering.

Kim and coworkers [169] have reported the synthesis of a linear-dendritic copolymer containing thermoresponsive poly(*N*-isopropylacrylamide) (PNIPAAm), hydrophobic and biodegradable poly(*L*-lactic acid) (PLLA), and hydrophilic poly(*L*-lysine) (PLL) dendrons (Fig. 4.14(b)). The linear-dendritic copolymer was synthesized by 1,3-dicyclohexylcarbodiimide (DCC) coupling reaction of three generation PLL dendron and PNIPAAm grafted with PLLA. The research results demonstrated that the linear-dendritic copolymer was thermoresponsive by showing a lower critical solution temperature whose value depended on the linear-dendritic copolymer concentrations. The viscosity and molar mass of the linear-dendritic copolymer decreased with time in PBS (pH = 7.4) solutions indicating that the linear-dendritic copolymer was degradable.

Gong et al. [172] designed and prepared a series of well-defined dumbbell-shaped tri-block copolymers (Fig. 4.13(c)) consisting of comb-like PLLA and linear PEG with narrow molecular weight distributions and varied PLLA arm lengths via the sequential preparation of terminal dendronized polyhydric PEG



**Figure 4.14** The structures of three dendritic copolymer examples of PLA

and ring-opening polymerization (ROP) of LA. Self-organized porous structures have been found in the copolymer films after solution casting and solvent evaporation. Honeycomb-like surface morphology could be achieved by adjusting the length of PLLA arms. Meanwhile, as for surface chemistry of the copolymer films, surface hydrophobicity and the capability of adsorbing protein increase with the length of PLLA arms. Controllable material properties have been correlated with the *in vitro* cell responses. No cytotoxicity of the dumbbell-shaped copolymers has been found using rabbit bone marrow stromal cells (BMSCs). Human embryonic kidney (HEK) 293T cells have been used to reveal the effect of surface characteristics on cell attachment and proliferation. It has

been found that cell proliferation has been enhanced significantly on the surfaces of the copolymers with longer PLLA arm lengths because of more favorable surface physicochemical properties.

### 4.2 PLA Blending

In many film applications, such as for grocery and garbage bags, bursting strength, elongation and tear strength are important properties. These properties can be improved to a certain extent by mechanical drawing, such as biaxial orientation and stretch blow molding. However, for other PLA parts where the use of mechanical orientation is not feasible (e.g., injection molded articles), blending of PLA with other polymers is a useful strategy to impart flexibility and toughness. Another motive for blending PLA with other polymers is to reduce the material cost since the cost of PLA is relatively higher compared to other petroleum plastics.

Various polymers have been used for improving the properties of PLA, including elastomers, thermoplastic starch, PEG, triacetin and tributyl citrate, and PHA. Lee and McCarthy modified the toughness of 4% *d*-PLA with poly(3-hydroxyoctanoate) (PHO). In order to overcome the process difficulties due to the large difference in melt viscosity between the two polymers, they modified the PHO with hexamethylene diisocyanate (HMDI) by reacting the hydroxyl group of PHO to form urethane linkages. HMDI of 2%–5.5% (w/w) was reacted with PHO using a counter-rotating screw at 40 r/min for 2 min at 100°C. The modified PHO was melt-blended with PLA at 40 r/min for 3 min at 175°C and then compression molded. Noda et al. prepared plastic films by melt compounding various proportions of PLA, PHA copolymer (copolymer of 3-hydroxybutyrate with 21 mol% of 3-hydroxyhexanoate), and poly(ethylene oxide). These authors claimed that the inherent tackiness of PHA polymer and brittleness of PLA can be overcome by this approach [173]. Recently, based on viscosity and gel permeation chromatography measurements, Conrad et al. reported that PLA/PHA blends degraded more rapidly as compared to the neat PLA. In another patent, Randall et al. blended PLA with epoxidized natural rubber in the presence of a compatibilizing agent (maleic anhydride/polybutadiene copolymer or maleic anhydride/polybutadiene/PS copolymer at 1–2 wt% relative to the epoxidized rubber). They observed an increased ultimate elongation from 72.6% to 295%, and an increase of izod impact value from 2.08 to 3.8 ft lbs/in. for injection molded test bars, as compared to the non-compatibilized control [174]. The blends were produced by extruding the polymers through a twin-screw extruder (150–175°C extruder zone temperatures; 250 r/min), cooling in a water trough, chopping the extruded strand into pellets, drying to remove water, and then injection molding into test bars. Randell et al. noted that reprocessing the polymer blends, i.e., passing them through the



extruder more than once, tended to increase the impact resistance of the resulting molded articles.

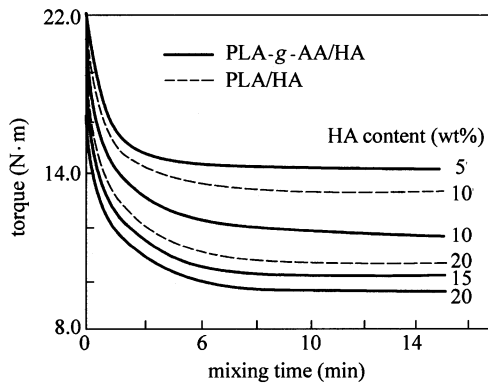
Averous attempted to blend thermoplastic starch, PEG, glycerol and oligomeric lactic acid by using a single-screw extruder equipped with a conical-shaped shear element. Glycerol was found to be the least efficient plasticizer, while oligomeric lactic acid and PEG provided substantial increases in elongation. Affinity of PLA and thermoplastic starch was poor, leading to blends that possessed much weaker mechanical properties as compared to the individual polymers [175]. Moura reported that the tensile strength, elongation, and damping for PLA blended with starch particles increased with average particle size of the starch granules, but declined when the granules were greater than 45  $\mu\text{m}$ . Moreover, crystallinity increased as the particle size decreased. The use of methylenediphenyl diisocyanate as a coupling agent dramatically improved the mechanical properties of the composite. Sheth et al. melt-blended PLA and PEG using a counter-rotating twin-screw extruder at 120–180°C. They reported that PEG could form miscible to partially miscible blends with PLA, depending on the blend concentration. Below 50% PEG, the plasticized PLA samples have high elongation with a concomitant reduction in modulus values. However, above 50% PEG content, the blend crystallinity increases, resulting in an increased modulus and a considerable decrease in the elongation at break [176]. Although PEG is effective in decreasing the stiffness of PLA, the use of low molecular weight plasticizer has a disadvantage in that it has a tendency to migrate in the PLA matrix. For instance, Hiltunen et al. reported that although PEG plasticized PLA could be extrusion blown to form film with a reasonable tensile strength, PEG tended to migrate out of the film after a few days or weeks. Ljungberg and Wesslen reported that the  $T_g$  of PLA could be effectively depressed by blending with triacetine and tributyl citrate up to about 25% (w/w), above which phase separation of plasticizer tended to occur. They also observed that phase separation of plasticizer accelerated at elevated temperature (50°C) due to the increased crystallinity of the PLA phase. During storage of triacetine and tributyl citrate plasticized PLA film, the migration of the plasticizer to the film surfaces and the concomitant increased crystallinity of the bulk material have been reported to cause difficulty in subsequent heat welding.

#### 4.2.1 PLA/HA

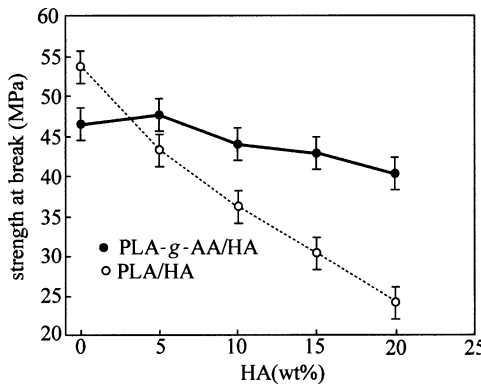
The hyaluronic acid (HA), a linear polysaccharide composed of repeating units of *N*-acetyl-glucosamine and *D*-glucuronic acid, is a component of extracellular matrix (ECM) and it has the high capacity of lubrication, water absorption and water retention. Recently, HA has been widely used in biomedical applications such as scaffolds for wound healing and tissue engineering, ophthalmic surgery, arthritis treatment, and utilized as a component in implant materials. Blending of PLA with biodegradable polymers, such as poly(3-caprolactone), poly(butylene

succinate) and poly(hydroxybutyrate), to produce fully degradable hybrids has been studied but there are no articles about the investigation of PLA/HA blends.

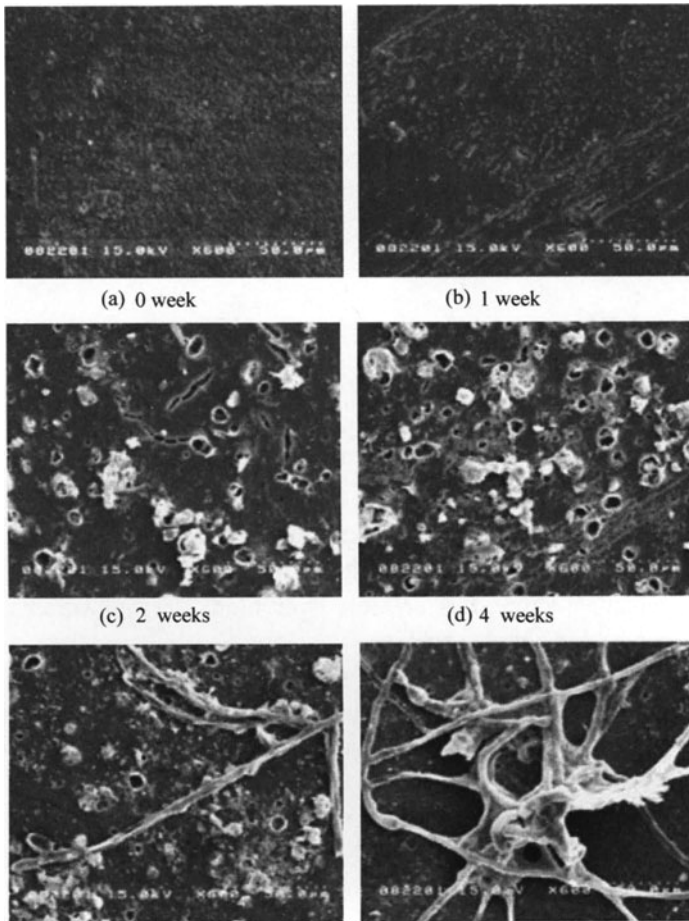
As the result, due to the poor compatibility between PLA and HA, the mechanical properties of PLA/HA composites are worse than that of PLA. Much better dispersion and homogeneity of HA in the polymer matrix can be obtained when PLA-g-AA is used in place of PLA in the composite. The PLA-g-AA/HA composites can markedly improve the mechanical properties of PLA/HA ones, and the former provides a plateau tensile strength at break when the HA content is up to 20 wt%. Furthermore, the PLA-g-AA/HA is more easily processed than PLA/HA because the former has lower viscosity than the latter as they are molten as shown in Fig. 4.15 and Fig. 4.16. Biodegradation tests of blends are also made under the enzymatic environment, and the result shows that the mass of blends reduces by about the HA content within 4 weeks. SEM micrographs of PLA/HA (10 wt%) are shown in Fig. 4.17.



**Figure 4.15** Torque value vs. mixing time for preparation of PLA/HA and PLA-g-AA/HA blends at various HA contents



**Figure 4.16** Tensile strength at breakpoint vs. HA content for PLA-g-AA/HA and PLA/HA blends



**Figure 4.17** SEM micrographs of PLA/HA (10 wt%) exposed to the enzymatic environment

By using PLA-*g*-AA to replace PLA for preparation of blends, the mechanical properties of a PLA/HA-type composite can be improved. The crystalline structure of PLA-*g*-AA/HA differs from that of PLA/HA due to the formation of an ester carbonyl functional group from the reaction between the —OH of HA and the —COOH of PLA-*g*-AA. For PLA/HA blends, the melting temperature ( $T_m$ ) and the melting enthalpy ( $\Delta H_m$ ) both decrease with increasing hyaluronic acid content. When PLA is replaced with PLA-*g*-AA, the PLA-*g*-AA/HA gives higher  $T_m$  and lower  $\Delta H_m$  than PLA/HA. Morphology of PLA/HA blends indicates that the hyaluronic acid phase size increases with increasing hyaluronic acid content, suggesting that the compatibility between PLA and hyaluronic acid is very poor. For PLA-*g*-AA/HA blends, the size of the hyaluronic acid phase is noticeably reduced and is always less than 36  $\mu\text{m}$ , is detectable only under higher

magnification. Tensile strength at breakpoint of PLA/HA blends decreases markedly and continuously as hyaluronic acid content is increased. The composite containing PLA-g-AA exhibits enhanced mechanical properties compared with that containing PLA, especially regarding tensile strength at breakpoint. The water resistance of PLA-g-AA/HA is better than that of PLA/HA. Finally, the effect of enzyme (tyrosinase) on biodegradation of PLA is slight but marked for HA [177].

### 4.2.2 PLA/PEG

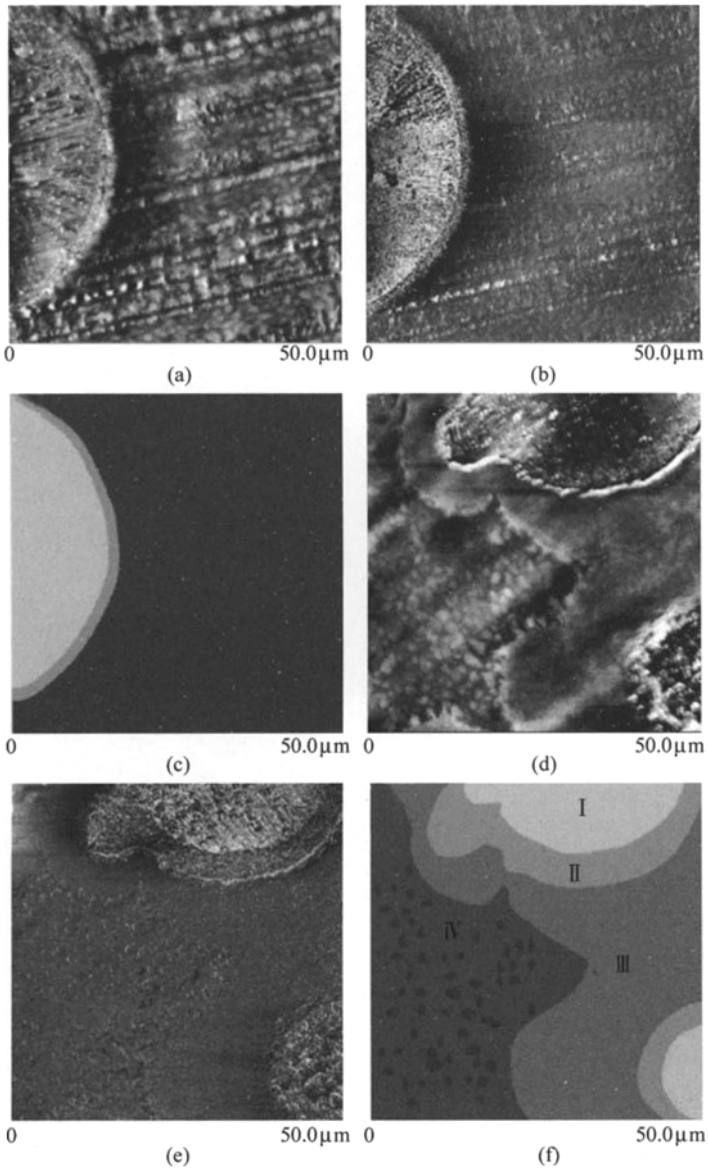
The tendency for PLA plasticized with PEG to lose properties with time at ambient temperature is a major obstacle to its application as a biodegradable packaging material. Without plasticizer, PLA is stiff and brittle. Blending with low molecular weight PEG improves elongation at break and softness. The desired mechanical properties are achieved in quenched PLA/PEG blends with 30 wt% PEG. However, the blends are not stable at ambient temperature and the attractive mechanical properties are lost over time. Crystallization and phase separation are possible aging processes.

The aging of homogeneous amorphous PLA/PEG blends that is obtained by quenching from the melt has been studied. The kinetics and mechanism of ambient temperature aging strongly depend on stereoregularity of PLA. Lower stereoregular PLA appears to be miscible with 30 wt% PEG at ambient temperature. Stiffening is caused by slow crystallization of PEG from the homogeneous matrix. As aging gradually depletes the amorphous matrix of PEG, the glass transition increases; aging ceases when the glass transition temperature reaches ambient temperature. Blends of higher stereoregular PLA with 30 wt% PEG phase-separate at ambient temperature before either constituent crystallizes. As formation of a PEG-rich phase depletes the matrix of PEG, the matrix becomes stiffer.

Higher stereoregular PLA readily crystallizes from blends with PEG if the blend is slowly cooled from the melt. Table 4.1 shows the effect of cooling rate on crystallization behavior of PLA and PEG in the PLA/PEG=70/30 blend. Blending with PEG reportedly decreases the nucleation density but increases spherulite growth rate of PLA. The PEG constituent also crystallizes under these conditions, but does not cocrystallize with PLA. The studies of quenched blends are extended to consider the effect of crystallinity on the ambient temperature aging of higher stereoregular PLA blended with PEG. The cooling rate from the melt is varied in order to vary the amount of PLA crystallinity. Changes in solid state structure during subsequent ambient temperature aging are compared with previous observations on quenched amorphous blends as shown in Fig. 4.18.

**Table 4.1** Effect of cooling rate on crystallization behavior of PLA and PEG in the PLA/PEG = 70/30 blend

Cooling rate (°C/min)	Cooling			Subsequent heating												
	PLA crystallization	PEG crystallization	PEG melting	PLA cold-crystallization	PLA melting	PLA cold-crystallization	PEG melting	PEG crystallization	PLA crystallization							
	$T_c$ (°C)	$\Delta H$ (J/g)	$\chi_c$ (%)	$T_c$ (°C)	$\Delta H$ (J/g)	$\chi_c$ (%)	$T_m$ (°C)	$\Delta H$ (J/g)	$\chi_c$ (%)	$T_m$ (°C)	$\Delta H$ (J/g)	$\chi_c$ (%)				
100	-	0	0	-	0	0	-	0	0	88	-26	38	151	29	43	
30	66	-3	4	8	8	-5	8	56	9	15	89	-14	21	150	29	43
20	70	-12	18	15	15	-16	27	58	20	34	89	-9	13	151	30	44
10	79	-22	32	26	26	-27	46	58	35	59	89	-1	1	150	30	44
5	90	-26	38	32	32	-35	59	59	36	61	-	0	0	151	29	43
2	98	-26	38	32	32	-35	59	59	36	61	-	0	0	151	30	44
1	105	-27	40	36	36	-36	60	59	37	63	-	0	0	151	30	44
PEG(1 °C/min)	-	-	-	42	-185	94	63	191	97	-	-	-	-	-	-	-



**Figure 4.18** AFM images showing the effect of ambient temperature aging on morphology of PLA/PEG=70/30 cooled at  $30^{\circ}\text{C min}^{-1}$ : (a) unaged, height image; (b) unaged, phase image; (c) unaged, schematic; (d) aged 2 h, height image; (e) aged 2 h, phase image; and (f) aged 2 h, schematic

Crystallization and aging of slowly cooled PLA/PEG blends have been studied. Although the blend constituents are crystallizable, the blends can be quenched from the melt to the homogeneous amorphous glass. Alternatively, the blends can also be crystallized by slowly cooling from the melt. The degree of crystallization

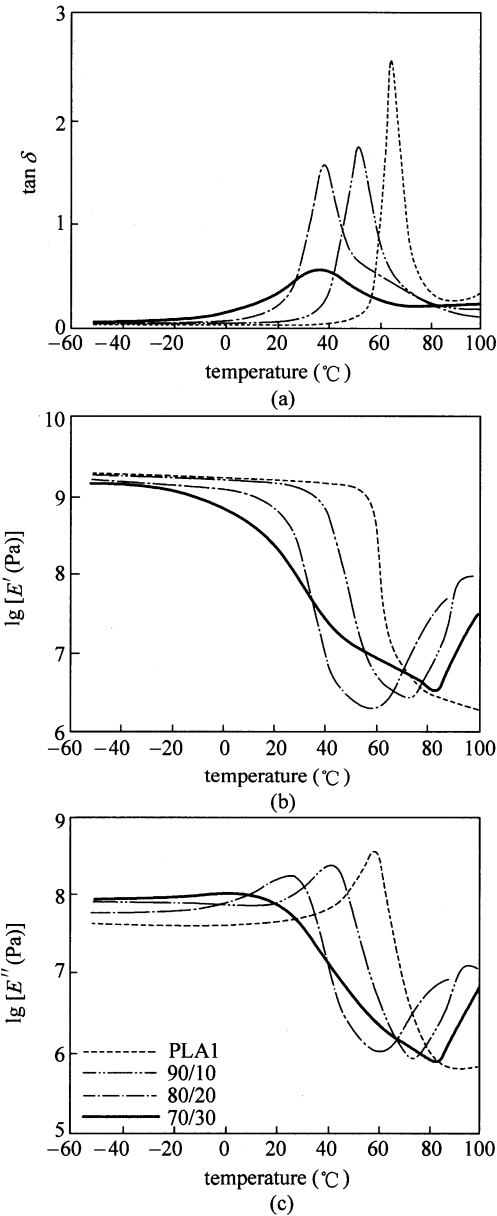
depends on the cooling rate. The maximum crystallinity of the PLA/PEG = 70/30 (wt/wt) blend is achieved with a cooling rate of 5°C/min or lower. Both PLA and PEG crystallize during slow-cooling. Proportionality between PEG crystallinity and PLA crystallinity indicates that PEG that is trapped in the intraspherulitic regions crystallizes much more rapidly than PEG in the interspherulitic amorphous regions. Crystallization of intraspherulitic PEG ceases as  $T_g$  of the intraspherulitic amorphous regions approaches ambient temperature. However, further crystallization of intraspherulitic PEG is possible by increasing the temperature.

In contrast to earlier studies that focused on aging of amorphous quenched blends, aging of crystalline blends has been studied. Partially crystallized blends consisting of large spherulites are dispersed in a homogeneous amorphous matrix. The solid state structure is not stable at ambient temperature if the amorphous phase is in the rubbery state, that is, the temperature is above its  $T_g$ : Epitaxial crystallization of PEG on the edges of spherulites depletes the surrounding region of that constituent, thereby increasing the  $T_g$  locally until vitrification essentially halts further crystallization of PEG. Regions of the amorphous phase that are more distant from the spherulites experience a different aging process. These regions undergo phase separation without crystallization. Formation of a PLA-rich matrix with dispersed PEG-rich domains is completely analogous to the aging process observed in completely amorphous quenched blends. Both aging processes alter the blend properties and increase stiffness. There is no indication that PLA crystallizes further during aging.

Attempts to improve the mechanical properties have focused on biocompatible plasticizers. Blending with PEG, the conventional name for low molecular weight (<20 000) PEO, improves elongation at break and softness of PLA. At ambient temperature, the desired mechanical properties are achieved by blending PLA with 30 wt% PEG. Table 4.2 shows the effect of PEG content on the thermal and mechanical properties of quenched PLA/PEG blends. However, there is evidence that the blend is not stable and the attractive mechanical properties are lost over time. The dynamic mechanical relaxation behavior and tensile stress-strain behavior of PLA and PLA/PEG blends are shown in Figs. 4.19 and Fig. 4.20 respectively.

**Table 4.2** Effect of PEG content on the thermal and mechanical properties of quenched PLA/PEG blends

Composition PLA1/PEG	$T_g$ from DSC (°C)	$T_g$ from E <sup>a</sup> (°C)	2% secant modulus (MPa)	Yield stress(MPa)	Fracture strain(%)
100/0	60	59	2500±200	68±2	3±0.5
90/10	39	40	900±50	26±1	180±10
80/20	21	24	150±20	4±0.5	260±20
70/30	12	–	20±2	–	300±30

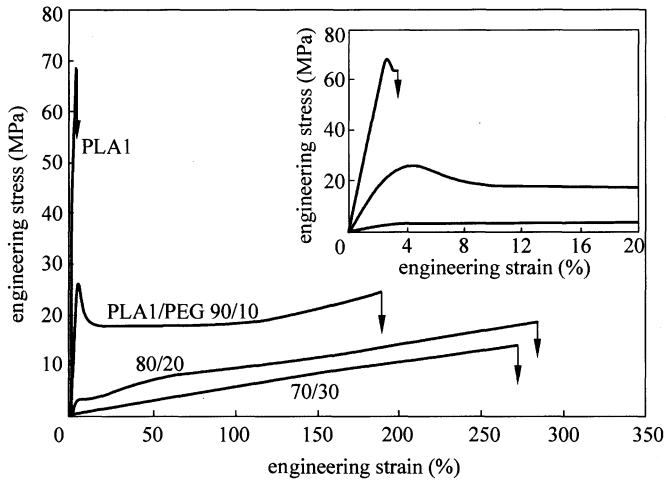


**Figure 4.19** Dynamic mechanical relaxation behavior of PLA and PLA/PEG blends: (a)  $\tan \delta$ ; (b)  $E'$ ; and (c)  $E''$

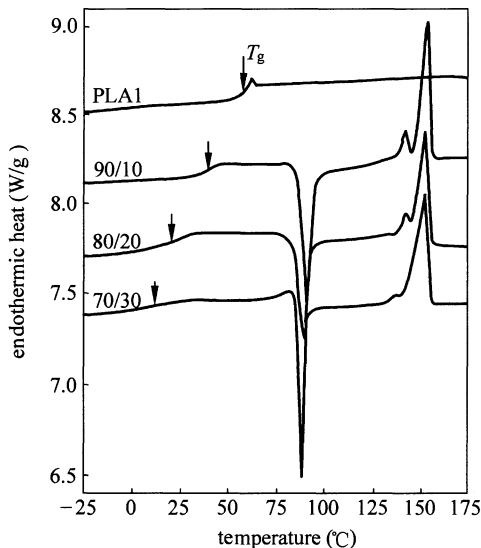
Stereoregularity of PLA may similarly affect miscibility with PEG and other plasticizers. The phase condition has important implications for aging. However, previous investigations have not addressed this possibility. Low stereoregular PLA and up to 30 wt% PEG are miscible at ambient temperature. Changes in mechanical properties over time are due to slow crystallization of PEG from the



homogeneous blend. Depletion of PEG increases the glass transition temperature ( $T_g$ ) of the amorphous phase until aging essentially ceases when  $T_g$  reaches the aging temperature [178]. The effect of stereoregularity on miscibility and aging of PLA/PEG blends has been investigated. Results obtained with blends of a high stereoregular PLA are compared with findings in the study of low stereoregular PLA as shown in Fig. 4.21.



**Figure 4.20** Tensile stress–strain behavior of quenched PLA and PLA/PEG blends at ambient temperature. The insert shows the modulus and yielding regions on an expanded strain scale



**Figure 4.21** Thermograms of quenched PLA and PLA/PEG blends with a heating rate of 10°C/min

Addition of 30 wt% PEG to PLA with low stereoregularity decreases  $T_g$  from above ambient temperature to below ambient temperature and thereby decreases the modulus and increases the ductility of this relatively rigid, brittle thermoplastic. Immediately after cooling from the melt, blends with up to 30 wt% PEG are amorphous and homogeneous with a single  $T_g$  that depends on composition in accordance with the Fox relationship. However, the blends with 20 wt% or more PEG are not stable at ambient temperature.

### 4.2.3 PLA/PHB

Polyhydroxyalkanoates (PHAs) are polyesters synthesized by many bacteria. These polymers are accumulated intracellularly under nutrient stress and act as a carbon and energy reserve. PHAs are non-toxic, biodegradable and biocompatible. They are produced from renewable sources. They have high degree of polymerization, are highly crystalline, isotactic and insoluble in water. Because of these properties, PHAs have a real potential in medical and pharmaceutical applications, such as drug delivery systems and tissue engineering.

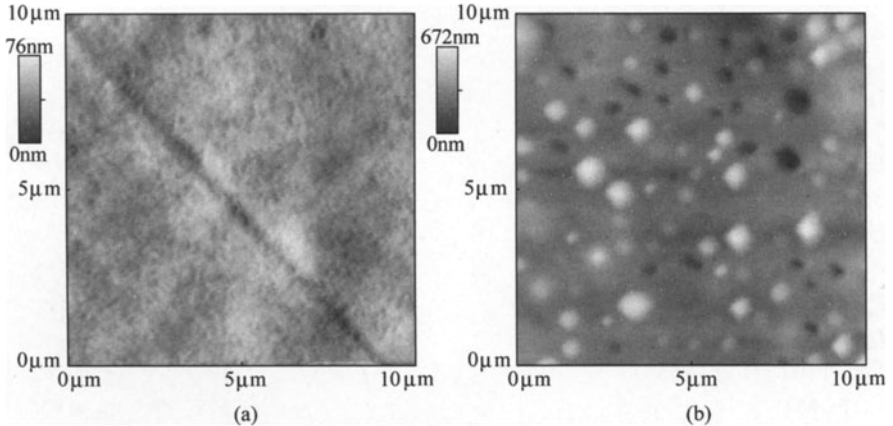
Solution blending has been used to study blending of PLA/PHB. For example, PHO and PLA50 blends are prepared by mixing different percentages w/w (100/0, 90/10, 80/20, 50/50 and 0/100) in chloroform solution (50 mg/mL) under vigorous agitation for 2 h. Polymer characteristics are shown in Table 4.3. The PHO/PLA solutions are then poured onto glass microscope slides and allow to crystallize at room temperature for 17 days, at which time the solvent is assumed to be completely removed from the films. The mixtures of PHAs with other polymers or oligomers are prepared by the same method. Cast PHA films measuring 3 cm×2.5 cm are detached from the glass slide having a mean thickness

**Table 4.3** Polymer characteristics

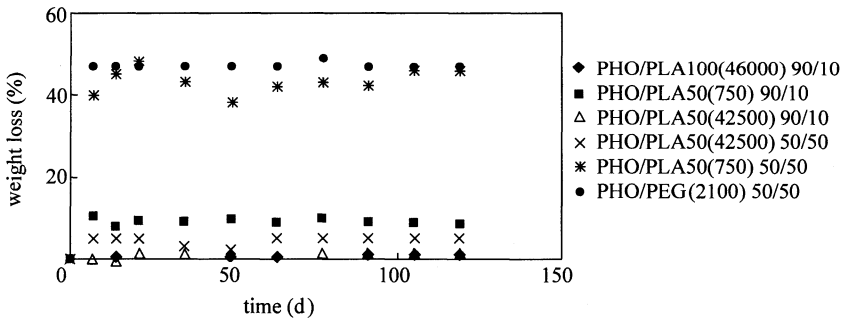
Polyme	$M_n$ (g/mol)	$I_p$	Chemical composition <sup>a</sup>
PHBHV	184 000	2.00	88HB, 12HV
PHO	50 000	1.93	85HO, 15HH
PHO—COOH	38 000	2.00	75HO, 25HO
PLA50	56 000	2.00	50LLA
PLA100	46 000	2.00	100LLA
PLA50	42 500	2.67	50LLA
PLA100	31 000	1.4	100LLA
PLA50	750	2.00	50LLA
PEG	2100	1.09	

<sup>a</sup> Determined by NMR 1H and 13C (HB = 3-hydroxybutyrate unit, HH = 3-hydroxyhexanoate unit, HO = 3-hydroxyoctanoate unit, HD = 9-carboxy-3-hydroxydecanoate unit, LLA = L-lactic acid).

of 70  $\mu\text{m}$  and a mean weight of 80 mg. The surface morphology is shown in Fig. 4.22 and weight loss of PHO blends at various incubation times is shown in Fig. 4.23. In the case of PHO—COOH, the polymer chloroform solution is cast directly into a flask (2.5 cm in diameter) [179, 180]. DSC data of PHO/PLA blends, DSC data of PHO/PLA50 blends and thermal characteristics of PHBVs blends are shown in Tables 4.4, 4.5 and 4.6, respectively.



**Figure 4.22** AFM images of the films: (a) PHO film; (b) blend of PHO/PLA 50 (750) 80/20



**Figure 4.23** Weight loss of PHO blends at various incubation time

Nodax<sup>TM</sup> is a registered trademark of a family of newly introduced PHA copolymers consisting of 3-hydroxybutyrate (3HB) and small amounts of other longer-chain 3-hydroxyalkanoate comonomer units [181]. Nodax<sup>TM</sup> materials are thermoplastic with properties comparable to highgrade polyethylene in terms of strength, flexibility, and toughness. On the other hand, Nodax<sup>TM</sup> has additional beneficial characteristics of polyesters, such as dyeability, printability, and compatibility with other materials. Although the target price of Nodax<sup>TM</sup> is

comparable to high-end commodity plastics, its compatibility with other materials suggest that it could be used as an additive to enhance the properties of other even less expensive materials. The structures of PLA and P(3HB-co-3HHx) are given in the next paragraph.

**Table 4.4** DSC data of PHO/PLA blends

PHO/PLA 100 ( $M_n = 31000$ ) <sup>a</sup>	100/0	90/10	0/100
$T_g$ (PHO) (°C)	-39	-39	-
$T_g$ (PLA) (°C)	-	+56	+57
$T_m$ (PHO) (°C)	+57	+51	-
$\Delta H_m$ (PHO <sup>b</sup> ) (J/g)	17	13	-
$T_m$ (PLA) (°C)	-	13	-
$\Delta H_m$ (PLA <sup>b</sup> ) (J/g)	-	18	52
PHO/PLA 100 ( $M_n = 4600$ )			
$T_g$ (PHO) (°C)	-39	-39	-
$T_g$ (PLA) (°C)	-	+57	+59
$T_m$ (PHO) (°C)	+57	+51	-
$\Delta H_m$ (PHO <sup>b</sup> ) (J/g)	17	10	-
$T_m$ (PLA) (°C)	-	+177	+180
$\Delta H_m$ (PLA <sup>b</sup> ) (J/g)	-	14	46

<sup>a</sup> Compositions mentioned in the table correspond to weight proportions.

<sup>b</sup> The values of enthalpy of fusion for blend components are normalized in compositions.

**Table 4.5** DSC data of PHO/PLA 50 blends

PHO/PLA 50( $M_n = 750$ ) <sup>a</sup>	100/0	90/10	80/20	50/50	0/100
$T_g$ (PHO) (°C)	-39	-39	-39	-35	-
$T_g$ (PLA) (°C)	-	-	-	-17	-17
$T_m$ (PHO) (°C)	+57	+51	+51	+54	-
$\Delta H_m$ (PHOb) (J/g)	17	18	16	15	-
PHO/PLA 50( $M_n = 750$ ) <sup>a</sup>					
$T_g$ (PHO) (°C)	-39	-39		-38	-
$T_g$ (PLA) (°C)	-	-		+46	+46
$T_m$ (PHO) (°C)	+57	-		+49	-
$\Delta H_m$ (PHOb) (J/g)	17	-		11	-
PHO/PLA 50( $M_n = 750$ ) <sup>a</sup>					
$T_g$ (PHO) (°C)	-39		-39		+53
$T_g$ (PLA) (°C)	-		+43		-
$T_m$ (PHO) (°C)	+57		+52		-
$\Delta H_m$ (PHOb) (J/g)	17		15		-

<sup>a</sup> Compositions mentioned in the table correspond to weight proportions.

<sup>b</sup> The values of enthalpy of fusion for blend components are normalized in compositions.

**Table 4.6** Thermal characteristics of PHBVs blends

	$T_g$ (°C)	$T_m$ (°C)	$\Delta H_f$ (J/g)
PHBV	+1	+160	78
PLA50	-17	–	–
PEG	–	+51	172
PHBV-PLA50(50/50) <sup>a</sup>	–	+117 +136 <sup>b</sup>	53c
PHBV-PEG(50/50) <sup>a</sup>	–	+50 +137 +153	n.d. 31°

n.d.: not determined.

<sup>a</sup> Compositions mentioned in the table correspond to weight proportions.

<sup>b</sup> Major peak.

<sup>c</sup> The values of enthalpy of fusion for blend components are normalized in compositions.

#### 4.2.4 PLLA/PDLA

The percentage of PLLA and PDLA in polymer blends affects the crystal structure, melting point, and glass-transition of PLA. A 50/50 PLLA/PDLA blend can have a different crystal structure from that of pure PLLA or PDLA. The 50/50 blend can form a stereocomplex, which is a complex between PLLA and PDLA. The stereocomplex structure of the 50/50 PLLA/PDLA blend has a glass-transition temperature of 65–72°C and a melting point of 220–230°C, which are both higher than those of pure PLLA and PDLA. The glass transition temperature of pure PLLA and pure PDLA is 50–65°C, and their melting point is 170–195°C.

The percentage of PLLA and PDLA in blends also affects the mechanical properties of PLA. Fibers made from a 50/50 PLLA/PDLA blend have been found to have relatively high Young's modulus (2.5–4.5 GPa) and tenacity (100–400 MPa), which increase with increasing take-up velocity from 1 to 5 km/min during melt spinning due to increased formation of stereocomplex crystallites and increased crystallinity from 8 to 36%. At a given molecular weight within  $1 \times 10^5 - 1 \times 10^6$  g/mol, a 50/50 blended film has been found to have greater tensile strength, Young's modulus, and elongation-at-break than a PLLA or PDLA film. PLA fiber has shown 40% strength loss at pH=4 and 110°C during dyeing, and it has exhibited complete strength loss at 130°C. Greater than 55% strength loss has been reported for PLA fiber at 110°C and pH=7–8, and pH=4–6 at the same temperature has resulted in 35%–40% strength loss for the fiber. Improved resistance of PLA to hydrolysis is therefore, desirable.

The percentage of PLLA and PDLA in blends is known to affect the enzymatic hydrolysis of PLA. For hydrolysis of PLA films at 20°C and pH=8.5, a well-stereocomplexed 50/50 PLLA/PDLA blend has shown a much lower rate of

hydrolysis than a semi-crystalline PLLA film, and PDLA film has given a much lower rate of hydrolysis compared to the PLLA film because the enzyme proteinase K has preference for PLLA. However, parameters other than the optical isomer content are varied in this case because PLLA has an 11% higher initial molecular weight than PDLA, and the percent crystallinity and orientation of the films are not reported. Differences in these parameters would affect the rate of hydrolysis.

Hydrolysis of PLA at 37°C and pH=7.4 without the use of enzymes is affected by the percentage of PLLA and PDLA in polymer blends. PDLA film has been observed to have an 11% higher hydrolysis rate constant and a greater extent of hydrolysis compared to a PLLA film. PDLA also has shown 23% weight loss after 24 months of hydrolysis while PLLA has only shown 10% weight loss. However, well crystallized PLLA and PDLA have given very similar hydrolysis behavior with both showing a 95%–96% drop in average molecular weight after 24 months of hydrolysis. A 50/50 PLLA/PDLA blend with pure PLLA and PDLA crystallites and no stereocomplex crystallites has given only a 15%–24% lower hydrolysis rate constant compared to pure PLLA and PDLA. In addition, these types of 50/50 blends have shown 14% weight loss after 24 months of hydrolysis, which is very close to the 10% loss for pure PLLA and 23% loss for pure PDLA. However, a well-stereocomplexed 50/50 blend has shown much better resistance to hydrolysis compared to well-crystallized pure PLLA and PDLA with a 53% reduction in the average molecular weight after 24 months of hydrolysis compared to a 95%–96% reduction for the pure homopolymers [182]. The contradictions in the studies are due to variability in parameters of the films other than the PLLA and PDLA content such as crystallinity, crystal structure, initial molecular weight, tenacity, Young's modulus, and elongation at break.

For studies where the percentages of PLLA and PDLA in blends are varied to study their effect on hydrolysis of PLA, it is difficult to hold the percent crystallinity, molecular weight, and other factors constant experimentally.

Molecular modeling has been used to explain how the percentages of PLLA and PDLA in PLA blends affect its resistance to hydrolysis. The 50/50 PLLA/PDLA blend is found to have the greatest resistance to hydrolysis among the blends included in the study, and this finding is supported by an earlier study finding that a 50/50 blended film is hydrolyzed to a lesser extent than a pure PLLA or PDLA film. The high potential energy of all the PLLA/PDLA blends before hydrolysis (9116–9156 kcal/mol) indicates that PLA is very unstable. The change in potential energy for hydrolysis,  $\Delta U$ , is found to decrease linearly (–83 to –45 kcal/mol) with increasing % PLLA or % PDLA within the range of 0–50%. Two blends have the same  $\Delta U$  when the % PLLA of one blend equals the % PDLA of the other blend, and for a given blend, the  $\Delta U$  for cleavage of one PLLA is equal to that for cleavage of one PDLA. This indicates that two blends have the same resistance to hydrolysis when the weight percentage and

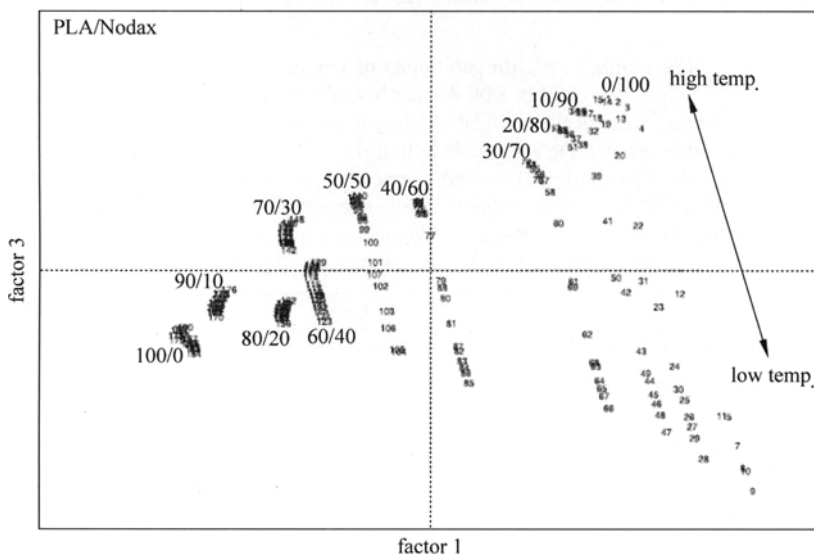
molecular weight distribution of PLLA in one blend is identical to that of PDLA in the other blend because the blends are mirror images of each other. Blending PLLA and PDLA in equal amounts improves the resistance of PLA to hydrolysis because the 50/50 blend is the most energetically stable blend before hydrolysis. The greater resistance to hydrolysis of the 50/50 blend is due to its stronger hydrogen-bonding and dipole–dipole interactions compared to that of pure PLLA and PDLA. This is based on the finding that the differences between the 50/50 blend and the pure homopolymers with respect to the  $\Delta U_{\text{electrostatic}}$  (42–44 kcal/mol), which account for the potential energy of the hydrogen-bonding and dipole–dipole interactions but not that of the dispersion forces or dipole-induced dipole interactions, are larger than their differences with respect to the  $\Delta U_{\text{van der Waals}}$  (3–4 kcal/mol). Additionally, the  $\Delta U_{\text{electrostatic}}$  is less negative for the 50/50 blend (–38 and –37 kcal/mol) than for pure PLLA (–80 kcal/mol) and PDLA (–81 kcal/mol). The stronger hydrogen-bonding and dipole–dipole interactions in the 50/50 blend are also based on the greater number of hydrogen-bonds and dipole–dipole interactions of lengths within 2.00 and 3.00 Å for the 50/50 blend and the shorter average length for its hydrogen-bonds and dipole–dipole interactions before hydrolysis. Of these intermolecular interactions, the hydrogen-bonding possibly has a greater effect than the dipole–dipole interactions on greater resistance of the 50/50 blend to hydrolysis because the 50/50 blend has more hydrogen-bonds than dipole–dipole interactions by a factor of about 9, and the average length of the 1952 shortest hydrogen-bonds (2.71 Å) in the 50/50 blend is lower than the average length of the 200 shortest dipole–dipole interactions in that blend (2.93 Å) as shown in Table 4.7.

**Table 4.7** The number of hydrogen-bonds of lengths within 3.00 Å (number of H-bonds  $\leq$  3.00 Å) and within 2.00 Å (number of H-bonds  $\leq$  2.00 Å), the average hydrogen-bond length of the shortest 1952 hydrogen-bonds (Avg H-bond length of 1952 shortest H-bonds), the average length of the 14 shortest hydrogen-bonds (Avg H-bond length of 14 shortest H-bonds), the number of dipole–dipole interactions of lengths within 3.00 Å (number of dipole–dipole interactions  $\leq$  3.00 Å), and the average length of the 200 shortest dipole–dipole interactions (Avg dipole–dipole length of 200 shortest dipole–dipole) for PLLA, PDLA, and the 50/50 blend before hydrolysis

	PLLA	PDLA	50/50
Number of H-bonds $\leq$ 3.00 Å	1953	1952	1992
Avg H-bond length of 1952 shortest H-bonds (Å)	2.72	2.72	2.71
Number of H-bonds $\leq$ 2.00 Å	14	14	17
Avg H-bond length of 14 shortest H-bonds (Å)	1.87	1.87	1.86
Number of dipole-dipole interactions $\leq$ 3.00 Å	202	200	216
Avg dipole-dipole length of 200 shortest dipole-dipole (Å)	2.94	2.94	2.93

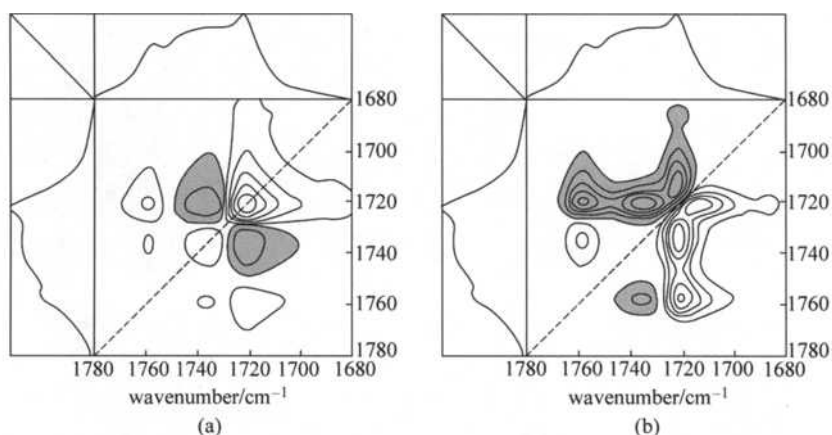
A combination of approaches, including peak positions, widths and intensities, principal components, and 2D correlation spectra, are used to analyze ATR FT-IR spectra collected as a function of temperature on a series of blends of poly(lactic acid) (PLA) and Nodax™ (P(3HB-co-3HHx) (3HHx = 13.4 mol%)). For the 40/60 PLA/Nodax™ blend, two types of crystalline Nodax™ C=O bands are observed. The band representing a more-ordered local C=O environment has a peak absorbance at a lower wavenumber than the second, less-ordered C=O species. The 2D IR correlation analysis also reveals that the more-ordered material disappears first upon heating of the sample and the amorphous Nodax™ C=O band formed before the lessordered P(3HB-co-3HHx) C=O band disappears. This observation is likely the result of the less-ordered crystalline form being replenished by thermally induced disordering of the more-ordered crystalline form [183]. Thus, the less-ordered crystalline material may be viewed as an intermediate form during the melting process. In the 80/20 PLA/Nodax™ blend, it is observed that the lower wavenumber peak in the PLA C=O doublet preferentially interacts with amorphous Nodax™.

These IR results suggest that Nodax™ has the potential to increase the toughness of PLA dramatically, thereby enlarging the design space of sustainable materials achievable by blending. This effect is expected to be most pronounced at 10%–20% Nodax™. At these compositions the crystallinity of Nodax™ is restricted, probably due to domain size restriction and inherent low nucleation density of Nodax™ as shown in Figs. 4.24 and 4.25.



**Figure 4.24** PCA score plot of factor 1 vs. factor 3 obtained from the entire mean-centered set of 179 IR spectra recorded as a function of temperature





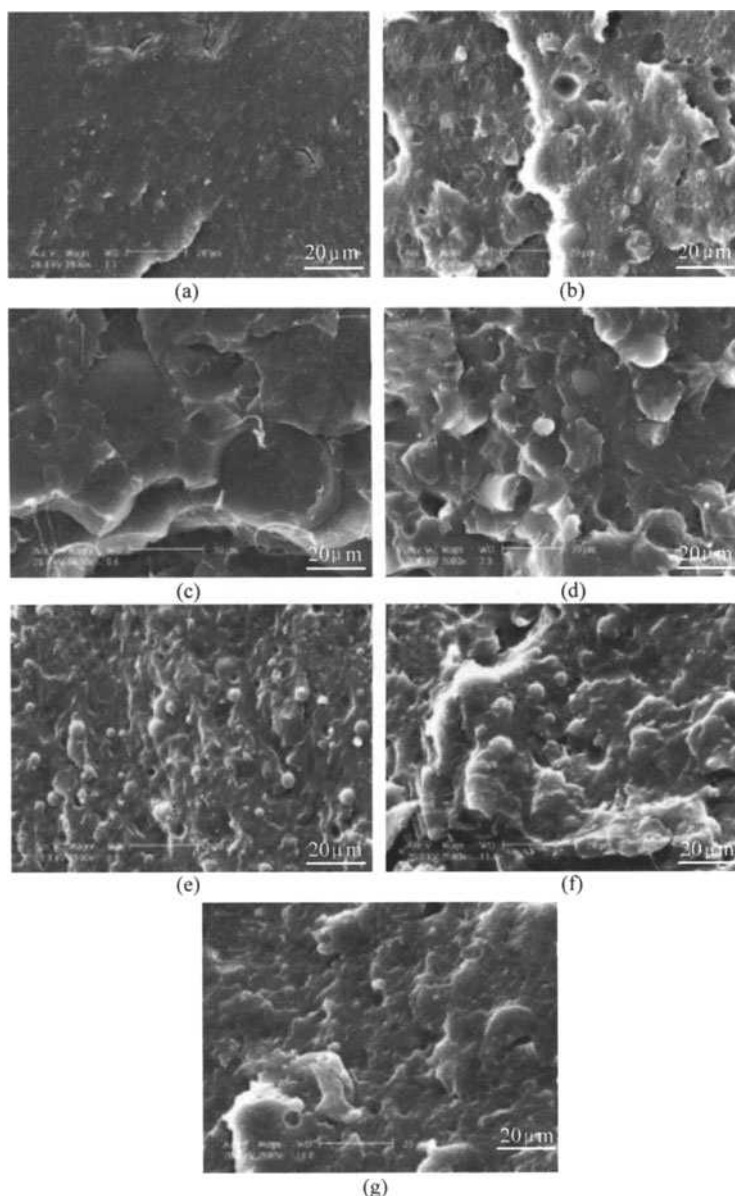
**Figure 4.25** Synchronous (a) and asynchronous (b) 2D IR plots of a set of 40/60 PLA/Nodax™ blend spectra recorded sequentially at 40, 60, 80, 100, 120, 140, and 160°C

#### 4.2.5 PLLA and PDLLA/PCL

Among those blends, PLA-blend-PCL materials are very interesting because of their wide variety of physical properties and biodegradability, in which the glassy PLA with high degradation rate shows better tensile strength, while the rubbery PCL with much slower degradation rate shows better toughness. The property complementarity between these two biocompatible polymers is very important to their blend materials because one can control the performance by adjusting the blending ratio and molecular characteristics as well as preparation conditions to meet requirements for various applications.

Hitherto many excellent works have been reported on the properties and applications of PLA/PCL blend. Favis's group prepared a co-continuous PLA/PCL blend and obtained a kind of microporous material with a single component structure through selective extraction of one of two components in this blend, which can be used as an ideal temporary scaffold for tissue engineering and drug delivery. Then, the evolution of this co-continuous morphology during annealing process was studied because it was pivotal to the interconnected porosity control. Tsuji's group also concentrated on the preparation of the microporous materials using PLA/PCL blend. Hence, the immiscible morphology, crystallization and enzymatic degradation behaviors of the blend have been investigated in detail. In addition, many other properties of the PLA/PCL blend, such as the thermal, mechanical and drug release properties, and non-enzymatic degradation have also been reported in the literature as shown in Fig. 4.26 [184].

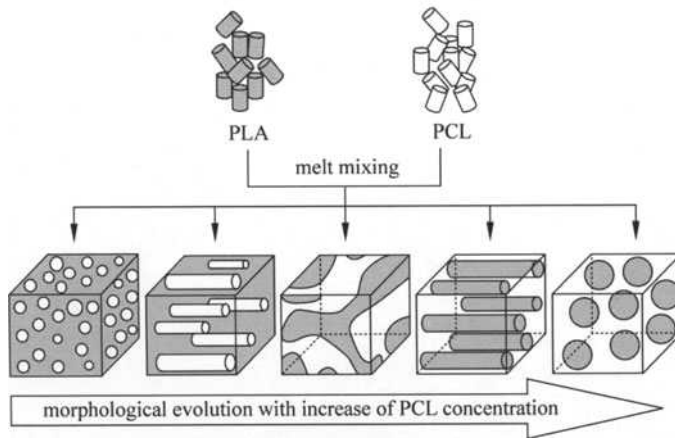
It is well known that for the immiscible polymer blends, their performance not only depend on properties of the polymer pairs used, but also highly on the



**Figure 4.26** SEM images for the PLA/PCL samples with various blending ratios (w/w): (a) 80/20, (b) 70/30, (c) 60/40, (d) 50/50, (e) 40/60, (f) 30/70 and (g) 20/80

morphology, which changes significantly during processing and as a result, is generally assumed to be a unique function of the flow history and of the properties of the polymer. Thus, it is very important to explore the rheological properties of the immiscible PLA/PCL blend as shown in Fig. 4.27. On the one hand, to optimize final properties of this blend material, good insight into the

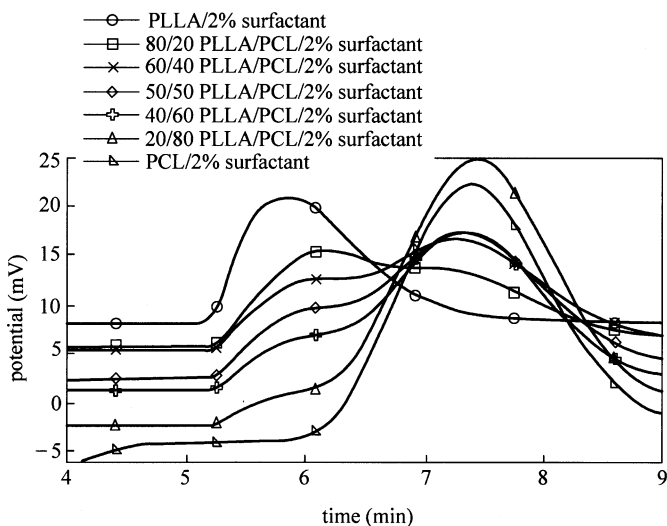
relation between the morphology development and rheological response is essential. On the other hand, from processing and application points of view, the rheological behavior of this multiphase system may provide some useful guidance to overcome the possible difficulties resulting from large changes in the viscoelastic properties during melt processing.



**Figure 4.27** Schematic diagrams of the morphological evolution for the PLA/PCL blend with increasing PCL concentrations. The white part is PCL phase and the gray part is PLA phase

The immiscible PLA/PCL blend, which has a high viscosity ratio between PLA and PCL components, is prepared by melt mixing for phase behavior and rheological measurements. The results show that phase inversion occurs at the region of about 60% PLA, in which the co-continuous morphology can be observed. Those viscous models present serious limitations to the viscosity ratio approach for the determination of phase inversion, indicating that elasticity has to be fully considered as an important factor also affecting the phase behavior. The Palierne model gives better fit to the linear viscoelastic properties of the blends compared with the G-M model, but both fail with prediction on the blend with co-continuous structure [185]. TTS is only valid for the co-continuous blend. The possible reason for this temperature independence is the relative low effective interfacial tension due to large characteristic size of the cocontinuous phase structure. The viscoelastic responses of the blends highly depend on the shear history and, show different sensitivity to the steady preshear, which is due to their different morphologies and the shear rate, as shown in Fig. 4.28. DSC data of PLLA/PDLLA blends (second heating), DSC data of PLLA/PDLLA/2% surfactant blends (second heating), DSC data of PLLA/PCL blends (second heating), DSC data of PLLA/PCL/2% surfactant blends (second heating), mechanical properties of PLLA/PDLLA blends, mechanical properties of 50/50

PLLA/PDLLA blends with different concentration of surfactant, mechanical properties of PLLA/PDLLA/2% surfactant blends, mechanical properties of PLLA/PCL blends and mechanical properties of PLLA/PCL/2% surfactant blends are shown in Table 4.8 – 4.16, respectively.



**Figure 4.28** GPC data of PLLA/PCL/2% surfactant blends

**Table 4.8** DSC data of PLLA/PDLLA blends (second heating)

PLLA/PDLLA	100/0	80/20	60/40	50/50	40/60	20/80	0/100
$T_g$ (°C)	57.4	58.1	56.6	57.6	53.3	52.2	51.6
$T_{cc}$ (°C)	109.9	116.8	120.7	123.4	130.2	–	–
$\Delta H_{cc}$ (J/g)	–39.1	–32.6	–24.1	–20.5	–13.6	–	–
$T_m$ (°C)	175.1	174	171.8	171.7	172.5	173.8	–
$\Delta H_m$ (J/g)	39.8	33.3	24.5	23.3	18	1.1	–

**Table 4.9** DSC data of PLLA/PDLLA/2% surfactant blends (second heating)

PLLA/PDLLA with 2% surfactant	100/0	80/20	60/40	50/50	40/60	20/80	0/100
$T_g$ (°C)	55	54.4	51.7	51.1	50	49.4	47.2
$T_{cc}$ (°C)	106.9	119.1	114.3	116	122.3	148.3	–
$\Delta H_{cc}$ (J/g)	–35.4	–32.3	–23.2	–17.5	–15.6	–2.3	–
$T_m$ (°C)	173.5	173.8	173.2	174.3	175.3	173.5	–
$\Delta H_m$ (J/g)	36.4	34.9	24.7	21.4	18	4.8	–

**Table 4.10** DSC data of PLLA/PCL blends (second heating)

PLLA/PCL	100/0	80/20	60/40	50/50	40/60	20/80	0/100
$T_g$ (°C)	57.3	56.4	–	–	–	–	–
$T_{cc}$ (°C)	109.9	91	91.3	90.2	91.1	91.1	–
$\Delta H_{cc}$ (J/g)	–42.5	–22.4	–16.5	–13.0	–14.3	–6.9	–
$T_m$ (PLLA) (°C)	175.1	170.3	170.1	170.5	171	171.7	–
$\Delta H_m$ (PLLA) (J/g)	39.7	33.9	28.1	22.4	22.4	12.1	–
$T_m$ (PCL) (°C)	–	–	52.0	52.3	52.3	52.8	53.1
$\Delta H_m$ (PCL) (J/g)	–	–	13.9	20.7	8.4	47.7	67.9

**Table 4.11** DSC data of PLLA/PCL/2% surfactant blends (second heating)

PLLA/PCL with 2% surfactant	100/0	80/20	60/40	50/50	40/60	20/80	0/100
$T_g$ (°C)	50.6	–	–	–	–	–	–
$T_{cc}$ (°C)	106.9	86.6	88.1	89.6	88.7	87.4	–
$\Delta H_{cc}$ (J/g)	–35.7	–19.3	–15.1	–13.4	–11.3	–3.7	–
$T_m$ (PLLA) (°C)	170.7	170.8	170.8	171.3	171.1	170.3	–
$\Delta H_m$ (PLLA) (J/g)	41.5	32.5	25.3	21.3	23.8	8.1	–
$T_m$ (PCL) (°C)	–	54.5	52.3	52.7	52.5	52.6	53.1
$\Delta H_m$ (PCL) (J/g)	–	2.0	5.9	14.3	27.5	41.9	69.5

**Table 4.12** Mechanical properties of PLLA/PDLLA blends

PLLA/PDLLA	100/0	80/20	60/40	50/50	40/60	20/80	0/100
Elastic modulus (MPa)	19.8±3.0	11.9±1.7	20.5±3.9	10.1±0.1	22.0±3.4	17.6±2.1	2.8±0.4
Yield strength (MPa)	31.5±4.5	34.5±2.5	39.2±7.7	35.8±1.3	38.5±5.4	32.3±2.0	25.9±3.3
Yield elongation (%)	11.9±0.0	13.8±2.7	8.2±0.9	11.9±1.9	10.9±3.8	6.3±1.4	11.4±1.0
Break strength (MPa)	34.1±2.5	35.2±2.4	41.1±8.1	36.2±1.5	39.2±5.4	32.6±2.1	26.9±3.3
Elongation at break (%)	56.3±1.9	59.8±9.3	38.1±4.6	56.2±3.4	60.8±6.6	62.5±9.0	54.6±3.8

**Table 4.13** Mechanical properties of 50/50 PLLA/PDLLA blends with different concentration of surfactant

Different conc. Surfactant (%)	0	0.5	1	2	3	5	10
Elastic modulus (MPa)	10.1±0.1	10.3±1.4	15.6±3.9	17.4±2.6	6.1±1.0	4.3±0.6	3.4±0.8
Yield strength (MPa)	35.8±1.3	32.4±1.6	32.4±0.8	29.8±1.5	20.9±1.7	14.1±0.6	11.2±0.5

(Continued)

Different conc. Surfactant (%)	0	0.5	1	2	3	5	10
Yield elongation (%)	11.9±1.9	26.7±8.9	21.3±0.7	15.3±1.0	49.7±5.3	21.8±4.7	44.2±1.8
Break strength (MPa)	36.2±1.5	32.6±1.5	30.8±3.9	30.7±1.9	21.3±1.7	14.5±0.7	11.7±0.6
Elongation at break (%)	56.2±3.4	76.8±4.4	43.9±4.9	86.4±12.9	98.9±10.1	92.2±6.7	61.6±6.3

**Table 4.14** Mechanical properties of PLLA/PDLLA/2% surfactant blends

PLLA/PDLA with 2% surfactant	100/0	80/20	60/40	50/50	40/60	20/80	0/100
Elastic modulus (MPa)	10.5±1.0	8.8±0.3	13.4±1.4	17.4±2.6	10.9±1.0	7.0±1.3	1.0±0.1
Yield strength (MPa)	25.2±3.1	22.1±4.2	26.4±1.3	29.8±1.5	23.4±1.2	24±0.2	16.7±1.9
Yield elongation (%)	7.1±1.8	16.9±4.9	10.2±0.9	15.3±1.0	19.2±2.6	14.6±2.1	44.6±11.3
Break strength (MPa)	25.4±3.0	22.3±4.2	26.9±1.5	30.7±1.9	23.8±1.3	24.5±0.5	16.8±1.9
Elongation at break (%)	84.7±2.2	53.2±5.7	62±13.2	86.4±12.9	85.6±6.3	89.6±22.1	114.6±11.3

**Table 4.15** Mechanical properties of PLLA/PCL blends

PLLA/PCL	100/0	80/20	60/40	50/50
Elastic modulus (MPa)	19.8±3.0	20.7±1.4	10.7±2.2	8.1±2.8
Yield strength (MPa)	31.5±4.5	40.4±1.6	18.9±1.9	16.3±1.3
Yield elongation (%)	11.9±0.0	12.1±4.3	15.0±3.4	18.3±3.7
Break strength (MPa)	34.1±2.5	41.2±1.5	19.3±1.9	16.9±1.3
Elongation at break (%)	56.3±1.9	129.5±32.9	152.1±11.8	139.6±17.4

**Table 4.16** Mechanical properties of PLLA/PCL/2% surfactant blends

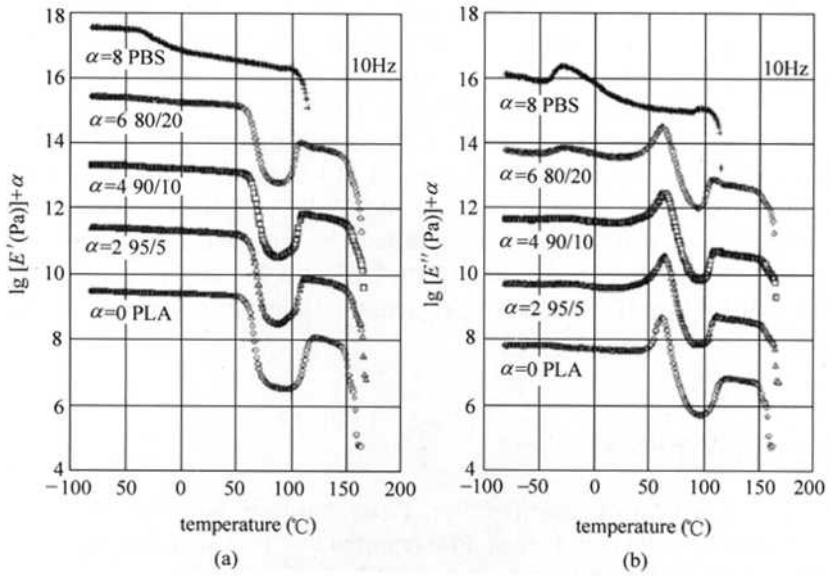
PLLA/PCL with 2% surfactant	100/0	80/20	60/40	50/50
Elastic modulus (MPa)	10.5±1.0	9.5±1.2	4.7±0.7	6.6±0.7
Yield strength (MPa)	25.2±3.1	19.3±2.2	12.7±0.8	9.9±0.5
Yield elongation (%)	7.1±1.8	14.7±1.4	28.9±10.6	4.6±1.7
Break strength (MPa)	25.4±3.0	20.1±1.4	12.9±0.8	10.4±0.5
Elongation at break (%)	84.7±2.2	129±4.8	130±14.2	123.7±13.3

Several observations in the last few paragraphs have shown that pure PLLA is hard and brittle, and that adding PDLLA or PCL can change its original properties. Solution-blending is an effective and easy way to achieve the purposes mentioned above. PLLA/PDLLA has poor miscibility, which can be significantly improved by addition of a copolymer of ethylene oxide and propylene oxide surfactant, and PLLA/PDLLA is hard and tough after adding the surfactant. The DMA data show that 40/60 PLLA/PDLLA is harder and tougher than PLLA, and that adding 2% surfactant to the blends can increase their miscibility, especially for the 50/50 PLLA/PDLLA blend. In comparison with PLLA/PDLLA blends, the PLLA/PCL blends have higher elongation and weaker mechanical properties [186,187].

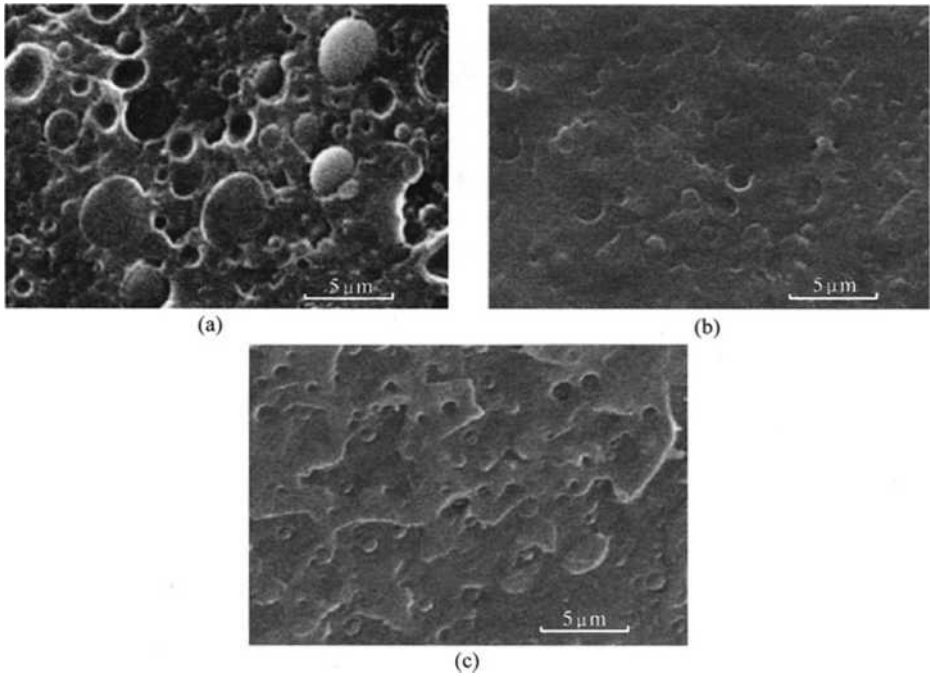
#### **4.2.6 PLA /PBS**

PBS is studied as a modifier for PLA, because both materials exhibit biodegradability. Although Park and Im reported that PLA was miscible with PBS in the amorphous region from the results of thermal analysis, recent studies have concluded that PLA is immiscible with PBS. Chen et al. found that a reactive organoclay with glycidyl functionality acted as a compatibilizer for PLA/PBS blends and enhanced the tensile properties such as tensile modulus and elongation at break. Furthermore, Takagi et al. and Shibata et al. clarified that adding PBS enhanced the cold-crystallization of PLA, i.e., increased the crystallization rate of PLA during heating process for a quenched sample. This phenomenon should be notified because PBS would act as nuclei for PLA crystallization, although the nucleating effect of PBS during the cooling process has not been directly detected. The result suggests that characteristics of phase-separated structure, such as the size and number of dispersed PBS particles in PLA matrix, have a significant influence on the crystallization rate of PLA and therefore the mechanical properties. In general, domain size of an immiscible polymer blend is determined by interfacial tension, viscosity ratio, and applied external force [188]. In other words, the morphology is predictable from the material parameters as well as the mixing condition. The interfacial tension between PLA and PBS is, however, unknown, which restricts the material design for the biomass based blends.

Structure and properties for binary blends of PLA and PBS are studied both in the solid and molten states. It is found that PLA and PBS are immiscible in the molten state and the blends exhibit phase-separated structure. The interfacial tension between PLA and PBS is estimated using a rheological emulsion model proposed by Palierne and found to be 3.5 mN/m as shown in Figs. 4.29, 4.30 and 4.31. Basic rheological parameters are also evaluated for PLA and PBS. It is suggested that the entanglement molecular weight of PLA is lower than that of PBS.

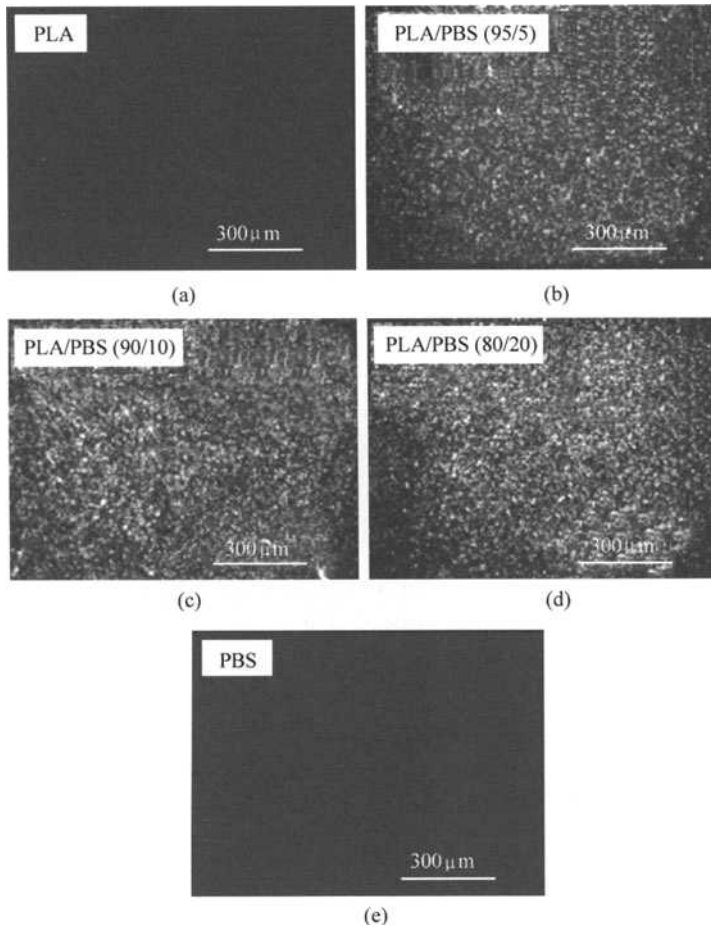


**Figure 4.29** Temperature dependence of (a) tensile storage modulus  $E'$  and (b) loss modulus  $E''$  at 10 Hz for PLA ( $\alpha=0$ ), PLA/PBS (95/5) ( $\alpha=2$ ), PLA/PBS (90/10) ( $\alpha=4$ ), PLA/PBS (80/20) ( $\alpha=6$ ), and PBS ( $\alpha=8$ )



**Figure 4.30** Scanning electron micrographs of (a) PLA/PBS (80/20), (b) PLA/PBS (90/10), and (c) PLA/PBS (95/5)





**Figure 4.31** Polarized optical micrographs under crossed polars at 100°C at the cooling process for PLA, PBS, and the blends

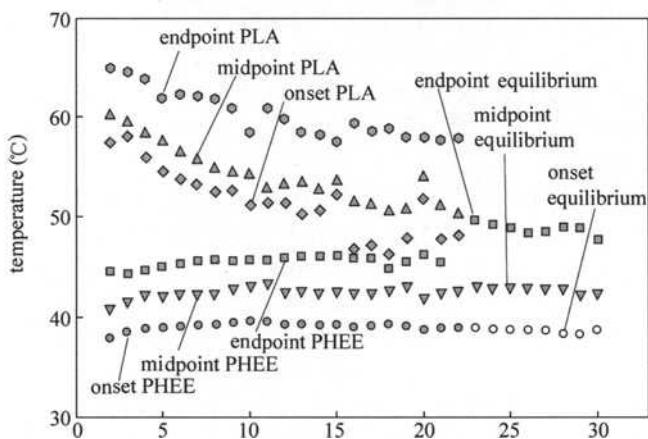
Further, there are distinct double peaks in the dynamic mechanical spectra ascribed to the glass transition of each component. Since the peak temperature of the  $E''$  curve is located at those of the individual pure components, mutual dissolution does not take place in the blends. Blending PBS, however, accelerates the crystallization of PLA, which is directly detected by DSC and optical microscope measurements at the cooling process. This is a significantly interesting phenomenon because molten PBS droplets act as crystallization nuclei for PLA. Furthermore, the PLA crystallites generated during the quench operation are responsible for the enhancement of the cold-crystallization behavior for the blends.

### 4.2.7 PLA /PHEE

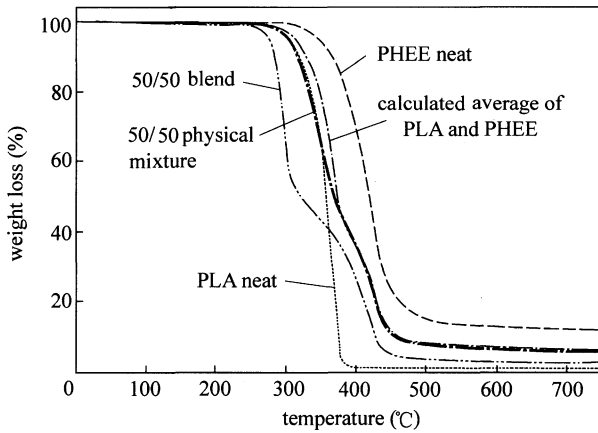
One of the most abundant polymeric materials from renewable resources is starch. While abundant and inexpensive, however, starch alone as a material does not offer satisfactory properties for many applications. Meanwhile, the synthetic biodegradable polymers with satisfactory properties are prohibitively expensive when compared to commodity non-biodegradable polymers. A common approach is to make blends/composites of starch and other biodegradable synthetic polymers to produce materials of satisfactory properties and a low overall cost.

Three-component blends of cornstarch, PLA, and poly(hydroxy ester ether) (PHEE), have been prepared with satisfactory properties and processibility [189]. Of the three biodegradable components, starch is used to reduce the overall cost, PLA provides thermal and mechanical properties, while PHEE acts as a processing aid and increases inter-component interactions.

The DSC thermograms (second heating) of PLA/PHEE blends, prepared by melt blending, show two distinguishable  $T_g$  as well as crystallization and melting enthalpies, corresponding to the  $T_g$  of the two neat polymers, and the crystallization and melting enthalpies of neat PLA, respectively. Such thermograms have traditionally been used as direct evidence that the two polymers are not miscible. However, the DSC cycling procedure shows that the  $T_g$ , as well as the enthalpies, are dependent on the number of DSC cycles to which the blends are subjected to. Eventually the two  $T_g$  merge into one single  $T_g$  and the enthalpies reach zero, i.e., PLA in the blends is no longer capable of recrystallizing, strongly suggesting that these two polymers are miscible as shown in Figs. 4.32 and 4.33.



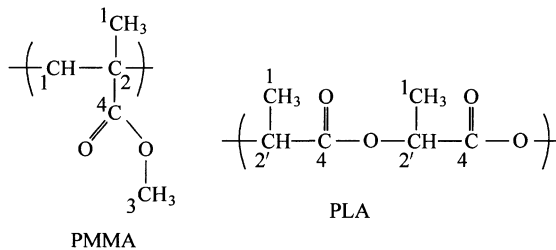
**Figure 4.32**  $T_g$  values for the 40/60 PLA/PHEE blend. Before nine cycles, two  $T_g$  values are distinguishable, afterwards only a single  $T_g$  is seen. The onset, endpoint as well as  $T_g$  (midpoint) are plotted to show the breadth of the transition



**Figure 4.33** Non-isothermal TGA tests on neat PLA, neat PHEE, 50/50 PLA/PHEE blend, and a physical mixture of equal amounts of the two neat polymers. A composed curve calculated from the average values of neat PLA and PHEE is also shown

#### 4.2.8 PLA /PMMA

PLA/PMMA blends as shown below are characterized by interesting bulk and surface properties, like their biodegradability, biocompatibility, and the possibility of using such materials for in vitro drug agent release materials. The literature references also the hydrolytic degradation kinetics of PLLA [190].



#### 4.2.9 PLA /PVA

PLA/poly(vinyl acetate) (PVAc) blends have been reported by Gajria et al. regarding their miscibility, physical properties, degradation and surface tension. The blends show a miscible phase, and the mechanical properties of the blends exhibit a synergism in the range of 5 to 30% PVAc content. However, the addition of PVAc to PLA leads to a dramatic decrease in the degradation rate for enzymatic degradation. On the contrary, the nonenzymatic and enzymatic hydrolysis of PLA is accelerated by the presence of the hydrophilic PVA, but these blends is

immiscible to induce a phase-separated system. Therefore, the blend of PLA and poly(vinyl acetate-co-vinyl alcohol) [P(VAc-co-VA)] is expected to have enhanced mechanical properties as well as a proper degradation rate if the blend forms a miscible phase at the specific vinyl alcohol content. In the case of P(VAc-co-VA) blends with other polymers, such as poly(*N,N*-dimethylacrylamide), poly(4-vinylpyridine) and poly(*b*-hydroxybutyrate) (PHB), the copolymer composition has been reported to be a major factor to affect their miscibility. Xing et al. have investigated the miscibility and morphology of blends of PHB and P(VAc-co-VA) with various copolymer composition in detail. At low vinyl alcohol content (9 mol%), the blend formed a miscible phase in molten state within whole composition range. But at higher vinyl alcohol content, the blends were partially miscible or immiscible systems.

Blends of PLA and PVAc [or P(VAc-co-VA)] are semicrystalline/amorphous systems. Generally in this system the morphology is known to depend on the extent of segregation of amorphous polymeric diluents. The diluent molecules can locate in interlamellar regions (between lamellar crystals), interfibrillar regions (between the fibrils or lamellar bundles in spherulites) or interspherulitic regions (between the spherulites). The amorphous diluents are often located at multiple sites, leading to coexistence of different types of morphology. These multiple location of the amorphous diluents results in multiple  $T_g$ -like transitions, although the polymers themselves are miscible at this temperature. Thermal characteristics of PLA/PVAc blends are shown in Table 4.17.

**Table 4.17** Thermal characteristics of PLA/PVAc blends

Mixing ratios of PLA/PVAc	$T_g$ (°C)	$T_m$ (°C)	$\Delta H_f$ (J/g)
100/0	62.8	176.1	27.1
90/10	58.1	171.0	26.3
80/20	49.4	168.0	19.0
70/30	46.5	166.7	14.3
60/40	44.9	166.4	9.0
50/50	42.9	166.6	4.8
30/70	38.9	166.0	–
0/100	35.3	–	–

The segregation of amorphous diluents is brought by the entropic force associated with the tendency to resume random-coiled conformations and the crystallization driving force of crystallizable components in the interlamellar regions [191]. In addition, these two entropic forces compete against the favorable interaction between the polymeric diluent and the amorphous portion of the crystalline polymer in the interlamellar regions. Therefore, the morphology in semicrystalline/amorphous blend is governed by the exclusion of amorphous components out of interlamellar regions and consequently governed by the

magnitude of interaction, the interlamellar distance, and the degree of supercooling. Kinetically, the chain diffusivity and the crystallization rate may also be important factors.

PLA can also be blended with PVAc. The miscibility, the crystallization behavior and morphology of P(VAc-co-VA) has been investigated by means of differential scanning calorimetry, synchrotron SAXS techniques, polarized optical microscopy and scanning electromagnetic microscopy.

PLA/PVAc blends were miscible systems for the entire composition range, but for the blends with even 10% hydrolyzed PVAc copolymer the phase separation and double glass transition are observed.

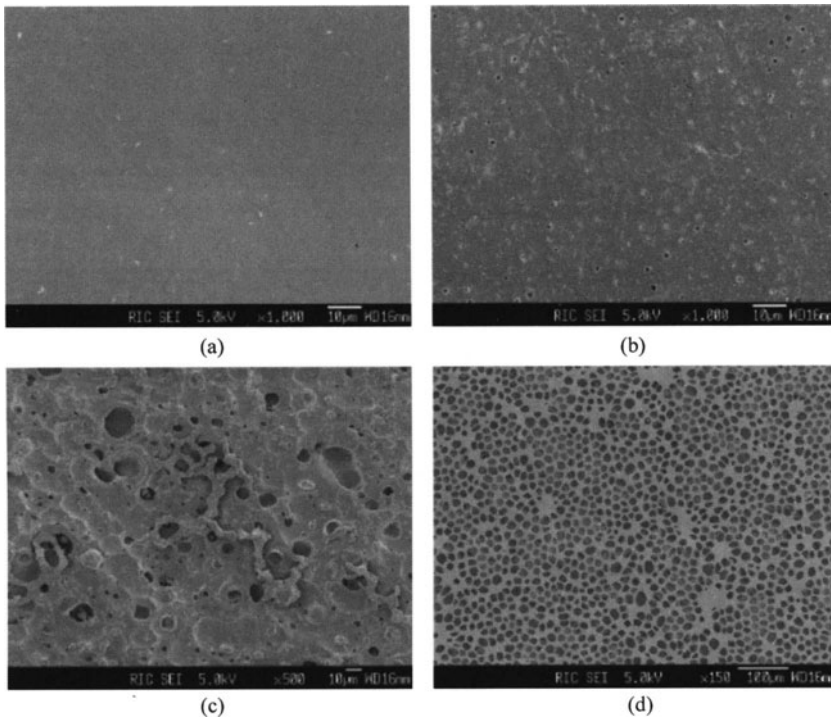
With increasing neat PVAc content, the heat of fusion decreases and the melting peaks shift to lower temperature in PLA/PVAc blends. The interaction parameters exhibit negative values for up to 10% hydrolyzed PVAc copolymer, but the values increase to positive ones with increasing the degree of hydrolysis. SAXS analysis and polarized optical microscopy observation indicate that a considerable amount of PVAc components is located in the interlamellar region. But P(VAc-co-VA) component is expelled out of the interfibrillar regions of the PLA spherulites in PLA/P(VAc-co-VA) blends.

SEM analysis reveals that the significant phase separation occurs at the high degree of hydrolysis. In the case of PLA/P(VAc-co-VA)<sub>30</sub> blend with 70/30 composition, the P(VAc-co-VA)<sub>30</sub> copolymer forms the regular domains with a size of about 10 nm as shown in Fig. 4.34.

### 4.2.10 PLA/ PBAT

Poly(butylene adipate-co-terephthalate) (PBAT) is an aliphatic-aromatic copolyester, which is fully biodegradable. It degrades within a few weeks with the aid of naturally occurring enzymes. The PBAT is a flexible plastic designed for film extrusion and extrusion coating. In the view of its high toughness and biodegradability, PBAT is considered as a good candidate of the toughener for PLA. PLA/PBAT blends show decreased tensile strength and modulus, however, elongation and toughness are dramatically improved. The failure mode changes from brittle fracture of the neat PLA to ductile fracture of the blends.

Generally, PLA is made into useful items using thermal processes, such as injection molding and extrusion. Therefore, its rheological properties, especially its shear viscosity ( $\eta$ ), have important effects on thermal processes, such as film blowing, paper coating, injection molding, sheet forming and fiber spinning. And the study of rheological properties of any polymeric melts is crucial to gain fundamental understanding of the processability of the materials. Melt rheology of amorphous and semicrystalline PLA and PLA/layered silicate nanocomposites have been reported, while relatively few studies on the rheology of PLA blends have appeared in the open literature. In the case of polymer blends, rheological



**Figure 4.34** SEM photographs of (a) PLA/PVAc 70/30, (b) PLA/P(VAc-co-VA)10 70/30, (c) PLA/P(VAc-co-VA)20 70/30, (d) PLA/P(VAc-co-VA)30 70/30

behaviors are strongly influenced by their structures and interfacial characteristics. The studies of melt rheological properties are not only important to understand the knowledge of the processability of these materials, but also are helpful to find out the structure-property relationship in blends [192].

PLA/PBAT blend is a kind of immiscible, two-phase system where PBAT disperses evenly in PLA matrix. It is revealed that linear viscoelastic limits of PLA/PBAT melts are smaller than that of neat PLA melt. At lower frequencies, storage moduli ( $G'$ ) of the blends increase with the increasing of PBAT content. But PBAT content has no significant effect on loss moduli ( $G''$ ) of the blends at all frequencies. The complex viscosities of PLA/PBAT melts show stronger shearthinning tendency at all frequencies. The slopes of  $G'(\omega)$  and  $G''(\omega)$  for all PLA/PBAT melts are considerably lower than those of neat PLA melt. Rheological characteristics of PLA and PLA/PBAT melts are shown in Table 4.18. The lower slope values and higher absolute values of dynamic moduli indicate the formation of entanglement structures in PLA/PBAT melts. The incorporation of PBAT results in a gradual increase of the viscosity and a decrease of flow activation energy. The relaxation moduli of the blends increase with the introduction of PBAT. The incorporation of PBAT results in a gradual increase of the steady viscosity of the blends. Besides, the incorporation of PBAT leads to a

decrease of flow index  $n$ .

**Table 4.18** Rheology characteristics of PLA and PLA/PBAT melts

Samples	PLA100	PLA95	PLA90	PLA85	PLA80	PLA70
Terminal region slope of $G(\omega)$	1.62	1.32	1.18	1.04	0.96	0.86
Terminal region slope of $G'(\omega)$	0.93	0.87	0.85	0.83	0.84	0.85
Flow activation energy $E_a$ (kJ/mol)	113.02	91.34	89.01	61.99	72.53	68.89
Flow index ( $n$ )	0.8555	0.8298	0.7374	0.7582	0.7260	0.7304

### 4.3 Composites

The commercial importance of polymers has been driving intense applications in the form of composites in various fields, such as aerospace, automotive, marine, infrastructure, military etc. Performance during use is a key factor of any composite material, which decides the real fate of products during use in outdoor applications. Whatever the application, there is often a natural concern regarding the durability of polymeric materials partly because of their useful lifetime, maintenance and replacement.

Commercially available PLA are copolymer of poly(*L*-lactide) with *D*-lactide. The amount of *D* enantiomers is known to affect the properties of PLA, such as melting temperature, degree of crystallinity and so on. PLA has good mechanical properties, thermal plasticity and biocompatibility, and is readily processed, and is thus a promising polymer for various end-use applications [193–196]. Even when burned, it emits no nitrogen oxide gases and generates only one-third of the combustible heat generated by polyolefins, and it does not damage the incinerator and provides significant energy savings [197]. So, increasing realization of the various intrinsic properties of PLA, coupled with knowledge of how such properties can be improved to achieve the compatibility with thermoplastics processing, manufacturing, and end-use requirements has fuelled technological and commercial interest in PLA. This section mainly discusses the preparative techniques so far used by various authors to produce PLA-based composites and their characterization.

Fibers are widely used in polymeric materials to improve mechanical properties. Vegetable fibers (e.g., cotton, flax, hemp, jute) can generally be classified as bast, leaf or seed-hair fibers. Cellulose is the major substance obtained from vegetable fibers, and applications for cellulose fiber-reinforced polymers have again come to the forefront with the focus on renewable raw materials [198–200]. Hydrophilic cellulose fibers are very compatible with most natural polymers.

The reinforcement of polymers using fillers is common in the production and processing of polymeric materials. The interest in new nanoscale fillers has

rapidly grown in the last two decades, since it is discovered that a nanostructure can be built from a polymer and a layered nanoclay. This new nanocomposite shows dramatic improvement in mechanical properties with low filler content. The reinforcement with filler is particularly important for polymers from renewable resources, since most of them have the disadvantages of lower softening temperatures and lower modulus. Furthermore, the hydrophilic behavior of most natural polymers offers a significant advantage, since it provides a compatible interface with the nanoclay.

### **4.4 Additives**

#### **4.4.1 Additives for PLA**

Additives are essential components in plastic formulations providing maintenance and/or modification of polymer properties, performance and long-term use. The extension of polymer properties by additives has played a substantial role in the growth of plastics. At the beginning of the plastics age additives were used mainly to maintain polymer properties and to help plastics to survive heat treatment during transforming processes. The next generation of additives provided extension of service life as well as modification of mechanical and physical properties. These well-established additives included antioxidants, heat stabilizers, light stabilizers and others addressing the requirements of modification for standard plastics and today's mass applications. The more recent developments of high-performance additives address more stringent or new requirements, more severe processing and use conditions and/or environmental concerns, but still with the main target of maintaining plastic properties. The future will introduce more and more new effects and functionalities through additives in plastic applications tailoring the properties of polymers and offering a vast potential of innovation in the plastics area. Recent examples of emerging technologies show that additives will not only modify the polymer itself and add new properties, but can also, when incorporated into the plastic, beneficially impact properties, which are of high value for user, as shown in Fig. 4.35. The role of additives used in plastics from the past to the present will be described with the focus on stabilization and performance of additives incorporated during melt processing, and future trends will be outlined.

Innovation in additives for plastics is unbroken. Due to the trend in plastics to larger volumes and less grades the importance of additives in plastics will not only sustain but also increase providing new applications and new effects. Even in the traditional area of polymer properties retention and extension new additives have been recently commercialized where improved performance for



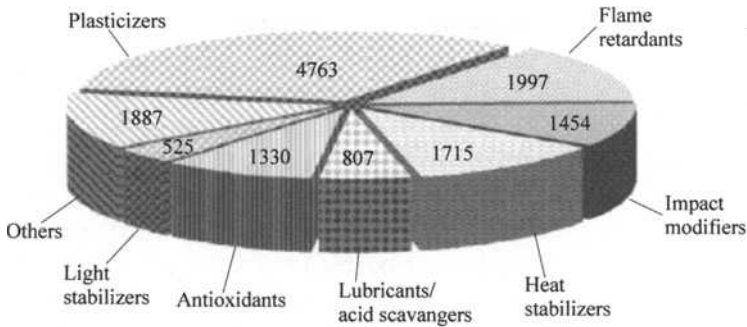


Figure 4.35 Turnover of additives (M\$) in 2004 [201]

demanding applications in selected use areas are required. Another driver for new additives is the increasing awareness of the environment protection. This area covers the introduction of oligomeric/polymeric stabilizers, graftable stabilizers, halogen free flame retardants as well as additives for the mechanical recycling of plastics. Beyond polymer properties extension additives will provide more and more functionalities to the polymer and to the product itself, taking over functionalities from the polymer (e.g. modification of polymers by reactive additives), being competitive to new polymer structures as well as introducing new effects (e.g. plant growth promoter). In a nutshell, plastic additives are and will be essential components in polymer formulations and will provide innovative solutions for the resin producer, the plastic converter and more and more value for the user of the plastic article.

#### 4.4.1.1 Flame retardants

Flame retardants play a vital role as additives for plastics. Improvements in flame retardant technology have continued to extend the areas where plastics can be used. Many good examples exist where high performance plastics have found new applications in automotive, electrical and electronic, and other industrial markets. For example, polyamides are now widely used in many of these high performance applications. Flame retardants are playing an increasingly important role in extending the use of polyamides in these areas as well as enhancing the material properties.

Selecting the right polymer, filler and additive combination for a particular application is key to any compounding operation. However, finding the correct relationship between performance and the final cost of the compound is critical if the application is ever likely to be successful.

In recently years, some researchers have given much attention on producing fully biodegradable biocomposites by compounding natural fibers with biodegradable polymers including PLA, starch plastics, soybean plastics and cellulosic plastics. Compared with traditional composites, these biocomposites have many advantages: totally biodegradable, lower density, higher tensile strength

## **Biodegradable Poly(Lactic Acid): Synthesis, Modification, Processing and Applications**

and modulus than common biodegradable polymers, lower cost and abundant renewable source. The fully degradable natural fibers/degradable polymer biocomposites have various applications such as automotive components, building materials, and the aerospace industry due to ecological and economical advantage over conventional composites.

However, there are still three factors limiting the applications of natural polymers and fibers in these fields: low compatibility with hydrophobic polymer matrices, thermal sensitivity at the temperature of compounding processes and flammability, which conflicts with the safety requirements. Compared with wide researches on surface treatment improving the compatibility and strengthening the interfacial interaction, there are few reports on the improvement of thermal stability and the fire retardancy. So improvement of flame retardancy of biocomposites becomes more and more important. Two general approaches to achieve flame retardancy in polymers are known as the additive and the "reactive" types, and the most expeditious method used to acquire flame retardancy is the incorporation of flame-retardants. The flame retardant is a kind of materials that can interfere with the combustion during a particular stage of the process so that the resulting system shows satisfactory flame retardancy. Flame retardants containing halogens and working by suppressing ignition and slowing flame spread are widely used for their high effect. However, during incineration, they evolve halogen acids that can act as irritants and what is more, halogen acids are also potential corrosive agents for metals. A growing demand to avoid these disadvantages has resulted in the development of non-halogen-containing flame retardants.

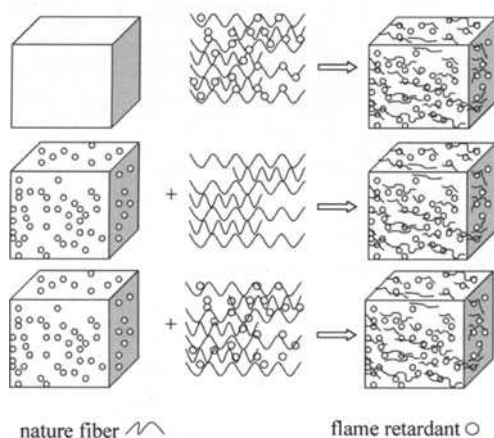
A kind of halogen-free flame retardant containing phosphorus -nitrogen has been extensively studied and reviewed in the literature for its low-toxicity and high efficiency. It is well known that most organophosphorus flame retardants form phosphoric acid at high temperature and prevent the burning of the substrate by condensed phase mechanism. Ammonium polyphosphate (APP), usually associating with char forming agent and nitrogen-containing components is generally called intumescent flame retardants and is widely researched and used.

The interface between flame retardant, fiber and polymers influences the mechanical properties and flame retardancy, so it is necessary to render the flame retardant, natural fibers and polymer compatibility to optimize the reinforcing properties and flame retardancy. Silane coupling agents are usually used to modify the interfacial region between the filler and organic polymer by forming a link between the components. At first, the hydrolysis reaction forms silanol groups, and then they react with hydroxyl groups found on filler surfaces to form siloxane bonds through a condensation reaction.

Halogen, phosphorus, antimony and metal oxide flame retardants and organosilicon are attracted one's attention. Effective additives are required to impart fire retardancy to polymeric materials used in a variety of applications. Traditionally, these have been gas-phase active additives, most commonly, organohalogen

compounds, or solid-phase active agents like organophosphorus compounds. Organophosphorus flame retardants are often very effective but may suffer from a cost disadvantage when compared with their organobromine counterparts. Organohalogen flame retardants are usually quite effective but their use is subject to several environmental concerns. The development of additives that could simultaneously promote both types of fire retardant action could make available flame retardants that are both more cost effective and more environmentally friendly than those currently in use. Several sets of compounds with the potential to display both solid-phase and gas-phase flame retardant activity have been prepared and evaluated.

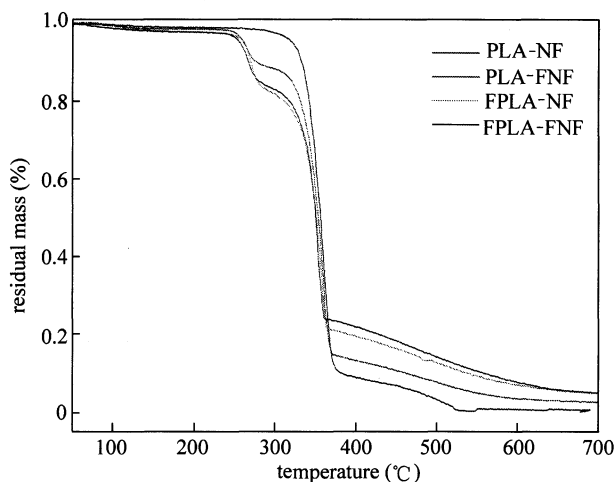
Ramie reinforced PLA biocomposite with flame retardancy by using APP on preserving the environmental friendly character of biocomposites has been studied. Here, natural fibers can be used as char formers in association with APP to increase the char yield of biocomposites. The flame retardancy of biocomposites is obtained by three means (Fig. 4.36). PLA is blended with APP, then the resulting flame-retarded PLA is combined with ramie fibers (ramie fibers with flame retardant treatment by APP is compounded with PLA) PLA and ramie both of which have been flame-retarded by APP are blended together.



**Figure 4.36** Schematic representation for fabricating the flame-retarded biocomposites: nature fiber and APP in PLA matrix [202]

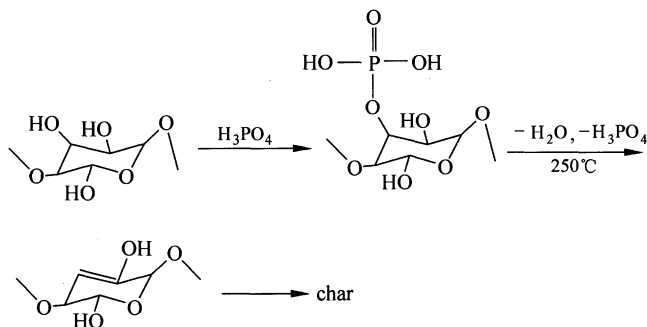
Figure 4.37 presents comparison of TGA curves of samples with different composition. In the case of PLA-NF, after initial loss of moisture and desorption of gases at about 50–150°C, a major decomposition occurs from 280 to 390°C. Nevertheless, the addition of APP changes the decomposition pattern. For PLA-FNF, FPLA-NF, FPLA-FNF (refer to Table 4.19 below), the starting decomposition temperature decreases markedly. At the same time, two significant mass loss stages appear on the curve from 240°C and 280°C and from 300°C to

385°C respectively, indicating that thermal stability is decreased. It is well known that APP releases phosphoric acid, poly-phosphoric acid and nonflammable gas when exposed to high temperature; the resulting acid is contributed to ramie intermolecular or intermolecular dehydration, then dehydrogenization, charring.



**Figure 4.37** TGA results of all the samples [202]

On the other hand, the acid from the pyrolysis of APP catalyzes the —C—O— bonding to break easily to produce many oligomers and small molecular substances at lower temperatures, as shown in Fig. 4.38. According to these facts, the first weight loss stage is due to the APP pyrolysis and advance decomposition of ramie fibers catalyzed by acid released from APP decomposition. The char residues for PLA-FNF, FPLA-NF and FPLA-FNF at 400°C are 13.31 wt%, 19.49 wt% and 21.90 wt%, respectively, which are obviously higher than that of 8.85 wt% for PLA-NF in the same experimental conditions. As for the flame-retarded composites, adding APP significantly increases residues at high temperature. The presence of APP enhances the charring process for composites. According to Holmes the materials treated with flame retardant produce fewer flammable gases and more chars and water, and eventually lead to dehydration and charring of the cellulose. Richard A. H. et al. has proposed that the char interaction or char bound effect has two stages. During 300–400°C, it is a consequence of initial physical interaction of both fiber and intumescent agent via partial liquefaction and subsequent mixing of adjacent contact zones. When the temperature increases to above 400°C, the matrix and the intumescent component begins to fully develop a bonded char structure. During the char formation, the heat and the amount of the volatile products are drastically reduced, and thermally stable char in high temperature contributes to the thermal and flame protection to matrix.



**Figure 4.38** Hypothetical charring process of phosphate ramie [202]

LOI and UL-94 tests are effective methods in evaluating the flame retardancy, and have become the main criterion in polymer industry. The results of flame retardancy (FR) measurement are presented in Table 4.20. PLA and ramie fiber are flammable materials, thus PLA-NF is completely consumed and shows melt dripping of material during UL-94 test. Although for PLA-FNF the fire is not extinguished after ignition, the flame spread is obviously slowed down. On the other hand, LOI values markedly increase from 19.1 for PLA-NF to 25 for PLA-FNF. These facts indicate that APP imparts the composites certain flame retardancy. However, the flame retardancy is not enough to extinguish fire itself, therefore higher APP content is needed to flame retard ramie reinforced PLA composites. The APP content in FPLA-NF and FPLA-FNF is 10.5 wt%, which is higher than that in PLA-FNF (4.5 wt%). From Table 4.20, it can be found that LOI values for FPLA-NF and FPLA-FNF are above 26 (28.1 and 35.6, respectively), and both FPLA-NF and FPLA-FNF achieve V-0 rating. Generally, when LOI value is greater than 26, materials can be considered to have flame retardancy [202]. The correspondingly high loading of APP in composites is beneficial to the enhancement of flame retardancy.

The PLA/ramie hybrid alone presents no efficient charring to protect matrix, however, the addition of APP in PLA/ramie hybrid enhances the formation of coherence of carbonaceous charring layer as protective shield and thermal barrier (as shown in Fig. 4.37). The TGA test demonstrates the increase of char. When cooperating with APP, ramie fiber being rich in polyhydric compound acts as a charring agent to form an intumescent flame retardant system. This intumescent mechanism has been discussed in the literature.

Compared to FPLA-NF, FPLA-FNF has a high LOI value and becomes completely non-flammable with 0 s burning time. This fact indicates FPLA-FNF has a better flame retardancy than FPLA-NF though they have the same APP loading. This can be explained by the “candlewick effect” caused by ramie fibers. There are two main reasons making the PLA-NF more flammable: (1) a continuous mass path can form to make the burning area fast spread to the flammable mass; (2) natural fibers have a larger heat conduction coefficient and

more flammable than PLA. The heat can easily transmit to PLA-NF underneath the burning area. This is so-called “candlewick effect”. The “candlewick effect” caused by ramie fibers imposes a big challenge for flame retardation. The time necessary for inflammation of PP/fiber, PP/fiber/APP system is decreased when compared to neat PP. The introduction of flax fiber into the polyolefin decreases the apparent stability and increases the conductivity of composite, thus the ignition becomes easy. The flame-retardant treatment of fibers prohibits the heat and flame transmission along the fibers, thus effectively preventing the “candlewick effect” and improving the flame retardancy of the composites. The formulation of the biocomposites is shown in Table 4.19 and the results of flame retardancy measurement are shown in Table 4.20.

**Table 4.19** The formulation of the biocomposites [202]

Sample	PLA(wt%)	F-PLA		NF(wt%)	F-NF(wt%)	
		PLA(wt%)	APP(wt%)		Ramie(wt%)	APP(wt%)
PLA-NF	70			30		
PLA-FNF	70				30	5.3
FPLA-NF		59.5	10.5	30		
FPLA-FNF		59.5	5.2		30	5.3

**Table 4.20** Results of flame retardancy measurement [202]

Sample	LOI	$t_1/t_2$ (s)	Dripping	UL94
PLA-NF	19.1	— <sup>a</sup>	Y	NC <sup>b</sup>
PLA-FNF	25	—	Y	NC
FPLA-NF	28.1	2/8	N	V-0
FPLA-FNF	35.6	0/3	N	V-0

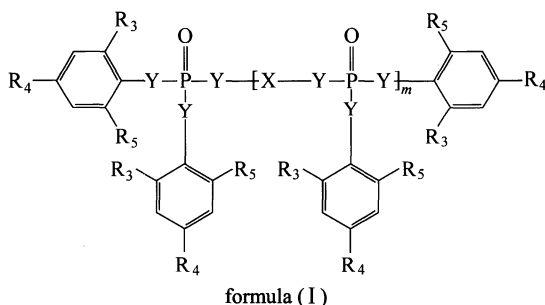
a. fire not extinguished after ignition; b. not classified by UL-94 rating.

Currently, there are three forces driving the development of new flame retardant for PLA. The first is the ever-increasing need to expand the use range of these materials, i.e., to utilize them in applications at the limits permitted by the properties of the materials—at high temperatures or high stress loads, for example. Flame retardants must be found which are effective under these conditions. Secondly, formulators wish to use as little flame retardant as possible to largely reduce the cost of the finished article. Thirdly, there is an ever-increasing demand for more environmentally benign (i.e. “greener”) flame retardants. Notwithstanding their superior effectiveness, limitations on the use of organohalogen flame retardants need to be addressed. Effective flame retardants that contain lower levels of halogen (or no halogen at all) are needed to be responsive to this concern.

All these considerations require more effective flame retardants be found. In particular, if compounds which would simultaneously promote char formation at the surface of the polymer and at the same time display effective gas-phase disruption of the flame propagating reactions could be found, a significant advance in flame retardant technology might be possible. In fact, there is some evidence that such agents might display a synergy of action (i.e., that the effectiveness of either mode of action might be enhanced in the presence of the other). This would mean that smaller amounts of total additive would be required to impart the desired level of flame retardancy. This should both lower the cost required to achieve an acceptable level of flammability and reduce the potential environmental impact that might accompany decomposition or release of the additive.

**Phosphorous Compound:** The phosphorous compound that can be used as fire retardant include a phosphoric acid ester compound, a phosphoamidate compound, an oxaphospholane compound, a carboxy phosphinic acid, phosphoric acid ester morpholide compound and a phosphazene compound. The phosphorous compounds are used alone or in combination. The phosphorous compound may be used in the amount of about 0.1 to 50 parts by weight based on 100 parts by weight of the base resin. The phosphorous compounds are described in detail as follows.

**Phosphoric acid ester compound and phosphoamidate compound:** The phosphoric acid ester compound and phosphoamidate compound are represented by the following chemical formula (I):



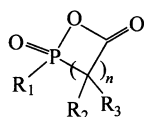
where  $R_3$ ,  $R_4$  and  $R_5$  are hydrogen or alkyl of  $C_{1-4}$ ,  $X$  is aryl of  $C_{6-20}$  or aryl of alkyl-substituted  $C_{6-20}$  that are derivatives from diol such as resorcinol, hydroquinol, bisphenol-A and bisphenol-S,  $Y$  is oxygen or nitrogen, and  $m$  is in the range of 0 to 4.

If  $m = 0$  in above formula, the compounds may be triphenyl phosphate, tricresyl phosphate, trixylenyl phosphate, tri(2,6-dimethylphenyl) phosphate, tri(2,4,6-trimethylphenyl) phosphate, tri(2,4-ditertiarybutylphenyl) phosphate, tri(2,6-ditertiarybutylphenyl) phosphate and the like, and if  $m = 1$ , the compounds may be resorcinol bis(diphenyl) phosphate, resorcinol bis(2,6-dimethylphenyl) phosphate, resorcinol bis(2,4-ditertiary butylphenyl) phosphate, hydroquinol(2,6-

## Biodegradable Poly(Lactic Acid): Synthesis, Modification, Processing and Applications

dimethylphenyl) phosphate, hydroquinol(2,4-ditertiarybutylphenyl) phosphate and the like. The phosphorous compounds are used alone or in combination.

**Oxaphospholane Compound:** The oxaphospholane compound is represented by the following chemical formula (II):

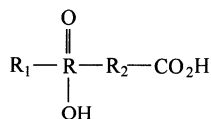


formula (II)

where  $R_1$  is hydrogen, alkyl of  $C_{1-6}$ , or aryl of  $C_{6-15}$ ,  $R_2$  and  $R_3$  are hydrogen or alkyl of  $C_{1-6}$ , and  $n$  is in the range of 1 to 3.

The examples of the oxaphospholane compound are 2-methyl-2,5-dioxo-1-oxa-2-phospholane and 2-phenyl-2,5-dioxo-1-oxa-2-phospholane. The oxaphospholane compounds are used alone or in combination.

**Carboxy phosphinic acid compound:** The carboxy phosphinic acid compound is represented by the following chemical formula (III):

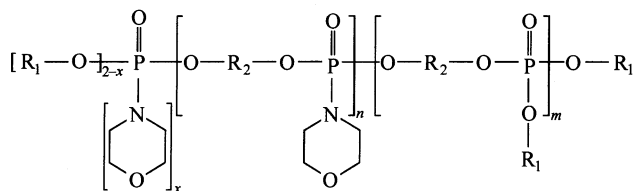


formula (III)

where  $R_1$  is hydrogen, alkyl of  $C_{1-12}$ , aryl of  $C_{6-10}$ , or alkyl-substituted aryl of  $C_{7-15}$ ,  $R_2$  is alkylene of  $C_{1-12}$ , ring type alkylene of  $C_{1-12}$ , aryl of  $C_{6-12}$ , or alkyl-substituted aryl of  $C_{6-12}$ .

The examples of the carboxy phosphinic acid compound are 2-carboxy-ethyl-methyl-phospanic acid, 2-carboxy-ethyl-phenyl-phospanic acid, and 2-carboxy-methyl-phenyl-phospanic acid. The carboxy phosphinic acid compounds are used in single or in combination.

**Phosphoric Acid Ester Morpholide Compound:** The phosphoric acid ester morpholide compound is represented by the following chemical formula (IV):

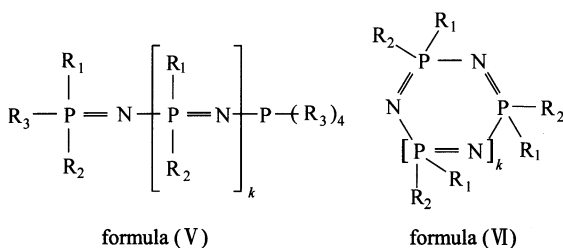


formula (IV)



where  $R_1$  is a  $C_{6-20}$  aryl group or an alkyl-substituted  $C_{6-20}$  aryl group,  $R_2$  is a  $C_{6-30}$  aryl group or an alkyl-substituted  $C_{6-30}$  aryl group,  $x$  is 1 or 2, and  $n$  and  $m$  are number average degree of polymerization and  $n + m$  is 0 to 5.

Phosphazene Compound: The linear phosphazene compound is represented by the following chemical Formula (V) and the cyclic phosphazene compound is represented by the following chemical Formula (VI):



where  $R_1$ ,  $R_2$ , and  $R_3$  are independently alkyl, aryl, alkyl substituted aryl, aralkyl, alkoxy, aryloxy, amino or hydroxyl, and  $k$  is an integer from 0 to 10. The alkoxy and aryloxy groups may be substituted with alkyl, aryl, amino, hydroxyl, nitrile, nitro, aryl with hydroxy, and the like.

CLARIANT's pigments and additives division, Sulzbach, Germany, launched two additions to its Exolit OP flame retardants range at the 11th Flame Retardants Conference in London, UK. These non-halogenated additives have been developed for use in glass fibre reinforced thermoplastics.

Exolit OP 1311 (TP) and 1312 (TP) are based on metal phosphinates. Both flame retardants are characterized by a high comparative tracking index (CTI) of 600 Volt and low compound density. Clariant claims that the Exolit OP additives have very little affect on the mechanical properties of the compound and that only small amounts are needed to achieve a flame retardant classification of UL 94 V0 or a glow wire flammability index (GWFI) of 960°C.

The two products are reported to be easily dispersed, have good rheological properties and can be easily coloured. They can be used in injection moulding processes, but the manufacture of complex shapes often requires high temperatures and high injection speeds. Exolit OP 1312 is a specially-stabilised system for polyamide 66 and its main applications are in flame retarded injection mouldings for the electrical and electronic industries.

#### 4.4.1.2 Impact Modifier

Degradable materials are being investigated for a wide variety of packaging applications to ameliorate the environmental problems associated with conventional, non-degradable packaging plastics, such as polypropylene, polyethylene, poly(vinyl chloride) and polyethylene terephthalate. A promising degradable packaging material is polylactide. When contacted with water, polylactide depolymerizes and decomposes into naturally occurring substances, such as lactic acid, and

ultimately can be reduced to water and carbon dioxide. This process is facilitated by heat such as is found in composting.

In typical packaging applications, a desirable degradable packaging material requires a high degree of flexibility and a high impact strength. The amorphous and semi-crystalline forms of polylactide lack these properties. Amorphous and semi-crystalline polylactide have a low impact strength. Both semi-crystalline and amorphous polylactide have a low degree of flexibility.

A degradable film having a high impact resistance that is particularly suitable for packaging applications can be prepared using impact modifiers. The degradable film consists of (a) at least about 50% by weight of a crystalline polylactide as the primary polymer; (b) a degradable impact modifier; and (c) a degradable plasticizer having a weight average molecular weight of no more than about 2000 Da.

Surprisingly, it has been discovered that the incorporation of both degradable impact modifier and plasticizer in the blend yields an attractive combination of high tensile and impact strengths on the one hand and high flexibility on the other. The degradable impact modifier for degradable PLA should have a glass transition temperature less than about 0°C to decrease the glass transition temperature of the degradable film and thereby provide increased impact strength. They should be a degradable, non-toxic elastomer or a degradable, non-toxic non-elastomer provided that the elastomer or non-elastomeric polymer are blend compatible with polylactide. Because of the lack of commercially available degradable elastomers, degradable non-elastomeric polymers can be used. Unlike elastomers which typically improve impact strength by absorbing the energy of the impact through deformation of the elastomer, non-elastomeric polymers having a low glass transition temperature decrease the glass transition temperature of the film, thereby softening the film and increasing the amount of energy that the film can absorb through deformation. Although the end groups on the non-elastomeric polymers can act as a plasticizer and decrease the film's tensile strength, the degree of end group plasticization is believed to decrease as the length of the elastomeric chain increases. This limits the amount of decrease in tensile strength relative to shorter chain, lower molecular weight elastomeric polymers. The impact modifiers include polymers such as: (a) PEG or PEO having a preferred weight average molecular weight ranging about 2000 to about 25 000 Da; (b) polycaprolactone having a preferred weight average molecular weight ranging from about 2000 to about 150 000 Da; (c) a copolymer of LA or ester thereof and caprolactone having a preferred weight average molecular weight ranging from about 2000 to about 200 000 Da; and (d) an oligomer of lactic acid having a preferred weight average molecular weight ranging from about 500 to about 10 000 Da. The content of the modifier in the degradable film preferably ranges from about 3% to about 25% by weight.

The degradable film can contain more than one impact modifier to realize improved impact and tensile strengths. The first degradable impact modifier is

PEG and/or PEO, which have been found to have a relatively high influence on impact strength compared to other degradable impact modifiers. The second degradable impact modifier is a polycaprolactone homopolymer or a copolymer of lactic acid or an ester thereof with caprolactone, which have been found to have a relatively high influence on tensile strength. It has been discovered that the use of two degradable impact modifiers as above mentioned produces a film having improved influence on tensile strengths compared to blends having only one degradable impact modifier. PEG and PEO have been found to have a greater influence on impact strength than polycaprolactone or the copolymers. However, polycaprolactone and the lactic acid/caprolactone copolymers have been found to provide significantly improved tensile strengths compared to PEG or PEO. The amounts of the various components used in the blend are important to realize these improved properties. The blend contains preferably from about 1 to about 15% by weight of poly(caprolactone) and/or lactic acid/caprolactone copolymer. The amounts of the polylactide and degradable plasticizer are as set forth above.

The molecular weight of the degradable impact modifier has a significant influence on the properties of the film. The preferred molecular weight depends on the kind of impact modifier. When the impact modifier is polycaprolactone, the impact modifier has a weight average molecular weight preferably ranging from about 3000 to about 140 000 Da. When the impact modifier is a copolymer of lactic acid or its esters with caprolactone, the impact modifier's weight average molecular weight preferably ranges from about 3000 to about 180 000 Da. When the impact modifier is an oligomer of LA, the impact modifier's weight average molecular weight preferably ranges from about 550 to about 9000 Da. To inhibit premature degradation of the polylactide, the end groups of the LA oligomers are preferably rendered less reactive by end capping. Finally, when the impact modifier is PEG and/or PEO, the impact modifier's weight average molecular weight preferably ranges from about 3000 to about 20 000 Da. At weight average molecular weights above 25 000 Da, PEG and PEO are typically not degradable in the environment.

The amount of the degradable impact modifier required to realize the desired film properties depends upon the degree of miscibility of the modifier in the polylactide. The properties of polymer blends are strongly dependent upon the degree of compatibility and/or miscibility of the components. Only a few blends are truly miscible at the microscopic level while most are semi-miscible. Typically, the amount of modifier in the film ranges from about 10 to about 25% by weight of the film.

Rohm and Haas improves the performance of green packaging with the launch of their new additive, PARALOID™ BPM-500, an impact modifier that broadens the usability of bioplastics by making them stronger without sacrificing clarity. PARALOID™ BPM-500 supports the packaging industry's movement toward sustainability by enhancing PLA polymer, an innovative bioplastic derived from

a renewable resource, such as corn, and used in some packaging applications.

The packaging industry's move toward PLA resin has been hampered by unmodified PLA being somewhat weaker and more brittle than traditional materials. Previous attempts to strengthen PLA packaging have sacrificed transparency in their efforts. Rohm and Haas' new PLA additive, PARALOID™ BPM-500, toughens PLA packaging while maintaining clarity, thereby fulfilling a key industry need.

Using dispersible nanoparticles that do not scatter light, PARALOID™ BPM-500 allows for the production of PLA packaging material that exhibits less than 10% haze at 5% loading, a significant advantage compared to other additives on the market. Combining this visual transparency with the stronger impact and tear-resistance achieved with PARALOID™ BPM-500 creates an improved consumer experience and an eco-friendly product. In addition, PARALOID™ BPM-500 complies with food contact requirements in Europe and with room temperature food contact requirements in the United States.

### **4.4.1.3 Heat Stabilizers**

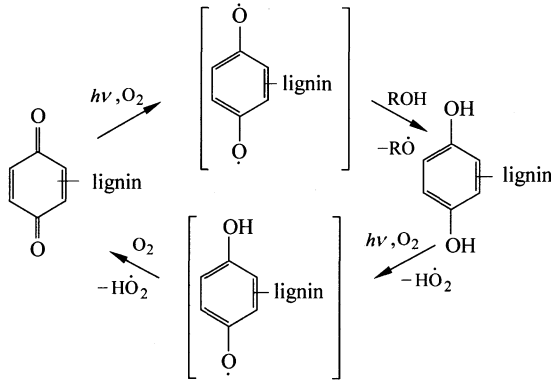
Heat stabilizers are used to prevent oxidation of plastics by heat, particularly during processing but also in application.

The stabilizers must be effective over long periods of time. It is important that they do not volatilize, can not be leached out or otherwise be removed from plastic materials. It is also important that the stabilizer is distributed in the polymer matrix where it is most needed, particularly on the surface of the amorphous fraction. In semicrystalline materials, the stabilizer is substantially excluded from the crystalline part and the spherulites of the polymer.

### **4.4.1.4 Photostabilizers**

Photostability of the polymers is one of their most important properties. To solve the problem of polymer stabilization, a number of different stabilizers have successfully been applied. Among them, both 2-hydroxyphenyl benzotriazoles and hindered amines such as 2,2,6,6-tetramethyl piperidines are of a great interest due to their high photostabilizing efficiency. These two groups differ in their action, although both are classed as photodegradation stabilizers. Hindered amine stabilizers are at present the most effective stabilizers for long-term stabilization of polyolefins, polystyrenes and polydienes, their copolymers and terpolymers. The 2,2,6,6-tetramethyl piperidines are multifunctional stabilizers. They inhibit the processes of autoxidation by transformation of the parent amines to *N*-oxil radicals either by reaction with peroxy radicals or occasionally by reaction with singlet oxygen. The *N*-oxil radicals stop oxidative degradation by coupling of alkyl radicals. In contrast to 2,2,6,6-tetramethyl piperidines, 2-hydroxyphenyl benzotriazoles prove to be UV-absorbers, as shown in Scheme 4.1. They are transparent to visible light and are believed to dissipate the absorbed

energy in a harmless manner, i.e. to convert the absorbed photon energy into heat without being chemically affected [203].



**Scheme 4.1** Phenoxo Quinone Redox Cycle involved in photoyellowing and photobleaching [203]

A great deal of efforts have been made in recent years for obtaining stabilizers with a better compatibility and higher molecular weight showing a lower migration tendency in comparison to the additives with low-molecular weights. Table 4.21 shows the photostabilizing additive description and formulations. The

**Table 4.21** Photostabilizing additive description and formulations [203]

Formulation #	Additive description	Trade name	Molecular mass (g/mol)
<b>Single additive</b>			
1	Low m.w. diester	Tinuvin 770	481
2	Medium m.w. diester	Tinuvin 123	737
3	High m.w. diester	Tinuvin 622	3100–4000
4	Tertiary amine triazine	Chimassorb 119	2286
5	Secondary amine triazine	Chimassorb 944	2000–3100
6	UVA (benzotriazole)	Tinuvin 360	659
7	UVA (benzophenone)	Chimassorb 81	326
<b>Combination additive formulation</b>			
8	UVA (benzotriazole) + low m.w. diester	Tinuvin 360 + Tinuvin 770	
9	UVA (benzophenone) + low m.w. diester	Chimassorb 81 + Tinuvin 770	
10	UVA (benzotriazole) + tertiary amine triazine	Tinuvin 360 + Chimassorb 119	

homopolymerization and copolymerization of the monomers containing functional groups with UV absorbing and antioxidizing properties represents the most widely applied methods for preparing the photostabilizers of high molecular weight. The chemistry of Mannich bases offers convenient and useful ways for the synthesis of various compounds mainly based on phenolic derivatives which can inhibit the formation of radical species [204, 205].

### 4.4.1.5 Plasticizer

A number of plasticizers have been investigated to be used with biodegradable polymers. Citrate plasticizers, being biodegradable esters, gained much attention. PLA, which has been extensively studied in medical implants, suture, and drug delivery systems since the 1980s due to its biodegradability, can be plasticized with four commercially available citrate plasticizers: triethyl, tributyl, acetyltriethyl and acetyltributyl citrate. The plasticizing effects on thermal and mechanical properties of PLA are satisfactory in that the citrate esters produce flexible materials. The high  $M_w$  citrates also reduce the degradation rate of PLA. However, a considerable amount of loss of plasticizer is encountered during processing, especially with the lower  $M_w$  citrates. Elsewhere, citrate esters are used to plasticize cellulose acetate, and the biodegradation rates increase dramatically with an increase in plasticizer content.

Polyols are another class of compounds which have been studied as plasticizers for biodegradable polymers. Glycerol, which is often used with biodegradable polymers, has been found to reduce degradation of thermoplastic starch (TPS). Starch, a polysaccharide found abundantly in plants, is not a thermoplastic material itself. But at moderately high temperatures (90–180°C), under pressure and shear stress, starch granules melt and flow to give an amorphous material called TPS, which can be processed just like a thermoplastic synthetic polymer. The utilization of TPS for the production of biodegradable plastics has grown and has been the object of several studies in the last decade. One of the problems associated with TPS processing is degradation of starch. The effects of glycerol in preventing degradation of TPS reinforced with cellulosic fibers, are observed. An increase in glycerol content reduces chain degradation considerably. However, an increase in the fiber content amplifies it [206].

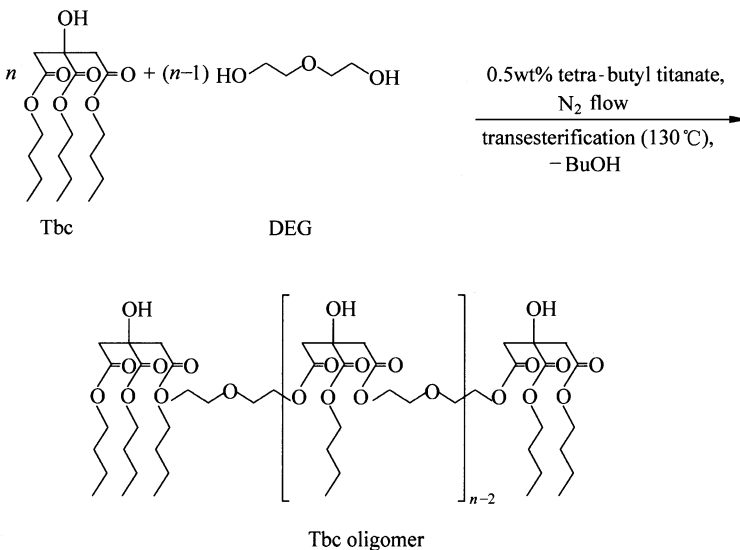
The extensive use of polymers in short-term packaging and disposable applications, and in food and pharmaceutical industries, has stimulated research interest in biodegradable plasticizers as an alternative to the conventional nondegradable ones. This is one of the major research interests in the plasticizer industry now. With the expansion of biodegradable plastic industry, owing to the growing global concern about the environmental impact of persistent plastics, biodegradable plasticizer research continues to grow.

The flexibility of PLA can be improved by modifying its physical properties,

e.g. through copolymerization. The mechanical properties can also be affected by blending PLA with a plasticizer or a second polymer. A large number of investigations have been performed on the blending of PLA with various polymers. Examples of such polymers are thermoplastic starch, PEO, PEG, poly (1-caprolactone), poly (vinyl acetate), poly (hydroxyl butyrate), cellulose acetate, poly (butylenes succinate) and poly (hexamethylene succinate). Low molecular weight compounds have also been used as plasticizers for PLA, e.g. oligomeric lactic acid, glycerol, triacetin and low molecular weight citrates.

The choice of polymers or plasticizers to be used as modifiers for PLA is limited by the requirements of the application. Only non-toxic substances approved for food contact can be considered as plasticizing agents in food packaging materials. For a low molecular weight plasticizer an important demand is that it should be miscible with PLA, thus creating a homogeneous blend. The plasticizer should not be too volatile so as not to evaporate at the elevated temperatures used during processing. Nor should the plasticizer be prone to migration as this would be a source of contamination of the food or beverage in contact with the plasticized PLA. Migration would also cause the blended material to regain the brittleness of neat PLA.

Two oligomeric plasticizers, one trimer (TbC-3) and one heptamer (TbC-7), are prepared by transesterification of TbC and DEG. The tertiary hydroxyl group on TbC seems to have participated in the reaction, causing uncontrolled branching as shown in Fig. 4.39.



**Figure 4.39** Synthesis path for the transesterification of TbC and DEG [206]

Blending PLA with the oligomeric plasticizers lowers the glass transition temperature. The plasticization effect is larger with low molecular weight plasticizers. TbC-3 is compatible with PLA at concentrations up to 20 wt% after the phase separation occurs. Materials containing 10 and 15 wt% TbC-3 that are aged at ambient temperature for 4 months display an additional peak in the loss modulus curves indicating phase separation. The cold crystallization temperature of the aged material remains the same as for the unaged one, suggesting that even though there is progressive phase separation the plasticizer remains in the bulk instead of migrating to the film surface. Aging of the 20 wt% TbC-3 film in the same manner generates further phase separation but also forces the plasticizer to migrate to the film surface. Thus the morphological stability of the PLA/TbC-3 blends is better when the plasticizer concentration is reasonably low.

Blends of PLA plasticized with TbC-7 display phase separation already at a concentration of 15 wt%, due to its higher molecular weight. Only a certain amount of plasticizer can be incorporated in PLA before becoming saturated and the higher the molecular weight of the plasticizer, the lower the saturation concentration.

Plasticizers form a major part of the plastic industry. The diversified applications of plastics in numerous fields of applications largely depend on the performance of the plasticizers incorporated. In the past century, the plasticizer industry came across a number of technical challenges. Leaching and migration of plasticizers have been reduced by methods including surface crosslinking, grafting, and surface extraction, the use of alternative and novel plasticizers and also the use of alternative polymers which do not require plasticizers. Many of these methods to prevent leaching and migration of plasticizers have been developed on a case-by-case basis, where different methods are successful for particular solvents or plasticizers. Research is being carried out worldwide in both academic and industrial laboratories to provide tunable solutions to the leaching and migration issues. Also, plasticizers are being sought to improve the biocompatibility of flexible plastics since they are widely used in medical applications [207, 208].

High temperature stable plasticizers are under investigation to provide materials that meet demanding work environments. New and modified plasticizers have also been developed to impart nonflammable properties to polymers. With the extensive growth in the biodegradable polymer market, a major portion of plasticizer research is now focused on materials, which are GRAS and are capable of providing flexibility to polymers. As the plastic industry continues to expand, new challenges arise for the plasticizer industry. Thus, different approaches to overcome the shortcomings of traditional plasticizers for use in a multitude of plastic materials have led to the continuing quest for specialty plasticizers.



#### 4.4.1.6 Colourant and Disperse Dyes

Colour is all around us. It is important in our daily lives and we learn from birth to react to colours logically or emotionally [209].

PLA fiber is most commonly dyed with disperse dyes. One major concern with PLA is that only a limited number of disperse dyes have been found to have good sorption on PLA at the appropriate dyeing temperature. PLA filaments with higher melting points have yielded greater dye sorption in the cross section of the filaments than that of PLA filaments with lower melting points. PLA fibers containing greater amounts of *D*-lactide units have shown higher dye sorption than fibers with smaller amounts of *D*-lactide, but the higher sorption is due to those fibers being more amorphous. High percentage dye sorption is important because it decreases the dye consumption required to obtain a given shade, especially a dark shade, and the lower dye consumption results in less pollution and a lower cost of dyeing. High dye sorption indicates that the dye has a high affinity for the fiber and, therefore, good colorfastness as shown in Figs. 4.40 and 4.41.

Because high percentage dye sorption on PLA is important, the sorption of disperse dyes onto PLA at 100°C and 110°C has been explained in earlier studies using the solubility parameter calculated according to the group contribution method. The solubility parameter of a chemical characterizes the interactions between its molecules due to dispersion forces, polar forces, and hydrogen bonding, and two chemicals tend to be mutually soluble if their solubility parameters are approximately equal. More than 11 dyes that have been found to have less than 70% sorption on PLA, 11 have solubility parameters greater than  $25.0 \text{ (J/cm)}^{0.5}$ , but one dye has a solubility parameter above this value. Six dyes that have been reported to have greater than 70% sorption on PLA have a solubility parameter less than  $25.0 \text{ (J/cm)}^{0.5}$ , which is close to that of PLA,  $20.2 \text{ (J/cm)}^{0.5}$ . However, a linear regression of the percentage sorption against the solubility parameters of the dyes gives an  $R^2$  of only 0.228, and the calculated solubility parameters of the dyes therefore have poor agreement with their percentage sorption on PLA [210]. Table 4.22 shows the decrease in the interaction energy ( $\Delta U_{\text{dye-PLA}}$ ) between various disperse dyes with a diphenyl monoazo or tetrahydrothiophenyl phenyl monoazo parent structure and PLA after a given substituent is removed (group removed) from the dye and replaced with an —H. Table 4.23 shows the decrease in the interaction energy ( $\Delta U_{\text{dye-PLA}}$ ) between various disperse dyes with an anthraquinone parent structure and PLA after a given substituent is removed (group removed) from the dye and replaced with an —H. Table 4.24 shows the decrease in the interaction energy ( $\Delta U_{\text{dye-PLA}}$ ) between various disperse dyes with various parent structures and PLA after removing a substituent (group removed) from the dye and replacing it with an —H.

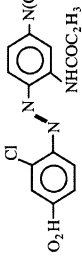
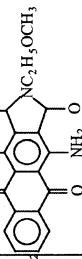
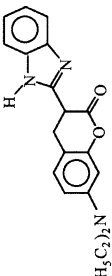
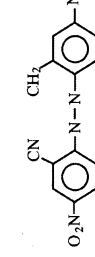
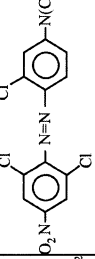
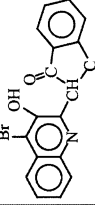
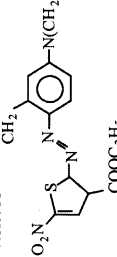
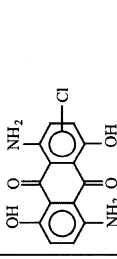
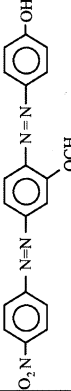
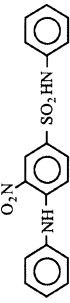
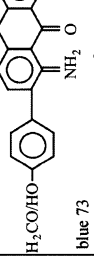
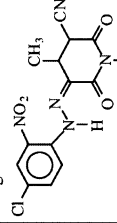
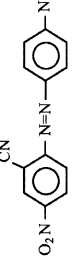
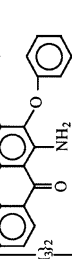
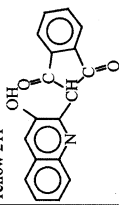
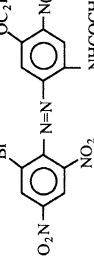
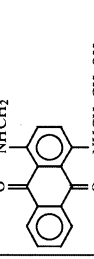
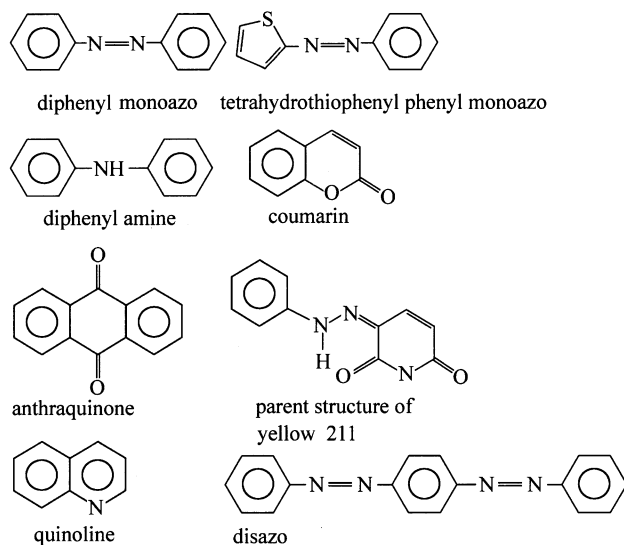
C.I. disperse dye	% sorption	C.I. disperse dye	% sorption	C.I. disperse dye	% sorption
 red 167	98.4[6]	 blue 60	58.4[6]	 (H <sub>5</sub> C <sub>2</sub> ) <sub>2</sub> N yellow 82	26.8[5]
 violet 33	98[1]	 brown 1	51.8[5]	 yellow 64	22.8[5]
 blue 356	92[6]	 blue 56	26.8[6]	 orange 29	22.1[6]
 yellow 42	85.4[5]	 blue 73	40.4[6]	 yellow 211	17.6[6]
 red 82	79.1[6]	 violet 26	35.6[5]	 yellow 54	10.9[5]
 blue 79	72.8[6]	 blue 3	30.7[5]		

Figure 4.40 Structures of the disperse dyes (C.I. Disperse Dye) and their percentage sorption (% sorption) on PLA fiber [210]



**Figure 4.41** Parent structures of the disperse dyes

**Table 4.22** Decrease in the interaction energy ( $\Delta U_{\text{dye-PLA}}$ ) between various disperse dyes with a diphenyl monoazo or tetrahydrothiophenyl phenyl monoazo parent structure and PLA after a given substituent is removed (group removed) from the dye and replaced with an  $\text{—H}$

Group removed	Decrease in $\Delta U_{\text{dye-PLA}}$ (kcal/mol)					
	Red 167	Violet 33	Blue 79	Blue 356	Red 82	Brown 1
Original $\Delta U_{\text{dye-PLA}}$	-135	-118	-117	-111	-111	-96
$\text{—N}(\text{C}_2\text{HOCOC}_2\text{H}_5)_2$	60	54	53	46	47	NA
$\text{—N}(\text{C}_2\text{H}_4\text{OH})_2$	NA	NA	NA	NA	NA	30
$\text{—NHCOC}_2\text{H}_5$	28	NA	NA	NA	NA	NA
$\text{—NHCOCH}_3$	NA	NA	26	NA	NA	NA
$\text{—COOC}_2\text{H}_5$	NA	NA	NA	20	NA	NA
$\text{—NO}_2$	18	17	14	15	11	22
$\text{—OC}_2\text{H}_5$	NA	NA	10	NA	NA	NA
$\text{—CH}_3$	NA	7	NA	6	NA	NA
$\text{—CN}$	NA	3	NA	NA	5	NA
$\text{—Cl/—Br}$	-1	NA	0	NA	NA	0

Note: Arranged from greatest decrease at the top to smallest decrease at the bottom.

**Table 4.23** Decrease in the interaction energy ( $\Delta U_{\text{dye-PLA}}$ ) between various disperse dyes with an anthraquinone parent structure and PLA after a given substituent is removed (group removed) from the dye and replaced with an —H

Group removed	Decrease in $\Delta U_{\text{dye-PLA}}$ (kcal/mol)					
	Blue 60	Blue 73 with —OCH <sub>3</sub>	Violet 26	Blue 73 with —OH	Blue 56	Blue 38
Original $\Delta U_{\text{dye-PLA}}$	-88	-88	-80	-79	-63	-59
—(CO) <sub>2</sub> NC <sub>3</sub> H <sub>6</sub> OCH <sub>3</sub>	42	NA	NA	NA	NA	NA
—C <sub>6</sub> H <sub>4</sub> OCH <sub>3</sub>	NA	32	NA	NA	NA	NA
—C <sub>6</sub> H <sub>4</sub> OH	NA	NA	NA	23	NA	NA
—OC <sub>6</sub> H <sub>5</sub>	NA	NA	15	NA	NA	NA
—NHC <sub>2</sub> H <sub>4</sub> OH	NA	NA	NA	NA	NA	11
—NHCH <sub>3</sub>	NA	NA	NA	NA	NA	8
—OH	NA	3	NA	2	5	NA
—NH <sub>2</sub>	4	0	0	0	3	NA
—Cl	NA	NA	NA	NA	1	NA

Note: Arranged from greatest decrease at the top to smallest decrease at the bottom.

**Table 4.24** Decrease in the interaction energy ( $\Delta U_{\text{dye-PLA}}$ ) between various disperse dyes with various parent structures and PLA after removing a substituent (group removed) from the dye and replacing it with an —H

Group removed	Decrease in $\Delta U_{\text{dye-PLA}}$ (kcal/mol)					
	Yellow 42	Orange 29	Yellow 82	Yellow 211	Yellow 64	Yellow 54
Original $\Delta U_{\text{dye-PLA}}$	-85	-82	-75	-75	-64	-59
—CN(NH)C <sub>6</sub> H <sub>4</sub>	NA	NA	33	NA	NA	NA
—CH(CO) <sub>2</sub> C <sub>6</sub> H <sub>4</sub>	NA	NA	NA	NA	30	26
—SO <sub>2</sub> NHC <sub>6</sub> H <sub>4</sub>	26	NA	NA	NA	NA	NA
—NO <sub>2</sub>	17	14	NA	20	NA	NA
—N(C <sub>2</sub> H <sub>5</sub> ) <sub>2</sub>	NA	NA	12	NA	NA	NA
—OH	NA	7	NA	NA	6	4
—C <sub>2</sub> H <sub>5</sub>	NA	NA	NA	7	NA	NA
—OCH <sub>3</sub>	NA	6	NA	NA	NA	NA
—CN	NA	NA	NA	5	NA	NA
—CH <sub>3</sub>	NA	NA	NA	3	NA	NA
—Br/—Cl	NA	NA	NA	1	5	NA

Note: Arranged from greatest decrease at the top to smallest decrease at the bottom.

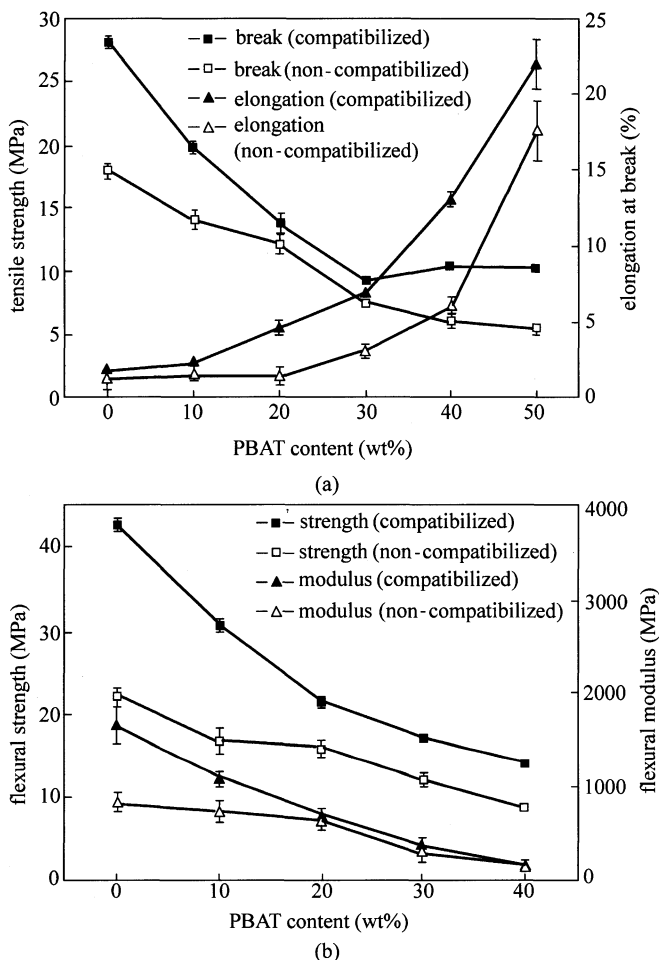
The interaction energies between various disperse dyes and PLA ( $\Delta U_{\text{dye-PLA}}$ ) calculated using molecular modeling agree with experimental data for the percentage sorption of the dyes onto PLA. A linear equation has been developed to predict the percentage sorption of disperse dyes onto PLA based on the  $\Delta U_{\text{dye-PLA}}$ , and the predicted percentage sorption for a dye has been shown to

agree with the actual percentage sorption of that dye on commercial PLA fabric and on PLA fiber extruded. According to this equation, dyes that form stronger interactions with PLA, which are indicated by a more negative  $\Delta U_{\text{dye-PLA}}$ , have greater percentage sorption on PLA. Among the substituents on the parent structures of the dyes, the substituents that form the strongest interactions with PLA are  $-\text{N}(\text{C}_2\text{H}_4\text{OCOCH}_3)_2$ ,  $-(\text{CO})_2\text{NC}_3\text{H}_6\text{OCH}_3$ ,  $-\text{SO}_2\text{NHC}_6\text{H}_5$ ,  $-\text{NO}_2$ ,  $-\text{CN}(\text{NH})\text{C}_6\text{H}_4$ , and  $-\text{CH}(\text{CO})_2\text{C}_6\text{H}_4$  in their respective dyes. The substituents that form the weakest interactions with PLA are  $-\text{Br}$  and  $-\text{Cl}$ . Substituting  $-\text{N}(\text{C}_2\text{H}_4\text{OCOCH}_3)_2$  groups onto various parent dye structures such as diphenyl monoazo, tetrahydrothiophenyl phenyl monoazo, anthraquinone, diphenylamine, methine, quinoline, and disazo are found to give those dyes  $\Delta U_{\text{dye-PLA}}$  values that correspond to a predicted percentage sorption greater than 90% [211].

#### 4.4.1.7 Compatibilizer

Binary and ternary blends of TPS, PLA and PBAT have been prepared using a one-step extrusion process. The concentration of TPS in both binary and ternary blends is fixed at 50 wt%, with the rest being PLA and PBAT. A compatibilizer with anhydride functional groups is used to improve the interfacial affinity between TPS and the synthetic polyesters. The addition of a small amount of compatibilizer greatly increases the mechanical properties of the blends. Mechanical properties of the blends exhibit a dramatic improvement in elongation at break with increasing PBAT content as shown in Fig. 4.42. Compared to the non-compatibilized blends, the morphology analysis of the blends shows that most of the TPS particles melt and are well dispersed in the polyester matrix for the compatibilized blends. The water absorption of the non-compatibilized blends increases more significantly than that of the compatibilized blends when PBAT content increases.

Polymer blending is an important way to obtain new materials that can meet different needs. Blending of TPS with other polymers represents an important route to overcome the limitations of TPS. PLA is a hydrophobic and semicrystalline polyester, also is a renewable material that can be utilized by microbes within 30 – 40 days. Its good physical properties and commercial availability makes it very attractive, not only as a substitute of non-biodegradable polymers for commodity applications, but also for specific applications in medicine and in agricultural areas. The main limitation of PLA is its high price that is caused by its complicated production process. Blending of PLA with TPS is a good way to balance the cost-effective issue and get a new material that has good performances. However, earlier studies have shown that TPS/PLA blend have rather poor mechanical properties due to the poor interfacial affinity of starch and PLA. Thus, compatibility is the vital problem that has to be dealt with when blending hydrophilic starch granules and hydrophobic PLA together. In order to increase the interfacial adhesion between TPS and PLA, polymers having functional groups capable of interacting with the hydroxyl groups on starch are



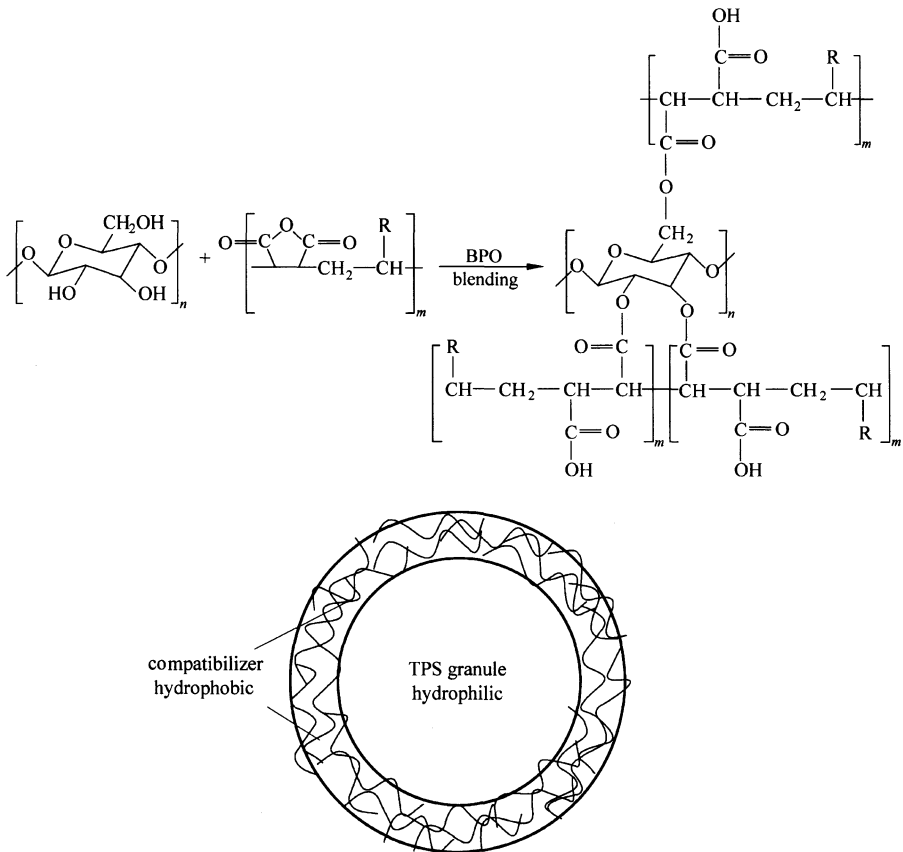
**Figure 4.42** Mechanical properties of TPS/polyester blends as a function of PBAT content (a) Tensile strength and elongation at break; (b) Flexural strength and flexural modulus [212]

desirable. It has been found that MAH-grafted PLA/starch blend shows much finer dispersed phase and exhibits a dramatic improvement in ductility than pure PLA/starch blend. Acrylic acid grafted PLA and starch composite has much better mechanical and thermal properties than PLA/starch blend. Bhattacharya et al. prepared starch/synthetic polymer blends by injection moulding and studied the effect of processing parameters on physical properties of the blends, evaluation of mechanical properties, effect of amylopectin on amylose ratio in starch, thermal and morphological properties. Their research shows that maleated synthetic polymers such as SMA, EPMA and EVAMA are effective compatibilizers for starch/synthetic polymer blends.

It has been found that the addition of PCL greatly increased the ductility of

PLA/TPS blends. So blending PLA/TPS binary blend with another flexible polymer could be a useful way to obtain a new kind of materials with excellent integrated performances. PBAT is a flexible copolyester which can be fully degraded within a few weeks with the aid of naturally occurring enzymes. PLA/PBAT blends show decreased tensile strength and modulus, however, increased elongation and toughness. The failure mode changes from brittle fracture of the neat PLA to ductile fracture of the blends. In this respect, PBAT could be considered as a good candidate for toughening rigid polymers such as TPS/PLA binary blend.

Here TPS/PLA/PBAT binary and ternary blends have been prepared via a one-step melt-processing. The morphology and properties of both compatibilized and non-compatibilized blends have been investigated. The TPS content of the blend is fixed at 50% by weight, the remaining being the synthetic polymers PLA and PBAT, which are varied in different ratios as shown in Fig. 4.43. One



**Figure 4.43** Formation of TPS and compatibilizer and the reaction between them [212]

anhydride functionalized polymer that has very high content of maleic anhydride is used as compatibilizer, and for the compatibilized blends its content is fixed at 1 wt% of the blends [212].

Biodegradable binary and ternary blends of TPS, PLA and PBAT give excellent properties when small amount of compatibilizer (an anhydride functionalized polyester) is added. For the TPS/PLA and TPS/PBAT binary blends the tensile strength increases by about 30% and 100% respectively after compatibilized. The elongation is drastically increased as the percentage of PBAT is increased; this is particularly true for the compatibilized blend where at 50% PBAT content the value of the elongation reaches 22.04%. The anhydride functionalized polyester reduces the size of the dispersed phase, thus enhancing the interaction between the two phases of TPS and polyesters. Better properties could also be found for the compatibilized blends in the results of MI and VST. DMA results show a decrease of the  $T_g$  of PLA as PBAT content increases, and storage modulus and loss modulus also decrease as PBAT contents increases. Compared with those containing more PLA, blends containing more PBAT have higher water uptake and took a longer time to reach equilibrium, which is in inverse proportion to the crystallinity of the polyester in the blend as shown in Figs. 4.44 and 4.45. After compatibilized, the water uptake of the blends is lower and the time required to reach the equilibrium water uptake is longer than those of non-compatibilized blends.

### 4.4.2 PLA Crystallization Behavior and Nucleating Agents

PLA has been currently received a lot of attention for commodity applications because of environmental degradability and sustainable biomass resources. The crystal structure, crystallization behavior and even nucleating agents can greatly determine the mechanical and thermal properties of PLA.

#### 4.4.2.1 PLA Crystal Structure

PLA has four optical enantiomers: PLLA, PDLA, PDLLA and *meso*-PLLA. The PLLA is most commonly used that has three crystal structures:  $\alpha$ ,  $\beta$  and  $\gamma$ .

The  $\alpha$ -phase PLLA is most common structure that can be obtained from crystallization in melt, solution and fiber spinning with low strain rate and temperature. Santis and Kovacs [213] first determined the conformation of  $\alpha$ -phase PLLA and PDLA. PLLA is left handed  $10_7$  helix, and a right handed  $10_3$  helix for the *d*-isomer PDLA. Both PLA are orthorhombic crystal systems with unit-cell parameters of  $a=1.06$  nm;  $b=0.610$  nm and  $c=2.88$  nm. The ratio of  $a$  and  $b$  is 1.737, which is nearly equal to  $\sqrt{3}$  indicating an almost hexagonal packing of helices. Figure 4.46 shows the crystal structure of  $\alpha$  phase PLLA.



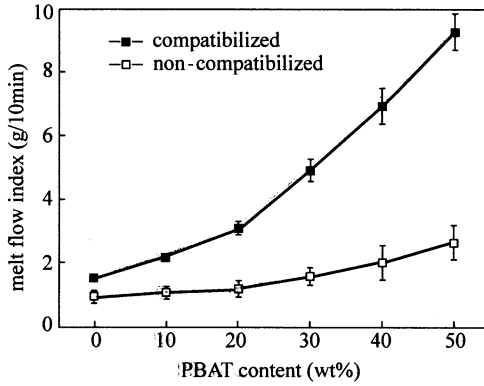


Figure 4.44 Melt flow index curves of TPS/polyester blends, as a function of PBAT content [212]

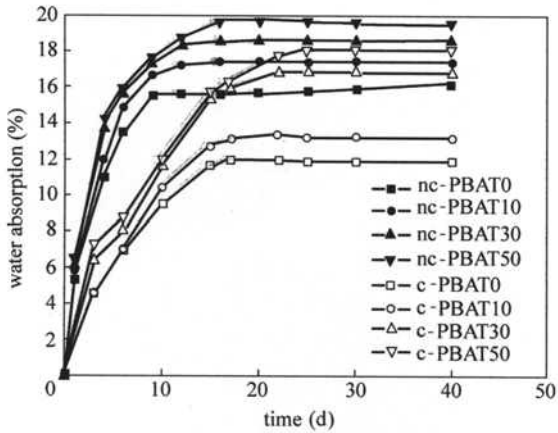


Figure 4.45 Water absorption of non-compatible and compatible blends [212]

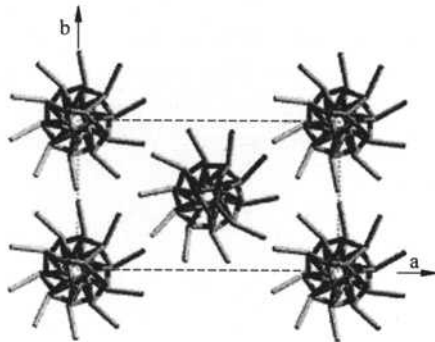
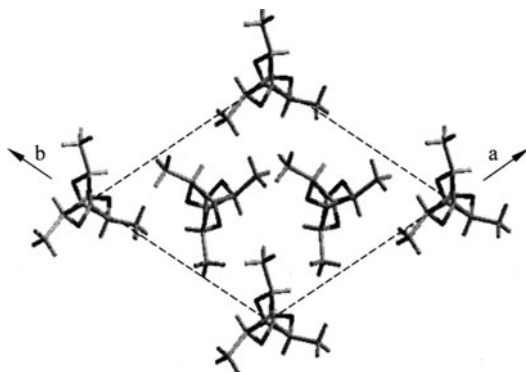


Figure 4.46 Model of the crystal structure of  $\alpha$ -phase PLLA with  $10_7$  helix conformation [214]

The  $\beta$ -phase was first observed by Eling et al. [215] upon tensile drawing of  $\alpha$ -phase PLLA in high drawing temperature and rate. Hoogsteen et al. [216] further observed that upon high drawing temperature and ratio, the PLLA fibers transformed from left handed  $10_3$  helix of  $\alpha$ -phase to left handed  $3_1$  helix of  $\beta$ -phase with an orthorhombic unit-cell with parameters of  $a=1.031$  nm,  $b=1.821$  nm,  $c=0.900$  nm, and transformed from a lamellar folded-chain structure to a fibrillar extended-chain structure. Differential scanning calorimetric (DSC) study shows that though  $\beta$ -phase has a lower melting temperature of  $175^\circ\text{C}$  than that of  $\alpha$ -phase ( $\approx 185^\circ\text{C}$ ),  $\beta$ -phase is much more stable than  $\alpha$ -phase. Based on the three-fold helical conformation, chirality and trigonal unit-cell with three helices of PLA, Cartier et al. [217, 218] further suggested that the helix packing was related to the frustrated crystal structures. Recently, Puiggalia et al. [219] has observed that  $\beta$ -phase is three three-fold helices in a trigonal unit-cell with parameters of  $a=b=1.052$  nm,  $c=0.88$  nm, the structure of which is shown in Fig. 4.47. However, the crystal structure and unit-cell parameters still need to be studied.

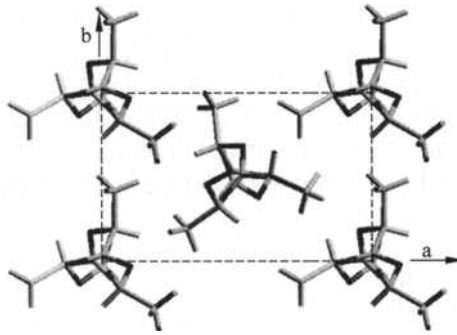


**Figure 4.47** Crystal structure of  $\beta$ -phase of PLLA with three parallel helices [219]

B. Lotza et al. [214] found that  $\alpha$ -phase PLLA was formed when growing epitaxially on hexamethylbenzene (HMB) at higher temperature of  $155^\circ\text{C}$ , which had the same unit-cell parameters as that observed by Santis and Kovacs [201]. While in lower temperature of  $140^\circ\text{C}$ , the  $\gamma$ -phase PLLA was formed, the structure of which is close to  $\beta$ -phase observed by Brizzolara et al. [220], the difference is that two anti-parallel helices are packed in an orthorhombic unit-cell with parameters of  $a=0.995$  nm,  $b=0.625$  nm,  $c=0.88$  nm. The structure of  $\gamma$ -phase PLLA is showed in Fig. 4.48.

#### 4.4.1.2 PLLA Crystallization Behavior

PLLA is semi-crystalline polymer. The glass transition temperature of PLLA is  $50\text{--}60^\circ\text{C}$ , the crystallization temperature is  $90\text{--}140^\circ\text{C}$ , and the melting temperature



**Figure 4.48** Crystal structure of  $\gamma$ -phase of PLLA with two anti-parallel helices

is 150–180°C [221], the equilibrium melting temperature is 203°C [222]. The crystallization behavior of PLLA is controlled by polymerization kinetics, blending with nucleating agents like organic and inorganic small molecules and also polymers.

#### (1) PLLA Isothermal and Non-Isothermal Crystallization Behaviors

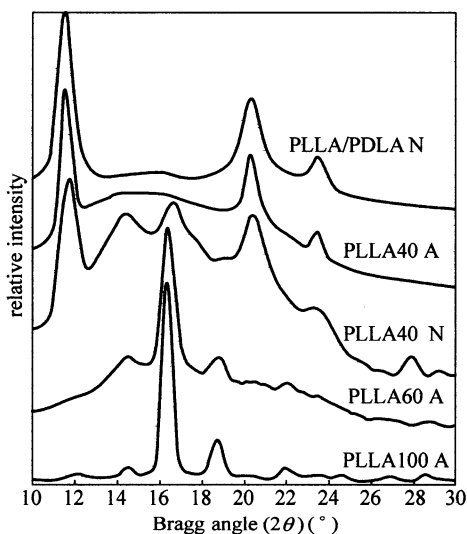
As for isothermal crystallization of PLLA, the spherulite growth rate is determined by crystallization temperature and molecular weight. As the crystallization temperature rises, the spherulite growth rate first increases and then decreases. As the molecular weight of PLLA increases, the spherulite growth rate decreases. The maximum of spherulite growth rate occurs at 120°C and isothermal overall crystallization rate occurs at 105°C [221].

The cooling rate is one of the factors that determine the crystallization behavior of PLLA. As the cooling rate decreases, the crystallization enthalpy and crystallinity increases. When cooling rate is higher than 10°C/min, PLLA hardly crystallizes. When cooling rate increases to 20°C/min, PLLA is amorphous. As for  $\alpha$ -phase PLLA, the density of monocryalline is 1.285g/cm<sup>3</sup>. Based on the linear relation between crystallization enthalpy and cooling rate and the density of monocryalline, Miyata et al. [221] observed that the maximum crystallization enthalpy of PLLA was 135J/g, and the crystallization enthalpy of PLLA was 60 J/g and crystallinity was 0.44 when cooling rate was 10°C/min. When PLLA was annealed at 140°C for 24 h, the crystallinity was 0.52. Therefore, the crystallinity of PLLA was generally less than 0.5.

#### (2) Effect of Optical Purity on the PLLA Crystallization Behaviors

As the optical purity of PLLA decreases, the melting peak becomes undiscernible, and the crystallinity also decreases. As for 100% optical purity of PLLA, the crystallization peak becomes undiscernible when cooling rate is less than 10°C/min. As for 80% optical purity of PLLA, the crystallization peak becomes undiscernible when cooling rate is less than 0.3°C/min. Meanwhile, compared with the single melting peak of 100% optical purity of PLLA, the PLLA with 80% optical purity shows two melting peaks. Moreover, when the optical purity is less than 80%, the multi-melting peaks occur that is due to multi-crystal structures and morphologies. In the DSC heating process, the

incomplete crystals melt and recrystallize, and remelt in higher temperature. Meanwhile, the multi-melting peaks are related to the stereocomplex structure formed during the polymerization. Figure 4.49 shows that the PLLA with 43% optical purity has the same wide angle X-ray diffraction(WAXD) peaks of 12°, 21° and 24° with that of blending PLLA/PDLA(50/50) when annealing at 111°C or 24 h which means they have the same crystal structure [223].



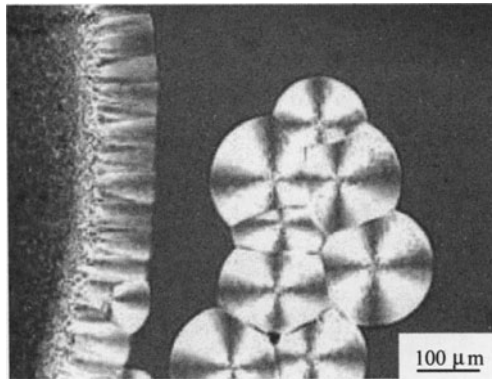
**Figure 4.49** X-ray diffraction curves of PLLA with optical purities of 43%, 61% and 100% and an equimolar mixture of PLLA and PDLA annealing at 111°C, 122°C and 120°C for 24 h [211]

### (3) Effect of Nucleating Agents on the Crystallization Behaviors of PLLA

Compared with common thermoplastics, PLLA has better mechanic properties like tensile strength, but the crystallization rate is extremely slow which results in the low heat-distortion temperature (HDT) and limits the application in high temperatures. One of the efficient methods to improve the crystallization behavior of PLLA is adding the nucleating agents, which have several advantages: providing more nucleation sites; shortening the induction time for crystallization; increasing the HDT and enhancing the tensile strength of polymer.

The inorganic particles are often used to improve the mechanical properties and lower the cost of polymer materials. It can also be added with small amount as the nucleating agents to improve the crystallization behavior of polymers. Angela and Lee observed that when 2 wt% talc was added in PLLA, the isothermal crystallization half times at 115°C were extremely decreased from 38.2 min for plain PLLA to 0.6 min and the crystallinity was increased [224]. Ruogu Liao et al. [225] used nano-CaCO<sub>3</sub>, nano-BaSO<sub>4</sub> and nano-TiO<sub>2</sub> as the nucleating agents for PLLA, the PLLA crystallinity was increased and the crystallization rate was also increased.

When the organic compounds are used as the nucleating agents for PLLA, the spherulite radius and induction time are decreased, and nucleation density and overall crystallization rate are increased and transcrystallization at interface between PLLA and nucleating agent occurs, which is showed in Fig. 4.50 [226]. Kawamoto et al. [227] synthesized a series of dicarboxylic disalicyloylhydrazide compounds as the nucleating agents, which markedly enhanced the crystallization ability of PLLA. Meanwhile the efficiency of nucleating agents can also be controlled by carbon length or benzene ring of hydrazide compounds. Jie Ren et al. [228] synthesized an N-aminophthalimide nucleating agent for PLLA, the results showed that it could increase the nucleation density and overall crystallization rate by epitaxial crystallization mechanism.



**Figure 4.50** Optical micrographs at interface between PLA and nucleating agent at  $T_c = 130^\circ\text{C}$  for 30 min

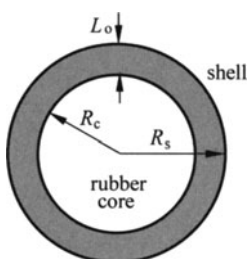
The PLLA crystallization ability can also be improved by adding the polymer molecules as nucleating agents. Hideto Tsuji et al. [229] observed that when the PDLA was added from 0.1 wt% to 10 wt%, the spherulitic size of PLLA was decreased when crystallized at  $135^\circ\text{C}$ . Meanwhile, the addition of small amounts of PDLA is effective to accelerate overall PLLA crystallization. The WAXD results show that the stereocomplex crystallites in the melt-quenched PLLA films are formed when PDLA contents is above 1 wt%.

## 4.5 New Modifiers for PLA

### 4.5.1 Core-Shell Impact Modifiers

For the core-shell impact modifiers of interest here, the rubber core can be regarded as an impenetrable wall where one end of each chain is grafted to this

wall. Since 1977, there has been an extensive discussion in the literature on polymer brushes showing their quite different conformational properties and mixing behavior compared with 'free' polymer chains. Even though SMA copolymers may be completely miscible with PMMA in the free state, the geometrical constraints of the shell layer limit the amount of SMA that can be solubilized into the grafted PMMA. The extent to which the conformational issues limit the solubilization of free polymer chains into the grafted chains forming the shell of core-shell impact modifiers has been theoretically examined. Tucker and Paul developed a thermodynamic model for the solubilization of SMA copolymers in the PMMA grafted chains of core-shell impact modifiers, or any similar system. To apply this model requires information about the polymer-polymer (i.e., SMA-PMMA) interaction energy, which, in principle, can be evaluated from separate experiments on blends where all chains are free. Other factors that can influence the solubilization limit like the grafted (PMMA) chain length, the molecular size of the added chains (SMA) and the shell thickness are included in the model. SMA is solubilized into the shell of some particular coreshell impact modifiers as shown in Fig. 4.51 and Fig. 4.52. This is done by examining the glass transition behavior of blends prepared by melt mixing and by transmission electron microscopy techniques [230, 231].



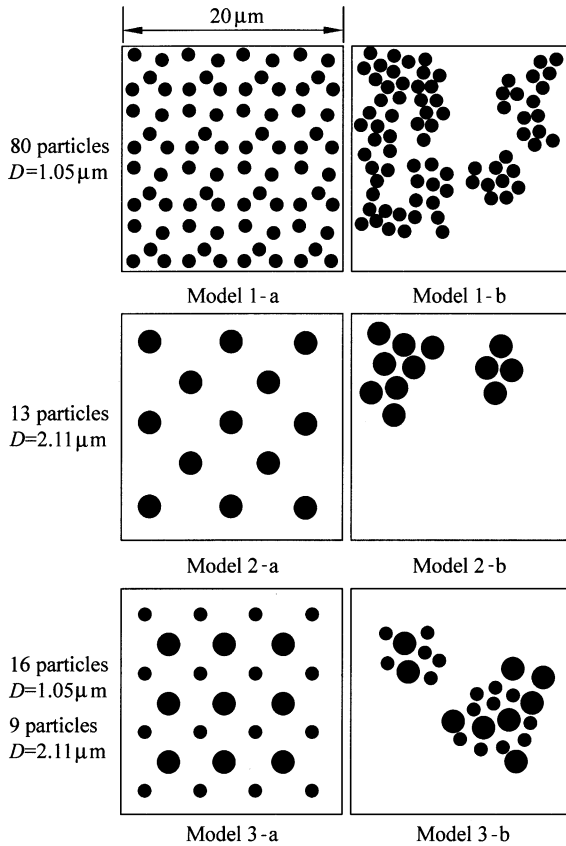
**Figure 4.51** Schematic illustration of an emulsion-made core-shell impact modifier particle

## 4.5.2 Nanocomposites

### 4.5.2.1 PLA-Silica Nanocomposites

For some application, PLA needs modification. High stiffness and brittleness at ambient temperature or below can be substantially improved by blending with biodegradable plasticizer such as PEG. However, other properties including tensile strength, thermal stability and gas barrier properties of the resulting PLA-based materials still need to be improved to fulfil for instance the requirements for food packaging applications.

In recent years, the PLA nanocomposites based on layered silicates, such as montmorillonite, smectite and mica has been actively investigated due to their

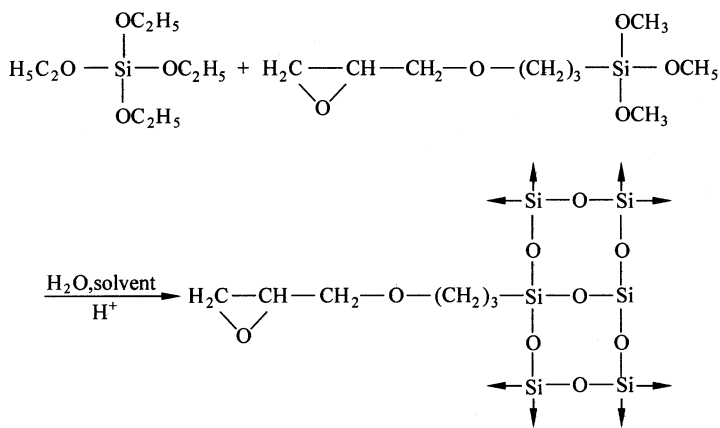


**Figure 4.52** Simple morphology models: Models 1 and 2 employ particles of the same size while Model 3 uses a mixture of two particles of different size. Model a shows a uniform spatial distribution while Model b shows a non-uniform spatial distribution

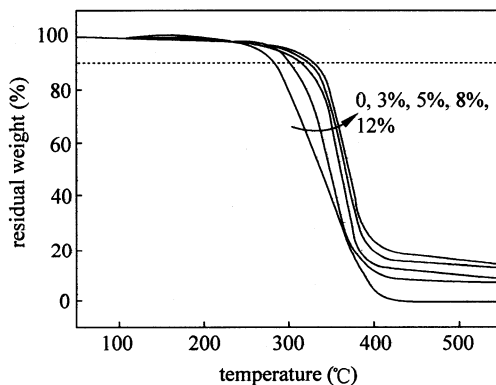
significant improvements to the virgin polymer in terms of mechanical, fire retardant, gas barrier and other properties. Nanocomposites from flexible plasticized PLA are also prepared by melt blending the PLA/PEG matrix with different amounts of organo-modified montmorillonites [232]. Thermal stability is greatly improved with the increase of montmorillonites content, but the mechanical properties are not discussed. No study on plasticized PLA-silica nanocomposites has been reported yet.

Plasticized PLLA-silica nanocomposite materials have been successfully fabricated by sol-gel method. IR and XRD measurements show that both the vibration of C—O—C group and the crystallization of PLA are confined by silica network as shown in Fig. 4.53. The presence of even a small amount of silica greatly improved the tensile strength of the samples. The thermal stability of samples is improved with silica loading as shown in Fig. 4.54.

## Biodegradable Poly(Lactic Acid): Synthesis, Modification, Processing and Applications



**Figure 4.53** Formation of silica network within PLA/PEG matrix



**Figure 4.54** TGA curve of PLA/PEG/silica nanocomposites with different silica contents

### 4.5.2.2 Multi-Wall Carbon Nanotube

The discovery of carbon nanotube has generated remarkable excitement in scientific communities around the world. Polymer nanocomposites containing carbon nanotubes also bring great interest both in academic and commercial fields. PLLA is linear thermoplastic polyester produced from renewable resources, and it is expected to be a suitable replacement for numerous petroleum-based polymers in the future. However, it has some weakness, such as poor gas barrier, low heat deflection temperature (HDT) and brittleness if crystallized completely, high production costs and others [233]. A water-crosslinking method has been proposed to achieve the improved interface between multi-wall carbon nanotube (MWCNT) and PLLA. The reaction scheme is shown in Fig. 4.55. This process is through free radical initiators and then subsequently via condensation of water, leading to the crosslinking of polymer matrix. Thermal mechanical and crystalline





properties of composite have been studied with the various carbon nanotube contents and different water-crosslinking time.

MWCNT/PLLA nanocomposite has been prepared successfully. X-ray diffraction results indicate that the crystalline of PLLA can be transformed to a natural PLA semicrystalline after water-crosslinking reaction. PLLA crystallization temperature decreases with the increase of water-crosslinking time, indicating a stable crystalline after water-crosslinking reaction. Thermal properties show that the introduction of water-crosslinking reaction would improve the thermal degradation properties by 12°C and 20°C, with and without carbon nanotube added, respectively. Mechanical property tests show that adding 1 phr MWCNT would improve the tensile strength of nanocomposite by 13%. After 7 h water-crosslinking reaction, the HDT of 1 phr MWCNT nanocomposite is 106°C, while that of virgin PLLA is 62°C.

### 4.5.2.3 Titanium Dioxide

Titanium dioxide (TiO<sub>2</sub>) nanoparticles have been investigated in recent years because of their photocatalytic effects. The nanoparticles is able to catalyze the decomposition of various organic chemicals such as aldehyde, toluene and polymers such as PE, PP, PVC and PS. The photocatalysis reaction is well known to active oxygen species, e.g. O<sub>2</sub><sup>-</sup>, HO<sub>2</sub> radicals, HO radicals, from H<sub>2</sub>O or O<sub>2</sub> by oxidative or reductive reductions under UV conditions. These active oxygen species lead to a degradation reaction by attacking polymer chains and accelerating chain cleavage [234].

Thus, if TiO<sub>2</sub> nanoparticles are introduced into PLA matrices, the above-mentioned disadvantages can be overcome. Earlier studies have revealed that the polymer TiO<sub>2</sub> composite could potentially be used as a photodegradable product. However, there still remain unresolved problems related to the uniform dispersion of photocatalyst in polymer matrices. The direct mixing of the nanoparticles with PLA often leads to their aggregation within PLA matrices. The micrometer-sized severe aggregation of TiO<sub>2</sub> nanoparticles can significantly reduce the efficiency of photodegradation by the decrease of interfacial areas between TiO<sub>2</sub> and the polymer chain. Thermal properties of pure PLA, and the nanocomposite (PLA-TiO<sub>2</sub>-1, PLA-TiO<sub>2</sub>-5 and PLA-TiO<sub>2</sub>-10) are shown in Table 4.25.

By effective surface modification of TiO<sub>2</sub> nanoparticles using carboxylic acid and long-chain alkyl amine, the TiO<sub>2</sub> nanoparticles can be uniformly dispersed into the PLA matrices without aggregation. As a result, photodegradability of nanocomposites can be efficiently promoted. The photodegradation rate of nanocomposites can be controlled by TiO<sub>2</sub> nanoparticles content. The development of PLA-TiO<sub>2</sub> nanoparticle nanocomposites can lead to an eco-friendly disposal of polymer waste.

**Table 4.25** Thermal properties of pure PLA, and the nanocomposite (PLA-TiO<sub>2</sub>-1, PLA-TiO<sub>2</sub>-5 and PLA-TiO<sub>2</sub>-10)

Samples	$T_g$ (°C)	Melting enthalpy (J/g)	Melting temperature, $T_m$ (°C)	Crystallization temperature, $T_g$ onset (°C)	Crystallization temperature, $T_c$ (°C)	Crystallization enthalpy (J/g)	Degree of crystallization (%)
Pure PLA As-casted file	40	-33.5	171	71	85	15.8	-
PLA-TiO <sub>2</sub> -1	41	-30.6	171	77	88	18.4	-
PLA-TiO <sub>2</sub> -5	Unkown <sup>a</sup>	-26.8	165,170 (two peaks)	78	89	15.0	-
PLA-TiO <sub>2</sub> -10	Unkown <sup>a</sup>	-24.3	165	82	99	12.7	-
Pure PLA With annealing (90°C/h)	-	-31.2	171	-	-	-	33.5 <sup>c</sup>
PLA-TiO <sub>2</sub> -1	-	-30.0	171	-	-	-	31.8
PLA-TiO <sub>2</sub> -5	-	24.0	170	-	-	-	25.8
PLA-TiO <sub>2</sub> -10	-	-21.7	169	-	-	-	23.3

Note a: Glass transition peak is too diffuse to evaluate  $T_g$ .

## References

- [1] Mohammadi-Rovshandeh J., Sarbolouki M. N. *Iran Polym. J.*, 10, 53 (2001).
- [2] Fredericks R. J., Melveger A. J., Dolegiewitz L. J. *J. Polym. Sci. Part B: Polym. Phys.*, 22, 57 (1984).
- [3] Lan P., Zhang Y. P., Gao Q. W., et al. *J. Appl. Polym. Sci.*, 92, 2163 (2004).
- [4] Grijpma D. W., Nijenhuis A. J., Pennings A. J. *Polymer*, 31, 2201 (1990).
- [5] Farnia S. M. F., Mohammadi-Rovshandeh J., Sarbolouki M. N. *J. Appl. Polym. Sci.*, 73, 633 (1999).
- [6] Dobrzynski P., Kasperczyk J., Janeczek H., et al. *Polymer*, 43, 2595 (2002).
- [7] Dobrzynski P., Kasperczyk J., Janeczek H., et al. *Macromolecules*, 34, 5090 (2001).
- [8] Rebert N. W. *Macromolecules*, 27, 5533 (1994).
- [9] Shen Y. Q., Zhu K. J., Shen Z. Q., et al. *J. Polym. Sci. Part A: Polym. Chem.*, 34, 1799 (1996).
- [10] Cai Q., Bei J. Z., Wang S. G. *Acta Polym. Sin.*, 761 (1999).
- [11] Perego G., Vercellio T., Balbontin G. *Makromolekulare Chemie-Macromolecular Chemistry and Physics*, 194, 2463 (1993).
- [12] Dobrzynski P. *J. Polym. Sci. Part A: Polym. Chem.*, 40, 3129 (2002).
- [13] Nalampang K., Molloy R., Punyodom W. *Polym. Advan. Technol.*, 18, 240 (2007).
- [14] Hiljanen-Vainio M., Karjalainen T., Seppälä J. *J. Appl. Polym. Sci.*, 59, 1281 (1996).
- [15] Bero M., Kasperczyk J., Adamus G. *Makromol. Chem.*, 194, 907 (1993).
- [16] Perego G., Cella G. D., Aldini N., et al. *Biomaterials*, 15, 189 (1994).
- [17] Jeon O., Lee S. H., Kim S. H., et al. *Macromolecules*, 36, 5585 (2003).
- [18] Kim J. K., Park D. J., Lee M. S., et al. *Polymer*, 42, 7429 (2001).
- [19] Kricheldorf H. R., Boettcher C., Tönnies K. U. *Polymer*, 33, 2817 (1992).
- [20] Brostrom J., Boss A., Chronakis L. S. *Biomacromolecules*, 5, 1124 (2004).
- [21] Yamaoka T., Hotta Y., Kobayashi K., et al. *Int. J. Biol. Macromol.*, 25, 265 (1999).
- [22] Kimura Y., Shirotani K., Yamane H., et al. *Polymer*, 34, 1741 (1993).
- [23] Zhao Y. C., Hu Y. J., Cheng S. J., et al. *Polym. Bull.*, 61, 35 (2008).
- [24] Wang W., Liu Y., Wang J., et al. *Tissue Engineering Part A*, 15, 65 (2009).
- [25] Wang L., Jia X., Yuan Z. *Polymer*, 47, 6978 (2006).
- [26] He B., Bei J. Z., Wang S. G. *Polymer*, 44, 989 (2003).
- [27] Chen X. H., McCarthy S. P., Gross R. A. *Macromolecules*, 31, 662 (1998).
- [28] Dobrzynski P., Kasperczyk J. *J. Polym. Sci. Part A: Polym. Chem.*, 44, 3184 (2006).
- [29] Yokoe M., Aoi K., Okada M. *J. Polym. Sci. Part A: Polym. Chem.*, 41, 2312 (2003).
- [30] Kricheldorf H. R. *J. Polym. Sci. Part A: Polym. Chem.*, 42, 4723 (2004).
- [31] Hwang Y., Kim H., Ree M. *Macromol. Symp.*, 224, 227 (2005).
- [32] Matsumura S., Tsukada K., Toshima K. *Int. J. Biol. Macromol.*, 25, 161 (1999).
- [33] Rokicki G. *Prog. Polym. Sci.*, 25, 259 (2000).
- [34] Plichta A., Florjanczyk Z., Rokicki G. *Polimery-w.*, 50, 537 (2005).
- [35] Agarwal S., Puchner M., Greiner A., et al. *Polym. Int.*, 54, 1422 (2005).
- [36] Jarrett P. K., Casey D. *J. U. S. Pat.* 5 376 102 (1994).
- [37] Roby M. S., Kokish L. K., Mehta R. M., et al. *U. S. Pat.* 6 235 869 (2005).

- [38] Schmidt P., Keul H., Hocker H. *Macromolecules*, 29, 3674 (1996).
- [39] Xie Z. G., Hu X. L., Chen X. S., et al. *J. Appl. Polym. Sci.*, 110, 2961 (2008).
- [40] Fan C. L., Li B., Liu Z. H., et al. *Chem. J. Chinese U.*, 16, 971 (1995).
- [41] Barrera D. A., Zylstra E., Lansbury P. T., et al. *J. Am. Chem. Soc.*, 115, 11010 (1993).
- [42] Lee R. S., Yang J. M. *J. Polym. Res. (Taiwan)*, 9, 45 (2002).
- [43] Deng X. M., Liu Y., Yuan M. L. *Eur. Polym. J.*, 38, 1435 (2002).
- [44] Gu S. Y., Wang Z. M., Zhang C. Y., et al. *Carbohydr. Polym.*, 74, 572 (2008).
- [45] Liu Y., Yuan M. L., Deng X. M. *Eur. Polym. J.*, 39, 977 (2003).
- [46] Ouchi T., Nozaki T., Ishikawa A., et al. *J. Polym. Sci. Part A: Polym. Chem.*, 35, 377 (1997).
- [47] Zhao J., Quan D. P., Liao K. R., et al. *Chem. J. Chinese U.*, 26, 1570 (2005).
- [48] Montaudo M. S. *Rapid Commun. Mass. Sp.*, 13, 639 (1999).
- [49] Agnihotri S. M., Vavia P. R. *Journal of Biomedical Nanotechnology*, 2, 239 (2006).
- [50] John G., Morita M. *Macromolecules*, 32, 1853 (1999).
- [51] Duan J. F., Du J., Zheng Y. B. *J. Appl. Polym. Sci.*, 103, 2654 (2007).
- [52] Hwang H. S., Park E. J., Jeong Y. T., et al. *Stud. Surf. Sci. Catal.*, 153, 389 (2004).
- [53] Yu G. H., Ji J., Shen J. C. *J. Mater. Sci-mater. M.*, 17, 899 (2006).
- [54] Kumar N., Ravikumar M. N. V., Domb A. J. *Adv. Drug Deliver. Rev.*, 53, 23 (2001).
- [55] Ferruti P., Pence M., Daddato P., et al. *Biomaterials*, 16, 1423 (1995).
- [56] Lee S. H., Kim S. H., Han Y. K., et al. *J. Polym. Sci. Part A: Polym. Chem.*, 40, 2545 (2002).
- [57] Jedlinski Z., Kurcok P., Walach W., et al. *Makromolekulare Chemie-Macromolecular Chemistry and Physics*, 194, 1681 (1993).
- [58] Xiong C. D., Cheng L. M., Xu R. P., et al. *J. Appl. Polym. Sci.*, 55, 865 (1995).
- [59] Lemmouchi Y., Perry M. C., Amass A. J., et al. *J. Polym. Sci. Part A: Polym. Chem.*, 45, 2235 (2007).
- [60] Yasugi K., Nakamura T., Nagasaki Y., et al. *Macromolecules*, 32, 8024 (1999).
- [61] Salem A. K., Cannizzaro S. M., Davies M. C., et al. *Biomacromolecules*, 2, 575 (2001).
- [62] Bae J. W., Lee E., Park K. M., et al. *Macromolecules*, 42, 3437 (2009).
- [63] Shim W. S., Kim S. W., Choi E. K., et al. *Macromol. Biosci.*, 6, 179 (2006).
- [64] Deng X. M., Xiong C. D., Cheng L. M., et al. *J. Polym. Sci. Part C: Polym. Lett.*, 28, 411 (1990).
- [65] Lee C. W., Kimura Y.: *B. Chem. Soc. Jpn.*, 69, 1787 (1996).
- [66] Li S. M., Rashkov I., Espartero J. L., et al. *Macromolecules*, 29, 57 (1996).
- [67] Rashkov I., Manolova N., Li S. M., et al. *Macromolecules*, 29, 50 (1996).
- [68] Deng X. M., Li X. H., Yuan M. L., et al. *Chinese J. Polym. Sci.*, 17, 265 (1999).
- [69] Yuan M. L., Liu D., Xiong C. D., et al. *Eur. Polym. J.*, 35, 2139 (1999).
- [70] Lee C. W., Bae K. S. *Polym-Korea*, 26, 582 (2002).
- [71] Huang M. H., Suming L. M., Coudane J., et al. *Macromol. Chem. Phys.*, 204, 1994 (2003).
- [72] Song C. X., Feng X. D. *Macromolecules*, 17, 2764 (1984).
- [73] Gu Z. W., Ye W. P., Yang J. Y., et al. *J. Control Release*, 22, 3 (1992).
- [74] Deng X. M., Zhu Z. X., Xiong C. D., et al. *J. Polym. Sci. Part A: Polym. Chem.*, 35, 703 (1997).
- [75] Qian H. T., Bei J. Z., Wang S. G. *Polym. Degrad. Stabil.*, 68, 423 (2000).
- [76] Shim W. S., Kim S. W., Lee D. S. *Biomacromolecules*, 7, 1935 (2006).

## Biodegradable Poly(Lactic Acid): Synthesis, Modification, Processing and Applications

- [77] Wei Z. Y., Liu L., Yu F. Y., et al. *Polym. Bull.*, 61, 407 (2008).
- [78] Hori Y., Suzuki M., Yamaguchi A., et al. *Macromolecules*, 26, 5533 (1993).
- [79] Hori Y., Takahashi Y., Yamaguchi A., et al. *Macromolecules*, 26, 4388 (1993).
- [80] Hiki S., Miyamoto M., Kimura Y. *Polymer*, 41, 7369 (2000).
- [81] Li B., Chen S. C., Qiu Z. C., et al. *Polym. Bull.*, 61, 139 (2008).
- [82] Abdouss M., Hoseini S. M., Mohammadi-Rovshandeh J., et al. *Materialwiss. Werkst.*, 40, 676 (2009).
- [83] Stridsberg K., Albertsson A. C. *Polymer*, 41, 7321 (2000).
- [84] Stridsberg K., Albertsson A. C. *J. Polym. Sci. Part A: Polym. Chem.*, 38, 1774 (2000).
- [85] Bhattarai N., Bhattarai S. R., Yi H. K., et al. *Pharmaceut. Res.*, 20, 2021 (2003).
- [86] Bhattarai N., Il Cha D., Bhattarai S. R., et al. *J. Polym. Sci. Part B: Polym. Phys.*, 41, 1955 (2003).
- [87] Bhattarai N., Kim H. Y., Lee D. R., et al. *Polym. Int.*, 52, 6 (2003).
- [88] Bhattarai S. R., Yi H. K., Bhattarai N., et al. *Acta Biomaterialia*, 2, 207 (2006).
- [89] Kim J. H., Lee S. Y., Chung D. J. *Polym. J.*, 32, 1056 (2000).
- [90] Nakayama Y., Yasuda H., Yamamoto K., et al. *React. Funct. Polym.*, 63, 95 (2005).
- [91] Xie Z. G., Guan H. L., Lu C. H., et al. *Acta Biomaterialia*, 1, 635 (2005).
- [92] Guan H. L., Xie Z. G., Zhang P. B., et al. *J. Polym. Sci., Part A: Polym. Chem.*, 43, 4771 (2005).
- [93] Wang Y. B., Hillmyer M. A. *J. Polym. Sci. Part A: Polym. Chem.*, 39, 2755 (2001).
- [94] Zhang S., Hou Z., Gonsalves K. E. *J. Polym. Sci. Part A: Polym. Chem.*, 34, 2737 (1996).
- [95] Kayaman-Apohan N., Karal-Yilmaz O., Baysal K., et al. *Polymer*, 42, 4109 (2001).
- [96] Bongiovanni R., Malucelli G., Messori M., et al. *J. Polym. Sci. Part A: Polym. Chem.*, 43, 3588 (2005).
- [97] Boudouris B. W., Frisbie C. D., Hillmyer M. A. *Macromolecules*, 41, 67 (2008).
- [98] Ho R. M., Chiang Y. W., Tsai C. C., et al. *J. Am. Chem. Soc.*, 126, 2704 (2004).
- [99] Wei Y. H., Pan C. Y., Li B. Y., et al. *J. Chem. Phys.*, 126, (2007).
- [100] Fu J., Luan B., Yu X., et al. *Macromolecules*, 37, 976 (2004).
- [101] Ho R. M., Tseng W. H., Fan H. W., et al. *Polymer*, 46, 9362 (2005).
- [102] Li J. B., Ren J., Cao Y., et al. *Reactive and Functional Polymers*, 69, 870 (2009).
- [103] Luo L. B., Ranger M., Lessard D. G., et al. *Macromolecules*, 37, 4008 (2004).
- [104] Xiong L., Jiang H., Wang D. *Journal of Polymer Research*, 16, 191 (2009).
- [105] Benahmed A., Ranger M., Leroux J. C. *Pharmaceut. Res.*, 18, 323 (2001).
- [106] Yang X. Z., Wang Y. C., Tang L. Y., et al. *J. Polym. Sci. Part A: Polym. Chem.*, 46, 6425 (2008).
- [107] Yang X. Z., Sun T. M., Dou S., et al. *Biomacromolecules*, 10, 2213 (2009).
- [108] Kohori F., Sakai K., Aoyagi T., et al. *J. Control Release*, 55, 87 (1998).
- [109] Liu S. Q., Yang Y. Y., Liu X. M., et al. *Biomacromolecules*, 4, 1784 (2003).
- [110] Liu S. Q., Tong Y. W., Yang Y. Y. *Biomaterials*, 26, 5064 (2005).
- [111] You Y. Z., Hong C. Y., Wang W. P., et al. *Macromolecules*, 37, 9761 (2004).
- [112] Spasova M., Mespouille L., Coulembier O., et al. *Biomacromolecules*, 10, 1217 (2009).
- [113] Sun J., Chen X. S., Lu T. C., et al. *Langmuir*, 24, 10099 (2008).
- [114] Lavik E. B., Hrkach J. S., Lotan N., et al. *J. Biomed. Mater. Res.*, 58, 291 (2001).

- [115] Deng C., Chen X. S., Yu H. J., et al. *Polymer*, 48, 139 (2007).
- [116] Yu H., Guo X. J., Qi X. L., et al. *J. Mater. Sci-mater. M.*, 19, 1275 (2008).
- [117] Luo W. J., Li S. M., Bei J. Z., et al. *J. Appl. Polym. Sci.*, 84, 1729 (2002).
- [118] Chen Y., Tan L., Zhou W., et al. *J. Therm. Anal. Calorim.*, 96, 307 (2009).
- [119] Chen W. N., Yang J., Wang S. G., et al. *Acta Polym. Sin.*, 695 (2002).
- [120] Teng C. Q., Kai Y., Ping J., et al. *J. Polym. Sci. Part A: Polym. Chem.*, 42, 5045 (2004).
- [121] Huang L. H., Zhuang X. L., Hu J., et al. *Biomacromolecules*, 9, 850 (2008).
- [122] Nagata M., Sato Y. *J. Polym. Sci. Part A: Polym. Chem.*, 43, 2426 (2005).
- [123] Wang W., Ping P., Chen X., et al. *Eur. Polym. J.*, 42, 1240 (2006).
- [124] Ojha U., Kulkarni P., Singh J., et al. *J. Polym. Sci. Part A: Polym. Chem.*, 47, 3490 (2009).
- [125] Yu T., Ren J., Gu S. Y., et al. *Polym. Int.*, 58, 1058 (2009).
- [126] Kricheldorf H. R., Rost S. *Macromol. Chem. Phys.*, 205, 1031 (2004).
- [127] Chen D. P., Sun B. Q. *Mat. Sci. Eng. C-bio. S.*, 11, 57 (2000).
- [128] Yan C. H., Zhang J. M., Lv Y. X., et al. *Biomacromolecules*, 10, 2013 (2009).
- [129] Dong H. Q., Xu Q., Li Y. Y., et al. *Colloid Surface*, B66, 26 (2008).
- [130] Hadano S., Maehara S., Onimura K., et al. *J. Appl. Polym. Sci.*, 92, 2658 (2004).
- [131] Chen L., Qiu X. Y., Xie Z. G., et al. *Carbohyd. Polym.*, 65, 75 (2006).
- [132] Kim J. Y., Ha C. S., Jo N. J. *Polym. Int.*, 51, 1123 (2002).
- [133] Yao F. L., Chen W., Liu C., et al. *J. Appl. Polym. Sci.*, 89, 3850 (2003).
- [134] Yao F. L., Chen W., Wang H., et al. *Polymer*, 44, 6435 (2003).
- [135] Yao F. L., Liu C., Chen W., et al. *Macromol. Biosci.*, 3, 653 (2003).
- [136] Cai Q., Bei J. Z., Wang S. G. *Acta Polym. Sin.*, 719 (2004).
- [137] Nagahama K., Mori Y., Ohya Y., et al. *Biomacromolecules*, 8, 2135 (2007).
- [138] Bang J. Y., Song C. E., Kim C., et al. *Arch. Pharm. Res.*, 31, 1463 (2008).
- [139] Lee C. T., Huang C. P., Lee Y. D. *Biomacromolecules*, 7, 1179 (2006).
- [140] Hrkach J. S., Ou J., Lotan N., et al. *Macromolecules*, 28, 4736 (1995).
- [141] Tasaka F., Miyazaki H., Ohya Y., et al. *Macromolecules*, 32, 6386 (1999).
- [142] Jeong B., Kibbey M. R., Birnbaum J. C., et al. *Macromolecules*, 33, 8317 (2000).
- [143] Chung Y. M., Simmons K. L., Gutowska A., et al. *Biomacromolecules*, 3, 511 (2002).
- [144] Jeong B., Wang L. Q., Gutowska A. *Chem. Commun.*, 1516 (2001).
- [145] Liu X. M., Wang L. S., Wang L., et al. *Biomaterials*, 25, 5659 (2004).
- [146] Krogman N. R., Weikel A. L., Nguyen N. Q., et al. *Macromolecules*, 41, 7824 (2008).
- [147] Joziassse C. A. P., Grablowitz H., Pennings A. J. *Macromol. Chem. Phys.*, 201, 107 (2000).
- [148] Wang J. L., Dong C. M. *Macromol. Chem. Phys.*, 207, 554 (2006).
- [149] Yu X., Tang X. Z., Pan C. Y. *Polymer*, 46, 11149 (2005).
- [150] Cui Y. J., Tang X. Z., Huang X. B., et al. *Biomacromolecules*, 4, 1491 (2003).
- [151] Yuan W. Z., Yuan J. Y., Huang X. B., et al. *J. Appl. Polym. Sci.*, 104, 2310 (2007).
- [152] Pan T., Zhang G. L., Ma J. B. *Acta Polym. Sin.*, 330 (2006).
- [153] Li Y. X., Kissel T. *Polymer*, 39, 4421 (1998).
- [154] Cai C., Wang L., Dong C. M. *J. Polym. Sci. Part A: Polym. Chem.*, 44, 2034 (2006).
- [155] Liu Q., Cai C., Dong C. M. *J. Biomed. Mater. Res. Part A*, 88, 990 (2009).
- [156] Lu D. D., Yuan J. C., Li H. G., et al. *J. Polym. Sci. Part A: Polym. Chem.*, 46, 3802 (2008).
- [157] Zhang Z. P., Feng S. S. *Biomacromolecules*, 7, 1139 (2006).

## Biodegradable Poly(Lactic Acid): Synthesis, Modification, Processing and Applications

- [158] Yuan W. Z., Ren J. J. *Polym. Sci. Part A: Polym. Chem.*, 47, 2754 (2009).
- [159] Yuan W. Z., Yuan J. Y., Zheng S. X., et al. *Polymer*, 48, 2585 (2007).
- [160] Kang N., Leroux J. C. *Polymer*, 45, 8967 (2004).
- [161] Sun J., Chen X. S., Guo J. S., et al. *Polymer*, 50, 455 (2009).
- [162] Han D. H., Pan C. Y. *J. Polym. Sci. Part A: Polym. Chem.*, 44, 2794 (2006).
- [163] Wei H., Zhang X. Z., Chen W. Q., et al. *J. Biomed. Mater. Res. Part A*, 83, 980 (2007).
- [164] Wei H., Chen W. Q., Chang C., et al. *J. Phys. Chem. C*, 112, 2888 (2008).
- [165] Yuan W. Z., Yuan J. Y., Zhou M., et al. *J. Polym. Sci. Part A: Polym. Chem.*, 44, 6575 (2006).
- [166] Han D. H., Pan C. Y. *J. Polym. Sci. Part A: Polym. Chem.*, 45, 789 (2007).
- [167] Shi P. H., Li Y. G., Pan C. Y. *Eur. Polym. J.*, 40, 1283 (2004).
- [168] Nagahama K., Nishimura Y., Ohya Y., et al. *Polymer*, 48, 2649 (2007).
- [169] Kim Y. S., Gil E. S., Lowe T. L. *Macromolecules*, 39, 7805 (2006).
- [170] Luan B., Pan C. Y. *Eur. Polym. J.*, 42, 1467 (2006).
- [171] Kong L. Z., Pan C. Y. *Polymer*, 49, 200 (2008).
- [172] Gong F. R., Cheng X. Y., Wang S. F., et al. *Polymer*, 50, 2775 (2009).
- [173] Noda I., Bond E. B., Melik D. H. U. S. Pat. 6808795 (2004).
- [174] Randall J. R., Ryan C. M., Lunt J., et al. U. S. Pat. 6495631 (2002).
- [175] Averous O. M. *Polymer*, 42 (12): 6209-6219 (2001) .
- [176] Sheth M., Kumar R. A., Dave V., et al. *J. Appl. Polym. Sci.*, 66(8),1495 (1997).
- [177] Wu C. S., Liao H. T. *Polymer*, 46(23), 10017 (2005).
- [178] Tsuji F. *Polymer*, 43(6), 1789 (2002).
- [179] Hu Y., Rogunova M., Topolkaev V., et al. *Polymer*, 44(19), 5701 (2002).
- [180] Hu Y., Hu Y. S., Topolkaev V., et al. *Polymer*, 44(19), 5711 (2002).
- [181] Hu Y., Hu Y. S., Topolkaev V., et al. *Polymer*, 44(19), 5681 (2003).
- [182] Renard E., Walls M., Guerin P., et al. *Polym. Degrad. Stabil.*, 85(2), 779 (2004).
- [183] Marcott C., Dowrey A. E., Van Poppel J., et al. *Vib. Spectrosc.*, 36(2), 221 (2004).
- [184] Karst D., Yang Y. Q. *Polymer*, 47(13), 4845 (2006).
- [185] Wu D. F., Zhang Y. S., Zhang M., et al. *Eur. Polym. J.*, 44(7), 2171 (2008).
- [186] Chen C. C., Chueh J. Y., Tseng H., et al. *Biomaterials*, 24(7), 1167 (2003).
- [187] Mi F. L., Shyu S. S., Lin Y. M., et al. *Biomaterials*, 24(27), 5023 (2003).
- [188] Yokohara T., Yamaguchi M. *Eur. Polym. J.*, 44(3), 677 (2008).
- [189] Cao X., Mohamed A., Gordon S. H., et al. *Thermochim. Acta*, 406(1-2), 115 (2003).
- [190] Cossement D., Gouttebaron R., Cornet V., et al. *Appl. Surf. Sci.*, 252(19), 6636 (2006).
- [191] Park J. W., Im S. S. *Polymer*, 44(15), 4341 (2003).
- [192] Gu S. Y., Zhang K., Ren J., et al. *Carbohydr. Polym.*, 74(1), 79 (2008).
- [193] Garlotta D. J. *Polym. Environ.*, 9, 61 (2002).
- [194] Fang Q., Hanna M. A. *Indus. Crops. Pds.*, 10, 47 (1999).
- [195] Palade L., Lehermeier H. J., Dorgan J. R. *Macromolecules*, 34, 1384 (2001).
- [196] Yamane H., Sasai K. *Polymer*, 44, 2569 (2003).
- [197] Lindblad M. S., Liu Y., Albertsson A. C., et al. *Adv. Polym. Sci.*, 157, 139 (2002).
- [198] Bledzki A. K., Gassan J. *Prog. Polym. Sci.*, 24, 221 (1999).
- [199] Wollerdorfer M., Bader H. *Ind. Crop. Prod.*, 8, 105 (1998).



- [200] Herrmann A. S., Nickel J., Riedel U. *Polym. Degrad. Stabil.*, 59, 251 (1998).
- [201] Pfaendner R. *Polym. Degrad. Stabil.*, 91(9), 2249 (2006).
- [202] Li S. M., Yuan H., Yu T., et al. *Polym. Advan. Technol.*, 20(12), 1114 (2009).
- [203] Muasher M., Sain M. *Polym. Degrad. Stabil.*, 91(5), 1156 (2006).
- [204] Bojinov V., Grabchev I. J. *Photoch. Photobio. A*, 150(1-3), 223 (2002).
- [205] Seliger H., Happ E., Cascaval A., et al. *Eur. Polym. J.*, 35(5), 827 (1999).
- [206] Martin O., Averous L. *Polymer*, 42(14), 6209 (2001).
- [207] Ljungberg N., Wesslen B. *Polymer*, 44(25), 7679 (2003).
- [208] Rahman M., Brazel C. S. *Prog. Polym. Sci.*, 29(12), 1223 (2004).
- [209] Takahashi M., Onishi H., Machida Y. *J. Control Release*, 100(1), 63 (2004).
- [210] Karst D., Nama D., Yang Y. Q. *J. Colloid Interf. Sci.*, 310(1), 106 (2007).
- [211] Vladislavljevic G. T., Williams R. A. *Adv. Colloid Interfac.*, 113(1), 1 (2005).
- [212] Ren J., Fu H. Y., Ren T. B., et al. *Carbohydr. Polym.*, 77(3), 576 (2009).
- [213] De Santis P., Kovacs A. J. *Biopolymers*, 6, 299 (1968).
- [214] Cartiera L., Okihara T., Ikadab Y., et al. *Polymer*, 41, 8909 (2000).
- [215] Eling B., Gogolewski S., Pennings A. J. *Polymer*, 23, 1587 (1982).
- [216] Hoogsteen W., Postema A. R., Pennings A. J., et al. *Macromolecules*, 23, 634 (1990).
- [217] Laurent Cartier, Bernard Lotz. *Macromolecules*, 31, 3049 (1998).
- [218] Laurent Cartier, Takumi Okihara, Bernard Lotz. *Macromolecules*, 31, 3303 (1998).
- [219] Puiggalia J., Ikadab Y., Tsujic H., et al. *Polymer*, 41, 8921 (2000).
- [220] Brizzolara Davide, Cantow Hans-Joachim, Diederichs Kay, et al. *Macromolecules*, 29, 191 (1996).
- [221] Tadakazu Miyata, Toru Masuko. *Polymer*, 39, 5515 (1998).
- [222] Vasanthakumari R., Pennings A. J. *Polymer*, 24, 175 (1983).
- [223] Jose-Ramon Sarasua, Robert E., Prud'homme, et al. *Macromolecules*, 31, 3895 (1998).
- [224] Angela M. Harris, Ellen C. Lee. *Journal of Applied Polymer Science*, 107, 2246 (2008).
- [225] Liao Ruogu, Yang Bin, Yu Wei, et al. *Journal of Applied Polymer Science*, 104, 310 (2007).
- [226] Joo Young Nam, Masami Okamoto, Hirotaka Okamoto, et al. *Polymer*, 47, 1340 (2006).
- [227] Kawamoto N., Sakai A., Horikoshi T., et al. *Journal of Applied Polymer Science*, 103, 198 (2007).
- [228] Ren Jie, Gui Baozhu, Yuan Weizhong, et al. *Polymer*(submitted).
- [229] Hideto Tsuji, Hiroki Takai, Swapan Kumar Saha. *Polymer*, 47, 3826 (2006).
- [230] Lu M., Paul D. R. *Polymer*, 37(1), 115 (1996).
- [231] Lu M., Keskkula H., Paul D. R. *Polymer*, 37(1), 125 (1996).
- [232] Yan S. F., Yin J. B., Yang J. Y., et al. *Mater. Lett.*, 61(13), 2683 (2007).
- [233] Kuan C. F., Chen C. H., Kuan H. C., et al. *J. Phys. Chem. Solids*, 69(5-6), 1399 (2008).
- [234] Nakayama N., Hayashi T. *Polym. Degrad. Stabil.*, 92(7), 1255 (2007).

## 5 Processing of PLA

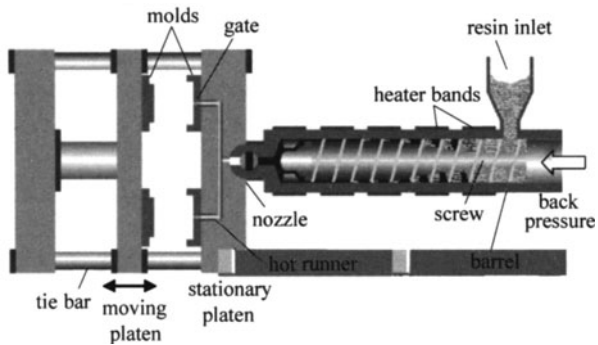
**Abstract** Processing method is important to broaden the application area of PLA materials. The processing technologies include injection molding, hot press molding, spinning, blow molding, foam molding and electrospinning. In this chapter, for different application, four processing methods are selected to discuss in detail including injection, spinning, blowing and foaming. And the structure development in the processes, mechanical properties and corresponding application are also discussed.

**Keywords** processing, injection, spinning, coaxial electrospinning, dry-jet-wet spinning, dry spinning, dry-wet phase-inversion spinning process, dyeability, melt spinning, wet spinning, blowing, foam molding, electrospinning

### 5.1 Injection

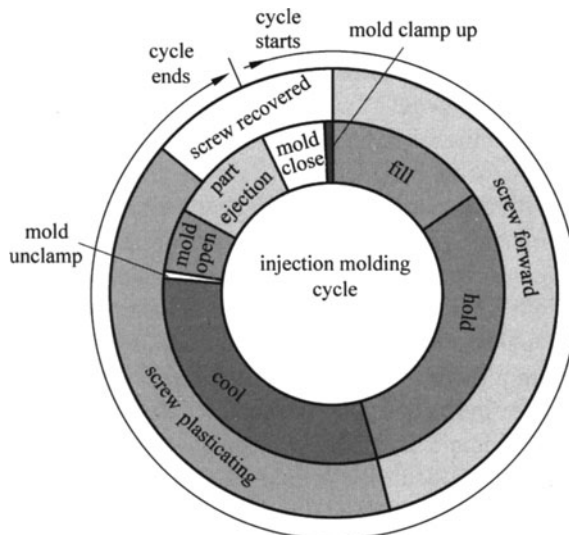
#### 5.1.1 PLA Injection Molding

Injection molding is the most widely used converting process for thermoplastic articles, especially for those that are complex in shape and require high dimensional precision. All injection molding machines have an extruder for plasticizing the polymer melt. Unlike a standard extruder, the extruder unit for injection molding machine is designed such the screw can reciprocate within the barrel to provide enough injection pressure to deliver the polymer melt into the mold cavities (Fig. 5.1). Most injection molding machines for PLA are based on the reciprocating screw extruder, although two-stage systems, which integrate a shooting pot and extruder in a single machine, have also been deployed for injection molding of preforms for PLA bottles. The two-stage system consists of an in-line extruder integrated to a shooting pot. The extruder plasticizes and feeds the melt into the shooting pot under relatively low injection pressure, from which the melt is injected into the hot runner under high pressure by a plunger in the shooting pot. While the reciprocating machine must stop the screw during the injection and packing phases, the screw for the two-stage machine can rotate during the majority of the cycle. The two-stage system presents some advantages over its reciprocating counterpart, including shorter cycle time, small screw motor drive, more consistent melt quality, and more consistent shot size [1].



**Figure 5.1** Major components of an injection molding machine showing the extruder (reciprocal screw) and clamp units [1]

A typical cycle for an injection molding machine is presented in Fig. 5.2. The beginning of mold close is usually taken as the start of an injection molding cycle. Immediately after the molds clamp up, the nozzle opens and the screw moves forward, injecting the polymer melt into the mold cavity. To compensate for the material shrinkage during cooling in the mold, the screw is maintained in the forward position by a holding pressure. At the end of the holding phase, the nozzle is shut off and the screw begins to recover, while the part continues to be cooled in the mold. During the recovery phase, the screw rotates and conveys the polymer forward along the screw. At the same time, the screw is allowed to slide backward within the barrel against a controlled back pressure exerted on the screw by a hydraulic cylinder. To ensure that the part is dimensionally stable enough



**Figure 5.2** Typical cycle for an injection molding process [1]

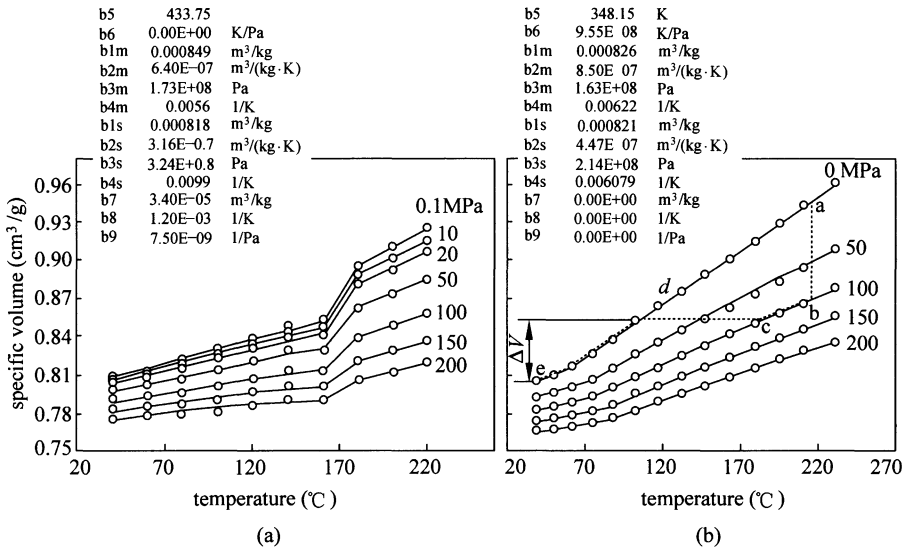
to withstand the opening stroke, sufficient cooling time must be given to the mold. In the molding cycle, heat removal takes place predominantly during the fill, hold and cool phases, although mold opening phase also contributes to partial cooling since one side of the part (core-contacting side) is still being cooled prior to ejection.

Cycle time is an important process parameter that is often minimized to maximize the production throughput. To reduce the cycle time, it is quite common to transfer the partially cooled injection molded article to a post-mold cooling device to provide an extended cooling of the part outside the molds, either by direct contact on a chilled surface and/or by forced air. From Fig. 5.2, it is also evident that minimizing the duration for non-process events, such as mold opening, part ejection and mold closing is also important for reducing the cycle time. Lowering mold temperature can also increase the heat extraction rate from the polymer. Nevertheless, the propensity of lactide condensation on the cold tooling surfaces, which can affect the surface finish and weight of the molded articles, limits the minimal temperature that can be used during injection molding of PLA to 25 – 30°C. The use of molds with polished surfaces, in conjunction with an increased injection speed during fill, can also reduce the deposition of the lactide layers.

The fill, hold and cool events that take place during injection molding have an important implication on the shrinkage of the injection molded articles. This effect can be best elucidated using a pressure-volume-temperature (PVT) diagram [2]. The different profiles shown here are likely due to the different grades of PLA used. During injection molding, the polymer is first subjected to isothermal injection of the polymer melt into the mold cavity, during which the pressure increases as the polymer is being injected and packed to the holding pressure (trace ab in Fig. 5.3). The polymer then undergoes isobaric cooling in the holding phase (trace bc), followed by isochoric cooling. When the polymer cools below the freezing point, the gate freezes and the pressure in the mold cavities drops to one atmospheric pressure (trace cd). In the last cooling phase, the article continues to cool isobarically to room temperature (trace de). The change in specific volume during the final isobaric cooling (trace de) dictates the extent of part shrinkage. The hold pressure and temperature play an important role in determining how much the molded article shrinks.

The PVT relationship can be modeled mathematically by using the modified two-domain Tait model. This model is often used for numerical simulation of injection molding processes involving finite element analysis for predicting the shrinkage behavior of injection molded articles. The estimated parameter values for the modified two domain Tait model are shown in the inserts in Fig. 5.3.

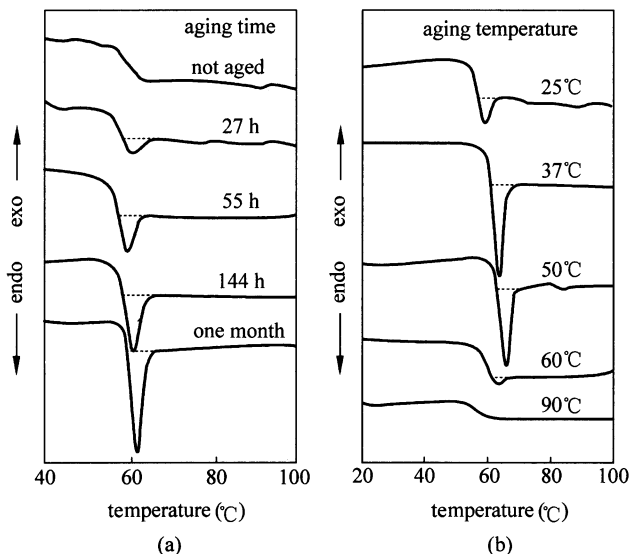
In general, injection molded PLA articles are relatively brittle. The brittleness of PLA has been attributed to the rapid physical aging of the polymer since ambient temperature is only about 25°C below the  $T_g$ . The aging of PLA can be evaluated by studying the  $T_g$  region of a DSC scan and measuring the development of



**Figure 5.3** PVT plots for PLA based on the data from Sato et al. and Natureworks LLC. The continuous lines represent the fitted results based on the two-domain modified Tait model [2]

endothermic enthalpy relaxation  $\Delta H_{rel}$  using DSC on injection molded samples made from PLA (96% *L*-lactide).  $\Delta H_{rel}$  increases with increasing aging time [3]. As the aging temperature increases towards the  $T_g$ , the rate of physical aging also becomes faster. However, when the aging temperature goes to above the  $T_g$  (60°C), the excess enthalpy relaxation is reduced, indicating that physical aging is no longer taking place when the aging temperature is above  $T_g$ . The extent of aging increases with decreasing molecular weight (i.e.,  $\Delta H_{rel}$  increases with decreasing molecular weight), which is attributed to the increased chain terminals that possess higher motional freedom than the internal chain segments, as shown in Fig. 5.4. In the physical implication of aging, the injection molded articles immediately after quenching to very cold temperatures exhibit a much larger extension to break. However, when the molded articles are aged at room temperature for 3 – 8 h, they become very brittle. This phenomenon is attributed to the reduction of free volume of the polymer due to rapid relaxation towards the equilibrium amorphous state. Aging below  $T_g$  is exclusively related to the amorphous phase of the polymer; accordingly, increasing the crystallinity of the polymer (e.g., by adjusting *D*-isomer composition or the use of nucleating agents) will reduce the aging effect. Furthermore, the crystallites formed also act like physical crosslinks to retard the polymer chain mobility. However, amorphous injection molded articles that are intended for further processing (e.g., preforms for stretch blow molding), the storage conditions prior to subsequent processing may need to be controlled. Moreover, process parameters such as mold temperature,

packing pressure, cooling rate, and post-mold cooling treatment are expected to influence the PLA aging behavior as well.



**Figure 5.4** Effects of temperature and time on the aging of injection molded 4% *D*-lactide PDLA specimens. (a) DSC curves of PLA aged at room temperature for various aging times; (b) DSC curves of PLA annealed for 24 h at different temperatures [4]

### 5.1.2 Controlling Crystallinity in Injection Molded PLA

Currently, use of PLA for injection molded articles is limited for commercial applications because PLA has a slow crystallization rate when compared with many other thermoplastics as well as standard injection molding cycle times. The overall crystallization rate and final crystallinity of PLA are controlled by the addition of physical nucleating agents as well as optimization of injection molding processing conditions [4].

It is well known that PLA crystallinity can play a significant role in the mechanical and durability performance in rigid molded applications. An increase in the polymer's overall crystallinity can lead to improvements in stiffness, strength, heat deflection temperature and chemical resistance. However, obtaining a highly crystalline, injection molded article of PLA remains difficult due to the slow crystallization rate. The crystallization half time,  $t_{1/2}$ , of a pure sample of PLA is reported in the literature to be in the range of 17 – 45 min, depending on crystallization temperature, stereochemistry, and molecular weight, whereas polypropylene homopolymers have half times that can be faster by an order of

magnitude at similar degrees of undercooling. To obtain a component with sufficient crystallinity to maximize physical property enhancements during injection molding, the cycle time would be extremely long or a post-annealing step would have to be added. Since a typical injection molding cycle time is 60–90 s, this would be impractical and economically unrealistic for high volume automotive use.

### 5.1.3 Mechanical Properties of Injection-Molded Poly (*L*-Lactic Acid)

For different applications, PLA can be easily processed using conventional polymer processing techniques like injection molding, sheet extrusion, blow molding, thermoforming, and fiber spinning. However, for different processing techniques, PLA resins need to be tailor made, e.g., branching is typically introduced to obtain high melt strength, which is suitable for processing like extrusion, coating, blow molding, and foaming. For thermoforming, 4%–8% *D*-isomer is introduced to avoid crystallization during stretching of the polymer below melting point [5]. Table 5.1 shows the injection molding processing parameters ( $T_m$ ,  $T_w$ ,  $Q_{inj}$ ,  $P_h$ ) and simulated thermomechanical variables ( $T_b$ ,  $\gamma$ ,  $\tau_w$ ,  $S_a$ ) of poly (*L*-lactic acid) (PLLA).

**Table 5.1** Injection molding processing parameters ( $T_m$ ,  $T_w$ ,  $Q_{inj}$ ,  $P_h$ ) and simulated thermomechanical variables ( $T_b$ ,  $\gamma$ ,  $\tau_w$ ,  $S_a$ ) of PLLA [7]

Run	$T_m$ (°C)	$T_w$ (°C)	$Q_{inj}$ (cm <sup>3</sup> /s)	$P_h$ (MPa)	$T_b$ (°C)	$\gamma$ (s <sup>-1</sup> )	$\tau_w$ (MPa)	$S_a$ (%)
I	165	24	7	7	171.7	2594	0.61	4.4
II	165	60	7	29	172	2592	0.61	2.8
III	165	24	28	29	177.8	21,550	0.82	2.7
IV	165	60	28	7	178.1	18,845	0.79	1.5
V	220	24	7	29	224.3	2505	0.46	4.4
VI	220	60	7	7	224.3	2510	0.46	2.8
VII	220	24	28	7	227.0	10,304	0.63	2.8
VIII	220	60	28	29	227.1	10,339	0.64	1.5
Variation (10%)					32	760	78	193

The development of different microstructures because of the applied thermomechanical conditions during injection molding depends upon the operative parameters involving melt processing temperature, mold temperature,

the injection flow rate, and holding pressure. For the particular case of high *L*-lactide content linear PLA, most of the injection-molded articles exhibit low degree of crystallinity because of its slow crystallization rate and the high cooling rates imposed during processing. Typically, a nucleating agent is added to enhance the rate of crystallization and to obtain higher crystallinity. In this regard, a recent review highlights the demanding technological importance and complexity of crystallinity development of stressed melt under intense flow field [6]. However, the effect of shear stress and shear rate on molecular orientation and crystallinity development of injection-molded PLLA products were not properly addressed so far.

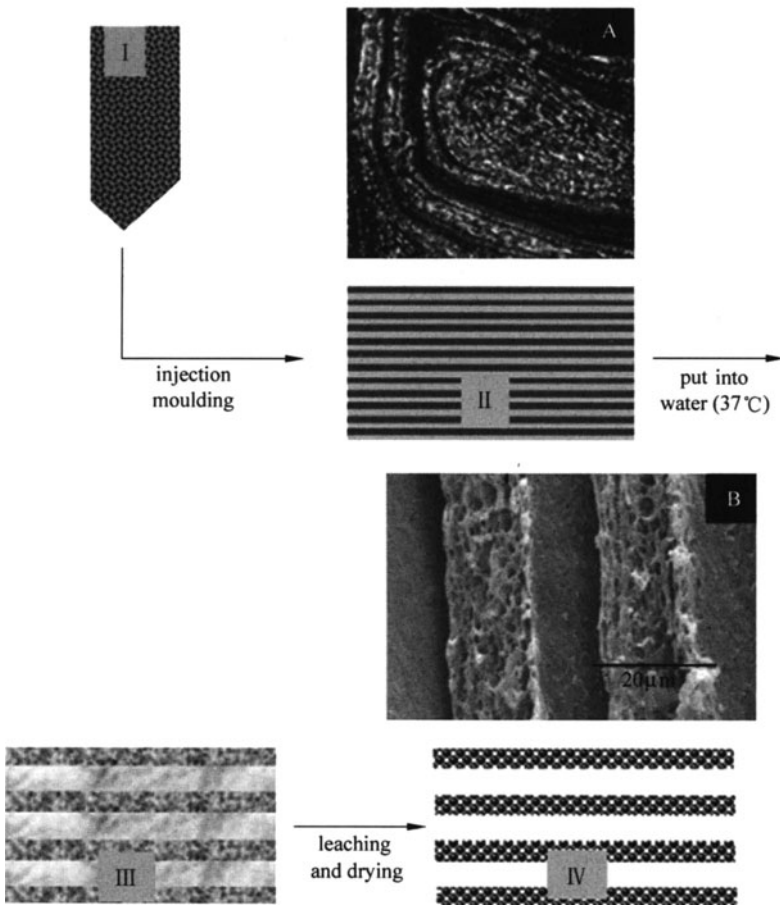
### **5.1.4 Porous Lamellar Poly (*L*-Lactic Acid) Scaffolds Made by Conventional Injection Molding Process**

A number of processing techniques based on textile technologies, including thermally induced phase separation, solvent casting/particulate leaching, fiber templating, melt extrusion and combinations of the above techniques have been used for the preparation of multi-tubular and simple tubular structures. Hollow conduit-like constructs can be fabricated by melt-based processing techniques, such as extrusion of polymer/salt followed by leaching of salt; radial alignment of internal pores across a hollow tube by spinning a polymer suspension followed by freeze drying and sublimation; formation of tubular scaffolds by rolling freeze-dried films into the form of a tube; bonding of non-woven polymer meshes wrapped around a mandrel and spraying a polymer solution onto them; or formation of hollow fabric tubes by knitting of prefabricated yarns followed by dipping in solution, freezing and sublimation. The multitubular porous scaffolds can also be prepared by phase-separation techniques, e.g. (I) freezing of polymer solution and sublimation of solvent; (II) freezing polymer/solvent with a uniaxial temperature gradient followed by sublimation of solvent; (III) injecting polymer suspension into a prefabricated multiple channel mold followed by sublimation of solvent; (IV) freeze-drying with a uniaxial thermal gradient; (V) fiber templating technique; and (VI) Solution coating and gas foaming by porogen decomposition. Scaffolds prepared by the freeze-drying process are limited to thin constructs and the dense outer wall of the scaffolds may not allow interaction between the cells in the lumen and the surrounding tissue. Moreover, the dense outer walls may prevent scar tissue from invading into the scaffolds and suppress tissue regeneration. The permeability of the tubular wall is an important requirement of such scaffolds as it facilitates the supply of oxygen and nutrients and the removal of metabolic waste substances. Moreover, the use of organic solvents in most of these fabrication processes and the potential toxicity of these solvents has already been reviewed.



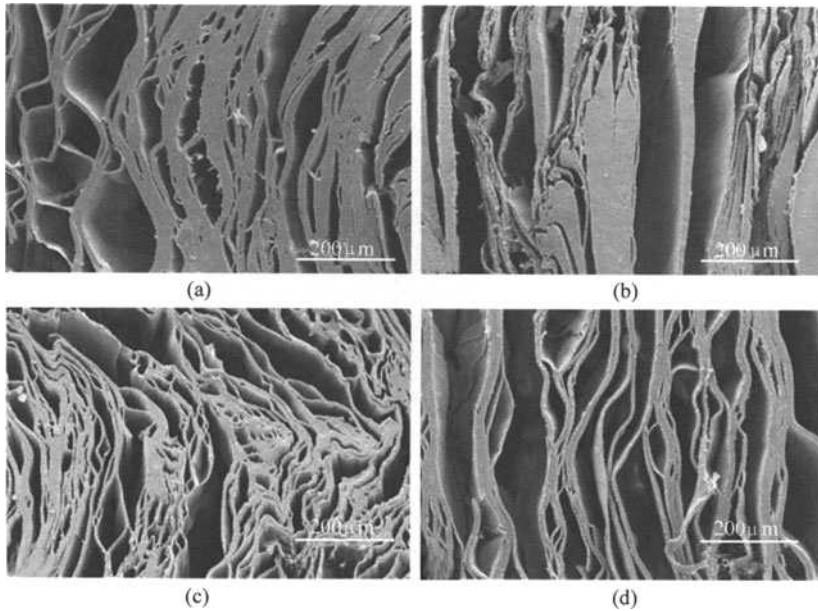
Three-dimensional porous scaffolds can also be produced from selective dissolution of a polymer from blends such as PLLA/polystyrene, PLLA/poly ( $\epsilon$ -caprolactone) and poly ( $\epsilon$ -caprolactone)/poly (ethyl-eneoxide) (PEO). It has been demonstrated that a layered structure can also be produced by injection molding of the partially miscible polymer blend. Injection molding is a versatile, efficient and highly reproducible process, capable of fast production of complex geometric shapes with tight dimensional tolerances. Injection molding has been used to prepare scaffolds by compounding polymer with a blowing agent. In that case sphere-shaped pores are obtained as shown in Fig. 5.5.

The 50/50 wt% PLLA and PEO was compounded in a tumbler mixer in solid form and put into the hopper. The lamellar structure is developed by injection molding of the blend above the melting temperature of PLLA and PEO, and the



**Figure 5.5** Scheme for preparing the porous lamellar scaffolds using a conventional injection molding process

morphology is maintained by quenching at 5°C. The molded specimens were immediately immersed in water at 37°C and the blend swells in water. The porous lamellar scaffolds are obtained by aqueous leaching of water-soluble porogen. The optical micrograph shows the lamellar structure of the compact injection molded specimen and the SEM micrograph shows the porous lamellar architecture as shown in Fig. 5.6 [7].



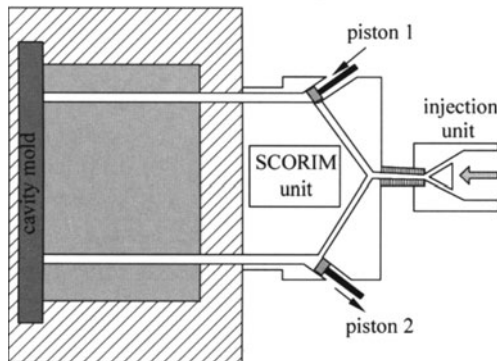
**Figure 5.6** SEM micrographs showing the lamellar architectures along the cross-section of PLLA scaffolds prepared from injection molding of a 50/50 wt % blend of PLLA and PEO followed by swelling and posterior leaching of porogen. (a) Melt processing temperature = 165°C, injection flow rate = 7 cm<sup>3</sup>/s; (b) melt processing temperature = 165°C, injection flow rate = 56 cm<sup>3</sup>/s; (c) melt processing temperature = 190°C, injection flow rate = 7 cm<sup>3</sup>/s; (d) melt processing temperature = 190°C, injection flow rate = 56 cm<sup>3</sup>/s

### **5.1.5 Shear Controlled Orientation in Injection Molding of PLLA**

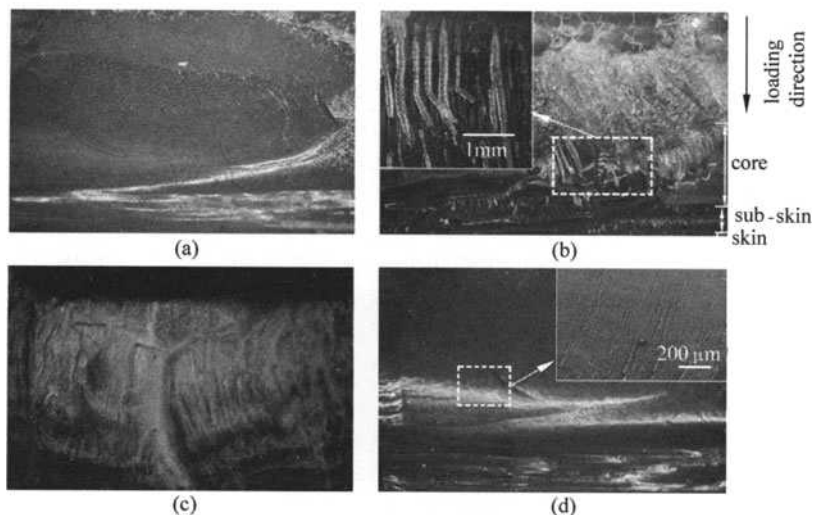
A technique based on injection molding, as it is a versatile, efficient and highly reproducible process, and capable of fast production of complex geometric shapes with tight dimensional tolerances has been studied. The mechanical property of PLLA can be optimized up to a certain level through manipulation of thermomechanical environment of conventional injection molding. Non-conventional injection molding processes like shear controlled orientation in

injection molding (SCORIM) have additional degrees of freedom over conventional injection molding (CIM), as SCORIM technique manipulates the structure development of a solidifying polymer melt through an in-mold shearing action, thereby tailoring the morphology and hence controlling the mechanical properties of polymers. SCORIM has already been successfully used to optimize the mechanical properties of starch/ethylene vinyl alcohol copolymer blends and composites based biomaterials intended for biomedical applications. Normally, this method is based on a conventional injection molding machine fitted with an externally controlled in-mold unit, the SCORIM unit, which has two cylinders and each cylinder is located on its own melt flow path leading to the corresponding gates (Fig. 5.7). The processing cycle begins with the filling of the cavity. The filling of the cavity is carried out with one gate. After the filling phase, the melt manipulation can be carried out with three modes of SCORIM operations. Mode-A, an out of phase reciprocation of the two pistons, causing the back and forth movement of the cylinders and thus manipulating the melt inside the mold; Mode-B, an in-phase operation, which pumps more melt into the cavity; and Mode-C, hydrostatic pressure applied by the two cylinders for offsetting volumetric shrinkage [8]. The cross-sectional fracture surfaces of the PLLA article detected by reflected light microscopy images are shown in Fig. 5.8. The flexural modulus, maximum stress, energy at break and hot recoverable strain of the CIM and SCORIM processed PLLA are shown in Table 5.2.

In conventional injection molding, the melt processing temperature plays the most significant role in regulating the thermomechanical state of PLLA. The melt viscosity of PLLA is higher at low temperature and decreases with increasing temperature and the higher stress associated with high viscosity melt induces more shear induced molecular orientation. The changes in mechanical properties of PLLA are mitigated when the SCORIM processing is carried out with the concomitant changes in melt processing temperature and mold temperature.



**Figure 5.7** Schematic diagram of SCORIM technique



**Figure 5.8** Reflected light microscopy images showing the cross-sectional (13 mm×8 mm) fracture surfaces of the PLLA specimens prepared with the mold temperature = 30°C. (a) conventional injection molding; (b) with SCORIM (shearing time = 3 s, number of strokes = 3), insets showing the fibril morphology in the core region; (c) with SCORIM (shearing time = 10 s, number of strokes = 10); (d) with SCORIM (shearing time = 15 s, number of strokes = 3), insets showing the fibril morphology in the core region. The scale bar = 4 mm

**Table 5.2** The flexural modulus, maximum stress, energy at break and hot recoverable strain of the CIM and SCORIM processed PLLA

Run	Elastic modulus (GPa)	Maximum stress (MPa)	Energy at break (J)	Hot recoverable strain (%)
A*	2.88±0.04	31±2	0.20±0.02	0.13±0.05
A1	2.83±0.06	68±5	1.26±0.14	0.84±0.24
A2	2.88±0.03	55±7	0.64±0.14	2.19±0.41
A3	2.92±0.04	45±9	0.58±0.16	2.67±0.39
B*	2.83±0.09	29±3	0.17±0.04	0.08±0.03
B1	2.86±0.07	50±2	0.54±0.05	0.32±0.12
B2	2.82±0.08	65±2	0.92±0.24	1.6±0.31
B3	2.96±0.07	68±1	0.94±0.02	1.9±0.42
Variations (10%)	5	134	641	3238

## 5.2 Spinning

PLA is an aliphatic polyester. It is a biodegradable thermoplastic and can be processed to become composites. Its monomer, lactic acid, is derived from

renewable plant sources, such as starch and sugar. PLA can be degraded into carbon dioxide and water by an action of suitable fungi. This means that biodegradable PLA fibers are environment friendly material even if the fiber is left in the natural environment. The demand for PLA fibers as a substitute for the present synthetic fibers has been growing greatly in recent years.

On the other hand, high water vapor transmission rate of PLA makes it a good candidate for fabricating fibers used in garments (e.g., shirts, dresses, underwear, shoes, etc.) to improve their “breathability”. While PLA fibers are not as wettable as cotton, they exhibit much greater water vapor transmission than aromatic polyesters or nylon fibers.

The manufacturing of PLA fiber is carried out by melt spinning, dry spinning, wet spinning, and dry-jet-wet spinning processes. Like other polyesters, such as polyethylene terephthalate (PET), PLA fibers can be manufactured by melt spinning owing to the thermoplastic nature of PLA. Melt spinning usually has advantages over wet spinning; i.e. it is a solvent-free process and provides a more economical and eco-friendly route. Production rate is normally higher than that in solution spinning. Sometimes, however, melt spinning is not possible, either because the polymer degrades while melting or the melt is thermally unstable. In dry spinning, solvents are removed by thermal evaporation while in wet spinning the coagulation of the polymer is carried out in another fluid that is compatible with the spinning solvent but is not itself a solvent for the polymer. Commercially PLA fibers are generally produced using the melt spinning technique. And ultra-fine PLA fibers can be produced by electrospinning.

### 5.2.1 Melt Spinning of PLA

Melt spinning of PLA was one of the first methods used to produce PLA fibers. Various research groups have studied the melt spinning of PLA fibers under various processing conditions. A range of production rates has been studied, from a few meters to a few thousand meters per minute. PLA fibers are typically melt-spun at approximately 185–240°C through spinnerets with  $L/D$  ratios of 2–10. The melting temperature used also depends on the optical purity of the polymer used. Lower processing temperatures can be used for polymer with lower optical purity (i.e., greater *D*-isomer content), which can help reduce the thermal and hydrolytic degradation. Fiber-grade PLA needs to be dried to contain moisture of less than 50 ppm before melting to minimize molecular weight drop.

In a 2-stage melt spinning process the polymer is first heated to temperature of above its melting point and then spun through spinneret. The solidification is achieved by cooling in the air and the take-up roller. In the second stage, the as-spun fibers undergo hot drawing where the filaments are pulled by a take-up roll with a specific speed to achieve fiber orientation, which is important to increase the tenacity and stiffness of the fibers. PLA can also be melt spun in a

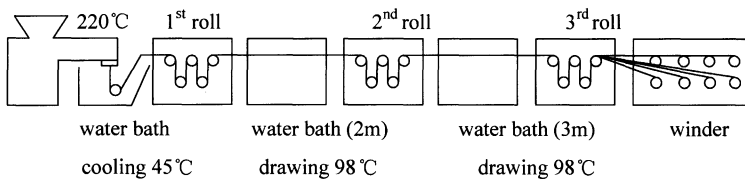
high-speed spinning process with take-up speed of up to 5000 m/min and a draw ratio of up to six. The degree of crystallinity of the fiber increases with spinning velocity due to stress-induced crystallization. While high speed spinning provides high fiber manufacturing output, manufacturing of fiber with uniform diameter is not a trivial task under high speed condition due to process instability caused by the draw resonance known as spinline neck-like deformation. The phenomenon is related to the spinline flow-induced crystallization [9, 10].

Melt spinning of PLA was first reported by Eling et al. [11]. PLLA with molecular weight below 300 000 was extruded at 185°C through a capillary with a diameter of 1 mm and length of 10 mm. The take-up speed was 250–350 mm/min. Hot drawing of the fibers was then carried out in an electric tube furnace of 500 mm in length with input speed 20 mm/min. 2-step melt spinning of PLLA with viscosity average molecular weight 330 000 was reported by Fambri et al. [12]. Monofilaments of 1 mm in diameter were spun from a single-screw extruder under an inert atmosphere at take-up speeds ranging from 1.8 to 10 m/min. The as-spun fibers were drawn at 160°C using a hot plate drawing apparatus at various drawing rates. The molecular weight of PLLA fibers fell to about 100 000. Ninety per cent of the molecular weight loss occurred during extrusion and ten percent during hot-drawing. At fixed extrusion rate, properties of as-spun fibers strongly depended on their collection rate. The higher the collection rate, the higher the modulus and strength, and the lower the strain at break. While almost amorphous fibers were obtained at lower collection rates (1.8 and 3.1 m/min), about 30% and 38% crystalline as-spun fibers were produced at rates of 5 and 10 m/min, respectively. Tensile modulus of 9.2 GPa and tensile strength of 0.87 GPa were obtained for fibers collected at 5 m/min and draw ratio of 10. PLLA. PLA of three viscosity-average molecular weights (494 600, 304 700, and 262 800) from Purac were melt spun by Yuan et al. [13]. Prior to melt spinning PLA was dried in a vacuum oven at 50°C for at least 48 h. PLLA fibers were prepared by a two-step melt spinning process, i.e., melt extrusion and hot drawing. The fibers were spun at the die temperature ranging from 200 to 240°C. The as-spun fibers were collected at a rate of 3.20 m/min on a sand blasted glass drum, and subsequently drawn in nitrogen atmosphere at 120°C in a self-constructed hot drawing apparatus at a feed velocity of 0.26 m/min and a take-up speed of 1.09 m/min (the second step). Another 10 min of heat treatment was conducted additionally in nitrogen atmosphere at 120°C to get the final hot-drawn fibers. The extent of decrease in viscosity average molecular weight of PLLA dropped sharply by 39.0%–69.0% during melt-extrusion. The hot-draw process in this study had a little effect on the viscosity-average molecular weight of PLLA. Smoother fibers could be obtained for the die temperature at least 230°C for raw materials with higher crystallinity (more than 75%) and at least 220°C for raw materials with lower crystallinity (about 60%). The as-spun fibers showed crystallinity of 16.5%–22.8% and the value increased to 50.3%–63.7% after hot drawing. Tensile moduli of the as-spun fibers were in

the range of 1.2–2.4 GPa which were raised to 3.6–5.4 GPa after hot drawing. The final PLLA fibers with diameters of 110–160  $\mu\text{m}$  showed tensile strengths of 300–600 MPa.

PLA supplied by Galactic (Belgium) was melt spun to produce multifilament continuous yarns by Solarski et al. Spin-drawing of PLA was realized with the spinning device Spinboy I from Busschaert Engineering. PLA pellets were first melted in a single screw extruder at temperatures from 220 to 225°C. Then molten PLA was passed through two dies consisting of 40 circular channels with a diameter of 400  $\mu\text{m}$  to produce a multifilament yarn which was coated with Filapan CTC, a spin-finish supplied by Boehme. At last, the multifilament yarns were hot drawn between two rolls with different speeds and temperatures. The feed rate was fixed at 150 or 200 m/min. The draw ratio (DR) varied between 2 and 4. The draw temperature was in the range of 60–70°C. Fibers with diameter in the range of 45 to 56  $\mu\text{m}$ , tensile strength in the range of 258 to 414 MPa and tensile modulus in the range of 4.2 to 5.7 were obtained [14].

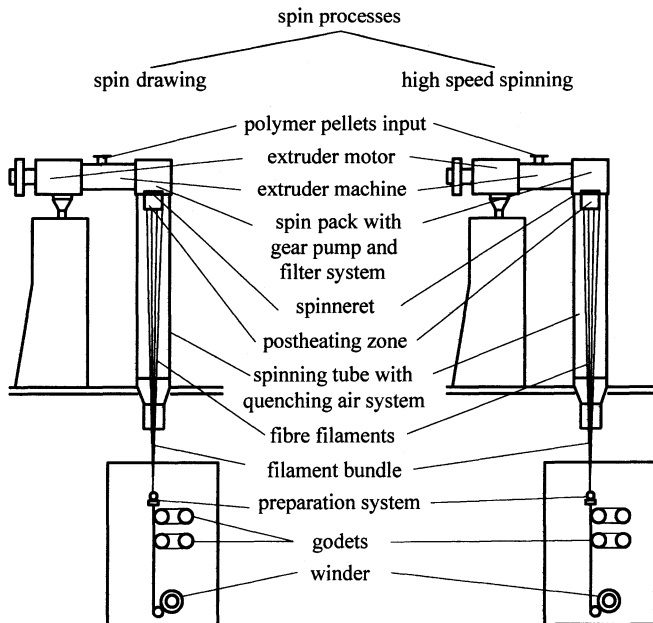
The melt spinning and melt drawing of PLLA were carried out with a melt spinning machine as shown in Fig. 5.9 by Nishimura et al. [15]. At the end of a 35 mm single-screw extruder (length/diameter = 28) a spinning nozzle with 12 holes (1.0 mm in diameter) was installed. The melt extrusion temperature was kept at 220°C. The molten PLLA was extruded into water (45°C) in a cooling bath. The take-up speed for the melt-spun fiber was 8 m/min. The as-spun fiber was then drawn on drawing machines with temperature kept at 98°C. Drawing ratios of 6–18 were employed. The diameter of the fibers was adjusted from 100 to 200  $\mu\text{m}$ . PLLA fibers with a tensile strength of 0.81 GPa were successfully obtained through two steps of drawing at a draw ratio of 18 in hot water.



**Figure 5.9** Outline of the production line for melt spinning and melt drawing [15]

All the above fiber forming studies have used processes that had typical fiber take-up velocities of a few centimeters to a few meters per minute, much too slow for industrial production. Schmack et al. [16, 17] investigated high-speed melt spinning and spin drawing process of type LA 0200 K PLA. The type LA 0200 K PLA is a copolymer of *L*-lactide (92 wt%) and *meso*-lactide (8 wt%). The pellets were dried in a drum dryer at a temperature of 120°C under a vacuum for 16 h and then filled and kept under a nitrogen atmosphere. The fibers were spun using a spinning device on an extruder (18-mm screw diameter), a spinning pump,

and a spin-pack, three heated godets, and two winders with take-up velocities up to 2000 m/min and with the range of 2000 – 6000 m/min as shown in Fig. 5.10. The geometry of the extruder screw was chosen in the usual way for PET and the conditions of extrusion (temperature profile) were adapted according to the lower melting temperature of type LA 0200 K PLA of 185°C. The spin-pack contained two double filter screens. A 12 hole spinneret was used and yarns with 12 filaments were spun. The diameter of a single spinneret hole was 0.3 mm and its length 0.6 mm. The spin drawing was carried out using the same equipment. The filaments were taken up at about 200 m/min and were drawn between the first and the second heated godets. The temperatures of the godets were set above the glass-transition area (65°C) and the temperature of the second godet was in the vicinity of the crystallization (110°C). The draw ratios were varied in a range of 4 – 6, which means that the velocities of the second godet were between 800 and 1200 m/min. Because of the crystallization the length of the filaments varied so that a tension between the second godet and winder was necessary during spinning. It was shown that the PLA of type LA 0200 K can be spun both in a high-speed spinning process with a take-up speed of up to 5000 m/min and in a spin drawing process up to a draw ratio of 6. The values for tensile strength, elongation at break, and Young’s modulus reached 460 MPa, 19.7% and 6.3 GPa, respectively.



**Figure 5.10** Spinning devices (spin drawing process, high speed spinning process) [16]



In their another report, PLA with different *D*-lactide contents, tacticities, molecular mass and molecular mass distribution was used in high-speed melt-spinning process [18]. The spinnability of PLA with broad mass distribution was extremely restricted. The crystallinity of fibers which was influenced by *D* content and the extent of orientation-initiated crystallization had a decisive influence on the tensile properties of the investigated PLA fibers.

PLLA was successfully melt spun at high spinning speed by Mezghani et al. In general, the structure and properties of the as-spun filaments change dramatically with spinning speed. The crystallinity and overall molecular orientation exhibit maxima at take-up velocities between 2000 and 3000 m/min. At take-up velocities below approximately 2100 m/min the crystallinity increases due to the increased crystallization rates caused by the increased molecular orientation (stress-induced crystallization). The oriented nucleation and growth of crystals resulting from stress-induced crystallization also contributes to the increase in birefringence observed in this range of spinning speeds. Above 3000 m/min the crystallinity decreases due to the increased rate of cooling of the filaments without a compensating increase in crystallization kinetics. It is likely that this produces a radial variation in the structure of the as-spun filaments. The dependence of crystallinity and overall molecular orientation on take-up speed is directly correlated to the variation of the boiling water shrinkage and the mechanical properties of the filaments. The maximum tensile strength and modulus of fibers obtained were 385 MPa and 6 GPa respectively. These values are quite sufficient for most textile applications of the fibers such as in nonwoven fabrics [19].

One of the most important morphological features of the fibers is their cross-sectional shape. Nowadays, the circular fiber cross-section is the most common shape of melt-spun man-made fibers. Other shapes are beginning to emerge for a variety of reasons such as performance, comfort, pilling propensity, bulkiness, tactility, processing etc. The filaments' cross-section can be easily varied by changing the spinneret hole shape. Synthetic fibers that are predominantly spun by the melt spinning method with spinnerets having the noncircular hole geometry are called profiled or noncircular fibers. Modifications of the fiber cross-section allow designing surface properties in yarn and fabric. PLA can also be melt spun into kinds of profiled fibers for its wide commodity usage. For example, trilobal profiled PLA fiber with a profiled degree of 52% was prepared from PLA with intrinsic viscosity 1.51 dL/g using trilobal profiled spinneret via melt spinning process by Yan et al.. The trilobal profiled PLA fibers had the breaking strength and initial modulus of 2.39 cN/dtex and 17.27 cN/dtex at 4 time drawing respectively [20].

### 5.2.1.1 Melting Spinning of PLA Blends

It is well known [21] that the melting temperature and the degree of crystallinity of PLA polymerized from *L*-lactide can be controlled by the thermoplastic processing and by the insertion of *D*-lactic acid units and other monomer units [22]

in the chain. The investigations of Cicero et al. illustrated two-step melt spinning of PLA fibers. Textile grade PLA with a 98:02 ratio of *L/D* stereochemical centers ( $M_w = 98\,500$ ) was dried at  $82^\circ\text{C}$  to reduce the water level to 100 ppm or lower. The molten polymer was extruded through a spinneret and quenched in a water bath. The melt draw-ratio was kept constant at 40. The take-up speed was varied from 2.3 to 18.3 m/min [23, 24].

Poly-*L, DL*-lactide 70/30 is an amorphous copolymer of *L*-lactide and *DL*-lactide that is more hydrophobic than polyglycolide. The degradation kinetics of this copolymer is between that of polyglycolide and poly-*L*-lactide, hence poly-*L, DL*-lactide 70/30 fibers appear promising for production of biodegradable scaffolds where the retention of properties for a few weeks is required. Fibers were produced by melt spinning in a single step process where orientation and drawing occur simultaneously using a commercial extruder Estru13 (Friulfiliere, Buia-UD, Italy) with a screw of 14 mm diameter (*L/D* 20 and RC 2.5) and a single-hole spinneret having holes of 1.0 mm diameter. The effect of drawing appeared evident above a certain critical draw ratio, experimentally determined as 50. The properties of fibers were found to be dependent on the draw ratio. Fibers drawn with draw ratio of 297 exhibited modulus and strength of 4.1 GPa and 183 MPa respectively. In vitro degradation showed the retention of adequate mechanical properties for up to 4 weeks, and a significant decrease of strength associated to water sorption and molar mass decrease at longer time. These poly-*L, DL*-lactide 70/30 fibers may be suitable for weaving meshes and/or fabrics for the production of biodegradable scaffold [25].

Although PLLA has a fairly high melting temperature in comparison with other biodegradable polyesters, its  $T_m$ , around  $180^\circ\text{C}$ , is not high enough for some applications. PLLA fibers and cloths have to be dyed at fairly low temperature ( $110^\circ\text{C}$ ) and ironing of PLLA cloths at high temperature ruins their softness. Carothers in DuPont synthesized various aliphatic polyesters in 1930s as the material for synthetic fibers. Unfortunately he finally gave up because of low thermal stability of these aliphatic polyesters. Most synthetic polymers for the synthetic fibers, such as nylon 66, nylon 6, and PET have a melting point higher than  $200^\circ\text{C}$ . One of the fundamental techniques to increase the melting point of PLA is to produce so called “stereocomplex-type crystal” which is formed by the equimolar blend of PLLA and PDLA. This stereocomplex crystal melts at a temperature of about  $50^\circ\text{C}$  higher than the melting point of PLLA [26].

There are some reports concerning the fiber processing of stereocomplex-type PLAs. Yamane reported the melt spun fibers from PLLA/PDLA blend with higher-order structure and high mechanical strength [27]. Glassy as-spun blend fiber drawn up to several times at  $110^\circ\text{C}$  resulting in the oriented fibers consisted of both homo- and stereocomplex crystals. Although an annealing process of the drawn fiber under tension at the temperature above  $T_m$  of the homocrystal gave a fiber mainly consisting of stereocomplex crystal, the crystal orientation and the mechanical properties were significantly deteriorated.

Takasaki et al. have published two papers on the high-speed melt spinning of PLLA/PDLA blends with various blend ratios [28, 29]. They found that the as-spun blend fibers with up to 16.4 wt% PDLA content have only homocrystals. However, PLLA/PDLA = 50/50 blend high-speed spun fibers obtained under high spinline tension contained a certain amount of stereocomplex crystal, and the annealing gave a fiber mainly consisting of highly oriented stereocomplex crystal. Equimolecular blends of PLLA and PDLA were melt spun into PLA fibers. Drawing and annealing processes were performed to form stereocomplex crystals [30]. WAXD patterns showed that three kinds of higher-order structure were observed in the drawn fibers depending on the drawing temperature: (1) oriented amorphous state in the fiber drawn at a lower temperature (60°C), at which crystallization does not occur significantly. (2) highly oriented homocrystal in the fiber drawn at an intermediate temperature (90°C), at which homocrystallization significantly occurs. (3) coexistence of homo- and stereocomplex crystals with a fairly low orientation at a higher temperature (120°C). DSC measurements revealed that the fiber drawn at an intermediate temperature range seems to have some pure PLLA or PDLA crystal which cannot be transformed to the stereocomplex crystal by annealing process. Annealing process at 190°C of the fibers drawn at 60°C and 120°C gave the fibers mainly consisting of stereocomplex crystals. Rest of the fibers still showed a coexistence of homo- and stereocomplex crystals. These results indicate that the higher-order structure of the drawn fiber strongly affects the crystalline form obtained in the annealed fiber. Unfortunately, the annealed fiber with high stereocomplex content does not show the superior mechanical properties.

### 5.2.1.2 Effect of Spinning Parameters on the Structure and Properties of PLA Fibers

Structure development of PLA fibers at various spinning conditions was investigated by Ghosh et al. [34]. PLA filaments were spun by melt-spinning at 500 and 1850 m/min, and further drawn and heat-set to modify the morphology of these PLA filaments. PLA yarns spun at 500 m/min are almost amorphous while the PLA filaments spun at 1850 m/min have about 6% crystallinity. This is different from PET filaments spun at the same speed that have almost no crystallinity. This crystallinity developed in *as*-spun PLA yarns spun at 1850 m/min is attributed to the orientation induced crystallization associated with the entropy of the amorphous, noncrystalline phase. At higher spinning speed a greater velocity gradient is created in the spin line, which causes stretching and alignment of macromolecules during the development of orientation. This process reduces entropy of the amorphous phase by a certain amount depending upon the degree of orientation created during spinning. This free energy for crystallization provides a driving force for the kinetics of crystal nucleation and growth of the crystallinity. Both drawn and heat-set PLA filaments showed much higher crystallinity (60%) than did *as*-spun fibers produced at 500 and 1850 mm<sup>-1</sup>, which

was also higher than the usual heat-set PET yarns. It appears that crystalline orientation rapidly reaches a value in the order of 0.95 at 1850 m/min and that drawn- and heat-set yarns have almost the same crystalline orientation values. Molecular orientation was relatively low for as-spun PLA yarn, and molecular orientation increased to 0.5 after drawing or heat-setting or both. This can be attributed to thermal as well as stress-induced crystallization. Since almost the same crystallinity was obtained for the PLA yarns after drawing and heat-setting, it was concluded that thermally induced crystallization had the greatest contribution to the development of filament crystallinity. However, the samples drawn with tension rolls without relaxation showed a slightly lower crystallinity than that of the filaments relaxed after drawing. At the heat-setting process less stable crystals occurs, and the short length molecules move to form more stable intermolecular bonds that provide better perfection of crystals. This local melting allows recrystallization into folded segments following the folds that are already present as nuclei for recrystallization. The amount of tension during heat-setting influences the amount of refolding. Very high tension inhibits the folding process and, consequently, disrupts the crystal perfection during the annealing treatment. Furthermore, the relative amounts of mobility of the molecular segments are low under that condition.

The drawing applied to filaments is known to improve the tensile properties of polymer. The drawing of the PLA filaments allows an alignment of macromolecules in the drawing direction, which provokes an increase in Young's modulus and tensile strength. At the same time, the elongation at break decreases greatly when the draw ratio increases. An increase of the degree of crystallinity is observed with increasing draw ratio, so it is consistent with the observed improvement of the mechanical properties of the PLA filaments [14].

Crystallization of PLA (4% *D*-lactic acid monomer) fibers drawn at different temperatures was investigated by Mahendrasingam et al. [32]. The samples drawn at the lower temperatures of 80, 90 and 100 °C show different drawing and crystallization behaviors from that drawn at the higher temperatures of 110 and 120 °C. The change in behavior above 100 °C is attributed to the onset of relaxations associated with chain retraction mechanisms. At the lower temperatures there is a rapid crystallization giving highly oriented crystals with the crystallization kinetics following a first order transformation process. Clear SAXS patterns can not be detected during 12 s for the time-resolved observations. This is partly due to the poor density contrast between crystalline and non-crystalline regions. Annealing treatment improves the contrast and gives rise to a clear four-point SAXS pattern suggesting a microfibrillar morphology in the as-drawn sample. At the higher temperatures, the draw is non-uniform and gives rise to less oriented crystals with a very slow growth rate. Prolonged crystallization after drawing at 120 °C gives a two-point SAXS pattern indicating a "shish-kebab" morphology. The WAXS fiber pattern after annealing shows a sampling on intermediate layer lines that is consistent with the crystal form with a 10<sub>3</sub> helix. However, prior to

annealing the sampling indicates a different helical configuration.

The effect of melt-spinning speed and heat treatment on the mechanical properties and biodegradability of PLA fibers were investigated by Park et al. [33]. PLA was spun at a high spinning speed of 2000 – 4000 m/min, and each specimen was heat-treated. Heat treatment of the PLA fibers increased the breaking stress and crystallinity. With increasing spinning speed, breaking stress and crystallinity also increased. An increase in spinning speed was more effective than an increase in heat treatment for enhancing the breaking stress.

High-speed melt spinning of racemate polylactide (*r*-PLA) that is a blend of equal amount of poly (*L*-lactide) and poly(*D*-lactide) was performed up to the take-up speed of 7.5 km/min. In the fiber structure analysis, particular attention was paid to the formation of stereocomplex crystals because this crystal form had a melting temperature about 60 °C higher than that of homocrystals. It was found that highly oriented and highly crystallized fibers containing the alpha-form and stereocomplex crystals were obtained when the take-up speed exceeded about 4 km/min. The amount of stereocomplex crystal was higher under the spinning conditions of higher take-up speed, lower throughput rate and lower extrusion temperature. Under these conditions higher tensile stress can be applied to the spinning line, and therefore, the orientation-induced crystallization is promoted. Annealing at a temperature between the melting temperatures of alpha-form and stereocomplex crystals of the fibers that was obtained at high-take-up speed, such as 6 km/min, and already had the crystalline structure with a certain amount of stereocomplex crystal yielded the fiber structure mainly consisting of highly oriented stereocomplex crystal. The annealed fibers showed fairly high mechanical properties and good thermal stability [29].

### 5.2.2 Dry Spinning of PLA

Another approach to form PLA fiber is based on dry spinning process that involves dissolving the polymer in a solvent (typically chloroform, toluene or a mixture of the two solvents) and extruding the polymer solution in air or inert gas. Evaporation of the solvent causes the extruded filaments to solidify. Although the melt spinning process is relatively straightforward, the process tends to induce molecular weight drop of the PLA polymer due to thermal-induced hydrolytic degradation during the melting step in the presence of residual water. Because PLA rapidly degrades at elevated temperatures, molecular weight loss during processing is an important issue. It has been observed that significant changes occur in the molecular weight of the polymer during the spinning and post-spinning operations. Previous fiber-spinning studies have found the losses between 28% and 43% [25, 26]. Yuan et al. [13] encountered losses of up to 69% and Schmack et al. [34] experienced a 31% molecular weight reduction. Similarly, melt spinning by Fambri et al. [12] resulted in losses of over 60%. Generally, thermal

degradation is more severe for melt spinning than for solution spinning. In contrast, the dry spinning technique is quite effective in preserving the molecular weight of the polymer due to the lower processing temperature used.

Very few studies have been reported on dry spinning of PLA. Leenslag et al. [35] produced high strength fibers by dry spinning and subsequent hot drawing from polymer solutions in chloroform/toluene mixtures near the temperature where PLA adopts an interrupted helical conformation. The spinning solutions were prepared by dissolving PLA in chloroform and subsequently adding toluene without mechanical stirring. Before extrusion, the PLA solutions were conditioned in the piston-cylinder apparatus at 70°C (PLLA/toluene at 90°C) for 3 h and the fibers were extruded through a stainless steel conical die. Hot drawing was carried out in a heated double-wall glass tube to obtain fiber with good tensile properties.

Solvent and nonsolvent compositions have been established for producing porous fibers by dry spinning. Solvent evaporates quickly and the nonsolvent causes coagulation of a porous structure. Horocek and Kalisek [36] prepared PLA fibers by a continuous dry spinning-hot drawing process. They dissolved the polymer in a chloroform/cyclohexane mixture and spun the solution at ambient temperature through an orifice (0.5 mm×7 mm) with an extrusion speed of 65 mm/min. The filament was continuously led on to a steel drum in 10 mm×300 mm drawing tube at the drawing temperature of 110–190°C, and the hot-drawn fiber was collected on another drum. The resulting fibers had an average mechanical strength of 0.7 GPa and porous morphology. The solvent composition played an important role in establishing the fiber morphology. The fibers obtained had average or poor mechanical properties and a porous structure with a pointed outer skin. As the cyclohexane content in the chloroform–cyclohexane mixture increased, phase separation occurred more rapidly and tensile strength decreased, irrespective of the heat setting temperature. Although the surface skin was slightly porous, the core did not coagulate rapidly and was very porous. At chloroform/cyclohexane volume ratio of 6:4 the process resulted in nearly hollow fiber structure. No increase of the degradation rate was observed except for the fibers formed from pure chloroform with a residual monomer at a drawing temperature of 110°C. Nonsolvent, such as methanol, ethanol or petroleum ether, formed a vapor in the chamber. PLA fibers were prepared by spinning in the vapor precipitant and were subsequently hot drawn. PLA was dissolved in chloroform and was spun at laboratory temperature through an orifice. The filament was led up through a glass tube and collected on a steel drum. The precipitant vapor was introduced at the bottom of the tube in a gentle stream of argon. After 48 h in a drawing tube at 90°C, the fibers were hot drawn to a maximum draw ratio ( $\lambda_{\max}$ ) at an entrance speed of 83 mm/min. Petroleum ether, by virtue of its high vapor concentration, behaves like a liquid precipitant. As a result, a skin layer and then a porous inner layer were formed [37].

The ambient temperature at the spin line has a profound influence on the

physical characteristics of the filament. The tensile strength increased with increasing temperature up to 25°C and then decreased drastically [38]. It is the solidification process that determines fiber structure and physical properties. At high temperature, the flash evaporation of the solvent (chloroform) is accelerated and then solidification (phase separation) impedes sliding of the molecular chains and chain reorientation where topological defects are numerous. Variation of this ambient temperature induced variation of the extrudate swell of the spinline, affected by the rate of solidification of PLLA. By way of phase separation, porous filaments were achieved in which the morphology depended on the applied ambient temperature. Hot drawing of these filaments led to tensile strengths varying between 1.1 and 2.2 GPa as shown in Table 5.3. An optimal tensile strength of 2.2 GPa was achieved by hot drawing of a filament which was spun into a surrounding at 25°C.

**Table 5.3** Heat of fusion of the *as*-spun fibers, maximum draw ratio, diameter of drawn fiber and tensile strength of PLLA filament, spun from 4 wt% solutions in chloroform/toluene (40/60) into surroundings at various temperatures [38]

Ambient temperature (°C)	Heat of fusion (J/g)	Draw ratio	Fiber diameter (μm)	Tensile strength (GPa)
9	48.8	12	27	1.3
20	44.6	14	23	1.5
22	41.2	13	21	1.8
25	54.8	13	17	2.2
30	45.6	14	22	1.9
37	53.5	13	19	1.8
45	34.9	12	26	1.4
60	49.3	13	28	1.1

The extrusion speed and winding speed play a dominant role in the development of fiber structure and fiber characteristics. Increasing extrusion speed leads to higher orientation and enhanced crystallization [12]. But Postema et al. [38–40] observed no correlation between the extrusion speed and the crystallinity of the fiber, and found that tensile strength decreased with increasing extrusion rate. PLLA fibers with tensile strengths of 2.3 GPa were produced. Although high shear rate may lead to significant chain scission, this was not a factor in these studies as the molecular weight of the polymer was not affected by the extrusion rate. Southern and Ballmann [41] proposed that the loss in tensile properties might be the outcome of flow instabilities which lead to the voiding and cavitation resulting in anisotropic structure, and hence to inferior fiber properties.

Leenslag et al. [42] obtained PLA fibers with a loosened fibrillar structure by solution spinning from a good solvent (chloroform) in the presence of various additives. Spinning was carried out at room temperature with chloroform as the

solvent. Polymer concentrations were in the range of 10% – 18% (w/v). Toluene, camphor, a copolymer PLLA-polyurethane and commercial medical grade polyurethane were used as additives at concentrations of 30% (v/v), 20% (w/w), and 5% (w/w) respectively for both polyurethanes. No orientation or degradation was found during the spinning of the fiber. Hot drawing was carried out in an electric tube furnace of 300 mm in length with draw ratios of 6–30 and input velocity of 20 mm/min. Gogolewski and Pennings [43] also reported solution spinning of PLLA fibers in solvents, such as dichloromethane and trichloromethane. Polymer concentrations were in the range 1% – 20% (w/v). Filaments were collected on a glass drum at a speed of 0.02–1.0 m/min. No orientation was introduced by spinning.

Unlike melt spinning, the molecular chain degradation in dry spinning is effectively controlled. If any degradation at all occurs, it may be during polymer dissolution, particularly in solvents like chloroform. The moisture ordinarily present in chloroform is sufficient to cause chain scission and may eventually lead to degradation in molecular weight as high as 23% after 1 week in solution [39]. However, a careful check on degradation is possible by using chloroform dried over  $P_2O_5$ .

### 5.2.2.1 Morphology and Structures

One important parameter that affects the fiber morphology during dry solution spinning is the composition of the solvent. Instead of using one solvent, several studies have successfully manipulated the morphology and physical properties of PLA fibers by using multiple or binary solvent systems. Postema et al. reported that PLA fibers spun from a solvent made up of 40/60 chloroform/toluene exhibited the highest tensile strength of 2.3 GPa after hot drawing among other chloroform/toluene proportions tested [38, 39]. Similar observations were reported by Leenslag and Pennings [44]. They postulated that under the 40/60 chloroform/toluene condition, the PLA adopted an interrupted helical conformation. Solidification of PLA from the solution during solvent evaporation caused the helical aggregates to form crystalline junctions that hampered re-entangling of polymer chains leading to crystalline polymer with good drawability [44]. In this binary system that contained a good PLA solvent (chloroform) and a poor PLA solvent (toluene) the greater tendency for chloroform to evaporate during spinning causes an increased PLA concentration with a concomitant decrease in solvent power, resulting in the formation of polymer-poor and polymer-rich phases. The polymer-rich phase underwent rapid solidification, thereby generating porous fiber structures [42].

The morphology of fiber is significantly affected by precipitant vapor. The structure of *as*-spun fiber in petroleum ether vapor as precipitant is characterized by an irregular skin and porous inner part due to very fast phase separation. In ethanol vapor phase separation rate is very slow, which gives a surface similar to that of dry-spun fiber. The fiber spun in methanol vapor as a precipitant has no



apparent skin; the surface is perforated and the fiber shape is regular [37]. The spinning rate also has a crucial impact on fiber morphology. A regular spiraling distortion of the extrudate is observed on the fiber surface. Increasing spinning rate via the pressure applied to the polymer solution also increases the pitch of the helical distortion [42].

Gogolewski and Pennings [43] observed that the morphology of PLLA fibers produced by dry spinning from dichloromethane or trichloromethane solutions at room temperature depended to a great extent on polymer concentration. Changing of the polymer concentration in the spinning solution gave rise to formation of fibers with different shape and porosity. Fibers spun from 10%–20% solutions at room temperature exhibited a regular structurization due to melt fracture. These fibers had knot strengths up to 0.6 GPa, whereas fibers with a smooth surface spun from more dilute solutions had weaker square knots of 0.3 GPa. The fibers obtained from 2% solution were flat and exhibited a smooth surface while the fibers spun from 10% to 20% solutions were cylindrical and had a characteristic “structured” surface. This surface structurization may very well be due to melt fracture, a phenomenon that has been observed for a number of polymers and is related to flow instabilities in the spinning die arising from the elastic character of polymer melts and solutions. Owing to the influence of elasticity on flow behavior, the fiber turned out to be regularly “coarse threaded”. For a given polymer concentration, the pitch of the thread decreased with increasing the pressure applied to the polymer solution. Even hot drawing at high draw ratios does not completely remove the surface structure. Fiber stretching causes an extension of the pitch of the helix, indicating that drawing does not proceed by neck formation. Between the helical pitch lines the surface of the fiber appears to be rather smooth and fibrillated, as may be seen by scanning electron micrographs (SEM). Hot drawing does not lead to a full reorganization at the molecular level, but a strong “memory effect” occurs that is likely associated with remnants of chain entanglement [43].

### 5.2.2.2 Mechanical Properties

In general, solution-spun fibers are superior to melt-spun fibers from the standpoint of mechanical properties. This is attributed to the lower chain entanglement of polymer molecules in the solution state as compared to the melt state. Therefore, the *as*-spun fibers tend to exhibit high draw ratios. For instance, Penning et al. reported that dry spinning followed by hot drawing resulted in low crystallinity fibers having a tensile strength of 1 GPa, whereas fibers prepared from melt spinning followed by hot drawing have much considerably lower strengths ranging from 0.19 for completely amorphous copolymer to 0.53 GPa for PLA homopolymer [22]. The major drawback to solution spinning is the use of organic solvents which can pose environmental problems.

The composition and nature of the solvent play an interesting role in the morphological development of the fiber and its mechanical properties. The

tenacity of PLLA fiber spun from 4% (w/v) polymer solution in various chloroform/toluene mixtures and then hot-drawn to different  $\lambda$  at 204 °C is shown in Table 5.4. The tensile strength  $\sigma_b$  of the fiber depends on the chloroform/toluene composition with a maximum of 2.1 GPa at a toluene volume fraction  $\phi_{\text{tol}}$  of 0.6 [44]. However, fibers spun from trichloromethane attain higher tensile strengths and moduli than those of similar initial molecular weight spun from toluene [43].

**Table 5.4** Typical properties of PLLA fibers ( $M_v=900\,000$ ) spun at 60 °C from various solvents (mixtures) and hot-drawn at 204 °C to  $\lambda_{\text{max}}$

Solvent composition		$\sigma_b$ (GPa)	$E$ (GPa)	$\varepsilon$ (%)	$\lambda_{\text{max}}$	Cross sectional area ( $\times 10^{10} \text{ m}^2$ )
Chloroform ( $\phi$ )	Toluene ( $\phi$ )					
1	0	0.75	9	20	5	11
0.5	0.5	1.45	10	23	10.5	3.45
0.4	0.6	2.10	16	23	20	1.36
0.3	0.7	1.40	11	23	14.5	2.67
0	1	1.05	10.5	23	13.5	4.21

The effect of polymer molecular weight on the ultimate tensile properties of the fiber is of obvious importance. As molecular weight increases, the complexity of the entanglement network also increases, hampering partial disentangling of the chains during dissolution and/or hot drawing. Less entanglement in the transient polymeric network during drawing enables proper alignment and extension of high molecular weight chains. Therefore, in dry spinning of high-MW flexible polymer, solidification (gelation) of the polymer should preferably take place near the onset of coil overlap in order to minimize the entanglement density in the filaments produced [35]. Tensile strength is independent of molecular weight in the range of 180 000 – 300 000, beyond which tensile strength increases linearly with reciprocal molecular weight. Tensile strength as a function of drawing temperature exhibits a maximum value of 2.0 GPa after drawing at 188 °C to a maximum draw ratio of 13. The low values of draw ratio leading to excellent fiber properties indicate that although the entanglements are mobile enough to slip into newly created disordered domains, disentangling is impeded by the rapid formation of fibrillar crystals between entanglement-rich domains [40]. The tensile strength is also dependent on an optimum drawing temperature which in turn depends on the molecular weight of the material. The maximum tensile strength was found after drawing at temperatures in the range of 197 – 200 °C for fibers with molecular weights above 400 000, while for the fibers with molecular weight in the range of 120 000 – 350 000, the maximum in the tensile strength was reached at 175 – 180 °C [43].

The ultimate tensile strength of fibers appears to be dependent on the ambient temperature during spinning which is usually set from 9 to 60 °C. Postema et

al. [38] obtained the filaments spun at 25°C with a maximum tensile strength of 2.2 GPa after hot drawing. At lower and higher ambient temperatures the ultimate tensile strength decreased drastically. The deformation rate in the drawing tube had no effect on strength of filaments spun at low and high ambient temperatures except near 25°C. This suggests that during spinning in surroundings above or below an optimal temperature, heterogeneous filaments are formed (possibly due to rapid phase separation) that leads to weak fibers after hot drawing [38].

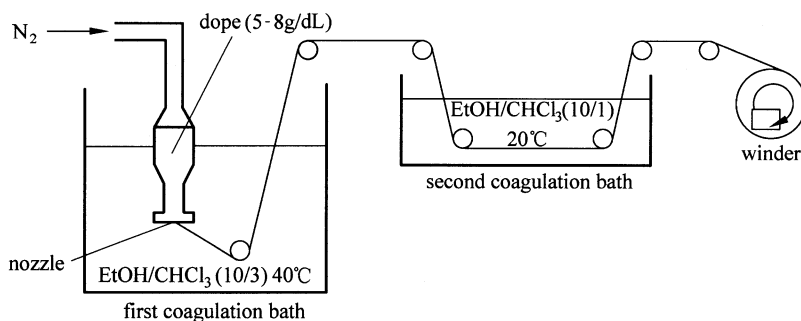
Spinneret design has a substantial effect on fiber properties. During extrusion, breakup of the molecular network causes flow instabilities. Extension of the molecular network over the sharp edges inside the orifice, combined with the acceleration of the solution at that point, might cause a rupture of the solution structure. Additionally, adsorption of polymer chains on the wall of die may originate topological constraints that are most likely the reason for the decrease in the tensile strength after hot drawing. Both entanglements and reduction of the entrance angle will result in a smaller velocity gradient in the orifice and thus may reduce partial crystallization and rupture of the molecular network due to phase separation. The hot drawing of PLA filament has been investigated by Postema and Pennings [40] at temperatures up to 180°C and above 190°C. In the former case (up to 180°C) the deformation takes place in the semicrystalline state of the polymer and in the latter case deformation proceeds in the amorphous fluid state of the polymer. In both cases, drawing of PLA resulted in moderately good mechanical properties and fibers with a tensile strength of 2.2 GPa were achieved. This seems to demonstrate not only that the deformation rate is responsible for the ultimate mechanical properties but also that harmonization of drawing temperature and deformation rate is needed for every selected molecular weight and molecular weight distribution in order to determine the correct drawing conditions leading to the ultimate mechanical properties [40].

### 5.2.3 Wet Spinning of PLA

The wet process is similar to the dry process except that the polymer solution is spun into a bath containing coagulating solution that causes the polymer filament to solidify. In wet spinning the polymer solution prepared in a suitable solvent is extruded as a fiber into a coagulation bath containing a nonsolvent. The limits of polymer concentration in the spinning solvent are determined by factors such as polymer solubility and solution spinning pressure limitations. The polymer concentration used for wet spinning is lower than that in dry spinning since the solution is spun at lower temperatures. The spinneret is submerged in the liquid coagulation bath, and the emerging filaments are coagulated in a precipitating bath or a series of baths of increasing precipitant concentration. This perhaps represents the most critical element in the solvent spinning process because of its

short residence time in the coagulation bath, the fiber forms and its structure takes shape as a result of complex interactions of numerous factors such as the particular solvent, polymer, temperature, and nonsolvents used as well as flow variables, etc. Interactions among these factors lead to the conditions in which counter diffusion of solvent and nonsolvent and phase separation of the polymer take place.

With this approach PLA is normally dissolved in chloroform and is then extruded into a toluene or methanol bath [11]. Tsuji et al. [45] reported wet spinning of stereocomplex PLA fibers. Chloroform solutions of PDLA and PLLA with a concentration of 5–10 g/dL were separately prepared and mixed in equimolar ratio. The coagulation was carried out in the first coagulation bath containing a mixture of nonsolvent and solvent, ethanol/chloroform 10/3 (v/v), at 40°C, and then further in the second coagulation bath [ethanol/chloroform=10/1 (v/v)] at 20°C to complete the desolvation, finally the fiber was wound. The apparatus for wet spinning is shown in Fig. 5.11 The tensile strength of the wet-spun complex fibers was very low and could not be drawn at high temperatures. The undrawn fiber surfaces are very irregular with an average diameter of about 50 μm and a large number of pores with various sizes ranging from sub-mm to 10 mm on its surface. The defective structure of the wet spun fibers is probably due to the rapid desolvation from the extruded dope during precipitation.



**Figure 5.11** Wet spinning apparatus [45]

## 5.2.4 Dry-Jet-Wet Spinning of PLA

In wet spinning, the *as*-spun fiber always has voids that cause deterioration of fiber properties, e.g., inferior mechanical properties due to easy fibrillation and low transparency. The formation of voids can be held to a minimum by extruding the dope stream from a dry jet and then coagulating as in conventional wet spinning. This process is known as dry-jet-wet spinning. The dry jet gap is varied from 3 to 5 mm. Dry-jet-wet spinning allows stress relaxation of polymer chains in the air gap of the orientation produced in the spinneret, so that the spun fiber is

less oriented and more uniform than that from the immersed jet. This permits orientation by subsequent drawing and gives fibers with higher tenacity.

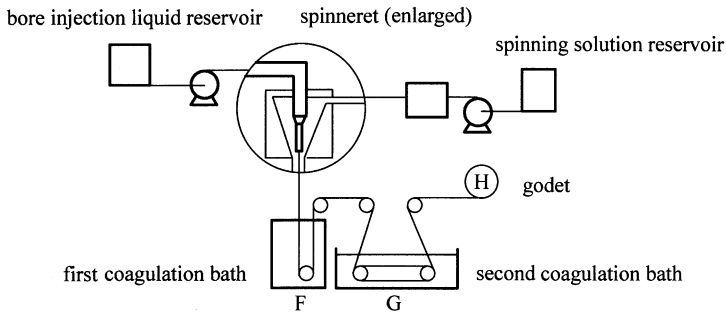
PLA fibers has been prepared by dry-jet-wet spinning of the polymer from chloroform solution and with methanol as the precipitating medium. The as-spun fibers are subsequently made into high strength fiber by two-step process of drawing at a temperature of 90°C and subsequent heat setting in the temperature of 120°C. The draw ratio has significant influence on crystallinity and tensile strength of the fibers. The fibers with the tenacity of 0.6 GPa and modulus of 8.2 GPa can be achieved at a draw ratio of 8. The differential scanning calorimetry reveals an increase in the glass-transition temperature with the increase in the draw ratio, which suggests the orientation of chains during the drawing process. The fibers are porous in nature, but a significant reduction in the porosity and pore size of the fiber is observed with the increase in the draw ratio.

The dry-jet-wet spinning of PLA produces the fibers where the molecular weight degradation during the spinning is slight and a significant advantage is achieved as compared with the melt-spinning process. The fiber acquires some orientation even before the coagulation process, which helps in further enhancing the fiber strength. The maximum draw ratio of 10 was achieved for the fibers. The draw ratio plays an important role in the structural development of the fiber. The orientation and crystallinity increase with the increase in the draw ratio. The tensile strength of the fiber also increases with the draw ratio. The drawing leads to collapse of the porous structure, the surface is still porous at higher draw ratio. The porosity becomes negligible and pores get stretched during the process [46].

The important parameters affecting properties of dry-jet-wet spun PLA fiber are the take-up speed, draw ratio, drawing temperature, and heat-setting temperature. When the take-up speed increases the wet stretch increases, which leads to better orientation of the as-spun fibers and results in improvement in the mechanical properties. The as-spun fibers show porous morphology. Both the drawing temperature and heat-setting temperature have significant effect on the structure and properties of the fibers. The strength of the fiber decreases beyond a drawing temperature of 90°C. The optimum drawing temperature and heat-setting temperature are observed to be 90 and 120°C respectively [47].

Eenink et al [48] reported spinning of hollow PLA fibers by a phase-inversion spinning process. The dry-wet phase-inversion spinning process is schematically shown in Fig. 5.12. The as-spun hollow fibers without post-spinning treatment were used as drug delivery devices. The fibers were characterized with respect to molecular weight, residual additive content, degree of crystallinity, and transition temperatures. It was found that no polymer degradation occurred during spinning from dioxane and chloroform solutions. Witte et al. [49] reported highly crystalline, porous, hollow PLLA fibers spun by the dry-wet spinning process. The pore structure of the fibers could be regulated by changing the spinning system and spinning conditions. The spinning system of PLLA-chloroform/toluene-methanol

yielded fibers with a very open, porous structure. An extensive study of dry-jet-wet-spun PLA fiber was reported by Gupta et al. [46, 47] using chloroform/methanol as the solvent/nonsolvent system.



**Figure 5.12** Scheme of dry-wet spinning process [48]

### **5.2.5 Dyeing of PLA Fibers**

Like other polyesters, PLA can be dyed with the same disperse dyes used to dye PET. The disperse-dyeability of PLA also leads to the possibility of transfer printing the synthetic suede if a high  $T_m$  PLA is used. Also important to its use in various apparel applications is PLA's dyeability. It can be disperse-dyed by using standard dyes for PET and dyeing procedure, but again there is a difference between PLA and PET. PLA's refractive index is lower than that of PET or nylon, so it can be dyed to deeper and brighter shades. Dyeability is admittedly of greater concern for knit or woven fabrics than for nonwovens, but there are nonwoven segments where dyeability is important.

Dyeing process of PLA fibers is also similar to those of synthetic fibers. Dyeing of PLA fibers is generally carried out with disperse dyes under high temperature and pressure because PLA fibers have low affinity to conventional water soluble dyes. Optimization of dyeing PLA fibers with vat dyes has been investigated by Sawada et al. [50]. Conventional method for dyeing cellulose fibers with vat dyes was able to be applied for dyeing PLA fibers. The prescribed amount of indigo dyes was previously dissolved in the same quantity of ethanol. Then exact amount of NaOH,  $\text{Na}_2\text{S}_2\text{O}_3$  and boiled distilled water was added with stirring. After the indigo dye was reduced to a leuco-form the dye solution was poured into a stainless steel dyeing vessel until the dyeing vessel was filled with the dye solution. The volume of the dyeing vessel was 500 mL. After the temperature of the dye solution became constant, PLA fabric specimens were then immersed into the dyeing vessel and completely sealed to avoid gases. Dyeing was carried out by using MINI-COLOUR12E (TEXAM Co. Ltd.) dyeing machine under exact

temperature and time. The bath ratio was adjusted to 1:50. After dyeing a fabric specimen was dried overnight under the stream of air for complete oxidation. The removal of un-dyed dyes on the fabric was attained by soaping in boiled water for 10 min under the presence of Marseille soap (1 g/L). The color depth of the dyed fabrics was estimated from the reflectance of the dyed fiber measured with the Minolta CM-1000 spectrophotometer (illumination diameter: 12 mm) under illuminant D65 by using 10° observer. The color depth of dyed PLA fabrics increased from 57°C and leveled off at higher temperature for 1 h. The temperature that improves the dyeability completely agrees with the glass transition temperature of the PLA fiber. An activation of molecular dynamics in an amorphous region by an increase in temperature obviously supports access of dye molecules into fibers. When the fiber gaps spread in the degree, which does not have evil for the penetration of dyes, further spread of them do not provide marked improvement of the dyeability of dyes. From these results the dyeing at 100°C that is the lowest temperature to obtain high color yield seems to be suitable from the view point of energy saving.

The color depth of the dyed PLA fabric gradually decreases with increasing dyeing time. This is quite different from dyeing behaviors of conventional dyeing processes. In general, the color depth of a dyed fabric would increase with increasing dyeing time until equilibrium dyeing is attained. After the dyeing reaches equilibrium the color depth of a dyed fabric does not vary. A decrease in the color depth of dyed fabric obtained may relate to a drop in the affinity of fibers on dyes or its contrary. Dealing with the first issue of a drop in the affinity of fibers, prolonged dyeing under high temperature may cause variations of the surface property of PLA fibers. As is generally known, softening temperature of PLA fibers at atmospheric pressure is about 127°C. On the other hand, the apparent softening temperature of PLA fibers may be reduced in this experimental condition because the pressure in a closed dyeing vessel is supposed to be high compared to that in an open vessel. As a result, prolonged dyeing under unsuitable dyeing condition may cause a drop in the dyeability of dyes. The second factor to be considered is a drop in the affinity of dyes on fibers. A part of a leucocompound may be decomposed in this dyeing condition. Chemical reactions with oxygen may be the most leading factor for a decomposition of a leucocompound. In order to avoid thermal decomposition of a leucocompound without causing a drop in the dyeability of dyes, adjustment between dyeing temperature and dyeing time may be necessary.

When concentrations of auxiliaries (NaOH and Na<sub>2</sub>S<sub>2</sub>O<sub>3</sub>) are kept at constant and dye concentration is ca. 5% owf, K/S value turns into the maximum. And then the color yield decreases at higher concentration of dyes. These results are quite different from the dyeing behaviors of conventional dyeing processes. Stoichiometric relationship between the dye and the auxiliaries seems to determine the dyeability of dyes in this system. In order to evaluate the effects of the auxiliaries on dyeing PLA fabrics, similar investigations have been carried out

changing the concentration of auxiliaries.

At the constant NaOH concentration the amount of  $\text{Na}_2\text{S}_2\text{O}_3$  that is required to obtain the deepest color depth increases with increasing concentrations of indigo. It is natural that higher amount of  $\text{Na}_2\text{S}_2\text{O}_3$  are required to reduce higher amount of indigo molecule. However, further addition of  $\text{Na}_2\text{S}_2\text{O}_3$  causes adverse effects on the dyeing property. The color depth of dyed PLA fabrics decreases after reaching the maximum and became constant. This would relate to the over reduction of indigo molecules. The leucocompound in the system may be over reduced by the presence of excess amount of  $\text{Na}_2\text{S}_2\text{O}_3$ . As a result, a drop in the affinity or the destruction of a leucocompound may occur. In addition, dyeing under high temperature may also participate in the decomposition of the dye. These assumptions are supported from the similar experimental results at the time of changing the amount of NaOH. A drop in the color depth of dyed fabrics in the range of high concentration of NaOH is remarkable. In particular, the color depth of the fabric dyed with 5% owf of the indigo dye has fallen to nearly 0.

These results suggest that a leucocompound in the system is completely decomposed to the extent at which it cannot be developed again. Stoichiometric relationship between indigo dyes and auxiliaries seems to be very important to attain successful dyeing of PLA fabrics. Overall, the PLA fabrics could be dyed in deep shade by a similar method for dyeing cellulose fibers with vat dyes. Effects of auxiliaries on the dyeability of dyes are remarkable and negative at the range of high concentration. Optimal concentrations of dyes and auxiliaries could be estimated with simple experimental equation.

Ten popular disperse dyes with different energy levels and chemical constitutions as shown in Table 5.5 have been used to compare their exhaustion, color yield, and colorfastness on PLA and PET. Based on the dyes examined (Table 5.6), PLA has relatively lower disperse dye affinity than that of PET. Only two out of the 10 dyes have exhaustion values higher than 80% on PLA at 2% owf. Five of the 10 dyes have exhaustion values less than 50%. All dyes have more than 90% exhaustion on PET with six of those having exhaustions of 98% or higher. There is no obvious pattern as to which energy level or which structure class provides better dye exhaustion. PLA has higher color yield than that of PET. Based on the regression study of all dyes examined, the color yield of PLA is about 30% higher than that of PET. Lower reflectance, or reflectivity of PLA, contributes to the higher color yield of PLA than that of PET. This means that although PLA may have lower dye uptake, it can still be dyed with the similar apparent shade depth to that of PET. A quantitative relation between the shade depth of PLA and PET and their dye sorption has been developed. Colorfastness to accelerated home laundering indicated that PLA has lower wash fastness than that of PET. Compared at the same 2% owf, wash fastness of disperse dyes on PLA is about 0.5 to 1.0 class lower than that of PET. Crock fastness of PLA is close to that of PET than wash fastness. Five of the 10 dyes have their crock fastness 0.5 to 1.0 class lower on PLA than that of PET. If the comparison is based on the same dye



uptake rather than the same initial dye concentration, the crock fastness on PLA probably would be worse. Colorfastness to light of PLA is very close to that of PET. Five of the 10 dyes have 0.5-class lower light fastness on PLA than that of PET. Four of the 10 dyes have the same light fastness on both fibers. Only disperse orange 29 has a substantially lower light fastness on PLA (Class 5) than that of PET (Class 8).

**Table 5.5** Characteristics of disperse dyes [51]

Dye	Energy level	Structure class
Disperse blue 56	Low	Anthraquinone
Disperse yellow 64	Low	Quinoline
Disperse yellow 86	Low	Nitrodiphenylamine
Disperse blue 60	Medium	Anthraquinone
Disperse blue 73	Medium	Anthraquinone
Disperse yellow 211	Medium	Monoazo
Disperse orange 29	Medium high	Dizao
Disperse blue 79	High	Monoazo
Disperse red 82	High	Monoazo
Disperse red 167	High	Monoazo

**Table 5.6** Colorfastness to crocking (AATCC Test Method 8) [51]

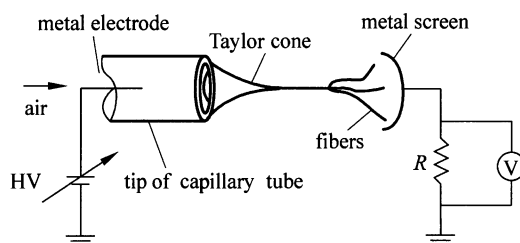
Disperse dye	Dye exhaustion <sup>a</sup> (2% owf) (PLA/PET) (%)	Gray scale rating for dry crockfastness <sup>a</sup> (PLA/PET)	Gray scale rating for wet crockfastness <sup>a</sup> (PLA/PET)
Disperse blue 56	42/97	4-5 / 4-5	4 / 4
Disperse yellow 64	23/99	4-5 / 4-5	4 / 4
Disperse yellow 86	89/93	4-5 / 5	4-5 / 5
Disperse blue 73	58/99	4-5 / 5	4 / 4-5
Disperse blue 60	40/96	4-5 / 4-5	4-5 / 4-5
Disperse yellow 211	18/99	4-5 / 4-5	4-5 / 4-5
Disperse orange 29	22/95	4-5 / 4-5	4 / 4
Disperse blue 79	73/99	4-5 / 5	4-5 / 4-5
Disperse red 82	79/98	4 / 4-5	3-5 / 4-5
Disperse red 167	98/100	4-5 / 4-5	3-5 / 4-5

a. First part of each value is for PLA and the second part is for PET. For example, a gray scale rating of yellow 86 of 4-5/5 means that the crocking fastness of PLA is 4-5 and that of PET is 5.

## 5.2.6 Electrospinning of PLA Fibers

One variant of dry spinning is known as electrospinning which utilizes an

electrostatic force to draw fiber. Electrospinning is a technique for producing fibers that are drastically thinner than those produced using conventional fiber preparation methods, such as melt, dry and wet spinning. Electrospun fibers typically have diameters ranging from micrometer to nanometer. Electrospinning involves application of an electric field between a capillary tip and a collector by a high voltage source. A pendant droplet of polymer solution at the capillary tip is transformed to a hemispherical shape and then into a conical shape, also known as Taylor cone by the electric field. When the effect of the electric field becomes stronger than the surface tension of the polymer solution, the solution is ejected towards the metallic collector. If the concentration of the solution is not suitable, the jet breaks up into droplets. However, if the viscosity is high enough, indicating that the polymer chains are entangled, a continuous jet is formed. The field accelerates the jet and it becomes unstable. Whipping instability is one of the possible instabilities that may occur in an electrified fluid jet. The rapidly whipping jet undergoes high stretching during its complicated path through the electric field. The initially single jet can also be divided into multiple filaments by radial charge repulsion, a process known as “splaying”, which can be responsible for the formation of fibers with diameters on the meso- and nanometer scales. The solvent evaporates during the spinning process, and then dry, thin fibers can be obtained on the collector plate using appropriate process parameters. The dry fibers accumulated on the surface of the collection screen form a nonwoven mesh of nanometer to micrometer diameter fibers even when operating with aqueous solutions at ambient temperature and pressure. The electrospinning process can be adjusted to control fiber diameter to some extent by varying the charge density and polymer solution concentration, while the duration of electrospinning controls the thickness of the deposited mesh. Due to their small diameter, electrospun fibers possess very large surface area, making them an ideal material for applications such as medical tissue scaffold, wound dressing, carrier for drugs, protective fabrics, high performance filter media, filler for nanocomposite materials, etc. [52]



**Figure 5.13** Experimental set up of the electrospinning process [53]

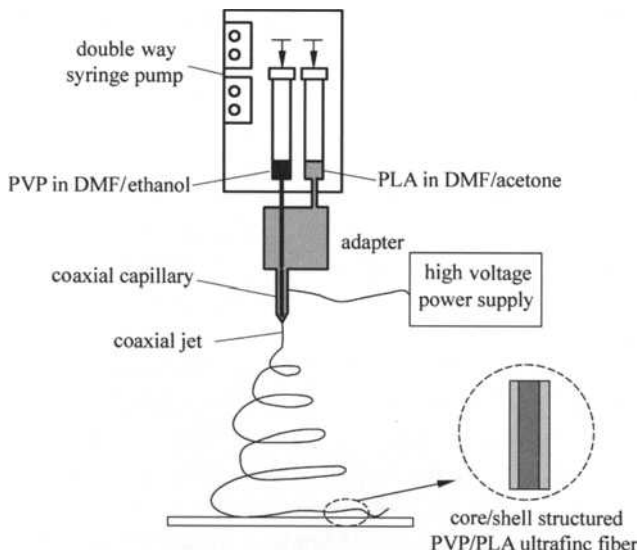
PLA has been successfully electrospun into fibers primarily for tissue engineering and biomedical applications. For instance, a number of studies show that scaffolds

for the regeneration of cardiac, neural, bone and blood vessel tissues can be fabricated from electrospun PLA fiber through post-spinning orientation and/or using rotating target collectors [54 – 57]. PLA has been electrospun into different forms of ultrafine fiber and used as carriers for bioactive agents including antibiotics [58], anticancer drugs [59, 60] and antibacterial silver nanoparticles [61].

Poly (*L,D*-lactide) (PDLA) can be electrospun to fibers with diameters ranging from 350 to 1900 nm. Morphology of fibers and distribution of fiber diameter has been investigated varying molecular weight, concentration and applied voltage. Molecular weight and concentration play an important role in the morphology of fibers. Lower molecular weight and lower concentration tend to facilitate the formation of beads or bead-on-string structures. Fiber diameter tend to increase with increasing polymer concentration and decrease with increasing applied voltage. Two-way analysis of variance has been carried out at the significance level of 0.05 to study the impact of applied voltage and concentration on average fiber diameter for a polymer with molecular weight of 100 000 g/mol. It is concluded that both concentration and applied voltage have significant impacts on average fiber diameter. But the impact of concentration is much greater. And there is some interaction between concentration and applied voltage. Applied voltage has less impact on average fiber diameter at lower concentration than at higher concentration. Process conditions can be chosen according to the model. Fibers with narrower diameter distribution can be obtained at lower concentration regardless of applied voltage. Fibers with uniform diameter and narrower distribution can be obtained at higher concentration and higher applied voltage [62].

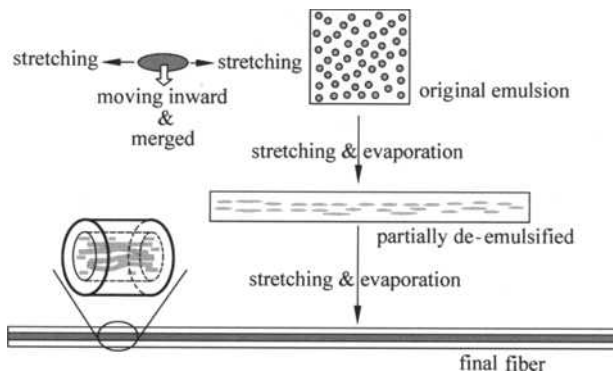
PLA solutions with lower polymer concentrations favor formation of small diameter fibers. But these fibers are less consistent in morphology and tend to form beads along their length. These defects can be overcome by incorporating an organic or inorganic salt, such as pyridinium formiate,  $\text{NaH}_2\text{PO}_4$ , or  $\text{NaCl}$ , in the fiber-forming solution to enhance electrical conductivity [63, 64]. The solvent used will affect the surface morphology of the fiber. Using dichloromethane as a solvent to prepare polymer solution of 5%, Bognitzki et al. observed that the surface exhibited regular pore structures, which were attributed to rapid phase separation of the solvent [65].

Core/shell PVP/PLA ultrafine fibers by coaxial electrospinning is shown in Fig. 5.14. The schematic setup of coaxial electrospinning is essentially the same as that of a conventional electrospinning setup except for replacing the single capillary with a coaxial spinneret consisting of two concentrically arranged capillaries that are flatted stainless steel needles. A certain amount of the two polymer solutions are contained separately in two medical syringes connected to the coaxial spinneret respectively. The flow rate in each capillary can be adjusted in a double-way syringe pump. Membranes made from the biodegradable core/shell ultrafine fibers could be potentially used in loading bioactive molecules for tissue regeneration [66].



**Figure 5.14** Schematic setup of coaxial electrospinning [66]

Core-sheath nanofibers of PEG-PLA and PEO can be prepared by electrospinning a water-in-oil emulsion in which the aqueous phase consists of a PEO solution in water and the oily phase is a chloroform solution of an amphiphilic PEG-PLLA diblock copolymer. The fibers obtained are composed of a PEO core and a PEG-PLA sheath with a sharp boundary in between. By adjusting the emulsion composition and the emulsification parameters the overall fiber size and the relative diameters of the core and the sheath can be changed. As shown in Fig. 5.15, a mechanism is proposed to explain the process of transformation from the emulsion to the core-sheath fibers, i.e., the stretching and evaporation induced de-emulsification. In principle, this process can be applied to other systems to



**Figure 5.15** Schematic mechanism for the formation of core-sheath composite fibers during emulsion electrospinning [67]

prepare core-sheath fibers in place of concentric electrospinning and it is especially suitable for fabricating composite nanofibers that contain water-soluble drugs [67].

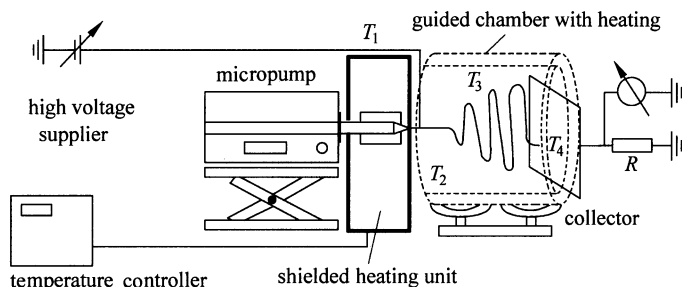
PLA/inorganic nanosize layered double hydroxides (LDH) has been successfully obtained by the method of electrospinning. LDH particles are dispersed evenly and uniformly in PLA matrix. The number average molecular weight of the electrospun PLA fibers does not change remarkably while the melting point of PLA decreases upon the increase of LDH content, which suggests that the PLA/LDH composite material may have prospective application as the basis of environmental friendly systems [68].

Other PLA composite fibers containing nano-components such as nanoclay (montmorillonite, MMT) and TiO<sub>2</sub> nanoparticles have also been successfully produced using the electrospinning technique [60, 69].

Levit et al. reported an electrospinning process assisted by supercritical CO<sub>2</sub>. Polymer fibers of high molecular weight PLA were produced using only electrostatic forces without the use of a liquid solvent. The fibers were formed between two electrodes in a high-pressure view cell. A polymer sample was placed on a grounded electrode and a second, counter electrode was placed at high potential. The polymer was observed as the thermodynamic conditions (e.g. temperature, CO<sub>2</sub> pressure) and potential difference was varied. At a CO<sub>2</sub> temperature and pressure above the critical point, but well below the single-phase region, polymer fibers formed between the grounded electrode and the high voltage counter electrode. The supercritical CO<sub>2</sub> reduces the polymer viscosity sufficiently to allow fibers to be electrostatically pulled from an undissolved bulk polymer sample. Unlike a conventional electrospinning process where the liquid solvent is replenished through a hypodermic needle connected to a syringe pump, the isolated droplets applied to the microelectrode contain a limited amount of liquid solvent which evaporates leaving behind a dry polymer microdot [70].

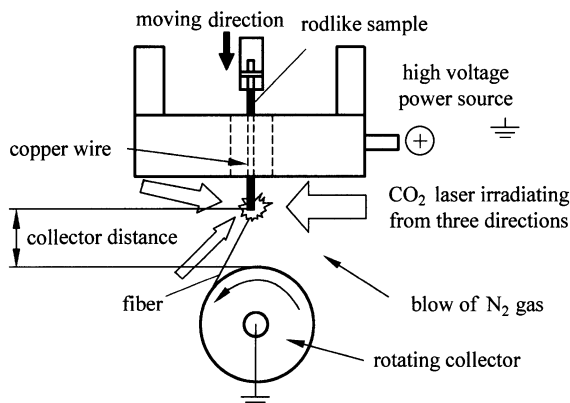
Melt electrospinning can be a feasible way to produce sub-micron scale PLA fibers as shown in Fig. 5.16. The setup includes basic components such as a digitally controlled syringe pump, a high voltage supplier and a collector and some critical components for melt electrospinning such as a heating oven for polymer melt reservoir ( $T_1$ ), a nozzle heater ( $T_2$ ), a heated guiding chamber ( $T_3$ ) and a temperature controllable collector ( $T_4$ ). This solvent-free approach to produce sub-micron scale fibers is more environmentally benign than common solution electrospinning processes, and has a potential to increase the production rate significantly. The temperatures at the spinneret and in the spinning region are critical to produce sub-micron size fibers: a high speed photographic investigation reveals that when spinning temperature is below glass transition temperature, whipping of the jet is suppressed by fast solidification in the spinning region leading to a larger jet diameter. Both thermal and mechanical degradations of PLA in melt electrospinning can be significant but no change in chemical composition is found. Due to rapid solidification, melt electrospun PLA fibers are mostly

amorphous, and the small presence of  $\beta$  crystals is noted in the sub-micron scale PLA fibers by XRD studies. The highly oriented structure of PLA fibers gives rise to cold crystallization at around  $95^{\circ}\text{C}$ , and the degree of crystallinity of fibers increases with increasing the degree of annealing. Melt electrospun PLA nanofiber mats with no residual solvent may serve as better filter media and tissue scaffolds than those obtained from solution electrospinning processes [71].



**Figure 5.16** Schematic diagram of the melt electrospinning setup [71]

In the case of the conventional melt-electrospinning process the molten polymer is exposed to long-term thermal degradation. Recently, an innovative technique was reported for electrospinning PLA in the melt phase by using a  $\text{CO}_2$ -laser as shown in Fig. 5.17. This technique relies on a laser beam to melt the PLA polymer locally, thus minimizing thermal degradation due to prolonged heat exposure, which has been observed previously for melt-electrospinning for other polymers based on the heat conduction melting approach. Moreover, the laser technique also eliminates the use of solvent, making the process more environmentally benign. This technique is capable of producing fibers with diameters smaller than 1  $\mu\text{m}$  [72].



**Figure 5.17** Schematic diagram of the melt-electrospinning system

While research on electrospinning has exploded in the past decade for fibers spun from various polymers, the commercial production of ultrafine PLA fibers using this technique has not been forthcoming due to the low production throughput, the requirement for the use of specific solvents, and variation in fiber diameter. Based on the present state-of-the-art of electrospinning, this technique is likely to find uses for products containing PLA-nanofibers in pharmaceutical and biomedical applications.

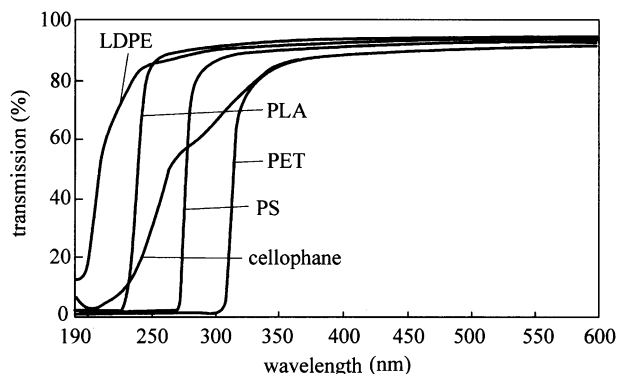
## 5.3 Blowing

### 5.3.1 Properties for Packaging

#### 5.3.1.1 Optical

The absorption of visible and UV light by polymers is one of the main factors affecting food quality [73, 74]. The protection of light sensitive foods such as vitamin, dairy products and edible oils from UV radiation when packaged in plastic containers has been widely investigated [75 – 77]. For example, light has been found to affect the flavor and, to a lesser degree, the nutritional content of milk [74, 78]. Therefore, the material used to produce the primary package is critical in minimizing product damage. PLA light barrier properties have been studied and compared with the visible and ultraviolet light transmission rates of standard commercial polystyrene, PET, low density polyethylene and cellophane films in the range 190 – 800 nm. Figure 5.18 shows the light transmission profiles for PLA and other standard commercial films. PLA shows almost no UV transmission in the lower range of UV-C (190 – 220 nm). However, at 225 nm the amount of UV light transmitted by PLA increases significantly. At 250 nm, 85% of the UV light is transmitted. At 300 nm, 95% of the UV light is transmitted. Thus, while UV-C is not transmitted, nearly all the UV-B and UV-A light passes through the film [79]. Therefore, the application of transparent PLA film to, for example, dairy products may require additives to block UV light transmission. Effective UV stabilizers are able to absorb UV light and thus prevent damage to light sensitive packaged food, resulting in retention of taste and appearance, extension of shelf life and improvement of product quality. PLA transmits less UV-C light than LDPE (Fig. 5.18), but PET, PS and cellophane transmit less UV-B and UV-A than PLA and LDPE. Moreover, PET does not transmit UV-C and UV-B wavelengths, which are the most damaging for food.

All polymers have a refractive index that is characteristic of the polymer structure. The refractive index can be calculated by different theoretical methods based on the molecular weight and molecular volume of the monomer or constitutional unit, the density of the polymer and the chemical structure of the



**Figure 5.18** Percent transmission versus wavelength for PLA (98% *L*-lactide), PS, LDPE, PET and cellophane films (PLA samples were obtained from Cargill Dow LLC)

polymer. The refractive index of PLA polymer and of common commercial polymers was calculated by the Lorentz and Lorentz, Gladstone and Dale and Vogel methods. Table 5.7 shows the experimental and calculated refractive indices for PE, PS, PVC, PET and PLA. Light refraction is directly correlated with the isotropy of the polylactide [80]. Tsuji et al. measured the optical rotation of PDLA and PLLA. The specific optical rotation,  $\alpha$ , of the polymers was measured in chloroform at a concentration of 1 g/dL at 25°C, using a polarimeter at a wavelength of 589 nm. Values of  $-156^\circ$  and  $156 \text{ deg}\cdot\text{dm}^{-1}\cdot\text{g}^{-1}\cdot\text{cm}^3$  were reported for PLLA and PDLA [81].

**Table 5.7** Theoretical and experimental refractive index for standard commercial polymers

Polymer	$n$ exp.	$n$ calculated		
		Lorentz and Lorentz <sup>b</sup>	Gladstone and Dale <sup>c</sup>	Vogel <sup>d</sup>
PE	1.490 <sup>a</sup>	1.479	1.478	1.469
PS	1.591 <sup>a</sup>	1.603	1.600	1.590
PVC	1.539 <sup>a</sup>	1.544	1.543	1.511
PET	1.63–1.68 <sup>a</sup>	1.581	1.580	1.560
PLLA <sup>e</sup>	–	1.482	1.492	1.500

a: Values obtained from Van Krevelen [82].

b: Values calculated according to Lorentz and Lorentz.

c: Values calculated according to Gladstone and Dale.

d: Values calculated according to Vogel.

e: Experimental value was not obtained.

### 5.3.1.2 Physical and Mechanical Properties

Physical properties of PLA polymers as well as other polymers depend on their



molecular characteristics as well as ordered structures such as crystalline thickness, crystallinity, spherulite size, morphology and degree of chain orientation. The physical properties of polylactide are related to the enantiomeric purity of the lactic acid stereocopolymers [83, 84]. The homopolymers poly (*D*-lactide) or poly- (*L*-lactide) and high *D*- or *L*-lactide copolymers have very regular structures and develop a crystalline phase. High molecular weight polylactides are either amorphous or semicrystalline at room temperature, depending on the amounts of *L*, *D* and *meso*-lactide in the structure. PLA can be produced totally amorphous or up to 40% crystalline. PLA resins containing more than 93% of *L*-lactic acid are semi-crystalline while PLA with 50% – 93% *L*-lactic acid is strictly amorphous. The presence of both *meso*- and *D*-lactide forms causes imperfections in the crystalline structure, reducing the percent crystallinity. For amorphous PLA, the glass transition temperature ( $T_g$ ) is one of the most important parameters since dramatic changes in polymer chain mobility take place at and above  $T_g$ . For semicrystalline PLA, both the  $T_g$  and melting temperature ( $T_m$ ) are important physical parameters for predicting PLA properties. The glass transition temperature is also determined by the proportion of different lactides. According to Ikada and Tsuji, melting temperature rises with an increase in molecular weight ( $M_w$ ) until the maximum practical value [85]. On the other hand, the crystallinity of the samples gradually decreases with increasing  $M_w$ . The glass transition temperature is also determined by the proportion of different lactides present. This results in PLA polymers with a wide range of hardness and stiffness values. The typical PLA glass transition temperature ( $T_g$ ) ranges from 50°C to 80°C while the melting temperature ranges from 130°C to 180°C. The glass transition temperature of PLLA is higher than PDLA but this may be partly due to the difference in crystallinity between the two polymers [86]. Table 5.8 presents the glass transition and melting temperatures and the enthalpy of fusion for two PLA and PET films. Polylactide films undergo an endothermic event superimposed on  $T_g$ , which is observed during first DSC heating. This endothermic relaxation, with an average enthalpy of 1.4 J/g, results from a secondary molecular reordering in the amorphous phase of semi-crystalline polymers. The endothermic peak is eliminated as the sample is heated above  $T_g$ .

**Table 5.8** Physical properties of PLA (98% *L*-lactide), PLA (94% *L*-lactide) and PET

	PLA(98% <i>L</i> -lactide)	PLA(94% <i>L</i> -lactide)	PET
$T_g$ (°C)	71.4	66.1	80
Relaxation enthalpy(J/g)	1.4	2.9	N/A
$T_m$ (°C)	163.4	140.8	245
Enthalpy of fusion(J/g)	37.5	21.9	47.7
Percent crystallinity	40	25	38

The tensile strength and the elastic modulus values for poly (98% *L*-lactide and 94% *L*-lactide) films are presented in Table 5.9. The higher content of *L*-lactide in the films contributes to a higher tensile strength. Although poly (98% *L*-lactide) has greater elongation at yield than poly (94% *L*-lactide), the latter has an elongation at break 7 times greater than poly (98% *L*-lactide), which indicates that poly (94% *L*-lactide) is more plastic.

**Table 5.9** Mechanical properties of poly (98% *L*-lactide) and poly (94% *L*-lactide)

	Poly (98% <i>L</i> -lactide)		Poly (94% <i>L</i> -lactide)	
	MD	CD	MD	CD
Tensile yield stress (MPa)	72	65	84	74
Percent elongation at yield	5	4	3	4
Percent elongation at break	11	5	78	97
Elastic modulus (GPa)	2.11	2.54	2.31	2.87

The thermal history of PLLA films strongly affects their physical properties since it induces changes in crystallinity (i.e., long physical aging time affects the ratio of the glassy amorphous phase). This phenomenon is clearly observed as the storage temperature approaches the glass transition temperature of the films. Celli and Scandola [87] found that the decrease in molecular weight of PLLA films increased the magnitude of the enthalpy of relaxation at the glass transition. Tsuji and Ikada [88] prepared PLLA films which they annealed. They found that PLLA polymer morphology strongly depended on the annealing temperature and time since it alters the spherulite size and morphology. In addition, annealing effects depend on pretreatments such as melting before annealing. Annealing studies of PLLA at 448 K showed an increase in melting temperature and heat of fusion with annealing time, suggesting an increase in lamellar thickness.

### 5.3.1.3 Time, Temperature and Humidity

In polymers that absorb very low amounts of water, such as PLA and PET, the effect of water on the physical properties can be crucial to the polymer's general performance. For example, in the case of PET, water plasticizes the amorphous phase, which leads to a decrease of the  $T_g$  from about 80°C in a dry state to about 57°C in a saturated state and a consequent reduction of the elastic modulus [89]. Besides the changes in the physical and mechanical properties, surprising changes in polymer barrier properties can occur as a result of the presence of relatively small quantities of absorbed water. Therefore, changes in the physical properties (i.e.,  $T_g$ ,  $T_m$  and enthalpy of fusion) as a function of the storage time at different temperatures and water activities can be used as an indicator of the change in the performance of the polymers under different environmental conditions. Variation in the glass transition and melting temperatures with time, temperature and humidity for two polylactide films of rectangular shape (5 cm×1 cm×25.4 μm),

poly (98% *L*-lactide) and poly (94% *L*-lactide), stored for 120 d at 5, 23 and 40°C, and 0.11, 0.53 and 0.94 water activities has been reported. In a study the glass transition and melting temperatures were monitored every week for the first month and after that every 30 d. For poly (98% *L*-lactide), the variation in  $T_g$  was statistically significant as a function of time. The major reduction in  $T_g$  as a function of time was reached prior to seven days. After this no statistically significant change was recorded. No statistically significant change of  $T_g$  as a function of storage temperature was found. Humidity also has an effect on  $T_g$ . It was found that the reduction of  $T_g$  as a function of time was statistically significant after seven days. The change in  $T_g$  as a function of storage temperature and the change of  $T_g$  with humidity were not statistically significant. Melting temperature was analyzed in the same way as the glass transition temperature and no significant changes were found for poly (98% *L*-lactide) and poly (94% *L*-lactide). In addition, the change in the enthalpy of fusion as function of time, temperature and humidity was evaluated. For poly (98% *L*-lactide), no statistically significant change in the enthalpy of fusion as a function of time, temperature and humidity was found. For poly (94% *L*-lactide), however, the change was statistically significant. One reason for the change in the enthalpy was likely to be the low molecular weight sealant layer.

#### 5.3.1.4 Heat Sealing Properties

Working with amorphous PLA sealant films, Gruber and O'Brien reported sealing temperatures of 80°C and 85°C and an ultimate tensile strength of 360 g/cm over a broad temperature range. They also reported a peak hot tack strength of 450 g/cm in a PLA made by co-extrusion [90]. Auras determined the best sealing conditions for poly (94% *L*-lactide) films and found that poly (94% *L*-lactide) had a constant peel force until the sealing temperature exceeded 115°C. At 120°C the peeling force increased by 25%, though the material failed before seal failure. The maximum and minimum peel forces did not differ much from the average values, which indicated uniform sealing of the PLA samples. When the heating temperatures exceeded 110°C, the shrinkage of the sample increased to 10% and then 20% at a temperature of 120°C. The best sealing condition for poly (94% *L*-lactide) was a temperature of around 110°C for one to five seconds. The strongest peel seal could be achieved at temperatures near the melting point of the inner sealant layer of the polymer film. Sealing at a temperature above the fusion temperature resulted in a weld seal and a high shrinkage rate. The dwell time for sealing did not result in any considerable difference in seal strength once the temperature at the interface reached the set temperatures. Sufficient pressure was required to bring the sealing surfaces together at the sealing temperature. Once achieved, however, a higher pressure did not add to the seal strength. The combination of the delamination failure mode shown in PLA with this peel strength value may indicate the potential for PLA to be incorporated into an "easy-open" package.

## **5.3.2 Process of Blown Film**

### **5.3.2.1 Raw Material Handling**

Although almost no LDPE, LLDPE or HDPE manufacturing line is equipped with desiccant bed dryers designed to dry down to less than 250 ppm of moisture, drying of PLA is necessary before extrusion. In addition, perhaps more importantly, once PLA material is dried, it needs to be conveyed to the extruder with dry air to keep the resin from regaining moisture. All the blending and holding hoppers also need to be sealed to keep a dry environment for the resin.

### **5.3.2.2 Extrusion**

While not ideally suited for melting PLA, a small percentage of extruders designed for processing polyolefins would be able to melt and process PLA at some level with acceptable performance. The remaining extruders will typically be limited by excessive power consumption. That is because of the significant density difference between the polymer families. PLA has a specific density of about  $1.24 \text{ g/cm}^3$ , which is much higher than polyolefins ( $0.91 - 0.96 \text{ g/cm}^3$ ). This represents an increase of between 30% and 35%. Considering all other factors such as feeding properties, heat capacity and rheology, this would require the motor to supply a minimum of 30% – 35% greater energy for a same screw speed. While PLA may be processed in extruders designed for polyolefins, if the extruder is already operating at close to maximum power of the screw, the extruder may not have enough power to process PLA due to the substantial higher density of PLA [91].

A second consideration is the screw design. Most of the commercial lines have extruder screws that have been optimized to run olefin resins at the maximum output for the diameter of the screw. To do this, they need to design for the specific melt flow properties (rheology) of the resin. PLA has a significantly different rheological behavior from olefin materials. It does not shear thin as readily and therefore typically requires additional power input from the drive. This additional power input manifests itself as an excessive increase in melt temperature. Quite often, if the drive has enough power to process PLA, it will be screw speed limited (and hence rate limited) by excessive melt temperature.

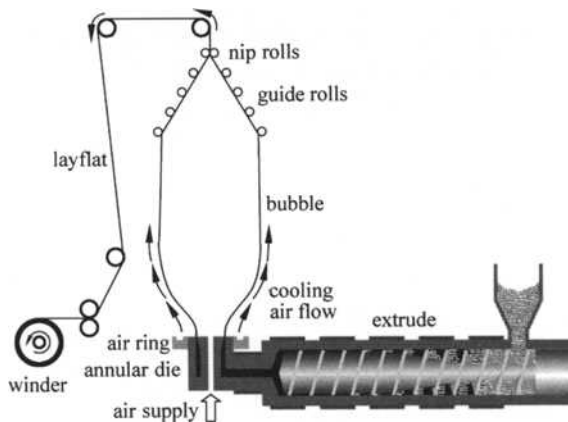
### **5.3.2.3 Blowing Film [92]**

In extrusion blow film process, molten PLA is extruded to form a tube with an annular die. By blowing air through the die head, the tube is inflated into a thin tubular bubble and cooled. The tube is then flattened in the nip rolls and taken up by the winder (Fig. 5.19). The ratio of bubble diameter to the die diameter is called the blow-up-ratio (BUR). BUR ratios of 2:1 – 4:1 with the die temperature of 190 – 200°C have been used for extrusion blowing of PLA films. By varying the BUR, screw speed, air pressure, and winder speed, films of different thicknesses (10 – 150  $\mu\text{m}$ ) and degree of orientation can be achieved [93, 94]. Compared to

polyolefins, PLA has weaker melt strength, and therefore, the formation of a stable bubble during extrusion blowing is more difficult. Depending upon the melt temperature, it could also limit the overall rate or maximum gauge film that could be produced.

By its nature, PLA is quite a stiff film. As it has a glass transition temperature ( $T_g$ ) higher than room temperature, it is stiff and glassy compared to an olefin material that has a  $T_g$  lower than room temperature. The PLA film is significantly stiffer film. In addition, the elongation of a PLA film is very low as it is in its glassy state compared to a LDPE film that has elongations of 200%–300%. These two facts make it very difficult to collapse a bubble of PLA film without creating a significant amount of wrinkles in the web. As PLA has excellent dead fold properties, these wrinkles will remain in the film and make further downstream converting difficult.

As an unoriented film, PLA has low elongation, poor tear initiation strength and poor tear propagation strength. These properties make handling of a PLA web difficult. The tension control through the web path must be excellent and all idler driven rolls must be maintained in top working condition. If the web is edge trimmed or slit, rotary shear trimming wheels are required to prevent web breaks.



**Figure 5.19** Extrusion blown film line

### 5.3.3 Modification of Blown Film

As a result, extrusion blowing of PLA film often requires the use of additives, such as viscosity enhancers to strengthen its melt strength. These additives protect the polymer from degradation and/or help couple polymer chains to attenuate overall loss of molecular weight and viscosity of the polymer melt. The formulation of coupling agents is often proprietary. One commercially available coupling agent for PLA is made up of copolymer of styrene, methyl methacrylate and

glycidyl methacrylate. Sodergard et al. [93] has disclosed a method to stabilize PLA and enhance its melt strength by adding an organic peroxy compound (e.g., tert-butylperoxybenzoate, dibenzoylperoxide, tert-butylperoxyacetate) during melt processing, wherein the peroxide is added in about 0.01%–3% by weight of PLA. Since PLA films are quite stiff and have much lower elongation than polyolefins, collapsing of bubble in the nips rolls tends to produce wrinkles which tend to permanently remain in the film due to the high dead-fold properties of PLA. This problem can be overcome by incorporating fillers into PLA during extrusion. To reduce the adhesion between films, Hiltunen et al. blended PLA with triacetin plasticizer (glycerol triacetate), together with various anti-adhesion agents, such as talc, TiO<sub>2</sub> and CaCO<sub>3</sub>. It was claimed that the bursting strengths of the resulting blown films were better than typical polyethylene and PP films [95]. Slip additives (e.g., oleamide, stearamide, *N,N*-ethylene bisstearamide, oleyl palmitamide) have also been added to reduce the coefficient of friction between overlapping films. Typically, slip additive of less than 0.5%–1.0% by polymer weight is used, as excessive amounts will compromise the ability for printing inks, stickers to adhere to the film surface. To avoid the use of copolymerization techniques, blending, or plasticizers, Tweed et al. developed a method to obtain PLA blown films by elevating the viscosity of PLA through successive steps in a polymer cooling unit or by internal cooling of the die mandrel using air or liquid fluid to control the temperature of the die. Mitsui Chemicals successfully developed PLA-based films by copolymerization technology [96], and it is commercializing it as one of the LACEA brand resins.

### 5.4 Foaming

PLA foams are first utilized in tissue engineering and medical implant applications [97–99], where the high cost of the materials is justified. Their processing must be relatively simple and inexpensive if they want to be suitable for industrial foaming applications [100]. However, thermal, oxidative, and hydrolytic degradations may occur during its processing—leading to the cleavage of polymer chains, and hence to a decrease in molecular weight [101]. All these degradation processes result in a deterioration of the rheological properties, which should be avoided for processing purpose, especially when high levels of extensional viscosity and elasticity are required for extrusion foaming [102]. Another shortcoming of PLA is its very low melt viscosity, which may also limit its blow molding and foaming processabilities. To overcome such shortcomings, many strategies to control the melt rheology of PLA and to increase the melt viscosity have motivated considerable research efforts. In particular, three different techniques are described in this chapter: (1) Modification of PLA resins with chain extenders to compensate for the molecular weight decrease caused by processing degradation. Generally, a commercial PLA product has been reactively modified in melt by

sequentially adding 1, 4-butanediol and 1,4-butane diisocyanate as low-molecular-weight chain extenders. (2) Blending with other natural or synthetic materials such as PEG, polycaprolacton (PCL), starch, poly (butylene adipate-co-terephthalate) (PBAT) and so on. To do so, blends/alloys with improved properties and cost effectiveness will be obtained. (3) Preparation of PLA nanocomposite foam. Well-dispersed nanoparticles in PLA matrix may serve as nucleation sites to facilitate the bubble nucleation process, reduce gas diffusivity in PLA matrix and enhance mechanical and physical properties of PLA foams.

### 5.4.1 Modification of PLA and Its Foam

As mentioned above, low thermal, oxidative, and hydrolytic stability may lead to a decrease of molecular weight during processing. Many strategies have been devoted to control the melt rheology by increasing the molecular weight to compensate for molecular weight decrease caused by processing degradation such as branching/ linking [103, 104], chain extension [105] and solid-state polymerization [106]. In the following paragraph, one method is utilized to extend PLA chain and the modified PLA foam is described.

It has been reported [107] that 1, 4-butanediol (BD) and 1, 4-butane diisocyanate (BDI) can be used as chain extender to modify commercial PLA in two steps. In first step, the commercial PLA melt is allowed to first react with BD in the presence of trace amount of tin (II) 2-ethylhexanoate to obtain hydroxyl terminated PLA (OH—PLA) [Fig. 5.20(a)]. And then, in the second step, BDI is added to react with hydroxyl end groups of OH—PLA to achieve chain-extended PLA, leading to the formation of urethane [Fig. 5.20(b)].

The —NCO groups of isocyanate readily react with every active hydrogen in the reacting system. Consequently, besides engaging in urethane formation, BDI can also react with carboxyl group residuals (because of equilibrium reaction) leading to amide bond [Fig. 5.21(a)]. The urethane and amide groups can further react with additional isocyanate. Such reactions can cause crosslinks in PLA [Fig. 5.21(b) and (c)].

Such modification also causes a dramatic increase in storage modulus and loss modulus. This is attributable to more entanglements and the pseudostructures through formation of physical networks at high molecular weights. That is, over a range of frequencies the balance between viscous and elastic properties is retained because of the existence of gel-like pseudostructures, which can withstand the shear force. Hence, chain interactions play a more important role and give rise to higher storage modulus. In general the melt elasticity has a direct relationship with the melt strength, which is an indication of the resistance for a melt to extension [108]. Accordingly, such chemical modification has improved both melt viscosity and elasticity/strength for PLA.

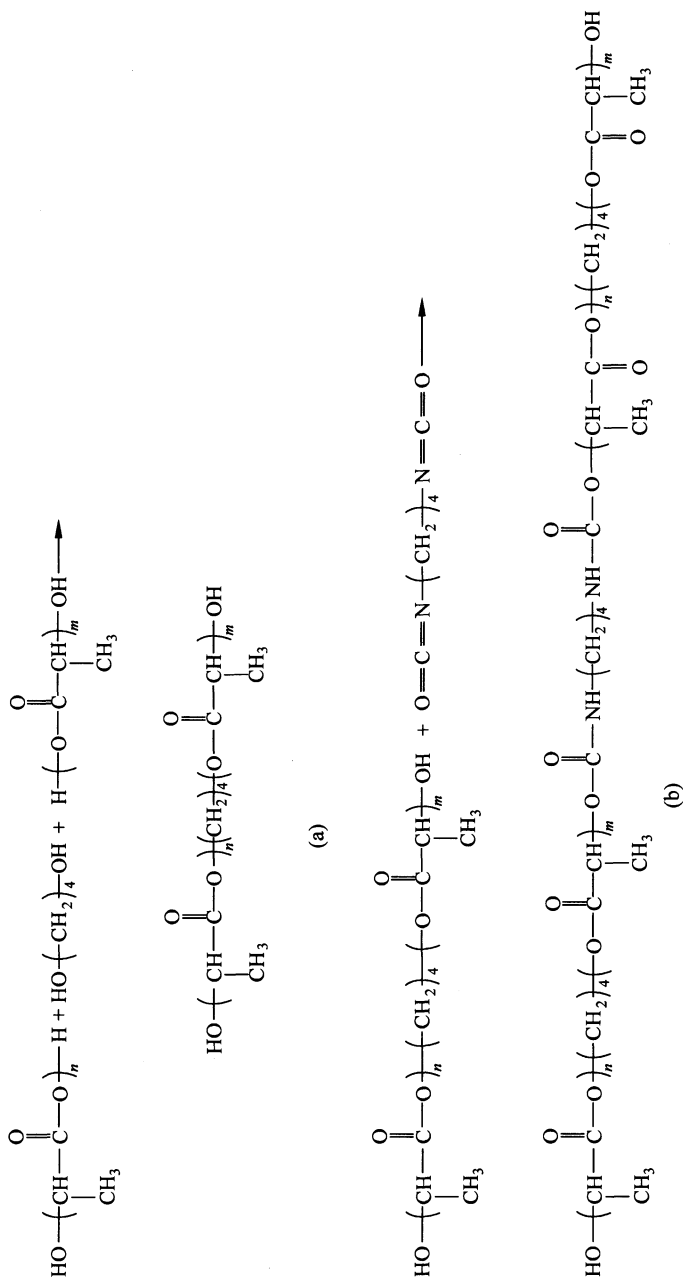
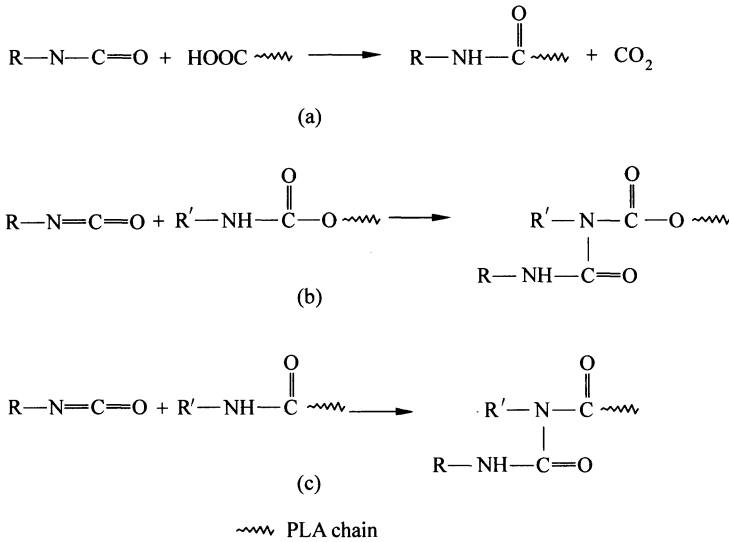


Figure 5.20 PLA chain extension process





**Figure 5.21** PLA chain crosslink process

The plain and modified PLA foaming (batch process) has been conducted in a high pressure stainless steel autoclave. The blowing agent used in the study is mixture of compressed CO<sub>2</sub> and N<sub>2</sub> (20/80). The pressure of blowing agent at 170°C is adjusted to the desired saturation pressure (16 MPa). The solubilization is maintained for about 4 h to ensure equilibrium absorption of blowing agent by the samples and then the temperature is cooled down at 5°C/min to the foaming temperature (110°C) and the pressure is rapidly reduced to atmosphere pressure by opening the valve of autoclave. After that the autoclave is opened and the foamed samples are cooled naturally to room temperature and kept in desiccator at room temperature.

Table 5.10 shows characteristics of plain and modified PLA foam. It is clearly shown that molecular weight of samples of modified PLA 1 and modified PLA 2 is increased compared to plain PLA because of chain extension. The excess of

**Table 5.10** Characteristics of plain and modified PLA foam

Sample	Plain PLA	Modified PLA 1 <sup>a</sup>	Modified PLA 2 <sup>b</sup>
$M_n/(10^3 \text{ g/mol})$	57	84	107
$M_w/(10^3 \text{ g/mol})$	124	225	308
$M_w/M_n$	2.2	2.7	2.9
Average cell size (μm)	227	37	24
Cell number density (10 <sup>8</sup> /cm <sup>3</sup> )	0.008	1.9	6.7
Foam density (g/cm <sup>3</sup> )	0.125	0.067	0.092

a: COOH/BD = 2:1, OH/BDI = 2:1, i.e. equimolar amount of BD and BDI relative to end groups —COOH and —OH of PLA;

b: COOH/BD = 2:1, OH/BDI = 1:1, i.e. BDI amount is excessive compared to Modified PLA 1.

BDI in modified PLA 2 sample results in materials with the higher molecular weight ( $M_w$ ) and broader molecular weight distribution. It is reasonable to conclude that due to the excess of BDI, the isocyanate groups can react with carboxyl groups of PLA leading to amide bond that can further react with additional BDI and cause cross-linking in PLA. The improved viscous and elastic properties of modified PLA samples results in foams with lower foam density and higher cell density.

### 5.4.2 Starch/PLLA Hybrid Foams

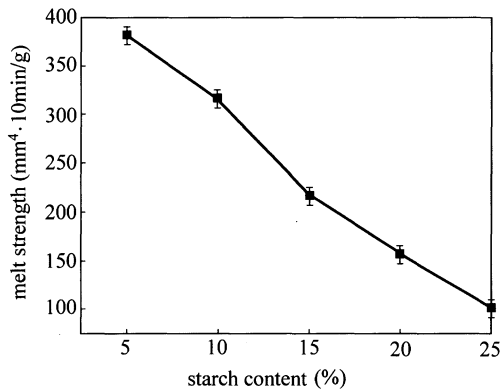
Researches on PLA foams have been reported by many authors [109, 110]. But, due to its high manufacturing price, it has long been restricted from being widely used in practice. On the other hand, PLA has very low melt strength; it means that PLA can be foamed only within a very narrow range of processing temperatures. So the reports about PLA foams are few so far. Starch is the second most abundant renewable polymer in nature next to cellulose [111]. Because of the low cost, starch-based foams have been investigated widely. Yogaraj Nabar and Ramani Narayan [112] investigated twin-screw extruded starch foams. Lawton et al. [113] produced baked cornstarch foams by using a laboratory baking machine, and they used aspen fiber as an additive to improve the mechanical properties. However, the starch foams have poor mechanical properties and hydrophobicity while the traditional petroleum-based foams are superior in these aspects. So there are many difficulties for the application of starch foams. Because of these shortcomings, starch has been combined with PLA to produce a new polymer hybrid foam applicable for a variety of purposes.

Dujdao et al. [114] prepared starch/ PLA hybrid foams by baking a mixture of starch, PLA, and other ingredients in a hot mold. Starch, guar gum (1 wt% of starch) and magnesium stearate (2 wt% of starch) were first dry-mixed. Distilled water was then added to the mixture and the batter was further mixed for 20 min. PLA or a plasticizer (i.e. glycerol, urea, or ammonium chloride) was also added to the batter. Starch/PLA foams were then prepared by first applying batter in a mold cavity. Slight pressure was applied just to close the mold. After 2 min of baking period, the mold was cooled down to room temperature. The ultimate tensile strength of the foam was shown to exhibit a maximum when the relative humidity was 42% (for a fixed storage time of 7 d) and when the storage time was 2 d (for a fixed relative humidity of 42%). Addition of PLA helped improve the ultimate tensile strength and the percentage of elongation at break of the hybrid foams. Resistance to water absorption of the starch/PLA hybrid foams was superior to that of pure starch foams.

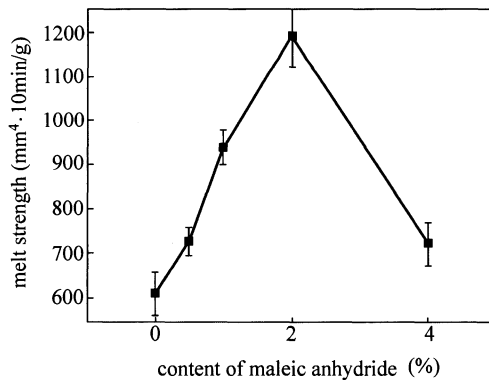
In the lab, starch/PLA composite foams have also been prepared by extruding. First, the modified starch is prepared by mixing the starch with maleic anhydride and montmorillonite in a homogenizer and PLA with SiO<sub>2</sub>, maleic anhydride (MAH), BPO and white titanium dioxide are extruded as the master batch by using

a laboratory twin-screw co-rotating extruder. The master batch is then extruded with starch, AC and 2, 5-dimethyl-2,5-di-(*tert*-butylperoxy) hexane (L101) to prepare the composite foams.

As shown in Fig. 5.22, it is observed that melt strength (MS) reduces with an increase in content of the starch. Addition of maleic anhydride can remarkably make MS increase (Fig. 5.23). But when the content rises to above 2%, MS would decrease. This is because that when maleic anhydride is excessive, the graft reaction is completed. The remaining maleic anhydride functions as lubricant that causes MS to decrease.



**Figure 5.22** MS of the composites as a function of starch content



**Figure 5.23** MS of the composites as a function of maleic anhydride content

Cell density reflects the compact degree of the cells. High cell density means more excellent mechanical and thermal properties in the same apparent density. As shown in Fig. 5.24 and Fig. 5.25, cell density increases as the content of starch increases. Modified starch has no different influence on cell density compared to starch. As can be seen from Fig. 5.25, the bubbles become larger when the content of starch increases.. This is because bubbles can grow more easily due to low MS.

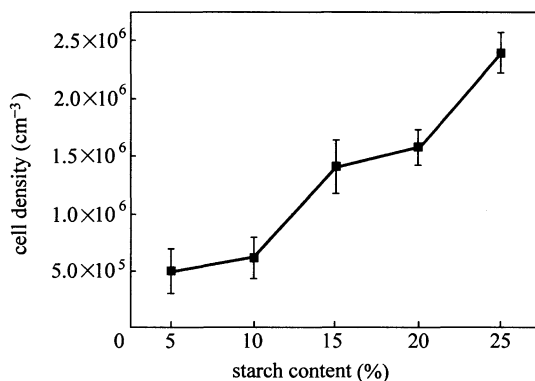


Figure 5.24 Cell density of the composite foams as a function of starch content

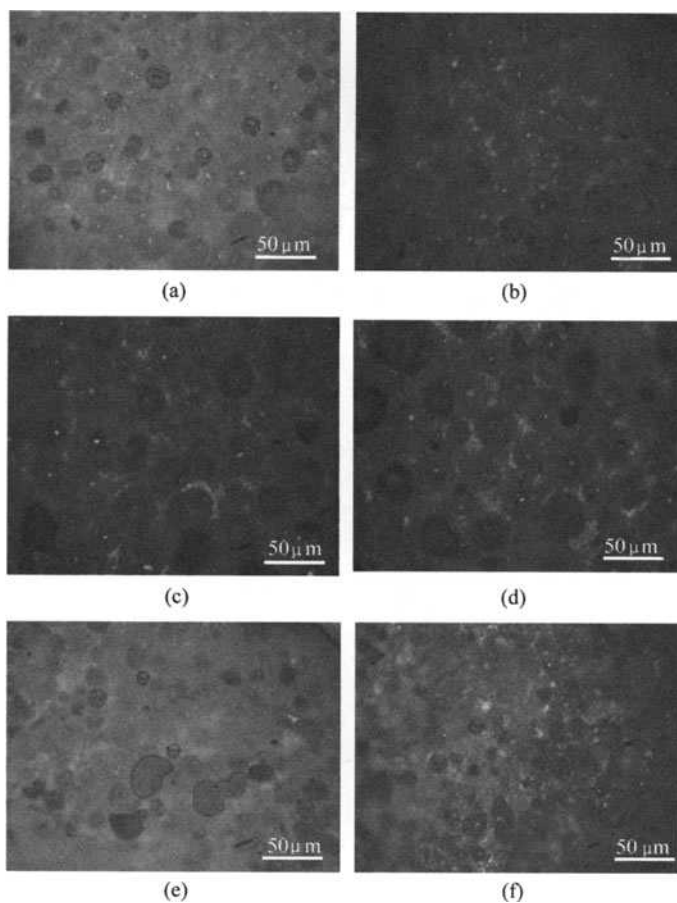
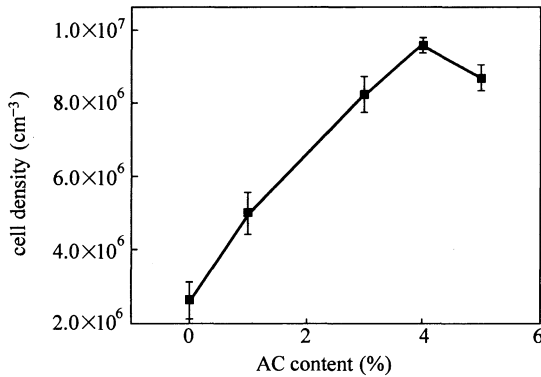
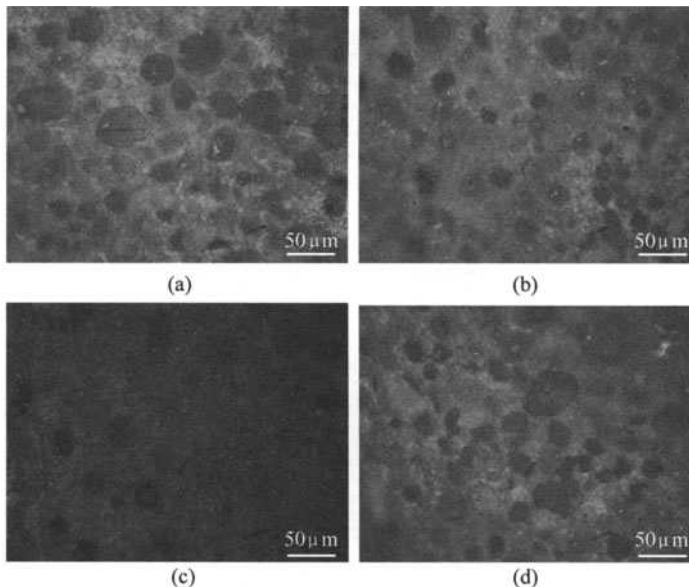


Figure 5.25 Micrograph of bubbles of starch/PLA composite foams. (a) starch5%; (b) starch10%; (c) starch15%; (d) starch20%; (e) starch25%; (f) modified starch

Cell density increases with the increase of AC content evidently, but may decrease slightly when the AC content increases to above 4% (Fig. 5.26, Fig. 5.27). As AC content increases, the amount of gas in the composites increases. However, when the content of gas is overfull, the bubbles may string to cause decrease of cell density.

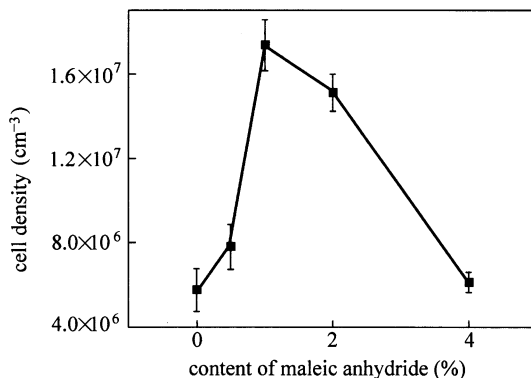


**Figure 5.26** Cell density of the composite foams as a function of AC content

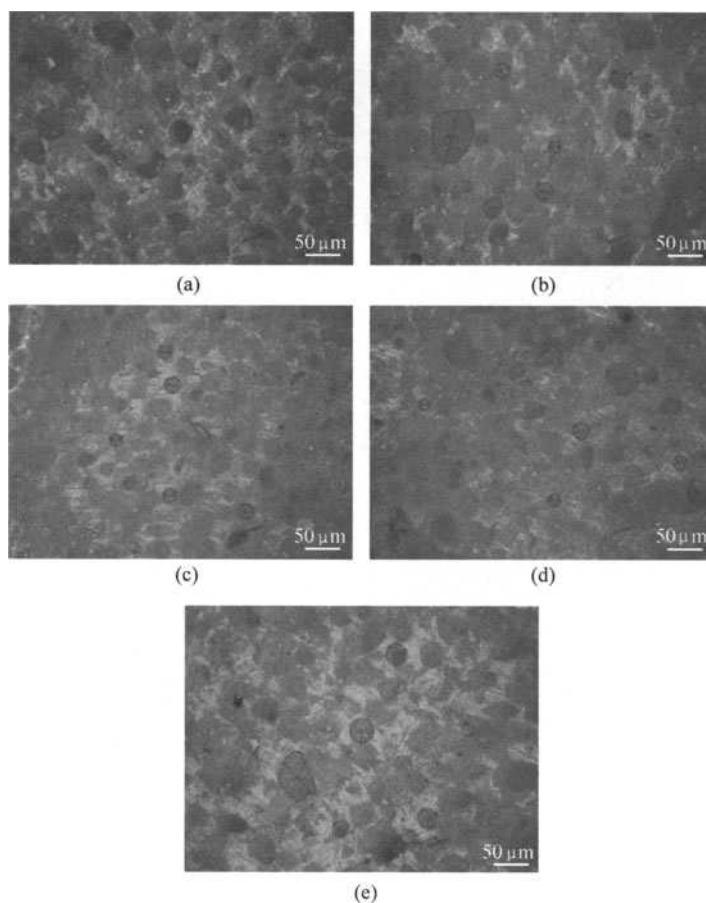


**Figure 5.27** Micrograph of bubbles of the composite foams. (a) AC = 1%; (b) AC = 3%; (c) AC = 4%; (d) AC = 5%

As shown in Fig. 5.28 and Fig. 5.29, cell density increases firstly and then decreases with increasing the content of maleic anhydride. Low content of maleic anhydride can increase the composites' MS, many small bubbles appear so that



**Figure 5.28** Cell density of the composite foams as a function of maleic anhydride content



**Figure 5.29** Micrograph of bubbles of the composite foams. (a) maleic anhydride 0%; (b) maleic anhydride 0.5%; (c) maleic anhydride 1%; (d) maleic anhydride 2%; (e) maleic anhydride 4%

cell density increases. But when the content of maleic anhydride is raised to above 2%, MS begins to decrease to cause bubbles to grow larger, and thus cell density decreases.

### 5.4.3 PLA /PBAT Blend Foams

Poly (butylene adipate-co-terephthalate) (PBAT) is an interesting polymer [116, 117] and has attracted more attention. PBAT is also a biodegradable polymer, which has proper viscosity and elasticity. Moreover, the balance of biodegradability (e.g., life time) and its physical properties (e.g., thermal and mechanical properties) can be adjusted by controlling the molar ratio of comonomers in the copolymer [118, 119]. It has been reported that the aliphatic/aromatic copolyester with aromatic units within the range of 35 – 55 mol% offers an optimal compromise of its biodegradability and physical properties.

Yuan et al. [120] has reported the research on PLA/PBAT blend foam. Maleic anhydride is used to enhance compatibility between PLA and PBAT. The compatibilization mechanism of maleic anhydride (MAH) is that MAH enhances intermolecular force by forming hydrogen bond between grafted MAH and polymer backbone. Grafting MAH onto PLA and PBAT is performed by reactive extrusion, which can improve the interfacial adhesion between PBAT and PLA matrix. In order to increase the maleicing reaction activity, a free radical initiator, 2, 5-dimethyl-2, 5-di-(*tert*-butylperoxy) hexane (L101), can be used.

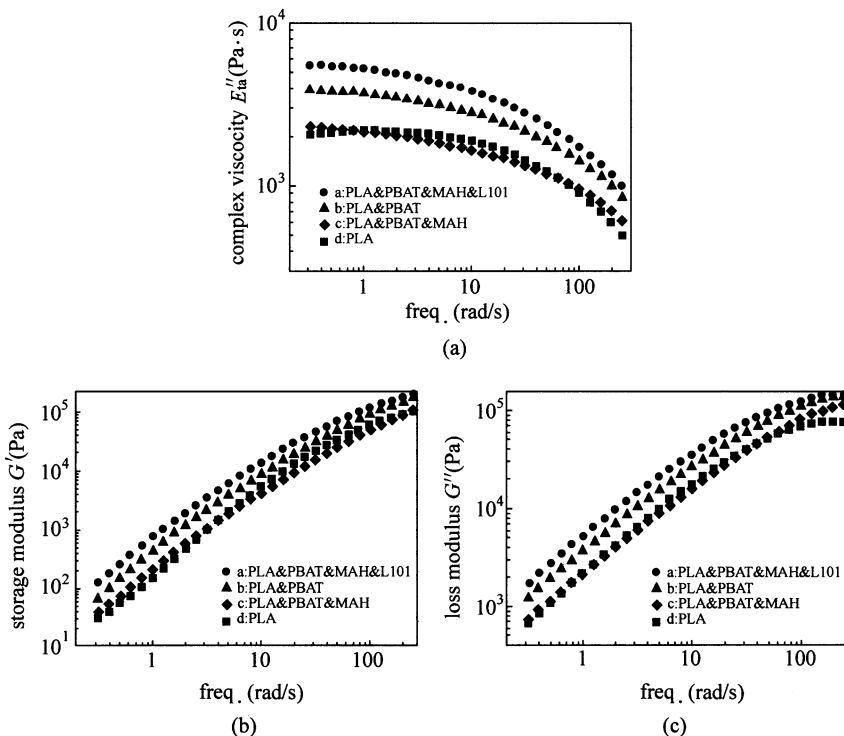
PLA and PBAT are premixed as pre-foaming master batches. Maleic anhydride and L101 are then added to PLA/PBAT blend pre-foaming master batches as a multi-compatibilizer. PLA/PBAT foams are prepared by reactive extrusion. AC is added as blowing agent and nano-SiO<sub>2</sub> as nucleation agents. The formulations for all experiments are shown in Table 5.11.

**Table 5.11** Formulations for experiments (wt%)

Materials Group	PLA	PBAT	AC	Nano-SiO <sub>2</sub>	MAH	L101
Plain PLA	100	0	2	0.5	0	0
PLA-PBAT	90	10	2	0.5	0	0
PLA-PBAT-M	90	10	2	0.5	2	0
PLA-PBAT-ML1	90	10	2	0.5	1	0.5
PLA-PBAT-ML2	90	10	2	0.5	2	0.5
PLA-PBAT-ML3	90	10	2	0.5	3	0.5
PLA-PBAT-ML4	90	10	2	0.5	4	0.5

Rheological properties are important for foam extruding process. Dynamic frequency scanning is performed at a definite temperature 170°C and strain range.

As can be seen from Fig. 5.30, the complex viscosity of PLA/PBAT blends is increased significantly compared with plain PLA both in low and high freq. This fully proves the effectiveness of PBAT in improving melt viscosity and elasticity of PLA. When only adding MAH, the complex viscosity of PLA/PBAT drops greatly. This phenomenon is probably caused by free MAH, which acts as plasticizer during extruding foam process. The blends with both 2 wt% of MAH and 0.5 wt% of L101 have the highest complex viscosity, which suggests that maleicing reaction could enhance the intermolecular force of polymer chains and improve the elasticity of blends significantly. At the same time, it is obvious that with increasing frequency, the complex viscosities of all blends drop, which indicates typical non-Newtonian fluid characteristics. On one hand, the screw speed should set as high as possible for uniform mixture. On the other hand, the screw speed should not be set too high in order to get enough melt viscosity for foaming process. In the study, the screw speed was set at 100 r/min. In addition, viscosity of Maleicing PLA/PBAT blends drops deeply at high frequency areas, which suggests that the vibration of polymer chains are increased under high alternate stress. The intermolecular force between them decreases as well. L101 probably plays its role mainly in initiating maleicing reaction rather than cross-linking reaction.



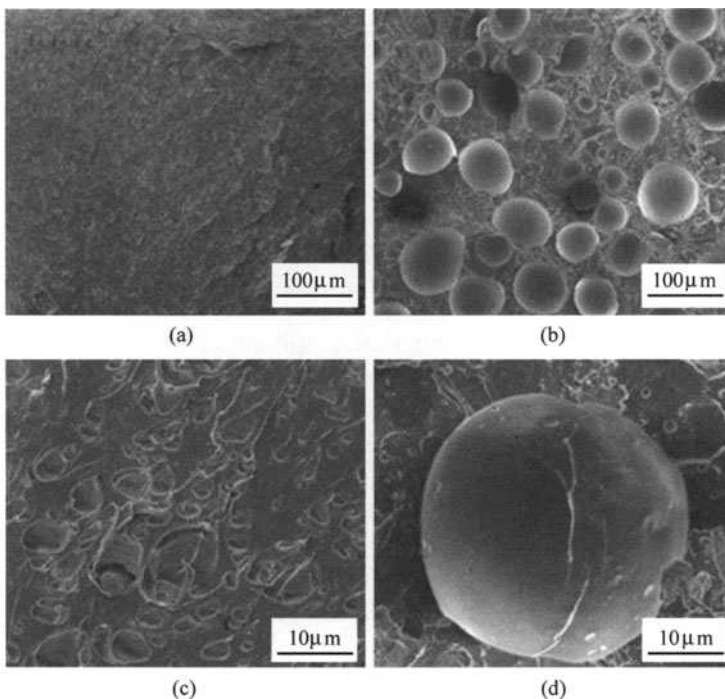
**Figure 5.30** Rheological properties of a: PLA-PBAT-ML2; b: PLA-PBAT; c: PLA-PBAT-M; d: pure PLA



Storage modulus reflects elasticity of materials. It is known that cell grows with the deformation and movement of polymer surrounding it. In cell growing process, cell wall will bear both internal and external pressures. The internal pressure mostly comes from the decomposition of foaming agent while the external one comes from the elasticity of polymer. If the elasticity and melt strength are not high enough to sustain cell growth, the cell will collapse and become an irregular minute one, which is not ideal phenomenon for foaming process. Figure 5.30 shows the frequency dependence of the dynamic properties of PLA/PBAT.

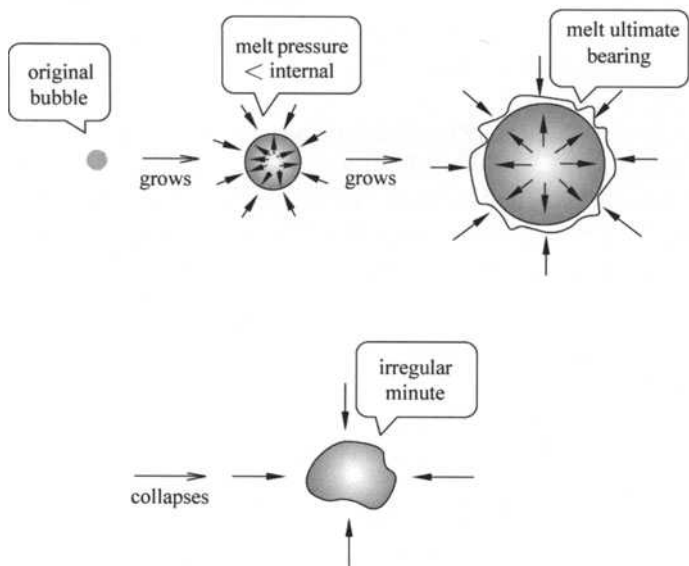
Loss modulus represents the loss of energy as heat during the deformation of materials. When loss modulus becomes low, damping loss factor decreases, which means the material is closer to ideal elastic material. The loss modulus of maleicing PLA/PBAT blends is higher than that of both PLA/PBAT blends without maleicing and plain PLA, which means that better impact resistance of modified PLA foams can be achieved.

Radial expansion ratio (RER) and unit density are important physical properties of the extruded foams. High RER and low unit density are ideal for foams because of the reduced cost. Because of the low elasticity of plain PLA, most of PLA foaming materials couldn't attain high RER. Scanning electron micrographs of the foam surfaces and cross-sections are shown in Fig. 5.31. The surfaces of



**Figure 5.31** SEM of (a) plain PLA foam; (b) PLA-PBAT-ML2 foam; (c) pure PLA foam; and (d) PLA-PBAT-ML2 foam

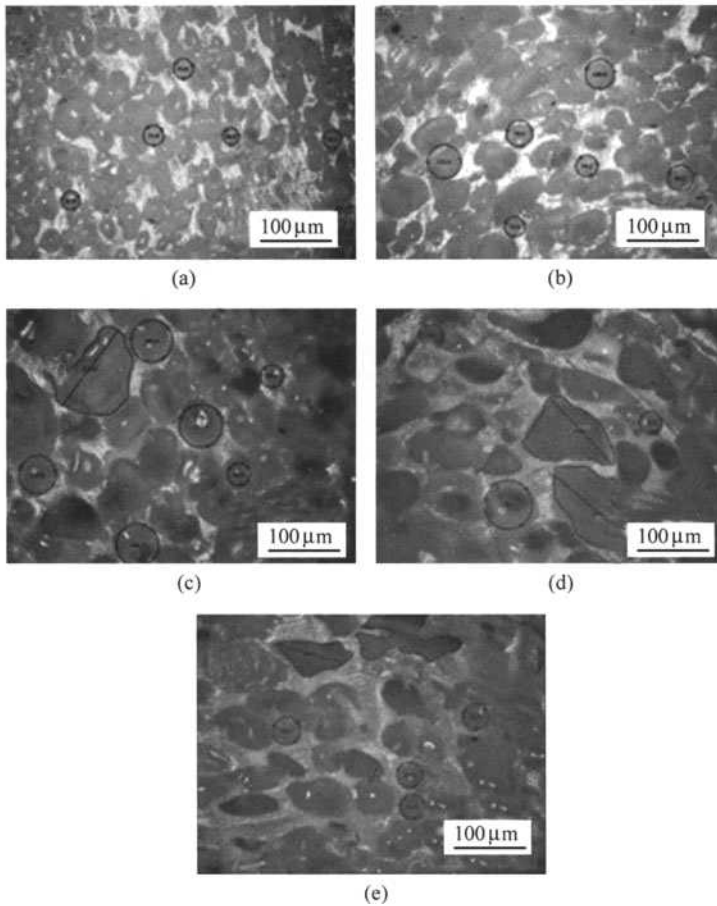
PLA foams containing no added polymer generally show many small cells. Cell sizes are about 10 – 100  $\mu\text{m}$ . Most of the cell shapes are anomalous. Cell sizes and shapes are closely related to melt properties. As the cell grows, cell walls would have to bear pressure coming from both inside and outside cells, which are shown in Fig. 5.32. When the internal pressure is higher than that of the external one, the cells would keep on growing. At the same time, the melt surrounding the cell walls would keep on deforming. Because of the low elasticity and high rigidity of PLA chain, the cell fails to survive the internal pressure. As the result, the PLA cell wall bursts during extrusion foaming.



**Figure 5.32** Schematic of cell growth

This situation is improved by maleicing PLA/PBAT blends. It was reported that extrusion condition and material compositions were main factors influencing cell structure and distribution [121]. The surfaces of PLA/PBAT blends foams containing MAH and L101 have much bigger cells. Cells are about 100 – 500  $\mu\text{m}$ . The shape of cells is approximately spherical and cells are uniform. Despite that PBAT molecule contains several aliphatic long chains, which increase the elasticity of the blends; it is not enough without MAH. By MAH grafting onto PLA and PBAT molecule chain, the intermolecular force between polymer chains is enhanced and the compatibility between PLA and PBAT is improved. By doing this, the cells can grow up to a much bigger size without burst. This means the modified PLA foams have a better ability to support their shapes. If the content of foaming agent increases, a higher foaming rate of PLA can be achieved and a lower cost can be realized as well.

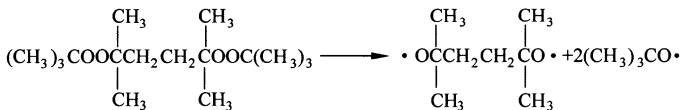
Figure 5.33 presents the microscopic pictures of PLA/PBAT foams with increasing content of MAH. Comparing the 5 pictures, it is obvious that the foam cells without MAH are small (30–50  $\mu\text{m}$ ). They get closely to each other and even some of them merge together. With increasing content of MAH, the cells grow up to a bigger size (50–100  $\mu\text{m}$ ). As the content of AC foaming agent is unchanged, the increasing cells size means that better elasticity is obtained. When the content of MAH is 2 wt%, the cells appear in regular spherical shape, but some of them begin to collapse and form a bigger cell. Above this content of MAH, structure of cells becomes irregular and the distribution of them becomes not uniform because of high enough melt elasticity but exorbitant melt strength. This is disadvantageous for mechanical properties of stress concentration.



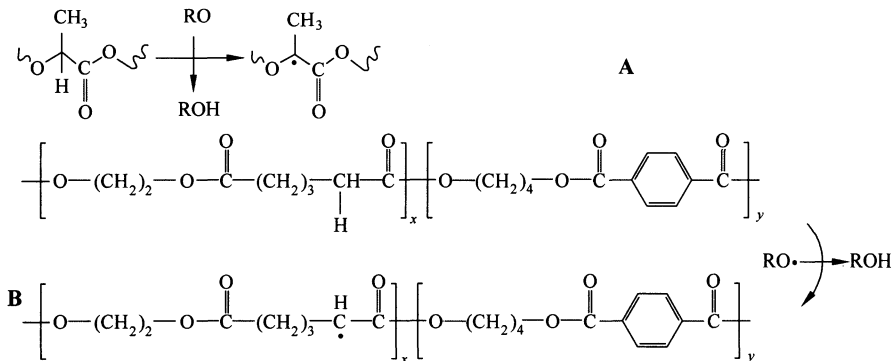
**Figure 5.33** Effects of MAH content on cell structure. (a) PLA-PBAT; (b) PLA-PBAT-ML1; (c) PLA-PBAT-ML2; (d) PLA-PBAT-ML3; (e) PLA-PBAT-ML4

As explained above, melt strength is very important for foaming process. In order to improve melt elasticity and viscosity, Y. W. Di and S. Iannace introduced 1,4-butanediol and 1,4-butane diisocyanate as low-molecular-weight chain extenders to modify the properties of PLA, but the dosage was hard to control [129]. In other experiment, MAH was used as a better choice. Table 5.12 shows the effect of MAH content on melt strength of the blend with the content ratio of PLA:PBAT:L101 fixed at 90:10:0.5. With increasing MAH content, the melt strength of blends increases correspondingly. A possible explanation is that molecular chain of PLA/PBAT undergoes partial cross-linking reaction (between products A and A, A and B, B and B) with the help of L101. This increases the elasticity of blends. Besides, the MAH grafted onto PLA and PBAT would possibly form hydrogen bond with hydroxyl terminated PLA and PBAT, which could increase intermolecular force. Actually, as shown in Fig. 5.34, cross-linking reaction and chain scission reaction often take place simultaneously. When the content of L101 is too much compared with the content of MAH (<2 wt%), chain scission reaction would dominate, and vice versa. With the increasing content of MAH, more and more free radicals take part in maleicing reaction rather than chain scission reaction, which is why the melt strength of PLA/PBAT blends increases.

(a) L101 decomposition



(b) Hydrogen atom capture



(c) Chain scission reaction

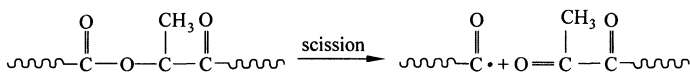


Figure 5.34 Reaction mechanism of L101

Strong correlation exists between cell density and MAH content. As shown in Table 5.12, cell density decreases with increasing MAH content. As mentioned above, maleicing blends have better viscosity and elasticity. The cell sizes increase with adding MAH, the quantity of cells in unit volume reduces accordingly. Similar correlations are observed between apparent density and MAH content. MAH content increases from 1 wt% to 4 wt%, the apparent density decreases by 30%. Considering the processing conditions of extrusion, high rate of screw speed reduces the residence time of blends. When the content of MAH exceeds 4 wt% with the content of L101 being 0.5 wt%, the result is not satisfactory.

**Table 5.12** Effects of MAH content on properties of PLA/PBAT blend

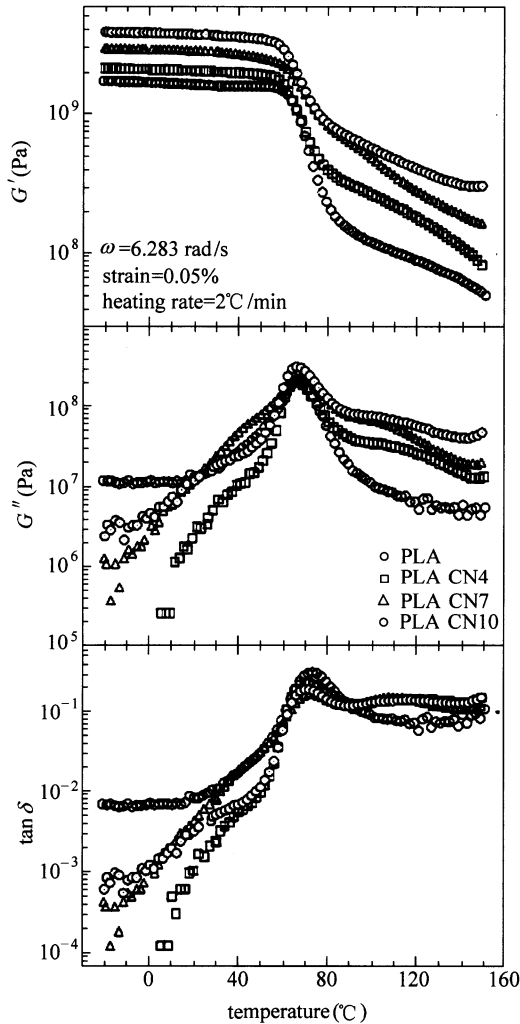
Performances Content of MAH (wt%)	Melt strength (mm <sup>4</sup> ·10min/g)	Cell density (cm <sup>-3</sup> )	Apparent density (g/cm <sup>3</sup> )
0	58.75	2270760	0.5986
1	116.05	1624820	0.4811
2	271.67	738053	0.4735
3	517.92	574462	0.4471
4	956.04	461061	0.404

#### 5.4.4 PLA Nanocomposite Foams

The field of polymer nanocomposites has become increasingly intriguing from scientists and industries. Polymer/layered silicate (PLS) and organically modified layered silicate (OMLS), such as montmorillonite or hectorite have got more attention because of their demonstrated significant enhancement of performances [122, 123]. The nanoscale distribution of such high aspect ratio fillers brings up marked improvements to the polymer matrix in term of mechanical, fire retardant, rheological, gas barrier and optical properties, especially at low clay content (1 – 10 wt%) in comparison with more conventional microcomposites (30 wt% of microfiller) [124, 125]. The main reason for these improved properties in nanocomposites is the stronger interfacial interaction between the matrix and layered silicate, compared with conventional filler-reinforced systems [126].

PLA nanocomposites (PLACN) have already been shown to exhibit a high modulus and, under uniaxial extension, a tendency toward strong strain-induced hardening. On the basis of these results, Sinha Ray et al. [127] prepared PLACNs with three different amounts of organically modified synthetic fluorine mica (OMSFM) of 4, 7, and 10 wt%, which were correspondingly abbreviated as PLACN4, PLACN7, and PLACN10, respectively. Figure 5.35 shows the temperature dependence of  $G'$ ,  $G''$  and  $\tan\delta$  for plain PLA and corresponding PLACNs. For all PLACNs, a significant enhancement of  $G'$  can be seen in the

investigated temperature range, indicating intercalated PLACNs have a strong influence on the elastic properties of the PLA matrix. It is well known that interconnected structures with anisometric fillers result in an apparent yield stress, which is visible in dynamic measurement.

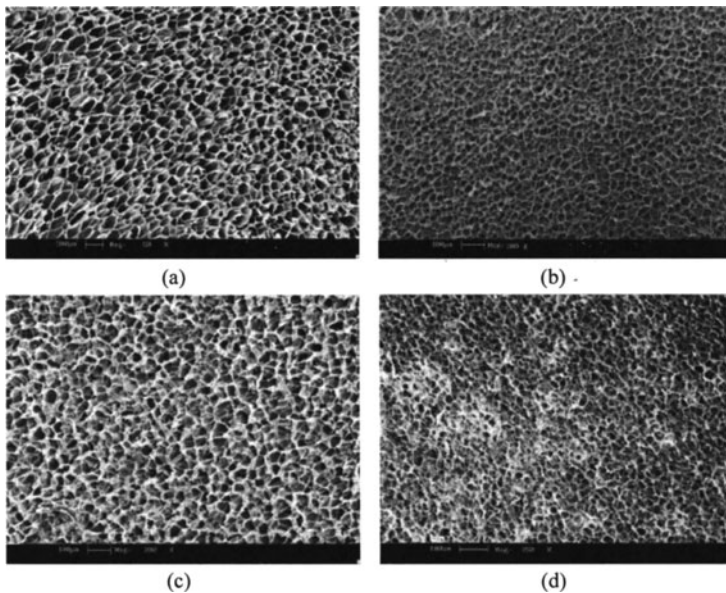


**Figure 5.35** Temperature dependence of storage modulus (GPa), loss modulus (GPa), and their ratio,  $\tan \delta$ , for plain PLA and various PLACNs

In another paper by Sinha Ray et al. [128] foam processing of plain PLA and PLACNs (PLA/MMT) was conducted by a physical foaming method, i.e., batch process. The samples were first saturated with  $\text{CO}_2$  at  $140^\circ\text{C}$  and 10 MPa, Samples were then kept under these conditions for 2 h. Subsequently, the  $\text{CO}_2$  was quickly released from the autoclave (within 1 s). After removing the  $\text{CO}_2$ -saturated plain

PLA and nanocomposite sheets from the autoclave, the samples were immersed in a silicone oil bath maintained at the desired temperature (165 °C) for a fixed time (30 s, known as foaming time). The foamed samples were next quenched in an ethanol/water (1:1) mixture, washed in ethanol. Rheological properties of plain PLA and various PLA/MMT nanocomposites were reported in detail. Dynamic measurements indicated the formation of a spatially-linked-structure in the case of PLA/MMT nanocomposite melts, and during shear measurements very strong rheopexy behavior of PLA/MMT nanocomposite melts under very slow shear field was observed. Under uniaxial extension flow, PLA/MMT nanocomposite melts exhibited very high viscosity and a tendency of strong strain-induced hardening, which may originate from the perpendicular alignment of the silicate layers towards the stretching direction. This strain-induced hardening behavior is an indispensable characteristic for foam processing due to its capacity to withstand the stretching force experienced during the latter stages of bubble growth.

Yingwei Di et al. [129] also reported PLA/organoclay nanocomposite foaming by using similar method. The organoclay they used is commercial product named Cloisite 30B. The SEM images of foamed PLA and PLA nanocomposites are shown in Fig. 5.36. It is noticed that the foams of PLA nanocomposites exhibit a nicely interconnected, closed-cell structure with pentagonal and hexagonal faces, which express the most energetically stable state of polygon cells.



**Figure 5.36** SEM micrographs for foams of PLA and PLA nanocomposites with different weight fraction of 30B: (a) PLA, original magnification 50 ×; (b) PLA, 1 wt% 30B, original magnification 200 ×; (c) PLA, 2 wt% 30B, original magnification 200 ×; (d) PLA, 5 wt% 30B, original magnification 250 ×

To summarize, the beneficial effect of nanometric fillers in thermoplastic foaming can be ascribed to [130]: (1) the enhancement of the strength of the polymer melt to prevent melt fracture and foam collapse during bubble growth; (2) the enhancement of the crystallization kinetics to facilitate foam setting immediately after the growth; and (3) the induction of the formation of numerous bubbles.

## References

- [1] Lim L. T., Auras R., Rubino M. *Prog. Polym. Sci.*, 33(8), 820 (2008).
- [2] Sato Y., Inohara K., Takishima S., et al. *Polym. Eng. Sci.*, 40(12), 2602 (2000).
- [3] Cai H., Dave V., Gross R. A., et al. *J. Polym. Sci. Pol. Phys.*, 34(16), 2701 (1996).
- [4] Harris A. M., Lee E. C. *J. Appl. Polym. Sci.*, 107(4), 2246 (2008).
- [5] Ghosh S., Viana J. C., Reis R. L., et al. *Polym. Eng. Sci.*, 47(7), 1141 (2007).
- [6] Kumaraswamy G. J. *Macromol. Sci-Pol. R*, C45(4), 375 (2005).
- [7] Ghosh S., Vianac J. C., Reis R. L., et al. *Acta Biomater.*, 4(4), 887 (2008).
- [8] Ghosh S., Viana J. C., Reis R. L., et al. *Mat. Sci. Eng. Struct.*, 490(1-2), 81 (2008).
- [9] Kohler W. H., Shrikhande P., McHugh A. J. *J. Macromol. Sci.*, B44, 185 (2005).
- [10] Shin D. M., Lee J. S., Jung H. W., et al. *Rheol. Acta.*, 45, 575 (2006).
- [11] Eling B., Gogolewski S., Pennings A. *J. Polymer*, 23, 1587 (1982).
- [12] Fambri L., Pegoretti R., Fenner R., et al. *Polymer*, 38, 79 (1997).
- [13] Yuan X., Mak A. F. T., Kwok K. W., et al. *J. Appl. Polym. Sci.*, 81, 251 (2001).
- [14] Solarski S., Ferreira M., Devaux E. *Polymer*, 46, 11187 (2005).
- [15] Nishimura Y., Takasu A., Inai Y., et al. *J. Appl. Polym. Sci.*, 97, 2118 (2005).
- [16] Schmack G., Tandler B., Vogel R., et al. *J. Appl. Polym. Sci.*, 78, 2785 (1999).
- [17] Schmack G., Jehnichen D., Vogel R., et al. *J. Biotechnol.*, 86, 151 (2001).
- [18] Schmack G., Tandler B., Optiz G., et al. *J. Appl. Polym. Sci.*, 91, 800 (2004).
- [19] Mezghani K., Spruiell J. E. *J. Polym. Sci.*, 36B, 1005 (1998).
- [20] Yan Y., Zhao Y., Zhan H., et al. *China Synth. Fiber Ind.*, 5, 11 (2006).
- [21] Dartee M. In: *Proceedings of the 5th Conference on Biodegradable Polymers*. Wurzburg, Germany, 1998, 1–9.
- [22] Pennings J., Dijkstra H., Pennings A. *J. Polymer*, 34, 942 (1993).
- [23] Cicero J. A., Dorgan J. R., Janzen J., et al. *J. Appl. Polym. Sci.*, 86, 2828 (2002).
- [24] Cicero J. A., Dorgan J. R. *J. Polym. Environ.*, 9, 1 (2001).
- [25] Fambri L., Bragagna S., Migliaresi C. *Macromol. Symp.*, 234, 20 (2006).
- [26] Zhang J., Sato H., Tsuji H., et al. *Macromolecules*, 38, 1822 (2005).
- [27] Yamane H. *Nihon Reoroji Gakkaishi*, 27, 213 (1999).
- [28] Takasaki M., Ito H., Kikutani T. *J. Macromol. Sci.*, 59B, 59 (2003).
- [29] Takasaki M., Ito H., Kikutani T. *J. Macromol. Sci.*, B42, 403 (2003).
- [30] Furuhashi Y., Kimura Y., Yoshie N., et al. *Polymer*, 47, 5965 (2006).
- [31] Ghosh S., Vasanthan N. *J. Appl. Polym. Sci.*, 101, 1210 (2006).
- [32] Mahendrasingam A., Blundell D. J., Parton M., et al. *Polymer*, 46, 6009 (2005).



- [33] Park C. H., Hong E. Y., Kang Y. K. *J. Appl. Polym. Sci.*, 103, 3099 (2007).
- [34] Schmack G. T., Vogel R., Beyreuther R., et al. *J. Appl. Polym. Sci.*, 73, 2785 (1999).
- [35] Leenslag J. W., Pennings A. J. *Polymer*, 28, 1602 (1987).
- [36] Horacek I., Kalisek V. *J. Appl. Polym. Sci.*, 54, 1751 (1994).
- [37] Horacek I., Kalisek V. *J. Appl. Polym. Sci.*, 54, 1767 (1994).
- [38] Postema A. R., Luiten A. H., Pennings A. J. *J. Appl. Polym. Sci.*, 39, 1265 (1990).
- [39] Postema A. R., Luiten A. H., Pennings A. J. *J. Appl. Polym. Sci.*, 39, 1275 (1990).
- [40] Postema A. R., Pennings A. J. *J. Appl. Polym. Sci.*, 37, 2351 (1989).
- [41] Southern J. H., Ballmann R. L. *Text. Res. J.*, 53, 230 (1983).
- [42] Leenslag J. W., Gogolewski S., Pennings A. J. *J. Appl. Polym. Sci.*, 29, 2829 (1984).
- [43] Gogolewski S., Pennings A. J. *J. Appl. Polym. Sci.*, 28, 1045 (1983).
- [44] Leenslag J. W., Pennings A. J. *Polymer*, 28, 1695 (1987).
- [45] Tsuji H., Ikada Y., Hyon S. H., et al. *J. Appl. Polym. Sci.*, 51, 337 (1994).
- [46] Gupta B., Revagade N., Anjum N., et al. *J. Appl. Polym. Sci.*, 100, 1239 (2006).
- [47] Gupta B., Revagade N., Anjum N., et al. *J. Appl. Polym. Sci.*, 101, 3774 (2006).
- [48] Eenink M. J. D., Feijien J., Olijslager J., et al. *J. Contr. Rel.*, 6, 225 (1987).
- [49] Witte P. E. H., Peters A. M. P., Dijkstra P. J., et al. *J. Contr. Rel.*, 24, 61 (1993).
- [50] Sawada K., Ueda M. *Dyes and Pigments*, 74, 81 (2007).
- [51] Yang Y., Huda S. *J. Appl. Polym. Sci.*, 90, 3285 (2003).
- [52] Huang Z. M., Zhang Y. Z., Kotaki M., et al. *Compos. Sci. Technol.*, 63, 2223 (2003).
- [53] Doshi J., Reneker D. H. *J. Electrostat.*, 35, 151 (1995).
- [54] Zong X., Bien H., Chung C. Y., et al. *Biomaterials*, 26, 5330 (2005).
- [55] Yang F., Murugan R., Wang S., et al. *Biomaterials*, 26, 2603 (2005).
- [56] Vaz C. M., van Tuijl S., Bouten C. V. C., et al. *Acta Biomaterialia*, 1, 575 (2005).
- [57] Kim H. W., Lee H. H., Knowles J. C. *J. Biomed. Mater. Res.*, 79A, 643 (2006).
- [58] Kenawy E. R., Bowlin G. L., Mansfield K., et al. *J. Control. Release*, 81, 57 (2002).
- [59] Xu X., Yang L., Xu X., et al. *J. Control. Release*, 108, 33 (2005).
- [60] Song M., Pan C., Li J., et al. *Electroanalysis*, 18, 1995 (2006).
- [61] Xu X., Yang Q., Wang Y., et al. *Eur. Polym. J.*, 42, 2081 (2006).
- [62] Gu S. Y., Ren J. *Macromol. Mater. Eng.*, 290, 1097 (2005).
- [63] Jun Z., Hou H., Schaper A., et al. *e-Polymers*, 009 (2003).
- [64] Zong X., Kim K., Fang D., et al. *Polymer*, 43, 4403 (2002).
- [65] Bognitzki M., Czado W., Frese T., et al. *Adv. Mater.*, 13, 70 (2001).
- [66] Sun B., Duan B., Yuan X. *J. Appl. Polym. Sci.*, 102, 39 (2006).
- [67] Xu X., Zhuang X., Chen X., et al. *Macromol. Rapid Commun.*, 27, 1637 (2006).
- [68] Zhao N., Shi S., Lu G., et al. *J. Phys. Chem. Solid*, 69, 1564 (2008).
- [69] Lee Y. H., Lee J. H., An I. G., et al. *Biomaterials*, 26, 3165 (2005).
- [70] Levit N., Tepper G. *J. Supercritical Fluids*, 31, 329 (2004).
- [71] Zhou H., Green T. B., Joo Y. L. *Polymer*, 47, 7497 (2006).
- [72] Ogata N., Yamaguchi S., Shimada N., et al. *J. Appl. Polym. Sci.*, 104, 1640 (2007).
- [73] Rappard P. *Packag. Rev. S. Afr.*, 23, 19 (1997).
- [74] Nelson K. H., Cathcart W. M. *J. Food Prot.*, 47, 346 (1984).
- [75] Pascall M. A., Harte B. R., Giacini J. R., et al. *Journal of Food Science*, 60(5), 1116 (1995).

## **Biodegradable Poly(Lactic Acid): Synthesis, Modification, Processing and Applications**

- [76] Erickson M. C. *Int. J. Dairy Technol.*, 50, 107 (1997).
- [77] Dunkley W. L., Pangborn R. M., Franklin J. D. *Milk Dealer*, 52, 52 (1963).
- [78] Bradley R. L. *J. Food Prot.*, 43, 314 (1980).
- [79] Auras R. Ph.D. Thesis, Michigan State University, East Lansing. 268 (2004).
- [80] Auras R., Harte B., Selke S. *Macromol. Biosci.*, 4, 835 (2004).
- [81] Tsuji H., Ikada Y., Hyon S. H., et al. *J. Appl. Polym. Sci.*, 51, 337 (1994).
- [82] VanKrevelen D. W. *Properties of Polymers* (Elsevier Science B.V.), Amsterdam, Netherlands (1997).
- [83] Witzke D. R. Ph.D. Thesis, Michigan State University, East Lansing, 389 (1997).
- [84] Tsuji H., Ikada Y. *Macromol. Chem. Phys.*, 197, 3483 (1996).
- [85] Ikada Y., Tsuji H. *Macromol. Rapid Commun.*, 21, 117 (2000).
- [86] Jamshidi K., Hyon S. H., Ikada Y. *Polymer*, 29, 2229 (1988).
- [87] Celli A., Scandola M. *Polymer*, 33, 2699 (1992).
- [88] Tsuji H., Ikada Y. *Polymer*, 36, 2709 (1995).
- [89] Launay A., Thominet F., Verdu J. *J. Appl. Polym. Sci.*, 73, 1131 (1999).
- [90] Gruber P. R., O'Brien M. in: *Biopolymers Polyesters III. Applications and Commercial Products* (1st ed.). Doi Y., Steinbüchel A. Eds., Wiley-VCH Verlag GmbH, Weinheim, 235 (2002).
- [91] Natureworks. *Production of Natureworks Polylactide Films on Blown Film Equipment Designed for Producing Low Density Polyethylene Film*. Minnetonka, MN: Natureworks LLC (2003).
- [92] Lim L. T., Auras R., Rubino M. *Progress in Polymer Science*, 33, 820 (2008).
- [93] Sodergard A., Selin J. F., Niemi M., et al. US Pat. 6 559 244 B1 (2003).
- [94] Tweed E. C., Stephens H. M., Riegert T. E. US Pat. Application, 0045940A1 (2006).
- [95] Hiltunen E., Selin J. F., Skog M. US Pat. 6 117 928 (2000).
- [96] Kawashima N., Ogawa S., Obuchi S., et al. In: Doi Y., Steinbüchel A. (ed.). *Biopolymers Polyesters III. Applications and Commercial Products*. Weinheim: Wiley-VCH Verlag GmbH. 251 (2002).
- [97] Mathieu L. M., Mueller T. L., Bourban P. E., et al. *Biomaterials*, 27, 905 (2006).
- [98] Maquet V., Martin D., Malgrange B., et al. *J. Biomed. Mater. Res.*, 52, 639 (2000).
- [99] Busby W., Cameron N. R., Jahoda C. A. B. *Polym. Int.*, 51, 871 (2002).
- [100] Lee Chau-Tarn. *Polymeric Foams*. Taylor & Francis Group, LLC (2009).
- [101] Tsuji H., Fukui I. *Polymer*, 44, 2891 (2003).
- [102] Di Y., Iannace S., Di Maio E., et al. *Macromol. Mater. Eng.*, 290, 1083 (2005).
- [103] Carlson D., Dubois P., Nie L., et al. *Polymer Engineering Science*, 38, 311 (1998).
- [104] Sodergard A., Niemi M., Selin J. F., et al. *Industrial and Engineering Chemical Research*, 34, 1203 (1995).
- [105] Zhong W., Ge J., Gu Z., et al. *Journal of Applied Polymer Science*, 74, 2546 (1999).
- [106] Shinno K., Miyamoto M., Rimura Y. *Macromolecules*, 30, 6438 (1997).
- [107] Di Y., Iannace S., Di Maio E., et al. *Macromol. Mater. Eng.*, 290, 1083 (2005).
- [108] Park C. B., Cheung L. K. *Polym. Eng. Sci.*, 37, 1 (1997).
- [109] Matuana L. M. *Bioresource Technology*, 99(9), 3643 (2008).
- [110] Laurent M. Matuana, Omar Faruk. *Bioresource Technology*, 100, 5947 (2009).

- [111] Guan Junjie, Kent M. Eskridge, Milford A. Hanna. *Industrial Crops and Products*, 22, 109 (2005).
- [112] Yogaraj Nabar, Ramani Narayan. *Polymer Engineering and Science*, 46, 438 (2006).
- [113] Lawton J. W., Shogren R. L., Tiefenbacher K. F. *Industrial Crops and Products*, 19, 41 (2004).
- [114] Dujdao Preechawong, Manisara Peesan. *Carbohydrate Polymers*, 59, 329 (2005).
- [115] Huneault M. A., Li H. *Polymer*, 48, 270 (2007).
- [116] Witt U., Einig T., Yamamoto M., et al. *Chemosphere*, 44(2), 289 (2001).
- [117] Gan Zhihua, Kazuhiro Kuwabara, Motonori Yamamoto, et al. *Polymer Degradation and Stability*, 83(2), 289(2004).
- [118] Hiroaki Sato, Mototake Furuhashi, Daniel Yang, et al. *Polymer Degradation and Stability*, 73(2), 327 (2001).
- [119] Tserki P., Matzinos E. Pavlidou. *Polymer Degradation and Stability*, 91(2): 367 (2006).
- [120] Yuan Hua, Liu Zhiyong, Ren Jie. *Polymer Engineering & Science*, 49(5), 1004 (2009).
- [121] Zhang Jianfeng, Sun Xiuzhi. *Polymer Degradation and Stability*, 106(2), 857 (2007).
- [122] Giannelis E. P., Krishnamoorti R., Manias E. *Adv. Polym. Sci.*, 118, 108 (1999).
- [123] Paul M. A., Alexandre M., Degée P., et al. *Polymer*, (44)2, 443 (2003).
- [124] Utracki L.A. *Clay-Containing Polymeric Nanocomposites*, Rapra Technology Limited, UK (2004).
- [125] Pluta M., Galeski A., Alexandre M., et al. *J. Appl. Polym. Sci.*, 86, 1497 (2002).
- [126] Suprakas Sinha Ray, Masami Okamoto. *Prog. Polym. Sci.*, 28, 1539 (2003).
- [127] Sinha Ray S., Yamada K., Okamoto M., et al. *Chem. Mater.*, 15, 1456 (2003).
- [128] Suprakas Sinha Ray, Masami Okamoto. *Macromol. Rapid Commun.*, 24, 815 (2003).
- [129] Di Yingwei, et al. *Journal of Polymer Science: Part B: Polymer Physics*, 43, 689 (2005).
- [130] Lee S. T. *Polymeric Foams*. Taylor & Francis Group, LLC (2009).

## 6 Application in the Field of Commodity and Industry Product

**Abstract** Because of numerous advantages such as excellent properties, varied modification and processing, PLA has wide applications as packaging, fibre, engineering plastic, disposable ware and adhesive. In this chapter, the applications of PLA in the five fields of commodity and industry as mentioned above are discussed. In addition, the modification and processing methods of PLA as well as prospects of its application are analyzed.

**Keywords** low carbon; environmental protection, packaging, fibre, mono-filaments, multiple filaments, nonwoven, engineering plastic, disposable ware, hot-melt adhesive

### 6.1 Packaging Materials

Due to its higher cost, the initial focus of PLA as a packaging material has been in high value films, rigid thermoforms, food and beverage containers and coated papers. PLA may have packaging applications for a broader array of product fields [1 – 4] as its production cost may be much lowered by using modern and emerging production technologies [5]. The production of PLA offers numerous advantages: (1) it can be obtained from a renewable agricultural source (corn); (2) its production consumes quantities of carbon dioxide; (3) it provides significant energy savings; (4) it is recyclable and compostable; (5) it can help improve farm economies and (6) the physical and mechanical properties can be manipulated through the polymer architecture. Early economic studies showed that PLA was an economically feasible material to use as a packaging polymer [6, 7]. Medical studies have shown that the level of lactic acid (LA) that migrates to food from packaging containers is much lower than the amount of LA used as common food ingredients. Therefore, polymers derived from lactic acid may be good candidates for packaging applications. By providing consumers with extra end-use benefits, such as avoiding paying a “green tax” in Germany or meeting environmental regulations in Japan, PLA has become a growing alternative as a packaging material for demanding markets. Currently, PLA is being used as a food packaging polymer for short shelf life products with common applications such as containers, drinking cups, sundae and salad cups, overwrap and lamination films and blister packages. Moreover, new applications include thermoformed

PLA containers being used in retail markets for fresh fruit and vegetables.

The properties of high molecular weight PLA are determined by the polymer architecture (i.e., the stereochemical makeup of the backbone) and the molecular mass, which is controlled by the addition of hydroxylic compounds. The ability to control the stereochemical architecture permits precise control over the speed of crystallization and finally the degree of crystallinity, the mechanical properties and the processing temperatures of the material. In addition, the degradation behavior strongly depends on the crystallinity of the material. Two of the pioneer companies in using PLA as a packaging material for yoghurt cups and cutlery were Dannon and McDonald's in Germany in yoghurt cups and cutlery, respectively.

Currently, PLA is used in compostable yard bags to encourage recycling and composting programs. In addition, new applications such as fibers, textiles, foamed articles and paper coatings are being pursued. Commercial brands like Ingeo concentrate on commercializing fabrics made from polylactide polymers.

Commercially available PLA films and packages provide better mechanical properties than polystyrene (PS) and have properties comparable to those of poly(ethylene terephthalate) (PET). The new commercially available PLA polymers have reduced the cost and the use of PLA is encouraged. In the next ten years, PLA production and consumption are expected to increase substantially.

PLA polymers are becoming a cost-effective alternative to commodity commercial petrochemical-based materials. The introduction of PLA will encourage the use and expansion of agricultural based materials. As the PLA price drops and new facilities produce higher volumes of PLA is produced from new facilities, new applications will be explored. Although PLA is a relatively new polymer, it is possible to manipulate its physical, mechanical and barrier properties by changing its chemical composition, and varying its molecular characteristics. It is also possible to blend PLA with other polymers, making it a good biodegradable alternative for use in plastic packaging.

## 6.2 Fiber and Nonwoven

### 6.2.1 PLA Fibers

PLA is an aliphatic polyester. It is a biodegradable thermoplastic and can be processed to become composites. Its monomer, lactic acid, is derived from renewable plant sources, such as starch and sugar. PLA can be degraded into carbon dioxide and water by an action of suitable fungi. This means that biodegradable PLA fibers are environment friendly material even if the fiber is left in the natural environment. The demand for PLA fibers as a substitute for the present synthetic fibers has been growing greatly in recent years.

On the other hand, high water vapor transmission rate of PLA makes it a good candidate for fabricating fibers used in garments (e.g., shirts, dresses, underwear, shoes, etc.) to improve their “breathability”. While PLA fibers are not as wettable as cotton, they exhibit much greater water vapor transmission than aromatic polyesters or nylon fibers.

### **6.2.2 Application of PLA Fibers**

PLA offers unique features of biodegradability, thermoplastic processibility and ecofriendliness that offer potential applications as commodity plastics as in packaging, agricultural products and disposable materials. On the other hand, the polymer also has a bright future for applications in medicine, surgery and pharmaceuticals. The fundamental polymer chemistry of PLA allows control of certain fiber properties that make the fiber suitable for a wide variety of technical textile fiber applications, especially for apparel and performance apparel applications:

- Low moisture absorption and high wicking, offering benefits for sports and performance apparel and products;
- Low flammability and smoke generation;
- High resistance to ultra violet (UV) light, a benefit for performance apparel as well as outdoor furniture and furnishing applications;
- A low index of refraction which provides excellent color characteristics;
- Lower specific gravity making PLA lighter in weight than other fibers;
- In addition to coming from an annually renewable resource base PLA fibers are readily melt-spun offering manufacturing advantages that result in greater consumer choice;

PLA finds applications in a variety of filament and nonwoven structures, such as monofilament, multifilament, trilobal BCF, staple fiber, bicomponent fiber, spun bonded nonwoven, needle punched nonwoven, knitted structure, woven structure, composite materials, etc. These structures may be produced by a variety of spinning techniques and mechanical processing. The fiber may be made into fabric by bonding, thermal bonding, carding, knitting and weaving. The versatility of the filament with respect to transformation into various shapes and morphology along with good mechanical properties has led to its wide range of applications, such as apparel, furnishings, fibers, agricultural products, hygiene products, sports wear, sutures, braided prostheses, pharmaceuticals and drug release system, support matrices, scaffolds for tissue engineering, etc. These areas ranged from apparel, furnishing and agricultural products to the world of biomaterials and artificial organs.

#### **6.2.2.1 Commodity Application**

PLA fibers offer sustainability, resilience, dyeability, comfort, softness, strength,

low flammability, and UV durability. Ingeo™ fiber is the first world's manufactured fiber made from 100% annually renewable plant resources instead of oil. Ingeo™ is made uniquely from Nature Works® biopolymer. Ingeo™ PLA fiber combines the qualities of natural and performance fibers, offering strength and resilience and good moisture management characteristics. All these are balanced with comfort, softness, making it an ingenious fabric innovation for both fashions, furnishings and fiberfill as well as in a new range of eco-performance nonwoven applications for personal care and garden textile applications. And the natural stain resistance that comes with Ingeo™ PLA fiber makes it ideal for carpets for the home, office, transportation and event trade show use.

The natural versatility of Ingeo PLA fibers gives us the opportunity to design new yarns, fabrics and garments for a contemporary wardrobe. Ingeo fiber works in both pure qualities and innovative blends for everything from dress shirts to draperies. Nature Works resins and a comprehensive range of Ingeo PLA fibers fit with all standard nonwoven technologies including spun lacing, thermo, chemical or resin bonding, calendaring, needle punch, wet laid and spun bond processes.

In Japan four companies, namely, Kanebo Gohsen Ltd., Unitika Fibers Ltd., Kuraray Co. Ltd. and Mitsubishi Plastics Inc. are receiving a supply of PLA resins from Nature Works. Of the four, the first three companies are synthetic fiber producers.

Kanebo Gohsen is manufacturing and marketing the PLA fiber "Lactron". "Lactron" products have expanded into multifilament yarn, staple fiber, spun bonded fabrics, monofilament yarn and flat yarn. Applications also cover a wide variety of sectors such as apparel, living materials, agriculture and horticulture, and civil engineering and building. "Lactron" is manufactured by the melt-spinning method just like nylon and polyester. Accordingly, conventional equipment can be used by remodeling it slightly and, therefore, a flexible expansion of production capacity becomes feasible. Initial physical fiber properties of "Lactron" are nearly equal to nylon and polyester fibers. The biodegradation of "Lactron" is milder than that of non-PLA biodegradable plastics. Decomposition hardly takes place when it used in normal conditions, but "Lactron" will lose its tenacity in two or three years when buried in the earth. Furthermore, "Lactron" gets decomposed by microorganisms within a month along with organic wastes at compost facilities. "Lactron" offers a silky feel and luster. As in the case of polyester, dyeing by diverse dyes is possible. When mix-woven with natural fibers "Lactron" imparts dimensional stability and wrinkle-resistant property to fabrics in the same way as polyester. "Lactron" itself does not possess water-absorbing property but offers good water-diffusion property. Consequently, double layered knits with "Lactron" on the skin side and cotton on the outer side exhibit excellent perspiration absorbing/fast-drying functions. The melting point of "Lactron" is quite lower than general synthetic fibers. Therefore, it is better to avoid ironing.

Unitika has been marketing PLA products in a wide range of areas including

films, sheets, fibers and nonwoven fabrics. Unitika has been marketing these PLA products as “eco-materials” which come from nature and go back to nature under the integrated trade name “Teramac”. “Teramac” fiber covers from monofilament to multifilament yarn and staple fiber as well as chopped fiber. As for its applications, Unitika is placing importance on industrial and lifestyle materials. As for apparel applications, Unitika has been marketing composite-fiber yarn for knits such as polo shirts made by covering the core of spun PLA yarn with cotton or lyocell.

Kuraray has developed PLA fiber with the brand name “Plastarch”. The firm started the development of PLA fiber by using the resin of Nature Works in 1998. Kuraray has been placing importance on the establishment of this development and know-how regarding its applications. It has promoted the development of applications for filament yarn and staple fiber made of homopolymer in order to grasp the essential characteristics of PLA in the first phase of development. Kuraray has been intending to promote the development of its original materials through combinations with other polymers such as vinyl acetate instead of PLA fiber made of homo-polymer.

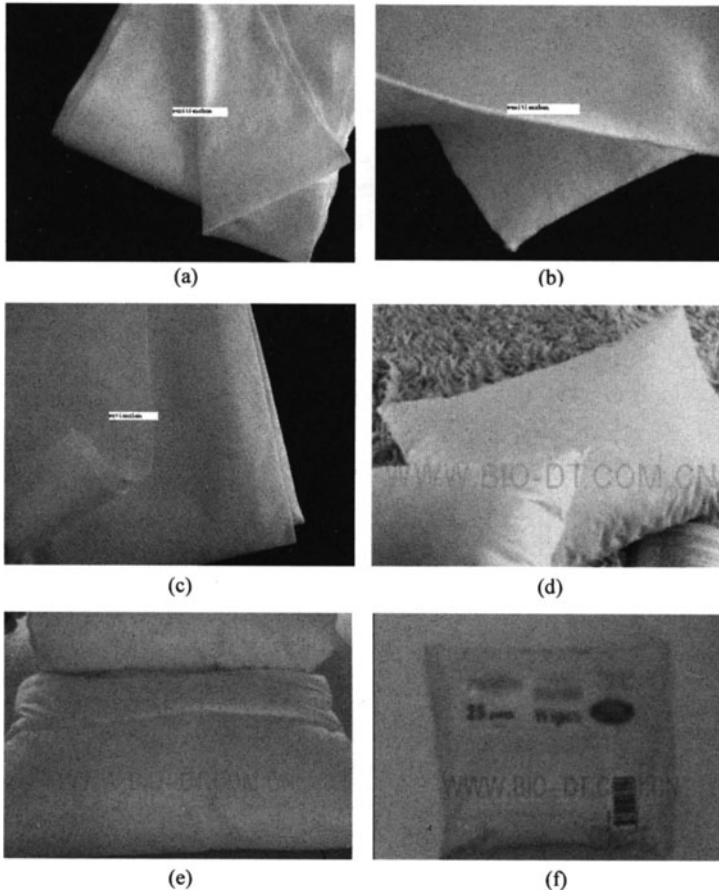
In China, Dalian Impex International Trading Co., Ltd. are dedicated to the marketing 100% biodegradable products, especially PLA series products, such as PLA fiber, yarn, nonwovens, baby wipes, home textiles, apparels and other terminal products of PLA as shown in Fig. 6.1. The stuffing of the pillow is 100% PLA fiber that is ecofriendly and biodegradable. The PLA pillow is smooth, light, soft and perfect in moisture absorption and perspiration. It makes your rest more comfortable. The PLA baby wipe is made of 100% PLA spun laced non-woven. It is soft and gentle for babies’ skin and no stimulation. It is safer than PET. No alcohol is contained. It is sturdy, no falling apart when you use. Other Chinese companies such as Jiangyin Gao Xin Chemical Fibers Co. Ltd., Trans-Pacific International Group, also supply the biodegradable PLA fiber fabric. The application is for packaging and agriculture and construction.

Future plans call for extracting dextrose from other plant sources such as sugar beets, wheat, rice and other products containing cellulose. Worldwide production is an implication of this renewable resource—a boon for farmers around the globe. A major new market for producers of agriculture crops is created, securing an employment base for rural workers [9].

### **6.2.2.2 Medical Applications**

The medical textile industry is one of the most diversified sectors representing the state-of-the-art in designing and developing innovative materials and devices that are redefining traditional approaches to human health care [10]. The attraction lies in specialized polymer materials and engineered structures dedicated to specific applications. This is where the term ‘biotextile’ is originated, signifying structures designed for use in specific biological environments (e.g., surgical implants, biomass reactors), where their performance measured in terms of their





**Figure 6.1** Kinds of terminal products of PLA fibers [8] (a) PLA Water-Embroidered Non-Woven Fabric; (b) PLA Needle-Punching Non-Woven; (c) PLA Thermal Calendaring Non-Woven Fabric; (d) PLA pillow; (e) PLA Quilt 100%; (f) PLA Baby Wipe

biocompatibility and biostability [11] depends on their interactions with cells and biological fluids. The applications of biotextiles range from pharmaceuticals to suture materials, implantable matrices and organ reconstruction. The medical applications of PLA fibers rest upon its biodegradability and the biocompatibility of the degradation products with the human body.

#### (1) Sutures

PLA is a biodegradable, bioresorbable polymer that can be assimilated by the body and has important applications in sustained-release drug delivery systems. The mechanical properties and absorbability of PLA make it an ideal candidate for implants in bone and soft tissue and for resorbable sutures.

Surgical sutures are wound closure filaments fabricated in various shapes. The basic requirement of sutures is that they hold tissues in place until natural healing

of a wound provides sufficient tissue strength. PLA has been approved by the Federal Drug Administration (FDA, USA) for its use as a suture material because of its features that offer crucial advantages [12, 13].

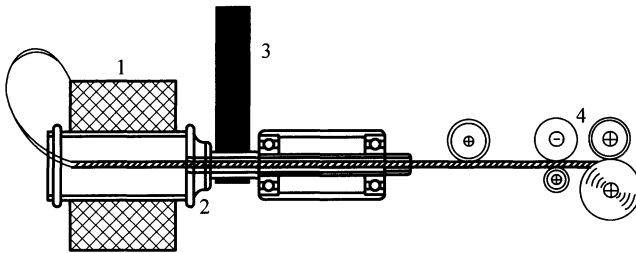
The intrinsic properties of unmodified PLA, such as its high crystallinity (ca. 40%) and brittleness and slow degradation, limit its use as suture materials. For this reason lactic acid is copolymerized with other biodegradable monomers to achieve precisely defined properties required. The comonomer unit interferes with the regular alignment of molecular chains and hence impedes the formation of highly ordered regions. Glycolic acid is the most widely used monomer for this purpose and a copolymer with a 90:10 mole ratio of glycolic acid to lactic acid has been commercialized as Vicryl by Ethicon. This suture material has a higher degradation rate than PLA filament. It is important to note that the copolymerization of lactic acid with a comonomer introduces significant changes in physical properties. Crystallite formation is impeded and the glass transition temperature is lowered depending on the amount of comonomer. The copolymer has a window of 24% – 66% glycolic acid in which it is amorphous. Therefore, a desired material may be tailored by copolymerization with glycolide. This approach helps in producing sutures with the required initial mechanical strength to hold wound tissues together. At the same time, the biological performance of the material must be maintained [14].

Implanted PLA material undergoes degradation and is reduced in weight by 63.2% within 168 days [15]. It has been estimated that complete degradation would need at least 1.5 years—an important consideration for surgical applications. This consideration leads to development of sutures based on polyglycolic acid (Dexon) and its copolymers (Vicryl) [16 – 18]. In an investigation of its degradation behavior it was observed that these suture undergoes drastic loss of physical properties under aqueous medium in vitro. The results are indicative of cleavage-induced crystallization during degradation [17, 18]. In this process the amorphous chains undergo scission, which leads to increased chain mobility and loss of tensile strength. Subsequently, crystallites are formed from these short chains at temperatures as low as ca.  $-40^{\circ}\text{C}$ . The  $T_g$  of shorter chains may fall significantly owing to the plasticization effect of absorbed water.

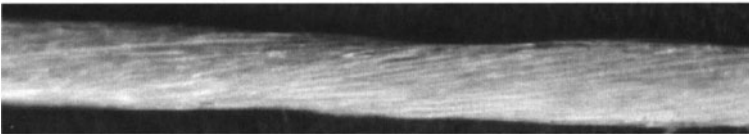
Sutures have been developed based on both poly (*D,L*-lactic acid) and poly (*L*-lactic acid) [19]. The filaments are produced by melt spinning carried out to get continuous filaments with a draw ratio of 4–12 so that appropriate strength would be achieved, i.e. 2.5 g/d under these spinning conditions. The sutures are manufactured by plying and twisting the filaments into 520 denier yarn. In vitro degradation has been investigated in sodium hydroxide solution at  $25^{\circ}\text{C}$ . The degradation is extremely high initially, as is evident from intrinsic viscosity measurements. Surgical evaluation of the sutures is carried out by intramuscular implantation. The tissue reaction is like that to stainless steel and Dacron.

In early 1998 Lin et al. [20 – 22] fabricated a rotor-twister that twisted multifilament to increase yarn strength. Enormous advances have been made in

recent years in the development of synthetic absorbable suture materials. The PLA multifilament was twisted by Lou et al. by using different twisting parameters and a rotor-twister to fabricate United States Pharmacopoeia (U.S.P.) size 5 – 0 and 7 – 0 surgical sutures as shown in Fig. 6.2. The best tensile strengths of the suture (Fig. 6.3) were 3.1 and 12.3 N and the coefficients of variation were 3.70% and 1.75%. The PLA suture was then scoured with 1 wt% sodium hydroxide to eliminate impurities, and the knot-pull strengths decreased to 1.66 and 6.84 N for 7 – 0 and 5 – 0 PLA sutures respectively, but still conforming to the U.S.P. knot-pull strength standard. An in vitro hydrolysis test was performed at 37°C by immersing 5 – 0 PLA suture in physiological saline (0.9 wt% NaCl aqueous solution); the knot-pull strength decreased by 12% after 28 days [23].



**Figure 6.2** The mechanism of the rotor-twister: 1-PLA yarn; 2-rotor twister; 3-driving belt; 4-take-up roller [23]



**Figure 6.3** The appearance of the PLA absorbable suture [23]

## (2) Drug Delivery

Biodegradable polymers provide sustained release of encapsulated drugs and degrade in the body to nontoxic, low-molecular weight products that are easily eliminated. Polymeric drug delivery systems have numerous advantages compared to conventional dosage forms, such as improving therapeutic effects, reducing toxicity, convenience, etc. In addition, a wide variety of polymers, polymer processing techniques, and fabrication techniques are being explored for incorporation of drug molecules into delivery vehicles of various geometries. Release of pharmaceutical dosage can be designed as rapid, immediate, delayed, pulsed, or modified dissolution depending on the polymer carriers used and other included additives. Microspheres formulations have been extensively investigated, and closed correlations have been quantitatively determined between release profiles and drug distribution in polymer matrix and matrix degradation [24]. Besides microspheres, biodegradable polymers have been made into hydrogels [25],

micelles [26], and fibrous scaffolds as drug carriers, each with certain advantages and disadvantages. The main advantage of fibrous carriers can offer site-specific delivery of any number of drugs from the scaffold into the body. In addition, the drug can be encapsulated directly into fibers with different sizes, and these systems have special properties and surprising results for drug release different from other formulations. Due to their high specific surface area and porous structure the electrospun nonwoven fabrics consisting of ultrafine fibers find wide applications as scaffolds for tissue engineering, tissue repair substitutes, wound dressing materials, and carriers for drug delivery [27]. Furthermore, unlike common encapsulation involving some complicated preparation process, therapeutic compounds can be conveniently incorporated into the carrier polymers using electrospinning. Electrospun nonwoven mats can be cut to almost any size and fabricated into other shapes (e.g., tubes) by using different target geometries. The resulting nanofibrous membrane containing drugs can be applied typically for skin and wound healing or post processed for other kinds of drug release. Thus, electrospinning show potential as an alternative polymer fabrication technique to drug release systems from particles to fibers.

Cui et al. assessed the potential use of electrospun fibers as drug delivery vehicles with focus on the different diameters and drug contents to control drug release and polymer fiber degradation [28]. An *in vitro* drug release study shows that a pronounced burst release or steady release phase is initially observed followed by a plateau or gradual release during rest of the time. Fibers with a larger diameter exhibits a longer period of nearly zero order release, and higher drug encapsulation leads to a more significant burst release after incubation. *In vitro* degradation shows that the smaller diameter and higher drug entrapment leads to more significant changes of morphologies. The electrospun fiber mat shows almost no molecular weight reduction, but mass loss is observed for fibers with small and medium size, which is characterized with surface erosion and inconsistent with the ordinarily polymer degrading form. Further wetting behavior analysis shows that the high water repellent property of electrospun fibers leads to much slower water penetration into the fiber mat, which may contribute to the degradation profiles of surface erosion. The specific degradation profile and adjustable drug release behaviors by variation of fiber characteristics make the electrospun nonwoven mat a potential drug delivery system rather than polymer films and particles.

The influence of the solubility and compatibility of drugs in the drug/polymer/solvent system on the encapsulation of the drug inside the PLLA electrospun fibers and the release behavior of this formulation were examined by Zeng et al. using paclitaxel, doxorubicin hydrochloride and doxorubicin base as model drugs. The burst release of the drugs can be avoided by using drugs compatible with polymers, and the drug release can follow nearly zero-order kinetics due to the degradation of the PLLA fibers in the presence of proteinase K [29].

Paclitaxel-loaded biodegradable implants in the form of microfiber discs and

sheets have been developed using electrospinning technique and investigated against malignant glioma *in vitro* and *in vivo*. The fibrous matrices not only provide greater surface area to volume ratio for effective drug release rates but also give the much needed implantability into tumor resected cavity in post-surgical glioma chemotherapy. poly(*D,L*-lactide-co-glycolide) (PLGA) 85:15 co-polymer is used to fabricate microfiber disc (MFD) and microfiber sheet (MFS) and PLGA 50:50 co-polymer is used to fabricate submicrofiber disc (SFD) and submicrofiber sheet (SFS) to avail different drug release properties. All the dosage forms show sustained paclitaxel release over 80 days *in vitro* with a small initial burst. Sheets exhibited a relatively higher initial burst compared to discs probably due to the lower compactness. Also, submicrofibers show higher release against microfiber due to higher surface area to volume ratio and higher degradation rate. Apoptosis study confirms the advantage of sustained release of paclitaxel from fiber matrices compared to acute Taxol administration. Animal study confirms inhibited tumor growth of 75%, 78%, 69% and 71% for MFD, SFD, MFS and SFS treated groups over placebo control groups after 24 days of tumor growth. Thus these implants may play a crucial role in the local chemotherapy of brain tumors [30].

Plasmid DNA is incorporated into a polymer scaffold using electrospinning. The non-woven, nano-fibered, membranous structures is composed predominantly of poly (lactide-co-glycolide) (PLGA) random copolymer and a poly(*D,L*-lactide)-poly(ethylene glycol) (PLA-PEG) block copolymer. Release of plasmid DNA from the scaffolds is sustained over a 20 day study period with maximum release occurring at 2 h. Cumulative release profiles indicate that amounts released are approximately 68%–80% of the initially loaded DNA. Variations in PLGA to PLA-PEG block copolymer ratio vastly affect the overall structural morphology as well as both the rate and efficiency of DNA release [31]. And proteins are also loaded into PLLA nanofiber nonwovens by electrospinning of emulsions composed of an organic PLLA solution and an aqueous protein solution. Nanofiber nonwovens with proteins have a mean fiber diameter of approximately 350 nm. The protein release is found to be dependent on the surface tension of the release medium [32].

Nanocomposites produced by the combination of PLA nanofibers with titanium dioxide (TiO<sub>2</sub>) nanoparticles have been utilized in the biomolecular recognition of antitumor or anticancer drug daunorubicin. Observations of electrochemical studies indicate that because of the relative large surface area of the blends, the new nano TiO<sub>2</sub>-PLA polymer nanocomposites could remarkably increase the detection sensitivity as well as the binding affinity of daunorubicin to DNA, which is also demonstrated in spectroscopic study. Besides, to further reveal the effect of the new TiO<sub>2</sub>-PLA polymer nanocomposites for the biorecognition the relative influence of nano TiO<sub>2</sub> or PLA themselves has also been explored. The results illustrate that the drug molecules and/or DNA can be more readily self-assembled on the surface of the blends of the nano TiO<sub>2</sub>-PLA nanofibers so that the new nanocomposites can efficiently facilitate the relative

biorecognition of daunorubicin [33]. Biodegradable PLLA ultrafine fibers containing nanosilver particles are prepared via electrospinning. These fibers show antibacterial activities (microorganism reduction) of 98.5% and 94.2% against *Staphylococcus aureus* and *Escherichia coli* respectively because of the presence of the silver nanoparticles [34].

Up to now, the degradation behavior of drug-loaded superfine fibers and the correlations between drug release and matrix degradation are still the hot topic for drug delivery system. The possibility of controlling drug release through degradation of matrix polymer and fiber characteristics represents an attractive feature for a drug delivery system.

### **(3) Tissue Engineering**

Tissue engineering is an interdisciplinary field that applies the principles of life science and engineering to the development of biological substitutes that aim to maintain, restore or improve tissue function. Initial developments were confined to the use of biostable materials as scaffolds culturing cells that were then harvested into tissue. More recently, biodegradable materials have found enormous interest as supports because of the fact that the support disappears from the transplantation site with the passage of time leaving behind a perfect patch of the natural tissue. The purpose of the scaffold is to act as an extracellular matrix (ECM) where cells can adhere and grow, and thus to guide the development of new, fully functional tissues [35]. A fibrous scaffold has significant advantages over polymer films in the high level of porosity needed to accommodate large number of cells. This is where the pore diameter (interstitial space) becomes important for cell growth, vascularization, and diffusion of nutrients.

PLA may be fabricated into various shapes (e.g., filament, braided, knitted, nonwoven or film) as required of the organ construction. A successful scaffold design must include: fiber bonding that provides the required porosity, the specified size and shape of the object, and the required physical properties, such as extensibility and strength. The nonwovens provide well-defined porous structure and have proved to be excellent support matrixes for the seeding of large variety of cells. In applications such as bladder reconstruction the knitted structures performing best as the scaffold material must be extensible during the transplantation stage [36]. PLA filaments have been fabricated into knittings for this purpose. Collagen can be immobilized on the PLA knitting by dip-coating to obtain a structural resemblance to human decellurized matrix. These protein-immobilized knittings are used for seeding urothelial and smooth muscle cells.

Steuer et al. developed PLA filaments for regeneration of nerves in paralyzed patients [37]. Although nerves do not grow at all, it is, however, possible to seed Schwann cells on a polymer support and grow them. The approach adopted has been to join distal and proximal ends of a nerve by an artificial segment which will allow the Schwann cells to grow and fill the gap between the two ends. With the passage of time the support disappears and leaves behind a continuous channel of nerve cells. Adhesion of Schwann cells on virgin PLA surfaces is very limited,

but plasma processing of PLA fiber is very effective in enhancing the adhesion. The plasma treatment introduces chemical functionalities that can interact with poly-Dlysine and render the surface bioreceptive to cell attachment. C17.2 nerve stem cells were seeded and cultured on electrospun PLGA nanofibers by Bini et al. The nerve stem cells were adhered and differentiated on all the scaffolds and supported neurite outgrowth. Interesting observation was seen in the aligned microfiber scaffolds where the C17.2 nerve stem cells were attached and differentiated along the direction of the fibers. The size and shape of the cell-polymer constructs remained intact. The study suggests that PLGA is a potential scaffold for nerve tissue engineering and predicts the orientation and growth of nerve stem cells on the scaffold [38].

Bhattarai et al. developed a novel biodegradable electrospun membrane as a scaffold for tissue engineering. A nanofibrous matrix of poly(*p*-dioxanone-co-*L*-lactide)-block-poly(ethylene glycol) (PPDO/PLLA-b-PEG) copolymer was evaluated for cell proliferation and its morphology of cell-matrix interaction. The electrospun structure composed of fibers with an average diameter of 380 nm, medium pore size 8  $\mu$ m, porosity greater than 80% and mechanical strength of 1.4 MPa is favorable for cell-matrix interaction [39].

Xu et al. developed aligned poly (*L*-lactid-co- $\epsilon$ -caprolactone) [P(LLA-CL)] (75:25) copolymer nanofibrous scaffold by electrospinning. The diameter of the generated fibers was around 500 nm with an aligned topography which mimics the circumferential orientation of cells and fibrils found in the medial layer of a native artery. A favorable interaction between the scaffolds with human coronary artery smooth muscle cells (SMCs) was demonstrated via MTS assay. The SMCs attached and migrated along the axis of the aligned nanofibers and expressed a spindle-like contractile phenotype; the distribution and organization of smooth muscle cytoskeleton proteins inside SMCs were parallel to the direction of the nanofibers; the adhesion and proliferation rate of SMCs on the aligned nanofibrous scaffold were significantly improved compared with that on the plane polymer films. The above results strongly suggest that this synthetic aligned matrix combines with the advantages of synthetic biodegradable polymers, nanometer-scale dimension mimicking the natural ECM and a defined architecture replicating the in vivo like vascular structure, and therefore, may represent an ideal tissue engineering scaffold, especially for blood vessel engineering [40]. Bone morphogenetic protein-2 (BMP-2) was encapsulated into a polymeric matrix by electrospinning and their individual performance was characterized in a nude mouse model. The PLGA/hydroxyapatite (HAp) composite scaffolds developed in the study exhibited good morphology/mechanical strength and HAp nanoparticles were homogeneously dispersed inside PLGA matrix. Results from the animal experiments indicate that the bioactivity of BMP-2 released from the fibrous PLGA/HAp composite scaffolds is well maintained, which further improves the formation of new bone and the healing of segmental defects in vivo. BMP-2 loaded PLGA/Hap composite scaffolds are promising for bone healing [41].

PLGA 85:15 and 75:25 electrospun polymer scaffolds for dermal replacement were developed by Blackwood et al.[42]

The hot topics in the tissue engineering are to functionalize the polymer matrix and to enhance its interaction with cells. For example, bioactive collagen is incorporated into PLA and PLGA nanofibrous scaffolds to improve its cellular behavior [43, 44].

#### (4) Others

Cigarette filter tows and filter rods can be produced from PLA by melt-spinning [45]. Magnetite ( $\text{Fe}_3\text{O}_4$ ) nanoparticles in the diameter range of 5–10 nm are incorporated into PLLA by electrospinning. Nanofibers with diameters ranging from 50 to 300 nm are obtained. Nanofibers containing up to 35 wt% magnetite nanoparticles display superparamagnetism at room temperature. Such composites are of potential interest for various applications in medicine, especially drug delivery to precise target areas [46]. A wide variety of materials have been incorporated in electrospun PLA fibers to tailor the fibers for particular end uses. Nanoscale clay particles have been incorporated in electrospun PLA fibers to control modulus and biodegradation rate for potential biodegradable packaging applications [47]. Carbon nanotubes have been incorporated in electrospun PLA fibers for potential use as bone graft materials [48]. Biotin is incorporated into PLA nanofibers through electrospinning to prepare membrane substrates for biosensors based on biotin–streptavidin specific binding. Preliminary biosensor assays confirm that streptavidin immobilized on the membrane surface can capture a biotinylated DNA probe [49].

## 6.3 Engineering Plastic

Engineering thermoplastics are sold in much lower quantities and are thus more expensive per unit weight. Despite this, they are widely used in everyday products. For example ABS is used to manufacture car bumpers and dashboard trim, polycarbonate is used in motorcycle helmets and polyamides (nylons) are used for skis and ski boots.

Typically, an engineering plastic is chosen for its range of enhanced physical properties, e.g., polycarbonate is highly impact resistant and polyamides are highly resistant to abrasion. In these types of applications, designers are looking for plastics that can replace traditional engineering materials such as wood or metal. The advantage gained is the inherent “formability” (ease of processing) of plastics as opposed to metal-working or fabrication.

Other properties exhibited by various grades of engineering plastics include high heat resistance, mechanical strength, rigidity, chemical stability and flame retardency.

PLA is obtained from agricultural products (for example, corn). The most prestigious advantage of PLA is biodegradable. It can be degraded by



micro-creatures in the nature under certain circumstances by giving out carbon dioxide and water. No air pollution is caused. Therefore, this is very helpful for environmental protection. It has been recognized as the most prospective plastics in the new century. Some researches have been conducted for this polymer. The general properties of PLA compared with some conventional polymers are shown in Table 6.1.

**Table 6.1** General property comparisons

	PLA	GPPS	PET	PP
Tensile strength (MPa)	53.1	45.5	58.6	35.9
Elongation at break (%)	4.1	1.4	5.5	350
Tensile modulus (GPa)	3.45	3.03	3.45	1.31
Izod impact (J/m)	16	21.4	26.7	48.1
Glass transition (°C)	60	102	74	-20
Melting point (°C)	130–170	–	270	165
Density (g/mL)	1.25	1.05	1.35	0.9



**Figure 6.4** FOMA(TM) N701iECO phone made of PLA bioplastics reinforced with kenaf fibres developed by NEC, UNITIKA and NTTDoCoMo © Paul Fowler [50]

PLA is a transparent plastic whose characteristics resemble common petrochemical-based plastics such as polyethylene and polypropylene. It can be processed on equipment that already exists for the production of conventional plastics. PLA is produced from the fermentation of starch from crops, most commonly corn starch or sugarcane in the US, into lactic acid that is then polymerized. Its blends are used in a wide range of applications including computer and mobile phone casings, foil, biodegradable medical implants, moulds, tins, cups, bottles and other packaging [50].



**Figure 6.5** The product made by PLA

## 6.4 Disposable Ware

Many quick service establishments use disposable products due to its convenience and low cost. Products like these save the labor and equipment used for washing reusable products, and they are perfect for takeout orders. However, these disposables are used just once and then thrown away creating a tremendous amount of harmful waste. Literally tons of paper, plastic and Styrofoam products end up in landfills every year. Unfortunately, products like these do not break down until hundreds of years later, and even then sometimes deposit toxins into the earth. Due to diminishing natural resources and rising energy costs, it is becoming increasingly important to commit to environmentally friendly products and habits [51 – 55].

The problem of landfills overflowing with non-biodegradable plastic bags and containers is a global one. Some countries are passing the cost of convenience on to customers in the form of a “plas tax”, whereby consumers pay a fixed amount for plastic bags. Reportedly, this has resulted in a 90% drop in consumption. But not all countries are in agreement with this approach. Either way, the best solution is to think of disposables as a luxury. Use them sparingly and try to rely on re-usable products as much as possible.

As the great debate over plastic containers and bulging landfills rages on, a new product has slipped into the marketplace: bioplastics. Made from renewable raw materials, including corn, wheat, potatoes, beets and a variety of other plants, bioplastics have been on the drawing board since the mid-1980s. They are often referred to as PLAs, or polylactic acid, because this is what the plant matter is ultimately converted into. They are available in the form of containers, dishes, utensils and “plastic” bags.

The advantages of bioplastics:

- Producing bioplastics uses 65% less energy than producing petroleum-based

plastics, making bioplastics the energy-efficient choice, hands down.

- Bioplastics generate 68% fewer greenhouse gases than fossil-fuel-based plastics. Clearly, they are better for the environment.
- Manufacturing petroleum-based plastics uses approximately 200 000 barrels of oil per day. Switching to bioplastics means being less dependent on Fossil fuel.
- As they degrade, bioplastics will remain non-toxic and will not leach dangerous chemicals into the soil. This means they are safer.
- The process of making bioplastics has finally become cost effective.
- Bioplastics can be recycled and this is always good news. In fact, certain grassroots recycling organizations are very excited by the prospect of bioplastics.

The Disadvantages:

- Despite the fact that bioplastics are a great improvement over fossil-based fuels, they are not yet the perfect solution. Here's the reason.
- Most recycling centers are not set up to handle large amounts of PLA. Presently, PLA products cannot be recycled in conjunction with petroleum-based products, which means sorting is critical.
- Bioplastics are “compostable”, but only under specific conditions. To biodegrade within 90 days, as described, the products have to reach 140° F for 10 consecutive days. This requires a special facility, which few consumers have access to. If your PLA products end up at the landfill, they will not degrade any faster than a petroleum-based product.
- Planting corn for non-food uses is problematic for a number of reasons. Most corn planted for industrial uses is genetically modified, raising the question of the potential contamination of conventional crops. Soil erosion is another problem.
- Plant-based bioplastics have a low melting point. This means that if you leave a corn-based takeaway container in your car on a warm day, when you return you might find that it has melted into a small puddle.

### 6.4.1 What Is the Difference Between Biodegradable and Compostable?

Biodegradable means that the products break down through a naturally occurring microorganism, such as fungi or bacteria over a period of time. Biodegradable products are usually made from plant or animal sources. Biodegradable products can generate methane, a greenhouse gas with 62 times the global warming potential of carbon dioxide when dumped into landfills. Also, biodegradable waste may contain toxins.

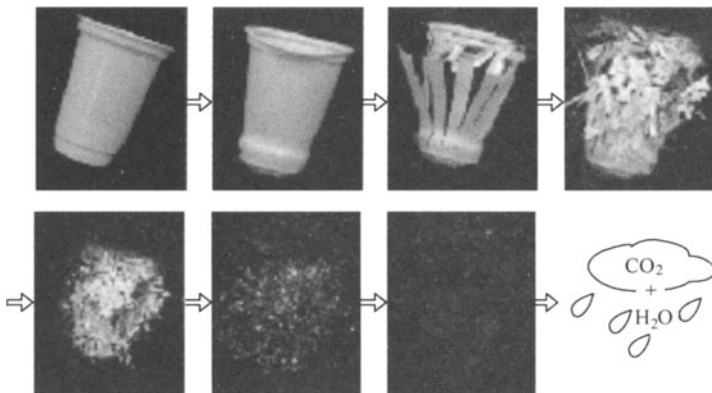
Compostable plastics mean that the products must be able to break down into

carbon dioxide, water, and biomass at the same rate as paper. Also, the broken down product should not produce any toxic material and should be able to support plant life. Compostable products are usually made from plant materials. Because biodegradable is used loosely with no legal enforced definition, compostability is more desirable for disposable products.

### 6.4.2 About PLA for Disposable Use

Poly(lactic acid), or polylactide, more commonly known as PLA, is a biodegradable polymer derived from 100% renewable resources. PLA, comparable to petroleum based plastic, is now used in a variety of industries including packaging, clothing, medicine and more. Classified as GRAS (generally recognized as safe) by FDA, PLA is a nonvolatile and odorless polymer [56 – 59].

PLA is fully compostable in municipal/industrial facilities (according to ISO, CEN, ASTM, BPI, DIN, BPS regulations) and can be disposed of by all traditional waste management methods such as incineration, landfill and mechanical recycling. CO<sub>2</sub> is removed from the atmosphere when growing the feed stock crop and is returned to the earth when PLA is degraded. PLA is much more sustainable than regular petroleum made plastic. Typically, PLA will completely degrade in commercial compost in roughly 30 – 45 d. In home composting bins they may take longer. Figure 6.6 shows the completely degradation process of PLA.



**Figure 6.6** Completely degradation process of PLA

#### Benefit of PLA:

- **Versatile:** Replaces many traditional package alternatives in a broad range of applications.
- **Clear:** Great optics and high gloss provides ideal product display.
- **Strong and Durable:** Protects your product appearance while guarding

## 6 Application in the Field of Commodity and Industry Product

against spoilage.

- **Printable:** Graphic imprint to present your design and message.
- **Secure:** Self-seals rapidly with heat, also compatible with a wide range of adhesive technologies.
- **Superior flavor & aroma barrier:** Keeps food tasting and smelling fresh. Tests prove excellent resistance to most oils and fats used in food preparation.
- **Uses 20% – 50% less fossil fuels** compared to traditional petroleum based plastics, reducing greenhouse gases and smog in our atmosphere.
- **Reduces burden on landfill.**
- **Cleaner production process** and thus reduces harmful pollutants emitted into the air.

PLA products require certain amounts of heat, moisture and air to compost. Regrettably typical landfills do not contain these necessary circumstances and the items dumped in the trash usually end up at these landfills. Also, landfills are typically sealed, which means that decomposition happens beneath the surface and what is thrown in the trash can is preserved for decades after.

You can dispose your PLA products at the closest composting facility. If you are in California, you can locate the closest facility. If you are located outside of California, you can find a facility near you.

PLA must be kept out of direct sunlight and in a cool, dry location. Keep the PLA products in the temperature below 110 °F and the humidity lower than 90% at all times. Although not required, refrigerated truck is highly recommended in transporting PLA products.

You can use PLA products for hot beverages if the beverage temperature does not exceed 110 °F. PLA products perform better when used with cold beverages although the typical heat tolerance of PLA products is 110 °F. And you can also do custom printed PLA cups.

The average cost of PLA compared to regular plastic products depends on the brand, type, and size of the order. Yet the cost compared to regular plastic products is becoming more competitive as the interest in biodegradable product rises. The disparity in prices is about 15%.

PLA is safe for food services and is classified as GRAS by the FDA. PLA also is certified by SGS HACCP for safe food management system. The person who is allergic to corn still can use PLA products because the heat used in the process of deriving the starch from corn destroys the immunologically reactive proflin. Proflin is the chemical that usually causes an allergic reaction and is not found in PLA products. But PLA products are not edible, yet are generally non-toxic. Small pieces of PLA will most likely pass harmlessly through the gastrointestinal tract. Once passed through the gastrointestinal tract it will be eliminated in the stool. Please consult a doctor if pain or discomfort arises.

### **6.4.3 Commercial PLA Disposable Ware**

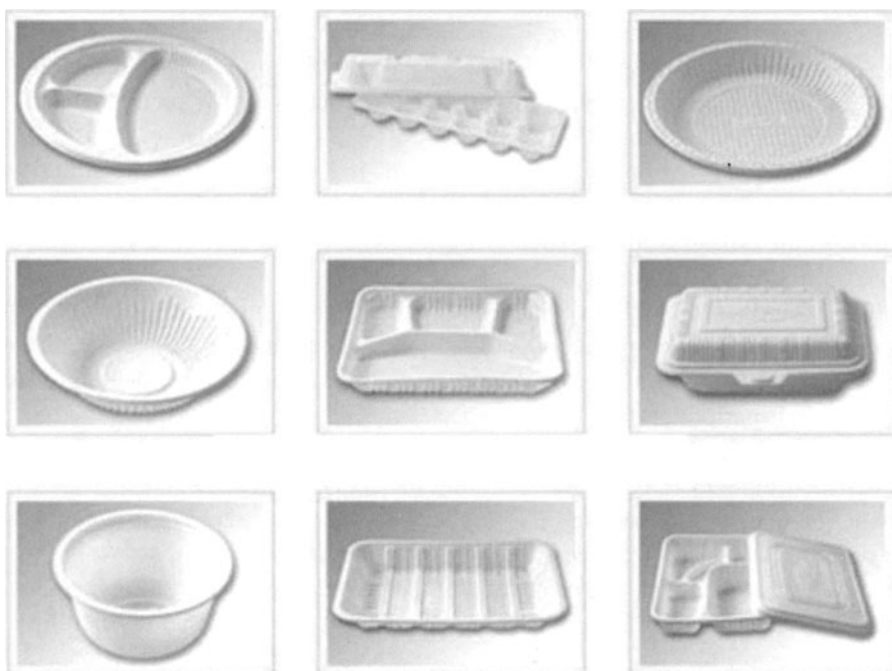
Based on the fully compostability and processability, PLA has been produced into series of commercial disposable ware such as dinnerware, cups and carryout containers [60, 61]. Although these products are made from corn, these plates are not edible and corn allergies are not an issue because no trace allergens remain in the finished product. PLA conserves energy by using only about half the resources that go into traditional plastics. PLA uses mainly renewable resources in their production unlike traditional plastics, which rely on petroleum products. Commercial PLA disposable ware is becoming more and more popular.

#### **6.4.3.1 PLA Disposable Tableware**

As shown in Fig. 6.7 and Fig. 6.8, PLA can be made into various tableware such as dish, ice tray, lunch box, knife, fork, scoop and so on.

#### **6.4.3.2 Clear Cup**

Based on the good processability and transparency, PLA can also be made into clear cups with a variety of size and capacity (see Fig. 6.9 and Table 6.2).



**Figure 6.7** Kinds of tableware made of PLA

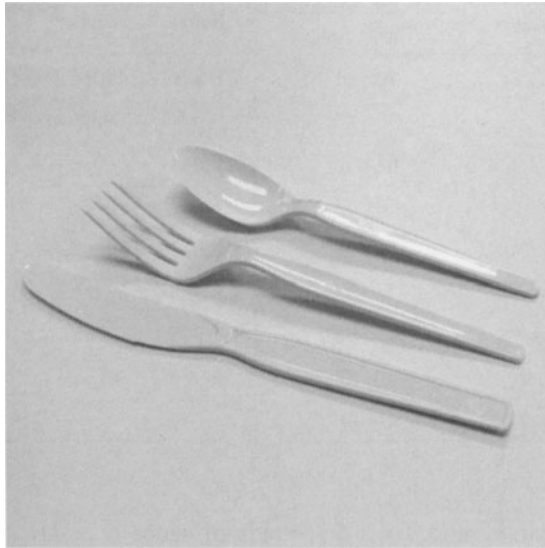


Figure 6.8 Knife, fork and scoop made of PLA

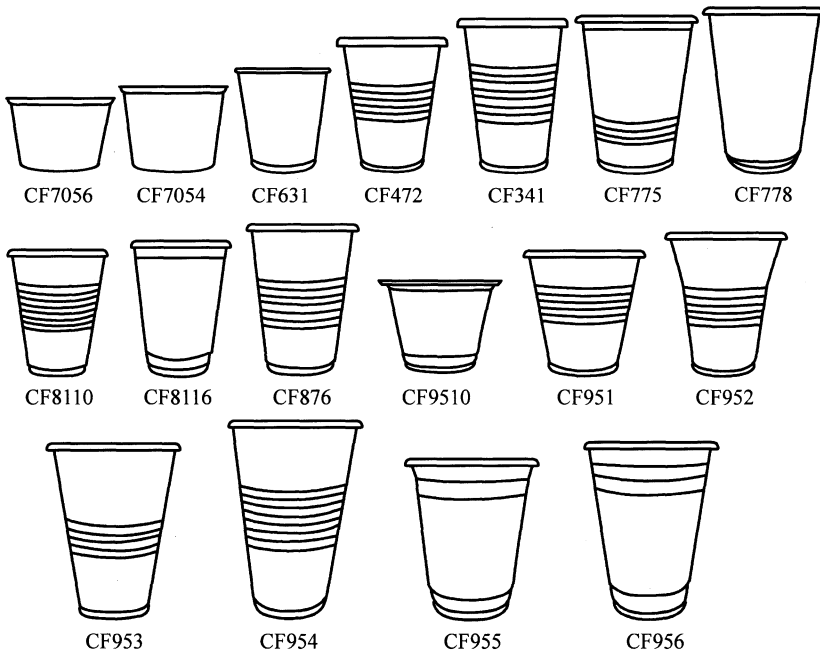


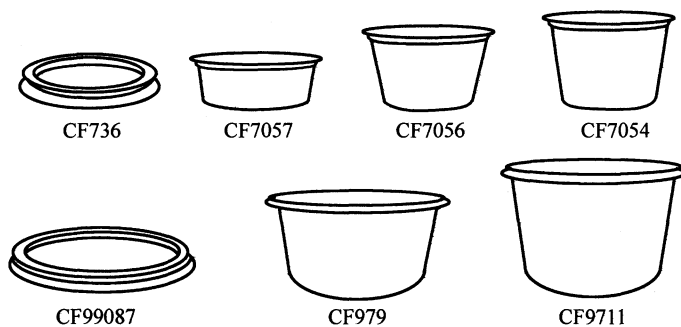
Figure 6.9 Disposable cups made of PLA

**Table 6.2** Parameters of PLA clear cups

Item	Capacity	Size (dia. ×height) (mm ×mm)	Item	Capacity	Size (dia. ×height) (mm ×mm)
CF 7056	80cc./ 3 oz	70×41	CF 876	420cc.	87×120
CF 7054	100cc./ 4 oz	70×48	CF9510	9oz	95×72
CF 631	3 oz	62×58	CF 951	360cc.	95×95
CF 472	170cc.	70×75	CF 952	400cc.	95×110
CF 341	200cc./ 7 oz	70×90	CF 953	500cc.	95×125
CF 775	260cc.	77×92	CF 954	600cc.	95×140
CF 778	9 oz	77×98	CF 955	14 oz	95×105
CF 8110	300cc.	80×100	CF 956	16 oz	95×122
CF 8116	12 oz	80×107			

**6.4.3.3 Sauce Cup**

As shown in Fig. 6.10 and Table 6.3, kinds of sauce cups are made of PLA by suction molding, and the assorted lids can also be made from PLA.



**Figure 6.10** Disposable sauce cups made of PLA

**Table 6.3** Parameters of PLA sauce cups

Item	Capacity	Size (dia. ×height) (mm ×mm)	Item	Capacity	Size (dia. ×height) (mm ×mm)
CF736	Flat lid	73×6	CF9907	Flat lid	99×7
CF7057	60c.c. /2 oz	70×26	CF979	200c.c. /7oz	97×45
CF7056	80c.c./3 oz	70×41	CF9711	250c.c. /8oz	97×58
CF7054	100c.c. /4oz	70×48			



## 6.5 Biodegradable Hot Melt Adhesive Based on PLA and Other Biodegradable Polymer

Hot-melt adhesive (HMA) is an important kind of adhesive, which is solid at room temperature and is molten state with high temperature. Until now, most of HMAs is not degradable. As a result, it is not good for environment protection and the material recycling. As more concerns on environment protection, environment-friendly biodegradability HMA with perfect adhesion becomes an important aim in the adhesive industry.

Biodegradable HMAs are prepared mainly based on biodegradable polyester (e.g., PLA, PCL, PHBV and PEA) and natural polymers (e.g., starch etc.). The applications of biodegradable HMAs have more than 10 years' history in developed countries, but is just beginning to be used in China.

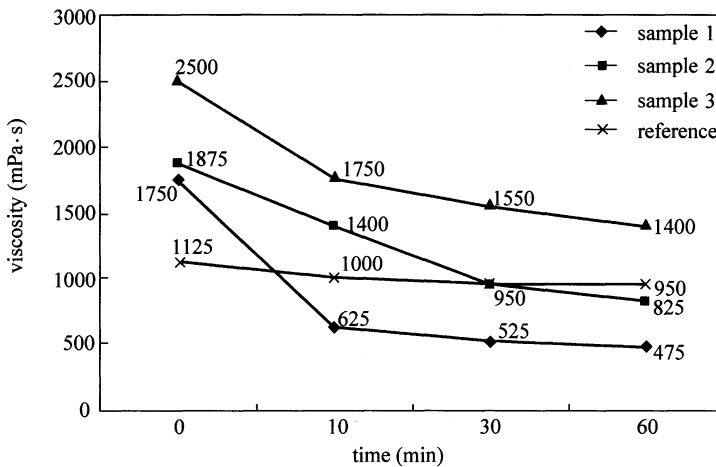
### 6.5.1 Biodegradable PLA and/or PCL Based Biodegradable HMAs

Currently, the polyester-based biodegradable HMAs are mainly based on PLA and/or PCL. PLA homopolymer has a glass transition temperature of about 170°C. Tensile strength and elongation at break are about 50 MPa and 2% [62], respectively, which means that flexibilizing components have to be incorporated in the polymer in order to make it suitable as an adhesive.

Polycaprolactone (PCL) is a biodegradable polyester that can be prepared by ring opening polymerization of  $\epsilon$ -caprolactone. Because its molecular chain has good flexibility, it has a low melting point of around 60°C and a glass transition temperature of about -60°C, so it is often used as an additive for resins to improve their processing characteristics and impact resistance.

Copolymer of PLLA and PCL are flexible polymers with low melting points. This can be attributed to the properties of PCL, which differs significantly from those of PLLA. PLLA, PCL and copolymers are degradable in biological environment [63, 64]. The degradation process in biological environment is complicated, which can be related to several different factors. However, the main mechanism is hydrolysis and this reaction can be catalysed by carboxyl end groups initially present or generated during the degradation process.

As the tide of moving toward use of degradable or reusable packaging products increases, it is of great interest to develop HMAs that not only have excellent mechanical properties but also meet the requirements related to biodegradability. Viljanmaa et al. [65 – 68] developed two PLA/PCL based HMAs for packaging. Both of the adhesives were based on PLLA and poly ( $\epsilon$ -caprolactone) (PCL) with molar ratio 81:19. Figure 6.11 is the testing result of viscosity. According to the results, they got the conclusion that PLLA/PCL copolymer was a potential candidate of HMA for the packaging use.



**Figure 6.11** Viscosity curves of the Samples 1a, 2, 3 and 4 [68]

Won Y. Choi et al. [69] developed a biodegradable HMA from PCL and soy protein isolate (SPI). The adhesive was synthesized from PCL/SPI mixture with plasticizers (coconut oil and PEG400) at varying ratios. The typical properties of the HMA, such as thermal properties, softening point, surface morphology, tensile strength, lap shear strength, were characterized. All the compositions were nontoxic, as shown in testing results. The adhesives can be used in nontoxic food packaging system.

Beside the application for packaging products, some PLA and/or PCL based on HMA can be used in disposable products, such as diapers, sanitary products. Carmine P. Iovine et al. [70] prepared a kind of HMA that contains PLA, polar tackifier, plasticizer, wax diluents, stabilizer and a polymer. Once the adhesive was in touch with the soil, it would be composted by bacteria, fungi, etc. If the HMA invented is prepared into non-pressure HMA, it can be used in bookbinding, bag ending, case and carton sealing; if prepared into pressure sensitive HMA, it can be used in the disposable industry. Garry J. Edgington et al. [71, 72] used a lower molecular weight material as a tackifier to formulate a kind of pressure sensitive HMA via PLA. At the same time, all the ingredients they used were biodegradable. The HMA were supposed to be used in packaging and the manufacturing of disposable articles.

Because of the good biocompatibility, the PLA and/or PCL based on HMA also can be applied in the biomedical use. Sze-Man Ho et al. [73] did some research work on synthesis, polymerization and degradation of poly (lactide-co-propylene glycol) dimethylacrylate adhesives. The adhesives can be put into biomedical applications. Gilad Lando et al. [74] synthesized lactide-based low molecular weight copolymers as tissue adhesives. The oligomers were composed of di- or tri-functional central connecting segments and lateral PLA blocks, besides, they inserted  $\epsilon$ -caprolactone (CL) molecules into the PLA blocks in order to produce longer biodegradable chains and improve the adhesive strength.

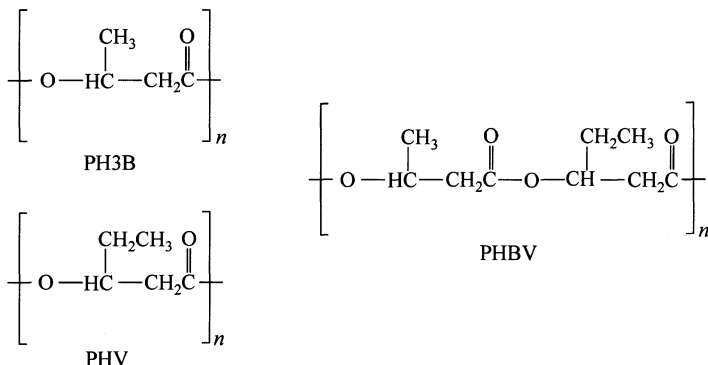
Ferreira et al. [75] synthesized a HMA for medical use. Urethanes based on polycaprolactone diol (PCL) were synthesized by reaction of the molecule either with isophorone diisocyanate (IPD-isocyanate) or hexamethylene diisocyanate (HDI-isocyanate). Nies Berthold et al. [76] tried out an adhesive composition based on polymers or polymer blends consisting of caprolactone copolymers or caprolactone copolymers and polycaprolactone. The adhesive can be utilized as HMA for temporarily gluing together biological tissue and other materials in medicine.

In addition, researchers have done a lot of attempts and experiments to enhance the HMA properties. Ming Yang et al. [77] synthesized the PLA/PCL-based biodegradable HMA by chain extending method, which has an excellent shear strength of as high as 6.788 MPa. Mikael Stolt et al. [78] prepared a product of PLA and a hydroxyl-terminated four-armed PCL through condensation reaction and studied its properties. They also determined the thermal stability and adhesive properties of the different formulations. Kitamura Tadashi et al. [79] prepared a PLA-based biodegradable HMA that consists of high-molecule PLA as thermoplastic resin and methyl lactate as the tackifier. Schoenberg Jules E. et al. [80] prepared polylactide or polyglycolide graft copolymers, which were suitable for use as the thermoplastic biodegradable hot melt adhesives.

The effects of adhesive composition on HMA properties were also investigated. Saara Inkinen et al. [81] discussed the stability of 70:24:6 (w/w/w) blends of a lactic acid-based hot melt adhesive (LHM), oxidized potato starch (dried or nondried), and polyethylene glycol (PEG). They used tensile test, water absorption, and scanning electron microscopy (SEM) to evaluate the adhesives. Lewis David Neal et al. [82, 83] invented several methods for preparing environmentally degradable polymeric compounds. The compounds are composed of PLA with molecular weight ( $M_w$ ) from 500 to 50 000 g/mol, to which a flexibilizing aliphatic polyester with molecular weight from 500 to 50 000 g/mol is incorporated. And the amount of lactic acid comprising groups in the polymeric compound ranges from 50% to 99% and the amount of flexibilizing polyester groups ranges from 1% to 50%.

### 6.5.2 PHBV and PEA Based on Biodegradable HMAs

PHB is produced by micro-organisms apparently in response to the conditions of physiological stress. The poly-3-hydroxybutyrate (P3HB) form of PHB is probably the most common type of polyhydroxyalkanoate, but many other polymers of this class are produced by a variety of polymers including poly-4-hydroxybutyrate (P4HB), polyhydroxyvalerate (PHV), polyhydroxyhexanoate (PHH), polyhydroxyoctanoate (PHO) and their copolymers. [84]



PHBV based biodegradable materials are also used to prepare various HMAs. Kauffman Thomas et al. [85, 86] developed a kind of HMA that contained linear polyester of 3-hydroxybutyric and 3-hydroxyvaleric acids, polar tackifier, plasticizer, wax diluent, stabilizer, and compatible polymer. Because the base polymer was derived from naturally occurring polymer and biodegradable copolymer, the HMA prepared was totally biodegradable. Sharak Matthew L. et al. [87] prepared a water sensitive or biodegradable thermoplastic adhesive. The adhesive was composed of biodegradable or water sensitive thermoplastic polymer, sucrose benzoate, plasticizing diluent, wax and antioxidant. They also prepared another biodegradable hot melt adhesives, which were prepared by thermoplastic methylol polyester prepared from the reaction of at least one dicarboxylic acid with a diglycidyl ether, a diglycidyl ester or a combination thereof, compatible tackifier, compatible plasticizer, compatible wax diluent and stabilizer [88].

PEA molecular chain contains both ester and amide bond, both of which are degradable in the microorganisms, enzymes catalytic solutions, so PEA is a good biodegradable HMA base materials. Timmermann Ralf et al. [89] prepared a biodegradable HMA by polyester amides consisting of 30% to 70% by weight aliphatic esters and 70% to 30% by weight amide segments. And Broos Rene et al. [90] offered nine different formulations to prepare biodegradable HMAs. The PEA used in the HMA formulation of the invention includes a short aliphatic dicarboxylic acid functionality and a short symmetrical, crystallizing amide diol functionality.

In order to enhance the property of the HMA, some proper additives are used. Grigat Ernst et al. [91] developed a kind of PEA-based biodegradable HMA. The ester segments of the PEA used consist of oligo-esters with  $M_n = 800 - 1300$  and 2 COOH end-groups obtained by melt condensation of diols with adipic acid; and the amide segments are preferably obtained by reaction of these COOH end-groups with hexamethylene diisocyanate. The ordinary additives such as plasticizers, fire retardants, and/or fillers were mixed into the system.

Besides, Sasaki Shingo et al. [92] prepared a biodegradable HMA. The HMA comprised aliphatic polyester resin, which was obtained by depolymerizing an aliphatic polyester resin. The test results suggested that the HMA had a well

balanced workability such as melt coatability, crushability and adhesion performance. And they synthesized the HMA comprising a polyester-added poly (vinyl alcohol)-poly (vinyl acetate) copolymer that was prepared by adding a terminal carboxyl group-forming aliphatic polyester to a poly (vinyl alcohol)-poly (vinyl acetate) copolymer [93].

### 6.5.3 Natural Polymer Based on Biodegradable HMAs

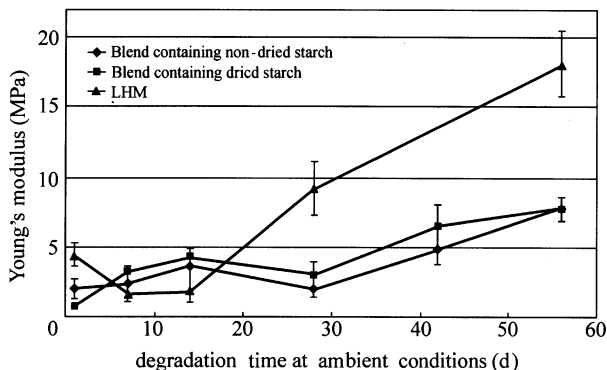
Starch is a fully biodegradable natural polymer, which has a wide variety and a wide range of resources, so it is an ideal natural renewable materials. Depending on the plant, starch generally contains 20% to 25% amylose and 75% to 80% amylopectin. [94]

As the molecular weight of the original starch is very high, original starch does not dissolve in water, but only swell. In order to use starch to prepare HMA, it should be degraded properly and modified. There are three main methods for starch degradation, that is, thermal degradation, acid degradation, biodegradation and oxidation degradation.

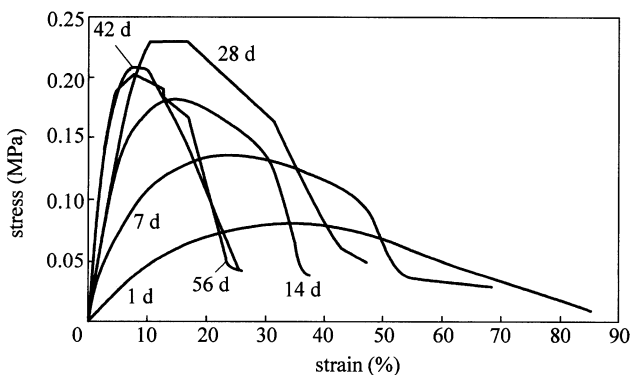
Similar to the PLA and/or PCL HMA, the natural polymer based HMA can also be applied in packaging. Saara Inkinen et al. [81] discussed the stability of blends of a lactic acid-based hot melt adhesive (LHM), oxidized potato starch (dried or nondried) and polyethylene glycol (PEG). Table 6.4 shows the stress and strain at maximum load values of the samples, and Figs. 6.12, 6.13 and 6.14 are several test results. The test results suggest that the HMA can meet the requirements for packaging. Blumenthal et al. [95] successfully prepared a

**Table 6.4** Stress and strain at maximum load values of pure LHM and the starch blends at the ageing periods tested [81]

Test day no.	Blend composition		
	LHM	Blend containing nondried starch	Blend containing dried starch
	Stress at maximum load (MPa) [Strain at maximum load (%)]		
1	0.08±0.01 (53.1±26.3)	0.07±0.00 (34.8±3.6)	0.08±0.00 (34.2±1.5)
7	0.03±0.01 (58.8±28.1)	0.13±0.01 (18.7±2.6)	0.13±0.01 (20.5±4.0)
14	0.04±0.01 (29.0±9.2)	0.17±0.01 (14.8±1.3)	0.18±0.01 (14.2±1.6)
28	0.24±0.05 (23.2±2.6)	0.21±0.01 (12.2±1.1)	0.24±0.02 (11.9±3.2)
42	–	0.20±0.01 (9.8±0.8)	0.20±0.01 (9.3±1.5)
56	0.61±0.06 (16.2±3.2)	0.21±0.01 (8.4±0.9)	0.20±0.01 (8.7±0.9)



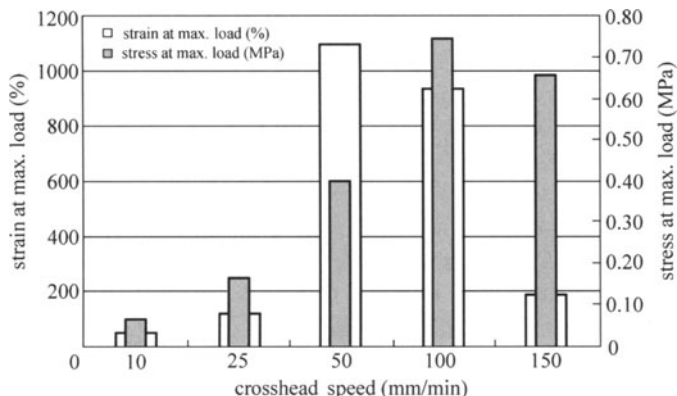
**Figure 6.12** Young’s moduli of pure LHM and starch blends versus degradation time at ambient conditions [81]



**Figure 6.13** Stress-strain curves of the blend containing dried starch [81]

starch-based hot melt that offer a potential alternative of repulpable and/or biodegradable adhesives with lower cost for packaging applications, such as case and carton sealing, bag ending, and roll wrap. The adhesive has excellent balance of hot and cold temperature adhesion properties, excellent repulpability, and comparable performance to conventional HMA.

Jansen, Johannes J. et al. [96, 97] found that a HMA composition could be prepared by mixing a starch product, urea and optionally water. They were mixed with each other to obtain a homogeneous composition, the starch product/urea weight ratio being selected within the range of 3/1 – 3/97 and the amount of water present being 3% – 20% by weight. The mixing process of the adhesive might not be carried out with heating, and the oxidative treatment was omitted. The adhesive of the invention is solid at room temperature but becomes fluid at elevated temperature and is supposed to be utilized in the manufacture of packaging and nonwoven articles.



**Figure 6.14** Stress and strain at maximum load of pure LHM versus crosshead speed [81]

Stein Winfried Chem et al. [98] prepared a HMA that was based on glutin glue, plasticiser optionally and other ordinary additives. The HMA can bond porous materials, especially wood, paper, cardboard or foamed plastics. It is useful in the production of packaging. The constituents of the HMA are not harmful when the bonded articles are recycled and are easily degraded in sewage plant.

Except for the application in the packaging production, the natural polymer based HMAs are also used in other ways. Kauffman, Thomas F. et al. [99] invented a starch based hot melt adhesives for cigarettes. The composition of the adhesive is intermediate or high degree of substitution (DS) starch ester and polar wax, plasticizing diluent, compatible tackifier and antioxidant. Because the HMA invented has sufficient fast-setting and acceptable taste and odor properties, it is used in commercial cigarette filter application. Santamaria Ibarburu et al. [100] used mixtures of starch and ethylene and vinyl acetate copolymer to prepare a HMA for bonding many materials (paper, textile, polyolefins), sealing cracks and fissures and repairing moulds. The mixtures of starch and ethylene and vinyl acetate copolymer (EVA copolymer) comprise natural and/or modified starch in a proportion between 1% and 90% by volume and EVA copolymer in a proportion of between 99% and 10% by volume.

Many researchers have done much work on the natural polymer based HMA. For example, Iovine Carmine et al. [101] prepared the HMA composed of PLA, polar tackifier, plasticizer, wax diluents, stabilizer and starch; Ueda Takashi et al. [102] developed a HMA consisting of a starch paste and starch plasticizer. The adhesive can be used as a water-soluble hot-melt adhesive with high adhesion and water-dissolution rate after the preliminary drying treatment; Miyamoto Yoshihiko et al. [103] prepared a composition of biodegradable HMA that was composed of PVA resin containing oxyalkylene group and starch. Preferably, the components form a sea-island structure and the average particle diameter of the dispersed starch is equal to or small than 10  $\mu\text{m}$ ; Dart Norman K. et al. [104]

provided a method to prepare a hot melt adhesive which contains a major amount of a meltable saccharide, and a minor amount of a polysaccharide that is derived from starch selected from pre-gelatinized converted starches, cold-water soluble dextrans, maltodextrins, and mixtures of more than one of such members of said group; Ishiguro Hideyuki et al. [105] developed a composition of HMA. This adhesive was obtained by mixing crude rosin, natural rubber and one or more vegetable or mineral waxes; Billmers Robert J. et al. [106] prepared a HMA that comprised selected modified starch esters as the main or base adhesive material and non-volatile, polar organic diluent to allow the composition to melt and have a low viscosity at the application temperature.

## Reference

- [1] Eling B., Gogolewski S., Pennings A. J. *Polymer*, 23, 1587 (1982).
- [2] Tsuji H., Smith R., Bonfield W., et al. *J. Appl. Polym. Sci.*, 75, 629 (2000).
- [3] Fambri L., Pegoretti A., Fenner R., et al. *Polymer*, 38, 79 (1997).
- [4] Perepelkin K. E. *Fibre Chem.*, 34, 85 (2002).
- [5] Drumright R. E., Gruber P. R., Henton D. E. *Adv. Mater.*, 12, 1841 (2000).
- [6] Sawyer D. J. *Macromol. Symp.*, 201, 271 (2003).
- [7] Bogaert J. C., Coszach P. *Macromol. Symp.*, 153, 287 (2000).
- [8] [http://www.fitfibers.com/summary\\_pages/PLA\\_fibers\\_s.htm](http://www.fitfibers.com/summary_pages/PLA_fibers_s.htm).
- [9] <http://www.dow.com>.
- [10] Dattilo Jr. P. P., King M. W., Cassill N. L., et al. *J. Textile Appl. Technol. Man.*, 2, 1 (2002).
- [11] King M. W. *Can. Text. J.*, 118, 34 (2001).
- [12] Benicewicz B. C., Hopper P. K. J. *Bioact. Compat. Polym.*, 5, 453 (1990).
- [13] Davis S. S., Illum L., Stolnik S. *Curr. Opin. Colloid. Interf. Sci.*, 1, 660 (1996).
- [14] Reed A. M., Gilding P. K. *Polymer*, 22, 494 (1981).
- [15] Brady J. M., Cutright D. E., Miller R. A., et al. *J. Biomed. Mater. Res.*, 7, 155 (1973).
- [16] Fu B. X., Hsiao B. S., Chen G., et al. *Polymer*, 43, 5527 (2002).
- [17] Chu C. C. *J. Appl. Polym. Sci.*, 26, 1727 (1981).
- [18] Zong X. H., Wang Z. H., Hsiao B. S., et al. *Macromolecules*, 32, 8107 (1999).
- [19] Kulkarni R. K., Moore E. G., Hegyeli A. F., et al. *J. Biomed. Mater. Res.*, 5, 169 (1971).
- [20] Lin J. H., Chang C. W., Lou C. W., et al. *Textile Res. J.*, 74, 480 (2004).
- [21] Lin J. H., Tsai I. S., Hsing W. H. *J. Textile Inst.*, 89, 266 (1998).
- [22] Lin J. H., Chiang S. H., Lou C. W. *J. Adv. Mater. Covina.*, 1, 82 (2006).
- [23] Lou C. W., Yao C. H., Chen Y. S., et al. *Textile Res. J.*, 78, 958 (2008).
- [24] Li X. H., Deng X. M., Huang Z. T. *Pharm. Res.*, 18, 117 (2001).
- [25] Mason M. N., Metters A. T., Bowman C. N., et al. *Macromolecules*, 34, 4630 (2001).
- [26] Hagan S. A., Coombes A. G. A., Garnett M. C., et al. *Langmuir*, 12, 2153 (1996).
- [27] Zhang Y. Z., Lim C. T., Ramakrishna S., et al. *J. Mater. Sci. Mater. Med.*, 16, 933 (2005).
- [28] Cui W., Li X., Zhu X., et al. *Biomacromolecules*, 7, 1623 (2006).



## 6 Application in the Field of Commodity and Industry Product

- [29] Zeng J., Yang L., Liang Q., et al. *J. Control Release*, 105, 43 (2005).
- [30] Ranganath S. H., Wang C. H. *Biomaterials*, 29, 2996 (2008).
- [31] Luu Y. K., Kim K., Hsiao B. S., et al. *J. Control Release*, 89, 341 (2003).
- [32] Maretschek S., Greiner A., Kissel T. *J. Control Release*, 127, 180 (2008).
- [33] Song M., Pan C., Li J., et al. *Electroanalysis*, 18, 1995 (2006).
- [34] Xu X., Yang Q., Wang Y., et al. *Euro. Polym. J.*, 42, 2081 (2006).
- [35] Kim B., Mooney D. J. *Tibtech.*, 16, 224 (1998).
- [36] Gupta B., Revagade N., Atthoff B., et al. *Polym. Adv. Technol.*, 18, 1 (2007).
- [37] Steuer H., Fadale R., Muller E., et al. *Neurosci. Lett.*, 277, 165 (1999).
- [38] Bini T. B., Gao S., Wang S., et al. *J. Mater. Sci.*, 41, 6453 (2006).
- [39] Bhattarai S. R., Bhattarai N., Yi H. K., et al. *Biomaterials*, 25, 2595 (2004).
- [40] Xu C. Y., Inai R., Kotaki M., et al. *Biomaterials*, 25, 877 (2004).
- [41] Fu Y. C., Nie H., Ho M. L., et al. *Biotech. Bioeng.*, 99, 996 (2008).
- [42] Blackwood K. A., Mckean R., Canton I., et al. *Biomaterials*, 29, 3091 (2008).
- [43] Chiu J. B., Liu C., Hsiao B. S., et al. *J. Biomed. Mater. Res.*, 83A, 1117 (2007).
- [44] Ma K., Chan C. K., Liao S., et al. *Biomaterials*, 29, 2096 (2008).
- [45] Yang L. X., Zhao S. Z., Chen X. S., et al. *Acta Polymerica Sinica*, 10, 959 (2007).
- [46] Tan S. T., Wendorff J. H., Pietzonka C., et al. *Chem. Phys. Chem.*, 6, 1461 (2005).
- [47] Zhou H., Kim K. W., Giannelis E. P., et al. *ACS Symposium Series Book*, 918 (2005).
- [48] Khan S. Carbon Nanotube Based Nanocomposite Fibril for Cartilage Regeneration, Drexel University (2002).
- [49] Li D., Frey M. W., Baeumner A. J. *J. Membrane Sci.*, 279, 354 (2006).
- [50] <http://www.thenakedscientists.com/HTML/articles/article/bioplastics/>
- [51] <http://www.smithsonianmag.com/science-nature/plastic.html>. Retrieved on 6 March 2008
- [52] <http://www.cfcup.com/>. Retrieved on 5 February 2009
- [53] Erwin T. H., Karl R., David A., et al. *Polymer Degradation and Stability*, 80, 403 (2003).
- [54] Kalea G., Auras R., Singha S. P., et al. *Polymer Testing*, 26, 1049 (2007).
- [55] Gruber P., O'Brien M. In: Doi Y., Steinbuchel A. (ed.). *Biopolymers in 10 volumes*, volume 4, *Polyesters III Applications and Commercial Products*. Weinheim: Wiley-VCH, 235 (2002).
- [56] ASTM D6400-04. Standard Specification for Compostable Plastics.
- [57] Kale G., Kijchavengkul T., Auras R., et al. *Macromol. Biosci.*, 7, 255 (2007).
- [58] Narayan R. Drivers and rationale for use of biobased materials based on life cycle assessment (LCA). In: *Global Plastics Environmental Conference*, Atlanta (2004).
- [59] Kale G., Auras R., Singh P. *J. Polym. Environ.*, 14, 317 (2006).
- [60] <http://www.foodservicewarehouse.com/going-green/c11836.aspx>, Retrieved on 5 February 2009
- [61] <http://www.cupdepot.com/pla-material-info.html>, Retrieved on 5 February 2009
- [62] Anders Soedergaard, Maria Niemi, Johan-Fredril Selin. *Industrial & Engineering Chemistry Research*, 34, 1203 – 1207 (1996).
- [63] Scott G., Gilead D. *Degradable Polymers*. London: Chapman &Hall, 43 (1995).
- [64] Fried J. *Polymer Science and Technology*. NJ: Prentice-Hall Inc., 140, 241-2, 246-9 (1995).

## **Biodegradable Poly(Lactic Acid): Synthesis, Modification, Processing and Applications**

- [65] Viljanmaa M., Sodergard A., Tormala P. *International Journal of Adhesion & Adhesives*, 22, 447 (2002).
- [66] Viljanmaa M., Sodergard A., Mattila R., et al. *Polymer Degradation and Stability*, 78, 269 (2002).
- [67] Viljanmaa M., Sodergard A., Tormala P. *International Journal of Adhesion & Adhesives*, 22, 219 (2002).
- [68] Viljanmaa M., Sodergard A., Tormala P. *International Journal of Adhesion & Adhesives*, 23, 151 (2003).
- [69] Choi Won Y., Lee Chong M., Park Hyun J. *LWT*, 39, 591 (2006).
- [70] Invine Carmine P., Kauffman Thoman F., Schoenberg Jules E., et al. US Patent, US5252646A.
- [71] Edgington Carry J., Ryan Christopher M. US Patent, US6365680B1.
- [72] Edgington Carry J., Ryan Christopher M. US Patent, US5753724A.
- [73] Ho Sze-Man, Young Anne M. *European Polymer Journal*, 42, 1775 (2006).
- [74] Gilad Lando, Daniel Cohn. *Journal of Materials Science: Materials in Medicine*, 14, 181 (2003).
- [75] Ferreira P., Antonio F. M. Silva, Pinto M. I., et al. *Journal of Materials Science: Materials in Medicine*, 19, 111 (2008).
- [76] Nies Berthold, Schilke Frank, Daum Ludwig. Germany Patent, DE10358779.
- [77] Yang Ming, Ren Tianbin, Gu Shuying, et al. *China Adhesives*, 16, 1 (2007).
- [78] Mikael Stolt, Mikko Viljanmaa, Anders Sodergard, et al. *Journal of Applied Polymer Science*, 91, 196 (2004).
- [79] Kitamura Tadashi, Doi Kiyoto, Kawasaki Eiichi, et al. Japan Patent, JP05339558A.
- [80] Harlan Robert D., Hatfield Stephen F., Samuel Johnson K., et al. US Patent, US5952405.
- [81] Saara Inkinen, Mikael Stolt, Anders Sodergard. *Journal of Applied Polymer Science*, 110, 2467 (2008).
- [82] Lewis David Neal, Schutte Gerrit, Westerhof Henk, et al. Europe Patent, EP1236753.
- [83] Lewis David Neal, Schutte Gerrit, Westerhof Henk, et al. US Patent, US7465770.
- [84] Steinbüchel Alexander. *Polysaccharides and Polyamines in the Food Industry (10 Volumes with Index)*. Wiley-VCH (2002).
- [85] Kauffman Thomas, Brady Francis X., Puletti Paul P., et al. Europe Patent, EP0553394.
- [86] Kauffman Thomas, Brady Francis X., Puletti Paul P., et al. US Patent, US5169889.
- [87] Paul Charles W., Sharak Matthew L. US Patent, US5574076.
- [88] Sharak Matthew L., Paul Charles W., Ray-Chaudhuri Dilip. US Patent, US5583187.
- [89] Timmermann Ralf, Grigat Ernst, Schulz-Schlitte Wolfgang. Germany Patent, DE19615899.
- [90] Cyberlink Corp. US Patent, US2010080384(A1).
- [91] Grigat Ernst, Dipl Chem D. R. Germany Patent, DE4234305A1.
- [92] Sasaki Shingo, Kamimura Tomohisa, Ueda Atsuko. Japan Patent, JP2004131675.
- [93] Sasaki Shingo, Kamimura Tomohisa, Miyake Munehiro. Japan Patent, JP2002088334.
- [94] Brown W. H., Poon T. *Introduction to Organic Chemistry (3<sup>rd</sup> Ed.)*. John Wiley & Sons Inc., (2005).
- [95] Blumenthal M., Paul C. W. *Tappi Journal*, 77, 193 (1994).
- [96] Jansen Johannes J., Veen Uko, Legters Johan. US Patent, US5454862.
- [97] Jansen Johannes J., Veen Uko, Legters Johan. Europe Patent, EP0609952.

## 6 Application in the Field of Commodity and Industry Product

- [98] Stein Winfried Dipl Chem, Engelbrecht Christoph R. Germany Patent, DE4225465.
- [99] Kauffman Thomas F., Wieczorek Jr. Joseph, Hatfield Stephen F. US Patent, US5498224.
- [100] Univ. Pais Vasco. Spain Patent, ES2112192.
- [101] Invine Carmine P., Kauffman Thoman F., Schoenberg Jules E., et al. US Patent, US5312850A.
- [102] Ueda Takashi, Takagi Shigeyuki. Japan Patent, JP2003020463.
- [103] Miyamoto Yoshihiko, Oohayashi Kazumichi. Japan Patent, JP04145181A.
- [104] Darp Norman K., Herenstreit William E., Hou Kwang-Chung. WIPO Patent, WO9222606.
- [105] Ishiguro Hideyuki, Tanaka Reiko. Japan Patent, JP07278510.
- [106] Billmers Robert J., Paul Charles W., Hatfield Stephen F., et al. US Patent, US5360845.

## 7 Application in the Field of Biomedical Materials

**Abstract** Much effort is currently being devoted to the development of biodegradable materials (such as PLA) for biomedical applications, such as tissue engineering scaffold, controllable drug delivery, bioabsorbable surgical sutures, soft tissue augmentation and mesh insertion for Groin Hernia repair. In this chapter, basic design principles for tissue engineering is briefly introduced and PLA materials and its modification for the application in tissue engineering scaffold and preparation methods of tissue engineering scaffold are discussed. Then a brief review of a modification method is made in which a biodegradable moiety (such as PLA) is incorporated into the molecular structure of functional polymers by different ways so that the biodegradability of the polymer obtained can be controlled.

**Keywords** biomedical material, biomedical application, compatibility, tissue engineering scaffold, controllable drug delivery, bioabsorbable surgical sutures

### 7.1 Tissue Engineering Scaffold

Tissue engineering is an interdisciplinary field that applies the principles and methods of engineering and life sciences toward the fundamental understanding of structure-function relationships in normal and pathological mammalian tissue and the development of biological substitutes that restore, maintain, or improve tissue function or a whole organ [1]. In tissue engineering technique, a 3-dimensional scaffold is critical to guide cell attachment and provide physical support for the formation of new three-dimensional tissue. In this chapter, we will firstly introduce basic design principles for tissue engineering. Then, we will discuss the PLA materials and modification for the application in tissue engineering scaffold. Finally, the preparation methods of tissue engineering scaffold are briefly reviewed.

#### 7.1.1 Design Principles of Tissue Engineering Scaffold

Scaffolds play a crucial role in tissue engineering applications. To design and prepare an appropriate scaffold, certain properties and factors must be taken into account [2]. The scaffold must also have certain physical characteristics in order to act temporary ECM and induce tissue growth. Porosity and pore size are

important physical characteristic.

A scaffold has to have high porosity and proper pore size [3 – 5]. The porosity should be maximal while not compromising the mechanical properties, and a suggestion of the porosity exceeding 90% has been made [6]. The pore size should be large enough to support cell migration and tissue ingrowth throughout the whole scaffold volume. Only a highly interconnected pore network can favor cell growth and flow transport of nutrients and metabolic waste. It can be expected that the rate and distribution of tissue ingrowth through the scaffold will be affected by the size and number of interconnecting channels. These requirements need that the materials for tissue engineering application should be easy to fabricate into a desired shape and have controlled pore architecture. The scaffolds also should be mechanically stable to keep their predesigned tissue structure during the tissue regeneration.

The materials for tissue engineering scaffolds should have controlled biodegradability or bioresorbability, so that scaffolds will be eventually replaced by the tissue [6]. It also should be safe and biocompatible, that is, no adverse inflammatory or immune response and no cytotoxicity to the cells and the degradation products should be non-toxic and easily resorbed in vivo through natural pathways by the action of living things, such as cellular activity or excreted by metabolic pathways. At last, the scaffold should positively interact with cells including enhanced cell adhesion, growth, migration, and differentiated function.

### 7.1.2 PLA Materials and Modification for Tissue Engineering Scaffold Application

The scaffolds for tissue engineering should be fabricated from biocompatible polymers that do not have the potential to elicit an immunological or foreign body reaction. The chosen polymer can degrade at a controlled rate in concert with tissue regeneration. The degradation products should not be toxic and must be easily excreted by metabolic pathways. Mechanical properties of the scaffold at various scales can determine the mechanotransduction within the developing tissue, and thereby the suitability of a particular scaffold for a particular tissue engineering application.

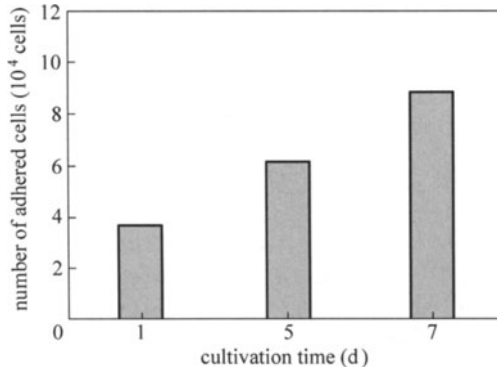
Synthetic polymers are that they are reproducible at large-scale production with consistent properties of strength, degradation rate, microstructure and their properties can be tailored for specific application. Therefore, synthetic biodegradable polymers have already been widely used as scaffolds for tissue engineering [7 – 11]. The most common of these polymers are the biodegradable polyesters, such as PLA, PGA and their copolymer (PLGA) that have been widely used in biomedical fields due to their good biodegradability, high mechanical properties and excellent processing properties [12 – 20]. These

polymers remain popular for a variety of reasons including the fact that these materials have properties that allow hydrolytic degradation through de-esterification [21]. Once degraded, the monomeric components of each polymer are removed by natural pathways: glycolic acid can be converted to other metabolites or eliminated by other mechanisms, and lactic acid can be cleared through the tricarboxylic acid cycle [22]. Thus, the body already contains highly regulated mechanisms for completely removing residual traces of the polymers. Due to these properties, PGA and PLA have been used in products such as degradable sutures for several decades and both have received approval for use by the U.S. Food and Drug Administration (FDA) [23]. Some studies have even indicated that these materials may not actively provoke an immune response since they lack peptide bonds [24]. One potential concern, however, arises from the local pH changes that can occur upon degradation due to the acidic nature of both the glycolide and lactide monomers.

Early work with polyester materials held much promise for cartilage tissue engineering. Cima et al. developed the first protocols for seeding chondrocytes onto degradable polymer meshes [25]. These meshes would act as scaffolding to support cell attachment and allow the chondrocytes to begin synthesizing cartilaginous extracellular matrix molecules. To further investigate the potential of polyesters in repairing cartilage defects, Vacanti et al. performed an expanded *in vivo* study on rabbits, Chondrocytes were extracted from rabbit hyaline cartilage, seeded onto 100  $\mu\text{m}$  thick nonwoven PGA meshes with 75 – 100  $\mu\text{m}$  interfiber spacing, and allowed to incubate in tissue culture conditions for 1 week [26]. Cartilage defects were then created in the knees of rabbits. After 7 weeks, neocartilage were observed in almost all of the experimental grafts. Within the control groups, only small amounts of fibrocartilage could be detected. Therefore, the thin PGA sheet was successful as a matrix for allowing chondrocytes an opportunity to resurface a cartilage defect in an articulating joint.

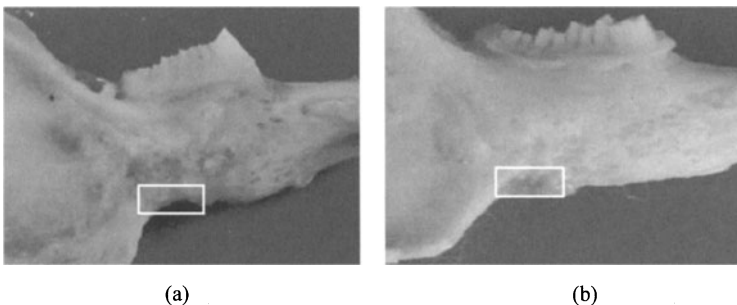
PLGA as the copolymers of PLA and PGA is a desirable and very attractive polymer due to the controllable hydrophilicity/hydrophobicity and degradation rate. It is one of the most commonly used biodegradable polymers and has been utilized for the regeneration of various tissues and organs including bone [27] and liver [28]. Ren et al. used PLGA scaffolds to fabricate *in vitro* tissue engineering bone and explored the potential to repair the mandibular defect using a rabbit model [29]. Firstly, the rabbit mesenchymal (MSC) stem cells were seeded to the polymer scaffold. The MSCs began to attach to the pore surface of the scaffold and grow 6 h after seeded into the scaffold. But only a fraction of cells could be attached to the polymer scaffold, and more MSCs were exuded from the pore of scaffold. After 1 day's culture, 37% of cells compared to initial seeding were attached to the scaffold (Fig. 7.1). Two days later, cells began to congregate on some area. After 7 days' culture, the number of cells was much more than 2 times that after 1 days' culture. Some small granules of calcification

could be seen within 2 weeks throughout the extracellular matrix and the degree of mineralization was increased with time.



**Figure 7.1** The numbers of MSCs attached in the PLGA scaffold with different times [29]

After the MSCs cultured, the scaffold was implanted into the mandibular defect site in rabbit. After 6 weeks of healing, some polymer still existed in defect site. After 12 weeks, polymer was completely degraded and absorbed, and no remnant of polymer was visible in the connective tissue (Fig. 7.2). The defect also had been completely filled with new bone for the PLGA/MSCs scaffolds group after 12 weeks. However, for the blank group (without scaffold), bone defect remains. So, the PLGA scaffolds fabricate in vitro tissue engineering bone with MSCs had demonstrated potential to offer an effective method for treating mandibular defects and other bone defects.



**Figure 7.2** The macroscopic analysis of bone defect repair: (a) the bone defect still remain after 12 weeks of healing for the blank group (without scaffold); (b) the defect has been filled with new bone for the PLGA/MSCs scaffolds group [29]

However, no single material can satisfy all the goals required for creating optimal scaffolding. For PLA, several drawbacks would be potential problems for further tissue engineering applications. Such as, the strong hydrophobicity

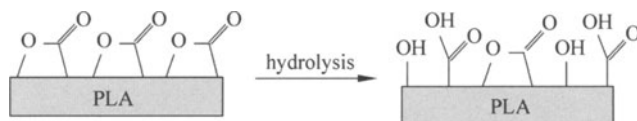
because of the lack of hydrophilic groups on its surface leads to its poor cell affinity; absence of suitable functional groups for covalently coupling with bioactive molecules restricts its application in tissue engineering [30, 31]; increased acidity of PLA during degradation causes serious inflammation and swelling. Therefore, in recent years, many research groups have focused on the chemical modifications of PLA attempting to overcome these drawbacks.

### 7.1.3 Surface Hydrophilicity Modifications

Several surface modification techniques have been developed to improve the wetting of PLA surfaces by introducing a variety of polar groups such as hydroxyl, carboxyl, amino and sulfate groups on polymer surfaces.

Plasma is a high-energy state of matter, in which a gas is partially ionized into charged particles, electrons, and neutral molecules. Plasma can provide modification of a polymer surface without using solvents or generating chemical waste. Different polar groups can be conveniently introduced to the surface of PLA using different reaction gases such as air,  $\text{NH}_3$ ,  $\text{SO}_2$ ,  $\text{CO}_2$  or other organic compounds [32 – 41]. The polar groups greatly improve hydrophilicity and biocompatibility of PLA surface. However, as-introduced groups show a tendency to rearrange over a period of time, thus the effect of plasma treatment is non-permanent.

Surface alkali hydrolysis treatment is also a convenient method to modify PLA polymer surface [42 – 47]. In general, biodegradable aliphatic polyesters, such as PGA and PLA, contain ester bonds. The polymer film or scaffolds are immersed into aqueous NaOH solution. The ester bonds at the surface can be hydrolyzed and results in the generation of carboxylic acid and hydroxyl groups at the polymer surface.



**Figure 7.3** Schematic illustration of alkali hydrolysis of PLA substrate

The hydrophilicity of the polymer is increased by introducing these carboxyl and hydroxyl groups, which can theoretically lead to better cell adhesion during seeding. Such as, Nam et al. [42] reported that the surface modification of PLGA and poly (*D,L*-lactic acid) in the NaOH solution could moderate the surface of the polymers and promote the adhesion of hepatocytes. Gao et al. [44] stated that the surface hydrolysis of PGA meshes in the NaOH solution could increase the attachment ability of vascular smooth muscle cells. However, strong alkali treatment is accompanied with extended bulk degradation of the polyester, and

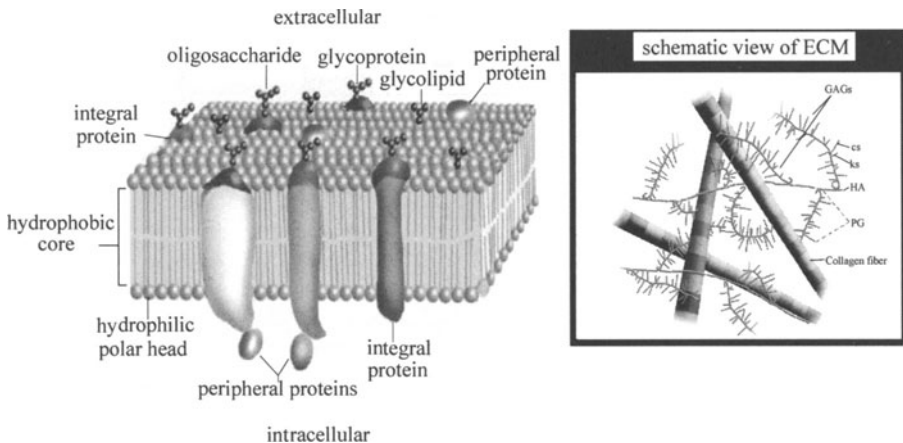


the residual alkali is not easily removed except by rinsing. It was shown that a mild alkali treatment could not break the ester bonds effectively in a short time.

Photo-induced grafting is another useful technique for the surface modification having advantages such as low cost of operation, mild reaction conditions, selectivity of UV light absorption without affecting the bulk polymer and permanent alteration of the surface chemistry [48]. Using this method a variety of polar groups could be introduced onto PLA film surface with relative ease [48 – 52]. The photoinduced grafting process generally consists of two steps. First, the PLA surface is activated to introduce surface radicals from where the photopolymerization of selected monomer would be initiated. Second, the polymerization of the selected monomer on the PLA surface occurs. These processes create peroxide functionalities on the surface, which lead to the formation of surface radicals.

### 7.1.4 Biomimetic ECM Modification

The extracellular matrix (ECM), surrounding cells in the body and comprised of a natural web of protein and polysaccharides, not only physically supports cells but also plays important functions to regulate cellular activities such as cell survival, migration, proliferation, and differentiation [53, 54].



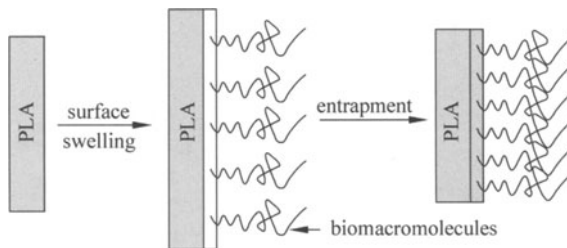
**Figure 7.4** Scheme of cell surrounding with the extracellular matrix in vivo; and the structure and component of the extracellular matrix

Therefore, as a temporary ECM for regenerative cells, scaffold needs to be developed for in vitro tissue reconstruction as well as for cell-mediated tissue regeneration in vivo. Although the hydrophilicity is improved by introducing polar groups onto the surface of PLA materials and the cell spread on materials,

it is not enough for PLA scaffold to play as an ideal ECM substitute. To serve as the temporary ECM for regenerative cells, scaffold must emulate certain advantageous features of natural ECM. As a result, biomimetic ECM modifications have been widely used to improve the cell biocompatibility of biomaterials [55 – 59].

So-called biomimetic ECM modification method is to engineer a component of ECM into synthetic substrate surfaces to generate biomimetic ECM surfaces. Due to the absence of functional groups at PLA materials, many groups have investigated methods for modifying the surface chemistry of these polymers and covalent grafting of ECM. Common approaches involve introducing reactive groups on existing polymer surfaces (surface hydrophilicity modifications).

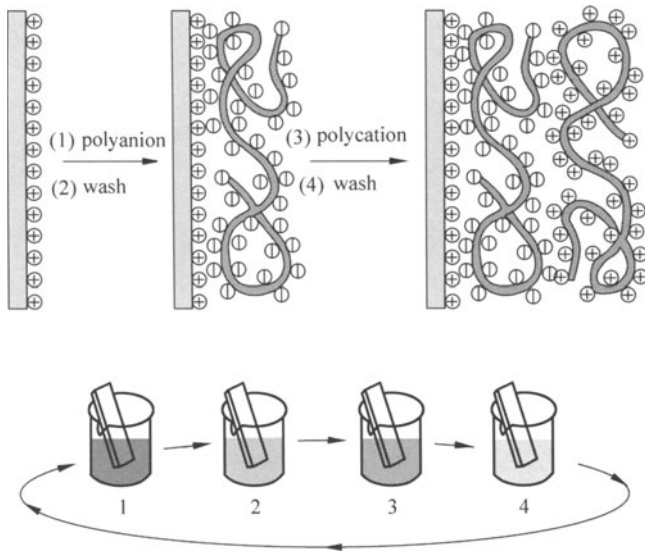
Wang et al. firstly used oxygen and ammonia plasma to treat poly (*D,L*-lactide) and then collagen treatment [60]. Effects of different modification methods including plasma treatment, collagen coating and combining plasma treatment with collagen anchorage have been investigated and compared. The results show that the hydrophilicity is improved and surface-free energy is reduced after the modification. The cell test results also indicate that cell affinity of PDLA modified by combining plasma treatment with collagen anchorage is greatly improved.



**Figure 7.5** Entrapment methods to immobilize the component of ECM on PLA material surface

The entrapment method, initially invented by Desai and Hubbell, appears promising to modify biomaterial surfaces to improve their hydrophilicity [61, 62]. With this method, the biomaterial surface can be non-covalently but stably modified with water-soluble polymers. The sketch map of this method is presented in Fig. 7.6. A PLA sample is immersed in an ECM solution in a solvent mixture (e.g., a good solvent of PLA and a non-solvent of PLA). Then PLA is moved to a non-solvent of the scaffold material. The ECM is successfully immobilized (entrapped) on the surfaces of PLA. The immersion of PLA in the ECM solution in the solvent mixture makes the PLA surfaces swelled to a certain extent, allowing the ECM molecules to at least partially penetrate into the swelled pore surfaces. The immersion in the non-solvent afterwards makes the porous PLA surfaces solidified, resulting in the entrapment of the ECM molecules

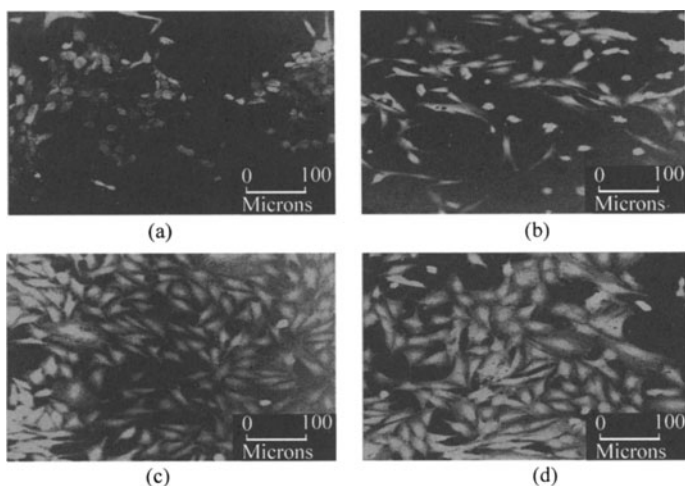
and formation of biomimetic ECM coating on the surface of PLA. This is a facile and permanent surface modification technique for PLA. This technique has been used to promote the cytocompatibility of polylactide by introducing different ECM or ECM-like molecules [63 – 68]. Most of the modifications of the polyester are evaluated by culturing osteoblast or chondrocytes. These ECM molecules could enhance osteoblast or chondrocyte adhesion, proliferation and function to a certain extent.



**Figure 7.6** Scheme of electrostatic assembly on a charged solid substrate by alternate adsorption of oppositely charged polyelectrolytes

The self-organization of polymers has been increasingly explored for the preparation of well-defined surfaces and interfaces in recent years [69 – 71]. Among these methods, ‘Electrostatic self-assembly’ coating has become a new and general way to functionalize polymer surfaces, which is based on the alternating physisorption of oppositely charged polyelectrolytes and represents a new, alternative solution for biomaterial coating [72 – 75]. The buildup is easy and the procedure can be adapted to almost any type of surface as long as surface charges are present. Since the components of the ECM are mostly charged protein and polysaccharide, the ECM or ECM-like molecules multilayer film coating could be formed on the PLA surface via this method. LBL method and the alternating physisorption of ECM molecules could generate a dense ECM coating on PLA surface and eliminate the effect of the bulk material surface. The layer-by-layer assembling applied for biomedical uses ensures not only the immobility of a biopolymer, but also its remarkable nanoscale control that can be exercised over the properties of the films i.e. their thickness, roughness, wettability

and swelling behavior by altering assembling conditions such as pH, ionic strength, polymer functionality and polymer concentration [76–78]. Recently, many groups used the ECM or ECM-like molecules multilayers to control cell adhesion [79–83]. Ji et al. constructed ECM-like biomacromolecule multilayers on a PLA surface [84]. PLA substrates were firstly activated with poly(ethylenimine) to obtain a stable positively charged surface. Then, polyelectrolytes such as alginate and poly (*L*-lysine) were alternately deposited onto the activated PLA substrates. The *in vitro* chondrocyte test indicates that the cell on the gelatin assembly PDLA substrate is spreading uniformly and completely covers the substrate surface, which is also similar with the chondrocyte on the TCPS substrate.



**Figure 7.7** Confocal laser scanning microscopy (CLSM) images of chondrocytes on different matrices: chondrocytes on (a) PDL-LA virgin substrate, (b) PEI-activated PDL-LA substrate, (c) PEI/gelatin multilayer modified PDL-LA substrate, and (d) tissue-culturing polystyrene [84]

### 7.1.5 PLA/Apatite Composite

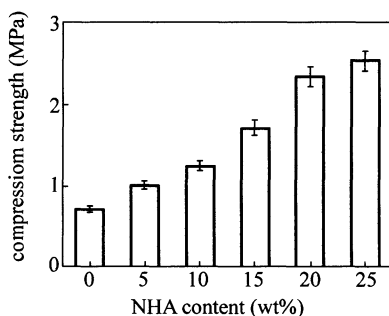
The cell biocompatibility problem of PLA materials can be resolved by Biofunctional modifications. However, such polymers on their own are too weak to be used in load bearing situations and not generally considered osteoinductive. PLA molecules would lower the *in situ* pH level, which raises difficulties in controlling its degradation rate and may induce an inflammatory reaction. In addition, PLA materials tend to be too flexible and of insufficient strength to meet the mechanical demands as hard tissue replacement.

Apatite, as an inorganic component of bone, has sufficient biocompatibility, high strength and excellent corrosion resistance [85–87]. Ceramics are very

brittle and difficulty to fabricate [88]. Therefore, development of composite scaffold materials is attractive because of their advantageous properties with combination of osteoconductive and high strength of bioceramics and the mechanical resilience and processing properties of polymers.

Among the composite, PLA or PLGA/calcium phosphate composites have been most extensively studied [89–93]. With the addition of calcium phosphate in composites not only the mechanical strength is improved, but also a more stable pH value than that for plain PLA or PLGA can be achieved; the acidic degradation byproducts of the PLA or PLGA is buffered by the calcium phosphate.

Ren et al developed a nano hydroxyapatite NHA/PLGA composite scaffold using thermally induced phase separation method and studied the effect of NHA on the mechanical properties of the scaffold [94]. Results suggest that by addition of inorganic component the compression strength of scaffolds is much improved and the compression strength of scaffolds increases with the increase in NHA contents as shown in Fig. 7.8. The compression strength of PLGA scaffold without NHA is 0.72 MPa, while the compression strength of PLGA scaffold with 25% NHA can reach 2.53 MPa.

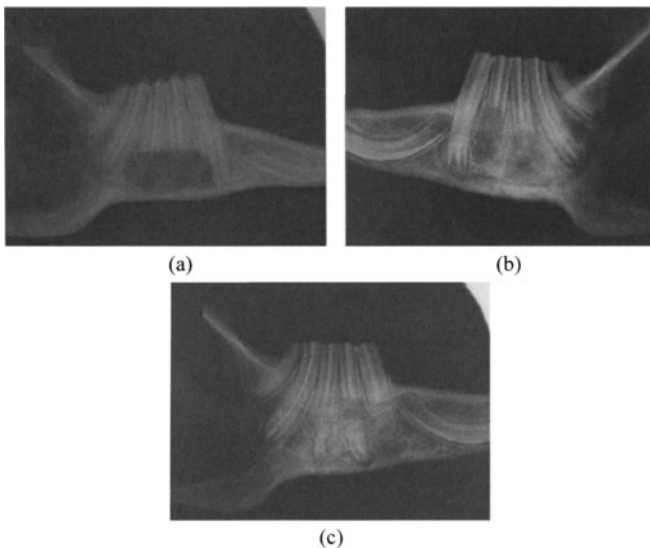


**Figure 7.8** Compression strength of PLGA/NHA scaffolds with different NHA contents [94]

Ren et al. also studied the cytotoxicity of PDLA/NHA composite using the cell relative growth rate (RGR) method and cell direct contact method [95]. Results indicate that the cytotoxicity of these scaffolds is rated grade I according to ISO 10993-1 and the PDLA/NHA composites show better hydrophilic ability, enhanced mechanical properties and excellent biocompatibility than PDLA materials. The inflammatory response of tissue after implanting, which may be caused by degradation products was also alleviated by introducing NHA in PDLA polymer matrix. So PLA/NHA nanocomposites are very attractive in tissue engineering field.

Ren et al. further demonstrated the osteogenic capabilities of cultured MSCs in PLGA/NHA composites scaffold using a rabbit mandibular defect model [96].

Polyethyleneimine (PEI) was used to create active groups on the poly (lactide-coglycolide)/nano-hydroxyapatite (PLGA/NHA) surface and Arg-Gly-Asp (RGD) was grafted on the active groups. Rabbit bone marrow stromal cells (MSCs) were seeded in the scaffolds materials and cultured for 3 days in vitro and then transplanted into the mandibular defect to regenerate the holes. The mandibular defect regeneration was observed with X-ray photography. Figure 7.9 shows the X-ray photograph of rabbit mandibular defect and the regeneration after repairing 12 weeks with both scaffolds. The dark area is the defect position and the white area is the original bone and the new bone formation from the implanted materials. It can be seen that the original defects are filled with new bone formed from cells/scaffolds constructs. There are still dark holes in the bone, but there is very uniform white area, which indicates the formation of the bone in the defect position. This demonstrates that mandibular defect implanted with PLGA/NHA-RGD scaffold is repaired more quickly than that implanted with PLGA/NHA during the 12 weeks. It can be concluded that the PLGA/NHA-RGD shows better ability to repair the bone defect.



**Figure 7.9** X-ray photography of rabbit mandibular defect after repairing 12 weeks with PLGA/NHA scaffold (b) and PLGA/NHA-RGD scaffold (c) and before implanting scaffolds (a)

### **7.1.6 Preparation of Tissue Engineering Scaffolds**

Fabrication technologies are critically important for tissue engineering in designing scaffolds. The scaffolds should have appropriate porosity, pores size

and pore structure, that is three-dimensional and interconnected macroporous network for cell growth and flow transport of nutrient metabolic waste. Different processing methods have been developed to fabricate interconnected porous PLA scaffolds. Some representative methods are reviewed in the following section.

### 7.1.7 Thermally Induced Phase Separation

Thermally induced phase separation (TIPS) technique is a versatile method to prepare porous biomaterials because different porous structures can be obtained by adjusting thermodynamic and kinetic parameters. This technique is based on the phase separation of a homogeneous polymer solution into polymer-rich and polymer-lean phases by changing the polymer solubility through changes either in temperature or solvent composition in the system. The final porous material contains a continuous rigid structure resulted from the polymer-rich phase, and a porous structure that is resulted from drying the polymer-lean phase [97, 98]. However, usually the scaffolds formed from this method have a pore size of 10–100  $\mu\text{m}$ . Using a coarsening process in the later stage of thermally induced phase separation, macroporous scaffolds with a pore diameter of greater than 100 $\mu\text{m}$  can be prepared [99].

### 7.1.8 Solvent Casting/Particulate Leaching

Solvent casting/particulate leaching is a simple and most commonly used method for fabricating porous biomaterials [100, 101]. The following steps are used to prepare a 3D porous polymer matrix by this method: (1) Add a water-soluble porogen, such as NaCl particles, to a polymer solution; (2) Evaporate solvent in air and vacuum; (3) Immerse the polymer/salt composite in distilled water to leach out the salt; (4) Dry the salt-free polymer and obtain a porous structure. This method has advantages of simple operation, easy control of pore size and porosity by salt/polymer ratio and particle size of the added salt. With 70 wt% salt and above, the pores exhibit high interconnectivity. However, the difficulty of removing soluble particles from the inside of a polymer matrix makes it hard to fabricate very thick 3D scaffolds [102]. The solvent casting/ particulate leaching method is seldom used to prepare polymer/ceramic scaffolds. A novel method has been developed to prepare composite scaffold with highly interconnected macroporosity through the process of particle fusion and particle leaching. In the method, the porogen is partially fused together prior to create a continuous polymer matrix [103].

### **7.1.9 Gas Foaming**

To eliminate the necessity to use organic solvents and solid porogens a technique with using gas as a porogen has been developed. This process involves the following steps: (1) saturate solid polymer discs with CO<sub>2</sub> by exposure to high pressure CO<sub>2</sub> gas. (2) Reduce the solubility of CO<sub>2</sub> in the polymer by rapidly decreasing the CO<sub>2</sub> gas pressure to atmospheric level and induce the thermodynamic instability of CO<sub>2</sub> dissolved in the polymer matrix. (3) Form polymer sponges with large pores due to nucleation and growth of gas cells in the polymer matrix.

Another approach to use gas as a porogen has been recently developed. The method involves both gas foaming and particulate leaching. The latter method is preferred because it does not result in the creation of a nonporous outer skin.

#### **(1) Emulsification/Freeze-Drying**

The use of a solid porogen like SCPL is not required in this technique. First a synthetic polymer is dissolved into a suitable solvent (e.g., polylactic acid in dichloromethane), then water is added to the polymer solution and the two liquids are mixed in order to obtain an emulsion. Before the two phases can separate, the emulsion is cast into a mold and quickly frozen by means of immersion into liquid nitrogen. The frozen emulsion is subsequently freeze-dried to remove the dispersed water and the solvent, thus leaving a solidified, porous polymeric structure. While emulsification and freeze-drying allows a faster preparation if compared to SCPL, and the time consuming leaching is not required, the use of solvents is still necessary, moreover pore size is relatively small and pores are often irregular. Freeze-drying by itself is also a commonly employed technique for the fabrication of scaffolds. In particular it is used to prepare collagen sponges: collagen is dissolved into acidic solutions of acetic acid or hydrochloric acid, then the solution is cast into a mold and frozen with liquid nitrogen to lyophilize.

#### **(2) CAD/CAM Technologies**

Since most of the above described approaches are limited to control porosity and pore size, computer assisted design and manufacturing techniques have been introduced to tissue engineering. First a three-dimensional structure is designed by using CAD software, then the scaffold is realized by using ink-jet printing of polymer powders or through Fused Deposition Modeling of a polymer melt.

#### **(3) Electrospinning Method**

Electrospinning is a polymer processing technique that has been revitalized with the advent of tissue engineering. The working principle of the technique involves applying a high-voltage electric field (of the order of 1 – 10 kV) between a metallic capillary containing a desired polymer solution/melt and a collecting electrode (usually a conductive plate) electrically grounded. When the electrical field overcomes the resistance of the surface tension of the polymer solution, the electrically charged solution is ejected from the capillary towards the counter electrode. The polymer solution jet stretches under the action of the electrostatic force and produces long and thin fibers. In practice, the polymer



solution is electrospun from a flat-ended needle of a syringe whose shaft is actuated by a programmable syringe pump that supplies the solution to the needle. In most of the cases reported in the literature, electrospinning is used to prepare mats of fibers to be used as scaffolds for tissue engineering with limited control in porosity and therefore in cell adhesion and growth. Nonetheless electrospinning offers the possibility to tune most geometrical and morphological properties on the entire hierarchy of scales of the scaffolds. Thus, besides controlling the fiber diameter, it is possible, for example, to modify the macro porosity by changing the confluence, the number of layers, or the alignment of the fibers in the network. Micro- and nanoporosity may also exist and be controlled.

## 7.2 Controllable Drug Delivery Based on PLA

### 7.2.1 Introduction to Drug Delivery Based on PLA

Normally, drugs are almost administered orally or injected at a site remote from the target tissue. With the development of more potent drugs, however, it is known that conventional therapeutic systems suffer from many drawbacks including adverse effects, strongly fluctuating drug levels in the body, and poor drug efficacy, so that the concentration, duration, and bioavailability of the pharmaceutical agents can not be controlled. Controlled release technology has been developed to overcome these problems.

The first polymeric devices developed for controlled drug release date back to the early 1960s. At that time, the idea of using degradable polymers as resorbable matrices in medical applications was introduced. In the 1960s, PGA and PLA was recognized as being highly interesting for use in temporary surgical implants and tissue repair [104 – 106]. In the early 1970s Yolles et al. took an innovative step towards controlled drug delivery by achieving sustained release of cyclazocine dispensed in PLA sheets [107, 108]. The following work included the systematic release of narcotic antagonists, fertility control agents, and anticancer drugs [108 – 112]. Furthermore, systems based on PLA were presented for long-term delivery of antimalarial drugs [110], contraceptives [111, 112], and eye drugs [113].

Although many scientists in academia and industry have been focused on the field of controlled drug delivery for the last 50 years, only a few products are available on the market and approved by the FDA of U.S. for use in a biological system [114]. This phenomenon might be caused by high cost and lengthy process of commercialization of a biomedical device. Chemical and physical properties, biocompatibility, purity, and reproducibility of the product must be maintained throughout the manufacturing process, packaging, and storage.

Moreover, regulatory requirements of design, performance, and safety must be considered throughout the development phase of medical devices. The time span for the development of a new drug product from the time of discovery of a new therapeutic substance to its commercial introduction is now likely 10 years or more, compared to an average of 2 years in the 1950s. Because of these limitations, only a limited number of drug delivery systems based on biodegradable polymers have so far been successfully commercialized. Among them, homopolymers and copolymers based on *L*-lactic acid, *D,L*-lactic acid have received great interests in the medical and pharmaceutical field because of their biodegradability and toxicological safety. One example is Lupron Depot; one-month injectable microspheres of PLGA containing leuprorelin acetate (LH-RH agonist) for the treatment of endometriosis and prostatic cancer [115, 116].

Nowadays, drug delivery is becoming an extremely demanding science. The reasons are essentially: (1) the emergence of the more challenging low-molecular-weight molecules and biomacromolecules with either poor aqueous solubility, poor tissue permeation, or both; (2) the increased use of biological materials with poorly understood physical properties or questionable shelf life issues, and (3) the realization that if the portion of the dose responsible for adverse effects could be directed away from sites where they originate, toxic side effects would become less frequent, thus benefiting the therapeutic index. Today's world requires that drug delivery systems be precise in their control of drug distribution and, preferably, respond directly to the local environment of the pathology in order to achieve a dynamic and beneficial interaction with the host pathology or physiology.

### **7.2.2 Science of Controllable Drug Delivery**

In general, the science of drug delivery may be described as the application of chemical and biological principles to control the *in vivo* temporal and spatial location of drug molecules for clinical benefit. Many methods have been developed by scientists in order to maximize drug activity and minimize side effects [117]. Among them, using stimuli-responsive polymers and molecular recognition technology is most known by their excellent properties.

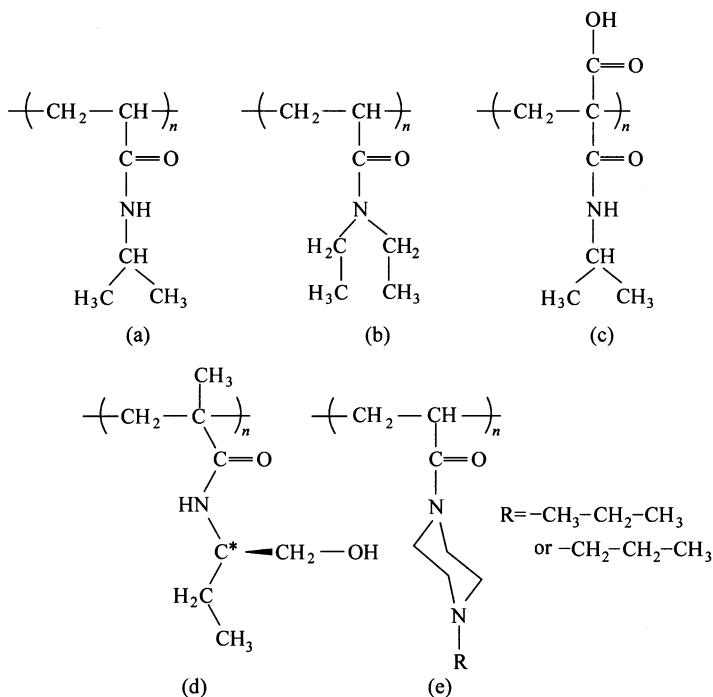
#### **7.2.2.1 Effect of Stimuli-Responsive Polymers**

Stimuli-responsive polymers are defined as polymers that undergo relatively large and abrupt physical or chemical changes in response to small external changes in the environmental conditions. It can provide a variety of applications for the biomedical fields, especially in drug delivery field. These stimuli could be classified as either physical or chemical stimuli. Chemical stimuli, such as pH, ionic factors and chemical agents, will change the interactions between polymer

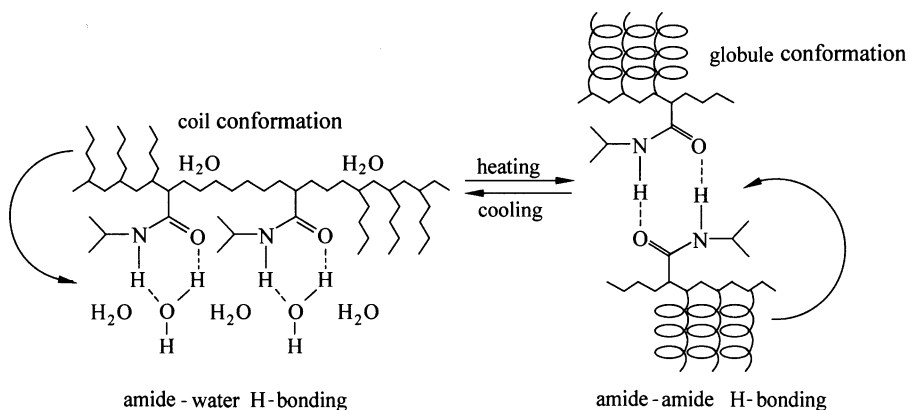
chains or between polymer chains and solvents at the molecular level. The physical stimuli, such as temperature, electric or magnetic fields, and mechanical stress, will affect the level of various energy sources and alter molecular interactions.

Temperature is the most widely used stimulus in environmentally responsive polymer systems [118–123]. The change of temperature is not only relatively easy to control, but also easily applicable both *in vitro* and *in vivo*. One of the unique properties of temperature-responsive polymers is the presence of a critical solution temperature. Critical solution temperature is the temperature at which the phase of polymer and solution (or the other polymer) is discontinuously changed according to their composition. This kind of phase separation or precipitation can occur for amphiphilic polymers as a consequence of an appropriate balance between hydrophilic and hydrophobic moieties. Below a critical temperature at which water is a good solvent for the polymer, the polymer-solvent interactions are stronger than the polymer-polymer interactions. At this point, the water is bound to the hydrophilic moieties through hydrogen bonds, and the presence of hydration water modifies the interaction between hydrophobic moieties so that the polymer exists in an extended “coil” conformation. The solvent quality decreases with increasing temperature, and the polymer-polymer interactions increase due to the hydrophobic interactions. Above this critical temperature, water becomes a poor solvent for the polymer. Here, the hydrogen bonds are disrupted, and water is expelled from the polymer coils, which start to collapse due to the interactions between hydrophobic moieties. This process results in aggregation and formation of compact globules. The temperature at which this phase separation occurs is called as lower critical solution temperature (LCST) or cloud point.

Poly (*N*-substituted acrylamide) is representative of the group of temperature-responsive polymers which have a LCST, defined as the critical temperature at which a polymer solution undergoes phase transition from a soluble to an insoluble state above the critical temperature. Figure 7.10 shows respective *N*-substituted polyamides according to the substitution groups. For example, Poly (*N*-isopropylacrylamide) (PNIPAAm) has a LCST at 32°C, at which it undergoes a reversible volume phase transition caused by the coil-to-globule transition (Fig. 7.11). When we mentioned LCST, it is influenced by hydrophobic or hydrophilic moieties in its molecular chains. In general, to increase the LCST of temperature responsive polymer (e.g., PNIPAAm), this polymer has to be random copolymer with a small ratio of hydrophilic monomers such as *N,N'*-dimethylacrylamide (DMAAm) [120]. In contrast, a small ratio of hydrophobic constituent was reported to decrease the LCST of NIPAAm as well as to increase its temperature sensitivity. What is the most important is that adjustment of LCST near body temperature is essential especially for the drug delivery application.

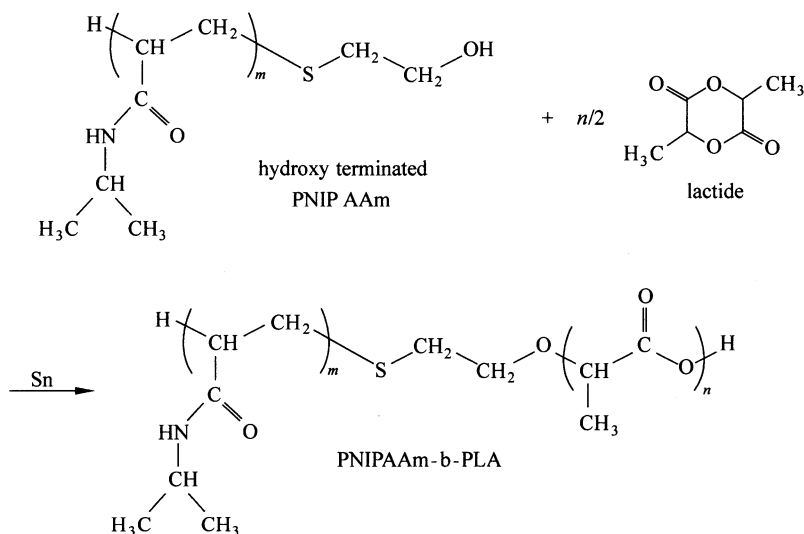


**Figure 7.10** Poly (*N*-substituted acrylamide) showing a LCST (a) Poly (*N*-isopropylacrylamide) (PNIPAAm); (b) Poly(*N,N'*-diethylacrylamide) (PDEAAm); (c) Poly(2-carboxyisopropylacrylamide) (PCIPAAm); (d) Poly(*N*-(*L*)-(1-hydroxymethyl), propylmethacrylamide) (P(*L*-HMPMAAm)); (e) Poly(*N*- acryloyl-*N'*-alkylpiperazine) [124]

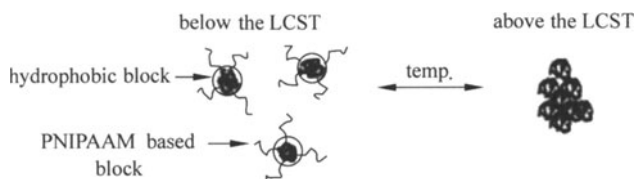


**Figure 7.11** The coil to globule transition of poly(*N*-isopropylacrylamide) (PNIPAAm) at its LCST [125]

PLA has been used as a hydrophobic and biodegradable segment to form temperature sensitive drug delivery system. For example, PNIPAAm-*b*-PLA can be synthesized by ring-opening polymerization of *D,L*-lactide using hydroxy-terminated PNIPAAm as the ring opening agent (Fig. 7.12). When we dissolve the copolymers and drug in elective solvent, a kind of amphiphilic drug-loaded micelles is formed. These micelles are able to undergo reversible thermal transition: when the temperature is below its LCST, micelles are stable, but when above LCST, the micelles are aggregated by the association of the hydrophobic surfaces, then the drug inside is released out (Fig. 7.13).



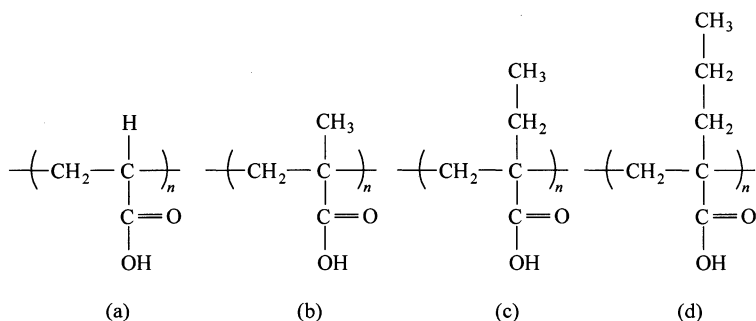
**Figure 7.12** Synthesis of poly (*N*-isopropylacrylamide-*block-D,L*-lactide) [126]



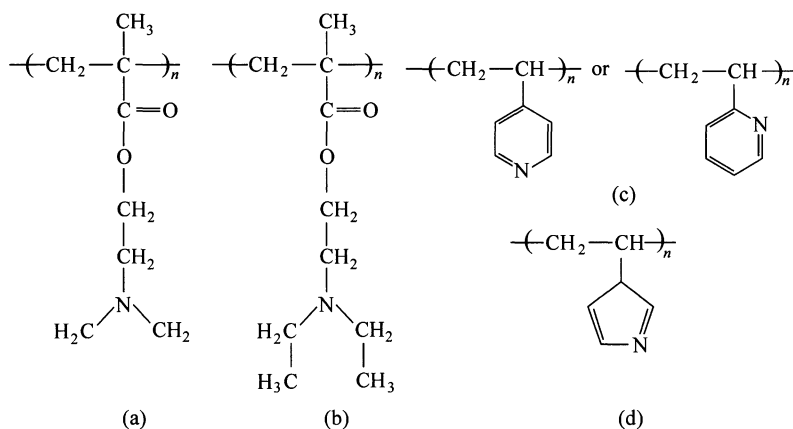
**Figure 7.13** Micellar structure of a block copolymer containing a temperature responsive polymer segment [127]

The pH-responsive polymers consist of ionizable pendants that can accept and donate protons in response to the environmental change in pH. As the environmental pH changes, the degree of ionization in a polymer bearing weakly ionizable groups is dramatically altered at a specific pH that is called pKa. This rapid change in net charge of pendant groups causes an alternation of the hydrodynamic volume of the polymer chains. The transition from collapsed state

to expanded state is explained by the osmotic pressure exerted by mobile counterions neutralizing the network charges [128]. The polymers containing ionizable groups in their backbone form polyelectrolytes in the aqueous system. There are two types of pH-responsive polyelectrolytes; weak polyacids (Fig. 7.14) and weak polybases (Fig. 7.15). The representative acidic pendant group of weak polyacids is the carboxylic group. Weak polyacids such as poly (acrylic acid) (PAA) accept protons at low pH and release protons at neutral and high pH [129]. On the other hand, polybases like poly (4-vinylpyridine) is protonated at high pH and positively ionized at neutral and low pH [130]. Therefore, the proper selection between polyacids and polybases should be considered for the desired application. Hydrophobically modified pH-responsive polymers have a sensitive balance between charged repulsion and hydrophobic interactions. When ionizable



**Figure 7.14** Representative pH-responsive polyacids. (a) PAA; (b) Poly (methacrylic acid) (PMAA); (c) Poly (2-ethyl acrylic acid) (PEAA); (d) Poly (2-propyl acrylic acid) (PPAA)



**Figure 7.15** Representative pH-responsive polybases. (a) Poly (*N,N'*-dimethyl aminoethyl methacrylate) (PDMAEMA); (b) Poly (*N,N'*-diethylaminoethyl methacrylate) (PDEAEMA); (c) Poly (4 or 2-vinylpyridine) (PVP); (d) Poly (vinyl imidazole)

groups are protonated and electrostatic repulsion forces disappear within the polymer network, hydrophobic properties dominate, introducing hydrophobic effects that cause aggregation of the polymer chains from the aqueous environment.

### 7.2.2.2 Effect of Molecular Recognition

Molecular recognition is an event that occurs everywhere in nature. It occurs when two molecules are both geometrically and chemically complementary; that is, when they can both “fit together” spatially as well as bind to each other using noncovalent forces including hydrogen bonds, electrostatic interactions, hydrophobic interactions and weak metal coordination [131]. Examples of this process include the binding of an enzyme to a substrate [132], a drug to a biological target [133, 134], antigen/antibody recognition in the immune system [135, 136].

The most widely recognized system of molecular recognition exists in the immune system of higher order organisms in the form of antigen/antibody recognition. Antibodies are globular proteins that have evolved to express specific binding sites that recognize and capture foreign materials in the bloodstream. These foreign materials, termed antigens, can range from simple proteins to large bacteria and viruses. Antibodies are composed of linear strands of amino acids consisting of two identical “heavy” polypeptide chains (55 kDa) and two identical “light” polypeptide chains (25 kDa) that are linked by disulfide bridges to form a “Y” structure [137]. At the *N*-terminus of the chains lies the variable region that contains an amino acid sequence that can recognize a particular portion of an antigen deemed the epitope.

A reversible antigen responsive polymer network has been obtained by immobilizing antigen and corresponding antibody onto the semi-IPN networks [138]. Antigen (rabbit immunoglobulin G (IgG)) and antibody (goat anti-rabbit IgG) are chemically modified by coupling respective antigen and antibody with *N*-succinimidylacrylate (NSA). The modified antibody monomers are copolymerized with acrylamide. Following this, the modified antigen monomers are then copolymerized with acrylamide and *N,N'*-methylenebisacrylamide (MBAAm) as a crosslinker in the presence of the polymer bearing the antibody, resulting in semi-IPNs containing antigen and corresponding antibody. Additional crosslinks are introduced by the binding between antigen and antibody in the network. The polymerized antibody shows a higher binding constant to the native antigen than to the polymerized antigen. Therefore, the presence of a free antigen causes swelling of the hydrogels by dissociating the non-covalent cross-links induced by the intra-chain antigen-antibody binding because the free antigen replaces the binding of antibody from the polymerized antigen to native antigen. The antigen responsive property can thus be specifically utilized in a drug delivery system.

### 7.2.2.3 Conclusion

The recent advances in the stimuli responsive polymers and their bioconjugates are summarized with a view towards their fundamental molecular designs as well

as their biomedical applications. The application of these “smart polymers” has undergone tremendous progress in the past few decades. Stimuli responsive behaviors of these polymers have attracted our attention as versatile bio-related intelligent systems such as gene or drug delivery, chromatography, microfiltration, actuator, sensor, injectable polymeric matrix, and artificial tissue or organs. The stimuli responsive system has broadened its application into different physical forms such as hydrogels, micelles, surface, and bioconjugates according to their desired applications.

The temperature and pH responsive polymers have been most intensively investigated in various laboratories and industries due to their relatively effective control in vivo as well as in vitro and their versatile application range. The stimuli responsive polymers should be designed at the molecular level before considering the desired applications. The LCST or critical pH ( $\text{pH}^*$ ) should be controlled to match the desired environmentally critical condition after selecting the appropriate polymers. Rapid response to stimuli is another important factor that can be adjusted by designing their molecular structures. Biocompatibility and biodegradability should be considered when these polymeric systems are applied into the physiological environment such as drug delivery system. Incorporating a biodegradable moiety (such as PLA) into the molecular structure of stimuli responsive polymers by different ways could control the biodegradability [139], which ranges from one day to long term depending on the specific applications. Once the desirable structure is developed, it could be applied to different physical forms, also resulting in its novel utilization.

### **7.3 Other Biomedical Appliances**

#### **7.3.1 PLA Used For Surgical Sutures**

Much effort is currently being devoted to the development of new biodegradable materials for biomedical applications. In this field, research on bioabsorbable surgical sutures is of particular relevance. Changes in composition, formulation and microstructure are usually investigated in order to improve polymer properties while maintaining the balance between degradation rate and temporary function. The addition of compounds with a pharmacological activity is a possibility to enhance suture performance and is a current topic of interest [140]. Thus, a suture made of copolymer of glycolide (90%) and LA (10%) that incorporates a biocide such as triclosan (2, 4, 40-trichloro-20-hydroxydiphenyl ether) onto the surface has recently been commercialized (vicryl plus 1). The antimicrobial effect has been evaluated and demonstrated. In a recent paper, many different ways to incorporate triclosan into sutures were proposed and the release was evaluated in different media and temperatures [141].



Synthetic absorbable sutures can be classified into monofilament and braided sutures on the basis of filament structure. The former group is advantageous if factors such as tissue drag [142], knot tie down [143] and risk of infection [144] are considered. Tissue drag can be minimized in braided sutures by using a coating that can be a degradable polymer of sticky nature. A copolymer based on lactide, caprolactone and trimethylencarbonate (PLA/PCA/PTMC 10/60/30) with suitable characteristics for use as a coating has recently been developed (Fig. 7.16) [141]. Furthermore, this copolymer shows a high miscibility with some hydrophobic drugs like triclosan, which allows them to be incorporated. Monofilaments can be coated in a similar way, but in this case the lubricant function of the copolymer is no longer necessary. Thus, it seems interesting to study the feasibility of incorporating a drug into the monofilament suture after the melt spinning process.

### 7.3.2 Ideal Filler for Soft Tissue Augmentation

Aging is a dynamic process determined, in fact, by the downward force of gravity associated with soft tissue depletion, loss of fat and muscle, and atrophy of skin and skeletal compounds [146, 147]. Soft tissue augmentation dates back more than 100 years, yet the search for an ideal filler continues [146].

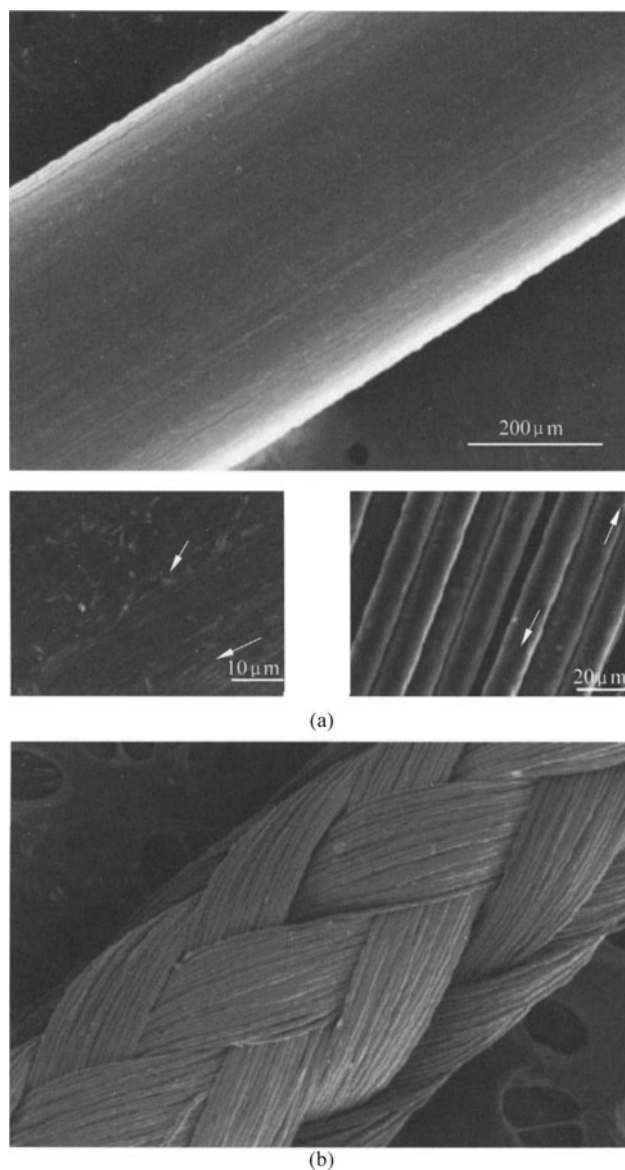
A variety of filling agents have been tried with varying success. Because aging changes are continuous, temporary fillers should be preferred over permanent ones. The industry and physicians are still looking for a filler that can last for years, in contrast to collagens and hyaluronic acids that last only months.

Like poly(glycolic acid), PLLA is a synthetic polymer that has been used in suture materials (vicryl) and in resorbable plates and screws. It is biocompatible and does not require skin testing [148 – 151].

PLLA comes in a powdered form of PLA microspheres that are reconstituted with sterile water to form a hydrogel with a methylcellulose carrier [152]. Injected PLA hydrogel stimulates a foreign body reaction, locally leading to collagen production, dermal fibrosis, and facial augmentation [153]. Undercorrection is performed, and a minimum of two treatments are required, usually 4 weeks apart [150]. The PLA particles are degraded over the first 6 months [154]. The thickened dermal layer producing the augmentation effect persists for 18 to 24 months or more [148, 154 – 156].

Originally marketed in Europe as Newfill (Biotech Industry SA, Luxembourg), PLA has been used for aesthetic indications since 1999 [151]. In 2004, the FDA of U. S. approved PLA under the name of Sculptra (Dermik Laboratories, Berwyn, PA, USA) for treatment of human immunodeficiency virus-related facial lipoatrophy [150, 155].

When injectable PLLA was produced by Biotech of Luxembourg, the particle size varied from 10 to 125 mg. However, the formulation currently marketed by



**Figure 7.16** SEM of a monofilament of poly (*p*-dioxanone) loaded with ibuprofen exposed for 24 h to a dichloromethane bath with a drug concentration of 10% (a) and a braided polyglycolide thread coated from an ethyl acetate bath containing 3% of PLA/PCA/PTMC 10/60/30 and 1% of ibuprofen (b). Insets correspond to higher magnifications that reveal the presence of some particles and striations (see arrows) on the surface of poly (*p*-dioxanone), and the coating on the polyglycolid threads (see arrows) [145]

Dermik Laboratories has a more uniform particle size, varying from 40 to 63  $\mu\text{m}$  in diameter [156].

Most common complications are small granulomas approximately 2 mm in diameter that show spontaneous remission in 3 years [150, 155, 156]. Despite the available publications considering the technical aspects of PLA filler and immediate results, concern remains about the long-term results and the durability of the procedure, mainly for cosmetic purposes [155, 156]. Salles [157] evaluated a 3 years follow-up investigation into the effect of PLA implant injection for the treatment of sunken nasolabial folds (Fig. 7.17).



**Figure 7.17** A 53-year-old patient who underwent PLLA filler injections for sunken nasolabial fold treatment. (a) Pretreatment; (b) After one session; (c) Attenuation of the nasolabial fold 6 months after treatment; (d) Still some degree of permanence of effect 36 months after treatment [157]

### **7.3.3 Mesh Insertion for Groin Hernia Repair**

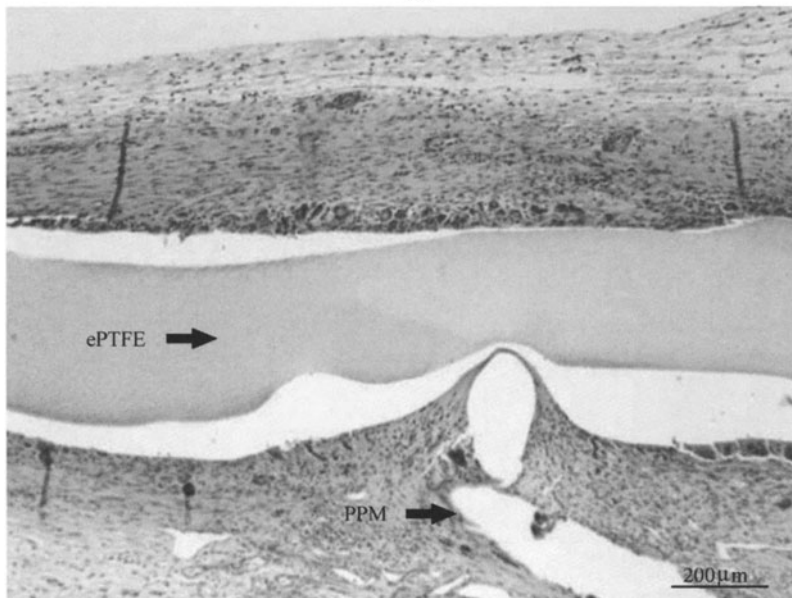
Inguinal hernia repair is the most common surgical procedure performed in the western countries. But evidence from several earlier studies reveals that primary repair has a high recurrence rate of 10%–15% [158]. This failure in hernia repair by conventional surgical techniques remains a major concern for general surgeons over the last decades and sustains research and development of prosthetic biomaterials to reinforce the closure of the muscular defect. Indeed, besides the 3-layered suture called “shouldice” procedure, which serves as the basic gold standard for comparison with all other new techniques [159], there exists the opportunity of prosthetic repair by performing a tension-free hernioplasty, called “lichtenstein” procedure [160]. The introduction of this tension-free technique in the so-called “open” procedures for groin hernia repair (to differentiate them from the “laparoscopic transabdominal pre-peritoneal” hernioplasties) is assessed to reduce recurrences [61]. Another progress seems to result from the use of per-fix plugs [162]. In this latter procedure the prosthetic material does not bridge the groin defect but plug the internal ring to avoid inguinal herniation.

The convenient prosthesis for this simpler procedure must comply with several requirements, i.e., be strong enough to compensate intra-abdominal pressure, have flexural rigidity for simple handling, serve as a framework for the ingrowth of connective tissue that first reinforces and then substitutes the foreign material and must be consequently slowly resorbed [163]. There is an adequacy between the rate of fibrosis induced by the biomaterial and the success of the hernia repair [163–165]. But the ideal prosthesis remains to be developed. As a matter of fact a chronic pain persisting after ending of healing with its train of paresthesias, neuritis, testicular atrophy, strain and reduced activity constitutes the major complication of all hernia-repair procedures [166–168] including plug application [169]. It was thought in the past to be rare but prospective studies give now the clear indication of a huge prevalence of either severe (6%) or mild (43%) chronic pain [168].

The strategy to avoid this serious long-term complication might be either to reduce the amount of foreign prosthetic materials or to use resorbable biocompatible products. As a matter of evidence, absorbable materials such as polyglactin or polyglycolic acid are not strong enough and/or are too quickly degraded to maintain a prolonged tensile strength high enough to counteract efficiently the abdominal pressure [170–172]. The use of current absorbable meshes cannot avoid recurrence of the inguinal hernia. Reducing the amount of non-resorbable material in the prosthesis may be the alternative. This strategy seems to be effective, as a 36% reduction of polypropylene (PP) amount does not affect tensile strength of the meshes *in vivo* [173]. It seems, however, that there exists a limit in reducing PP amount, as observed by Klosterhalfen et al. [173], who tested the properties of a 75%-PP reduced mesh. We must also consider another parameter

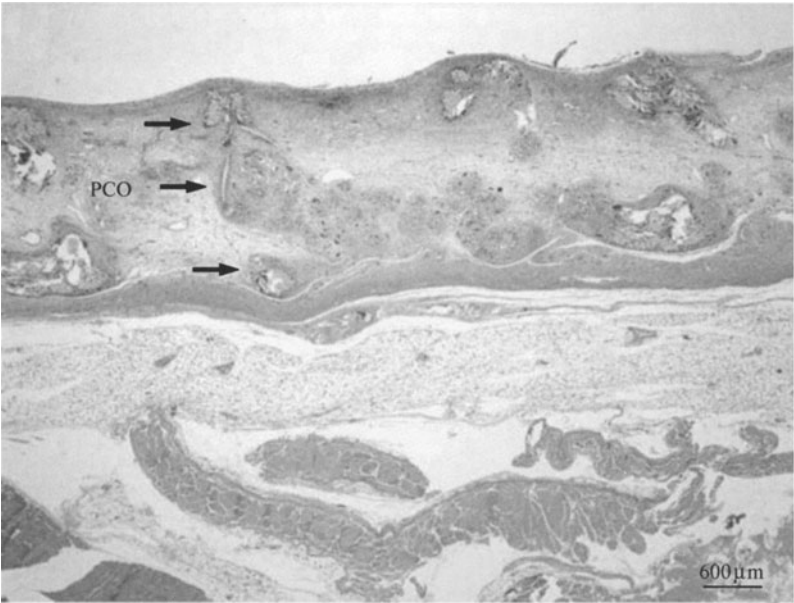


(a)

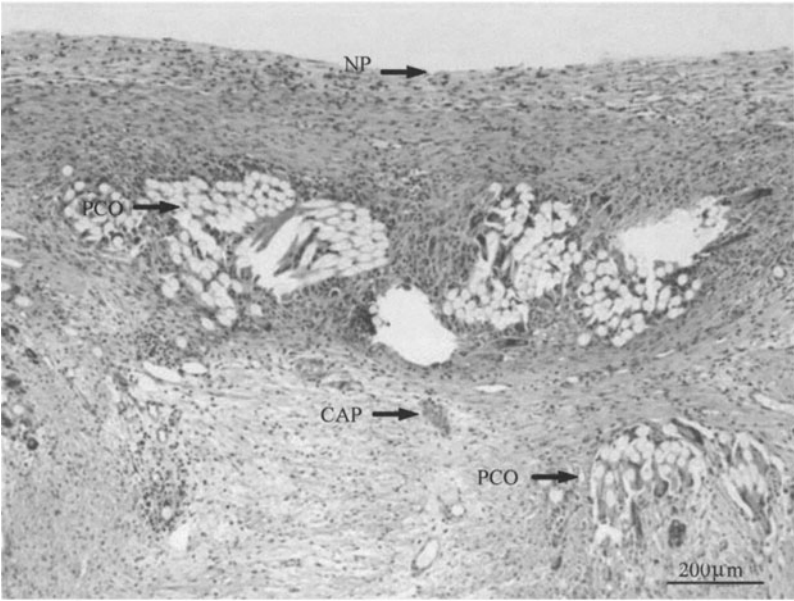


(b)

**Figure 7.18** A low-power micrograph of BC mesh (ePTFE-polypropylene composite). (a) Connective tissue ingrowth and inflammatory response are noted around the PPM (polypropylene) fibers; (b) High-power view of BC mesh. Superficial to the ePTFE layer is an inflammatory layer. The ePTFE layer is delaminated from the PPM and displays no tissue incorporation [187]



(a)



(b)

**Figure 7.19** A low-power micrograph of PCO (collagen-coated polyester mesh). (a) Connective tissue ingrowth and inflammatory response are noted around the polyester fibers; (b) High-power PCO with capillary neovascularization (CAP) and a neoperitoneal layer (NP) [187]

consisting in mesh shrinking. Shrinkage is more or less observed with all kind of non-resorbable materials in vivo [174 – 176] and seems linked to the ubiquitous inflammatory response to a foreign body [177]. Thus, it can be hypothesized that reducing the amount of non-resorbable materials should decrease the rate of shrinkage.

To find a good compromise between material tightness and stiffness has to be addressed by amending mesh composition. This objective should be achieved by using a composite prosthetic material designed with resorbable component balancing a low amount of permanent material. This kind of composite mesh, knitted with both resorbable and non-resorbable materials and named Vypro (Ethicon, a Johnson & Johnson company, Somerville, NJ) is currently under evaluation [178, 179]. It is designed with equal proportions of polypropylene and polyglactin. Recent works demonstrated that it was possible to use safely composite materials designed with less permanent component, and researchers investigated the experimental in vivo properties of a composite mesh designed with hugely less polypropylene (only 10% of the total) and PLLA, an absorbable biopolymer of constitutive lactate amino acid, which is widely applied as a scaffold [180 – 182] for tissue engineering allowing successful bone [183], vessels [184], nerves [185] and muscle [186] guided regeneration in vivo (Fig. 7.18, Fig. 7.19).

## Reference

- [1] Langer R., Vacanti J. P. *Science*, 260, 920 (1993).
- [2] Ma P. X. *Tissue Engineering*. In: Kroschwitz J. I. (ed.). *Encyclopedia of Polymer Science and Technology* (3rd Ed.). NJ: John Wiley & Sons Inc., (2004).
- [3] Rizzi S. C., Heath D. J., Coombes A. G. A., et al. *J. Biomed. Mater. Res.*, 55, 475 (2001).
- [4] Wang M. *Biomaterials*, 24, 2133 (2003).
- [5] Karageorgiou V., Kaplan D. *Biomaterial*, 26, 5474 (2005).
- [6] Widmer M. S., Puneet K., Gupta P. K., et al. *Biomaterials*, 19, 1945 (1998).
- [7] Shi F. Y., Gross R. A., Rutherford D. R. *Micromolecules*, 29, 10 (1996).
- [8] Shi F. Y., Ashby R., Gross R. A. *Macromolecules*, 29, 7753 (1996).
- [9] Yang Y., Basu S., Tomasko D. L., et al. *Biomaterials*, 26, 2585 (2005).
- [10] Ma P. X. *Materials Today*, 30 (2004).
- [11] Gopferich A., Mikos A. G. *Biomaterials*, 22, 291 (2001).
- [12] Kronenthal R. L. In: Kronenthal R. L., User Z., Martin E. (ed.). *Polymers in Medicine and Surgery*. New York: Plenum, 119 (1974).
- [13] Wang S. G., Cai Q., Bei J. Z. *Macromol. Symp.*, 195, 263 (2003).
- [14] Vert M., Li S., Spenlehauer G., et al. *J. Mater. Sci. Mater. Med.*, 3, 432 (1992).
- [15] Wang S. G., Cai Q., Hou J. W., et al. *J. Biomed. Mater. Res.*, 66A, 522 (2003).
- [16] Lu L. C., Garcia C. A., Mikos A. G. *J. Biomed. Mater. Res.*, 46, 236 (1999).

- [17] Migliaresi C., Fambri L., Cohn D. J. *Biomed. Sci. Polym.*, 6, 591 (1994).
- [18] Ge Z., Yang F., Goh J. C. H., et al. *J. Biomed. Mater. Res.*, 77A, 639 (2006).
- [19] Hollinger J. O., Schmitz J. P. J. *Oral Maxillofac. Surg.*, 45, 594 (1987).
- [20] Freed L., Marquis J. C., Nohria A., et al. *J. Biomed. Mater. Res.*, 27, 1 (1993).
- [21] Li S. *J. Biomed. Mater. Res.*, 48, 342 (1999).
- [22] Brady J. M., Cutright D. E., Miller R. A., et al. *J. Biomed. Mater. Res.*, 7, 155 (1973).
- [23] Yaszemski M. J., Payne R. G., Hayes W. C., et al. *Biomaterials*, 17, 175 (1996).
- [24] Kulkarni R. K., Moore E. G., Hegyesi A. F., et al. *J. Biomed. Mater. Res.*, 169, 5 (1971).
- [25] Cima L. G., Vacanti J. P., Vacanti C., et al. *J. Biomech. Eng.*, 113, 143 (1991).
- [26] Vacanti C. A., Kim W., Schloo B., et al. *Am. J. Sports Med.*, 22, 485 (1994).
- [27] Thomson R. C., Yaszemski M. J., Powers J. M., et al. *J. Biomater. Sci. Polym.*, 7, 23 (1995).
- [28] Mooney D., Sano K., Kaufmann P., et al. *J. Biomed. Mater. Res.*, 37, 413 (1997).
- [29] Ren T. B., Ren J., Jia X. Z., et al. *J. Biomed. Mater. Res.*, 74A, 562 (2005).
- [30] Khang G., Lee S. J., Jeon J. H., et al. *Polymer*, 24, 869 (2000).
- [31] Tjia J. S., Aneskievich B. J., Moghe P. V. *Biomaterials*, 20, 2223 (1999).
- [32] Inagaki N., Narushima K., Lim S. K. *J. Appl. Polym. Sci.*, 89, 96 (2003).
- [33] Wang Y. Q., Qu X., Lu J., et al. *Biomaterials*, 25, 4777 (2003).
- [34] Wan Y. Q., Yang J., Yang J. L., et al. *Biomaterials*, 24, 3757 (2003).
- [35] Wade W. L., Mammone R. J., Binder M. J. *J. Appl. Polym. Sci.*, 43, 1589 (1991).
- [36] Occhiello E., Morra M., Morini G., et al. *J. Appl. Polym. Sci.*, 42, 551 (1991).
- [37] Favia P., Agostino R. *Surf. Coat. Tech.*, 98, 1102 (1998).
- [38] Kang E. T., Tan K. L., Kato K., et al. *Macromolecules*, 29, 6872 (1996).
- [39] Qiu Y. X., Klee D., Plüster W., et al. *J. Appl. Polym. Sci.*, 61, 2373 (1996).
- [40] Hsu S. H., Chen W. C. *Biomaterials*, 21, 359 (2000).
- [41] Ryu G. H., Yang W. S., Roh H. W., et al. *Surface & Coatings Technology*, 193, 60 (2005).
- [42] Nam Y. S., Yoon J. J., Lee J. G., et al. *J. Biomater. Sci. E.*, 10, 1145 (1999).
- [43] Miller D. C., Thapa A., Haberstroh K. M., et al. *Biomaterials*, 25, 53 (2004).
- [44] Gao J. M., Niklason L., Langer R. J. *Biomed. Mater. Res.*, 42, 417 (1998).
- [45] Yuan X. Y., Mak A. F. T., Yao K. D. *Polym. Degrad. Stab.*, 79, 45 (2003).
- [46] Croll T. I., O'Connor A. J., Stevens G. W., et al. *Biomacromolecules*, 5, 463 (2004).
- [47] Yang J., Wan Y. Q., Wang S. G., et al. *Polym. Int.*, 52, 1892 (2003).
- [48] Ma H., Davis R. H., Bowman C. N. *Macromolecules*, 33, 331 (2000).
- [49] Janorkar A. V., Proulx S. E., Metters A. T., et al. *J. Polym. Sci. Polym. Chem.*, 44, 6534 (2006).
- [50] Zhu A., Zhang M., Wu J., et al. *Biomaterials*, 23, 4657 (2002).
- [51] Ranby B. *Int. J. Adhes.*, 19, 337 (1999).
- [52] Yang W., Ranby B. *Eur. Polym. J.*, 35, 1557 (1999).
- [53] Lukashev M. E., Werb Z. *Trends Cell Biol.*, 8, 437 (1998).
- [54] Ross J. M. Cell–extracellular matrix interactions. In: Patrick C. M., et al. (eds.). *Frontier in Tissue Engineering*. Elsevier, 15-27 (1998).
- [55] Dimilla P. A., Stone J. A., Wuinn J. A. *J. Cell Biol.*, 122, 729 (1993).
- [56] Massia S. P., Hubbell J. A. *J. Biomed. Mater. Res.*, 25, 223 (1991).
- [57] Lin H., Sun W., Mosher D. F., et al. *J. Biomed. Mater. Res.*, 28, 329 (1994).



- [58] Drumheller P. D., Ebert D. L., Hubbell J. A. *Biotech. Bioeng.*, 43, 772 (1994).
- [59] Otsuka H., Nagasaki Y., Kataoka K. *Biomacromolecules*, 1, 39 (2000).
- [60] Yang J., Bei J. Z., Wang S. G. *Biomaterials*, 23, 2607 (2002).
- [61] Desai N. P., Hubbell J. A. *Macromolecules*, 25, 226 (1992).
- [62] Desai N. P., Hubbell J. A. *Biomaterials*, 12, 144 (1991).
- [63] Zhu H. G., Ji J., Lin R. G., et al. *J. Biomed. Mater. Res.*, 62, 532 (2002).
- [64] Cui Y. L., Di Q. A., Liu W. G., et al. *Biomaterials*, 24, 3859 (2003).
- [65] Zhu H. G., Ji J., Shen J. C. *Macromol. Rapid Commun.*, 23, 819 (2002).
- [66] Cai K. Y., Yao K. D., Cui Y. L., et al. *Biomaterials*, 23, 1603 (2002).
- [67] Yuan L. C., Xin H., Ai D. Q., et al. *J. Biomed. Mater. Res. A*, 66, 770 (2003).
- [68] Quirk R. A., Davies M. C., Tendler S. J. B., et al. *Macromolecules*, 33, 258 (2000).
- [69] Ulman A. *Chem. Rev.*, 96, 1533 (1996).
- [70] Sano M., Lvov Y., Kunitake T. *Annu. Rev. Mater. Sci.*, 26, 153 (1996).
- [71] Laschewsky A. *European Chemistry Chronicle ECC*, 2, 13 (1997).
- [72] Decher G. *Science*, 277, 1232 (1997).
- [73] Picart C., Lavalle Ph., Hubert P., et al. *Langmuir*, 17, 7414 (2001).
- [74] Houska M., Brynda E. *Journal of Colloid and Interface Science*, 188, 243 (1997).
- [75] Brynda E., Houska M. *Journal of Colloid and Interface Science*, 183, 18 (1996).
- [76] Decher G., Schlenoff J. B. *Multilayer Thin Films: Sequential Assembly of Nanocomposite Materials*. Weinheim: Wiley-VCH (2002).
- [77] Mendelsohn J. D., Yang S. Y., Hiller J. A., et al. *Biomacromolecules*, 4, 96 (2003).
- [78] Kim B. Y., Bruening M. L. *Langmuir*, 19, 94 (2003).
- [79] Chua P. H., Neoh K. G., Kang E. T., et al. *Biomaterials*, 29, 1412 (2008).
- [80] Zhang J., Senger B., Vautier D., et al. *Biomaterials*, 26, 3353 (2005).
- [81] Fukuda J., Khademhosseini A., Yeh J., et al. *Biomaterials*, 27, 1479 (2006).
- [82] Johansson J. A., Halthur T., Herranen M., et al. *Biomacromolecules*, 6, 1353 (2005).
- [83] Zhu H., Ji J., Shen J. C. *Biomacromolecules*, 5, 1933 (2004).
- [84] Zhu H., Ji J., Tan Q. G., et al. *Biomacromolecules*, 4, 385 (2003).
- [85] Wilson J., Pigott G. H., Schoen F. J., et al. *J. Biomed. Mater. Res.*, 15, 805 (1981).
- [86] Ohura K., Yamamura T., Nakamura T., et al. *J. Biomed. Mater. Res.*, 25, 357 (1991).
- [87] Hench L. L. *J. Am. Ceram. Soc.*, 74, 1487 (1991).
- [88] Wang M., Hench L. L., Bonfield W. J. *Biomed. Mater. Res.*, 42, 577 (1998).
- [89] Bonfield W., Guild F. J. *Biomater.*, 14, 985 (1993).
- [90] Seal B. L., Otero T. C., Panitch A. *Materials Science and Engineering*, 34, 147 (2001).
- [91] Soriano I., Evora C. *Journal of Controlled Release*, 68, 121 (2000).
- [92] Thomson R. C., Yaszemski M. J., Powers J. M., et al. *Biomaterials*, 19, 1935 (1998).
- [93] Flahiff C. M., Blackwell A. S., Hollis J. M., et al. *Journal of Biomedical Materials Research*, 32, 419 (1996).
- [94] Huang Y. X., Ren J., Chen C., et al. *J. Biomater. Appl.*, 22, 409 (2008).
- [95] Ren J., Zhao P., Ren T. B., et al. *J. Mater. Sci. Mater. Med.*, 19, 1075 (2008).
- [96] Huang Y. X., Ren J., et al. *Journal of Biomedical Materials Research: Part A*, DOI: 10.1002/jbm.a.32922 (in press).
- [97] Boccaccini A. R., Maquet V. *Composites Science and Technology*, 63, 2417 (2003).

## **Biodegradable Poly(Lactic Acid): Synthesis, Modification, Processing and Applications**

- [98] Hua F. J., Kim G. E., Lee J. D., et al. *J. Biomed. Mat. Res.*, 63, 161 (2002).
- [99] Nam Y. S., Park T. G. *J. Biomed. Mater. Res.*, 47, 7 (1999).
- [100] Mikos A. G., Thorsen A. J., Czerwonka L. A., et al. *Polymer*, 35, 1068 (1994).
- [101] Ma Z. W., Gao C. Y., Gong Y. H., et al. *J. Biomed. Mater. Res. Part B: Appl. Biomater.*, 67B, 610 (2003).
- [102] Nam Y. S., Park T. G. *J. Biomed. Mater. Res.*, 47, 7 (1999).
- [103] Guan L. M., Davies J. E. *J. Biomed. Mater. Res.*, 71A, 480 (2004).
- [104] Kulkarni R. K., Pani K. C., Neuman C., et al. *Arch. Surg.*, 93, 839 (1966).
- [105] Schmitt E. E., Polistina R.A. US Patent 3 463 158 (1969).
- [106] Schneider A. K. US Patent 3 636 956 (1972).
- [107] Yolles S., Eldridge J. E., Woodland J. H. *R. Polym. News*, 1, 9 (1971).
- [108] Yolles S. *Polym. Sci. Technol.*, 8, 245 (1975).
- [109] Higuchi T. US Patent 3 625 214 (1971).
- [110] Wise D. L., McCormick G. J., Willet G. P. *Life Sciences*, 19, 867 (1976).
- [111] Schindler A., Jeffcoat R., Kimmel G. L., et al. *Cont. Topics Polym. Sci.*, 2, 251 (1977).
- [112] Beck L. R., Cowsar D. R., Lewis D. H., et al. *Am. J. Obstet. Gynecol.*, 135, 419 (1979).
- [113] Michaels A. S. US Patent 3 962 414 (1976).
- [114] Davis S. S., Illum L., Stolnik S. *Curr. Opinion Coll. Int. Sci.*, 1, 660 (1996).
- [115] Okada H., Ogawa Y., Yashiki T. US Patent 4 652 441 (1987).
- [116] Okada H., Yamamoto M., Heya T., et al. *J. Control Rel.*, 28, 121 (1994).
- [117] McIlwain C. *Nature*, 405, 983 (2000).
- [118] Liu Yunhai, Wu Jibing. *Journal of Biomedical Materials Research Part B: Applied Biomaterials*, 85B, 435 (2007).
- [119] Wei Hua, Zhang Xianzheng, Zhuo Ren-Xi. *Biomaterials*, 28, 99 (2007).
- [120] Masamichi Nakayama, Teruo Okano. *Journal of Controlled Release*, 115, 46 (2006).
- [121] Lo Chun-Liang, Lin Ko-Min, Hsiue Ging-Ho. *Journal of Controlled Release*, 104, 477 (2005).
- [122] Cheng Chenga, Wei Hua, Zhuo Ren-Xi. *Biomaterials*, 29, 497 (2008).
- [123] Wan Shun, Jiang Ming. *Macromolecules*, 40, 5552 (2007).
- [124] Gil E. S., Hudson S. M. *Prog. Polym. Sci.*, 29, 1173 (2004).
- [125] Zakir M. O. Rzaev, Sevil Dincer, Erhan Piskin. *Prog. Polym. Sci.*, 32, 534 (2007).
- [126] Kohori F., Sakai K., Aoyagi T., et al. *J Control Release*, 55, 87 (1998).
- [127] Konak C., Oupicky D., Chytrý V., et al. *Macromolecules*, 33, 5318 (2000).
- [128] Tonge S. R., Tighe B. J. *Adv. Drug Deliv. Rev.*, 53, 109 (2001).
- [129] Philippova O. E., Hourdet D., Audebert R., et al. *Macromolecules*, 30, 8278(1997).
- [130] Pinkrah V. T., Snowden M. J., Mitchell J. C., et al. *Langmuir*, 19, 585 (2003).
- [131] Chen B. N., Piletsky S., Turner A. P. *F. Comb. Chem. High Throughput Screen*, 5, 409 (2002).
- [132] Tulinsky A. *Semin Thromb Hemostasis*, 22, 117 (1996).
- [123] Britschgi M., von Greyerz S., Burkhart C., et al. *Curr. Drug Targets*, 4, 1 (2003).
- [134] Cudic P., Behenna D. C., Kranz J. K., et al. *Chem. Biol.*, 9, 897 (2002).
- [135] Sundberg E. J., Mariuzza R. A. *Protein Modules Protein-Protein Interact*, 61, 119 (2003).
- [136] Jimenez R., Salazar G., Baldrige K. K., et al. *Proc. Natl. Acad. Sci. USA*, 100, 92 (2003).

- [137] Glick B. R., Pasternak J. J. *Molecular Biotechnology: Principles and Applications of Recombinant DNA* (2nd Edition). Washington DC: ASM Press, 235 (1998).
- [138] Miyata T., Asami N., Uragami T. *Nature*, 399, 766 (1999).
- [139] Ren Jie, Hong Haiyan, Ren Tianbin, et al. *Reactive and Functional Polymers*, 66, 944 (2006).
- [140] Rothenburger S., Spangler D., Bhende S., et al. *Surg. Inf.*, 3, 79 (2002).
- [141] Zurita R., Puiggal J., Rodriguez-Galan A. *Macromol. Biosci.*, 6, 58 (2006).
- [142] Homsy C. A., McDonald K. E., Akers W. W. J. *Biomed. Mater. Res.*, 2, 215 (1968).
- [143] Rodeheaver G. T., Thacker J. G., Owen J., et al. *J. Surg. Res.*, 35, 525 (1983).
- [144] Blomstedt B. *Acta Chir. Scand.*, 144, 269 (1978).
- [145] Zurita R., Puiggal J., Rodriguez-Galan A. *Macromol. Biosci.*, 6, 58 (2006).
- [146] Fagien S. *Plast. Reconstr. Surg.*, 105, 362 (2000).
- [147] Rohrich R. J., Rios J. L., Fagien S. *Plast. Reconstr. Surg.*, 112 (2003).
- [148] Perry C. *Am. J. Clin. Dermatol.*, 15, 361 (2004).
- [149] Vleggaar D. *Dermatol. Surg.*, 31, 1511 (2005).
- [150] Vleggaar D. *Plast. Reconstr. Surg.*, 118(Suppl.), 46S (2006).
- [151] Vleggaar D., Bauer D. J. *Drugs Dermatol.*, 3, 542 (2004).
- [152] Jansen D. A., Graivier M. H. *Semin. Plast. Surg.*, 17 (2003).
- [153] Lemperle F., Morhenn V., Charrier U. *Aesth. Plast. Surg.*, 27, 354 (2003).
- [154] Valantin M. A., Aubron-Olivier C., Ghosn J., et al. *VEGA. AIDS*, 17, 2471 (2003).
- [155] Lam S., Azizzadeh B., Graivier M. *Plast. Reconstr. Surg.*, 118(Suppl), 55S (2006).
- [156] Bauer U., Vleggaar D. *Plast. Reconstr. Surg.*, 118, 265 (2006).
- [157] Salles A. G., Lotierzo P. H., Gimenez R., et al. *Aesth. Plast. Surg.*, 32, 753 (2008).
- [158] Fashid T., Heikkinen T. J., Wollert S., et al. *Ann. R. Coll. Surg. Engl.*, 82, 396 (2000).
- [159] Hay J. M., Boudet M. J., Fingerhut A., et al. *Ann. Surg.*, 222, 719 (1995).
- [160] Lichtenstein I. L., Shulman A. G., Amid P. K. *Am. J. Surg.*, 157, 188 (1989).
- [161] Mcgillicuddy J. E. *Arch. Surg.*, 133, 974 (1998).
- [162] Read R. C. *Hernia*, 8, 8 (2004).
- [163] Goldstein H. S. *Hernia*, 3, 23 (1999).
- [164] Bellon J. M., Bujan J., Contreras L. *Biomaterials*, 16, 381 (1995).
- [165] Klosterhalfen B., Junge K., Hermanns B. et al. *J. Surg.*, 89, 1043 (2002).
- [166] Koninger J., Redecke J., Butters M. *Langenbeck Arch. Surg.*, 389, 361 (2004).
- [167] Bay-Nielsen M., Perkins F. M., Kehlet H., et al. *Hernia Database Ann. Surg.*, 233, 1 (2001).
- [168] Courteney C. A., Duffy K., Serpell M. G. *Br. J. Surg.*, 89, 1310 (2002).
- [169] Pelissier E. P., Blum D., Damas J. M., et al. *Hernia*, 4, 201 (1999).
- [170] Lamb J. P., Vitale T., Kaminski D. L. *Surgery*, 93, 643 (1983).
- [171] Tyrell J., Siberman H., Chandrasoma P., et al. *Surg. Gynecol. Obstet.*, 168 (1989).
- [172] Klinge U., Schumpelick V., Klosterhalfen B. *Biomaterials*, 22, 1415 (2001).
- [173] Klosterhalfen B., Klinge U., Schumpelick V. *Biomaterials*, 19, 2235 (1998).
- [174] Amid P. K. *Hernia*, 1, 15 (1997).
- [175] Lowham A. S., Filippi C. J., Jr Fitzgibbons R. J., et al. *Ann. Surg.*, 225 422 (1997).
- [176] Klinge U., Klosterhalfen B., Muller M. *Eur. J. Surg.*, 164, 965 (1998).

## **Biodegradable Poly(Lactic Acid): Synthesis, Modification, Processing and Applications**

- [177] Klosterhalfen B., Klinge U., Hermanns B., et al. *Chirurg*, 71, 43 (2000).
- [178] Junge K., Klinge U., Rosch R., et al. *World J. Surg.*, 26, 1472 (2002).
- [179] Bringman S., Heikkinen T. J., Wollert S., et al. *Hernia*, 8 127 (2004).
- [180] Ren Tianbin, Ren Jie, Jia Xiaozhen, et al. *Journal of Biomedical Materials Research Part A*, 562 (2005).
- [181] Gu Shu-Ying, Zhan Hui, Ren Jie, et al. *Polymers & Polymer Composites*, 5, 137 (2007).
- [182] Ren Jie, Ren Tianbin, Zhao Peng, et al. *Journal of Biomaterials Science-Polymer Edition*, 18, 505 (2007).
- [183] Kellomaki M., Niiranen H., Puumanen K., et al. *Biomaterials*, 21, 2495 (2000).
- [184] Furukawa K. S., Ushida T., Toita K., et al. *Cell Transplant*, 11, 475 (2002).
- [185] Evans G. R., Brandt K., Katz S., et al. *Biomaterials*, 23, 841 (2002).
- [186] Fuchs J. R., Pomerantseva I., Ochoa E. R., et al. *J. Pediatr. Surg.*, 38, 1348 (2003).
- [187] Duffy A. J., Hogle N. J., LaPerle K. M., et al. *Hernia*, 8, 358 (2004).

## 8 Standard and Test Methods

**Abstract** The standards and test methods of properties of PLA have an important function as they facilitate communication between producers, authorities and consumers. This chapter provides a general overview of the biodegradability, standard and test method of properties of PLA. At first, biodegradation of PLA is reviewed, including definition of biodegradation, factors affecting the biodegradation behavior of PLA and biodegradability of PLA. Then, biodegradation standards and certification systems are introduced. Finally, some test methods are given.

**Keywords** biodegradation behavior, biodegradation standard, composting, abiotic degradation, biotic degradation, anoxic degradation, aerobic degradation

As mentioned in the previous chapters, PLA has received much attention as a bio-based and biodegradable plastic to replace other nondegradable, petroleum-based plastic materials. Much research devoted to it has mainly focused on its synthesis, modification, processing and property, great achievements have been made. Now PLA is commercially available. It has come to be used in many applications that utilize its properties, including degradability, transparency after being formed into film, and ease of fabrication. However, it has not gained widespread use. PLA with other biodegradable plastics only represents a tiny market as compared with the conventional petrochemical materials. One of the main limitations is higher cost compared to synthetic polymers such as LDPE, PP, PS, and PET. Another serious obstacle is a lack of suitable infrastructure for sorting, recycling and composting solid wastes [1]. One of the major tasks to be taken before the widespread application of PLA is the fundamental understanding of its degradation mechanisms and to give uniform, unbiased and scientific ways for measuring degradation, namely standards and test methods of biodegradation. Since these issues carry strong implications for the service life of plastic items, it is important to agree on common standards that distinguish degradable from non-degradable (environmentally stable) polymers and plastics. In fact, standards and test methods also have an important function as they facilitate communication between producers, authorities and consumers. This chapter provides a general overview of the biodegradability of PLA, the standard and test methods of biodegradability polymer.

## **8.1 Biodegradation of PLA**

### **8.1.1 Definition of Biodegradation**

Biodegradation is a natural process by which organic chemicals in the environment are converted to simpler compounds, mineralized and redistributed through elemental cycles such as the carbon, nitrogen and sulphur cycles. Biodegradation can only occur within the biosphere as microorganisms play a central role in the biodegradation process.

A number of standards authorities have sought to establish definitions for biodegradable plastics and some of these are provided below:

ISO 472: 1988—A plastic designed to undergo a significant change in its chemical structure under specific environmental conditions resulting in a loss of some properties that may vary as measured by standard test methods appropriate to the plastics and application in a period of time that determines its classification. The change in chemical structure results from the action of naturally occurring microorganisms.

ASTM sub-committee D20.96 proposal—Degradable plastics are plastic materials that undergo bond scission in the backbone of a polymer through chemical, biological and/or physical forces in the environment at a rate, which leads to fragmentation, or disintegration of the plastics.

Japanese Biodegradable Plastic Society 1 draft proposal—Biodegradable plastics are polymeric materials which are changed into lower molecular weight compounds where at least one step in the degradation process is through metabolism in the presence of naturally occurring organisms.

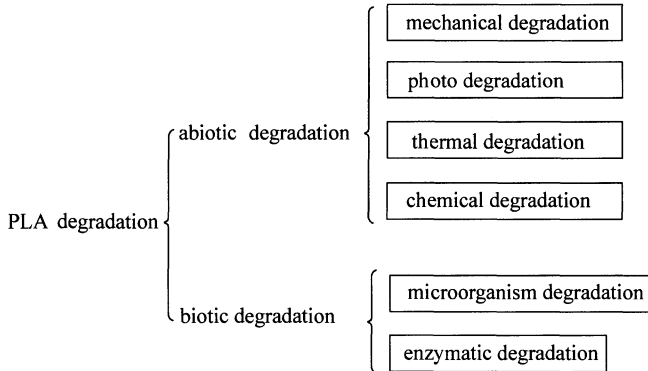
DIN 103.2 working group on biodegradable polymers—Biodegradation of a plastic material is a process leading to naturally occurring metabolic end products.

General definition of biodegradation—It is a process whereby bacteria, fungi, yeasts and their enzymes consume a substance as a food source so that its original form disappears. Under appropriate conditions of moisture, temperature and oxygen availability, biodegradation is a relatively rapid process. Biodegradation for limited periods is a reasonable target for the complete assimilation and disappearance of an article leaving no toxic or environmentally harmful residue.

The term “biodegradation” indicates the predominance of biological activity in this phenomenon. Several studies about biodegradation of PLA show that the abiotic degradation precedes microbial assimilation [2,3]. Consequently, in nature, biotic and abiotic factors act synergistically to decompose PLA (Fig. 8.1).

### **8.1.2 Factors Affecting the Biodegradation Behaviour of PLA**

PLA are water-insoluble, solid polymeric materials. PLA degradation takes place



**Figure 8.1** Abiotic and biotic involvement in PLA degradation

through the scission of the main chains or side chains of PLA. Different degradation mechanisms whether chemical or biological can be involved in the degradation of PLA. The biodegradability of PLA depends on the structure, the morphology, the crystallinity, the molecular weight, introduction of functionality, additives and environmental conditions.

Several reports showed that the crystalline part of the PLA was more resistant to degradation than the amorphous part, and that the rate of degradation decreases with an increase in crystallinity [4–7]. The degradation behavior of polymers also depends on their molecular weight ( $M_n$ ). High molecular weight PLA are degraded at a slower rate than those with low molecular weights [8]. The melting temperature ( $T_m$ ) of polyesters has a great effect on enzymatic degradability. In general, the higher the melting point is, the lower the degradability tends to be [9, 10]. Li and MacCarthy [11] studied the effects of the stereoisomeric content of PLA on the degradation rate of PLA films using proteinase K. They reported that the initial degradation occurred at the surface and that the degradation rate increased with high content of *L*-lactate unit. Likewise, the degradation of lactide oligomers and dimers and LA monomers with different stereofoms has been investigated by using *Fusarium moniliforme* and *Pseudomonas putida*. The low molecular weight oligomers were totally degraded regardless of enantiomeric composition. The *L*-dimer was consumed rapidly whereas the racemic oligomers were slowly assimilated [12].

### 8.1.3 Abiotic Degradation

#### 8.1.3.1 Mechanical Degradation

This process involves the application of compression, tension and/or shear forces to break apart the plastics. It is a notable method for size reduction. Mechanical factors are not predominant during biodegradation process, but mechanical

damages can activate it or accelerate it [13].

### 8.1.3.2 Photo Degradation

The energy carried by photons can create unstable states in various molecules. Photo-sensitive additives sometimes are added intentionally into polymer. These additives, when exposed to the sun's UV rays, release free radicals, which randomly attack and break the polymeric bonds that are susceptible to be oxidized under aerobic conditions. In abiotic degradation, the action of light radiation is one of the most important parameters [14]. Most of the synthetic polymers are susceptible to degradation initiated by UV and visible light. Normally the near UV radiations (290 – 400 nm) in the sunlight determine the lifetime of polymeric materials in outdoor applications [15]. The research [16] shows that the photo degradation of PLLA films proceeds via a bulk erosion mechanism, meaning that UV penetrates the specimens with no significant reduction in its intensity, irrespective of the chemical structure and the crystallinity of biodegradable polyesters. Although PLLA chains are photodegradable even in the crystalline regions, their photodegradability is lower than that in the amorphous regions. The significant increase in  $M_w/M_n$  is observed for PLLA-A, even when the decrease of  $M_n$  by UV irradiation is small. The Norrish reactions express photodegradation that transform the polymers by chain scission (Norrish II) (Fig. 8.2).

### 8.1.3.3 Thermal Degradation

The heat provides the required energy for promoting the oxidation of the carbon in the polymer backbone of molecules constituting the plastics. Generally, thermal degradation of PLA occurs at 159 – 178°C depending on its molecular weight and its crystallinity.

A very detailed study of thermal PLA degradation was carried out by McNeill and Leiper [17, 18]. They used TG, DSC and thermal volatilization analysis (TVA) in combination with H-NMR, IR and MS for product identification. Jamshidi et al. [19] and Zhang et al. [20] discussed inter- and intramolecular transesterifications as causes for the reduction of the molar mass when heated above the melting point. Five mechanisms have been postulated (Fig. 8.3).

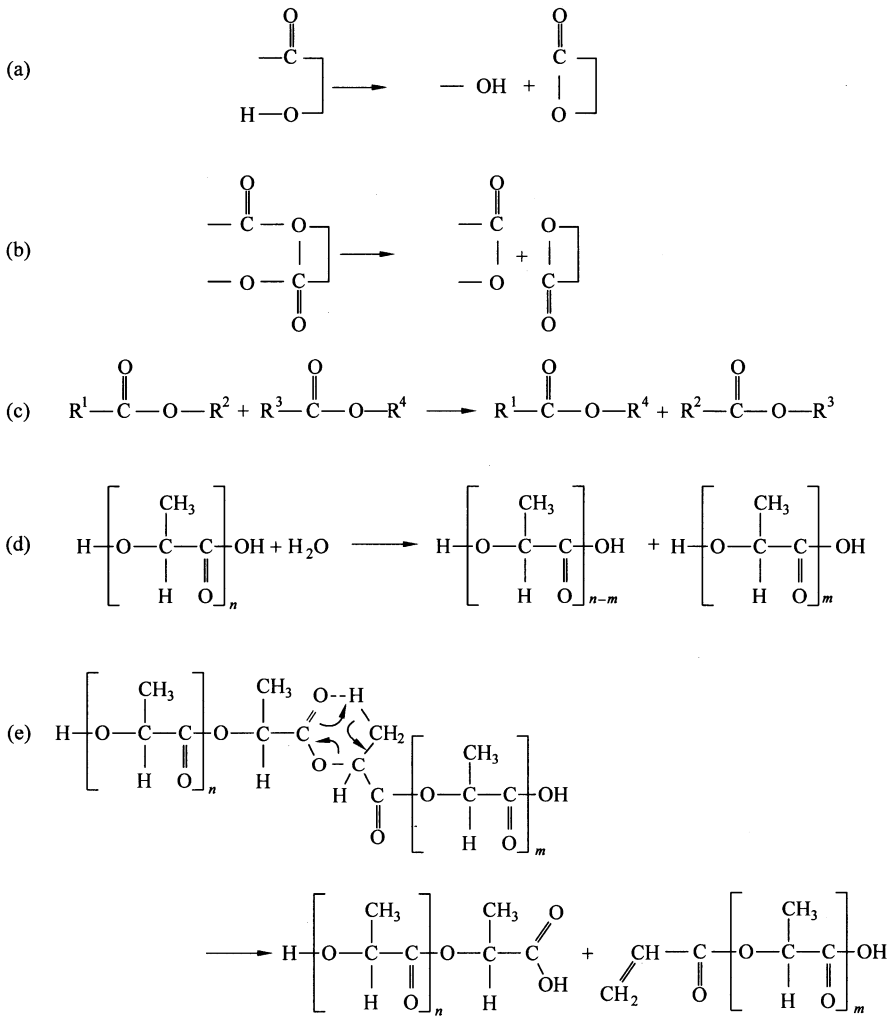
Combining liquid chromatographic methods (LACCC and SEC) with matrix-assisted laser desorption/ionisation time-of-flight mass spectrometry (MALDI-TOF-MS) and post-column derivatisation, Wachsen and Reichert [21] studied on the thermal degradation of oligo-*L*-lactide at 200°C under nitrogen atmosphere. It shows that PLA is highly sensitive to thermal treatment because of its small value of the activation energy.

### 8.1.3.4 Chemical Degradation

Chemical transformation is the other most important parameter in the abiotic degradation. Atmospheric pollutants and agrochemicals may interact with polymers







**Figure 8.3** Postulated reactions of polylactide degradation. (a) Intramolecular transesterification (back-biting); (b) Intramolecular transesterification; (c) Intermolecular transesterification; (d) Hydrolysis; (e) Pyrolytic elimination

of LA. The intramolecular degradation occurs by a random alkaline attack on the carbon of the ester group, followed by the hydrolysis of the ester link. Thus, new molecules with low molecular weight are produced. In acidic conditions [28] (Fig. 8.3), the protonation of the hydroxyl end-group forms an intramolecular hydrogen bond. The hydrolysis of the ester group allows the release of a lactic acid molecule leading to the decrease of the degree of polymerisation of the PLA. An intramolecular random protonation of carbon in the ester group conduces also to the hydrolysis of ester linkages. This hydrolysis gives different fragments of lower molecular weights.

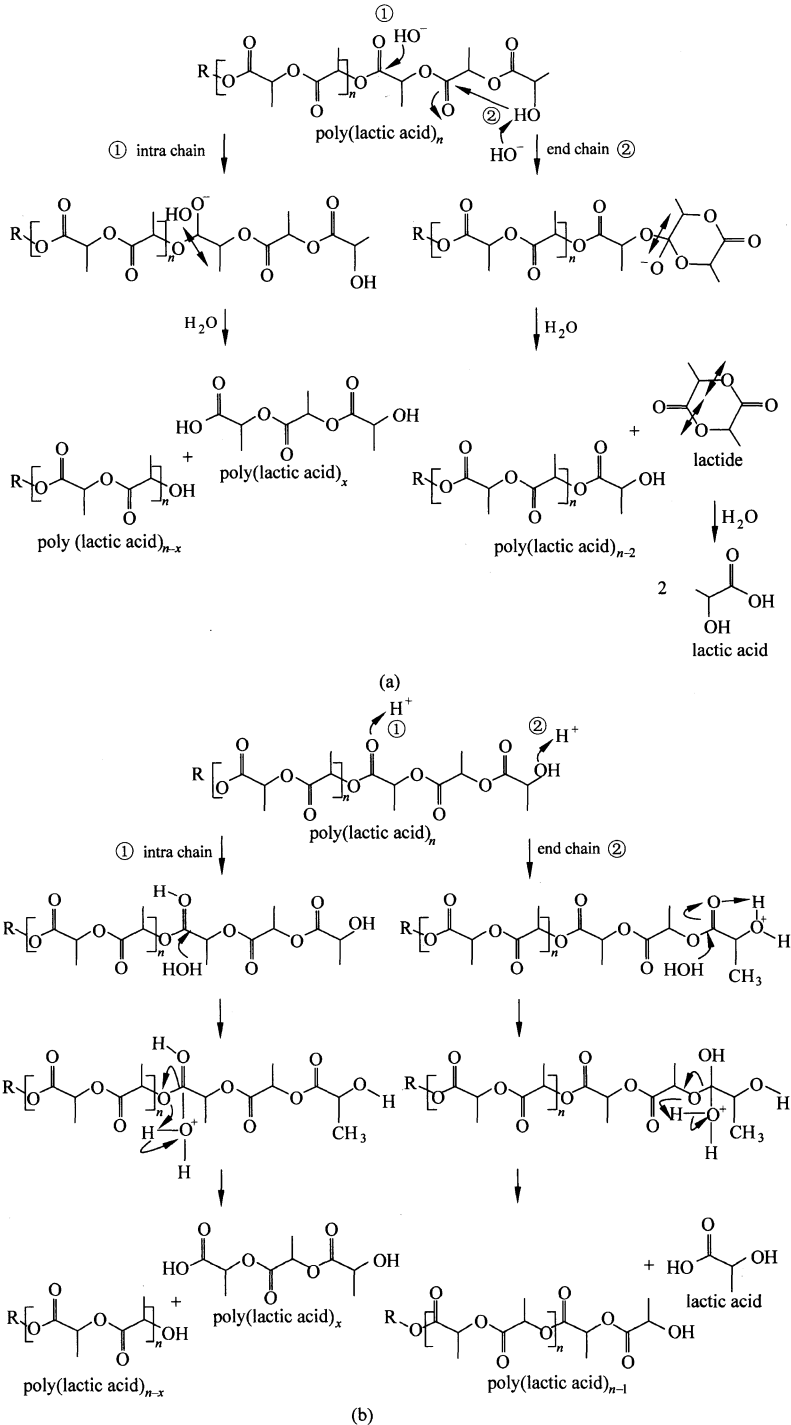


Figure 8.4 PLA hydrolysis. (a) in alkaline conditions; (b) in acidic conditions

## 8.1.4 Biotic Degradation

### 8.1.4.1 Microbial Degradation of PLA

Microbial degradation results from the action of naturally occurring microorganisms such as bacteria, fungi, algae, etc. Polymers are degraded in the soil by the action of a wide variety of microorganisms. The plate count and the clear zone methods using emulsified polyester agar plates are very efficient methods in the evaluation of the population of polymer-degrading microorganisms in the environment [29]. By applying the clear zone method, it was confirmed that the population of aliphatic polyester-degrading microorganisms at 30°C and 50°C decreased in the order of PHB = PCL > PBS > PLA [30]. A burial test comparison of PLA and other polyesters, e.g., PHB, PCL and PBS, indicated that PLA was not readily degraded when the PLA samples were buried under soil for 20 months. Degradation of these polyesters in the soil burial test also decreased in the same order as above on the distribution of polyester-degrading microorganisms. These results show that PLA-degrading microorganisms are not widely distributed in the natural environment and thus, PLA is less susceptible to microbial attack in the natural environment than other microbial and synthetic aliphatic polyesters. For the above reasons, it is very important to study the biodegradation of PLA and to develop treatment processes for plastic waste containing PLA. Biological degradation is chemical in nature but the source of the attacking chemicals is from microorganisms. These chemicals are of catalytic nature, e.g., enzymes. The susceptibility of the PLA to microbial attack generally depends on enzyme availability, availability of a site in the PLA for enzyme attack, enzyme specificity for that polymer and the presence of coenzyme if required [31]. Table 8.1 lists some isolated PLA-degrading microorganisms, their enzyme and substrate specificities.

**Table 8.1** Typical PLA-degrading microbes and their PLA-degrading enzymes and substrate specificities and detection methods used for degradation test [32]

Strain	Type of enzyme	Substrate specificity	Detection method for PLA degradation
Amycolatopsis sp. strain HT 32	Protease	<i>L</i> -PLA	Film-weight loss; monomer production (lactic acid)
Amycolatopsis sp. strain 3118	Protease	<i>L</i> -PLA	Film-weight loss; monomer production (lactic acid)
Amycolatopsis sp. strain KT-s-9	Protease	Silk fibroin, <i>L</i> -PLA	Clear-zone method
Amycolatopsis sp. strain 41	Protease	<i>L</i> -PLA, silk powder, casein, Suc-(Ala) <sub>3</sub> -pNA	Film-weight loss; monomer production (lactic acid)
Amycolatopsis sp. strain K104-1	Protease	<i>L</i> -PLA, casein, fibrin	Turbidity method

(Continued)

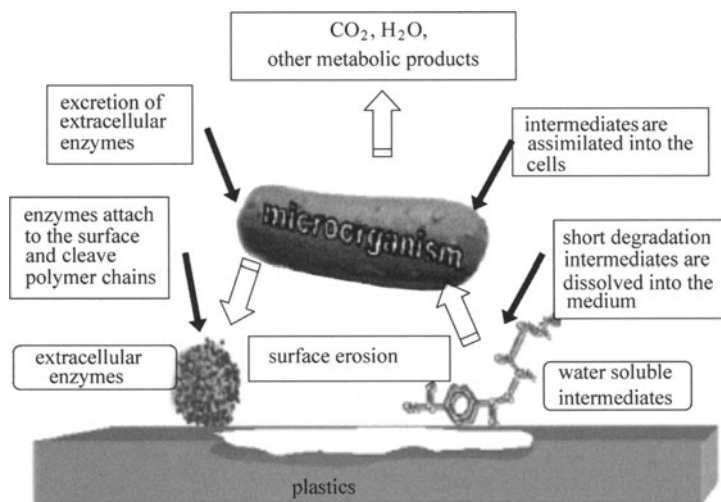
Strain	Type of enzyme	Substrate specificity	Detection method for PLA degradation
Lentzea waywayandensis (formerly Saccharothrix waywayandensis)	Protease	L-PLA	Film-weight loss; monomer production (lactic acid)
Kibdelosporangium aridum	Protease	L-PLA	Film-weight loss; monomer production (lactic acid)
Tritirachium album ATCC 22563	Protease	L-PLA, silk fibroin, elastin	Film-weight loss; monomer production (lactic acid)
Brevibacillus (formerly Bacillus brevis)*	Protease	L-PLA	Change in molecular weight and viscosity
Bacillus stearothermophilus*	Protease	D-PLA	Change in molecular weight and viscosity
Geobacillus thermocatenulatus*	Protease	L-PLA	Change in molecular weight and viscosity
Bacillus sinithii strain PL 21*	Lipase (Esterase)	L-PLA, pNP-fatty Acid esters	Change in molecular weight
Paenibacillus amylolyticus strain TB-13	Lipase	D,L-PLA, PBS, PBSA, PES, PCL, triolein, tributyrin	Turbidity method
Cryptococcus sp. strain S-2	Lipase (Curtinase)	L-PLA, PBS, PCL, PHB	Turbidity method

\* Thermophilic PLA-degrading microorganisms.

Dominant groups of microorganisms and the degradative pathways associated with polymer degradation are often determined by the environmental conditions. When O<sub>2</sub> is available, aerobic microorganisms are mostly responsible for destruction of complex materials, with microbial biomass, CO<sub>2</sub>, and H<sub>2</sub>O as the final products. In contrast, under anoxic conditions, anaerobic consortia of microorganisms are responsible for polymer deterioration. The primary products will be microbial biomass, CO<sub>2</sub>, CH<sub>4</sub> and H<sub>2</sub>O under methanogenic (anaerobic) conditions (Barlaz et al., 1989) (e.g., landfills/compost) (Fig. 8.5).

#### 8.1.4.2 Enzymatic Degradation of PLA

Enzymes are essentially biological catalysts. By lowering the activation energy they can induce an increase in reaction rates in an environment otherwise unfavourable for chemical reactions. Enzymes play a significant role in the degradation of polymers, although they are not solely responsible for the hydrolysis of polymers. The enzymatic degradation of aliphatic polyesters by hydrolysis is a two-step process. The first step is adsorption of the enzyme on the surface of the substrate through surface-binding domain and the second step is hydrolysis of the ester bond.



**Figure 8.5** General mechanism of plastic biodegradation under aerobic conditions [33]

Williams [34] first reported the degradation of *L*-PLA by proteinase K from *T. album*. Since then, this enzyme has been used in studying the degradation characteristics of PLA [35], copolymers of PLA [36], and PLA blends [37]. Oda et al. [38] examined the enzymatic degradation of *L*-PLA at 50°C using 56 commercially available proteases. They found out that acid and neutral proteases had a little or no effect on *L*-PLA degrading activity but some alkaline proteases derived from *Bacillus* spp. showed appreciable *L*-PLA degrading activity. Recently,  $\alpha$ -chymotrypsin was purified and compared its PLA-degrading activity with other serine proteases such as trypsin, elastase, subtilisin, and proteinase K. All tested serine proteases were able to hydrolyze *L*-PLA. Pranamuda et al. [39] purified a *L*-PLA depolymerase from *Amycolatopsis* sp. The purified enzyme has a molecular weight of 43 kDa. The optimum pH and temperature for *L*-PLA depolymerase activity were 6.0 and 37–45°C, respectively. In addition to high molecular weight *L*-PLA, the enzyme can also degrade casein, silk fibroin, succinyl-(*L*-alanyl-*L*-alanyl-*L*-alanine)-*p*-nitroanilide (suc-(ala) 3-pNA), but not PHB and PCL. The ability of the purified enzyme to degrade silk fibroin might be due to its capability to cleave the *L*-alanine unit in which the stereochemical structure is similar to *L*-lactate unit of *L*-PLA. The *L*-PLA-degrading activity was significantly inhibited by the addition of phenylmethylsulfonyl fluoride (PMSF), indicating the presence of serine residues in its active site. The enzyme was not inhibited by pepstatin, aprotinin, and ethylene diamine tetraacetic acid (EDTA). From these results, *L*-PLA degrading enzyme from *Amycolatopsis* sp. is considered as a kind of protease.

## 8.2 Biodegradation Standards and Certification Systems

### 8.2.1 Biodegradation Standards

There are a lot of organizations that have established standards or testing. The main international organizations are

- American Society for Testing and Materials (ASTM) ([www.astm.org](http://www.astm.org));
- European Standardisation Committee (CEN) ([www.cenorm.be](http://www.cenorm.be));
- International Standards Organisation (ISO) ([www.iso.org](http://www.iso.org));
- Institute for Standards Research (ISR);
- German Institute for Standardisation (DIN); and
- Organic Reclamation and Composting Association (ORCA) (Belgium).

The committee D20 in ASTM is responsible for Standardization on Plastics, whereas the subcommittee D20.96 is working on items related specifically to environmentally degradable plastics and biobased products. ASTM standards can be divided into three families. One addresses physical property deterioration in a variety of specific environmental conditions including simulated composting (D5509, D5512), simulated landfill (D5525), aerobic microbial activity (D5247) and marine floating conditions (D5437). The second addresses CO<sub>2</sub> generation in aerobic environments including sewage sludge (D5209), activated sewage sludge (D5271), and controlled composting (D5338). The third addresses CH<sub>4</sub>/CO<sub>2</sub> evolution in anaerobic environments such as anaerobic sewage sludge (D5210), anaerobic biodegradation (D5511), and accelerated landfill (D5526). D6400 differentiates between biodegradable and degradable plastics, and D5152 addresses environmental fate.

There are active ASTM standards on biodegradable plastics as shown in Table 8.2.

**Table 8.2** List of standards by ASTM

ASTM active Standards	Description
D5071-06	Standard practice for exposure of photodegradable plastics in a xenon arc apparatus
D5208-09	Standard practice for fluorescent ultraviolet exposure of photodegradable plastics
D5209-92	Standard test method for determining the aerobic biodegradation of plastic materials in the presence of municipal sewage sludge
D5210-92 (2007)	Standard test method for determining the anaerobic biodegradation of plastic materials in the presence of municipal sewage sludge
D5247-92	Standard test method for determining the anaerobic biodegradability of degradable plastics by specific microorganisms
D5271-02	Standard test method for determining the anaerobic biodegradation of plastic materials in an activated-sludge-wastewater-treatment system

## Biodegradable Poly(Lactic Acid): Synthesis, Modification, Processing and Applications

(Continued)

ASTM active Standards	Description
D5272-92 (1999)	Standard practice for outdoor exposure testing of photodegradable plastics
D5338-98 (2003)	Standard test method for determining aerobic biodegradation of plastic materials under controlled composting conditions
D5510-94 (2001) <sup>a</sup>	Standard practice for heat aging of oxidatively degradable plastics
D5511-02	Standard test method for determining anaerobic biodegradation of plastic materials under high-solids anaerobic-digestion conditions
D5526-94 (2002)	Standard test method for determining anaerobic biodegradation of plastic materials under accelerated landfill conditions
D5951-96 (2002)	Standard practice for preparing residual solids obtained after biodegradability standard methods for plastics in solid waste for toxicity and compost quality testing
D5988-03	Standard test method for determining aerobic biodegradation in soil of plastic materials or residual plastic materials after composting
D6002-96 (2002)e1	Standard guide for assessing the compostability of environmentally degradable plastics
D6003-96	Standard test method for determining weight loss from plastic materials exposed to simulated municipal solid-waste (MSW) aerobic compost environment
D6340-98(2007)	Standard test methods for determining aerobic biodegradation of radiolabeled plastic materials in an aqueous or compost environment
D6400-99e1 <sup>a</sup>	Standard specification for compostable plastics
D6691 e 01	Standard test method for determining aerobic biodegradation of plastic materials in the marine environment by a defined microbial consortium
D6692 e 01	Standard test method for determining the biodegradability of radiolabeled polymeric plastic materials in seawater
D6776-02	Standard test method for determining anaerobic biodegradability of radiolabeled plastic materials in a laboratory-scale simulated landfill environment
D6852-02	Standard guide for the determination of bio-based content, resources consumption, and environmental profile of materials and products
D6866-08	Standard test methods for determining the bio-based content of natural range materials using radiocarbon and isotope ratio mass spectrometry analysis
D6868-03	Standard specification for biodegradable plastics used as coatings on paper and other compostable substrates
D6954-04	Standard guide for exposing and testing plastics that degrade in the environment by a combination of oxidation and biodegradation
D7026-04	Standard guide for sampling and reporting of results for the determination of bio-based content of materials via carbon isotope analysis
D7081-05	Standard Specification for Non-Floating Biodegradable Plastics in the Marine Environment
F1635-04a	Standard Test Method for in vitro Degradation Testing of Hydrolytically Degradable Polymer Resins and Fabricated Forms for Surgical Implants



(Continued)

ASTM active Standards	Description
F2027-08	Standard Guide for Characterization and Testing of Raw or Starting Biomaterials for Tissue-Engineered Medical Products
F2150-07	Standard Guide for Characterization and Testing of Biomaterial Scaffolds Used in Tissue-Engineered Medical Products
G114-07	Standard Practices for Evaluating the Age Resistance of Polymeric Materials Used in Oxygen Service
F2502-05	Standard Specification and Test Methods for Bioabsorbable Plates and Screws for Internal Fixation Implants
D7075-04	Standard Practice for Evaluating and Reporting Environmental Performance of Biobased Products

The European Committee for Normalisation (CEN) established the norm (CEN prEN 13432) in 1999. The Technical Committees CEN TC261-Packaging and CEN TC249-Plastics are responsible for standardization on items based on polymeric materials. The TC261 comprises the Subcommittee SC4 working on environmental matters and also having an ad hoc group on heavy metal and dangerous substances. Plastic products can provide proof of their compostability by successfully meeting the harmonised European standard, EN 13432 or EN 14995. This standard can apply to other packaging materials in addition to polymers, and incorporates the following tests and standards:

- ISO 14855;
- ISO 14855 (respirometric);
- ISO 14852;
- ASTM D5338-92;
- ASTM D5511-94;
- ASTM D5152-92;
- ASTM E1440-91;
- Modified OECD 207; and
- CEN TC 261/SC4/WG2.

The standard specifies scope of test under EN 13432 / EN 14995 includes:

- Chemical test which discloses all constituents, threshold values for heavy metals are to be adhered to;
- Biodegradability in watery medium (oxygen consumption and production of CO<sub>2</sub>): Proof must be made that at least 90% of the organic material is converted into CO<sub>2</sub> within 6 months. In addition, the material must not exceed a heavy metals content above 50% of that for “normal” compost, as follows: Zn 150 ppm; Cr 50 ppm; Cu 50 ppm; Mo 1 ppm; Ni 25 ppm; Se 0.75 ppm; Cd 0.5 ppm; As 5 ppm; Pb 50 ppm ; F 100 ppm ; Hg 0.5 ppm.
- Disintegration in compost: After 3 months’ composting and subsequent sifting through a 2 mm sieve, no more than 10% residue may remain, as compared to the original mass.

## Biodegradable Poly(Lactic Acid): Synthesis, Modification, Processing and Applications

- Practical test of compostability in a semi-industrial (or industrial) composting facility: No negative influence on the composting process is permitted.
- Compost application: Examination of the effect of resultant compost on plant growth (agronomic test), ecotoxicity test.

The norm provides the European Commission's European Directive on Packaging and Packaging Waste with appropriate technical regulations and standards. This norm is a reference point for all European producers, authorities, facility managers and consumers.

The CEN TC249 comprises the working group WG9 entitled to propose standards on "Characterization of Degradability" of plastics. (Table 8.3). Many of the CEN standards are based on ISO standards. The adoption of CEN standards and norms is legally required for all EU member countries.

**Table 8.3** List of eight standards by CEN TC261 committee related to testing of biodegradable plastics

CEN standard	Description
EN 13432:2000	Packaging—requirements for packaging recoverable through composting and biodegradation—test scheme and evaluation criteria for the final acceptance of packaging
EN 14045:2003	Packaging—evaluation of the disintegration of packaging materials in practical oriented tests under defined composting conditions
EN 14046:2003	Packaging—evaluation of the ultimate aerobic biodegradability of packaging materials under controlled composting conditions—method by analysis of released carbon dioxide
EN 14047:2002	Packaging—determination of the ultimate aerobic biodegradability of packaging materials in an aqueous medium—method by analysis of evolved carbon dioxide
EN 14048:2002	Packaging—determination of the ultimate aerobic biodegradability of packaging materials in an aqueous medium—method by measuring the oxygen demand in closed respirometer
EN14806:2005	Packaging—Preliminary evaluation of the disintegration of packaging materials under simulated composting conditions in a laboratory-scale test
EN 14995 :2007	Plastics—evaluation of compostability—test scheme and specifications
EN ISO 14851:2004	Determination of the ultimate aerobic biodegradability of plastic materials in an aqueous medium—method by measuring the oxygen demand in a closed respirometer (ISO14851:1999)
EN ISO 14852:2004	Determination of the ultimate aerobic biodegradability of plastic materials in an aqueous medium—method by analysis of evolved carbon dioxide (ISO14852:1999)
EN ISO 14855:2004	Determination of the ultimate aerobic biodegradability and disintegration of plastic materials under controlled composting conditions—method by analysis of evolved carbon dioxide (ISO14855:1999)
EN ISO 14856:2004	Plastics—determination of the ultimate aerobic biodegradability in soil by measuring the oxygen demand in a respirometer or the amount of carbon dioxide evolved (ISO 14856:2003)
EN ISO 20200:2005	Plastics—determination of the percentage disintegration in a laboratory composting environment

The International Organization for Standardization (Organisation internationale de normalisation), widely known as ISO, is an international-standard-setting body composed of representatives from various national standards organizations. Founded on Feb. 23, 1947, the organization promulgates worldwide proprietary industrial and commercial standards. Most standards relevant to degradation of plastics under ISO are issued under the committee T61/SC5/WG22 (technical committee TC61 working on plastics, subcommittee SC5 on physical and chemical properties, and working group WG22 on biodegradable plastics). There are currently 23 active standards (Table 8.4).

**Table 8.4** List of 23 published standards by ISO TC61/SC5 committee

ISO standard	Description
ISO 7827:1994	Water quality—evaluation in an aqueous medium of the “ultimate” aerobic biodegradability of organic compounds—method by analysis of dissolved organic carbon (DOC)
ISO9408:1999	Water quality—evaluation of ultimate aerobic biodegradability of organic compounds in aqueous medium by determination of oxygen demand in a closed respirometer
ISO9439:1999	Water quality—evaluation of ultimate aerobic biodegradability of organic compounds in aqueous medium—carbon dioxide evolution test
ISO9887:1992	Water quality—evaluation of ultimate aerobic biodegradability of organic compounds in aqueous medium—semi-continuous activated-sludge method (SCAS)
ISO9888:1999	Water quality—evaluation of ultimate aerobic biodegradability of organic compounds in aqueous medium—static test (Zahn-Wellens method)
ISO 10634:1995	Water quality—guidance for the preparation and treatment of poorly water-soluble organic compounds for subsequent evaluation of their biodegradability in an aqueous medium
ISO 10707:1994	Water quality—evaluation in an aqueous medium of the “ultimate” aerobic biodegradability of organic compounds—method by analysis of biochemical oxygen demand (closed-bottle test)
ISO 10708:1997	Water quality—evaluation in aqueous medium of ultimate aerobic biodegradability of organic compounds determination of biochemical oxygen demand in a two-phase closed-bottle test
ISO 11266:1994	Soil quality—guidance on laboratory testing for biodegradation of organic chemicals in soil under aerobic conditions
ISO 11733:2004	Water quality—determination of the elimination and biodegradability of organic compounds in an aqueous medium—activated-sludge simulation test
ISO 11734:1995	Water quality—evaluation of the “ultimate” anaerobic biodegradability of organic compounds in digested sludge—method by measurement of the biogas production

## Biodegradable Poly(Lactic Acid): Synthesis, Modification, Processing and Applications

(Continued)

ISO standard	Description
ISO 14592-1:2002	Water quality—evaluation of the aerobic biodegradability of organic compounds at low concentrations—part 1: shake-flask batch test with surface water or surface water/sediment suspensions
ISO 14592-1:2002	Water quality—evaluation of the aerobic biodegradability of organic compounds at low concentrations—part 2: continuous flow river model with attached biomass
ISO 14593:1999	Water quality—evaluation of the aerobic biodegradability of organic compounds in aqueous medium—method by analysis of inorganic carbon in sealed vessels (CO <sub>2</sub> headspace test)
ISO 14851:1999	Determination of the ultimate aerobic biodegradability of plastic materials in an aqueous medium—method by measuring the oxygen demand in a closed respirometer
ISO 14852:1999	Determination of the ultimate aerobic biodegradability of plastic materials in an aqueous medium—method by analysis of evolved carbon dioxide
ISO 14855:1999	Determination of the ultimate aerobic biodegradability and disintegration of plastic materials under controlled composting conditions—method by analysis of evolved carbon dioxide
ISO/TR15462:1997	Water quality—selection of tests for biodegradability
ISO 15473:2002	Soil quality—guidance on laboratory testing for biodegradation of organic chemical in soil under anaerobic conditions
ISO 16221:2001	Water quality—guidance for the determination of biodegradability in the marine environment
ISO 16929:2002	Plastics—determination of the degree of disintegration of plastic materials under defined composting conditions in a pilot-scale test
ISO 17556:2003	Plastics—determination of the ultimate aerobic biodegradability in soil by measuring the oxygen demand in a respirometer or the amount of carbon dioxide evolved
ISO 20200:2004	Plastics—determination of the degree of disintegration of plastic materials under simulated composting condition in a laboratory-scale test

Currently European biodegradable plastics are assessed by three ISO standards: ISO14855, ISO14852 and ISO15985. ISO14855 is a controlled aerobic composting test, and ISO14851 and ISO14852 are biodegradability tests specifically designed for polymeric materials. An important part of assessing biodegradable plastics is testing for disintegration in the form in which it will be ultimately used. Either a controlled pilot-scale test or a test in a full-scale aerobic composting treatment facility can be used. Due to the nature and conditions of such disintegration tests, the tests cannot differentiate between biodegradation and abiotic disintegration, but instead demonstrate that sufficient disintegration of the test materials has been achieved within the specified testing time.

The committee responsible in DIN is the DIN FNK 103.3. There are currently nine active standards as shown in Table 8.5.

**Table 8.5** List of nine standards DIN FNK 103.3 committee

DIN Standards	Description
DIN V 54900-1	Testing of compostability of plastics—part 1: chemical testing
DIN V 54900-2	Testing of compostability of plastics—part 2: testing of the complete biodegradability of plastics in laboratory tests
DIN V 54900-3	Testing of compostability of plastics—part 3: testing under practice—relevant conditions and a method of testing the quality of the composts
DIN V 54900-4	Testing of compostability of polymeric materials—part 4: testing the ecotoxicity of the composts
DIN EN 13432	Requirements for packaging recoverable through composting and biodegradation—test scheme and evaluation criteria for the final acceptance of packaging
DIN EN 14045	Evaluation of the disintegration of packaging materials in practical oriented tests under defined composting conditions
DIN EN 14995	Plastics—evaluation of compostability—test scheme and specifications
DIN EN ISO 14851	Determination of the ultimate aerobic biodegradability of plastic materials in an aqueous medium—method by measuring the oxygen demand in a closed respirometer (ISO 14851:1999)
DIN EN ISO 14852	Determination of the ultimate aerobic biodegradability of plastic materials in an aqueous medium—method by analysis of evolved carbon dioxide (ISO 14852:1999)

The performance of biodegradable plastics in composting facilities and under laboratory conditions has been studied by ISR. ISR has determined that plastics need to meet the following three criteria in order to be compostable:

- They must biodegrade at the same rate and to the same extent as known compostable material such as garden waste and paper, and leave no persistent or toxic residues.
- They must disintegrate during active composting so there are no visible or distinguishable fragments found on the screens.
- They must have no ecotoxicity or phytotoxicity that may impact on the ability of the compost to support plant growth.

## 8.2.2 Different Certification Systems

Certification enables consumers to easily identify that a certain product has been independently verified as meeting particular performance requirements, usually through a clearly recognisable logo.

There are several overseas certification programs for degradable plastics.


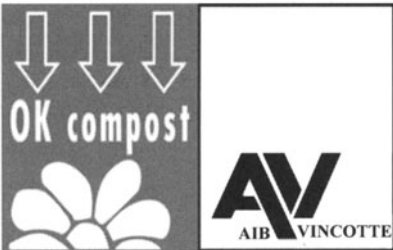
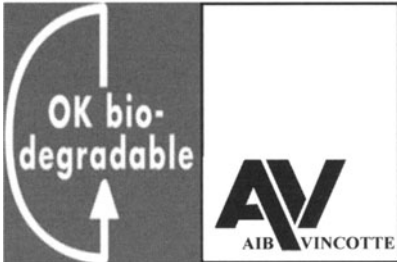
The German, United States and Japanese certification schemes are cooperating to enable international cross-certification of products, so that a product certified in one of these countries would automatically be eligible for certification in another. This would substantially reduce delays and costs for degradable plastics manufacturers and suppliers because the tests required for certification typically

## Biodegradable Poly(Lactic Acid): Synthesis, Modification, Processing and Applications




take around six months, and can be quite costly.

Some examples of overseas certifications programs and their logos are listed below. Please be aware that Australian Government does not in any way endorse these programs; they are provided for reference only:

The intensive work and development of international standards related to biodegradability and compostability of bioplastics and packaging materials are an important and vital element in the market development and breakthrough of these materials. Still, this is only the first step in the communication and build-up of credibility towards customers and authorities. The next step required is the formation of an independent and reliable certification system linked to a logo. The certification body is needed to evaluate the often complex information and make a correct judgement on the overall characteristics of a given material. In a way one could see it as standards being the theory and certification systems turning the theory into practice.

Certification systems	Logo	Organization	Based standard
DIN-Certco compostability certification scheme		DIN-Certco, Germany	the EN ISO/IEC 17025-1 standard for quality control and assurance in test laboratories.
OK Compost		AIB-vinçotte international (AVI), Belgium	EN 13432
OK Biodegradable		AIB-vinçotte international (AVI), Belgium	a certification scheme prepared by AVI itself

(Continued)

Certification systems	Logo	Organization	Based standard
BPI Logo	 The logo for BPI (Biodegradable Products Institute) features the letters 'BPI' in a large, bold, sans-serif font. To the right of 'BPI' is the text 'Biodegradable Products Institute' in a smaller font, with a circular icon containing a stylized globe. Below the main text is the tagline 'promoting biodegradable products throughout the world'.	International biodegradable products institute (BPI) and the US composting council (USCC), USA	ASTM D6400 and ASTM D6868
GreenPla Certification System	 The logo for GreenPla Certification System is a vertical rectangular emblem. At the top is a stylized green apple with a leaf. Below the apple is the Japanese text 'グリーンプラ' (GreenPla) in a bold, sans-serif font. At the bottom of the emblem is the Japanese text '生分解性プラスチック' (Biodegradable Plastic).	the biodegradable plastics society (BPS), Japan	a certification scheme prepared by BPS itself
the apple-logo	 The logo is a stylized, cartoonish illustration of an apple core. The apple has a smiling face with two dots for eyes and a curved line for a mouth. It has a short stem with a single leaf at the top. The bottom of the apple is shaded to represent the core.	the Jätelaitosyhdistys (Finnish solid waste association, organization coordinating activities of composting facilities), Finland	EN 13432

## 8.3 Introduction to Some Test Methods

### 8.3.1 Visual Observation

Polymer degradation usually leads to roughening of the surface, formation of holes or cracks, de-fragmentation, changes in color, or formation of bio-films on the surface. In order to obtain more information, X-ray photoelectron spectroscopy (XPS), SEM, atomic force microscopy (AFM), X-ray Diffraction (XRD), contact angle can be used to explain the degradation mechanism. A number of other techniques can also be used to assess the biodegradability of polymeric material such as Fourier transform infrared spectroscopy (FTIR), differential scanning calorimetry (DSC), nuclear magnetic resonance spectroscopy (NMR), XPS and

water uptake. Use of these techniques is generally beyond the scope of this book, although some are mentioned in the text.

### **8.3.2 Gravimetry**

Gravimetric method is the most widely used technique with a long history of success. The mass loss of test specimens is widely applied in degradation tests (especially in field- and simulation tests). By combining a structural analysis of the residual material and the low molecular weight intermediates, detailed information regarding the degradation process can be obtained, especially if a defined synthetic test medium is used.

### **8.3.3 Enzyme Assays**

In enzyme assays, the polymer substrate is added to a buffered or pH-controlled system, containing one or several types of purified enzymes. These assays are very useful in examining the kinetics of depolymerisation, or oligomer or monomer release from a polymer chain under different assay conditions. The method is very rapid (minutes to hours) and can give quantitative information. However, mineralisation rates cannot be determined with enzyme assays.

### **8.3.4 Plate Tests**

Plate tests were initially developed to assess the resistance of plastics to microbial degradation. They are now also used to see if a polymeric material will support growth. The principle of the method involves placing the test material on the surface of a mineral salts agar in a petri dish containing no additional carbon source. The petri dishes are sealed and incubated with known bacteria and/or fungi at a constant temperature between 21 and 28 days. This results in the agar having an opaque appearance. The formation of the clear halo around the colony indicates that the organisms are at least able to depolymerize the polymer. The test material is then examined for the amount of growth on its surface and a given rating.

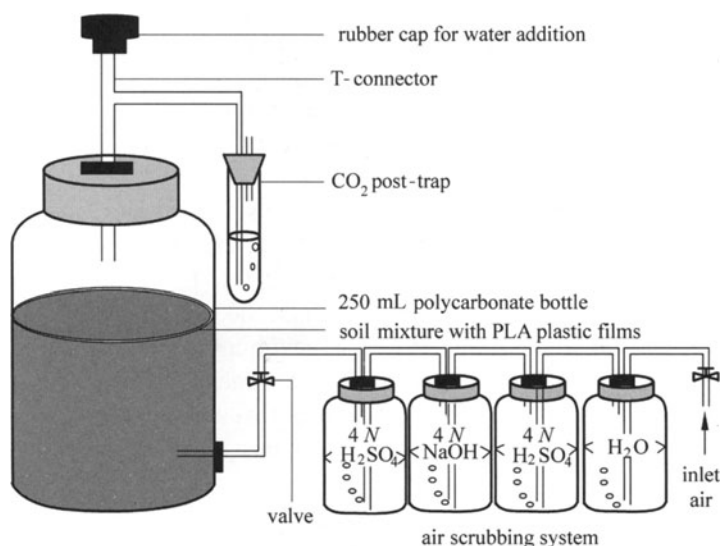
### **8.3.5 Respiration Tests**

This method measures either CO<sub>2</sub> produced or O<sub>2</sub> consumed or both of them in an enclosed system with proper maintenance or regulation of air or oxygen



supply. This is the most often used method to measure biodegradation in laboratory tests, especially suitable for confirmation on the extent of mineralization. Besides conventional trapping of  $\text{CO}_2$  in  $\text{Ba}(\text{OH})_2$  solution, followed by manual titration, infrared and paramagnetic  $\text{O}_2$  detectors can also be used to monitor  $\text{O}_2$  and  $\text{CO}_2$  concentrations in the air stream. The mixture is stirred in the closed flask of a respirometer. The biodegradation is calculated as the ratio of the biological oxygen demand (BOD) to the theoretical oxygen demand (TOD). The evolution of carbon dioxide or methane from a substrate represents a direct parameter for mineralisation.

Ho and Pometto reported respirometer system used to analyze the degradation of PLA plastic film in soil (Fig. 8.6) [40]. The respirometric system consisted of airconditioning pretraps, the soil reactor, and a  $\text{CO}_2$  posttrap. The  $\text{CO}_2$ -free humidified air was generated by sequentially scrubbing through carboys of deionized water, 4 *N* sodium hydroxide ( $\text{NaOH}$ ), and 4 *N* sulfuric acid ( $\text{H}_2\text{SO}_4$ ). Each respirometer consisted of a heat-sterilized 250 mL wide-mouth screw-capped polycarbonate bottle modified with air inlet and outlet ports. The outlet port was a T-connector fitted with a rubber septa for water addition. A 200 g homogeneous soil mixture of potting soil: manure soil: sand [1:1:1 (w/w)] and 1.5 g of  $1 \times 1 \text{ cm}^2$  plastic films were added to each bottle in layers. The respirometers were placed in a 28, 40, or 55°C water bath for 182 days. Exit air from each reactor was passed through a  $\text{CO}_2$  trap of 10 mL 4 *N*  $\text{NaOH}$  in a test tube with a bubble retention disk at 15 mL/min. It was determined that each trap would hold 240 mg carbon as  $\text{CO}_2$ . The  $\text{CO}_2$  traps were changed weekly and the amount of  $\text{CO}_2$  trapped was determined by pH titration (pH 8.3 to 4.2) with



**Figure 8.6** Schematic diagram showing the respirometer setup

standardized 0.4 *N* hydrochloric acid (HCl) using two autotitrators. Mineralization of PLA plastic films was indicated by the cumulative CO<sub>2</sub> (mg) liberated from each respirometer. The mineralization rate of each PLA plastic film at different temperature was determined by measuring the slope on the steepest region of the  $M_w$  versus time curve.

### 8.3.6 Controlled Composting Test

Compost may be the key to maximising the real environmental benefit of biodegradable plastics. Mature compost is a very heterogeneous and complex material. Therefore, it can be difficult to quantify the residual polymeric material left in the bed at the end of the test, to detect possible low-molecular-mass molecules released into the solid bed by the polymeric material during degradation, and to assess the biomass. As a result, it can be difficult to perform a complete carbon balance. Another difficulty which is sometimes encountered with mature compost is a “priming effect”: the organic matter present in large amounts in the mature compost can undergo polymer-induced degradation, known as the “priming effect”, which affects the measurement of the biodegradability. To overcome these difficulties and to improve the reliability of the method, the mature compost can be replaced by a solid mineral medium which is used as the composting bed. The treatment of solid waste in controlled composting facilities or anaerobic digesters is a valuable method for treating and recycling organic waste. The test method determines the ultimate biodegradability and degree of disintegration of test material under conditions simulating an intensive aerobic composting process. The inoculum used consists of stabilized, mature compost derived, if possible, from composting the organic fraction of solid municipal waste. The test material is mixed with the inoculum and introduced into a static composting vessel where it is intensively composted under optimum oxygen, temperature and moisture conditions for a test period not exceeding 6 months.

For ISO14855, the CO<sub>2</sub> produced is continuously monitored, or measured at regular intervals, in test and blank vessels to determine the cumulative CO<sub>2</sub> production. The percentage biodegradation is given by the ratio of the CO<sub>2</sub> produced from the test material to the maximum theoretical amount of CO<sub>2</sub> that can be produced from the test material. The maximum theoretical amount of CO<sub>2</sub> produced is calculated from the measured total organic carbon (TOC) content. The percentage biodegradation does not include that amount of carbon converted to new cell biomass which is not metabolized in turn to carbon dioxide during the course of the test.

To meet the ASTM D5338–93 standard, 60% of single polymer materials must mineralise in six months, and 90% must do so in blends. Materials should give way to intense microbial activity and be converted from carbon to CO<sub>2</sub>,

biomass and water. Materials also should begin to fragment, at which point disintegration begins. In this phase, the material must completely physically and visually disintegrate. 90% of the disintegrated material must not adversely affect the quality of the compost. Finally, even after land application, remaining materials should be safely converted into CO<sub>2</sub> by microorganisms. The resultant compost should not be toxic and should not deter plant growth.

## Reference

- [1] Zheng Ying, Ernest K. Yanful, Amarjeet S. Bassi. *Critical Reviews in Biotechnology*, 25, 243 (2005).
- [2] Kister G., Cassanas G., Bergounhon M., et al. *Polymer*, 41, 925 (2000).
- [3] Proikakis C. S., Mamouzelous N. J., Tarantili P. A., et al. *Polym. Degrad. Stab.*, 91(3), 614 (2006).
- [4] McDonald R. T., McCarthy S., Gross R. A. *Macromolecules*, 29, 7356 (1996).
- [5] Cai H., Dave V., Gross R. A., et al. *J. Polym. Sci. B. Polym. Phys.*, 34, 2701 (1996).
- [6] Iwata T., Doi Y. *Macromolecules*, 31, 2461 (1998).
- [7] Tsuji H., Miyauchi S. *Polym. Degrad. Stab.*, 71, 415 (2001).
- [8] Tokiwa Y., Suzuki T. *Agric. Biol. Chem.*, 42, 1071 (1978).
- [9] Tokiwa Y., Suzuki T. *J. Appl. Polym. Sci.*, 26, 441 (1981).
- [10] Tokiwa Y., Suzuki T., Ando T. *J. Appl. Polym. Sci.*, 24, 1701 (1979).
- [11] Li S., McCarthy S. *Macromolecules*, 32, 4454 (1999).
- [12] Torres A., Li S. M., Roussos S., et al. *J. Environ. Polym. Degrad.*, 4, 213 (1996).
- [13] Briassoulis D. *Polym. Degrad. Stab.*, 92, 1115 (2007).
- [14] Nathalie Lucas, Christophe Bienaime, Christian Belloy, et al. *Chemosphere*, 73, 429 (2008).
- [15] Ranby B. J. *Anal. Appl. Pyrolysis*, 15, 237 (1989).
- [16] Tsuji H., Echizen Y., Nishimura Y. *Polym. Degrad. Stab.*, 91, 1128 (2006).
- [17] McNeill I. C., Leiper H. A. *Polym. Degrad. Stab.*, 11, 267 (1985).
- [18] McNeill I. C., Leiper H. A. *Polym. Degrad. Stab.*, 11, 309 (1985).
- [19] Jamshidi K., Hyon S. H., Ikada Y. *Polymer*, 29, 2229 (1988).
- [20] Zhang X., Wyss U. P., Pichora D., et al. *Polym. Bull.*, 21, 623 (1992).
- [21] Wachsen O., Reichert K. H. *Polym. Degrad. Stab.*, 55, 225 (1997).
- [22] Briassoulis D. *Polym. Degrad. Stab.*, 86, 489 (2005).
- [23] Duval C. *Matériaux Déggradables In Matières Plastiques et Environnement–Recyclage, Valorisation, Biodégradabilité, écoconception*. DUNOD, Paris (2004).
- [24] Muller R. J., Witt U., Rantze E., et al. *Polym. Degrad. Stab.*, 59, 203 (1998).
- [25] Tsuji H., Ikada Y. *Polym. Degrad. Stab.*, 67(1), 179 (2000).
- [26] He Yi, Qian Zhiyong, Zhang Hailian, et al. *Colloid Polym. Sci.*, 282(9), 972 (2003).
- [27] De Jong, S. J., Arias E. R., Rijkers D. T. S., et al. *Polymer*, 42, 2795 (2001).
- [28] Nathalie Lucas, Christophe Bienaime, Christian Belloy, et al. *Chemosphere*, 73, 429 (2008).
- [29] Nishida H., Tokiwa Y. *J. Appl. Polym. Sci.*, 46, 1467 (1992).

## **Biodegradable Poly(Lactic Acid): Synthesis, Modification, Processing and Applications**

- [30] Yutaka Tokiwa, Buenaventurada P. Calabia. *Appl. Microbiol. Biotechnol.*, 72, 244 (2006).
- [31] Baljit Singh, Nisha Sharma. *Polymer Degradation and Stability*, 93, 561 (2008).
- [32] Yutaka T., Buenaventurada P. *Appl. Microbiol. Biotechnol.*, 72, 244 (2006).
- [33] Mueller R. J. In: Steinbüchel A. (ed.). *Biopolymers* (vol. 10). Weinheim: Wiley-VCH (2003).
- [34] Williams D. F. *Eng. Med.*, 10, 5 (1981).
- [35] McDonald R. T., McCarthy S., Gross R. A. *Macromolecules*, 29, 7356 (1996).
- [36] Moon S. I., Urayama H., Kimura Y. *Macromol. Biosci.*, 3, 301 (2003).
- [37] Tsuji H., Miyauchi S. *Polym. Degrad. Stab.*, 71, 415 (2001).
- [38] Oda Y., Yonetsu A., Urakami T., et al. *J. Polym. Environ.*, 8, 29 (2000).
- [39] Pranamuda H., Tsuchii A., Tokiwa Y. *Macromol. Biosci.*, 1, 25 (2001).
- [40] Ho K. G., Pometto III A. L. *Journal of Polymers and the Environment*, 7(2), 242 (1999).

# Index

## A

acidic 5,6,25,55,242,249,252,258,278,279  
adiabatic crystallization 11  
additives 12,30,38,100-103,109,112,113,  
163,164,179,185,186,215,232,235,275,276  
aerobic 273,276,281-284,286-289,294  
alpha hydroxy acid (AHA) 5  
alkaline 35,277-279,282  
alternating copolymer 39  
American Society for Testing and Materials  
(ASTM) 283  
ammonium lactate (NH<sub>4</sub>LA) 10  
amphiphilic 46,50,51,55,59,60,62,64,176,255  
anionic polymerization 47,49  
anisotropic structure 163  
annealing 50,85,128,158-161,178,182,  
anoxic 273,281  
application 1-3,6,12,13,24,32,33,38-44,  
48-51,53-57,59,64-66,68,69,78,85,87,  
94,99-102,106,109,110,112,114-116,121,  
124,128,130,142,146,147,151,157,158,  
170,174,177,179,186,190,206,208-214,  
216,218,220,221,224,229,230,234-237,  
240,241,243,244,253-255,258,260,264,  
271,273-276,295  
*Arg-Gly-Asp* tripeptide (RGD) 42  
as-spun fibers 153,154,163,165,169  
atom transfer radical polymerization  
(ATRP) 52,60,62  
atomic force microscopy (AFM) 291  
azeotropic dehydrative polycondensation 15,  
21,22  
azeotropic distillation technique 21

## B

bioabsorbable surgical suture 240  
biodegradable 1,4,6,12,20,32,33,38,39,41,  
44,47-49,51-56,59,61,64,66,69,72,78,94,97,  
101,102,114,116,121,124,130,152,153,158,  
175,195,204,209,211-216,218-225,229-235,  
240-242,244,254,257,260,273,274,276,283,  
284,286-289,291,294  
biomedical 1,2,24,32,33,40,42,51,55-57,59,  
64,65,69,137,151,174,179,230,240,241,243,  
245,247,249,251,253-255,257,259-261,263,  
265,267,269-272  
biotextile 212,213  
biotic degradation 280  
blending 38,68,69,72,75,78,83-86,93,94,  
115,116,121,123,127,128,130,131,184,186,  
187  
block copolymer 45-48,50-52,57,59,61,62,  
64,217,257  
blowing 3,97,142,149,179,184,185,189,195  
branched copolymer 54  
bulk polycondensation 16,21,22  
1,4-butane diisocyanate (BDI) 187,200  
1,4-butanediol (BD) 187  
butanol 10

## C

calcium salt 10  
 $\epsilon$ -caprolactone (CL) 24,40,47,48,57,58,62,  
149,229,230  
*N*-carboxyanhydride (NCA) 44,52,56,61  
catalyst 3,7,10,12,15-23,26,27,32-35,  
39-41,43-45,47,48,50,54,55,59,134,281  
cationic polymerization 24,26

## Biodegradable Poly(Lactic Acid): Synthesis, Modification, Processing and Applications

- cellulose 33,54,99,104,114,115,170,172, 190,212  
chain oligomer 17  
chemical degradation 276,277  
chitin 55  
chitosan 55  
chondroitin sulfate 55  
cigarette filter tows 220  
coaxial electrospinning 142,175,176  
cold-crystallization 91,93  
colorfastness 117,172,173  
comb polymer 62  
commodity application 121,124,210  
comonomer 39,40,43,45,51,79,195,214  
cooling crystallization 10,11  
coordination-insertion mechanism 28-31  
copolymerization 3,38-41,43-46,48,49,54, 57,58,114,115,186,214  
core-sheath composite fibers 176,177  
core-sheath nanofiberscoupling agent 176  
cross-sectional shape 157  
crystallization 4,10,11,14,18,38,50,57,61, 72,74-76,85,91,93,94,96,97,116,124,126, 127-129,131,134,146-148,154,156,157,159- 161,163,167,178,204,209,214  
cyclic oligomer 17,20  
cyclodextrin (CD) 59  
cyclophosphazene 58
- D**
- degree of polymerization (DP) 6,17,24,33, 61,109  
dehydration equilibrium 16,17  
dendrimer 59,60,62,66  
dendritic copolymer 67  
dendron 38,59,66  
depolymerization 16-18,21,32,41  
dextran 55  
dibenzoyl peroxide(BPO) 186  
dicyclohexyldimethylcarbodiimide (DCC) 52,66  
differential scanning calorimetry (DSC) 291  
*N,N'*-Dimethylacrylamide (DMAAm) 255  
4-dimethylaminopyridine (DMAP) 19,54  
2,5-dimethyl-2,5-di-(*tert*-butylperoxy) hexane (L101) 191,195  
2,2-dimethyltrimethylene carbonate (DTC) 49  
1,5-dioxepan-2-one (DXO) 25  
*p*-dioxanone (PDO) 49,262  
direct polycondensation 3,15-23,52,53,55  
disperse dyes 117,119,120,170,172,173  
disposable ware 208,222,226  
D-lactic acid 4,13,15,16,157,160  
3-*s*-[(dodecyloxycarbonyl)methyl]-1,4- dioxane-2,5-dione (DMD) 41  
draw ratio 154-156,158,160,162-166,169, 214  
driving force 11,24,96,159  
drug delivery 38,44,48,50,51,56,59,62,66, 78,85,169,213,215,216,218,220,240,253, 254,257,259,260  
dry spinning 142,153,161,162,164-167,173  
dry-jet-wet spinning 142,153,168,169  
dry-wet phase-inversion spinning process 142,169  
dyeability 79,142,170-172,210  
dyeing 81,117,170-172,211
- E**
- ecofriendliness 210  
electro-dialysis 4,9  
electrospinning 142,153,173-179,216-220, 252,253  
end group 21,29,57,110,111,187,189  
engineering plastic 3,208,220  
environmental protection 208,221  
enzymatic 33,35,70,71,81,85,95,275,281,282  
enzyme-catalyzed polymerization 15  
enzymes catalyze 33  
equilibrium constants 17  
ester 2,4,6,9,10,17,25,26,28,29,32,40,41, 42,47,56,71,94,107,108,110,111,114,232, 235,236,244,245,277,278,281  
esterification 4,6,7,9,10,16,18,19,21,62,242  
ethylene diamine tetraacetic acid (EDTA) 282

European Standardisation Committee (CEN)  
283  
evaporation crystallization 11  
extracellular matrix (ECM) 55,242,243,245  
extrusion 2,69,97,121,147,148,154-156,161,  
162,163,167,184,185,186,195,198,201

**F**

fermentation 4,6-10,12,13,15,221  
flame retardant 101-107,109  
fibre 109,208,221,236  
foaming 3,142,147,148,186,189,196-200,  
202-204,252  
foam molding 142  
Fourier transform infrared spectroscopy  
(FTIR) 291  
frustrated crystal structure 126

**G**

gas foaming 148,252  
gel permeation chromatography (GPC) 68  
German Institute for Standardisation (DIN)  
283  
glycolic acid (GA) 39,40  
glycolide (GA) 48,58  
glycolysis 8,9  
graft copolymer 54,56,64,231

**H**

heat deflection temperature (HDT) 3,38,  
132,146  
heat sealing property 183  
helical conformation 61,126,162,164  
heteroarm 63  
high-speed melt spinning 159,161  
hollow fiber structure 162  
hot-drawing 154  
hot-melt adhesive 208,229,235  
hydrogen cyanide 7  
hydrolysis 2,4,7,9,10,29,35,81,82,83,95,97,  
102,215,229,244,277,278,279,281  
hydrophilicity 2,39,41,47,51,52,59,60,  
244-246  
hydroxyl terminated PLA (OH-PLA) 21,200

hyperbranched 59

**I**

initiator 24-29,32,35,39,40,43,45-48,53,54,  
57-60,62,132,195  
injection 2,3,68,97,109,122,142-152,263,  
injection molding 2,68,97,142,143,144,146,  
147,148,149-152  
Institute for Standards Research (ISR) 283  
International Standards Organisation (ISO)  
283  
isothermal crystallization 127,128  
itaconic acid 21

**J**

Jacobson-Stockmayer theory 17

**K**

kinetic 15,23,72,95,127,157,158,159,160,  
204,216,251,292  
knot-pull strength 215  
Krebs cycle 8

**L**

lactide (LA) 1,3,12,15-35,38,39,41-47,52,  
54-56,144,191,193,195,199,242,275,277  
ligand 30,31,33  
*L*-lactic acid 4,6,8,13,15,17-22,40,41,42,44,  
45,50,54-56,66,78,147,148,181,214,254  
*L*-lysine (lys) 45  
low carbon 208  
low-density polyethylene (LDPE) 179,206  
lower critical solution temperatures (LCST)  
51,66,255

**M**

macromolecule 35-37,56,136-141,159,160,  
204,206,236,267,268-270,277,295,296  
maleic anhydride (MAH) 64,124,190,191,  
193,194,195  
matrix-assisted laser desorption/ionisation  
time-of-flight mass spectrometry MALDI-  
TOF-MS) 276  
measure molecular weight (MW) 231

## Biodegradable Poly(Lactic Acid): Synthesis, Modification, Processing and Applications

mechanical degradation 177,275  
medical applications 1,6,44,53,212,253  
melt polycondensation 18,22  
melt spinning 1,81,142,153,154,155,157-159,161,162,164,214,261  
melt strength (MS) 38,147,185,186,187,190,191,197,199,200,201  
melt-electrospinning 178  
melting peak 97,127  
melting temperature 48,71,126,127,149,153,156-158,161,181,182,183,275  
methanol 7,31,55,162,164,168,169  
*N,N'*-methylenebisacrylamide (MBAAm) 259  
micelle 38,50,51,54-57,59,62,216,257,260  
microbial degradation 280,292  
microfibrillar morphology 160  
miktoarm 63,64  
molecular distillation (MD) 4,11,12  
molecular weight distribution (MWD) 2,19,27,28,66,83,167,190  
monofilaments 154,261  
monomer 3,12,18,19,24-30,32,34,35,39,40-46,48,52,114,152,157,160,162,179,209,214,242,245,255,259,275,280,281,292  
multi-block copolymer 52,53  
multi-walled carbon nanotube (MWCNT) 132  
multiple filaments 174,208

### N

nano hydroxyapatite (NHA) 249  
nanocarrier 59,61  
nanocomposite 97,100,130-132,134,174,187,201,203,207,217,237,249,269  
neutralization 9  
nitroxide mediated radical polymerization (NMP) 61  
non-isothermal crystallization 127  
nonwoven 3,157,170,174,208-212,216,217,218,234,242  
nuclear magnetic resonance (NMR) 291  
nucleation 50,72,84,128,129,157,159,187,195,252

### O

octanoic acid 31  
oligo(*L*-lactic acid) (OLLA) 17,55  
optical purity 20,27,127,128,153  
organic reclamation and composting association (ORCA) 283  
organic solvent 9,22,23,32,44,148,165,252  
organically modified layered silicate (OMLS) 201  
organically modified synthetic fluorine mica (OMSFM) 201  
oxaphospholane compound 107,108

### P

packaging 1,3,6,53,72,109-112,114,115,130,179,208-210,212,220,221,224,229,230,233-235,253,285,286,289,290  
2,2-(2-pentene-1,5-diyl)trimethylene carbonate (cHTC) 43  
phase separation 52,69,75,97,116,148,162,163,164,167,168,249,251,255  
phenylmethylsulfonyl fluoride (PMSF) 282  
photo degradation 276  
photoelectron spectroscopy (XPS) 291  
PLA nanocomposites (PLACN) 130,201,203  
poly (2-ethyl acrylic acid) (PEAAc) 258  
poly (2-propyl acrylic acid) (PPAAc) 258  
poly (4 or 2-vinylpyridine) (PVP) 258  
poly (acrylic acid) (PAAc) 258  
poly (butylene adipate-co-terephthalate) (PBAT) 187,195  
Poly (*D,L*-lactide) (PDLLA) 15,40  
poly (glycolic acid) (PGA) 39,47,261  
poly (lactic acid) (PLA) 1,4,84  
poly (methacrylic acid) (PMAAc) 258  
poly (*N,N'*-diethylaminoethyl methacrylate) (PDEAEMA) 258  
poly(2-carboxyisopropylacrylamide) (PCIPAAm) 256  
poly(3-*r*-hydroxybutyrate) (*r*-PHB) 48  
poly(3-hydroxyalkanoates) (PHA) 48  
poly(*D,L*-lactic acid) (PDLLA) 15,40  
poly(dimethylsiloxane) (PDMS) 46,49



- poly(*D*-lactic acid) (PDLA) 175  
poly(ethylene glycol) (PEG) 3,47,231,233  
poly(ethylene oxide) (PEO) 59,64,  
poly(lactic acid) (PLA) 1,4,84  
poly(lactic acid) fibers 1,117,153,157-159,  
161-164,168-171,173,177-179,209-211,213,  
220  
poly(*L*-lactic acid) (PLLA) 6,15,66,147  
poly(*L*-lysine) (PLL) 66,248  
poly(*N*-(*L*)-1-hydroxymethyl) propylmeth-  
acrylamide (P(*L*-HMPMAAm)) 256  
poly(*N,N'*-diethylacrylamide) (PDEAAM)  
256  
poly(*N,N*-dimethylamino-2-ethyl methacrylate)  
(PDMAEMA) 51  
poly(*N*-acryloyl-*N'*-alkylpiperazine) 256  
poly(*N*-isopropylacrylamide) (PNIPAAm)  
51,62,66,255,256  
poly(*N*-vinyl-2-pyrrolidone) (PVP) 50  
poly(*p*-dioxanone) (PPDO) 48,262  
poly(tetramethylene ether glycol) (PTMG) 47  
poly( $\epsilon$ -caprolactone) (PCL) 40,47,229  
polycaprolacton (PCL) 187  
polycondensation 3,15-24,38,39,42,46,47,  
52,53,55  
polydepsipeptide 44  
polydispersity index (PDI) 27  
polyethylene glycol (PEG) 231,233  
polyethylene terephthalate (PET) 109,153  
polyethylenimine (PEI) 250  
polymer/layered silicate (PLS) 201  
polymerization 3,6,12,15-35,38-42,44,46-  
64,67,78,109,127,128,187,229,230,245,257  
polyphosphazene 56  
polyphosphoester (PPE) 51  
polypropylene (PP) 109,146,221,264,265,267  
polystyrene (PS) 18,112,179,209,248  
porous filaments 163  
precipitant vapor 162,164  
processing 3,9,10,38,48,54,68,86,87,94,  
99,100,112,114,115,122,142,145,146,147,  
148,150,151,153,157,158,161,162,184,186,  
187,190,201-203,208,209,210,215,219,220,  
229,241,249,251,252,273  
 $\beta$ -propiolactone (PL) 24
- Q**
- quenching 72,145,150
- R**
- radial expansion ratio (RER) 197  
random copolymer 39,44,45,217,255  
raw material 12,22,99,154,184,222  
reaction temperature 18,25,31  
reflux 17  
reversible addition fragmentation chain  
ransfer (RAFT) 51,61,63,64  
rheological 57,86,87,91,97,98,109,184,  
186,201  
ring-chain equilibrium 16,17  
ring-opening polymerization (ROP) 3,15,18,  
23,24,26,28,29,33,34,35,38,39,42,44,46,47,  
48,49,51,52,54,56,57,58,59,61,62,63,67,257
- S**
- scanning electron microscopy (SEM) 231  
self-condensation 20  
sodium lactate 13  
solid-state polycondensation 18  
solution polycondensation 17,22  
solvent evaporation 164  
splaying 174  
spinning 1-3,81,97,124,142,147,148,153-  
159,161-170,173,174,177,210,214,220,261  
stannous octoate 40,45,47,55  
star polymer 24,57,64  
starch 1,3,33,38,54,68,69,94,101,114,115,  
121,122,151,153,187,190,191,192,209,221,  
225,229,231,233,234,235,236  
star-shaped copolymer 56,57  
stereocomplex crystals 158,159,161  
stereoregularity 16  
succinyl- (*L*-alanyl-*L*-alanyl-*L*-alanine)-*p*-  
nitroamillide (Suc-(Ala) 3-pNA) 282  
sulfuric acid 4,9,293  
supercritical carbon dioxide (scCO<sub>2</sub>) 19  
suspension crystallization 10

## Biodegradable Poly(Lactic Acid): Synthesis, Modification, Processing and Applications

sutures 1,6,44,57,210,213-215,240,242,  
260,261  
synthesis 3,4,7,9,15,16,19,20,21,24,28,33,  
35,39,40,41,42,43,44,45,47,48,50,52,53,54,  
55,56,58,59,61,62,63,64,66,114,115,230,  
257,273  
syringe pump 175,177,253

### T

take-up roll 153,215  
tensile strength 2  
the biological oxygen demand (BOD) 293  
the rabbit mesenchymal (MSC) 242  
the theoretical oxygen demand (TOD) 293  
the US Food and Drug Administration (FDA)  
2,242  
thermal degradation 24,178,233,276  
thermal volatilization analysis (TVA) 276  
thermally induced phase separation (TIPS)  
148,249,251  
thermodynamic 2,5,24,59,130,177,251,252  
thermoreponsive 51,62,66  
tissue engineering 3,41,42,48,51,53-56,69,  
78,136,174,186,210,216,218,219,220,240,  
241,243,244,249,250,252,253,267,268  
titanium dioxide 134,190,217  
toluene sulfonic acid 20  
total organic carbon (TOC) 294  
*trans*-4-hydroxy-*N*-benzyloxycarbonyl-*L*-  
proline (*N*-CBz-Hpr) 45

transmission electron microscopy (TEM) 130  
trimethylene carbonate (TMC) 43,44,49  
two-step melt spinning process 154

### U

ultrafine 175,179,216,218  
ultraviolet (UV) 179,210,283

### V

valerolactone (VL) 24  
vinyl acetate 95,115,212,233,235  
viscosity average molecular weight 154

### W

water-crosslinking reaction 134  
wet spinning 142,153,167,168,174  
whipping instability 174

### X

xanthation 6  
X-ray diffraction (XRD) 128,291  
X-ray photoelectron spectroscopy (XPS) 291

### Y

Y-shaped copolymer 61,62

### Z

zinc(II) lactate (Zn(Lact)<sub>2</sub>) 33  
zirconium 39,40,44  
zirconium(IV) acetylacetonate 40,44